

Sociedad Mexicana de Ciencias y Tecnología
de Superficies y Materiales A.C.

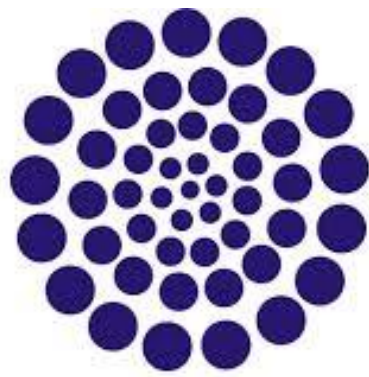


XII
*International Conference on
Surfaces, Materials and Vacuum*



September 23-27 2019, San Luis Potosí, S.L.P. México

PROCEEDINGS



CONACYT



IPICYT
INSTITUTO POTOSINO DE
INVESTIGACIÓN CIENTÍFICA
Y TECNOLÓGICA, A.C.



Cinvestav
Departamento de Física



Sponsored
Topical
Conference
www.avsp.org

AAA
Casa abierta al tiempo



XII International Conference on Surfaces, Materials and Vacuum

September 23rd to 27th, 2019 / San Luis Potosí, México



ORGANIZING COMMITTEE

Servando Aguirre Tostado
CIMAV

Emmanuel Haro Poniatowski
UAM-Iztapalapa

Eduardo Martínez Guerra
CIMAV

Mildred Quintana
UASLP

Leticia Pérez Arrieta
UAZ

Cristóbal Manuel Yee Rendón
UAS

Gregorio Hernández Coccoletzi
IFUAP

LOCAL COMMITTEE

Esteban Cruz Hernández
CIACYT, UASLP

Hugo R. Navarro Contreras
CIACYT, UASLP

Edgar López Luna
CIACYT, UASLP

Daniel U. Campos Delgado
Facultad de Ciencias, UASLP

Martha E. Compeán Jasso
Facultad de Ciencias, UASLP

Héctor E. Flores Reyes
Facultad de Estomatología, UASLP

Armando Encinas Oropesa
IPICYT

Edgar A. Cerdá Méndez
IICO, UASLP

INTERNATIONAL SCIENTIFIC COMMITTEE

Michael Springborg
Physical and Theoretical Chemistry,
University of Saarland, Germany

Talat S. Rahman, Department of Physics
University of Central Florida,
USA

Sergio E. Ulloa Department of Physics,
Ohio University, USA

Rubén Barrera Pérez Instituto de Física,
UNAM, México

Isaac Hernández Calderón
Departamento de Física, CINVESTAV,
IPN, México

Pedro Serena
Instituto de Ciencia de Materiales de
Madrid, España

Advanced and Multifunctional Ceramics

Jesús Heirás Aguirre (CNYN-UNAM)
José Trinidad Elizalde Galindo (UACJ)

Atomic Layer Deposition

Pierre Giovanni Mani González (UACJ)
Edgar López Luna (UASLP)

Hugo Tiznado:(CNYN-UNAM)

Biomaterials and Polymers

César Marquez Beltrán (BUAP)
Amir Maldonado Arce (USON)

Characterization and Metrology

Roberto Machorro (CNYN-UNAM)

Luminescence Phenomena: Materials and Applications

Salvador Carmona Téllez (CICATA LEGARIA-IPN)

Gilberto Alarcón Flores (CICATA ILEGARIA-IPN)

Microelectronics and MEMS

Norberto Hernandez Como (Centro de
Nanotecnología, IPN)

Israel Mejía Silva (CIDESI))

Nanostructures

Yenny Casallas (UPIITA-IPN)
Ángel Gabriel Rodríguez Vázquez (CIACYT -UASLP)

Plasma and Vacuum

José G. Quiñones-Galván, (CUCEI, UdeG)

Miguel Ángel Santana-Aranda, (CUCEI, UdeG)

Renewable Energy: Solar Cells and Materials

Issis Claudette Romero Ibarra (UPIITA-IPN)

Mario Fidel García Sánchez (UPIITA-IPN)

Semiconductors

Salvador Gallardo (CINVESTAV-DF)

Surfaces and Interfaces

Leonardo Morales de la Garza (CNyN-UNAM)

Mario Farás Sánchez (CNyN-UNAM)

Theory and Simulation of Materials

Raul Esquivel (IF-UAM)

María Teresa Romero de la Cruz (FCFM-UAdE)

Ariadna Sanchez (UAEH)

Thin Films

Alberto Duarte Moller, CIMAV-Chihuahua

Tribology

Enrique Camps Carvajal (ININ)

Giovanni Ramirez (Bruker Nano Surfaces)

Science Outreach

Wilfrido Calleja (INAOE),

Dolores García Toral (BUAP)

Josefina Robles Aguilar (BUAP)

Dalia Alejandra Mazón Montijo (CIMAV-Monterrey)

XII International Conference on Surfaces, Materials and Vacuum

September 23rd to 27th, 2019 / San Luis Potosí, México



Dear Colleagues,

From the very beginning the Annual Conference of the Sociedad Mexicana de Ciencia y Tecnología de Superficies y Materiales (SMCTSM, Mexican Society of Science and Technology of Surfaces and Materials) has been an important forum used by the Mexican scientific community for the discussion of scientific and technological topics related to research in the areas of surface and materials science.

In these occasion we are pleased to welcome you to participate in the XII International Conference on Surface, Materials and Vacuum (ICSMV) which will held in San Luis Potosí , S.L.P. 23th to the 27th of September 2019.

The scientific program of the Conference is divided into plenary conferences, short courses and the different symposia with oral and poster contributions. Additionally, to the scientific program, there is a symposium of Science Divulgation which is a traditional forum for the bringing together of students and the general public with the work undertaken and developed within our Society.

We hope that the efforts of the organizing committee, sponsors and colleagues will result in an interesting friendly meeting, providing the opportunity for closer and new interactions between researchers coming from the diverse institutions.

The SMCTM acknowledge the financial support of Consejo Nacional de Ciencias y Tecnología (CONACYT) for the realization of XII ICSMV.

The XII ICSMV
Organizing Committee SMCTSM
September 2019, San Luis Potosí , S.L.P México



XII -ICSMV
September 23rd to 27th, 2019 / San Luis Potosí, México

**XII INTERNATIONAL
CONFERENCE IN SURFACES,
MATERIALS AND VACUUM
PLENARY LECTURES**



OPENING TALK

Defects in 2D Metal Dichalcogenides: Doping, Alloys, Interfaces, Vacancies and Their Effects in Electronics, Catalysis, Optical Emission and Bio-Applications

Mauricio Terrones

Pennsylvania State University/USA

Semiconducting two-dimensional transition metal dichalcogenides (TMDs) such as MoS₂, MoSe₂, WSe₂, and WS₂ hold great promise for many novel applications. Recent years have therefore witnessed tremendous efforts on large scale manufacturing of these 2D crystals. A long-standing puzzle in the field is the effect of different types of defects in their electronic, magnetic, catalytic and optical properties.

In this presentation an overview of different defects in transmission metal di-chalcogenides (TMDs) will be presented [1,2]. We will define the dimensionalities and different atomic structures of defects, and discuss how these defects could be imaged with novel optical-driven techniques. We will emphasize doping and alloying in monolayers of MoS₂ and WS₂, and describe their implications in electronic and thermal transport. We will also describe the catalytic effects of edges, vacancies and local strain observed in Mo_xW(1-x)S₂ monolayers by correlating the hydrogen evolution reaction (HER) with aberration corrected scanning transmission electron microscopy (AC-HRSTEM) [3]. Our findings demonstrate that it is now possible to use chalcogenide layers for the fabrication of more effective catalytic substrates, however, defect control is required to tailor their performance. By studying photoluminescence spectra, atomic structure imaging, and band structure calculations, we also demonstrate that the most dominating synthetic defect—sulfur monovacancies in TMDs, is responsible for a new low temperature excitonic transition peak in photoluminescence 300 meV away from the neutral exciton emission [4]. We further show that these neutral excitons bind to sulfur mono-vacancies at low temperature, and the recombination of bound excitons provides a unique spectroscopic signature of sulfur mono-vacancies [4]. However, at room temperature, this unique spectroscopic signature completely disappears due to thermal dissociation of bound excitons [4]. One-dimensional hetero-interfaces in TMDs will be shown by AC-HRSTEM in conjunction with their non-linear optical emission, constituting a new way to image 1D defects [5]. Finally, the electronic effects of C-H defects within TMDs will be discussed, as p-type doping could be controlled by the presence of C within TMDs [6].



References:

- [1] Z. Lin, M. Terrones, et al. "Defect engineering of two-dimensional transition metal dichalcogenides". *2D Materials* **3** (2016) 022002.
- [2] R. Lv, M. Terrones, et al. "Two-dimensional transition metal dichalcogenides: Clusters, ribbons, sheets and more". *Nano Today* **10** (2015) 559-592.
- [3] Y. Lei, M. Terrones, et al. "Low temperature synthesis of heterostructures of transition metal dichalcogenide alloys ($W_xMo_{1-x}S_2$) and graphene with superior catalytic performance for hydrogen evolution". *ACS Nano*, **11** (2017), 5103-5112.
- [4] V. Carozo, M. Terrones, et al. "Optical identification of sulfur vacancies: Bound excitons at the edges of monolayer tungsten disulfide", *Sci. Adv.* **3** (2017), e1602813
- [5] B. R. Carvalho, M. Terrones, L. M. Malard, et al. "Imaging of 1D defects in monolayer dichalcogenides", submitted (2019).
- [6] F. Zhang, M. Terrones, et al. "Carbon Doping of WS₂ Monolayers: Band Gap Reduction and P-type Doping Transport", *Sci. Adv.* **5** (2019), eaav5003.



XII -ICSMV

September 23rd to 27th, 2019 / San Luis Potosí, México

PLENARY LECTURE I

Spectromicroscopy as a powerful tool for Investigating nanostructures

Carla Bittencourt

Mons University /Belgium

Limitations in characterization and theoretical modelling tools have been a major obstacle for the engineering of novel functional materials with properties enhanced by their nanoscale morphology, because detailed understanding of the structure–property–operando relationships are required. In this perspective technology has entered in a period of convergence between theory and characterization tools, traditional spectroscopic techniques such as Near Edge X- Ray Absorption Fine Structure (NEXAFS) and X-ray Photoelectron Spectroscopy (XPS) are being combined with microscopy to study individual nano-objects. In this context advances in the design and fabrication of x-ray focusing systems allow modifying conventional X-ray spectroscopies using synchrotron light to be used to study individual nanostructures and selected regions of a nanoscale sample. These spectroscopies are amongst the most powerful tools in material science providing elemental, electronic, structural and chemical information.

Recent trends include in-operando analysis of individual nanostructures. In my talk I will overview the development of spectromicroscopy techniques such as Nanoscale NEXAFS and Nanoscale XPS. Recent results on the doping of nanomaterials and their application will be presented.



PLENARY LECTURE II

Nonlocal response of metal-dielectric photonic metamaterials

Felipe Pérez-Rodríguez

Benemérita Universidad Autónoma de Puebla/México

An all-frequency homogenization theory, based on the Fourier formalism and the form-factor division approach, is applied to metal-dielectric photonic crystals (PCs). The theory provides explicit expressions for the nonlocal effective permittivity tensor for PCs with arbitrary Bravais lattice and any form of the dielectric and metallic inclusions inside the unit cell. Besides, it allows to describe the photonic band structure at any frequency and arbitrary Bloch wave number. As will be shown, the effective bianisotropic metamaterial tensors (permeability and crossed magneto-electric tensors) can be extracted from the nonlocal effective dielectric response via the redefinition of the average displacement vector and magnetic field. It turns out that the exact photonic band structure of the periodic metal-dielectric system can be reproduced by using both the original nonlocal dielectric response parameters and the new bianisotropic metamaterial ones even far beyond the long wavelength limit. The optical spectra (reflection and transmission) of a finite-size PC are calculated by applying the nonlocal homogenization approach together with the method of expansion into photonic bulk-modes (Bloch waves). In the talk, we compare the predictions of the developed all-frequency homogenization theory with exact theoretical results for the photonic band structure and optical spectra of one-dimensional PCs (regular multilayer structures) and with measured experimental optical spectra of two- (arrays of thin metal wires) and three-dimensional PCs (arrays of metallic split-ring resonators and crosses).



PLENARY LECTURE III

The promise of anisotropic 2D materials: the transition metal trichalcogenide

P. A. Dowben

Department of Physics and University of Nebraska-Lincoln

/U.S.A.

To develop new semiconductor technologies and, in fact, surpass silicon technology, the scaling of devices to transistor widths below 10 nm is essential. This poses problems for most materials, as few are perfect. Imperfections abound and in the limit of the very small, imperfections can have disastrous effects, especially on device performance (in say a transistor). As transistor dimensions decrease, in principle, 2D semiconductor channel materials are highly desirable because this reduced the leakage currents, but edge effects become significant. In aiming for 2D semiconductor channel materials, here lies a challenge for materials science: *to engineer a 2D material in which edge effects are not detrimental to transport as the channel width shrinks below 20 nm*. Here, we discuss possible 2D materials, with highly anisotropic band structure, and with promising edge structure and chemistry. Transition metal trichalcogenide (TMT), like MX₃ (M=Ti, Zr, Hf; X=S, Se, Te), and In₄X₃ (X=Se, Te) titanium trisulfide (TiS₃) are possible candidates for a semiconductor channel for a field effect transistor (FET) on the scale of a few nanometers. The band structure of titanium trisulfide (TiS₃) [1], ZrS₃ and In₄Se₃ [2] are both found to be highly anisotropic, consistent with transport measurements, and accompanied by few edge imperfections. TMT also have band gaps comparable to that of silicon (1.1 eV): ~ 1 eV for TiS₃; a direct band gap of about 1.3 eV and an indirect gap of about 0.6 eV for In₄Se₃. Such anisotropic 2D materials have great promise, indeed greater promise than graphene or the metal dichalcogenides, such that fabrication of ribbons for devices can be done reliably and reproducibly, for the production of high performance 2D devices with sub-20 nm dimension.

These anisotropic 2D materials will be discussed in the context of developing novel device concepts that will greatly extend the practical limits for energy-efficient computation. The general approach is to exploit the antiferromagnetic (AFM) order parameter, in materials with large boundary polarization, as a state variable to ensure nonvolatile device operation in a number of different devices concepts [3]. This approach to writing the magnetic information allows for a decrease in energy consumption per write operation by two orders of



magnitude, as compared to the relevant schemes associated with magnetic tunnel junctions. This is spintronics without ferromagnetism.

- [1] H. Yi, et al. *Applied Physics Letters* **112** (2018) 052102 [2] Ya. B. Losovyj, et al., *Applied Physics Letters* **92** (2008) 122107 [3] P. A. Dowben, et al., *IEEE Journal of Exploratory Solid-State Computational Devices and Circuits* **4** (2018) 1-9

This work was supported through the National Science Foundation grant NSF-ECCS—1740136, the Semiconductor Research Corporation through the E2CDA Center for Antiferromagnetic Magneto-electric Memory and Logic (AMML) under Task ID 2760.001, 2760.002 and 2760.003. This is an SRC Nanoelectronic COnputing REsearch (nCORE) program project. This work has been undertaken with D. Nikonov, Ch. Binek, U. Singisetti, J. Bird, S. Gilbert, M. Asensio, H. Ye, J. Avila, T. Komesu, W. Echtenkamp, P. V. Galiy, A. Kumar, B. Barut, T. M. Nenchuk, A. J. Yost, A. Sinitskii, M. Randle, C.-P. Kwan, S. Yin, A. Lipatov, N. Vorobeva, J. Nathawat, N. Arabchigavkani, K. He



PLENARY LECTURE IV

Atomic layer deposition: recent developments and new insights

W.M.M. (Erwin) Kessels

Department of Applied Physics, Eindhoven University of Technology, The Netherlands

E-mail: w.m.m.kessels@tue.nl

Current trends in semiconductor device manufacturing impose extremely stringent requirements on nanoscale processing techniques, both in terms of accurately controlling material properties and in terms of precisely controlling nanometer dimensions. For this reason atomic-scale processes have become vital in the area of the semiconductor industry [1,2]. Most particularly, the method of atomic layer deposition (ALD) has enabled the materials- and 3D-enabled scaling which has been necessary to continue Moore's law over the last decade.

ALD is a vapor-phase deposition technique that relies on the cyclic dosing of precursor molecules (A) and a co-reactant (B) in an ABABAB-type fashion. These exposures are separated by purge steps and result in self-limiting surface reactions. The self-limiting behavior of ALD can offer uniform and conformal films on large-area substrates and 3D structures, and allows for very precise thickness control.

In this presentation these features of ALD will be highlighted and the underlying surface chemistry will be discussed for prototypical processes and materials. This will include some latest insights in the surface reactions as well as some recent developments in terms of applications. Furthermore, some recent trends will be discussed such as the interest in area-selective ALD which is motivated by its potential application in self-aligned fabrication schemes. Finally also the demand for atomic layer etch (ALE) processes – basically the reverse of ALD processes – will be addressed. This includes both anisotropic and isotropic ALE processes in order to define and (re-)shape complicated 3D-structures on a wafer surface.

[1] R. Clark, K. Tapily, K.-H. Yu, T. Hakamata, S. Consiglio, D. O'Meara, C. Wajda, J. Smith, and G. Leusink, *APL Materials* 6, 058203 (2018)

[2] W.M.M. Kessels, *The dawn of atomic-scale processing*, www.atomiclimits.com, 2017.



PLENARY LECTURE V

The amazing optical properties of Metal Halide Perovskites: applications in photonics

Juan P. Martínez Pastor

Universidad de Valencia/ Spain

Metal halide perovskites (MHPs) have emerged as a very high promising materials for optoelectronics and photonics, mostly due to their large absorption coefficient and excellent photoluminescence quantum yield (PLQY) at room temperature. The optical properties of MHPs are comparable to those measured in III-V monocrystals and epitaxial films, the reason why MHPs are known as the “poor man’s high performance semiconductors” 1. The tetragonal phase of lead halide perovskites is characterized by a low exciton binding energy against the low temperature orthorhombic phase, making possible their good efficiency in solar cells. However, the carrier recombination dynamics of MHPs is mostly limited by the existence of shallow non-quenching traps under relatively low excitation powers 2, even if surface recombination and diffusion can play a relevant role in polycrystalline thin films. Under high excitation power these traps are filled and bimolecular recombination is the main radiative recombination channel, which makes possible the observation of stimulated emission with very low thresholds in MHP films integrated on polymer waveguides both on rigid 3 and flexible substrates 4. Similar and new applications can be obtained by using MHPs in the form of nanocrystals, from single photon emitters to lasers 5. Furthermore, if long aliphatic organic molecules are combined with methylammonium, strictly 2D with very high exciton binding energies and 2D/3D-MHP materials can be achieved, whose optical properties can lead to more efficient emitting devices and solar cells with higher stability 6.

1. Stoumpos, C. C. & Kanatzidis, M. G. Halide Perovskites: Poor Man’s High-Performance Semiconductors. *Adv. Mater.* 5778–5793 (2016). doi:10.1002/adma.201600265
2. Chirvony, V. S. *et al.* Delayed Luminescence in Lead Halide Perovskite Nanocrystals. *J. Phys. Chem. C* **121**, 13381–13390 (2017).
3. Suárez, I., Juárez-Pérez, E. J., Bisquert, J., Mora-Serò, I. & Martínez-Pastor, J. P. Polymer/Perovskite Amplifying Waveguides for Active Hybrid Silicon Photonics. *Adv. Mater.* **27**, 6157–6162 (2015).



XII -ICSMV

September 23rd to 27th, 2019 / San Luis Potosí, México

4. Suárez, I. *et al.* Integrated Optical Amplifier–Photodetector on a Wearable Nanocellulose Substrate. *Adv. Opt. Mater.* **6**, (2018).
5. Tang, X. *et al.* Room temperature single-photon emission and lasing for all-inorganic colloidal perovskite quantum dots. *Nano Energy* **28**, 462–468 (2016).
6. Rodríguez-Romero, J. *et al.* Tuning optical/electrical properties of 2D/3D perovskite by the inclusion of aromatic cation. *Phys. Chem. Chem. Phys.* **20**, 30189–30199 (2018).



XII -ICSMV

September 23rd to 27th, 2019 / San Luis Potosí, México

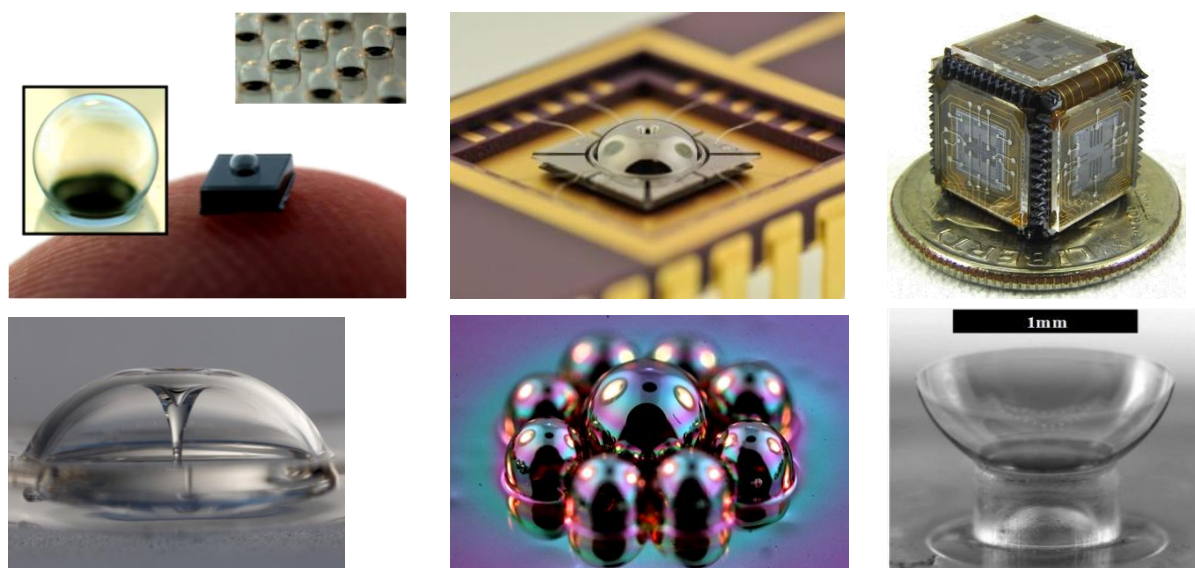
PLENARY LECTURE VI

MEMS are becoming 3D and atomically precise

Professor Andrei M. Shkel

University of California- Irvine/USA

Microtechnology comes of age. Clearly, some significant advances have been made, and we see a footprint of the technology in an ever-growing consumer electronics market full of interactive products enabled by microtechnology. These products include, for example, accelerometers for gaming, gyros for auto safety, resonators for clocks, and more. The questions remain, however: Is the technology really on the level of what we consider to be precision sensing? Is making sensors small necessarily result in degradation of performance? Why do we need the precision of sensing for our daily life and what are the opportunities if we have the precision at our fingertips? I will talk about some of the recent developments in my research group toward precision sensing, including solid-state 3D shell gyroscopes, spin-polarized atomic micro sensors, and the futuristic concept of the Ultimate Navigation Chip (uNavChip).





PLENARY LECTURE VII

Solar Photovoltaic system evolution and silicon-based solar cell technology

Yasuhiro Matsumoto

Centro de Investigación y de Estudios Avanzados del IPN/México.

Solar photovoltaic systems (PVS) became as one of the cleanest alternative energy production in several countries. The Electric energy generation is safe, reliable with a low-maintenance cost, without any on-site pollutant emissions. Nowadays, the utility grid-connected PVS are increasing rapidly in the world and the estimated global PV market grew to over 100 GW during 2018, and about 500 GW cumulatively installed capacity at the end of same year [1]. The underlying deployment scenario assumes 8,500 GW of cumulative installed PV capacity by 2050. The Renewables are expected to be a key driver of electrification with a global installed capacity of 20 TW where solar and wind are forecast to make a cumulative 8.5 and 6 TW, respectively. The renewable energy capacity would be responsible for around 86% of electric demand, with 60% covered by solar and wind [2].

First, an explanation about the general photovoltaic development and situation in Mexico and in the world will be given. Considerations about bulk and thin-film based technologies will be briefly reviewed for solar cell energy conversion by silicon technologies.

Some of the obtained silicon-based solar cells are analyzed through its light interaction, mostly, for the visible range for thin-films and for down-shift conversion approaches in bulk-silicon technology. An implementation for new solar cell structures and properties as using microcrystalline, and nanocrystalline silicon-based materials as SiO_x, SiC_x and SiO_xC_y by using Catalytic chemical vapor deposition methods are discussed [3].

References:

[1] PV activities in Japan, and global PV highlights, January 2019, RTS Japan.

[2] Global solar may reach 8,500 GW by 2050 – IRENA

<https://www.pv-magazine.com/2019/04/09/global-solar-may-reach-8500-gw-by-2050-irena/>

[3] Y. Matsumoto, et. al. "Luminescence study of Si/SiC nano-particles embedded in SiO_xC_y matrix



XII -ICSMV
September 23rd to 27th, 2019 / San Luis Potosí, México

deposited using O-Cat-CVD”, Physica E: Low-dimensional Systems and Nanostructures 111 (2019) 179–184.



PLENARY LECTURE VII

III-nitride quantum structures for device applications

S. Nikishin

Texas Tech-University/, USA

Gas source molecular beam epitaxy (GSMBE) and metallorganic chemical vapor deposition (MOCVD) were used for the growth of III-Nitride compounds and their random and digital alloys on different substrates. Using GSMBE with ammonia on (0001) sapphire substrates, AlN/AlGaN nanostructured SLs (digital alloys), with period from 1.25 to 2.25 nm, have been shown to have energy gaps in the deep UV suitable for light emitting diodes (LEDs) and photodetectors (PDs) operating down to \sim 240 nm. It was shown that the performance of LEDs and PDs is limited by factors including efficiency of radiative recombination and absorption in the active region and electrical resistivity (including contact resistance) of p-type wide bandgap SLs.

Using MOCVD approach, two types of selective area epitaxy (SAE) to grow quantum structures were realized. By patterning SiO₂ hard mask materials on planar sapphire substrates, we have grown various shapes including pyramidal stripes with In_xGa_{1-x}N multiple quantum wells. Using combined wet and dry etching to form structured fins on Si substrates, with (111) oriented sidewalls, we have demonstrated sidewall SAE of GaN layers for future electronic devices.



XII -ICSMV

September 23rd to 27th, 2019 / San Luis Potosí, México

PLENARY LECTURE IX

Generation and investigation of fermionic atomic superfluids

Jorge Amin Seman Harutinian

National Autonomous University of Mexico

In recent years, quantum gases have become a very active field of research. These systems represent an excellent scenario for studying macroscopic quantum phenomena, such as superfluidity, Bose-Einstein condensation and collective quantum excitations. At the same time, thanks to the extraordinary degree of control that ultracold atoms offer, they have been used as ideal quantum simulators of many-body and condensed matter systems.

The case of ultracold fermions is especially interesting thanks to the possibility of creating atomic pairs by means of Feshbach magnetic resonances, giving the possibility of creating different superfluid regimes across the BEC-BCS crossover: from Bose-Einstein condensates formed by tightly bound molecules, to BCS-like superfluids composed by loosely coupled Cooper pairs.

Very recently, at the Ultracold Matter Laboratory, we have been able to create for the first time in Mexico ultracold quantum samples using fermionic atoms of Lithium-6 across the BEC-BCS crossover. In this talk I will make a general description of our experimental setup and the techniques used to produce these ultracold systems, with special emphasis on the generation of different superfluid states.

Finally I will discuss the future perspectives of our laboratory and provide details about the ongoing experiments concerning the generation and study of collective excitations in fermionic superfluids.



PLENARY LECTURE X

The importance of solvent parameters in the large scale exfoliation of layered crystals

Antonio Esau Del Rio Castillo

Istituto Italiano di Tecnologia/ Italy

antonio.delrio@iit.it

The discovery of graphene in 2004[1] triggered the research in two dimensional (2D) materials. The outstanding properties of these thin materials awoke the imagination of hundreds of scientists. Giving as a result, multiple possible applications for these materials, ranging from polymer composites for aircraft to quantum computers, through applications in biology, electronics, and medicine.[2] It was clear that the announced 2D revolution requires efficient production methods and put in the market commercial applications. Although many production techniques developed[2] the most promising methods for large scale production of 2D materials relies on liquid phase exfoliation (LPE).[3] The process consists of mixing the bulk material in a solvent, and give energy to the mixture. Usually, the energy is applied in the form of sonic waves (or shear forces).

Up to now, the production of two-dimensional (2D) crystals is facing critical issues related to the transition from the lab to the industry,[2], e.g., heterogeneity of the flake size distribution and random type of defect, low-production rate, and so forth.[4] Recently, the high-pressure homogenisers (HPH) have emerged as attractive options for the large scale production of 2D crystals,[5,6] overcoming the low-production rate characteristic of the LPE methodologies.[5] Additionally, inside the HPS processor, the solvent flow reaches shear-rates $> 10^6$ s⁻¹, and the exfoliation process occurs in a few μ s's, thus reducing the impact of cavitation (explosion-implosion of solvent bubbles). These phenomena promote the peeling-off of large flakes (up to few μ m in lateral size) and reduce the damage induced in the flakes during the exfoliation.[7] However, the control of the flake sizes and defects (from the exfoliation) have not been demonstrated yet.

A possible route to achieve the size and defect tuning is to adjust the parameters that affect the shear rate and cavitation, i.e., the solvent viscosity, density, and vapour pressure.

In this talk will be presented the state-of-the-art results on the large scale exfoliation of layered materials (i.e., production rate more than 20 g h⁻¹) in the wet-jet mill,[5] a commonly used HPH technique in the industry.



Additionally, the first steps towards the on-demand control of the flakes morphology and defects, obtained by selecting solvents with different viscosities and vapour pressures will be presented. Finally, the last studies regarding the physicochemical process involved during the exfoliation and the importance of size selection will also be discussed.

a) Scheme of a high-pressure homogeniser used for the exfoliation of layered materials. b) shear stress (represented as red arrows) and cavitation (bubbles implosion), responsible for the exfoliation. c) Raman mapping on a drop of graphite exfoliated using dichloromethane, showing the presence of few-layers graphene (intensity of the 2D1 band, orange/red zones).

1. Novoselov, et al., Science, 306 (2004) 666.
2. Ferrari, et al., Nanoscale, 7 (2015) 4598.
3. Hernandez, et al., Nat. Nano., 3, (2008) 9, 563., Nicolosi, et al., Science, 340, (2013) 6139., Paton, et al., Nat. Mat., 13 (2014) 624
4. Del Rio and Bonaccorso. Carbon. Accepted manuscript.
5. Del Rio, et al., Mater. Horizon, 5 (2018) 890
6. Del Rio, et al, FlatChem, 2019. Accepted manuscript
7. Del Rio, et al. Manuscript in preparation



XII -ICSMV

September 23rd to 27th, 2019 / San Luis Potosí, México

PLENARY LECTURE XI

Study of the basic properties of InGaN in cubic phase and development of photovoltaic devices

Miguel A. Vidal Borbolla

CIACyT Universidad Autónoma de San Luis Potosí / México

In the past decades, nitride semiconductors have been used to fabricate different electronic and optoelectronic devices, among them the most important applications are blue laser and solid-state lighting, both with great economic impact and in people's daily lives. The success of these hexagonal phase devices has been possible due to the mastery in the construction of good heterostructures between GaN and AlGaN and InGaN in spite of the excessive quantity of dislocations present in the films. On the other hand, the cubic phase of GaN, InGaN and InN has some advantages over the hexagonal phase, such as the lack of spontaneous and piezoelectric polarization, greater symmetry, and greater structural strength. However, until a few years ago, the main physical properties of cubic GaN and the InGaN alloys including InN were unknown. In this conference we present the results of several years of work to synthesize GaN and ternary alloy InGaN in the cubic phase without hexagonal phase inlays and find their main physical properties without the perturbation of hexagonal GaN imbedded in the crystals. We present results of quantum wells of heterostructures among InGaN/GaN with different indium concentrations. In order to build a photovoltaic structure, we show the results of n and p-type doped GaN and the first solar cell of GaN in the cubic phase.



PLENARY LECTURE XI

De José Alfredo a Carl Sagan: explorando los *mundos raros* de la cristalográfica sincrotrónica

Luis E. Fuentes-Cobas

CIMAV-Chihuahua/ México.

luis.fuentes@cimav.edu.mx

El auditorio está invitado a un “viaje” alrededor del mundo de la cristalografía de sincrotrón.

Como recurso motivador, apelamos a un paralelo con los *mundos raros* del compositor mexicano José Alfredo Jiménez.

El viaje comienza con una muestra rápida de materiales avanzados, con propiedades extraordinarias. Descubrimos aleaciones con memoria de forma, superconductores de levitación magnética, materiales super-hidrófobos, neuronas artificiales, súper-aislantes térmicos, sistemas auxéticos y materiales invisibles.

Las propiedades físicas tienen su origen en la estructura de los materiales. La idea central de nuestro recorrido es una visita al mundo de las grandes instalaciones que ha hecho el hombre para investigar en detalle las estructuras de los materiales, en particular las estructuras cristalinas. Se observa el funcionamiento y rendimiento de los microscopios electrónicos, reactores de investigación y sincrotrones. Visitamos Chihuahua, *La Dama del Desierto*. Allí, en CIMAV, los microscopios SEM, TEM y STEM nos muestran desde los componentes de la micro-anatomía muscular hasta los átomos individuales de una cerámica superconductora. Volamos hacia el Oeste. Aterrizamos cerca del *Golden Gate*, en San Francisco. En el *Sincrotrón de Stanford* exploramos la perfección de los cristales gigantes de Naica con técnicas de difracción y absorción de rayos X. Cruzamos América del Norte y volamos sobre el océano Atlántico en dirección al Reino Unido. Desde el avión, si tenemos suerte, identificamos el anillo de *Stonehenge*. Aterrizamos en la Fuente de Luz *Diamond*. Luis Jr. Nos muestra muestra difractómetros con haces de rayos X tan intensos que evaporan las muestras biológicas en fracciones de segundo. A partir de



experimentos de difracción instantáneos, los investigadores de Diamond pueden descifrar estructuras biológicas de alta complejidad. Luego nos dirigimos a Europa continental, al sur de Francia. Sobrevolamos el *Mont Blanc* y aterrizamos en Grenoble. Allí visitamos a nuestro amigo Juan en el *Instituto Laue- Langevin* (ILL), un reactor de investigación con haces de neutrones lo suficientemente intensos como para descifrar (entre otras cosas) las estructuras magnéticas y las ubicaciones de los átomos ligeros. Al lado de la ILL encontramos la gran *Instalación Europea de Radiación de Sincrotrón* (ESRF). El espectro de energía de los

fotones ESRF es tan amplio como el de las investigaciones realizadas allí. Afortunadamente, México tiene a Hiram, nuestro facilitador para investigaciones de microabsorción. De Grenoble al sur. Aterrizamos en *Venecia* en nuestro camino hacia el *Sincrotrón de Elettra*. Estudiamos espectros, difractogramas, imanes, cerámicas, materiales sometidos a altas temperaturas y bajo campos eléctricos. En resumen, llevamos a cabo investigaciones de vanguardia utilizando los sincrotrones a nuestro alcance.

Nuestra siguiente etapa es un mundo de abstracción o fantasía: las matemáticas de la cristalográfica.

Los cristalógrafos nos movemos en el espacio recíproco (o *espacio de Fourier*), algo parecido a la imagen oscura de la cámara de Vera Lutter. Los espacios recíprocos y de difracción nos llevan a

descifrar las estructuras directas de los cristales. El mundo abstracto de los grupos matemáticos de Galois nos proporciona herramientas indispensables, desde la caracterización sistemática de la simetría estructural de cualquier objeto hasta las reglas de selección para espectroscopia infrarroja y Raman. Los grupos cristalográficos clásico y magnético nos permiten predecir la existencia o no, y la estructura tensorial, de las propiedades físicas. El Principio de Neumann es evidente en la anisotropía de las propiedades del cristal, tal como se describe en la Base de Datos Abierta de Propiedades de los Materiales (<http://mpod.cimav.edu.mx>).

A nivel atómico, el mundo cristalino es uno de competencia continua entre orden y desorden. Con nuestro arsenal de sincrotrón trabajamos para descifrarlo. Los máximos de difracción agudos nos proporcionan la estructura cristalina general de los materiales más diversos, monocrystalinos y policristalinos, desde inorgánicos simples hasta fármacos complicados y objetos biológicos. La



dispersión difusa nos informa sobre las estructuras amorfas y los trastornos locales (térmicos, elásticos, electromagnéticos).

La espectroscopia de absorción de rayos X nos permite observar estructuras a nivel local, con un enfoque diferente. XANES, EXAFS y otras técnicas nos muestran los estados de valencia iónicos, la función de distribución de pares, con selectividad elemental y la identificación de fases amorfas.

La luz sincrotrón nos ilumina los laberintos del *espacio de Euler*, que es el espacio de las orientaciones cristalinas, en un policristal texturado. Medimos las funciones de distribución de orientación y aplicamos herramientas que modelan la influencia de la textura en las propiedades de los policristales.

Perspectiva a futuro

La curiosidad humana escapa a los límites del planeta Tierra. La cristalográfica ya tiene informes detallados sobre las estructuras de los minerales de la Luna y Marte. El trabajo se ha realizado con muestras traídas a la Tierra por la expedición del Apolo 11 (hace exactamente 50 años) y está en curso hoy en día por el explorador marciano Curiosity. Se explica la detección de agua en arcillas marcianas de los difractogramas 2D obtenidos *in situ* por Curiosity e interpretados por el método de Rietveld en la Tierra. Recientemente (2017) se cumplieron 40 años del lanzamiento de la misión Voyager en el espacio interestelar. Esta estación automática, alimentada por un generador termoeléctrico de radioisótopos, ha enviado a la Tierra abundante información sobre los planetas exteriores del Sistema Solar (SS). Ya está fuera de las SS y lleva un saludo de la humanidad a las posibles civilizaciones extraterrestres. La presentación concluye con comentarios humanistas del reconocido astrofísico Carl Sagan (1934-1996).

Agradecimientos:

Las investigaciones de estructura y propiedades físicas por el Grupo de Cristalografía CIMAV han sido apoyadas por los Proyectos 257912 de CONACYT "Representación y pronóstico de las propiedades físicas de los materiales mono- y policristalinos" y 183706 "Influencia del ambiente sobre los cristales gigantes de selenita de Naica". Se han realizado experimentos de sincrotrón en los sincrotrones SSRL, Elettra, Diamond y ESRF. Se aprecia el soporte multifacético recibido por la Red Temática de Usuarios de Luz Sincrotrón (RedTULS).



XII -ICSMV
September 23rd to 27th, 2019 / San Luis Potosí, México



XII -ICSMV
September 23rd to 27th, 2019 / San Luis Potosí, México

ADVANCED AND MULTIFUNCTIONAL CERAMICS (AMC)

Chairmen: Jesus Heiras Aguirre (CNYN-UNAM)

José Trinidad Elizalde Galindo (UACJ)



XII -ICSMV
September 23rd to 27th, 2019 / San Luis Potosí, México

ADVANCED AND MULTIFUNCTIONAL
CERAMICS (AMC)
ORAL SESSIONS



XII -ICSMV

September 23rd to 27th, 2019 / San Luis Potosí, México

[AMC-31] Magnetic interaction between copper deposited over a strontium hexaferrite template

Azdrubal Lobo-Guerrero (azdlobo@gmail.com)³, Manuel Mirabal-García¹, Jesús García-Gallegos², Fabiola Santos-López³

¹ Instituto de Física. Universidad Autónoma de San Luis Potosí

² Universidad Tecnológica de San Juan del Río

³ Área Académica de Ciencias de la Tierra y Materiales. Universidad Autónoma del Estado de Hidalgo

This work explores the magnetic behavior of the copper deposition on the surface of strontium hexaferrite compound. Copper is a conductive and non-magnetic metallic material, while the strontium hexaferrite is a semiconductive and ferrimagnetic ceramic compound. Several systems based on the strontium hexaferrite as bulk and highly porous structures were analyzed when copper covers the ceramic surface. The copper deposition was done using chemical electrodeposition and magnetron sputtering. Experimentally, it was observed a strong interaction between copper and the strontium hexaferrite. This interaction improves the magnetic properties of the strontium hexaferrite. Results suggest that the interaction among the copper with the interstitial iron cations of the hexaferrite occurs through the oxygen cations through a superexchange interaction. Then, copper fixes the magnetic moments of iron, which makes difficult its magnetization switching. As this is surface phenomena, the deposition way on the hexaferrite is an important parameter to be account as well as the morphological characteristics of the hexaferrite template.



[AMC-187] SYNTHESIS OF TUNGSTEN TRIOXIDE DOPED WITH Ag AND Au BY THE MODIFIED COMBUSTION METHOD AND ITS APPLICATION IN DEGRADATION OF COLORANTS

Mirian Yoceline Herrera Herrera (m_y_herrera2@hotmail.com)¹, Rubén Jonatan Aranda García (jonatan_izucar@hotmail.com)¹, Daniel Cruz González¹

¹ BUAP

Tungsten trioxide (WO_3), also known as tungsten oxide (VI) or volphramic anhydride, is a naturally occurring material in the form of hydrates, which include minerals such as tungstite ($\text{WO}_3 \cdot \text{H}_2\text{O}$), meymacita ($\text{WO}_3 \cdot 2\text{H}_2\text{O}$) and hydrotungstite (of the same composition as meymacita). WO_3 has several uses, among which it stands out as a pigment in the ceramic and paint industry, in the manufacture of tungstates for X-ray screens, as a gas sensor, as a photocatalyst for degrading dyes in wastewater, among other applications.

Due to the diverse applications of WO_3 and the conventional industrial method that uses dangerous reagents and long reaction times to obtain it, in this work, it is proposed to synthesize it from tungsten recovered from incandescent waste bulbs. Since the filament of the bulbs is made of pure tungsten, it's possible to recover it and at the same time it contributes in the decrease of the waste of bulbs disposed in landfills which contaminate the water, soil and air. In addition, a novel method called Modified Combustion-Gelification is proposed, it's a simple method, it doesn't use hazardous materials, since urea, alanine and / or glycine are used as fuels, and metals in the form of nitrates, using short reaction times (approximately 5 minutes).

To study the materials obtained, the following characterization techniques were carried out: X-ray diffraction (XRD) to determine the molecular structure of the crystals and identify the different phases obtained, scanning electron microscopy (SEM) analysis to obtain information about the morphology and surface texture of the particles, the size distribution of the crystals and the composition of the samples synthesized. X-ray Energy Dispersion Spectrometry (EDS) to obtain chemical composition information, and Thermogravimetric Analysis (TGA) to study thermal stability.

Finally, degradation tests were performed on methylene blue dye of each of the materials, in dark and irradiated with ultraviolet light (UV), the results were studied by UV-VIS spectroscopy.

Keywords: Synthesis, Tungsten Trioxide, Modified Combustion Method, Degradation.



XII -ICSMV

September 23rd to 27th, 2019 / San Luis Potosí, México

[AMC-551] Comparison Between Physical Methods to Characterize the Composition of Lithium Niobate Powders

Rurik Farias (*rurik.farias@uacj.mx*)³, Oswaldo Sánchez-Dena², Carlos J. Villagómez², César D. Fierro-Ruiz¹, Artemio S. Padilla-Robles², Enrique Vigueras-Santiago⁴, Susana Hernández-López⁴, Diana María Carrillo Flores³, Jose Trinidad Elizalde Galindo³, Jorge Alejandro Reyes Esqueda²

¹ Departamento de Mecátronica y Energías Renovables, Universidad Tecnológica de Ciudad Juárez, Avenida Universidad Tecnológica 3051, Colonia Lote Bravo II, 32695 Ciudad Juárez, Chihuahua, México.

² Instituto de Física, Universidad Nacional Autónoma de México, 04510 Mexico City, México

³ Instituto de Ingeniería y Tecnología, Universidad Autónoma de Ciudad Juárez, Av. Del Charro 450 Norte, 32310 Ciudad Juárez, Chihuahua, México.

⁴ Laboratorio de Investigación y Desarrollo de Materiales Avanzados, Universidad Autónoma del Estado de México, Paseo Colón esquina Paseo Tollocan, 50120 Toluca, Estado de México, México.

X-Ray Diffraction (XRD), Raman Spectroscopy (RS), UV-vis Diffuse Reflectance (DR), and Differential Thermal Analysis (DTA) are the most accepted methods to characterize the composition of lithium niobate (LN) LiNbO_3 . A comparison between these physical methods is made. These methods are used in good acceptance in single crystals, nevertheless, for powders, some corrections are needed due to strong scattering effects and randomness. In this work, new linear equations for each method are proposed for the determination of the composition of LN powders. To validate our results, we compare several samples synthesized by the standard and inexpensive method of mechanochemical synthesis with powders obtained by the trituration of single crystals (commercial obtained).



XII -ICSMV

September 23rd to 27th, 2019 / San Luis Potosí, México

[AMC-538] Fabrication of hydroxyapatite-silica fibers by electrospinning for cadmium and lead removal from aqueous solution

*José Hafid Roque-Ruiz (jhroqueruiz@hotmail.com)², Jesús Alberto Garibay-Alvarado²,
Jonatan Torres-Pérez², Nahum Medellín-Castillo¹, Simón Yobanny Reyes-López²*

¹ Centro de Investigación y Estudios de Posgrado, Facultad de Ingeniería, Universidad Autónoma de San Luis Potosí

² Instituto de Ciencias Biomédicas, Universidad Autónoma de Ciudad Juárez

Water pollution by heavy metals represents a serious threat to the environment and human health. Interest in the adsorption process has increased as a simple and low-cost option to remove heavy metals from aqueous media. A hydroxyapatite-silica composite with morphology of continuous fibers was prepared by sol-gel process and electrospinning, in order to be used for removal of cadmium (Cd^{+2}) and lead (Pb^{+2}) present in aqueous solution. Adsorption equilibrium studies were conducted using two series of solutions with concentration between 60 and 500 mg/L of the corresponding metal. Cadmium and lead solutions with concentration of 200 mg/L were used for adsorption kinetic studies. Samples of the composite fibers were added to each solution in a ratio of 0.5 g/L. Changes in concentration were determined by atomic absorption spectroscopy. The highest amount of each metal adsorbed per gram of material (q) was 93.30 and 466.98 mg/g for cadmium and lead, respectively. Freundlich isotherm is the model showing the best correlation with experimental data, indicating that the adsorption process takes place on a heterogeneous surface. Furthermore, the adsorption process follows the pseudo-second order model. Results showed that the hydroxyapatite-silica fibers present a high capacity for adsorption of heavy metals and a greater affinity towards lead ions.



[AMC-682] MAGNETIC PROPERTIES AND STRUCTURAL CHARACTERIZATION OF MnFe₂O₄ NANOFIBERS OBTAINED BY ELECTROSPINNING

DIANA MARIA CARRILLO FLORES (*diana.carrillo@uacj.mx*)¹, ISAAC PANTOJA RODRIGUEZ¹,
JOSE TRINIDAD ELIZALDE GALINDO (*jose.elizalde@uacj.mx*)¹, JOSE RURIK FARÍAS MANCI-
LLA¹, CARLOS ELIAS ORNELAS GUTIERREZ²

¹ Departamento de Física y Matemáticas del Instituto de Ingeniería y Tecnología, Universidad Autónoma de Ciudad Juárez, Ave. Del Charro 450 norte, Partido Romero, 32310, Ciudad Juárez, Chihuahua, México.

² Laboratorio Nacional de Nanotecnología, Centro de Investigación en Materiales Avanzados, S.C., Miguel de Cervantes 120, Complejo Industrial Chihuahua, 31136, Chihuahua, Chihuahua, México.

Electrospinning technique has been used to produce MnFe₂O₄ nanofibers with diameters in the nanometer to submicron range. The precursor solution was prepared in water-ethanol with 20% PVP and nitrates (Mn, Fe). The fibers obtained were annealed at 700°C for 1 h in an argon atmosphere. Crystalline phases, microstructure, nanostructure and magnetic properties were studied by using X-ray diffraction (XRD), scanning (SEM) and transmission electron microscopy (TEM) and vibrational magnetometry (VSM). From XRD patterns it was found a pure phase MnFe₂O₄. From SEM was determined a heterogeneous morphology and an average grain size of 35nm. From TEM, was observed a high structural ordered nanostructure inside the grains conforming the fiber and characteristic peaks of electron energy-loss spectroscopy(EELS) for the low loss region 0-80 eV. Finally, the hysteresis loops showed a characteristic ferrimagnetic behavior, with a maximum magnetization value equal to 77 emu/g at 150 K.

Keywords: Electrospinning, Manganese ferrite, EELS.



XII -ICSMV
September 23rd to 27th, 2019 / San Luis Potosí, México

ADVANCED AND MULTIFUNCTIONAL
CERAMICS (AMC)
POSTER SESSIONS



[AMC-345] Effects of temperature on magnetic properties of SrFe₁₂O₁₉ synthesized by the Pechini method

Maria de los Angeles Urbano Peña (mariangeles137@hotmail.com)¹, Salvador Palomares Sanchez¹, Facundo Ruiz¹

¹ Facultad de Ciencias. Universidad Autónoma de San Luis Potosí. Av. Parque Chapultepec 1570, 78210. San Luis Potosí, México.

Permanent magnets are essential components in the industry, medicine, and research. Today, there is an undeniable need to find alternatives that allow us to improve their properties, reduce their size and increase their efficiency without the use of rare earths. Strontium hexaferrite (SrFe₁₂O₁₉) is the most widely used magnetic material due to its low production cost and its multiple applications as permanent magnets (electronic devices, gas sensors), catalytic supports, and in the field of biomedicine (drug delivery systems, cancer treatments, hyperthermia, magnetic resonance, etc.).

In this work, Strontium hexaferrite powders were synthesized by Polymeric Complex Method(Pechini). The samples were calcined at temperatures of 800 °C, 850 °C, 900 °C, 1000 °C, and 1050 °C during 1 hour. In addition, the presence of a secondary phase of hematite (α -Fe₂O₃) was detected in all samples. The influence of temperature and synthesis technique was analyzed to control grain growth and size. The phase and crystal structure of the samples were analyzed by X-ray diffraction, the morphology was observed using the scanning electron microscope (SEM) and transmission electron microscopy (TEM). While the magnetic properties were measured at room temperature using a vibrating sample magnetometer (VSM) with an applied field up to 20 KOe. The results show that the sample calcined at 900°C with a crystal size of 245 nm, exhibited the best magnetic properties of the entire series with an Ms=99.3 emu/g, Mr=49.1 emu/g, Hc= 6.15 kOe. This can be attributed to the exchange coupling interactions between the soft and hard phases of the sample.



[AMC-360] Influence of Fe³⁺ doping on the structural, ferroelectric, dielectric and optical properties of BaTiO₃

Fernando Daniel Cortes Vega (danielcv87@gmail.com) ¹, J. Martin Yañez Limón ¹

¹ CINVESTAV

In this work, we present a study of the structural, optical, ferroelectric and dielectric properties of BaTiO₃ doped with diluted quantities of iron ($x = 0, .01, 02, .04$; BaFe_xTi_{1-x}O₃). Pure and doped BaTiO₃ were prepared by mechanical milling and conventional solid state reaction method. The XRD revealed the formation of a hexagonal phase activated by the addition of Fe³⁺. The microstructure and morphology were analyzed by SEM, confirming the presence of the hexagonal phase as well as an important refinement of the grain size. The optical band-gap remained almost unchanged with the addition and increase of Fe³⁺, being observed a minimum decrease from 3.49 to 3.37 for pure BaTiO₃ and the sample doped with the highest amount of dopant, respectively. The ferroelectric performance was severely affected by the incorporation of dopant, deteriorating the remnant polarization from a maximum value of 9.42 $\mu\text{C}/\text{cm}^2$ for pure BaTiO₃ and up to 0.2 $\mu\text{C}/\text{cm}^2$ for the sample with the largest amount of dopant. Dielectric measurements allowed us to determine the Curie temperature that shows a continuous reduction as the amount of Fe increased. Similarly, the dielectric constant undergoes a significant reduction by the incorporation of Fe³⁺ into the host structure.



[AMC-533] Magnetocaloric effect and transition order of La_{0.67}Ca_{0.28}Sr_{0.05}MnO₃ compound

Verónica E. Salazar-Muñoz (veronica.salazar900203@gmail.com)², Salvador A.

Palomares-Sánchez², Azdrubal L. Guerrero-Serrano⁴, J. Israel Betancourt-Reyes⁵, A.

Alberto Torres-Castillo³, Javier G. Caval-Velarde¹

¹ Instituto Tecnológico Superior de Irapuato, Carretera Irapuato - Silao km 12.5, 36821
Irapuato, Guanajuato, México.

² Universidad Autónoma de San Luis Potosí, Facultad de Ciencias, Av. Salvador Nava s/n,
78290, San Luis Potosí, SLP, México.

³ Universidad Autónoma de San Luis Potosí, Instituto de Metalurgia, Av. Sierra Leona #550,
78350, San Luis Potosí, SLP, México

⁴ Universidad Autónoma del Estado de Hidalgo, Área Académica de Ciencias de la Tierra y
Materiales, Carr. Pachuca-Tulancingo Km. 4.5, 42039 Pachuca de soto, México.

⁵ Universidad Nacional Autónoma de México, Instituto de Investigaciones en Materiales,
Círculo Exterior, Ciudad Universitaria, Coyoacán, 04510, Ciudad de México, México.

There has been growing interest in the development of materials for magnetic refrigeration applications as they provide an environmentally friendly option to replace chlorofluorocarbons and hydrochlorofluorocarbons as refrigerants. Magnetic refrigeration (MR) technology is based on the magnetocaloric effect (MCE). The lanthanum manganite with Ca and Sr substitutions is an advanced ceramic which can become an alternative material for magnetic refrigeration. It has high chemical stability, it is easy to process, and cheaper than the gadolinium (Gd), considered the material with magnetocaloric

ΔS_M effect near room temperature par excellence. The magnetic entropy change (ΔS_M) is the physical property that describes the MCE, and its maximum value occurs with the ferromagnetic-paramagnetic (FE-PA) transition at Curie temperature. In this work are presented the results of the study of the order of FE-PA transition in submicron La_{0.67}Ca_{0.28}Sr_{0.05}MnO₃ particles, synthesized by Pechini method, using the phenomenological model proposed by Hamad. The effect of magnetic interactions on the MCE of the compound when the particles distance is varying, was also analyzed. In addition, the results of the structural characterization by X-ray diffraction and infrared spectroscopy of compound are presented, and morphological characterization by scanning electron microscopy.



XII -ICSMV

September 23rd to 27th, 2019 / San Luis Potosí, México

[AMC-593] Strontium Titanate Nanofibers by Electrospinning

Tania Beatriz Izquierdo-Almaguer (al157281@alumnos.uacj.mx)², Zabdy Jacqueline Ruvalcaba-Martínez², Rurik Farias², Miguel Melendez-Lira¹, Simon Yobanny Reyes-López (yobannyr@yahoo.com.mx)²

¹ Physics Department, CINVESTAV-IPN,

² Universidad Autónoma de Ciudad Juárez

An alternative methodology was obtained for the synthesis of strontium titanate fibers, which combines the sol-gel and electrospinning technique to produce a fibrillar ceramic composite. Two sol-gel solutions starting from Strontium nitrate and titanium tetraisopropoxide were prepared and then mixed and homogenized with polyvinylpyrrolidone polymeric solution. A mean diameter of 103 ± 39 nm for fibers was obtained using a 0.30 M precursor solution. Precursor concentration influenced morphology and stability of samples, as homogenous and smooth fibers were obtained from more concentrated solutions. The characteristic bands of strontium titanate of perovskite structure were identified in Infrared and Raman spectroscopy. The presence of tetragonal titania and strontium titanate was demonstrated at 800 °C by thermal analyses and X-ray diffraction. At 1200 °C, tetragonal TiO₂ decreased and pure and crystalline strontium titanate was observed.



[AMC-600] Synthesis of Lithium Niobate-Silica Nanofibers

Zabdy Jaqueline Ruvalcaba-Martínez (al166660@alumnos.uacj.mx)¹, Jesús Alberto Garibay-Alvarado¹, Rurik Farias¹, Tania Beatriz Izquierdo-Almaguer¹, Simón Yobanny Reyes-López (yobannyr@yahoo.com.mx)¹

¹ Universidad Autónoma de Ciudad Juárez

An alternative methodology was obtained for the synthesis of Lithium niobate-silica fibers, which combines the sol-gel and electrospinning technique to produce a fibrillar ceramic composite. Two sol-gel solutions starting from niobium-lithium ethoxide and tetraethyl orthosilicate were prepared and then mixed with polyvinylpyrrolidone; the solutions were electrospun in a coaxial setup. The obtained lithium niobate-silica polymeric fibers were approximately 760 nm in diameter. Raman spectroscopy confirmed the composite composition by showing signals corresponding to lithium niobate and silica. Scanning electron microscopy showed coaxial fibers with a diameter of around 330 nm arranged as a fibrillar membrane at 800 °C. At 1000 °C the continuous shape of fibers was preserved; the structure is composed of silica and lithium niobate nanoparticles within the fibers. The formation of crystalline lithium niobate and amorphous SiO₂ phase was also confirmed by Raman and XRD.



[AMC-644] Synthesis and analysis of ferroelectric properties of KNN-based ceramics ($K0.5Na0.5Nb03$) doped with copper

Jocelyne Marissa Estrella Núñez², Jesus Serralta-Macias¹, Karla Mariela Moya Canul², Rivelino Flores-Farias¹, Jose Martín Yañez-Limón¹

¹ Cinvestav-Unidad Querétaro. Libramiento Norponiente No. 2000 Fracc. Real de Juriquilla Querétaro Qro., México

² Yachay Tech, School of Chemical Sciences & Engineering, 100119-Urcuquí, Ecuador

The ferroelectric behavior of the $K0.5Na0.5Nb03$ system and the effect of doping with Cu in concentrations of 0.5 and 1 mol% were studied. In this range of copper concentrations the sample with 0.5%mol of Cu showed an antiferroelectric behavior, in this state, these materials have high saturation polarization and low remnant polarization values, which are very appropriate for energy storage. The synthesis was carried out using a mixture of oxides and carbonates ($K2CO3$, $NaCO3$, $NbO5$ and CuO), by the conventional ceramic method with high energy milling in a spex-8000 mill. The powders were mixed stoichiometrically and milled in the spex-mill for 6 hours, then calcined at $900^{\circ}C$ for 4 hours. The calcined powders were milled again for 15 minutes and uniaxially pressed at 385 MPa to obtain 0.95 cm diameter pellets, which were sintered under the following conditions: at $1100^{\circ}C$ for 4 hours (without encapsulation), 3 hours (with encapsulation) and 1 hour (with encapsulation). The formation of the orthorhombic phase in the KNN calcined powders was observed by DRX, however the presence of secondary phases in small concentrations is also observed, which in turn decreases with the encapsulation of the samples, during sintering. The SEM micrographs of the sintered samples show regions with grain size between 1-2 μm , as well as areas with not well defined grain edges probably due to incipient fusion. However, the majority presence of the orthorhombic phase with a very small concentration of the secondary phase is notable. Through hysteresis curves, (polarization vs applied field) a ferroelectric behavior was observed in samples of pure and doped KNN with 1% mol of Cu, in contrast the sample with 0.5% mol of Cu, showed a double hysteresis loop, behavior characteristic of antiferroelectric materials. Finally, the dielectric characterization was performed using impedance spectroscopy as a function of temperature, with which it was possible to determine the transition temperatures of the different phases of the KNN, namely orthorhombic-tetragonal and tetragonal-cubic transitions, which are presented around $200^{\circ}C$ and $400^{\circ}C$, respectively. The higher temperature corresponds to the Curie temperature, where the material changes its behavior from the ferroelectric state to paraelectric.

Keywords: Antiferroelectric, hysteresis, dielectrics.

References:

- [1] S. M. Ke, H. T. Huang, H. Q. Fan, H. K. Lee, L. M. Zhou, and Y.-W. Mai. "Antiferroelectric-like properties and enhanced polarization of Cu-doped $K0.5Na0.5Nb03$ piezoelectric ceramics". *American Institute of Physics*, (2012).
- [2] Dunmin Lin, K. W. Kwok, and H. L. W. Chan. "Double hysteresis loop in Cu-doped $K0.5Na0.5Nb03$ lead-free piezoelectric ceramic" *American Institute of Physics*, (2007).



XII -ICSMV

September 23rd to 27th, 2019 / San Luis Potosí, México

[AMC-645] Characterization of thin films of PZT doped in sites A and B obtained by sputtering

María Dolores Durruthy-Rodríguez², Rebeca Castanedo-Pérez¹, Gerardo Torres-Delgado¹, Moisés Hernández-García², Carlos Alberto Avila Herrera¹, José Martín Yáñez-Limón¹

¹ Cinvestav-Unidad Querétaro. Libramiento Norponiente No. 2000 Fracc. Real de Juriquilla Querétaro Qro., México

² Facultad de Humanidades, Universidad Nacional Evangélica, UNEV, Paseo de los Periodistas # 54, Ensanche Miraflores, Santo Domingo D.N., Republica Dominicana, CP 10230

The ferroelectric films with perovskite structure (ABO_3) take advantage of their multifunctional properties, being a versatile material for use in charge storage nonvolatile ferroelectric random access (FRAM) capacitors with high dielectric constant, etc. Their piezoelectric and dielectric properties are important for the integration of ferroelectric films in micro-electromechanical systems (MEMS), in energy harvesting devices, nano-actuators and complex systems for robotics and radio frequency (RF) small-scale applications. In this work thin films are obtained by the RF sputtering method, using PZT ceramic targets at the morphotropic phase boundary and doped with La, Nb and La + Nb and without doping, to produce changes in sites A, B and A + B of the perovskite structure of ABO_3 on two types of substrates: $\text{SiO}_2 / \text{Cd}_2\text{SnO}_4$ and $\text{SiO}_2 / \text{ITO}$.

The deposit was made using argon gas flow at 100 W of power for 30 minutes. The films were characterized through XRD, SEM, Uv-vis and current vs. voltage measurements. The thickness of the films were about 200 nm.

Key words: thin films, Sputtering, dielectric films, ferroelectric materials.



XII -ICSMV

September 23rd to 27th, 2019 / San Luis Potosí, México

[AMC-663] Study of the optical, structural properties and thermal stabilization of silica xerogel matrix with carrot juice

DIANA LETICIA ESPERICUETA GONZÁLEZ (*diana.espericueta88@hotmail.com*)¹, GERARDO ORTEGA ZARZOSA³, JOSÉ REFUGIO MARTINEZ MENDOZA³, AZDRUBAL LOBO GUERRERO², DORA ERIKA ESPERICUETA GONZÁLEZ³

¹ INSTITUTO TECNOLÓGICO DE SAN LUIS POTOSÍ CAPITAL

² UNIVERSIDAD AUTÓNOMA DE ESTADO DE HIDALGO

³ UNIVERSIDAD AUTÓNOMA DE SAN LUIS POTOSÍ

Using the techniques of X-ray diffraction, IR spectroscopy, scanning electron microscopy and emission fluorescence, optical and structural properties of thermal stabilization of samples synthesized from carrot juice within a silica matrix were studied. The organic components induce structural changes in the ceramic matrix, decreasing the sintering temperature at which stable forms of amorphous silica are formed, such as β -tridymite, and crystalline structures, including the presence of stishovite at room temperature. The results also show a stabilization of the organic components, the xerogel being a protector of the components at high temperatures.



XII -ICSMV

September 23rd to 27th, 2019 / San Luis Potosí, México

ATOMIC LAYER DEPOSITION SYMPOSIUM (ALD)

Chairmen: Pierre Giovanni Mani González (UACJ)

Edgar López Luna (UASLP)

Eduardo Martínez Guerra (CIMAV-MTY)



XII -ICSMV

September 23rd to 27th, 2019 / San Luis Potosí, México

ATOMIC LAYER DEPOSITION
SYMPOSIUM (ALD)
ORAL SESSIONS



[ALD-124] Effect of the fabrication processes in Al/HfO₂/n-Si MOS structures in the electrical properties

Dulce María Guzmán Bucio (guzmndulce@gmail.com) ², Marisol Mayorga Garay ¹,
Alberto Herrera Gómez ¹, Andrés de Luna Bugallo ¹, Orlando Cortazar Martínez ¹,
Joaquín Gerardo Raboño Borbolla ¹

¹ Cinvestav-Unidad Querétaro

² Instituto Tecnológico Superior de Ciudad Hidalgo

Hafnium based MOS (metal-oxide-semiconductor) structures have emerged as one of the preferred high-k dielectrics for development in nanoelectronics. Characterization of the structure and electrical properties of HfO₂ is fundamental to propose strategies for the improvement of electronic devices. The fabrication procedure may highlight the properties of the dielectric; or, it might degrade electrical performance of the devices, providing unreliable results about the behavior of the different layers in the stack.

In this work we evaluated the influence of the hard bake step from the photolithography process in the quality of the gate-metal contacts. Samples with 10 and 15 nm of the HfO₂ was deposited on n-type silicon substrates through ALD (using TDMAHf as the hafnium precursor). Aluminum contact was deposited using an ultra-high vacuum sputtering on the top of the dielectric film. The photolithography process was done as follows: deposit of positive photoresist; soft bake; alignment to positive mask and exposition; development; hard bake for different times from 0-60 seconds 2, 5 and 10 minutes. Then, the wet etching of aluminum, and finally the removal of the resist. The better capacitance values and less dispersion of the maximum capacitance (C_{max}) and threshold voltage (V_{TH}) of the C-V curves was found for the sample without hard bake, and the calculated dielectric constant was of ~9. The hard bake makes more difficult to remove the photoresist and affects the Al etching. This process presents many interconnected contacts and a thick film of resist over the surface, leading to no reliable measurements of the electrical properties of the devices, which is the cause of the low dielectric constant. Samples with hard bake do not saturate in the accumulation region, show dispersion of the C_{max} y V_{TH} and giving as a result very low dielectric constant values (~2) compared with the samples without hard bake.

Keywords: MOS, photolithography, dielectric, nanoelectronics



[ALD-164] Impact of the metal deposition technique on structural and electrical properties of Al/HfO₂/Si structures

Marisol Mayorga-Garay (*marisol.mayorga@cinvestav.mx*) ¹, Dulce María Guzmán-Bucio ², Alberto Herrera-Gómez ¹, Andrés De Luna Bugallo ¹

¹ CINVESTAV Unidad Querétaro.

² Instituto Tecnológico Superior de Ciudad Hidalgo

HfO₂ is one of the most promising high-k dielectrics to replace SiO₂ in MOS devices in order to improve device performance and miniaturization. Usually, the MOS fabrication process involves different techniques and each one of these microfabrication stages have a direct influence on the structural and electrical properties of the final device. Especially metal deposition when a sputtering process is used which may cause a change in the HfO₂ ultra-thin film properties due to the high energetic ions involved. In this work, we show the impact of the metal contact deposition technique on MOS capacitors based on Al/HfO₂/Si structures using two different physical vapor deposition (Sputtering and e-beam).

HfO₂/Si structures were processed using standard RCA cleaning on Si n-type (100) substrates followed by the growth of different thickness of HfO₂ (3, 5 and 8 nm) using ALD. The samples obtained were analyzed with angle-resolved X-ray photoemission spectroscopy (ARXPS) to determine the chemical composition and thickness of the HfO₂ layer by mean of the multilayer method (MLM). Results shows two components in the Hf 4f spectra related to hafnia and silicate respectively, suggesting the presence of a Hf_xSi_yO₂ interfacial layer. The chemical composition obtained is x≈0.3-0.5 and y≈0.7-0.5 in the Hf_xSi_yO₂ interface, with an oxide thickness between 0.5 nm and 1 nm.

A 200 nm layer of aluminum was deposited using sputtering or e-beam on top of HfO₂/Si structures. Electrical properties of the HfO₂ layer were studied by fabricating MOS type devices using a typical photolithography process to form 5.625x10⁻³ μm² capacitors.

Maximum capacitance (C_{max}) and leakage current were measured on different devices. C_{max} and threshold voltage in the sputtered samples show a large dispersion. This effect is lower for devices with contact deposited by e-beam. The C_{max} was 0.25 μF/cm² for the 3 nm sputtered samples and 1.2 μF/cm² for the 3 nm with Al deposited by e-beam, whilst samples with 5 nm and 8 nm shows a C_{max} two times bigger for the Al deposited e-beam samples. Breakdown voltage was not clear for the sputtered samples whereas for e-beam samples was between 2 V and 3 V. Leakage current was ~1x10⁻³ A/cm² for all the samples at 2 V. The dielectric constant was calculated using the thickness obtained with the MLM, obtaining a k value approximately 10 times lower for the sputtered samples (k=0.3) than for the samples with Al deposited by e-beam (k=3).



XII -ICSMV

September 23rd to 27th, 2019 / San Luis Potosí, México

In conclusion the technique used for the deposit of the Al contacts has an important impact on ultra-thin HfO_2 films suggesting that the high energetic ions involved in the sputtering process cause some defects and charges inside the HfO_2 and the interfacial layer. On the other hand, samples with the Al deposited by e-beam show better electrical properties because the process is softer decreasing the number of defects in the HfO_2 and interfacial layer.



XII -ICSMV

September 23rd to 27th, 2019 / San Luis Potosí, México

[ALD-183] Study of band structure by XPS of SnO₂ thin films deposited by ALD and PEALD

Marcelo Ademir Martínez Puente (marcelo.martinez@cimav.edu.mx)¹, Luis Gerardo Silva Vidaurre¹, Eduardo Martínez Guerra¹

¹ *Centro de Investigación en Materiales Avanzados S.C. Unidad Monterrey*

SnO₂ has been used as electron transport layer in solar cells based on hybrid perovskite with chemical formula MAPbX₃ due to the excellent compatibility of the heterojunction formed between SnO₂ and MAPbX₃. Additionally, SnO₂ has a 3x10² S/cm conductivity and a water vapor transmission rate with a value about 10₋₆ g/(m₂ day), being this value in the magnitud order used in OLED encapsulation. In this work different oxidizing agents were evaluated in ALD and PEALD as H₂O, O₃ in thermal ALD and H₂O and O₂ y PEALD using Remote and Direct Plasma. Depending of the oxidizing agent used, different kind of defects were found in the thin films, and these modify the work function and band gap. This variety of defects are obtained due to the oxidant agents reactivity and growth mechanism involved in each case. Using XPS and analyzing high kinetic energy electrons is possible obtain information about valence band, low kinetic energy electrons are used to obtain the work function and inelastic scattered electrons in O1s region give information about band gap. In dependence of the solar cell structure, is possible identify which is the best oxidizing agent to use for the SnO₂ deposition as ETL



[ALD-291] O₂-plasma effect on structural and optical properties of ZnO thin films prepared by PEALD at room temperature

Gonzalo Alonso Velázquez Nevárez (gonzalo.velazquez@cimav.edu.mx) ¹, Beatriz Ortega García ¹, María Isabel Mendivil Palma ¹, Marcelo Ademir Martínez Puente ¹, Eduardo Martínez Guerra ¹, Francisco Servando Aguirre Tostado (servando.aguirre@cimav.edu.mx)

¹

¹ Centro de Investigación en Materiales Avanzados S.C. (Unidad Monterrey), Av. Alianza Norte 202, Parque PIIT, Apodaca CP 66628, Nuevo León, México.

Zinc oxide (ZnO) is an n-type semiconductor, one of the most cost-effective, with wide direct band gap (3.37 eV). The application of ZnO films on thermo-sensitive substrates such as perovskites and biomaterials require deposition process operating at low temperature to avoid degradation of the substrates. Plasma-enhanced atomic layer deposition (PEALD) is a variation of ALD that allows lower deposition temperature. In this case, reactive plasma species are used as co-reactants.

In this study, the authors report ZnO films growth on glass and silicon substrates by PEALD at room temperature increasing O₂-plasma pulse, in order to improve the ZnO crystallinity and optical properties, as an alternative to avoid high-temperature synthesis. Diethylzinc (DEZ) and oxygen were used as precursor and oxidant, respectively. The O₂-plasma pulse was varied from 6 to 21 s, and the plasma power was kept at 150 W. The ZnO films exhibited a polycrystalline nature with a (100)-preferential orientation and crystal size around 18 nm. The XPS analysis reveals a trend to stoichiometry (Zn/O) and lower OH⁻ species as O₂-plasma pulse increases. A free exciton emission (375 nm) with a defect-band emission (525 nm) in the visible region was observed at room temperature by photoluminescence measurements. Longer O₂-plasma pulses exhibited a higher intensity of defect-band emission. The optical band gap decreases in ZnO films as O₂-plasma pulse increases (from 3.28 to 3.21 eV). The possibility to tune crystal structure, band gap, and stoichiometry of ZnO films by varying oxygen plasma pulse was demonstrated.

Keywords: PEALD, ZnO films, room temperature.



[ALD-301] Influence of the ALD synthesis process for Al₂O₃ in the passivation and degradation of a hybrid MA-PbBr₂Cl perovskite surface.

Fatima Paloma Reyes Ixta (fatima.reyes@cimav.edu.mx) ¹, Paul Horley ¹, Marcelo Ademir Martínez Puente ¹, Jesus Uriel Balderas ¹, María Isabel Mendivil Palma ¹, Francisco Servando Aguirre Tostado ¹, Eduardo Martínez Guerra (eduardo.martinez@cimav.edu.mx)
¹

¹ Centro de Investigación en Materiales Avanzados S.C., Unidad Monterrey, Alianza Norte 202, Parque PIIT, 66-628 Monterrey, Nuevo León, México

Hybrid lead halide perovskites have received enormous attention recently due to their interesting optoelectronic properties and high efficiency of power conversion in photovoltaic solar cells of up to 20% [1]. However, they present instability under different conditions such as humidity [2], light [3], temperature [4] and oxygen [5] supposing a great challenge for practical applications. Surface passivation is essential for properties not to be affected and to allow applications in solar cells. Due to the compatibility with perovskite and the reduction of atmospheric diffusion, alumina (Al₂O₃) was selected for synthesis [6]. The hybrid perovskites used MAPbBr₂Cl present greater stability than the perovskites of MAPbI₃ and MAPbBr₃ [7], which have a cubic structure of symmetry [8]. In this work, we study the degradation caused by the precursor TMA (trimethylaluminum) because it degrades MAPbBr₂Cl [9], the oxidizing agent (H₂O) and exposure to UV light in the perovskite hybridized MAPbBr₂Cl. The study of degradation and surface passivation was performed by ALD (Atomic Layer Deposition). The topography of the surface was evaluated by atomic force microscopy (AFM). X-ray photoelectron spectroscopy (XPS) was used to estimate the stoichiometry of Al₂O₃ and the elemental composition of our samples. The modification of the structural parameters of the material was studied by means of X-ray diffraction, confirming the presence of cubic phase with symmetry of in our samples.

The results of the XPS analysis indicate that the deposition of an Al₂O₃ layer on the perovskite should be performed with a pulse less than 50 ms of TMA without causing complete degradation, DRX shows that the perovskite has degraded to become PbBr₂ of orthorhombic phase with Pnma symmetry, AFM shows different phases caused by degradation.

[1] Zardetto, V., Williams, B. L., Perrotta, A., Di Giacomo, F., Verheijen, M. A., Andriessen, R., ... & Creatore, M. (2017). Atomic layer deposition for perovskite solar cells: research status, opportunities and challenges. *Sustainable Energy & Fuels*, 1(1), 30-55.

[2] Yang, J., Siempelkamp, B. D., Liu, D., & Kelly, T. L. (2015). Investigation of CH₃NH₃PbI₃ degradation rates and mechanisms in controlled humidity environments using in situ techniques. *ACS nano*, 9(2), 1955-1963.

[3] Xu, R. P., Li, Y. Q., Jin, T. Y., Liu, Y. Q., Bao, Q. Y., O'Carroll, C., & Tang, J. X. (2018). In situ observation of light illumination-induced degradation in organometal mixed-halide perovskite films. *ACS applied materials & interfaces*, 10(7), 6737-6746.



- [4] Kim, I. S., & Martinson, A. B. (2015). Stabilizing hybrid perovskites against moisture and temperature via non-hydrolytic atomic layer deposited overlayers. *Journal of Materials Chemistry A*, 3(40), 20092-20096.
- [5] Luo, B., Naghadeh, S. B., & Zhang, J. Z. (2017). Lead Halide Perovskite Nanocrystals: Stability, Surface Passivation, and Structural Control. *ChemNanoMat*, 3(7), 456-465.
- [6] Choudhury, D., Rajaraman, G., & Sarkar, S. K. (2016). Self limiting atomic layer deposition of Al_2O_3 on perovskite surfaces: a reality?. *Nanoscale*, 8(14), 7459-7465.
- [7] Hieulle, J., Wang, X., Stecker, C., Son, D. Y., Qiu, L., Ohmann, R., ... & Qi, Y. (2019). Unraveling the Impact of Halide Mixing on Perovskite Stability. *Journal of the American Chemical Society*, 141(8), 3515-3523.
- [8] Domanski, K., Correa-Baena, J. P., Mine, N., Nazeeruddin, M. K., Abate, A., Saliba, M., ... & Grätzel, M. (2016). Not all that glitters is gold: metal-migration-induced degradation in perovskite solar cells. *ACS nano*, 10(6), 6306-6314.
- [9] Koushik, D., Hazendonk, L., Zardetto, V., Vandalon, V., Verheijen, M. A., Kessels, W. M., & Creatore, M. (2019). Chemical Analysis of the Interface between Hybrid Organic-Inorganic Perovskite and Atomic Layer Deposited Al_2O_3 . *ACS applied materials & interfaces*, 11(5), 5526-5535.



[ALD-346] Aluminum Infiltration of Poly(2-vinylpyridine) via Atomic Layer Deposition

Matthew Snelgrove ⁴, Pierre Giovanni Mani-Gonzalez (pierre.mani@uacj.mx) ², K. Lahtonen ⁵, Ross Lundy ¹, Gregory Hughes ³, Pravind Kumar Yadav ¹, J. Saari ⁵, Michael Morris ¹, Enda McGlynn ³, Robert O'Connor ⁴, Pierre Giovanni Mani-Gonzalez ⁴, Enda McGlynn ⁴, Gregory Hughes ⁴

¹ AMBER, Trinity College Dublin, College Green, Dublin 2, Ireland

² Instituto de Ingeniería y Tecnología, Departamento de Física y Matemáticas, Universidad Autónoma de Ciudad Juárez, Ave. Del Charro 450, Cd. Juárez C.P. 32310, Chihuahua. México.

³ National Centre for Plasma Science and Technology, Dublin City University, Glasnevin, Dublin 9, Ireland

⁴ School of Physical Sciences, Dublin City University, Dublin 9, Ireland

⁵ Surface Science Laboratory, Tampere University of Technology, P.O. Box 692, FIN-33101 Tampere, Finland

The polymer Poly(2-vinylpyridine) (P2vP) is a significant material in Area Selectivity Deposition (ASD) and Block Copolymer (BCP) research, reported to have favorable properties that facilitate metal interaction and infiltration. Recent studies undertaken in assessing the ability P2vP has in incorporating metal via a salt solution and Atomic Layer Deposition (ALD) process have reported on successful infiltration.

Comparing the salt solution and ALD infiltration processes may present cheaper, more efficient alternatives in obtaining future high dielectric materials. In this work, we report on the infiltration of P2vP via a standard ALD process and by a salt infiltration process via spin coating. X-ray Photoelectron Spectroscopy (XPS) is used to assess the chemical environment of the polymer, while Energy Dispersive X-ray (EDX) mapping is implemented to assess the infiltration technique. A low pressure, O plasma technique is then implemented to oxidize the infiltrated metal and subsequently remove the polymer film. The P2vP-infiltrated samples were prepared for Transition Electron Microscopy (TEM) via a Focus Ion Beam (FIB), finding evidence of aluminum was infiltrated and it was distributed into P2vP film.



[ALD-516] In situ XPS Characterization of AlxOy growth by ALD

*Jesus Alfredo Hernandez Marquez (al114688@alumnos.aucj.mx)¹, Matthew Snelgrove³,
Kyle Shiel³, Gregory Hughes³, Gregory Hughes², Robert O'Connor³, Pierre Giovanni
Mani Gonzalez³, Pierre Giovanni Mani Gonzalez¹*

¹ *Instituto de Ingeniería y Tecnología, Departamento de Física y Matemáticas, Universidad Autónoma de Ciudad Juárez, Ave. Del Charro 450, Cd. Juárez. C.P. 32310, Chihuahua, México.*

² *National Centre for Plasma Science and Technology, Dublin City University, Glasnevin, Dublin 9, Ireland*

³ *School of Physical Sciences, Dublin City University, Dublin 9, Ireland*

An in situ Atomic Layer deposition (ALD) spherical system coupled with X Ray Photoelectron Spectroscopy (XPS) as surface characterization was developed for the growth of AlxOy layers. Silicon was detected into AlxOy films . 0.08s for Trimethylaluminum (TMA) and 0.08s for the oxidant agent H2O were used as aperture-time in each precursor. XPS was used to analyze the Si (100) as substrate sample after 1, 2, 3, 5, 10, 20, 50, 100 and 200 cycles of TMA and H2O. Another Si (100) as substrate samples were exposed to 10 cycles in a multi exposure. Both multi-step and single-step samples were heated at 150°C for each ALD cycle with a base pressure of 5x10-3 mBar . Each ALD cycle in TMA and H2O pressure increased the pressure to 50x10-1 and 45x10-1 torr respectively. The in situ surface characterization of samples using XPS shows that it was obtained layer mostly composed of Al2SiO5.



[ALD-673] Plasma-surface interaction during plasma-enhanced ALD and how it can be used to tailor film properties

W.M.M. (Erwin) Kessels (w.m.m.kessels@tue.nl)¹

¹ Department of Applied Physics, Eindhoven University of Technology, The Netherlands

Plasma-based processing remains key in next-generation device manufacturing and in the field of atomic scale processes plasma-enhanced atomic layer deposition (PEALD) has gained a very prominent position in obtaining ultrathin films with atomic scale precision [1]. Although the plasma-surface interaction has been investigated for conventional plasma-enhanced chemical and physical vapor deposition in great detail, very little is known about the effects of plasma-surface interaction during PEALD.

In this presentation, the plasma-surface interaction during PEALD will be addressed in detail. In particular the role of ion-surface interaction during PEALD will be addressed by analyzing the flux and energy of ions arriving at the surface and by linking these results with the material properties obtained [2]. Moreover, it will be demonstrated how the properties of materials (in particular oxides and nitrides of Ti, Hf and Si) can be tailored by controlling the kinetic energy of the ions impinging on the films with RF substrate biasing. This will be shown for planar substrates (up to 200 mm in size) as well as for 3D surface topologies yielding intriguing effects of inducing differing material properties at different surfaces of the nanostructures [3].

[1] H.C.M. Knoops, T. Faraz, K. Arts, and W.M.M. Kessels, J. Vac. Sci. Technol. A 37, 030902 (2019).

[2] F. Faraz, K. Arts, S. Karwal, H.C.M. Knoops, and W.M.M. Kessels, Plasma Sources Sci. Technol. 28, 024002 (2019).

[3] T. Faraz, H.C.M. Knoops, M.A. Verheijen, C.A.A. van Helvoirt, S. Karwal, A. Sharma, V. Beladiya, A. Szeghalmi, D.M. Hausmann, J. Henri, M. Creatore, and W.M.M. Kessels, ACS Appl. Mater Interfaces, 10, 13158, (2018).



XII -ICSMV

September 23rd to 27th, 2019 / San Luis Potosí, México

ATOMIC LAYER DEPOSITION
SYMPOSIUM (ALD)
POSTER SESSIONS



[ALD-121] XPS study of the composition of HfO_xN_y films obtained by remote plasma soft-nitridation as a function of the nitriding gas

Abraham Jorge Carmona Carmona (abraham.carmona@cinvestav.mx)², Marisol Mayorga Garay², Dulce María Guzmán Bucio¹, Orlando Cortazar Martínez², Alberto Herrera Gómez²

¹ Instituto Tecnológico Superior De Ciudad Hidalgo, v. Ing. Carlos Rojas Gutiérrez 2120, Fracc. Valle De La Herradura, 61100 Cd Hidalgo, Mich.

² LPCN, CINVESTAV unidad Querétaro Unidad Querétaro, Lib. Norponiente 2000, Fraccionamiento, Real de Juriquilla, Querétaro, Qro.

Performance of MOS devices depends in the composition of gate oxide and the distribution of the species in the films, which can change during fabrication of the electronic devices. High k dielectrics based on transient metal oxides, such as HfO₂, are currently employed for MOS device fabrication because of its excellent properties. Nitridation of MOS structures bases on HfO₂ can improve electric properties of the dielectric gate by substituting oxygen vacancies and preventing other issues related to, as dopant diffusion and low thermal stability¹⁻⁵.

In this work, we report the XPS characterization of 2 nm oxide hafnium layers that were nitrided by a remote plasma system attached to an ultra-high vacuum (UHV) sputtering. The growth of HfO₂ was done on clean Si(001) n-type substrate (cleaned with the standard RCA process) in an ALD Cambridge 100 tool using tetrakis (dymethylamido) hafnium (IV) as Hf precursor. The nitridation process was done in the UHV sputtering using one of two different gases (N₂ or N₂+H₂) in a remote plasma (Litmas). The gas flow was kept at 20 sccm of N₂ or N₂ + H₂. The power for the Litmas was fixed at 2500 W and substrate temperature at 300°C.

The film was characterized with an X-ray photoelectron spectroscopy (XPS) instrument with a monochromatic X-ray aluminum source (XR5, from ThermoFisher) and a 7-channeltron hemispherical spectrometer (Alpha110, from ThermoFisher) assembled by Intercovamex. Angle-resolved XPS (ARXPS) was employed to assess the thickness and composition of the HfO₂ and HfO_xN_y films. The initial thickness of the hafnia layer was 1.68 nm and was reduced to 1.4 nm and 1.58 nm after the nitridation process with forming gas and nitrogen, respectively. The N 1s signal was observed at 395.7 eV associated to Hf-N bond suggest a substitutional incorporation of nitrogen into the hafnia layer^{6,7}. ARXPS data of the Si 2p indicates that two compounds coexist in the same layer, HfO_xN_y and Hf₂Si_wO_xN_y, supporting the substitutional incorporation of N species. Also, an amount of interstitial nitrogen was found in the layers. Based

Keywords: Thin films, Atomic layer deposition, X-ray photoelectron spectroscopy.



[ALD-182] Study of band structure by XPS of SnO₂ thin films electron transport layers deposited by ALD and PEALD: compatibility with perovskite layer in solar cells

Marcelo Ademir Martínez Puente (marcelo.martinez@cimav.edu.mx)¹, Luis Gerardo Silva Vidaurre¹, Eduardo Martínez Guerra¹

¹ Centro de Investigación en Materiales Avanzados S.C. Unidad Monterrey, Alianza Norte # 202, Parque de Investigación e Innovación Tecnológica. (PIIT), Autopista Monterrey-Aeropuerto Km. 10, Apodaca, Nuevo León, México, C.P. 66628

SnO₂ has been successfully used as electron transport layer (ETL) in solar cells based on hybrid perovskite MAPbX₃ due to its excellent compatibility. Additionally, SnO₂ has a conductivity of 3×10^2 S/cm and a water vapor transmission rate of about 10^{-6} g/(m² day). This value is comparable to that used in OLED encapsulation (1). In this work, different oxidizing agents were evaluated for ALD and PEALD processes, including H₂O, O₃ for thermal ALD as well as H₂O, O₂ for PEALD using Remote and Direct Plasma modes. Depending on the oxidizing agent used, different kind of defects were found in these thin films, which influenced material work function and band gap. These defects are formed due to the reactivity of the oxidizing agents and with the particular growth mechanism involved in each case. The XPS analysis of high kinetic energy electrons permitted to obtain information about the valence band. Low kinetic energy electrons were used to obtain the work function and inelastic-scattered electrons in O1s spectra provided information about the band gap. Depending on solar cell structure, it was possible to identify the best oxidizing agent to be used for the SnO₂ layer serving as an ETL.

(1) A. Behrendt *et al.*, "Highly Robust Transparent and Conductive Gas Diffusion Barriers Based on Tin Oxide," *Adv. Mater.*, vol. 27, no. 39, pp. 5961–5967, Oct. 2015.



[ALD-266] Study of the chemical reactions between TDMA_n ALD precursor and MAPbX₃ perovskite

Marcelo Ademir Martínez Puente Marcelo Ademir Martínez Puente

(marcelo.martinez@cimav.edu.mx)¹, Jesús Uriel Balderas Aguilar¹, Fátima Paloma Reyes Ixta¹, María Fernanda Jasso Jasso¹, Servando Aguirre Tostado¹, Eduardo Martínez Guerra¹

¹ Centro de Investigación en Materiales Avanzados S.C. Unidad Monterrey, Alianza Norte # 202, Parque de Investigación e Innovación Tecnológica. (PIIT), Autopista Monterrey-Aeropuerto Km. 10, Apodaca, Nuevo León, México, C.P. 66628

Low chemical stability of the hybrid perovskite MAPbX₃ served as one of the main obstacles for commercialization of solar cells based on it. The efficiency of a solar cell depends on the quality of heterojunction formed by the perovskite with electron and hole transport layers (ETL and HTL). To achieve this, the deposition techniques should provide the lowest possible defects concentration, conformal deposition and good interfacial properties. Namely for these reasons, ALD was used par excellence for ETL deposition. SnO₂ deposited in this way demonstrates excellent material properties for p-i-n solar cell architecture: conductivity of 3×10^2 S/cm, water vapor transmission rate about 10^{-6} g/(m² day), and density of 5.2 g/cm³ (1). However, interfacial and surface reactivity problems between perovskite and ALD precursors remain to be solved. In this work, we studied the initial growth stages of SnO₂ deposited on MAPbBr_{3-x}Cl_x and the chemical mechanisms involved in the interaction of the TDMA_n molecule with MAPbBr_{3-x}Cl_x. Surface mechanical properties were analyzed using AFM phase images, showing non-uniformity of SnO₂ deposition. Additionally, XPS thickness measurement shows a low growth per cycle of SnO₂ deposited on the perovskite surface, suggesting the island growth mechanism. XPS chemical analysis shows a low surface degradation of perovskite in ALD conditions used in this research. RGA analysis in situ was unable to detect byproducts of the TDMA_n and perovskite interaction. When the TMA precursor was used, we identified that one of three methyls belonging to TMA was lost due to interchange reaction with methylammonium, forming dimethyl-aluminum and methylamine.

(1) A. Behrendt *et al.*, "Highly Robust Transparent and Conductive Gas Diffusion Barriers Based on Tin Oxide," *Adv. Mater.*, vol. 27, no. 39, pp. 5961–5967, Oct. 2015.



XII -ICSMV

September 23rd to 27th, 2019 / San Luis Potosí, México

[ALD-353] Electrical, optical and morphological properties of Al₂O₃ thin films grown by PE-ALD at low temperature

Jhonathan Castillo (*jhonathan.castillo@uabc.edu.mx*)¹, Jhonathan Castillo², Eduardo Martínez², Benjamín Valdez¹, Isabel Mendiola², David Mateos¹, Marcelo Martínez², Nicola Nedev¹

¹ a Instituto de Ingeniería, Universidad Autónoma de Baja California, Blvd. Benito Juárez s/n, C.P. 21280, Mexicali, B.C., México.

² b Centro de materiales avanzados CIMA V unidad Monterrey, Alianza Norte 202. Parque de Investigación e Innovación Tecnológica, C.P. 66600, Apodaca, Nuevo León, México.

Al₂O₃ layers with thicknesses of 50, 80 and 110 nm were deposited by Plasma Enhanced Atomic Layer Deposition (PE-ALD) at 70 and 80 °C. Trimethylaluminum (TMA) was used as organometallic precursor, O₂ and H₂O as oxidant agents and Ar as a purge gas. The deposition cycle consisted of 50 ms TMA pulse, 10 s purge time and 6 s of plasma oxidation at 200 W. The optical constants and thicknesses of the grown layers were determined by spectroscopic ellipsometry, while the roughness was measured by atomic force microscopy, giving RMS values in the 0.25 - 0.37 nm range for films deposited under different conditions and having different thicknesses. High transmittance, above ~95 %, was measured by UV-Vis spectroscopy. X-ray photoelectron spectroscopy revealed that films obtained with both types of precursors have stoichiometric composition and are with high purity, no C was detected. Electrical characterization was carried out using Keythley 4200 Semiconductor Characterization System. The obtained excellent optical, morphological, compositional and electrical properties of the deposited films, comparable to that of thermally grown Al₂O₃ at 200 °C, make them a promising candidate for electronic and optoelectronic applications, which require low temperature processes.

Keywords: PE-ALD, Al₂O₃, low temperature, thin films



[ALD-372] Synthesis of controlled Al₂O₃ deposited by ALD as an oxidation layer in a thermal barrier system

Andres Felipe Molina Torres (andres.molina@cimav.edu.mx)², Ana Arizmendi Morquecho (ana.arizmendi@cimav.edu.mx)², Eduardo Martínez Guerra², Renee Joselin Saenz Hernández¹

¹ Cimav unidad Chihuahua

² Cimav unidad Monterrey

Thermal barrier coatings (TBC) have been used in the aeronautic industry to reduce the heat effect on some turbine components. A conventional TBC deposited on a superalloy substrate is conformed by two different layers: the first one known as bond coat formed by M-CrAlY, and a second layer composed by YSZ. Between these layers an oxidation layer is grown during thermal cycles (TGO). The control and stability of this last layer is very difficult resulting in the formation of a thicker layer during the operation at high temperature, leading to the coating failure.

In this work, the synthesis of controlled and conformal Al₂O₃, deposited by ALD as an oxidation layer in a thermal barrier system was studied, varying the thickness and its effect on the mechanical and thermal stability. The Spark Plasma Sintering (SPS) technique was used to prepare the CoNiCrAlY superalloy substrates. Ultra-thin α-Al₂O₃ coatings were deposited by ALD using TMA/H₂O as organometallic precursor and oxidizing agent, respectively. 40 to 250 ALD-cycles and heat treatment were used as variable parameters to control the layer thickness. The composition and microstructure of α-Al₂O₃ were investigated using scanning electron microscopy (SEM), X-ray photoelectron spectrometry (XPS) and X-ray diffraction (XRD) analysis. The uncoated and coated substrates were exposed to isothermal oxidation at 1100°C for different times to study the oxidation kinetics and the mechanical stability of the coating.

Keywords: Thermal barrier coatings, ALD, spark plasma sintering, oxidation kinetics.



XII -ICSMV
September 23rd to 27th, 2019 / San Luis Potosí, México

BIOMATERIALS AND POLYMERS (BIO)

Chairmen: César Marquez Beltrán (BUAP)

Amir Maldonado Arce (USON)



XII -ICSMV
September 23rd to 27th, 2019 / San Luis Potosí, México

BIOMATERIALS AND POLYMERS (BIO) ORAL SESSIONS



[BIO-24] Thermal and biocompatibility properties of chitosan/mimosa tenuiflora/zinc oxide films

Santos Adriana Martel-Estrada (mizul@yahoo.com)¹, Claudia Lucía Vargas-Requena², Imelda Olivas-Armendáriz³, Claudia Alejandra Rodríguez-González³, Amanda Carrillo-Castillo³, Hortensia Reyes-Blas³, Mónica Cecilia Ruiz-Ramírez³, Adán Eduardo Arreola-Reyes³

¹ *Instituto de Arquitectura, Diseño y Arte, Universidad Autónoma de Cd. Juárez, Av. Del Charro 450 Norte. Col. Universidad, C.P: 32310, Cd. Juárez, Chihuahua, México*

² *Instituto de Ciencias Biomédicas, Universidad Autónoma de Ciudad Juárez, Henri Dunant 4016, Zona Pronaf. Cd. Juárez, Chihuahua, México, C.P. 32310.*

³ *Instituto de Ingeniería y Tecnología, Universidad Autónoma de Cd. Juárez, Av. Del Charro 450 Norte, Col. Universidad, C.P. 32310, Cd. Juárez, Chihuahua, México.*

The purpose of this study is to examine the thermal and biocompatibility properties of Chitosan/Mimosa Tenuiflora/Zinc Oxide films produced by casting method. Morphology, viability, chemical, and thermal properties were obtained by scanning electronic microscopy (SEM), MTT assay, FT-IR analysis and TGA/DSC. Our results thus show that Chitosan/ Mimosa Tenuiflora/Zinc Oxide films are suitable for biological applications. The results showed that the composite materials could be used in tissue engineering, with particular control of zinc oxide concentrations to avoid cytotoxicity.



[BIO-28] Biosynthesis of Metallic Nanoparticles for Biosensing Applications

Dulce Natalia Castillo (dulce.castillolo@correo.buap.mx)¹, Umapada Pal², Luz del Carmen Gómez¹, Arnulfo Luis¹

¹ Facultad de Ciencias de la Electrónica, Benemérita Universidad Autónoma de Puebla, 18 Sur y Av. San Claudio, Col. San Manuel, Apdo. postal J-48, C.P. 72570, Puebla, Pue., Mexico

² Instituto de Física "Luis Rivera Terrazas", Benemérita Universidad Autónoma de Puebla, 18 Sur y Av. San Claudio, Col. San Manuel, Apdo. postal J-48, C.P. 72570, Puebla, Pue., Mexico

In the last years, studies concerning the application of nanostructures have increased, this because of the potential and promising applications in various fields of research ranging from electronics to biology [1]. Regarding the latter application, biosensors based on metallic nanoparticles (NPs) have been widely explored by many researchers, this due to the surface-enhanced Raman scattering (SERS) phenomenon that they present [2-4]. In this work, we present a green method for synthesis of metallic NPs and their application in biosensing. The fabricated biosensors were tested for detection of methylene blue, rhodamine, and the hormone human chorionic gonadotropin (HCG) at different concentrations.

Keywords: nanoparticles, SERS, biosensing.

References

- [1] Guozhong C. and Ying W., Nanostructures and Nanomaterials: Synthesis, Properties, and Applications., 2nd Edition., 2011.
- [2] Sebastianx S., Surface-enhanced Raman spectroscopy: concepts and chemical applications., Angewandte Chemie International., 53, 4756-4795, 2014.
- [3] Bhavya S., Renee R. F., Anne-Isabelle H., Emilie R., and Richard P.V D., SERS: Materials, applications, and the future, materialstoday, 15, 2012.
- [4] Umapada P., Dulce Natalia C. L., Moisés Graciano C.M, Lucía L.-R, Pablo D.N., and Ovidio P. R., Nanoparticle-Assembled Gold Microtubes Built on Fungi Templates for SERS-Based Molecular Sensing, Applied Nano Materials, 2, 2019.



[BIO-59] Morphology, swelling behavior, mechanical properties and antibacterial activity of edible coatings based on chitosan nanoparticles and propolis

Zormy Nacary Correa-Pacheco¹, Silvia Bautista-Baños², Margarita de Lorena Ramos-García³

¹ CONACYT-Centro de Desarrollo de Productos Bióticos, Instituto Politécnico Nacional, Carretera Yautepec-Joxtla, km 6, calle CEPROBI, No. 8, San Isidro, Yautepec, Morelos, 62731, Mexico

² Centro de Desarrollo de Productos Bióticos, Instituto Politécnico Nacional, Carretera Yautepec-Joxtla, km 6, calle CEPROBI, No. 8, San Isidro, Yautepec, Morelos, 62731, Mexico

³ Universidad Autónoma del Estado de Morelos, Facultad de Nutrición, Calle Iztaccíhuatl S/N, Col. Los Volcanes, Cuernavaca, Morelos, C.P. 62350, Mexico

Nowadays, due to environmental concerns, the search of new alternatives of packaging based on biodegradable polymers for postharvest fruit preservation is necessary. In this work, the morphology, swelling behavior, mechanical properties and antibacterial activity of edible coatings based on chitosan nanoparticles and propolis for possible use in strawberries were evaluated. Five edible coatings' formulations were elaborated: chitosan solution (F1), chitosan nanoparticles in a chitosan solution (F2) and chitosan nanoparticles with ethanolic extract of propolis (EP) at concentrations of 10, 20 and 30% (F3, F4 and F5, respectively). Chitosan average particle size of 28 nm was observed from transmission electron micrographs. From contact angle measurements, samples with the most hydrophilic behavior were F1 and F4. Addition of chitosan nanoparticles caused an increase in hydrophobicity. Thickness of the edible coating on strawberries, were below 350 µm as observed by optical microscopy. Nanoparticles addition and increase of propolis content in the different formulations, decreased the water solubility and the degree of swelling. From FTIR spectra, interactions among components were observed. EP containing formulations showed a higher value of elastic modulus as measured by nanoindentation tests and were more homogeneous having the lowest value of roughness as observed by atomic force microscopy. The antibacterial activity was evaluated for three bacteria: *Escherichia coli*, *Listeria monocytogenes* and *Salmonella typhi*. A bactericidal effect was observed against *L. monocytogenes* and *E. coli* after 24 h for the EP formulations and only a bacteriostatic effect was seen after 48 h. Therefore, the use of edible coatings based on chitosan nanoparticles and propolis, could represent a good alternative for strawberry protection against foodborne pathogens.



XII -ICSMV

September 23rd to 27th, 2019 / San Luis Potosí, México



[BIO-82] SYNTHESIS OF CARBON SPHERES/POLY (METHYL METHACRYLATE) COMPOSITE FIBERS

Jael Madaí Ambriz-Torres³, Carmen Judith Gutiérrez-García³, Diana Litzajaya García-Ruiz³, Jaime Abraham Guzmán-Fuentes³, José de Jesús Contreras-Navarrete², Francisco Gabriel Granados-Martínez¹, Nelly Flores-Ramírez³, Ezequiel Huipe-Nava³, Orlando Hernández-Cristóbal¹, Yesenia Arredondo-León¹, Lada Domratcheva-Lvova³

¹ Escuela Nacional de Estudios Superiores Unidad Morelia, UNAM, Antigua Carretera a Pátzcuaro 8701, Ex-Hacienda de San José de La Huerta, Morelia, Mich., 58190, México.

² Instituto Tecnológico de Morelia, Av. Tecnológico, S/N, Lomas de Santaguito, 58160 Morelia, Michoacán, México

³ Universidad Michoacana de San Nicolás de Hidalgo, Av. Francisco J. Mújica S/N, Morelia, Mich., México, 58030, México.

Electrospinning fibers based on carbon nanomaterials and polymeric matrices are attractive multifunctional nanomaterials because they combine the remarkable mechanical and electrical properties of carbon nanomaterials and polymer properties within the nanofiber structure, which could improve the mechanical, electrical and thermal properties of the fibers. Carbon nanostructures/polymer fibers with improved properties are outstanding candidates for many applications, including reinforcement, tissue engineering, energy and environment. The electrospinning technique is an effective and attractive method that has been investigated extensively during the last few decades to fabricate nanofibers from a polymer solution. It produces a variety of polymer fibers or fiber sheets with diameters ranging from a few nanometers to several micrometers and that have a high surface area-to-volume ratio. In this study, fibers of carbon spheres/poly (methyl methacrylate) were produced by electrospinning. Poly (methyl methacrylate) (PMMA) solutions with different carbon spheres (CSs) concentration previously dispersed by sonication method during 20 minutes, were put in syringe pump at 4.2 mL/h. High voltage of 30 kV was applied at the tip of a syringe needle. The separation between the tip of the needle and the collector was kept at 7 cm and dry/semidry fibers resulted from solvent evaporation of the jet, which randomly deposited onto the collector. Scanning electron microscopy showed fibers with diameters around 85-900 nm. Particles with major diameters can be observed along the fibers. Characteristic CSs bands (D and G) and other signals corresponding to PMMA (2956.8, 1729.5 and 1458.6 cm⁻¹) were observed by Raman spectroscopy. Electrical conductivity was improved in four order of magnitude, being 1.51×10^{-6} cm⁻¹ the maximum value. Vickers microhardness increased 3.5 times in contrast with pristine polymeric fibers. In summary, CSs/PMMA fibers were successfully produced by electrospinning technique. CSs/PMMA fibers demonstrated enhanced properties in comparison to the pristine PMMA fibers. These type of fibers could be used for multiple future applications in several areas. **Acknowledgement** to Scientific Research Coordination of UMSNH and CONACyT for the financial support.



XII -ICSMV

September 23rd to 27th, 2019 / San Luis Potosí, México

[BIO-89] A review of the experimental progress of composites beams as light-weight structures and their in and out-of-plane properties

Omar Camilo Hortua Diaz (oc.hortuadiaz@ugto.mx)¹, Victor Alfonso Ramirez Elias
(va.ramirezelias@ugto.mx)¹

¹ Universidad de Guanajuato

This paper reviews several studies about the progress of mechanical properties and through-the-thickness reinforcements into the primary structural sections, I-beam, T-beam and T-joint comprised of FRP composites. Longitudinal, out-of-plane, flexural, fracture, fatigue, tensile, compressive, stiffness properties and delamination behaviour are reported and lead to identifying similarities and differences, hence, to obtain the knowledge of the optimum configuration for these structures and discuss the viability of the use as light-weight structures and suggest the fields where further researches are required. Many studies reached similar conclusions, whereas there is a similarity in how interlaminar reinforcements affects the mechanical properties and a slight difference between z-pinning and stitching. However, the effects produced depend on a variety of factors, including the type of composites, place of the load applications, and reinforcing parameters. Future work was proposed based on the reinforcements that are not being studied and critical points of failure.



[BIO-529] Cell viability on SiO₂-HA and Al₂O₃-SiHA ceramic composites.

Jesús Alberto Garibay Alvarado (*garibay.jesus@gmail.com*) ¹, Pamela Nair Silva Holguín

¹, Idahli Alejandra Meléndez Estrada ¹, León Francisco Espinosa Cristóbal ¹, Simón Yobanny Reyes López (*simon.reyes@uacj.mx*) ¹

¹ Instituto de Ciencias Biomédicas, Universidad Autónoma de Ciudad Juárez, Envolvente del PRONAF y Estocolmo s/n, Ciudad Juárez, Chih., México C.P. 32300.

Ceramic composites of SiO₂-HA (Hydroxyapatite) and Al₂O₃-SiHA (Silicon-substituted hydroxyapatite) were obtained through the sol-gel method and electrospinning technique and tested for their influence over cell viability. Precursors of SiO₂, HA, Al₂O₃ and SiHA were synthetized through the sol-gel method and then incorporated into a PVP polymeric matrix; then the solutions were processed by electrospinning in a single and coaxial fashion to obtain fibers which were thermally treated to obtain the final fibrillar ceramics. The ceramics were characterized with techniques such as ATR-FTIR, XRD and SEM, and ultimately tested for their influence on cellular viability using the MTT viability assay with incubation times of 24, 48 and 72 h. The chemical composition was confirmed as bands belonging to SiO₂, HA, SiHA and Al₂O₃ were observed in the infrared spectrums of the ceramics. The XRD showed that the fibers containing SiO₂-HA had a large amorphous zone mixed with peaks of crystalline HA, while the fibers containing Al₂O₃-SiHA showed that Al₂O₃ was α -Alumina while the SiHA peaks matched those of pure HA. The obtained fibers had diameters between 110 and 300 nm and showed random orientation and smooth surface. The MTT assay showed that the viability of cells was increased up to 300 % at 48 h on the SiO₂-HA composite and this material had the best performance of all of the tested materials.



[BIO-587] Compounds of PCL-CuONPs as an alternative to antibiotics.

*Antonio Muñoz-Escobar (al171425@alumnos.uacj.mx)¹, León Espinoza-Cristóbal¹, Idahli Alejandra Meléndez-Estrada¹, Simón Yobanny Reyes-López (yobannyr@yahoo.com.mx)
¹, Ayodeji Precious-Ayanwale,¹*

¹ Universidad Autónoma De Ciudad Juarez

Excess antibiotics in the environment could lead to antibiotic resistance by microorganisms and could harm many aquatic organisms. This has elicited an interest in the application of alternative antimicrobial agents, metal oxide ions being an attractive target. Copper oxide nanoparticles are considered by their catalytic and antifungal/antibacterial characteristics that are not observed in commercial copper. Therefore, the objective of this study is to prepare and characterize polycaprolactone fibers with copper oxide nanoparticles (PCL-CuONPs), and to evaluate their antimicrobial properties against Gram-negative and Gram-positive bacteria, and against fungi. The fibers are prepared by the cupric ion reduction method with the addition of the polycaprolactone polymer in solution for electrospinning. The results of Dynamic light scattering, UV-Vis Spectroscopy and Raman Spectroscopy confirmed the presence of copper oxide II nanoparticles with diameters of 85 to 95 nm. Energy-dispersive X-ray Spectroscopy and Scanning Electron Microscopy confirms the presence of CuONPs distributed in PCL nanofibers with an average size of 900 nm. Antibacterial activity against *E. coli*, *S. mutans*, *K. oxytoca*, *S. aureus*, *P. aeruginosa* and *B. subtilis* was evaluated. The results show the sensitivity of *P. aeruginosa* and *E. coli* but not *K. oxytoca* or Gram positive bacteria. The antifungal effect was greater than the antibacterial effect showing more than 50% inhibition against *C. albicans*, *C. tropicalis* and *C. glabrata*. The compounds of PCL-CuONPs have a high potential as alternative to antibiotics, reducing the risks involved in the discharge of antibiotics to aquatic bodies.



[BIO-602] Poly- ϵ -caprolactone hydroxyapatite-alumina-silver as an alternative to antibiotics.

Liliana Medina-Ochoa (al141804@alumnos.uacj.mx)¹, Antonio Muñoz-Escobar¹,
Pamela Nair Pamela Nair Silva-Holguín¹, Leon Espinosa-Cristobal¹, Simón Yobanny
Reyes-López (yobannyr@yahoo.com.mx)¹

¹ Universidad Autónoma de Ciudad Juárez

Currently, water pollution is growing alarmingly caused by various factors, such as the direct contamination generated by garbage, the discharge of liquids by the industry and can also be caused by the remains of antibiotics, due to its impact with the environment is currently studying new methods of degradation since due to the contamination generated by antibiotics in water, bacterial resistance is currently growing. It is due to the resistance that seeks to obtain a new method of inhibition of bacterial growth, by means of composites of poly- ϵ -caprolactone (PCL) -hydroxyapatite-alumina-silver composed of PCL a biodegradable polymer that allows the material to have firmness in addition to the fact that in its degradation process non-toxic products are obtained, hydroxyapatite and alumina work as ceramics and finally the silver which, being a noble and active metal, when found at a nanometric level can generate the release of ions which generates that has a bactericidal effect, caused by the interaction with the membrane of the bacterium, inhibiting the replication function, it can also generate pores in the membrane because when it is at a nanometer level it is very easy to cross the membrane, which would cause the colloidal stability of the bacteria is broken, finally the positively charged ions can interact with the sulphydryl groups of the genetic code of the bacterium, causing bacterial lysis as replication is inhibited, that is why it seeks to create a material that causes the use of antibiotics to decrease.



XII -ICSMV

September 23rd to 27th, 2019 / San Luis Potosí, México

[BIO-607] Compounds of PVA/PEO/HAp/NPsAg as an alternative to antibiotics

Michelle Gerardo Lang-Salas (gerardo.lang@uacj.mx)¹, Jesús Alberto Garibay-Alvarado¹, Juan Carlos Cuevas-González¹, Alejandro Donohué-Cornejo¹, León Francisco Espinosa-Cristóbal¹, Simón Yobanny Reyes-López (yobannyr@yahoo.com.mx)¹

¹ Universidad Autónoma de Ciudad Juárez

Antibiotics are used to prevent and treat bacterial infections. Antibiotic resistance occurs when bacteria mutate in response to the use of these drugs. It is bacteria, and not human beings or animals, that become resistant to antibiotics. These drug-resistant bacteria can cause infections in humans and animals and these infections are more difficult to treat than non-resistant ones. Antibiotic resistance increases medical costs, prolongs hospital stays and increases mortality. The objective of this work is to elaborate a polymer-ceramic composite from PVA, PEO with hydroxyapatite and silver nanoparticles in the form of a membrane that maintains stable the release of silver nanoparticles propitiating a bactericidal character for biomedical application and thus Avoid infection caused by pathogenic bacteria.



[BIO-608] Compounds of alumina-hydroxyapatite-silver nanoparticles with an antibacterial effect

Pamela Nair Silva Holguín¹, Idahli Alejandra Meléndez-Estrada¹, León Francisco Espinosa-Cristóbal¹, Simón Yobanny Reyes-López (yobannyr@yahoo.com.mx)¹

¹ Universidad Autónoma de Ciudad Juárez

The indiscriminate use of antibiotics in medical, veterinary and agricultural practices results in the unloading of antibiotics into the environment, which causes the bacteria to become increasingly resistant to antibiotics, due to their impact on the environment. looks for new alternative antibacterial agents. Therefore, in the present investigation we present the obtaining of porous alumina spheres coated with hydroxyapatite and doped with silver nanoparticles with antibacterial effect . In the present project, hydroxyapatite powders doped with silver nanoparticles were synthesized at concentrations of 0.5, 1, 2.5 and 5 mM. The obtaining of spheres of alumina-HA-NpsAg of $4.08 \times 3.25 \text{ mm}^2$ with a sphericity of 0.8 was by ionic encapsulation, the spheres obtained were coated with hydroxyapatite obtained from calcium nitrate and triethylphosphite by the sol-gel method and were doped by simple adsorption with a 10 mM NpsAg solution with a size of $5.6 \pm 2.9 \text{ nm}$. The antimicrobial susceptibility was with agar and turbidimetric diffusion methods in Gram-negative bacteria (*Escherichia coli*, *Klebsiella oxytoca* and *Pseudomonas aeruginosa*) and Gram-positive (*Streptococcus mutans*, *Staphylococcus aureus* and *Bacillus subtilis*). All the bacteria used were susceptible to the HA-NpsAg powder, obtaining a maximum inhibition of 42.34% for *P. aeruginosa* at the concentration of 5 mM; however, the alumina-HA-NpsAg spheres only showed susceptibility in *E. coli*, *P. aeruginosa* and *S. aureus*, obtaining a maximum inhibition of 20% in *S. aureus*.



XII -ICSMV
September 23rd to 27th, 2019 / San Luis Potosí, México

BIOMATERIALS AND POLYMERS (BIO) POSTER SESSIONS



XII -ICSMV

September 23rd to 27th, 2019 / San Luis Potosí, México

[BIO-17] Antibacterial, antifungal and immune response of gold nanorods embedded in a chitosan matrix hydrogel by photothermal therapy

Carlos Omar Bermúdez Jiménez (carlosbj8@gmail.com)⁴, Carlos Omar Bermúdez Jiménez¹, Gabriel Alejandro Martínez Castañón⁴, Nereyda Niño Martínez³, Marc G. Romney², Horacio Bach¹

¹ Department of Medicine, Division of Infectious Diseases, University of British Columbia, Vancouver, BC, Canada

² Division of Medical Microbiology, St. Paul's Hospital, Providence Health Care, Vancouver, BC, Canada

³ Facultad de Ciencias, Universidad Autónoma de San Luis Potosí, San Luis Potosí, S.L.P., México

⁴ Laboratorio de Nanobiomateriales, Facultad de Estomatología, Universidad Autónoma de San Luis Potosí, San Luis Potosí, S.L.P., México

Plasmonic photothermal therapy (PPTT) has been used as an alternative to chemotherapy for the elimination of resistant microorganisms; however, its in situ evaluation has not been well studied. In the present study, we assessed the antimicrobial activity of a chitosan-based hydrogel embedded with gold nanorods (Ch/AuNRs) using a low power infrared diode laser. The antibacterial activity was measured in both Gram-positive and –negative strains, including clinical isolates of multidrug-resistant pathogens. The cytotoxic effect, cellular proliferation, and the expression of the pro-inflammatory (IL-6 and TNF- α) and antiinflammatory (IL-10) cytokines were quantified in a murine model of macrophages. Results showed a potent antimicrobial activity of the Ch/AuNRs with MICs \leq 4 μ g/mL, very low cytotoxicity with cell viability above 80%, and the macrophage proliferation was not affected for a period of 48 h. These results suggest that our Ch/AuNR-embedded hydrogel could be an option to locally control chronic nosocomial infections using PPTT.



XII -ICSMV

September 23rd to 27th, 2019 / San Luis Potosí, México

[BIO-25] Physicochemical properties of chitosan/starch/extract of croton lechleri films for skin tissue engineering

Santos Adriana Martel-Estrada (mizul@yahoo.com)², Diego Javier Olivares-Ochoa³, Amanda Carrillo-Castillo³, Claudia Alejandra Rodríguez-González³, Perla Elvia García-Casillas³, Mónica Mendoza-Duarte¹

¹ Centro de Investigación en Materiales Avanzados, Miguel de Cervantes 120, Complejo Industrial Chihuahua, C.P. 31109, Chihuahua, México

² Instituto de Arquitectura, Diseño y Arte, Universidad Autónoma de Cd. Juárez, Av. Del Charro 450 Norte. Col. Universidad, C.P: 32310, Cd. Juárez, Chihuahua, México

³ Instituto de Ingeniería y Tecnología, Universidad Autónoma de Cd. Juárez, Av. Del Charro 450 Norte, Col. Universidad, C.P. 32310, Cd. Juárez, Chihuahua, México.

The purpose of this study is to examine the chemical, optical, morphology and mechanical properties of films produced by casting method. The properties were obtained by FT-IR analysis, UV-vis, SEM and DMA. The cumulative results obtained from IR, UV-vis and DMA suggest that there is a chemical interaction between the components of the composite. Our results thus show that Chitosan/ Starch/Extract of Croton Lechleri films could be suitable for biological applications but it is important to improve the mechanical properties of the film.



[BIO-35] Antimicrobial properties of starch/mimosa tenuiflora/zinc oxide films

Santos Adriana Martel-Estrada (adriana.martel@uacj.mx)¹, Edgar Eduardo Mendoza-Zubia³, Claudia Lucía Vargas-Requena², Amanda Carrillo-Castillo³, Lorena Rivera-Rios³, Imelda Olivas-Armendáriz³, Hortensia Reyes-Blas³, Claudia Alejandra Rodríguez-González³

¹ *Instituto de Arquitectura, Diseño y Arte, Universidad Autónoma de Cd. Juárez, Av. Del Charro 450 Norte. Col. Universidad, C.P: 32310, Cd. Juárez, Chihuahua, México*

² *Instituto de Ciencias Biomédicas, Universidad Autónoma de Ciudad Juárez, Henri Dunant 4016, Zona Pronaf. Cd. Juárez, Chihuahua, México, C.P. 32310.*

³ *Instituto de Ingeniería y Tecnología, Universidad Autónoma de Cd. Juárez, Av. Del Charro 450 Norte, Col. Universidad, C.P. 32310, Cd. Juárez, Chihuahua, México*

The purpose of this study is to examine the chemical, morphological, optical and antibacterial properties of starch/mimosa tenuiflora/zinc oxide films produced by casting method. The properties were obtained by FT-IR analysis, XRD, UV-vis, SEM and turbidimetry. The cumulative results obtained from IR, XRD, UV-vis SEM and turbidimetry test suggest that there is a physical interaction between the components of the composite. Our results thus show that Starch/mimosa tenuiflora/zinc oxide films could be suitable for biological applications.



[BIO-67] Development of a predictive model for an experimental plant that generates biogas from biomass resulting from agricultural and livestock activities.

Arturo Hernández Hernández (arturo.hernandez@upq.mx)³, Ruben Velázquez Hernández (rvelazquez@mail.itq.edu.mx)², María Guadalupe López Granada¹, María Blanca Becerra Rodríguez², Antonio Joaquin Nava Pineda³

¹ *JOR Solutions*

² *Tecnológico Nacional de México Campus Querétaro*

³ *Universidad Politécnica de Querétaro*

The present project consists of the development of a predictive model for an experimental plant that generates biogas from the biomass product of agricultural and livestock activities. The main problem that currently occurs is the low efficiency in energy generation, and there are few studies about the parameters of the raw material to make efficient the production of biogas, such as the mechanical, physical and chemical parameters necessary for the optimization, taking into account that not all customers have the same demand for biogas production, the transfer of equipment to take the device to places where access is complicated should also be considered. For the project experiments were carried out with cow excreta and cricket excreta with different portions of water to evaluate the feasibility of using some of the proportions based on the production of biogas from the production of bubbles.



[BIO-74] SYNTHESIS AND CHARACTERIZATION OF HYDROGEL WITH NANOCOMPSITES (Ag and TiO₂) FOR MENISCO PROSTHESIS BY 3D PRINTING

Karí Guadalupe Hortensia Martínez Reyna (kari_mr@alumnos.uaslp.edu.mx) ¹, Ma. Guadalupe García Valdivieso ¹, Hugo Ricardo Navarro Contreras (hnavarro@uaslp.mx) ¹

¹ Coordinación para la Innovación y Aplicación de la Ciencia y la Tecnología (CIACYT-UASLP), Av. Sierra Leona #550, Col. Lomas 2a. Sección, CP 78210, San Luis Potosí, S.L.P., MÉXICO.

Millions of people suffer from injuries or damage to organs or tissues, being the transplantation the solution to these problems at present. This is the reason why tissue engineering develops materials with the ability to create artificial tissues. One of the main injuries in developing countries is osteoarthritis, which causes disability after 40 years, reducing up to seven healthy years in men, in women the reduction is up to thirteen years.

One of the biomaterials used in tissue engineering is hydrogels because of their unique properties such as high water content, softness, flexibility and biocompatibility. As well as the nanocomposites, such as the silver nanoparticles used in biomedical applications due to their characteristic antibacterial property, or the nanotubes of titanates that, besides being biocompatible, have very favorable mechanical properties.

The objective of this work is the synthesis of a hydrogel with Ag nanoparticles and TiO₂ nanotubes, as a biocompatible polymer, as well as its characterization, in order to be used in 3D prosthesis printing. The purpose of making an antibacterial hydrogel is that in addition to being biocompatible prosthetic infections are avoided.

To obtain the hydrogel the AMPS monomer was dispersed under rigorous agitation, adding MBBA (cross-linker), I2959 (photoinitiator) and previously synthesized nanocomposites (TiO₂ nanotubes synthesized by hydrothermal method and Ag nanoparticles). Finally, Laponite is added to the solution in a percentage of 10-15% w/v. To create a double network hydrogel, Chitosan was used as the next monomer. The hydrogel Poly (AMPS / Chitosan) / Laponite with nanostructures will be used to build a model piece with the 3D printer, performing the curing by UV radiation to provide rigidity to the piece.

It is proposed to characterize the rheological properties of viscosity and the modules G', G''. The viscosity obtained is between 10-14.6 kPa, which guarantees the viability in 3D printing. The morphology is proposed to be characterized by Transmission Electron Microscopy (TEM), the polymerization process by Reflectance and RAMAN spectroscopy, the mechanical properties by Mechanical Tests.

Key Words

Biocompatible hydrogel, TiO₂ nanotubes, Ag nanoparticles, 3D printing.



XII -ICSMV

September 23rd to 27th, 2019 / San Luis Potosí, México

[BIO-78] Surface modification of Ti6Al4V alloys from phosphonic acid and UHMW-PE films to inhibit the corrosion process in emulated biological media

Karely Anaya Garza (*karelyanaya_grz@pm.me*)¹, Miguel Antonio Domínguez Crespo
(*mdominguezc@ipn.mx*)¹, Aidé Minerva Torres Huerta¹

¹ Instituto Politécnico Nacional, CICATA-Altamira, CIAMS, km 14.5 carretera Tampico – Puerto Industrial Altamira, Tamps., México CP 89600

The Ti6Al4V alloy, is commonly used in the production of medical implants. This work aims to prove that the surface modification of this alloy through the formation of thin films over its surface, will relieve the corrosive effects of the biological medium by decelerating the corrosion process. The superficial preparation of the Ti6Al4V alloys was made using emery paper grade 400, 600, 1000 and 1500, then degreased with deionized water, ethanol and acetone for 10 minutes in ultrasonic bath, each. The thin films formation was accomplished through dip-coating from octadecylphosphonic acid (in 1 mM octadecylphosphonic acid dissolved in ethanol at 40 °C) or UHMW-PE (in a dissolution of 5 wt% UHMW-PE powder in decalin at 160 °C). To optimize the preparation method, the influence of the process time was investigated: OPA 20h and OPA 30h and UHMW-PE 20s and UHMW-PE 30s, respectively. XRD patterns of the coated Ti6Al4V alloys showed the rising of new peaks not seen in the XRD patterns of the bare alloys, indicating the presence of the films coating the alloys. It was found that the octadecylphosphonic acid and UHMW-PE films presented less porosity and a better performance as protective barriers over the surface of the metallic substrates, to inhibit the corrosion process in an emulated biological medium, at 30 h and 30 s of process time, respectively.



[BIO-136] Use of *Agave tequilana*-xylans and multiwalled carbon nanotubes as scaffolds for *in vitro* culture of neurons

Jaime Agustin Torres Castro (bio.august.10@gmail.com)², Marcos Alfredo Escalante Álvarez², Graciela Gudiño Cabrera¹, Guillermo Toriz González², José Manuel Gutiérrez Hernández (manuel.gutierrez@academico.udg.mx)², Jaime Agustin Torres Castro¹

¹ *Department of Cellular and Molecular Biology, University Guadalajara, 45110, Guadalajara, Mexico.*

² *Department of Wood, Cellulose and Paper Research, University Guadalajara, 45110, Guadalajara, Mexico.*

In this work we explore the use of *Agave tequilana*-xylans in combination with functionalized multiwalled carbon nanotubes (MWCNTs) as an original biomaterial and suitable scaffold for neurons culture. At a first step, the development of hydrogels with *Agave tequilana*-xylans (AX) through a conjugation process with tyramine (TA) was used to enable enzymatic crosslinking. Then, functionalized MWCNTs were mixed in distinct concentrations with AX-TA obtained from agave bagasse with the aim of increase different properties of AX-TA hydrogels and obtain a novel hybrid material. The results indicate that AX-TA/MWCNTs scaffolds support neurons viability, adhesion and proliferation at higher levels as compared to traditional culture substrates. These results suggest the potential for this combination of biomaterials, i.e. agave xylans and carbon nanomaterials, as scaffolds for *in vitro* neurons culture.



[BIO-146] EFFECT OF THE TEMPERATURE IN THE MAGNETITE FILMS SYNTHESIS ON Ti6Al4V-Eli BY ELECTRODEPOSITE

Adriana Montiel García², Edgar Onofre Bustamante (edonofre73@yahoo.com.mx)³,
María Lorenza Escudero Rincón¹, Juan Pablo León González (jpleonglez@gmail.com)³,
Greta de Monserrat Tavarez Martínez³

¹ Centro Nacional de Investigaciones Metalúrgicas. Av. de Gregorio del Amo, 8, 28040 Madrid, España.

² Centro de Investigación en Ciencia Aplicada y Tecnología Avanzada del Instituto Politécnico Nacional Unidad Altamira, Altamira Tamaulipas, México. Km. 14.5 Carretera Tampico-Puerto Industrial Altamira, Altamira Tamaulipas C.P. 89290

³ Centro de Investigación en Ciencia Aplicada y Tecnología Avanzada del Instituto Politécnico Nacional Unidad Altamira, Altamira Tamaulipas, México. Km. 14.5 Carretera Tampico-Puerto Industrial Altamira, Altamira Tamaulipas C.P. 89290.

Titanium alloys have been widely employed as orthopedic and odontological implant materials due to its biocompatibility. The main limitations of these materials are the poor performance in applications involving surfaces in mutual contact and under load or relative motion (e.g. joint replacement), because of its low wear resistance, and the possible dissolution into the human body, by corrosion. Recently, new studies have been performed with a Ti6Al4V-Eli (Extra Low Interstitial) alloy with less oxygen content, as this improves corrosion resistance. However, its low wear resistance remains a disadvantage of this alloy, so it is necessary to modify its surface improving its resistance to wear and increasing its corrosion resistance. In this work it is proposed to evaluate the effect of temperature on their electrochemical properties of films obtained by potentiostatic pulse-assisted co-precipitation (PP-CP) deposited over Ti6Al4V-Eli. The anticorrosive properties will be determined by electrochemical techniques such as open circuit potential (OCP), electrochemical impedance spectroscopy (EIS) and polarization curves in a physiological solution of Hank's. The results are complemented by compound identification using X-ray diffraction. The effect of temperature plays an important role in obtaining the oxidation state of iron, since a slow heating ramp provides a coating in the form of iron oxide (Fe_3O_4), however, the films obtained on the titanium substrate correspond to iron oxy-hydroxides d- Fe^{3+} -O(OH) because of a rapid heating ramp. Through XRD, the presence of the magnetite film with particle sizes of 8-10 nm was determined for the plane (311), on the other hand, d- Fe^{3+} -O(OH) presents its characteristic planes in (010), (011) (012) (110) and (103). The electrochemical response (EIS) for M1 samples and M2 of Titanium + film presents impedances of greater magnitude ($1.0\text{E} + 20 \Omega * \text{cm}^2$) with respect to the reference ($5.26\text{E} + 4 \Omega * \text{cm}^2$), it is necessary to carry out continuous immersion to corroborate these results and see their behavior. In time, through the polarization curves, it was determined that the samples of Ti6Al4V-Eli (Reference) and Ti6Al4V-Eli + Fe_3O_4 , are not susceptible to prick corrosion within the polarization range evaluated.



[BIO-148] Influence of Polymer Modified Asphalt on the Compaction of the Asphalt Pavements using X-Ray Computed Tomography (CT)

Anyi Maritza Tacumá Garzón (anyi.tacuma@alumno.buap.mx)¹, Jorge Raúl Cerna Cortez
¹, César Marquéz Beltrán²

¹ Facultad de Ciencias Químicas, Benemérita Universidad Autónoma de Puebla, Ciudad Universitaria, Puebla 72570

² Instituto de Física, Benemérita Universidad Autónoma de Puebla, Ciudad Universitaria, Puebla 72570

Compaction is the process of densifying, or reducing the volume of, a mass of material. Most practitioners consider achieving appropriate compaction critical to the performance of an asphalt pavement. For asphalt mixtures, compaction locks the asphalt-coated aggregate particles together to achieve stability and provide resistance to deformation (or rutting) while simultaneously reducing the permeability of the mixture and improving its durability. In this research we have studied the degree of porosity of asphalt cement (AC) when polymers are added in the asphaltene. We have characterized the internal structure of this material by means of X-ray computed tomography. Particularly we analyzed the vacuum distribution in the AC mixtures and the volume fraction of porosity which can influences the mechanical properties. This work aims to correlate microstructural details and mechanical behavior of the conventional asphalt cement AC20 (pavement used in the road of the cities) with those polymer-modified asphalt cements. Image analysis on the tomograms obtained was used to determine the form of the compaction. The results showed that this parameter is depending of the type and concentration of the polymer used.



XII -ICSMV

September 23rd to 27th, 2019 / San Luis Potosí, México

[BIO-181] Parameters calculation in the plastic injection molding process

Samuel de la Luz Merino (samuel.delaluz@utpuebla.edu.mx)¹, José Victor Sandoval Ramos¹, Lucio Martínez Rodríguez¹

¹ Universidad Tecnológica de Puebla, Antiguo Camino a La Resurrección 1002-A, Zona Industrial, Puebla, Pue. México. C.P. 72300

Injection molding is an efficient processes where plastic devices production through automation is feasible, however, the products manufactured by using the current injection molding method usually have defects, such as short shot, jetting, sink mark, flow mark, burn mark, flash, warping, weld lines etc. These defects may be difficult or costly to address, however could be eliminated in a high percentage taking into account the parameters and variables associated with the experimental process doing correct calculations before starting process. To achieve the above, it is necessary a fundamental understanding of phenomena which are carried out in the plasticizing unit of the molding machine such as melt generation, solids transport, flow as well as the product shaping which takes place in the mold cavity. In this work experimental tests were made by using a Krauss Maffei injection molding machine CX 80-380, polypropylene cups were obtained. The injection parameters were adjusted according to the possibility of high production rates and the manufacture of articles with high quality standards.



[BIO-262] The influence of chitosan on the properties of an edible biopolymer based in native corn starch

Z. I. Hernández-Rufino (zaira-1224@hotmail.com)², A. Cortés-Mendoza², A.L. Atanacio-Gelover², C. Bravo-Rangel², M.B. Ortúñoz-López (mbortuno@mail.itq.edu.mx)², C.G. Flores-Hernández², J.M. Yáñez-Limón³, J.L. Rivera-Armenta¹

¹ Centro de Investigación en Petroquímica; Tecnológico Nacional de México / I. T. Ciudad Madero ; Prol. Bahía de Aldahir y av. de las bahías, parque de la pequeña y mediana industria, C. P. 89600, Altamira Tams. México.

² Departamento de Metal-Mecánica; Tecnológico Nacional de México / I. T. Querétaro; Av. Tecnológico s/n esq. Gral. Mariano Escobedo. Colonia Centro Histórico C.P. 76000, Querétaro, Qro. México.

³ Laboratorio Nacional de Investigación y Desarrollo Tecnológico de Recubrimientos Avanzados, LIDTRA; CINVESTAV; Libramiento Norponiente #2000, Fracc. Real de Juriquilla. C.P. 76230, Querétaro, Qro. México

The mechanical, thermal and thermomechanical properties of a biopolymer based on native corn starch and chitosan were investigated. For the study, some formulas were designed by varying the proportion of chitosan, and by casting, films of edible starch biopolymers were produced. On the other hand, samples of identical starch/chitosan proportions were processed by extrusion forming technology. For characterization, Differential Scanning Calorimetry experiments were used to monitor the thermal behavior of these biopolymers, using a dynamic heating program. By Infrared Spectroscopy, the chemical nature of the manufactured materials was investigated and confirmed, and changes due to oxidative degradation processes were monitored. Evidence shows that chitosan has antimicrobial, antibacterial and antifungal properties, which could promote the lifespan of this biopolymers. Chitosan also substantially improves the mechanical, thermal and thermomechanical properties of the starch biopolymer. The results of samples obtained by extrusion tests are consistent with the results obtained in the films. The edible biopolymers developed in this study showed many desirable characteristics, which could potentially be used in industrial applications, for the replacement of synthetic polymers in conventional products that are in contact direct with food.



XII -ICSMV

September 23rd to 27th, 2019 / San Luis Potosí, México

[BIO-278] Determination of functional groups by XPS on chitosan biofilms

Erick Saúl Aranda González (nt694722@iteso.mx)¹, Kevin Guzmán Chapa², Milton Vázquez Lepe (milton.vazquez@cucei.udg.mx)³

¹ Instituto Tecnológico de Estudios Superiores de Occidente

² Instituto Tecnológico de Matamoros

³ Universidad de Guadalajara

Chitosan is a biopolymer obtained by a process of deacetylation of chitin derived from the shell of crustaceans, insects, and fungi, with broad properties and applications in various sectors such as water treatment, biomedicine, the food industry, agriculture, among others. This work presents the chemical components of different chitosan solutions, were then the films can be used for antimicrobial applications. Films were characterized with X-ray Photoelectron Spectroscopy (XPS) and Scanning Electron Microscopy (SEM) with the objective of understanding how the surface morphology and their carbon components vary when the biopolymer is dissolved in acetic acid (C₂H₄O₂). By exposing the solutions to the evaporation of the solvent at room temperature and how this factor influences the viscosity and its chemical components. Selecting the solution that presents the best stability of amino groups (NH₂) for the films, subsequently, silver nanoparticles (AgNPs) are added as an additional agent in the inhibition of bacterial growth.



[BIO-293] GRAPHENE OXIDE COMPOSITE HYDROGEL FOR TRANSDERMAL DELIVERY OF METFORMIN.

LORENA GÁRATE-VÉLEZ (*lorena.garate.v@gmail.com*)³, RUBÉN OMAR URBINA-RODRÍGUEZ², TERESA NERI-GÓMEZ², ALMA GABRIELA PALESTINO-ESCOBEDO², MILDRED QUINTANA RUIZ¹

¹ CENTRO DE INVESTIGACIÓN EN CIENCIAS DE LA SALUD Y BIOMEDICINA

² DEPARTAMENTO DE CIENCIAS QUÍMICAS

³ DOCTORADO INSTITUCIONAL EN INGENIERÍA Y CIENCIA DE MATERIALES

The most prescribed medication for the treatment of diabetes mellitus type II as first-line oral therapy is Metformin HCl [1, 1-dimethylbiguanide hydrochloride], due to decrease insulin resistance, mainly in the skeletal muscle and the liver. Nevertheless, an important site of action and reaction to metformin HCl is the gastrointestinal tract, due to the intolerance of the formula. Often gastrointestinal tract limits its dosage are related with the alteration of such mechanisms as the altered transport of serotonin or histamine, local accumulation of the drug in the enterocytes, increased exposure to bile acids in the colon and alteration of the intestinal microbiome. Furthermore, another associated side effects are lactic acidosis, vomiting, diarrhea, abdominal pain, drowsiness, stomach pain, flatulence and loss of appetite. Hence, in this study we investigate the ability of graphene oxide as a vehicle for the transdermally administration route of Metformin HCl, through an hydrogel made of poly(ethylene glycol) diamine (PEGD):Citric Acid/Gelatin (PEGD:CA/GEL) which it acts as a strong elastic matrix. In other words, this composite could help to minimize some side effects associated with the oral administration route.



XII -ICSMV

September 23rd to 27th, 2019 / San Luis Potosí, México

[BIO-294] GRAPHENE OXIDE COMPOSITE HYDROGEL FOR TRANSDERMAL DELIVERY OF METFORMIN.

LORENA GÁRATE-VÉLEZ (*lorena.garate.v@gmail.com*)³, RUBÉN OMAR URBINA-RODRÍGUEZ², TERESA NERI-GÓMEZ², ALMA GABRIELA PALESTINO-ESCOBEDO², MILDRED QUINTANA RUIZ (*quintanamildred@gmail.com*)¹

¹ CENTRO DE INVESTIGACIÓN EN CIENCIAS DE LA SALUD Y BIOMEDICINA

² DEPARTAMENTO DE CIENCIAS QUÍMICAS

³ DOCTORADO INSTITUCIONAL EN INGENIERÍA Y CIENCIA DE MATERIALES

The most prescribed medication for the treatment of diabetes mellitus type II as first-line oral therapy is Metformin HCl [1, 1-dimethylbiguanide hydrochloride], due to decrease insulin resistance, mainly in the skeletal muscle and the liver. Nevertheless, an important site of action and reaction to metformin HCl is the gastrointestinal tract, due to the intolerance of the formula. Often gastrointestinal tract limits its dosage are related with alteration of such mechanisms as altered transport of serotonin or histamine, local accumulation of the drug in the enterocytes, increased exposure to bile acids in the colon and alteration of the intestinal microbiome. Furthermore, another associated side effects are lactic acidosis, vomiting, diarrhea, abdominal pain, drowsiness, stomach pain, flatulence and loss of appetite. Hence, in this study we investigate the ability of graphene oxide as a vehicle for the transdermally administration route of Metformin HCl, through an hydrogel made of poly(ethylene glycol) diamine (PEGD):Citric Acid/Gelatin (PEGD:CA/GEL) which it acts as a strong elastic matrix. In other words, this composite could help to minimize some side effects associated with the oral administration route.



[BIO-298] Synthesis of electrospun polycaprolactone based membranes for the treatment of drug residues in water using ZnO nanoparticles as active agent.

M.A. Juarez-Sanchez ³, J. Rangel-Rivera ², M. Melendez-Zamudio ², J. Cervantes ², S.Y. Reyes-Lopez ⁴, M. Melendez-Lira (mlira@fis.cinvestav.mx) ¹

¹ Departamento de Fisica, CInvestav-IPN, Zatenco, CDMX, Mexico

² Division de Ciencias Exactas, Universidad de Guanajuato, Guanajuato, Mexico

³ Escuela Nacional de Ciencias Biologicas, Instituto Politecnico Nacional, Santo Tomas, CDMX, Mexico

⁴ Instituto de Ciencias Biomedicas, Universidad Autonoma de Ciudad Juarez, PRONAF, Ciudad Juarez, Chihuahua, Mexico

Water pollution due to drug residues is a severe problem that may cause irreversible environmental damages. It has been reported that usual water treatment methods are not able to cope with the problem and an advanced oxidation process is required to degrade residual drugs[1]. A methodology useful to degrade chemical residues is photocatalysis employing compound semiconductors. ZnO is a semiconductor broadly employed in photocatalysis due to both its electronic properties and easy methodologies to produce nanoparticles. ZnO nanoparticles were synthesized from a colloidal suspension using zinc acetate and NaOH. In order to improve the re-use and reactivity of ZnO nanoparticles we prepared electrospun membranes mixing different ratios of ZnO nanoparticles with polycaprolactone. Membranes were characterized by UV-Vis, IR, Raman and X-ray spectroscopies and electron scanning microscopy. The photocatalytic response of membranes was first tested employing methylene blue to choose the best ZnO composition and then applied to polluted water with a controlled content of the drug bezafibrate. The degradation results are discussed in terms of fiber diameter, ZnO nanoparticle distribution and their surface exposure.

[1] Barceló, D. Emerging pollutants in water analysis, TrAC Trends in Analytical Chemistry. **22**, 14-15(2003).
*. Work partially supported by CONACyT



[BIO-302] SOMATROPIN CHARACTERIZATION AS EXAMPLE MODEL PROTEIN IN ENCAPSULATION BY SPRAY DRYER

Elvia Zárate (elvia.zarate@alumnos.uaslp.edu.mx)¹

¹ Facultad de Ciencias Químicas

Somatropin is a growth hormone, approved in 1980 as a treatment in cases of dwarfism, the dosage regimen of this drug is a daily injection, making it difficult to follow a long-term treatment. A new delivery system is needed that extends the half-life, without compromising the integrity and quality of the protein. Alginate is a polymer of natural origin, the pharmaceutical industry uses alginate for its high tolerability and a null pharmacological effect. In this work, we propose a new nano system of delivery for Somatropin with alginate as polymer by Spray dryer. Due high temperature is needed have information about quality parameters before and after of processes. The somatropin is a biologic drug, this protein need a characterization to guarantee its quality and uniformity. The characterization of protein included primary sequence by spectrometry mass coupled a time of flight (ESI-Q-TOF-MS), molecular weight, secondary structure by Circular Dichroism (CD), impurity and aggregates by Size-Exclusion-Chromatography. In this work, the analysis was performed with 6 batches of Genotropin® as a reference drug. In 6 batches the N-Terminal sequence is same in the 18 aminoacid with a molecular weight of 1821 Da. The molecular weight of native protein by ESI-Q-TOF-MS in 6 batches is 22 124 Da, this result is comparable with theoretical data (22 129 Da; DrugBank, 2018). The secondary sequence by CD in the region 270 to 290 nm, not show difference in the patterns, for this reason the lateral chains of aromatic aminoacid is not different. The determination of soluble aggregates by SEC-UPLC does not show the presence of protein fragments or cellular debris from the production system of the biopharmaceutical. The characterization of somatropin contained in a reference medicine shows a great uniformity of content and high quality in the production and storage process. These data will serve as a basis to begin the process of microencapsulation by spray drying (Spray-dryer) in a biocompatible polymer matrix.



XII -ICSMV

September 23rd to 27th, 2019 / San Luis Potosí, México

[BIO-338] Hydrophilic behavior of synthetic hydroxyapatite and fluids used in tissue culture in vitro

Andrés Rodolfo Serrano Castro¹, María Guadalupe González Morgado², María Magdalena Méndez-González¹

¹ *Physics department, ESFM-IPN, U.P. Adolfo López Mateos, Edif. 9, Lindavista 07738 CDMX, México*

² *UPIBI-IPN, Av. Acueducto 550, La Laguna Ticoman, 07340, CDMX, México*

Through the contact angle, the hydrophilic behavior of synthetic hydroxyapatite was determined using distilled water, saline solution and bovine fetal serum as wetting liquids, because these are the fundamental fluids used in tissue culture in vitro to determine the biocompatibility of synthetic hydroxyapatite. The contact angle provided information related to surface energy, surface roughness and heterogeneity in chemical composition of hydroxyapatite. This was measured as the angle formed between the surface of the hydroxyapatite, when coming into contact with the liquid and the line tangent to the point of contact of the drop of it. The three liquids used presented a desired hydrophilic behavior since they have a contact angle less than 65°, which is a necessary condition for cell cultures in vitro.



XII -ICSMV

September 23rd to 27th, 2019 / San Luis Potosí, México

[BIO-493] Obtaining resin based on unicel waste

*Abigail Ponce González (abiponglez@gmail.com)*¹

¹ Facultad de Ingeniería Química, BUAP

Expanded polystyrene (EPS), commonly known in Mexico as unicel, is a foamed plastic material obtained from polystyrene, is employed in the construction and packaging sector. It is characterized by its lightness, resistance to moisture and above all hygiene, but being one of the least environmentally friendly materials to take up to 500 years to degrade, currently looking for alternatives for recycling.

In the present work an alternative to its recycling is proposed from the manufacture of a resin based on unicel, whose production consists in the dilution of unicel residue, previously collected and washed, to dilute in an organic solvent (ethyl acetate). Different concentrations were tested until obtaining the most suitable one based on a liquid silicone consistency, in a proportion of 3:6 g/ml, after this it was allowed to dry for approximately 5 days. The material obtained was studied by scanning electron microscopy (SEM) to obtain information on the morphology and size of the samples prepared, an X-ray dispersive energy spectroscopy (EDS) analysis was performed to obtain information on the chemical composition of the samples prepared. In addition, hardness tests were carried out to measure some mechanical properties of the different samples obtained.



[BIO-531] Production of non-expensive hydrophobic and magnetic melamine sponges for the removal of hydrocarbons and oils from water

Jesús Iván Tapia (jesus.tapia@ipicyt.edu.mx)¹, Elizabeth Alvarado¹, Armando Encinas¹

¹ Instituto Potosino de Investigación Científica y Tecnológica A.C., Camino a La Presa de San José 2055, Lomas 4 sección, 78216 San Luis, S.L.P., México

Key Words: Melamine, super-hydrophobic, magnetic-nanoparticles, water, oil.

Water contamination by oils and heavy metals is an important problem, since environmental, economic and health issues can be caused. It can mainly damage the aquatic ecosystem as well as the biodiversity of the land, affecting the long-term health of population who live near to affected regions [1]. Furthermore the emission sources are multiple such as oil spill from oil platforms and the discharge of organic chemicals from industrial activities. Therefore, it is necessary to implement simple and non-expensive methods for the removal pollutant oils from water [2,3].

In this sense, we studied the use of melamine sponge, a porous structure, and a natural organic hydrophobic coating (stearic acid) in order to develop a hydrophobic porous material with high absorption capability. The material was also functionalized with magnetic nanoparticles. This material has potential applications to remove oils and toxic heavy metals from water using magnetic separation techniques. The material obtained was characterized using Scanning Electron Microscopy, Fourier Transform Infrared, water contact angles, oil absorption properties and magnetic properties.

References

[1] V., Environ. Sci. Technol. 40, 7914-7918 (2006).

[2] T. T., Sci Rep. 7, 17761-17769 (2017).

[3] X., Ind. Eng. Chem. Res. 55, 3596–3602, (2016).



[BIO-532] Synthesis and characterization of a collagen-alginate-graphene oxide aerogel-based scaffold

Abraham Israel Muñoz Ruiz (*a.israel.mr@gmail.com*) ¹, Diana Escobar Garcia ¹, Mildred Quintana ¹, Amaury Pozos Guillen ¹, Hector Flores Reyes ¹

¹ UASLP

Introduction. The loss and damage of organs and tissues due injuries/diseases has been a concern of clinicians for years, this has motivated the development of regenerative strategies. The aim of this study is to develop a highly porous aerogel-based collagen-alginate-graphene oxide scaffold for tissue engineering. **Methods.** The synthesis of the graphene oxide (GO) was performed according to hummers' method; the characterization was performed by Raman, FTIR, UV-Vis and TEM. For the aerogel a supercritical dryer was handcrafted; then a collagen-alginate-GO hydrogel was synthesized and was put under supercritical conditions into the dryer to produce an aerogel; the aerogel was evaluated by TEM and FTIR. **Results.** The supercritical process produced a scaffold with a stable structure; The aerogel FTIR shown that the aerogel conserve the functional groups of collagen and GO, meaning that both preserves their mechanical and biological properties. The SEM evaluation shown a three-dimensional highly porous structure. **Conclusion.** Here is presented a technique to synthesize a new collagen-alginate-GO aerogel-based scaffold. The scaffold produced presents adequate properties to be used for cell culture and tissue engineering.



[BIO-537] ALGINATE MICROBEADS FOR 3D CELL CULTURE

Noé Martín Carreón Aguiñaga (noecarreon_0611@outlook.com)¹, Héctor Flores Reyes¹,
Amaury de Jesús Pozos Guillén¹, Roel Cruz Gaona¹

¹ Universidad Autónoma de San Luis Potosí

Tissue engineering has been introduced as an alternative for medical applications. Even though many options have been widely studied, a few have reached the clinical stage and, moreover, they still present gaps to be filled to fully work on a clinical scenario.

One of the recent developed techniques is microencapsulation, a process that involves the use of biomaterials to provide a niche for the cells. This biomaterial must fulfill biological and mechanical requirements to be considered for the microencapsulation process. Such requirements involve mechanical and chemical stability, biocompatibility, non-toxic when applied or degraded, and able to allow the exchange of nutrients in a physiological environment.

Alginate is currently the most used biomaterial for microencapsulation. Its mechanical properties and chemical structure make it a top candidate for the process. In addition to this, its biocompatibility represents a great advantage for medical applications. By crosslinking alginate with divalent cations, stable microcapsules can be formed.

The objective of this project is to standardize a microencapsulation culture technique for its application in a dynamic culture device.

1.5% alginate solution was used for the microencapsulation process. Crosslinking solution was 104mM calcium chloride (CaCl_2). Human osteoblasts derived from third molar extraction sites were cultured until confluence was achieved. 10^5 cell density was resuspended in 1ml alginate solution and droplets were carefully poured into the crosslinking solution using a 29 gauge needle and under stirring (450 rpm). Encapsulation was achieved and confirmed by optical observation. Live dead test was performed at days 7, 14, 21 and 28. MTS assay kit was used to evaluate cell proliferation at 24 and 48 hours. Morphological changes were also reported by optical microscope observation. Thermal Gravimetric Analysis was performed to determine mass changes. Results showed cell viability and biocompatibility after 21 days. MTS and optical observation also showed cell proliferation. TGA results showed similar behavior in alginic acid salt and alginate solution.

Osteoblast microencapsulation using alginate showed promising results for its application as a 3D culture technique. Results may also suggest a possible in vivo application or the encapsulation process using different cell lines.



XII -ICSMV

September 23rd to 27th, 2019 / San Luis Potosí, México

[BIO-547] Novel Dog Hair Sponges Functionalized With Recycled Expanded Polystyrene For Oil Removal From Water

Sofia Vilchis Sanchez (sofi_svs96@gmail.com)¹, Daniel Esteban Camacho Martínez
(daniel.camacho@ipicyt.edu.mx)², Armando Encinas²

¹ Departamento de Matemáticas y Física, Instituto Tecnológico y de estudios Supérieures de Occidente, Periférico Sur Manuel Gómez Morín 8585, Colonia ITESO, 45604 Tlaquepaque, Jalisco, México

² División de Materiales Avanzados, Instituto Potosino de Investigación Científica y Tecnológica A. C., Camino a la Presa San José 2055, 78216 San Luis Potosí, SLP, México.

Due to humans activities oil contamination in water has become a huge problem for ecosystems. As a result, research for novel materials that can contribute to solving this issue has gained significant interest. Many of the materials that have been proposed have good properties and performance, they also have complicated, expensive, they are usually non-scalable and their synthesis is not ecofriendly. Therefore, it is imperative to identify and study for novel materials that circumvent these issues. In this sense, a new sponge made of dog hair (DHS) covered by a varnish made of expanded polystyrene waste, with a selective affinity for oil in an aqueous medium is presented in this work. These sponges are low-cost, easy to make, bases on a facile scalable manufacturing, can have any shape or size and are made of recycling materials that are simple to get with a practically endless supply. The Physicochemical and structural properties of the DHS's were determinate using Scanning Electron Microscopy and Fourier transform infrared spectroscopy. The absorption capacity was evaluated before and after coating with varnish, noticing a clear improvement in the selectivity of absorption between water and oil. The ability of the sponges to separate the water from the oil have been evaluated by performing concentration tests once the mechanical removal of the oil in the water was carried out.



[BIO-577] Natural hydrophobic luffa sponge to remove oil from water and its restoration

Elizabeth Alvarado Gómez (elizabeth.alvarado@ipicyt.edu.mx) ¹, Jesús Iván Tapia ¹,
Armando Encinas ¹

¹ Instituto Potosino de Investigación Científica y Tecnológica, Camino a la Presa San José #2055, 78216, San Luis Potosí, S.L.P., México

Water contamination by oils is a complex and persistent trouble, since the emission sources can be different; such as crude oil spills or daily activities as fuels, pharmaceutical, alimentary products, etc. Furthermore, the environmental impact is important, since aquatic and terrestrial ecosystems are affected, including human health. There have been many researching efforts about oil / water separation [1]. Nevertheless most of the proposals result expensive, dangerous in the use of new technologies or produce more residues. In this work, we propose a natural luffa sponge, functionalized with stearic acid (natural fatty acid), in order to obtain a hydrophobic sponge capable to absorb selectively oil from water. Moreover, the process is designed to generate no waste in agreement with the circular economy principles.

The functionalization process was done by the simple immersion of clean cubes of luffa (2.5x2.5.x2.5 cm), in a solution of stearic acid (SA) at different concentrations with ethanol and dried at room temperature. The characterization was done by water contact angle, pore size distribution, SEM, EDS, FTIR, XRD. Oil absorption capacity (Q), recyclability, and separation test were evaluated by using motor, vegetal and burned oil. The concentration of motor oil remnants in water was calculated by UV-Vis. Finally an L-SA impregnated with motor oil, was completely washed with hot soapy water, during 20 minutes, and with fresh tap water to remove oil and SA; its weights were recorded.

Luffa has polyporous structure, and the functionalized Luffa sponge with SA (L-SA) had the maximum contact angle ($133 \pm 4.03^\circ$) with 2 % of SA, which indicates that L-SA is hydrophobic. The physic-chemical characterization, reveals that luffa was covered by SA, without chemical changes in the original materials. The absorption capacity (Q) of L-SA increases with time increment, until 4 min, with a Q value of 12.6 ± 3.2 , 15.6 ± 1.7 and 14.5 ± 1.7 g/g for motor, vegetal and burned oil respectively. L-SA could be used to absorb oil as far as 12 times. It can remove more than 99 % of oil, since the concentration of oil remnants in water was 48.5 ± 9.7 mg/L from the initial 62,500 mg/L. A cube of L-SA impregnated with oil was restored to a normal luffa sponge by a simple cleaning method.

REFERENCE

- [1] B. Doshi, M. Sillanpää, and S. Kalliola, "A review of bio-based materials for oil spill treatment," *Water Research*, vol. 135, pp. 262-277, 2018.



XII -ICSMV

September 23rd to 27th, 2019 / San Luis Potosí, México

[BIO-609] Compounds of PCL-CeO₂ as an alternative to antibiotics.

Idahli Alejandra Meléndez-Estrada (al133887@alumnos.uacj.mx)¹, Pamela Nair Silva Holguin¹, Antonio Muñoz-Escobar¹, Juan Carlos Cuevas-González¹, Alejandro Donohué-Cornejo¹, León Francisco Espinosa-Cristóbal¹, Simón Yobanny Simón Yobanny (yobannyr@yahoo.com.mx)¹

¹ Universidad Autónoma de Ciudad Juárez

Currently, bacterial resistance is a problem worldwide. Bacteria have developed the ability to survive stress conditions with various mechanisms against drugs causing infections with higher morbidity, mortality and generating high costs for their treatment. This has elicited an interest in the application of alternative antimicrobial agents, metal oxide ions being an attractive target. The objective of this work is to elaborate a polymer-ceramic composite from poly-epsilon-caprolactone with ceria nanoparticles in the form of a membrane that maintains stable the release of ceria nanoparticles, propitiating a bactericidal character for the biomedical application in the coating of Cutaneous wounds and thus avoid infection caused by pathogenic bacteria.



XII -ICSMV

September 23rd to 27th, 2019 / San Luis Potosí, México

[BIO-615] Polymeric structures incorporated with iron and silver nanoparticles

Martha Eugenia Compeán Jasso², Martha Eugenia Compeán Jasso

(martha.compean@gmail.com)¹, Armando Encinas Oropesa², Idania De Alba Montero

¹, Nereyda Niño Martínez¹, Facundo Ruiz¹

¹ Facultad de Ciencias de la Universidad Autónoma de San Luis Potosí

² Instituto Potosino de Investigación Científica y Tecnológica, A.C.

Actually, the biocompatible and no toxic polymers are an option to obtain structures with potential applications in pro of the nature, considering that when they are mixed with additives their properties change or are added increasing their specific propose of world interest as in biomedical or waste water treatment areas. Silver nanoparticles are studied by their antibacterial properties, and the magnetic properties are characteristics of the iron oxide species. Membranes and nanofibers are structures than potentiate the relationship between area and volume. Homogeneous nanofibers of polyvinyl alcohol incorporated with iron and silver nanoparticles were obtained with electrospinning technique, as well as membranes of chitosan and polyvinyl alcohol. These polymers have affinity to the silver and iron species, they are not toxic, biocompatible and have functional groups. To obtain the structural properties, size distribution, morphology and composition, the polymeric structures were characterized by X-ray diffraction, dynamic light scattering, scanning electron microscopy, and energy dispersive X-Ray spectroscopy. The microbial activity was analyzed to obtain the antibacterial properties.



[BIO-630] Characterization of PLA/TiO₂ scaffold via air jet spinning

Margarita Linares (*ortodoncia.linares@gmail.com*) ¹, Carlos Alvarez ², Marco Antonio Alvarez ⁴, Amaury de Jesús Pozos ¹, Vicente Garibay ³

¹ *DICIM. UASLP. SierraLeona No. 550 Col. Lomas 2da. Sección, Planta Baja. C.P. 78210. San Luis Potosí*

² *Dental Materials Laboratory. UNAM. Investigación Científica 1853, C.U., 04360 Ciudad de México*

³ *Instituto Mexicano del Petróleo. Eje Central Lázaro Cárdenas No152 Col. San Bartolo Atepehuacan; 07730,Ciudad de México.*

⁴ *Tissue Engineering Laboratory. UNAM. Investigación Científica 1853, C.U., 04360 Ciudad de México*

The objective of this present study was to produce poly(lactic) acid (PLA) scaffolds / TiO₂ of different concentration, using technique air jet spinning. Structural, chemical, mechanical and biological characterizations were performed.

Introduction.

Biodegradable polymers have been recognized as alternative materials for tissue engineering applications, due to their ability to degrade through simple hydrolysis to products which can be accomplished through enzymatic activities in human body. We synthesized a scaffold with PLA (7% and 10%) and titanium dioxide (0.1% and 0.3%) to observe the mechanical, physical-chemical and biological properties and the effect in a cell line of human macrophages (U937 / A).

Results

The TiO₂ nano has no significant influence on the characteristic spectroscopy (IR and Raman), but has high impact on the elastic module of these systems. The degree of elasticity was significantly increases for PLA (10%) nanocomposites loaded with 0.1 and 0.3 % TiO₂, while the fiber size was analyzed by SEM, increased in the same way with the increase in the concentration of PLA (10%) and TiO₂ (0.1 and 0.3%). The degradation of the prepared composites was evaluated in PBS solution measure the pH. We found significant differences in the physicochemical and mechanical characterization of the scaffolds with different concentrations of PLA and TiO₂, as well as in the response to the macrophage cell line.

Conclusion

The concentration of PLA and TiO₂, directly modify the mechanical properties of the scaffold as well as the biological response.

References

1. Buzarovska, A., Gualandi, C., Parrilli, A., & Scandola, M. (2015). Effect of TiO₂ nanoparticle loading on Poly(L-lactic acid) porous scaffolds fabricated by TIPS. *Composites Part B: Engineering*, 81, 189-195. <https://doi.org/10.1016/j.compositesb.2015.07.016>
2. Hutmacher DW, Sittiger M, Risbud MV. Scaffold-based tissue engineering: rationale for computer-aided design and solid free-form fabrication systems. *Trends Biotechnology*. 2004;22:354–362. doi: 10.1016/j.tibtech.2004.05.005
3. Guntillake PA, Adhikari R. Biodegradable synthetic polymers for tissue engineering. *Eur Cell Mater*. 2003;5:1–16. doi: 10.22203/eCM.v005a01



[BIO-636] Nanotechnologies for neurodegenerative disorders: Targeted sgp130Fc functionalized MWCTNs (sgp130Fc-MWCNTs-T*) for the treatment of psychopathologies associated with inflammatory response triggered by sIL-R6/IL-6 complex.

*Lorena Gárate-Vélez², Marco Atzori³, Mildred Quintana-Ruiz
(quintanamildred@gmail.com)¹*

¹ *Centro de Investigación en Ciencias de la Salud y Biomedicina, Universidad Autónoma de san Luis Potosí, Av, Sierra Leona 550, Lomas de San Luis, 78210 San Luis, S.L.P.*

² *Doctorado Institucional en Ciencia e Ingeniería de materiales, Universidad Autónoma de San Luis Potosí, Sierra Leona #550, Lomas de San Luis, 78210 San Luis, S.L.P.*

³ *Facultad de Ciencias, Universidad Autónoma de San Luis Potosí, Av. Parque Chapultepec 1570, 78210 San Luis, S.L.P.*

Neurodegenerative disorders have been put in relation to increased inflammation of proinflammatory cytokines such as interleukin-6 (IL-6) by a trans signaling route whom the sIL-6R / IL-6 complex is involved in the pathogenesis of chronic inflammatory diseases, and it has been associated with different psychopathologies. One example is post-traumatic stress disorder (PTSD) caused by potentially disturbing events beyond a typical stressor. Evidence suggests that inflammatory reactions, as well as sleep disturbances present in PTSD may increase the risk of suffering from some type of dementia. In the search for treatments to neutralize the sIL-6R / IL-6 complex, have been developing a sgp130Fc chimeric protein with a fusion protein of the extracellular part of sgp130 and the constant Fc portion of the human IgG1 antibody, and it has greater affinity for the sIL-6R / IL-6 complex of trans signaling, selectively inhibiting it. Unfortunately, this protein is not able to cross the blood-brain barrier (BBB) so that, it could be modified to facilitate its entry into the SNC. In this direction, the use of CNTs as a mechanism of administration for the treatment of CNS pathology is based on its structural characteristics, especially its improved solubility in physiological solvents due to its functionalization, large surface area, easy modification capacity with drug molecules for obtaining the desired cellular response, biocompatibility with neural system and its penetration through the plasma membrane. The aim of this project is to synthesize and characterize MWCNTs conjugated with the chimeric protein sgp130Fc (sgp130Fc-MWCNTs) for the treatment of neurodegenerative diseases. The sgp130Fc-MWCNTs nanohybrids might inhibit the action of proinflammatory cytokines in biological models *in vitro* and *in vivo*, by crossing the BBB is favoring the future clinical application of sgp130Fc-MWCNTs as an active therapeutic for neurodegenerative diseases in the CNS. In addition, the high surface area of MWCNTs allows the further functionalization of sgp130Fc-MWCNTs with specific targeting ligands increasing their therapeutic efficiency.



XII -ICSMV

September 23rd to 27th, 2019 / San Luis Potosí, México

[BIO-667] Influence of pH on the synthesis of silver nanoparticles using fructose as a reducing agent

Daniela Alvarez Sánchez (dani.06_14@hotmail.com) ¹

¹ Blvd. Gral. Marcelino García Barragán #1421. Guadalajara, Jalisco

Se estima que las nanopartículas de plata (AgNP) son las que tienen el mayor nivel de comercialización de todos los nanomateriales utilizados en productos de consumo, esto se debe a que son útiles en diferentes áreas, como ropa, pinturas, cosméticos, electrónica, bactericidas, biofungicidas, Aplicaciones biomédicas, en la industria médica-farmacéutica y alimentaria. Las nanopartículas emergen a través de la capacidad de manipular la materia, por lo que estamos buscando métodos económicos y simples para la síntesis de nanopartículas con diferentes tamaños y formas. Los métodos que nos permiten sintetizar nanopartículas de manera simple y económica son en medio acuoso.

La espectrofotometría ultravioleta visible (UV-vis), la microscopía electrónica de barrido (SEM), la microscopía electrónica de transmisión (TEM) y la dispersión dinámica de luz (DLS) son métodos que nos permiten caracterizar las propiedades fisicoquímicas de las nanopartículas de plata.

Este trabajo estudia la influencia del pH en las nanopartículas de plata, los azúcares reductores tienen un carbono libre en su estructura y pueden reducir en ciertas condiciones a sales metálicas, el método de síntesis se llevará a cabo por "de abajo hacia arriba".



XII -ICSMV

September 23rd to 27th, 2019 / San Luis Potosí, México

CHARACTERIZATION AND METROLOGY (CHM)

Chairman: Roberto Machorro (CNYN-UNAM)



XII -ICSMV

September 23rd to 27th, 2019 / San Luis Potosí, México

CHARACTERIZATION AND METROLOGY (CHM) ORAL SESSIONS



[CHM-76] USE OF ALUMINUM ALLOY SERIES 6XXX-T6, TO RETARD THE CORROSION SPEED IN RECEIVER DRYER BOTTLE OF HEAT EXCHANGERS FOR THE AUTOMOTIVE INDUSTRY

ENRIQUE GALARZA GALARZA (enrique.galarza@valeo.com)², LUIS SANTIAGO ORTIZ MONRROY², EDGAR DE JESUS VEGA VALDES², ITZEL ESTEFANIA GALINDO IDROGO (itzel.galindo@valeo.com)², ALBERTO TORRES CASTILLO¹

¹ UNIVERSIDAD AUTONOMA DE SAN LUIS POTOSI

² VALEO ENGINE COOLING

Valeo design a new heat exchanger for the automotive industry, during the development of this product (Design Validation), it was selected a 6XXX alloy series with a T5 Heat treatment for extruded bottle for receiver dryer. During SWAAT (Sea Water Acetic Acid Test) Validation, it's detected a premature failure in this component, during failure analysis it's observed an intergranular corrosion failure mode in several points of receiver dryer bottle promoting a leak in the heat exchanger. According with the analysis done, it's proposed a change of alloy with different chemical composition with a T6 heat treatment, it's develop a new comparative corrosion study speed between these components detecting that corrosion resistance was improved considerably. The present work describes the comparative analysis of these bottles and the improvement in corrosion resistance after changing receiver dryer bottle from 6XXX-T5 to 6XXX-T6 and the impact to retard failures by intergranular corrosion, this results was confirmed during PACT (Polarized accelerate corrosion) tests, showing and improvement in corrosion resistance during SWAAT test up to 5 times in heat exchanger receiver dryer bottle.



[CHM-85] CARBON SPHERES RANDOM GROWTH DIAMETER ANALYSIS BY COMPUTATIONAL MODELING

José de Jesús Contreras-Navarrete¹, Carmen Judith Gutiérrez-García², Jaime Abraham Guzmán-Fuentes², Jael Madaí Ambriz-Torres², Diana Litzajaya García-Ruiz², Francisco Gabriel Granados-Martínez³, Ezequiel Huipe-Nava², María de Lourdes Mondragon-Sánchez¹, Lada Domratcheva-Lvova (ladamex@yahoo.es)²

¹ Instituto Tecnológico de Morelia, Morelia, Mich. México

² Universidad Michoacana de San Nicolás de Hidalgo, Av. Francisco J. Mújica S/N, Morelia, Mich., México, 58030, México.

³ Universidad Nacional Autónoma de México, ENES, Campus Morelia, 58190 Morelia, Mich.

One of the most useful nanomaterials obtained from a carbon source are the spheres. This carbon allotropic form has been used in several applications due to outstanding electrical, mechanical and chemical properties. Carbon spheres growth diameter presents a randomness pattern avoiding spheres sizes standardization. Monte Carlo simulation could be used to analyze the randomness and evaluate the experiment results. In the present research carbon spheres were synthetized by Chemical Vapor Deposition (CVD) technique using four aromatic carbon precursors (anthracene, benzene, naphthalene and pyrene) as carbon source and a stainless-steel bar as catalyst. The temperatures synthesis was 850 °C and reaction time 45 minutes. Once the carbon spheres synthesis was concluded, Scanning Electron Microscopy (SEM) was applied to measure the shape. ImageJ software were used to evaluate spheres diameter. The experimental conditions were set up to be analyzed by Monte Carlo computer simulation using ImageJ data (341-1591 nm) and synthesis settings. Statistical parameters like: diameter average, standard deviation, kurtosis and skewness coefficient the carbon spheres were acquired considering 1000, 5000, 15000 and 20000 trials for each carbon source. Carbon spheres diameters presented values around 340 to 1560 nm in Monte Carlo Simulation. The skewness coefficient for each: anthracene, benzene, naphthalene and pyrene were 0.0027, -1.1912, 1.2011, -1.1961 respectively. Kurtosis values present different values indicating that carbon spheres diameter follows a random and non-standardized behavior. Monte Carlo simulation allowed identify statistical parameters in several trials providing confinable results minimizing sources and costs. Acknowledgment to CIC of Universidad Michoacana de San Nicolás de Hidalgo and CONACYT Mexico for the financial support.



[CHM-105] Thermal lens spectroscopy. A theoretical and experimental study of low optical absorption models for very small thermal lens signal relative change.

Michel Alonso Isidro Ojeda (michel.isidro15@gmail.com)¹, Ernesto Marín Moares¹

¹ Instituto Politécnico Nacional, Centro de Investigación en Ciencia Aplicada y Tecnología Avanzada, Unidad Legaria, Legaria 694, col. Irrigación, Mexico City 11500, Mexico

Thermal lens spectroscopy (TLS) is a powerful photothermal technique. Due to its high sensibility it has been used in many areas of research, showing a time evolution in both the development of associated theoretical models and of the experimental set-up. In this technique, a refractive index periodical change is produced by the absorption of intensity modulated laser beam (called a pump), which affects the intensity of another laser beam (the probe) passing through the same heated region of the sample. The intensity changes are measured by a photodetector and are named the thermal lens signal.

If all the pump beam energy absorbed by the sample is transformed into heat (e.g. neglecting radiative effects such as fluorescence), the relative change of the thermal lens signal is given by:

where P_e is the excitation beam power, dn/dT is the absolute value of the photothermal parameter or the temperature (T) coefficient of the refractive index (n), λ_p is the probe beam wavelength, α is the optical absorption coefficient, k is the thermal conductivity and L is the optical path length of the sample. The time dependence of the thermal lens signal is a complex function that depends on ϑ , on the thermal diffusivity of the sample and on optical geometrical parameters of the pump and probe beams such as Rayleigh parameters and waist positions relative to the sample.

Usually, low optical absorption models are used that simplify the expression of the thermal lens signal, making data processing procedures simpler and fast. In this work, we analyze the predictions of the most important low absorption models for very small values of ϑ , i.e. when $\vartheta \ll 1$, for a sample that only shows optical and thermal activity (i.e. neglecting effects such as light scattering, mass diffusion, fluorescence, etc). These results are compared with those of computational simulations using the Finite Elements Method and with those of measurements performed in a pure water sample. Finally, we discuss some issues that must be considered experimentally to guarantee the fulfillment of the conditions imposed by the theoretical model.



XII -ICSMV

September 23rd to 27th, 2019 / San Luis Potosí, México



[CHM-108] Effect of the microstructure on impact toughness in HSLA steel joints welded by laser beam process

Miguel Ágel Hernández Méndez (miguel.hdz@alumnos-comimsa.mx)¹, Melvyn Álvarez Vera (melvyn.alvarez@comimsa.com)¹, Rita Muñoz Arroyo¹

¹ Corporación Mexicana de Investigación en Materiales

The influence of the microstructure during the solidification in the joints welded with the laser beam process in HSLA-80 steel was studied. The microstructures will be related to the different heat inputs by varying the powers in each sample during welding. The impact toughness results were affected by the microstructure on the fusion zone (FZ) and the heat affected zone (HAZ) due to welding process. Also was analyzed the influence of temperature on the impact toughness of the present microstructures. The microstructural analysis was performed by optical microscopy (MP) and scanning electron microscopy (SEM) to analyze the phases present and to observe the type of failure of the Charpy test results.



[CHM-140] Effect of the heat input in microalloyed steel welded by laser-GMAW hybrid welding

Ana Patricia SoriaBotello (ana.soria@alumnos-comimsa.mx)¹, Melvyn Alvarez Vera (melvyn.alvarez@comimsa.com)¹

¹ Corporación Mexicana de Investigación en Materiales SA de CV

The microstructure of a base metal processed by welding causes important changes that affect the mechanical properties of the joint. The aim of this work is to determinate the microstructure obtained in a micro alloyed steel joined by a hybrid laser arc welding process according with different heat inputs. The specimens microstructure were characterized by scanning electron microscopy (SEM) and their mechanical properties were evaluated by Vickers Hardness test and tension testing. The microstructure in the fusion zone area was acicular ferrite while in heat affected zone a mixture of plate and lath martensite were identified. The mechanical properties of the weld and their relationship with the microstructure are discussed.



XII -ICSMV

September 23rd to 27th, 2019 / San Luis Potosí, México



[CHM-184] Microstructural characterization of zinc-coated steel and aluminum AA7075 dissimilar lap joint welded by GTAW.

Jorge Antonio Rodríguez-Chávez (jorge.rdz@comimsa.com)³, Rocio Saldaña-Garcés (rocio.saldana@comimsa.com)¹, Rocio Saldaña-Garcés³, Gladys Yerania Pérez-Medina³, Felipe de Jesús García-Vázquez⁴, Emmanuel José Gutiérrez-Castañeda², Rubén García-Jacobo³

¹ Catedrática CONACYT-Corporación Mexicana de Investigación en Materiales (COMIMSA),
Saltillo 25290, Coahuila, México

² Catedrático CONACYT-Instituto de Metalurgia de la Universidad Autónoma de San Luis Potosí (UASLP), San Luis Potosí 78210, San Luis Potosí, México

³ Corporación Mexicana de Investigación en Materiales (COMIMSA), Saltillo 25290, Coahuila, México

⁴ Facultad de Ingeniería, Universidad Autónoma de Coahuila (UAdeC), Arteaga 25354, Coahuila, México

Dissimilar lap joining was made between zinc coated steel and aluminum alloy (AA7075) with thicknesses of 1.2 mm and 6.35 mm by gas tungsten arc welding (GTAW) with two types of filler metals (AA4043 and AA5356). The microstructural analysis and distribution of elements in the joint were carried out by means of scanning optical microscopy (SEM) and X-ray energy dispersion spectrometry (EDS). The increase in the current had a direct effect on the thickness of the intermetallic interface (IMA), which showed a variation of Al-Fe compounds. The increase in thickness resulted in a decrease in tensile strength.



[CHM-269] Development of Dual-Phase Steels by Austenitization, and Intercritical Heat Treatment Processes

Luis Alberto Mendoza-delaRosa (lamendozar@gan.com.mx)¹, Alberto Ignacio Perea Garduño¹, Rubén Menchaca Jiménez¹, Luis Antonio Silva Guajardo²

¹ *Investigación y Desarrollo, Altos Hornos de México S. A. B. de C. V., Prolongacion Juárez S/N, Las Lomas, Monclova, Coahuila*

² *Vinculación y Gestión Tecnológica, Altos Hornos de México S. A. B. de C.V., Prolongacion Juárez S/N, Las Lomas, Monclova, Coahuila*

Based on the analysis of the needs and realities of the steel industry, and given that in the northern region of the country, specifically in Coahuila, the steel industry is one of the main promoters of economic development, Altos Hornos de México, S. A. B. de C. V. (AHMSA), has taken the initiative towards the development of advanced steels, mainly for obtaining Dual Phase steels; which represent the largest amount of demand for the production of automotive steel, because of this type of metallic material has greater tensile strength and good formability qualities. This work focuses on the development of advanced Dual Phase steels at laboratory scale, so that initially the analysis of the chemical compositions of all steel types produced in the company, was carried out in order to determine the feasibility of obtaining them by comparing the behavior of the TTT and CCT curves of all grades currently produced by the company, these curves were obtained by simulating the chemical properties using the JMatPro V10 software. Later, the grade with greater feasibility was selected, which was obtained by hot rolling in a Steckel Mill; then the Production Department and the Central Laboratory were asked to section a fragment of the plate of this grade into smaller sections with dimensions of 2.5x6x100 mm. Once the samples were obtained, an experimental design was carried out so that later the samples received a heat treatment of austenitization at higher temperatures of Ac_3 ; later it received isothermal treatment by means of molten salts $NaCl/BaCl_2$ in a stoichiometric ratio, which formed a eutectic point in the biphasic range between Ac_3 and Ac_1 . Finally, the materials received an accelerated cooling to obtain the final microstructure. When analyzing the microstructure, the formation of the ferrite and martensite phases is observed, in addition to the bainite phase and a small portion of retained austenite. By characterizing their physical properties through uniaxial stress tests, ultimate tensile strength values above 1000 MPa and fracture elongation values of around 20% were obtained, so these steels are excellent candidates for diverse applications. Although it was obtained on a laboratory scale, it was successful, the real challenge will be industrial scale-up.

Keywords: advanced steels, Dual Phase steels, TTT and CCT curves.



[CHM-347] Tuning the work function and resistivity of transparent conducting sol-gel Cd₂SnO₄ electrode through annealing in an Ar/CdS atmosphere

Carolina Janani Diliegros-Godines (janani.diliegros@gmail.com)⁴, Rebeca Castanedo-Pérez², Gerardo Torres-Delgado², Osmany García-Zaldivar³, Francisco Javier Flores-Ruiz¹

¹ CONACYT-Instituto de Física, 4 Instituto de Física Benemérita Universidad Autónoma de Puebla, Apdo. Post. J-48, Puebla, Pue, 72570, Mexico

² Centro de Investigación y de Estudios Avanzados del Instituto Politécnico Nacional, Unidad Querétaro, A.P.1-798, Querétaro, Qro. 76230, México

³ Instituto de Física Benemérita Universidad Autónoma de Puebla, México-IMRE, Universidad Habana, Cuba

⁴ Tecnológico de Monterrey, School of Engineering and Science, Ave. Eugenio Garza Sada 2501, Monterrey, N.L., México

In multilayer solar cells, the charge flow from the low work function of transparent conductive oxide to the deep energy level of the metallic (top) electrode. A match in the energy levels between adjacent layers reduce the probability of Schottky barriers formation, which is essential for optimizing the efficiency of the photovoltaic cell. Here, sol-gel Cd₂SnO₄ (260 nm-thick) electrode films were sintered at 550°C, with a transmittance >90% and resistivity of ~2×10⁻². The films were annealed from 450°C to 650°C, with 50°C steps, in an Ar/CdS atmosphere in order to reduce the resistivity values and tuning the work function for their use in a solar cell with structure CTO/CdS/CdTe/top-contact. The cubic spinel Cd₂SnO₄ phase and high transmittance, were preserved during the Ar/CdS annealing treatment. Frequency modulation kelvin probe force microscopy was employed to measure simultaneously topography and the local contact potential difference (CPD). A calibration of the AFM-tip work function allowed determine the work function of the samples, which decrease from 4.74 to 4.52 eV as the annealing temperature increases. The resistivity shows a similar tendency of the work function, decreasing from ~2×10⁻³ to ~6×10⁻⁴ with the annealing temperature. Impedance measurements were carried out on the samples to evaluate the resistive stability at high frequencies, which will establish the frequency limits for determining the dynamic mechanisms of transport in solar cells.

Acknowledgements

The authors acknowledge CONACyT FOINS FC-2016-01-2488 for the financial support. C. J Diliegros-Godines thanks to Tecnológico de Monterrey Campus Puebla and the Strategic Research Group: Nanotechnology for Devices Design.



[CHM-348] Operation modes of Kelvin Probe Force Microscopy

*Francisco Javier Flores-Ruiz (fcojfloresr@gmail.com)*¹

¹ CONACYT-Instituto de Física, Benemérita Universidad Autónoma de Puebla, Apdo. Post. J-48, Puebla, Pue, 72570, Mexico

Kelvin Probe Force Microscopy (KPFM) is a non-destructive technique that allows scan the sample topography and simultaneously determine the local potential difference (LCPD) between the tip and a sample. The tip-sample system interacts electrically as a capacitor while the DC tip bias required to nullify the electrostatic force between them is recorded. The electrostatic force is generated between the tip and sample due to the difference in their Fermi levels. This work presents a comparative study between two operation modes of KPFM, amplitude modulation (AM) and frequency modulation (FM), both present in our AFM system. The samples used for this study were a KPFM standard sample and a transparent conductive oxide of Cd_2SnO_4 . We found, in agreement with other reports, that FM has higher spatial resolution than AM. However, FM requires to provide a higher AC bias to the AFM tip than AM, to provide the same LCPD resolution. This results was to be expected since AM aims to eliminate the electric force that requires a relatively low energy to be excited, while FM aims to remove the electrostatic force gradient; excitation of gradients requires more energy. In terms of applications, to study cross sections of solar cells, for example, FM will provide a high resolution to map the nanoscale potential distribution. In addition, it is less prone to certain imaging artifacts, such as crosstalk from topography or stray electric fields.

Acknowledgement

The author acknowledge to CONACyT FOINS FC-2016-01-2488 for the financial support.



[CHM-641] Artificial Vision System to identify and classify corn seeds

Hermenegildo Cisneros Carrillo (hermes.cisneros82@gmail.com)¹, Claudia Hernández

Aguilar (clauhaj@yahoo.com)¹, Flavio Arturo Domínguez Pacheco¹

¹ Instituto Politécnico Nacional, Sepi – Esime Zácatenco. Unidad professional Adolfo López Mateos, colonia Lindavista. Ciudad de Méxic, C.P. 07738, México

The objective of this research was to evaluate an image preprocessing method, an optimal features vector and the Support Vector Machines (SVM) to identify and classify varieties of corn seeds. Two varieties were used: hybrid H70 of crystalline type dyed of green color and crystalline creole of natural yellow color. five seeds of each variety were used for training (Fig. 2) and five for testing (Table 2).

The results indicated that it is possible to identify and classify maize varieties using an optimal feature vector and the SVM. The perimeter, the compactness, the kurtosis and the RGB colors space had a highest significant difference in relation to the elongation and the standard deviation to identify the varieties of corn seeds (Table 1).

In this way, the geometrical and color measurements were efficient to obtain a sufficiently robust vector to identify and classify maize seeds.

The authors thank the IPN through the support SIP, EDI, COFFA, etc. Hermenegildo Cisneros Carrillo thank for the support, for Doctorate studies, through the grant awarded by Conacyt.



XII -ICSMV

September 23rd to 27th, 2019 / San Luis Potosí, México

CHARACTERIZATION AND METROLOGY (CHM) POSTER SESSIONS



[CHM-19] Computational model for the estimation of porosity through images of microscopy of solid materials

Maria Raquel Ortiz-Alvarez (raquel.tyemelane@gmail.com)¹, Enrique Rocha-Rangel (erochar@upv.edu.mx)¹, Jose Amparo Rodríguez-García¹, Said Polanco-Martagón¹

¹ Universidad Politécnica de Victoria

In material science, porosity study of solid samples is of great importance, since it interacts within physical and chemical properties of such materials. For its study, different characterization techniques are used such as: optical microscopy, archimedes method, X-ray scattering, liquid intrusion, among others. However, these techniques depend to a large extent on the experience and underlying factors of researchers. Therefore, this work presents a computational method to estimate the amount of porosity from solid material samples, using optical microscopy images of study areas, which through digital image processing and machine learning techniques, results in the estimation of the average porosity of solid samples. Prior to obtaining images, the samples carried a metallographic preparation (progressive roughing from 80 caliber to the 1500 grit, followed by a polishing with diamond paste and ending with a chemical attack). The results obtained by means of the computational method and corresponding to a ceramic sample (CaAl_2O_4), give an estimate of 26.13% of porosity, while experimentally a 28.16% of porosity is registered. It can be seen that the difference between the proposed computational method and the experimental one is insignificant.



[CHM-30] CHARACTERIZATION POLYMER PURGES FOR OBTAINING PYROLYtic OIL

Alejandra Arias San Elías (ale.arias@mail.itq.edu.mx) ¹

¹ Instituto Tecnológico de Querétaro

The cleaning wastes of the injection process called purges were characterized, these are irregular masses can be combinations of polymers, colors or materials with a slight degradation, this makes it not possible to use them in the process again, it is suggested to use pyrolysis to obtain an oil with characteristics similar to diesel or kerosene.

The pyrolysis process requires that material to be processed is dry and particles are less than 5 cm, so that the reactions inside the reactor use the least fuel.

Three samples were analyzed, the 1st composed of 80% HDPE and 20% PP, the 2nd is 100% HDPE and the 3rd is the change between the previous ones. Different tests were carried out such as: hardness with Shore D, water absorption, moisture loss and RFDA (Resonant Frequency and Damping Analyzer), to see necessary energy required in crushing and drying time.

The results obtained show that the highest hardness is found in sample 3 with 64,367 Shore D and deviation of 1,159, water absorption is from sample 1, increasing its weight by 3.2%, with respect to loss of moisture they all need 3 hours to eliminate any residue, the RFDA indicates that when there is a PP the Young's modulus increases making the material less rigid, sample 1 had a reading of 0.111MPa with a deviation of 0.048 being the largest of the 3 cases analyzed



[CHM-39] DESIGN AND FABRICATION OF LOW EMISSIVITY OPTICAL FILTERS BASED ON COPPER.

Diego Germain Mejia Gonzalez (germain.mejia@uabc.edu.mx)³, Lorena Conchita Cruz Gabarain³, Noemi Abundiz Cisneros (nabundiz@cnyn.unam.mx)², Roberto Sangines de Castro², Juan Aguila Muñoz², Julio Cruz Cardenas¹, Roberto Machorro Mejia¹

¹ *Centro de Nanociencias y Nanotecnología, Universidad Nacional Autónoma de México, Km 107, Carr. Tijuana-Ensenada, Ensenada, B.C. C.P. 22800*

² *Cátedras CONACyT- Centro de Nanociencias y Nanotecnología, Universidad Nacional Autónoma de México, Km 107, Carr. Tijuana-Ensenada, Ensenada, B.C. C.P. 22800*

³ *Facultad de Ingeniería, Arquitectura y Diseño, Universidad Autónoma de Baja California, Carr. Transpeninsular Ensenada-Tijuana No. 3917, Col. Playitas, Ensenada, B.C. C.P. 22860*

One application of optical filters in the industry are the Low Emissivity (Low-E) filters on windows, usually based on metal thin layers. Thin films of metals like aluminum (Al), copper (Cu), silver (Ag) and gold (Au) exhibit visual transmission that gradually shifts to high infrared reflectance with longer wavelengths (infrared wavelengths longer than 700nm), this transparent metallic coating allows the visible light pass through a window, but blocks infrared-wavelength radiation. Low-E glass coatings can reflect up to 90 percent of the long-wave thermal energy, allowing much of the shorter-wave visible light to pass through [1]–[3].

Currently, most Low-E coatings are made of Ag that have the infrared properties, between two dielectric layers. However, Ag is expensive. Similarly, Au exhibits optimum reflectivity spectrum of heat reflecting coating, but its potential is greatly reduced by the high price. On the other hand, copper (Cu) and aluminium (Al) has a similar propertias than the Ag on the infrared radiation and low market price compared with the Ag and Au [4], [5].

In this work, Low-E optical filters based on multilayers structure have been designed and synthesized, using copper as an alternative material instead to silver. Thin copper layers were combined with Tin oxide (SnO_2) and titanium oxide (TiO_2) to fabricate $\text{TiO}_2/\text{Cu}/\text{TiO}_2$, $\text{SnO}_2/\text{Cu}/\text{TiO}_2$ and $\text{TiO}_2/\text{Cu}/\text{SnO}_2$ multilayers. Thin films were grown by magnetron sputtering technique and deposited onto BK7 glass, this process was monitored in real time by optical emission spectroscopy (OES) and ellipsometric-spectroscopy to obtain the optical properties of growing films. A comparison was made between the designed models and the experimental ones by means of spectrophotometry in the ultraviolet, visible and near infrared range. These measurements were made at different times and temperatures to see if there were changes in the films that affected their performance. $\text{TiO}_2/\text{Cu}/\text{TiO}_2$ structure exhibited the best optical properties experimentally with maximum transmission of 76% in the visible region (634 nm) and 40% in the near-infrared region (900 nm).

References:

- [1] S. Z. Wang y M. Guan, "Windows—the key of building energy efficiency", *Constr. Glas. Glas. Ind.*, vol. 4, pp. 3–8, 2005.



- [2] J. Mohelnikova, "Materials for reflective coatings of window glass applications", *Constr. Build. Mater.*, vol. 23, núm. 5, pp. 1993–1998, 2009.
- [3] A. Piegari y F. Flory, *Optical thin films and coatings: From materials to applications*. Woodhead Publishing, 2018.
- [4] G. K. Dalapati *et al.*, "Color tunable low cost transparent heat reflector using copper and titanium oxide for energy saving application", *Sci. Rep.*, vol. 6, p. 20182, 2016.
- [5] H. A. Macleod y H. A. Macleod, *Thin-film optical filters*. CRC press, 2010.



[CHM-57] Recycling of polymeric industrial materials, the technological challenge.

Ma. Guadalupe Plaza (guadalupe.plaza@live.com.mx)¹, María Luisa Mendoza López¹

¹ Programa Doctorado en Ingeniería, TecNM campus Querétaro, av. Tecnológico s/n col Centro, c.p. 76000 Querétaro, Qro.

The constant change in the environment has forced the entire world economy to develop technologies that allow the recycling of various post-consumer waste; However, industrial waste presents great challenges that have hampered the implementation of viable strategies. The present work focuses on the reincorporation of polymeric purges into industrial processes, as part of the circular economy. A large part of the problems for the recycling of purges derives from the irregular shape, size and mixture of materials, which can be of different composition or with additives. The characterization of three types of purges with a higher frequency index within the company dedicated to recycling was carried out, considering hardness and pyrolysis as part of the characterization. On the other hand, a thermal behavior test was carried out using two ways, heating in muffles and with a Fresnel-type solar concentrator. A temperature range of 230-280 ° C was determined for the softening of the material for the cutting process; It should be mentioned that the softening is not done until fluidity. The results show a minimum change in hardness for which the change of form was achieved without affecting the material.



[CHM-61] Synthesis of antireflective multilayer SiO₂/SnO₂/SiN_xO_y by DC reactive magnetron sputtering technique

Lorena Conchita Cruz Gabarain (*lorena.cruz@uabc.edu.mx*)³, Noemi Abundiz Cisneros²,
Diego G. Mejia Gonzalez³, Roberto Sangines de Castro², Roberto Machorro Mejia¹,
Juan Aguila², Julio Cruz Cardenas¹

¹ Centro de Nanociencias y Nanotecnología, Universidad Nacional Autónoma de México,
Km 107, Carr. Tijuana-Ensenada, Ensenada, B.C. C.P. 22860

² Cátedras CONACyT- Centro de Nanociencias y Nanotecnología, Universidad Nacional
Autónoma de México, Km 107, Carr. Tijuana-Ensenada, Ensenada, B.C. C.P. 22860

³ Facultad de Ingeniería, Arquitectura y Diseño, Universidad Autónoma de Baja California,
Carr. Transpeninsular Ensenada-Tijuana No. 3917, Col. Playitas, Ensenada, B.C. C.P. 22860

The use of cell phones, televisions, computers, lenses, building windows, which are made up of different components such as transistors, processors, coatings, etc., has a great impact on the daily life of man. The thin films coatings have different properties such as hardness, color, transparent layers or antireflective properties. The antireflective filters are usually used in eyeglasses, telescopes and solar cells to increase performance [4]. Currently, in the industry it is important to improve the performance of this kind of coatings. In this work, the design and synthesis of antireflective optical filter are presented using DC reactive magnetron sputtering technique [1]. The materials used are silicon dioxide (SiO₂), silicon oxynitride (SiN_xO_y) and tin oxide (SnO₂) synthesized on BK7 glass, obtaining a reflectance of 0.13% at 550 nm in the design [3]. The optical characterization of each layer was monitoring by in-situ ellipsometric analysis, plasma optical emission spectroscopy (OES) [2] and spectrophotometry (UV-Visible) in order to determine the optimal conditions of growth of the layers and its reproducibility. The final optical response of the synthesized filter was 99.4% of transmittance and 0.6% in reflectance at 550 nm.

Acknowledgments: This work was supported by the National Council of Science and Technology of Mexico, CONACyT (CB-2015-254494, PAPIIT-UNAM IT101017)

References:

- Depla, D., Mahieu, S., & Greene, J. E. (2010). Sputter deposition processes. En Handbook of Deposition Technologies for Films and Coatings (Third Edition) (pp. 253–296). Elsevier.
- Hernandez Utrera, O., Abundiz-Cisneros, N., Sanginés, R., Diliegros-Godines, C. J., & Machorro, R. (2018). Cleaning level of the target before deposition by reactive direct current magnetron sputtering. Thin Solid Films, 646, 98–104.
- Larouche, S., & Martinu, L. (2008). OpenFilters: open-source software for the design, optimization, and synthesis of optical filters. Applied Optics, 47(13), C219
- Macleod, H. A., & Macleod, H. A. (2010). Thin-film optical filters. CRC press.



[CHM-63] Novel Low-E filter for architectural glass pane with aluminum

Noemí Abundiz Cisneros (nabundiz@cnyn.unam.mx)¹, Roberto Sanginés De Castro¹, Ramon Rodriguez López², Miriam Peralta Arriola², Lorena Gabarain Cruz⁴, Diego Mejía Gonzalez⁴, Julio Cruz Cardenas³, Juan Aguila Muñoz¹, Roberto Machorro Mejía³

¹ CONACYT, Centro de Nanociencias y Nanotecnología, Universidad Nacional Autónoma de México. Apartado Postal 14, Ensenada, B.C., 22800, México

² Centro de Investigación Científica y de Educación Superior de Ensenada, Carretera Ensenada-Tijuana No. 3918, Zona Playitas, C.P. 22860, México

³ Centro de Nanociencias y Nanotecnología, Universidad Nacional Autónoma de México. Apartado Postal 14, Ensenada, B.C., 22800, México

⁴ Facultad de Ingeniería, Arquitectura y Diseño, Universidad Autónoma de Baja California, Carr. Transpeninsular Ensenada-Tijuana No. 3917, Col. Playitas, Ensenada, B.C. C.P. 22860

A good Low-Emissivity (Low-E) filter coated on glass reduces the amount of heat coming from solar light into the building, thus the expenses in electricity for air conditioning are reduced [1]. Standard Low-E filters contain a Silver layer between two dielectric thin films due to its high reflectance of infrared wavelengths; however, one of the major silver drawbacks are its chemical and mechanical weakness which reduces the filter mean lifetime. In this paper, we investigate alternative materials to be a substitution of Ag, and they were compared with commercial filters. It was found that an aluminum-based filter has a good cost-benefit performance with peak transmittance better than 80% in the visible, while having less than 20% transmittance for wavelengths longer than 1500 nm. A simulation of the filters construction was made providing a tolerance of each layer thickness, so the filter keeps its optical performance [2,3].

Acknowledgments

This work was supported by the National Council of Science and Technology of Mexico, CONACyT (Cátedras CONACyT, 1081; CB-2015-254494, PAPIIT-UNAM IT101017). J. Cruz acknowledges his postdoctoral fellowship from UNAM. R. Rodriguez-Lopez and M. Peralta-Arriola acknowledges their scholarship from CONACyT

References

- [1] M. Miyazaki and E. Ando, "Durability improvement of Ag-based Low-Emissivity coatings," Journal of Non-Crystalline Solids, vol. 178, pp. 245-249, 1994.
- [2] L. Martinu, "Plasma deposition of optical films and coatings: A review," Journal of Vacuum Science & Technology A, vol. 18, no. 6, p. 2619, 2000.
- [3] H. A. MacLeod, Thin-Film Optical Filters, 4 ed., CRC Press Taylor & Francis Group, 2010.



XII -ICSMV

September 23rd to 27th, 2019 / San Luis Potosí, México

[CHM-75] USE OF ALUMINUM ALLOY SERIES 4XXX (FOLDED TUBE) TO RETARD THE CORROSION SPEED IN HEAT EXCHANGERS FOR THE AUTOMOTIVE INDUSTRY

ENRIQUE GALARZA GALARZA (enrique.galarza@valeo.com)², LUIS SANTIAGO ORTIZ MONRROY (luis-santiago.ortiz@valeo.com)², EDGAR DE JESUS VEGA VALDES², ITZEL ESTEFANIA GALINDO IDROGO², ALBERTO TORRES¹

¹ UNIVERSIDAD AUTONOMA DE SAN LUIS POTOSI

² VALEO ENGINE COOLING

During a warranty claim on heat exchangers with extruded tube used in air conditioning, the client reports spikes of guarantees due to inter-granular corrosion. The Valeo R & D department, further analysis was perform to find a reduction to the corrosion on brazing process, proposing a change of technology from extruded tube to folded tube (4XXX Series alloy). Analysis on brazing Valeo Process confirm a phenomenon of atomic diffusion of the Si occurs in the alloy of the 4XXX series, this atomic diffusion forms a micro-structural layer of brown color. This brown layer retards inter-granular corrosion due to the corrosion takes a longitudinal direction to the tube and retards the speed in the transverse direction. The use of this band of brown color (silicon diffusion), minimizes failures by guaranteee in field. The present work presents a comparative PACT (Polarized accelerate corrosion) tests between heat exchangers manufactured with extruded tubes (Series XXX) vs folded tubes (4XXX series), confirming that investigation about brown band layer (presented in previous article) reduce the corrosion rate, describing the impact to retard failures by intergranular corrosion in heat exchangers, showing and improvement in corrosion resistance up to 7 times in heat exchangers with folded tube.



[CHM-84] PLASTIC SEPARATION WITH SIMILAR DENSITY FOR RECYCLING PROCESS, AN INDUSTRIAL CHALLENGE.

TERESA HERNANDEZ DE LA CRUZ (teresahdez17@gmail.com) ², MARÍA LUISA MENDOZA LÓPEZ ², J PÉREZ BUENO ¹

¹ *2Centro de Investigación y Desarrollo Tecnológico en Electroquímica, S.C., Parque Tecnológico Querétaro Sanfandila, Pedro Escobedo, Querétaro, C.P. 76703, México.*

² *Doctorado en Ingeniería, TecNM Campus Querétaro, Av. Tecnológico S/N, Col. Centro. Querétaro, Qro. C.P. 76000, México.*

Recycling is an effective and available way to diminish the negative impacts of plastic waste, the increase of these results in great environmental and social pressures, for which it represents one of the most dynamic areas in the plastics industry at present. Since plastic mixtures are difficult to recycle because of their intrinsic characteristics, the separation of mixed plastics is the key problem for recycling. The methods currently used are based on taking advantage of the physical and chemical properties of these plastics, procedures such as flotation focused on a specific feature such as polymer density, has given great and beneficial results. However some polymers such as: Acrylonitrile butadiene styrene (ABS), Polycarbonate (PC), Polypropylene, Polyethylene, Polybutylene terephthalate (PBT), Polyamide (PA) and Styrene, have a very similar density (0.90-1.20 gr/cm³), which represent a problem for separation.

This work studied polymers from a recycling company considering density as a similar property that makes it difficult to separate them. Pyrolysis, density and contact angle tests were performed with different solvents. The results show the possibility of using different liquids for separation of polymeric mixtures and allowed identified other separation process.



XII -ICSMV

September 23rd to 27th, 2019 / San Luis Potosí, México

[CHM-106] Microstructural characterization of dissimilar joints between steel and ductile iron by laser welding

Mario Alberto Alvarado Veloz (mario.alvarado@alumnos-comimsa.mx)¹, Melvyn Álvarez Vera (melvyn.alvarez@comimsa.com)¹, Héctor Manuel Hernández García¹

¹ COMIMSA

Laser welding process investigations are important to the manufacturing industry for better understanding of the physical, thermal properties and mechanical changes on the components to be joined specially in dissimilar welds. The aim of this study is the characterization of a butt weld joined by different laser power, between 20MnCr5 steel and ASTM A536 65-45-12 ductile iron with ER330 as filler metal and their effect on the microhardness in the present zones for the analysis of the mechanical properties of the weld joint. The techniques of optical microscopy, scanning electron microscopy (SEM) and X-Ray diffraction (XRD) were used to identify and analyze the microstructures and their changes for each laser welding power. The microstructural changes, microhardness profiles and thermal gradients present between steel and ductile iron are discussed.



[CHM-129] Thermal Lens to Determine the Thermal Diffusivity of Mezcal Cupreata

Jose Luis Jiménez-Pérez (jimenezp@fis.cinvestav.mx)², Genaro Gamboa-López³, Zormy Nacary Correa-Pacheco¹, Jose Luis Luna-Sánchez², Angel Netzahual-Lopantzi², Zulema Navarrete-Meza²

¹ CONACYT-Instituto Politécnico Nacional-Centro de Desarrollo de Productos Bióticos. Carretera Yautepec-Joxtla, Km. 6, calle CEPROBI No. 8, Col. San Isidro, Yautepec, Morelos, México CP 62730.

² UPIITA-Instituto Politécnico Nacional, Av. Instituto Politécnico Nacional No. 2580, Col. Barrio la Laguna Ticomán, Del. Gustavo A. Madero, Mexico

³ Universidad Politécnica del Valle de Toluca (UPVT) km 5.7 Carretera Almoloya de Juárez, Santiaguito Tlalcilalcali, C.P. 50904 Edo. México, México.

The thermal diffusivity of mezcal type Agave cupreata which is elaborated with exotic fruits, pomegranate, cranberry and pure mezcal was determined. These values of diffusivity were compared with the values obtained for pure mezcal agave. The photothermal technique used in this work to measure the thermal diffusivity was the time-resolved mode- mismatched dual-beam thermal lens technique, in which a temperature gradient is induced in the sample using non-radiative decay process followed of an optical excitation. An excitation laser and a probe laser were positioned in the mismatched mode to obtain high sensitivity of the thermal lens signal. The accuracy of the measurements was compared with literature values. The different type of mezcal were monitored at different wavelengths, using UV-vis spectroscopy to identify the maximum peaks corresponding to the absorption signal at 350 nm wavelength. Infrared spectra were subsequently used to determine the functional groups of the mezcal. As a result, this paper proposes a new, fast, low-cost, friendly and potentially new method to calculate the thermal diffusivity of mezcal with possible application in beverage industry.



[CHM-130] Study of Moringa Oleifera extract by thermal lens spectroscopy

Rigoberto Carbajal-Valdés⁴, José Luis Jiménez-Pérez (jimenezp@fis.cinvestav.mx)⁴,
Claudia Hernández-Aguilar³, José Luis Luna-Sánchez⁴, Alfredo Cruz-Orea¹, Zormy
Nacary Correa-Pacheco², Mario Pérez-González¹

¹ CINVESTAV, Av. Instituto Politécnico Nacional 2508, Col. San Pedro Zacatenco, Delegación Gustavo A. Madero, Mexico D.F. Código Postal 07360, Mexico

² CONACYT-CEPROBI, Instituto Politécnico Nacional, Carretera Yautepec-Joxtla, Km. 6, calle CEPROBI No. 8, Col. San Isidro, C.P. 62731, Yautepec, Morelos, Mexico

³ Instituto Politécnico Nacional, Sepi-Esime, Zacatenco, Unidad Profesional "Adolfo López Mateos". Col. Lindavista. México D.F., CP 07738, México

⁴ UPIITA-Instituto Politécnico Nacional, Avenida Instituto Politécnico Nacional No. 2580, Col. Barrio la Laguna Ticomán, Gustavo A. Madero, CP 07340, DF, Mexico

In this work, the method used to obtain Moringa oleifera extract and its characterization are presented. Moringa oleifera is a fast-growing softwood tree found in the Middle East areas, African and Asian countries. Recent studies have demonstrated that moringa has excellent oxidative stability, high antibacterial activity and healthful properties. Therefore, the use of analytical techniques are necessary to determine their characterization and composition for authentication purposes. Among the alternative techniques, photothermal techniques can be used to determine the thermal properties such as diffusivity, effusivity and thermal conductivity. In this work, the variation of the diffusivity of Moringa oleifera extract with the concentration was studied. Also, the Moringa oleifera leaf powders were characterized by the XPS technique and the aqueous extract was characterized by different techniques: UV-vis absorption spectroscopy, Fourier transform infrared transmission spectroscopy (FTIR) and thermal lens spectroscopy (TLS).



[CHM-138] On the sensitivity of the thermal lens technique and the use of a passive optical resonator to increase it.

Enrique Cedeño (enriqueced_b@hotmail.com)², Michel Isidro-Ojeda², Ernesto Marin (emarin63@yahoo.es)², Antonio Manoel Mansanares¹

¹ Gleb Wataghin Physics Institute, U. of Campinas-UNICAMP, 13083-859, Campinas, SP, Brazil

² Instituto Politécnico Nacional, Centro de Investigación en Ciencia Aplicada y Tecnología Avanzada, Unidad Legaria, Legaria 694, col. Irrigación, Mexico City 11500, Mexico

In the thermal lens technique, a refractive index periodical change is produced by the absorption of an intensity modulated laser beam (called a pump), which affects the intensity of another laser beam (the probe) passing through the same heated region of the sample. The intensity changes are measured by a photodetector and are named the thermal lens signal. Assuming that all the pump beam energy absorbed by the sample is transformed into heat (e.g. neglecting radiative effects such as fluorescence), the relative change of the thermal lens signal is given by:

(1)

where P_e is the excitation beam power, α is the absolute value of the photothermal parameter or temperature (T) coefficient of the refractive index(), λ_p is the probe beam wave-length, a is the optical absorption coefficient at the pump wave-length, k is the thermal conductivity, L is the optical path length of the sample. The parameter E is called the enhancement factor. The quotient:

. (2)

is a sample's constant parameter that can be consider as a figure of merit determining the sensitivity of the method. Several people chose a sample with a high photothermal parameter to increase the enhancement factor but forgot to consider the effects of the thermal conductivity value. Comparing some often-used solvents, here we will show that the figure of merit has the largest value for that with a lowest thermal conductivity (Carbon Tetrachloride) but, the solvent with the highest photothermal parameter (Benzene) is not that with the highest figure of merit. Therefore, Eq. (2) doesn't imply that the highest figure of merit can be achieved for a sample with the highest photothermal parameter and the lowest thermal conductivity. On the other hand, the figure of merit for water is at least 20 times lower than that of the other solvents analyzed here. Water is the most universal solvent, and there are experiments in which it is not possible to substitute water by a solvent with a higher F , for example in applications related to the determination of traces of contaminants in this substance. Therefore, it is important to find variants to increase the enhancement factor. One obvious way to do that is increasing the power of the excitation beam. But this variant has some disadvantages, for example convective and non-linear effects can be produced at high laser energies and the boundary conditions imposed by the theoretical models (often low absorption theories) used for data analysis cannot be well fulfilled. Adding to water some amounts of higher F substances such as ethanol is another often used method to improve the enhancement factor, as well as changing the sample temperature. But these artifacts can cause secondary effects such as non-desirable chemical reactions. Recently, a method has been proposed [1, 2] that avoids these limitations. It consists in enclose the sample's cell within a passive optical



XII -ICSMV

September 23rd to 27th, 2019 / San Luis Potosí, México

resonator so that the effective path length is increased due to the multiple reflections within the optical cavity that experiences the probe beam before reaching the detector. This approach is discussed in the present work. The cavity induced amplification factor will be determined for different reflections orders and compared with the theoretical awaited value. Advantages and disadvantages of using higher than two reflections orders will be analyzed too.

[1] H Cabrera et al Laser Physics Letters 13 (2016) 055702.

[2] E. Cedeño et al Talanta 1702 (2017) 260.



[CHM-268] Development of Dual-Phase Steels by Austenitization, and Intercritical Heat Treatment Processes

Luis Alberto Mendoza-delaRosa (lamendozar@gan.com.mx)¹, Alberto Ignacio Perea Garduño¹, Rubén Menchaca Jiménez¹, Luis Antonio Silva Guajardo²

¹ *Investigación y Desarrollo, Altos Hornos de México S. A. B. de C. V., Prolongacion Juárez S/N, Las Lomas, Monclova, Coahuila*

² *Vinculación y Gestión Tecnológica, Altos Hornos de México S. A. B. de C. V., Prolongacion Juárez S/N, Las Lomas, Monclova, Coahuila*

In recent decades in Mexico, the research in advanced materials have had very significant development, especially in the area of ceramics and polymers; however, in the area of metals, specifically in steel, some difficulties have arisen, because the research efforts were directed towards the demands of the steel industry for the production of steel with typical commercial qualities as structural applications, given that they were aimed at meeting these needs. However, in other parts of the world, the realities were different, mainly in the United States, China, and India. In recent times, the industry in Mexico has undergone a paradigm shift, because, with the opening of the markets, the economy has grown by increasing investment in various areas of production: as in the automotive industry, in the pipes production industry for the petrochemical, up to the production of the steel structure for wind towers. So, the growth in the need for steel production that satisfies these markets is evident, and since Mexico does not currently have the capacity to meet these needs, the import increase of advanced steel was required, leaving the production of steel at a disadvantage, because of the production systems are not designed for the production of these steels, and it requires a large amount of investment in technologies for the production of advanced steels. Another problem is the competitiveness of international prices, given that the protectionist strategies of other countries such as The United States and China have caused severe damage to the national and the international market for the national steel industry.

Based on the analysis of the needs and realities of the steel industry, and given that in the northern region of the country, specifically in Coahuila, the steel industry is one of the main promoters of economic development, Altos Hornos de México, S. A. B. de C. V. (AHMSA), has taken the initiative towards the development of advanced steels, mainly for obtaining Dual Phase steels; which represent the largest amount of demand for the production of automotive steel, because of this type of metallic material has greater tensile strength and good formability qualities. This work focuses on the development of advanced Dual Phase steels at laboratory scale, so that initially the analysis of the chemical compositions of all steel types produced in the company, was carried out in order to determine the feasibility of obtaining them by comparing the behavior of the TTT and CCT curves of all grades currently produced by the company, these curves were obtained by simulating the chemical properties using the JMatPro V10 software. Later, the grade with greater feasibility was selected, which was obtained by hot rolling in a Steckel Mill; then the Production Department and the Central Laboratory were asked to section a fragment of the plate of this grade into smaller sections with dimensions of 2.5x6x100 mm. Once the samples were obtained, an experimental design was carried out so that later the samples received a heat treatment of austenitization at higher temperatures of Ac_3 ; later it received isothermal treatment by means of molten salts $NaCl/BaCl_2$ in a stoichiometric ratio, which formed a eutectic point in the biphasic range between Ac_3 and Ac_1 . Finally, the materials received an accelerated cooling to obtain the final microstructure. When analyzing the microstructure, the formation of the ferrite and martensite phases is observed, in addition to the bainite phase and a small portion of retained austenite. By characterizing their



XII -ICSMV

September 23rd to 27th, 2019 / San Luis Potosí, México

physical properties through uniaxial stress tests, ultimate tensile strength values above 1000 MPa and fracture elongation values of around 20% were obtained, so these steels are excellent candidates for diverse applications. Although it was obtained on a laboratory scale, it was successful, the real challenge will be industrial scale-up.

Keywords: advanced steels, Dual Phase steels, TTT and CCT curves.



[CHM-274] Calibration process of sputtering growth thin film filters controlled by optical emission spectroscopy

Ramón Rodriguez⁴, Roberto Sanginés de Castro², Noemi Abundiz Cisneros², Amaidaly García Cabrera³, Julio Cruz Cárdenas¹, Juan Aguilera Muñoz², Roberto Machorro Mejía
(roberto@cnyn.unam.mx)¹

¹ CNyN UNAM, Km. 107 Carretera Tijuana-Ensenada, BC

² CONACyT, Cátedra adscrita al CNyN UNAM, Km. 107 Carretera Tijuana-Ensenada, BC

³ Licenciatura en Nanotecnología, Universidad Tecnológica de Querétaro

⁴ Maestría en Nanociencias, CICESE, Km. 107 Carretera Tijuana-Ensenada, BC

There are several plasma assisted deposition techniques, but only pulsed laser deposition (PLD) uses optical emission spectroscopy (OES) to analyze the plasma optical spectra on a regular basis. Studying the plasma properties is also a very important tool in astrophysics, and many tricks have been transported to PLD with great success. In this paper we use OES to monitor and control sputtering deposition, assuming two hypothesis: at the same plasma configuration we will get same (similar) thin films; Second, once we get the calibration of the physical properties of the films relative to lines spectra conditions, we will be able to reproduce the properties at any time. Furthermore, we can vary the plasma conditions, for example, changing the reactive gas flux continuously to obtain any desired physical property profile.

Our goal is to grow inhomogeneous optical thin film multilayers, that is, instead of high and low refractive index multilayer, with discrete optical properties, we deposit films with refractive index changing smoothly along the growing direction. For this purpose, a careful calibration of the refractive index as a function of reactive Oxygen high purity gas flux is required. The procedure is similar to a hysteresis curve described by Berg (Ref. [1, 2]), but measuring the optical spectra via OES as well as voltage, the optical properties of the film is measured with a spectral ellipsometer. With a silicon target and a silicon wafer substrate, we bring the chamber to torr then, closing the valve, we reach torr including a 20 sccm Argon and 10 sccm Nitrogen flux. Prior to the real deposition, we perform a cleaning process, to remove any poisoning on the target surface, we monitor this step with OES (Ref. [3]). The Oxygen is introduced by 0.05 sccm steps, at each stage we grow a film for 3 minutes. Real-time acquisition of the ellipsometric parameters of the film are recorded every second, and a model to the substrate-film is fitted to data to obtain thickness, deposition rate, and refractive index. The Oxygen flux range is from 0 to 2 sccm and then reverse, from 2 to 0 sccm.

A correlation of refractive index - deposition rate - O flux - line spectral ratio is obtained (Ref. [4]) and used to prepare a data set to feed a microcomputer which control and monitor a prescribed refractive index profile as a function of thickness, creating inhomogeneous filters. We report some results of the Gaussian index profile and a simple notch filter.

Acknowledgments

CONACyT for Catedras Patrimoniales to RSC, NAC, JAC, also for the 254494 CB-2015-01 grant, and for RR scholarship. DGAPA-UNAM for PAPIIT grant IT101017, and JC postdoc scholarship.

References

- 1.- Fundamental understanding and modeling of reactive sputtering processes S. Berg, T. Nyberg, Thin Solid Films **476** (2005) 215 – 230



XII -ICSMV

September 23rd to 27th, 2019 / San Luis Potosí, México

2.- Upgrading the “Berg-model” for reactive sputtering processes, S. Berg, E. Särhammar, T. Nyberg, Thin Solid Films **565** (2014) 186–192

3.- Cleaning level of the target before deposition in a reactive DC magnetron sputtering, Oscar Hernandez, Noemi Abundiz Cisneros, Roberto Sangines de Castro, Carolina Janani Diliegros Godines, Roberto Machorro Mejia, Thin Solid Films, **646**, (2018) 98–104

4.- Plasma emission spectroscopy and its relation to the properties of silicon oxynitride thin films deposited by reactive magnetron sputtering, Sangines, Roberto, et al. Journal of Physics D: Applied Physics, **51**, (2018)



[CHM-304] Characterization of gold nanostars by Small Angle X-Ray Scattering (SAXS)

Elihu Sánchez-Martínez (elihuuhazels@yahoo.com.mx)¹, Esteban Cruz-Hernández¹,
Joazet Ojeda-Galván¹

¹ Coordinación para la Innovación y la Aplicación de la Ciencia y la Tecnología (CIACYT-UASLP), Sierra Leona 550, C. P. 78210, San Luis Potosí, S.L.P., México

The success of nanotechnology is based, to a large extent, on the characterization techniques either of microscopy or spectroscopy, from which primordial information of the nanostructures is obtained. The SAXS technique allows the characterization of a wide variety of nanostructures ranging in size from 1 to 100 nm, such as nanoparticles, biological materials, polymers, colloids, chemicals, nanocomposites and metals, SAXS may be used to determine a particle's size, size distribution, shape, and organization into hierarchical structures [1].

In this work, we report the SAXS characterization of gold nanoparticles with star-like morphology (the nanostars). We used a Bruker SAXS system with a K α x-ray source. The SAXS experiments were realized with three samples of different concentrations. These samples were sealed in glass tubes, the sample to detector distance was 106cm and the time exposition of X-ray with the samples was 2000 seconds using a power of 40kV and 35mA. The analysis of the SAXS intensity profile was performed with the help of a commercial software [2]. The results were then contrasted with direct images obtained from the nanostars by scanning electron microscope (SEM).

[1] Tao Li, Andrew J. Senesi, and Byeongdu Lee, Chem. Rev. 2016, 116, 11128–11180

[2] <https://www.sasview.org/links.html>



[CHM-617] Diseases detection and hydric stress of sugar cane leaves using photoacoustic spectroscopy and multispectral photography

Edwin Alejandro Enríquez Valdés³, David Barrera del Ángel³, Sergio Osbaldo José García³, Ahtziry Guadalupe Alvarado Estrada (princesa_ahtziry@live.com.mx)³, Noé Sierra Romero³, Álvaro Anzueto³, Blanca Estela Zendejas Leal², Francisco Hernández Rosas¹, Alfredo Cruz Orea², Juan Hernández Rosas³

¹ Colegio de Postgrados, Campus Córdoba, Km.348 Carretera Federal Córdoba-Veracruz, Congregación Manuel León, Amatlán de los Reyes, Ver., 94946, México

² Departamento de Física, Centro de Investigación y de Estudios Avanzados del IPN, Apartado Postal 14-740, Ciudad de México, 07360, México

³ Instituto Politécnico Nacional UPIITA, Av. IPN, No. 2580, Col. La Laguna Ticomán, Del. Gustavo A. Madero, Ciudad México, 07340, México

In this work, we have used the photoacoustic spectroscopy (PAS) technique with the purpose to obtain the optical properties of health status of sugar cane leaves. The spectra of the samples under PAS study have been leaves of sugar cane taken from small plants growth in laboratory; some of them became infected, intentionally, with the fungus *Curvularia spp.* We have also study sugar cane leaves using multispectral photography in a cane field using a drone that took pictures at several heights. The images were merged in order to get an orthomosaic, which is nothing other than a complete picture of the field under study. On the orthomosaic we have used several techniques of image processing searching for visual patterns indicating diseases or even hydric stress.



[CHM-629] Determining the etching rate of silicon oxide by XPS

Juan Ignacio Cira-Esquivel (juancirae@gmail.com)³, Brayan González-Castro², José Antonio Rivera-Mayorga¹, Milton Vázquez-Lepe (milton.vazquez@academicos.udg.mx)¹

¹ CUCEI, Universidad de Guadalajara

² Instituto Tecnológico de Huachinango, Puebla

³ Instituto Tecnológico de Matamoros, Tamaulipas

X-ray photoelectron spectroscopy (XPS) is a surface-sensitive quantitative spectroscopic technique that measures the top nanolayers, the obtained spectra help to propose and empirical formula, chemical state and electronic state of the elements that exist within a material.

A silicon wafer 001 was heated at 800 °C during five minutes into a quartz tube, the growth of the silicon oxide was determinate by tilting the sample using Angle-Resolved XPS technique. Data obtained with a Specs detector and a monochromatic Al κ source at different angles were deconvoluted with AAnalyzer software to determinate de intensity ratios of SiO₂/Si. The data analyzed can be used to assess the thickness of silicon oxide layer growth on the silicon wafer.

The etching rate can be determinate using the same procedure when the exposure time is controlled with the etching energy applied. With the correct data analysis, the thickness is calculated and by differences between each experiment, is reducing the thickness sample.

This method can extend by understanding the etching in silicon oxide, then to control a specific thickness using an etching device, for example during the manufacture of photovoltaic solar panels which must have a specific thickness for its proper functioning, and in case it is overcome, to be able to reduce until obtaining effective conditions in order to optimize the efficiency.



[CHM-633] Thermal analysis and artificial vision of laser irradiation on crystalline type corn grains

Hermenegildo Cisneros Carrillo (hermes.cisneros82@gmail.com) ¹, Claudia Hernández Aguilar (clauhaj@yahoo.com) ¹, Flavio Arturo Domínguez Pacheco ¹

¹ Instituto Politécnico Nacional, Sepi – Esime Zácatenco. Unidad professional Adolfo López Mateos, colonia Lindavista. Ciudad de México, C.P. 07738, México

The objective of this research work was to analyze the thermal effects of laser irradiation on crystalline-type corn grain and get characteristic patterns of color and geometrical measurements using an Artificial Vision System (AVS). Three color categories were implemented: intense, middle and transparent of the same variety. The temperature variation of corn grains caused by laser light exposition during 60 s was realized according to Hernández (2015a).

The results point out to a time of 60 s, it is not possible to identify significant variations in the increase temperature when the three maize grains category implemented were compared. The highest variation of temperature was obtained by corn kernels of intense color with 1.075 °C with respect to the initial temperature, attained at 60 s of exposure of laser light, where the temperature reached to 23.975 °C, having an increment of 4.69% with respect to its initial temperature and an average increase of 0.1075 °C (Table 1). Likewise, the results of AVS (Table 2) indicated that the grains, with the original color, had higher difference in color intensities than the thermal images color intensities in RGB space and greater difference than the results of the thermal analysis. In this way, the results obtained by AVS, could be a useful strategy to identify and classify crystalline corn grains.

The authors thank the IPN through the support SIP, EDI, COFFA, etc. Hermenegildo Cisneros Carrillo thank for the support, for Doctorate studies, through the grant awarded by Conacyt.

1. C. Hernandez-Aguilar, A. Dominguez-Pacheco, A. Cruz-Orea, Int J Thermophys (2015) 36:2401–2409
DOI 10.1007/s10765-015-1882-7
2. Claudia Hernández Aguilar, Flavio Arturo Domínguez Pacheco, Alfredo Cruz Orea and Rumen Ivanov Tsonev, Int. Agrophys., 2015, 29, 147-156 doi: 10.1515/intag-2015-0028
3. A.Yu. Popov, N.A. Popova, A.V. Tyurin, Optics and Spectroscopy, 2007, Vol. 103, No. 4, doi:10.1134/S00304000X07100232



[CHM-639] Phonon-Plasmon coupling in InGaAsSb identified by Multiwavelength Raman

Yenny Lucero Casallas Moreno ¹, Gerardo Villa Martínez ², Manolo Ramírez López
(mrlopez.ipn@gmail.com) ², Alejandro Molina Bermúdez ², Patricia Rodríguez Fragoso ³,
Jose Luis Herrera Pérez ², Julio G. Mendoza Álvarez ³

¹ CONACYT, Instituto Politécnico Nacional - UPIITA, Av. IPN 2580, Col. Barrio la Laguna Ticomán, Ciudad de México, C.P. 07340, México

² Instituto Politécnico Nacional - UPIITA, Av. IPN 2580, Col. Barrio la Laguna Ticomán, Gustavo A. Madero, Ciudad de México, C.P. 07340, México

³ Physics Department, Centro de Investigación y de Estudios Avanzados del Instituto Politécnico Nacional, Av. IPN, 2508, Ciudad de México, C.P. 07360, México

Corresponding email: mrlopez.ipn@gmail.com, mramirezlo@ipn.mx

Keywords : Multiwavelength Raman, phonon, Antimonide, surface space-charge region.

Raman Spectroscopy is a powerful technique to analyze crystalline materials by identifying the vibrational modes that produce inelastic scattering of photons. Ordinarily, sample is illuminated with a laser beam of a fixed wavelength and the scattered beam is collected to a monochromator, where the raman shift is measured. The use of multiple wavelengths in Raman Spectroscopy allows to identify composition and dopants gradients, lattice mismatch, multilayer formation and changes of crystalline quality by phonon behavior analysis at different depths of the sample. In this work, quaternary samples of $\text{In}_{0.145}\text{Ga}_{0.855}\text{As}_y\text{Sb}_{1-y}$ with a small variation of the As content (0.134 to 0.143) were studied by Multiwavelength Raman Spectroscopy. Measurements were performed at room temperature in the backscattering geometry by using three excitation wavelengths, 473, 532 and 632 nm at normal incidence. The beams were focused to a diameter of 6 μm at the sample employing a 100 μm of aperture microscope objetivo. The nominal laser power used in these measurements was 20 mW for 532 nm, and 50 mW for 473 and 632 nm. The quaternary crystals show two intense peaks centered at 230 and 244 cm^{-1} originated by TO (GaSb-InAs)-like and LO (GaSb-InAs)-like modes, respectively [1]. The presence of the forbidden TO mode is related to breaking of the selection rules in the backscattering geometry due to tilt and rotations of the crystals with respect to the (100) growth direction. It is important to point out that the integrated intensity of these phonon modes decreases as As content increases because As content decreases the active phonon density.

Results of mutiwavelength spectroscopy were normalized with respect to the maximum intensity of the LO mode for a comparative analysis, and the integrated intensity and the FWHM of the LO and TO modes were determined using a lorentzian line shape analysis. In the spectra is observed that the integrated intensity of the forbidden TO (GaSb-InAs)-like mode increases as the excitation wavelength increases; while the integrated intensity of the LO (GaSb-InAs)-like mode remains constant regardless of wavelength used to measure. Raman signal for excitation wavelenghts shorter than 600 nm is mainly originated from the surface space-charge region (SSCR), in our case, for the spectra measured with excitation wavelengths of 473 and 532 nm; while for the Raman spectrum measured with an excitation of 632 nm comes from the bulk region. The increase of the integrated intensity of the TO mode can be explained due to that in the bulk region the phonon-plasmon



coupling is greater than in the SSCR, and this coupling has almost the same frequency shift than TO phonon modes. Besides, the Raman spectra of all samples measured with excitation wavelengths of 473 nm reveal two peaks at 198 and 263 cm⁻¹, respectively. These modes are associated to the LO-mode of the InSb and TO-mode of GaAs, respectively, which are activated by a carrier mechanism on the surface, so they are essentially manifested in short wavelengths.

[1] J. Díaz-Reyes, et. al., *Characterization of highly doped GaInAsSb grown by liquid phase epitaxy*, Revista Mexicana de Física 63, n.1. 55-64 (2017).

This work was partially supported by SIP-IPN project No. 20195413 and 2019 Innovation Project of Instituto Politécnico Nacional.



[CHM-655] Weldability analysis and microstructural evolution in forging die coupons AISI/SAE L6 repaired by flood welding process.

ING. CECILIA RODRÍGUEZ CABRERA (cecilia.rdz@becarios-comimsa.mx)¹, DR. FERNANDO MACÍAS LÓPEZ¹, DR. JOSÉ JORGE RUÍZ MONDRAGÓN¹

¹ COMIMSA, CALLE CIENCIA Y TECNOLOGÍA NÚMERO 790, COLONIA SALTILO 400

Flood welding process has been investigated as a method for repairing forging die. An experimental investigation has been made with welding coupons of AISI/SAE L6 (Ni, 1.25-2.0%, Cr, 0.6-1.2 %, Mn, 0.25 – 0.80 %) with a groove square slot milled into the upper surface.

Two hot work flux cored wire were deposited into the grooves. The deposition parameters were analyzed in terms of mass deposition rate, microstructure, mechanical properties (micro hardness) and microanalysis using SEM.

In this work, the results allow the general weldability of the repair process to be related to the flood welding process. The results show that the process can produce high quality repairs without metallurgical changes that affect the mechanical properties; however, it is necessary to have the correct selection of deposition parameters.



XII -ICSMV

September 23rd to 27th, 2019 / San Luis Potosí, México

LUMINESCENCE PHENOMENA: MATERIALS AND APPLICATIONS (LPM)

Chairmen: Salvador Carmona Téllez (CICATA LEGARIA-IPN)

Gilberto Alarcón Flores (CICATA LEGARIA-IPN)



XII -ICSMV

September 23rd to 27th, 2019 / San Luis Potosí, México

LUMINESCENCE PHENOMENA:
MATERIALS AND APPLICATIONS (LPM)
ORAL SESSIONS



[LPM-73] Solid state anion exchange on CsPbBr₃ nanostructured thin films by spray coating method

Raúl Ivan Sánchez Alarcón (ivanalarcon67@yahoo.com.mx)³, Rafael Abargues López², Vladimir Chirvony², Soosaimanickam Ananthakumar², Juan Navarro Arenas², Juan Francisco Sánchez Arroyo², Pedro Javier Rodríguez Canto², Miguel Aguilar Frutis¹, Gilberto Alarcon Flores¹, Juan Martínez Pastor²

¹ Instituto Politécnico Nacional, Centro de Investigación en Ciencia Aplicada y Tecnología Avanzada Unidad Legaría. Legaría #694 Col. Irrigación, Ciudad de México, México

² UMDO Instituto de Ciencia de los Materiales- Universidad de Valencia, Catedrático José Beltrán, 2, PO Box 22085, 46071, Valencia, España

³ b Instituto Politécnico Nacional, Centro de Investigación en Ciencia Aplicada y Tecnología Avanzada Unidad Legaría. Legaría #694 Col. Irrigación, Ciudad de México, México

Cesium lead halide perovskites CsPbX₃ (X=Cl, Br, I or mixture) have gained attention owing to astonishing properties as photoluminescent high quantum yields and tunable optical properties as a function of its chemical compositions. Although anion exchange reaction can be done on different phases because of its high anionic mobility, there is a few report of this process in solid phase. Here we report at first time a new strategy to obtain mixed halide CsPb_{1-X}Br_{3-X} thin films by solid state anion exchange using dynamic spray coating method. By mean of spraying of different volumes of HI precursor solution on the top of CsPbBr₃ thin films, it is possible to cover a fully gamut of wavelengths between 520 nm and 650 nm. These perovskite thin films are composed of nanocubes with a mean particle size of 13.7 nm which shape and size is preserved after spray processing. CsPbBr₃ and red shifted CsPb_{1-X}Br_{3-X} thin films are polycrystalline, and their X ray diffractions peaks could be indexed to the cubic phase of perovskite (JCPDS No. 54-0752). Also, it was observed that lattice parameter increase as a consequence of a major bromide substitution by iodide, and which change may be explained by Vegard's law, being the estimated composition of red shifted thin films of CsPbBr_{1.2}I_{1.8}. The photoluminescent quantum yield determined for CsPbBr₃ and CsPbBr_{1.2}I_{1.8} were of 60 % and 70 % respectively.



[LPM-92] Optical amplifiers based on Metal Halide Perovskites

Juan P. Martínez Pastor (martinep@uv.es) ¹

¹ Instituto de Ciencia de los Materiales, Universidad de Valencia, c/Catedrático J. Beltrán,
2, Paterna 46980, Spain

During the last years, Metal Halide Perovskites (MHPs) have attracted special attention as an efficient conversion films for photovoltaics, or excellent gain media to construct optical sources. Particularly, most of the works have been focused on $\text{CH}_3\text{NH}_3\text{PbI}_3$ polycrystalline thin films, where stimulated emission was observed under pulsed excitation and power density thresholds as low as $1 \mu\text{J}/\text{cm}^2$ at room temperature [1,2]. More recently, laser emission under continuous wave excitation have been also demonstrated [3] and even an integrated optical amplifier-photodetector on a flexible substrate was recently reported [4]. MHPs can be also synthesized as colloidal nanocrystals. In particular, CsPbX_3 nanocrystals (NCs) revealed extraordinary properties for optoelectronics. In this work, thin films of CsPbX_3 NCs are properly optimized to enhance the generation of photoluminescence, and with it the optical gain. In particular, Amplified Spontaneous Emission (ASE) is demonstrated with three different compositions ($X_3=\text{Br}_3$, $X_3=\text{Br}_{1.5}\text{I}_{1.5}$, $X_3=\text{I}_3$). Indeed, these films can demonstrate ASE thresholds less than $5 \mu\text{J}/\text{cm}^2$ at cryogenic temperatures under nanosecond excitation. These preliminary results pave the road towards the development of an active photonics technology based on a CsPbX_3 NCs.

REFERENCES

- [1] I. Suárez, E. J. Juárez-Pérez, I. Mora-Seró, J. Bisquert and J. P. Martínez-Pastor, "Polymer/perovskite amplifying waveguides for active hybrid silicon photonics", *Advanced Materials* **27**, 6157(2015).
- [2] T. T. Ngo, I. Suarez, G. Antonicelli, D. Cortizo-Lacalle, J. P. Martinez-Pastor, A. Mateo-Alonso and I. Mora-Sero, "Enhancement of the Performance of Perovskite Solar Cells, LEDs and Light Amplifiers by Anti-Solvent Additive Deposition", *Advanced Materials* **29**, 1604056 (7 pp) (2017).
- [3] Z. Li, J. Moon, A. Gharajeh, R. Haroldson, R. Hawkins, W. Hu, A. Zakhidov Y Q. Gu, "Room-Temperature Continuous-Wave Operation of Organometal Halide Perovskite Lasers" *ACS Nano*. **12**, 10968-10976 (2019).
- [4] I. Suarez, E. Hassanabadi, A. Maulu, N. Carlino, C. A. Maestri, M. Latifi, P. Bettotti, I. Mora-Sero and J. P. Martínez-Pastor, "Integrated Optical Amplifier-Photodetector on a Wearable Nanocellulose Substrate", *Advanced Optical Materials*, 1800201 (8 pp) (2018).



[LPM-93] Fluorolytic sol gel synthesis of red phosphor Mn⁴⁺ doped K₂TiF₆

Raúl Iván Sánchez Alarcón (ivanalarcon67@yahoo.com.mx)², Gilberto Alarcon Flores (alarfbeto@hotmail.com)², Ismael Arturo Garduño Wilches², Miguel Aguilar Frutis², Nicola Pinna¹

¹ Institut für Chemie, Humboldt-Universität zu Berlin, Brook-Taylor-Str. 2, 12489 Berlin, Germany

² Instituto Politécnico Nacional, Centro de Investigación en Ciencia Aplicada y Tecnología Avanzada Unidad Legaría. Legaría #694 Col. Irrigación, Ciudad de México, México

Mn⁴⁺ activate fluoride phosphors have drawn attention owing to its blue light broadband absorption and narrow band red emission, being compatible for applications in warm light emitting diodes (WLED). Also, these non lanthanide based phosphors have shown high photoluminescent quantum yields and good thermal stability. In this work we report the non- hydrolytic synthesis of Mn⁴⁺: K₂TiF₆ phosphors by microwave irradiation. Mn⁴⁺: K₂TiF₆ phosphors can be obtained since 150 °C because of thermal decomposition of ammonium fluoride, which substituting the use of highly toxic HF that is traditionally used as a fluorination source for synthesis of fluoride based phosphors. These phosphors are polycrystalline and their diffraction peaks could be indexed in the hexagonal phase (ICOD 01-070-4699 card). Three interplanar distances (4.698 Å, 4.662 Å and 2.816 Å) were determined from Transmission Electron Microscopy (TEM) which correspond to (001), (100) and (110) planes of the hexagonal phase of K₂TiF₆. Mn⁴⁺ doping were carried out using K₂MnF₆ at different molar ratios. Different organic solvents (benzyl alcohol and acetophenone), as well as different temperature synthesis was tested in order to obtain Mn⁴⁺: K₂TiF₆ phosphors. Photoluminescence and quantum yield measurements were carried out in order to analyze the optical properties of as synthesized materials.



[LPM-281] RE³⁺ based phosphors embedded into organic polyethylene films

*Salvador Carmona Téllez (scarmonat81@gmail.com)³, Raúl Iván Sánchez Alarcón¹,
Rosendo Leovigildo Lozada Morales⁴, Abraham Nehemías Meza Rocha³, Gilberto
Alarcón Flores¹, Ciro Falcony²*

¹ CICATA-IPN Legaria

² CINVESTAV

³ CONACyT-FCFM BUAP

⁴ FCFM-BUAP

In the present work the synthesis and characterization of polyethylene/phosphors composites are studied. RE³⁺-based inorganic phosphors were blended with the low-density polyethylene (LDPE) and then thin films were deposited by means of the dip coating technique. Their optical structural and luminescent properties were evaluated. All composites were made from virgin polyethylene, but easily scalable to waste-polyethylene and high volumes. FTIR measurements confirm the formation of polyethylene/phosphors composites, UV-Vis allows to characterize the transparency of the LDPE matrix after the incorporation of the phosphors. Finally, a complete luminescent study was carried out to characterize the optical properties of the composites and the possibility to use them in technological applications.



XII -ICSMV

September 23rd to 27th, 2019 / San Luis Potosí, México



[LPM-310] Improvement of emission on IR of CaF₂ codoped of lanthanides (Tb - Yb) through antenna based on octafluoroantrhaquinone (OFA).

Jessica De Anda Gil (jessica.deanda@cinvestav.mx)², Ciro Falcony Guajardo², Uriel Balderas¹

¹ *Centro de Investigación en Materiales Avanzados. Alianza Norte 202. Parque de Investigación e Innovación Tecnológica. Apodaca, Nuevo León, México. C.P. 66600*

² *Departamento de física, CINVESTAV, Av Instituto Politécnico Nacional 2508, San Pedro Zácatenco, 07360 Ciudad de México, CDMX.*

Luminescent materials based on lanthanides have been widely studied as spectral converter materials to harvest energy. Lanthanides can transfer energy between different energy states, hence, it permits to have emissions in different wavelengths, moving over electromagnetic spectra, however, one of the limits of lanthanides is narrow absorption bands. Fortunately, some chromophores have a broader absorption than lanthanides and they could be used as an organic ligand to work as an antenna.

In this work, nanocomposites of CaF₂ were synthesized and functionalized with different concentrations OFA to improve the emission intensity in the IR (973 nm) associated with the Yb ($^2F_{5/2} \rightarrow ^2F_{7/2}$) intra-electronic energy levels transition over an excitation of Tb with 485 nm light.



[LPM-369] Tunable white light emission in zinc phosphate glasses activated whit Ag⁺-Ag⁰ and Ag⁰+Ag⁺ and Eu³⁺

Omar Soriano Romero (omar.soriano.romero@gmail.com) ², Ulises Caldiño ³, Rosendo Lozada-Morales ², Antonio Méndez-Blas ¹, Salvador Carmona Telléz ², Abraham Meza Rocha ²

¹ Benemérita Universidad Autónoma de Puebla, Instituto de Física Luis Rivera Terrazas, Av. San Claudio y Av. 18 sur, Col. San Manuel Ciudad Universitaria, Puebla, Pue. C.P. 72570, México

² Benemérita Universidad Autónoma de Puebla, Postgrado en Física Aplicada, Facultad de Ciencias Físico- Matemáticas, Av. San Claudio y Av. 18 sur, Col. San Manuel Ciudad Universitaria, Puebla, Pue. C.P. 72570, México

³ Departamento de Física, Universidad Autónoma Metropolitana-Iztapalapa, P.O. Box 55-534, México, D.F. 09340, México

Keywords: ZnO-P₂O₅, Eu³⁺ emission, Absorption

Zinc phosphate glasses activated with Ag⁺-Ag⁰ and Ag⁰+Ag⁺ pair species and Eu³⁺, were prepared by the conventional melt-quenching method [1]. X-ray diffraction patterns in all cases showed broad bands, indicating lacks of long range order typical of a glassy structure. Such fact is verified by Raman scattering, which displays vibrational related modes with a Zn₃(PO₄)₂ in amorphous phase. From optical absorption data, the band gap energy calculated by the Tauc equation [2], results to be around 3.7 eV. The absorption spectra Eu³⁺ doped glasses display the Eu³⁺: 286 nm (⁷F_{0,1} → ⁵I₆), 297 nm (⁷F_{0,1} → ⁵F₂), 318 nm (⁷F_{0,1} → ⁵H₆), 361 nm (⁷F_{0,1} → ⁵D₄), 381 nm (⁷F_{0,1} → ⁵G₂), 393 nm (⁷F_{0,1} → ⁵L₆), 414 nm (⁷F_{0,1} → ⁵D₃), 463 nm (⁷F_{0,1} → ⁵D₂) and 534 nm (⁷F_{0,1} → ⁵D₁) absorption transitions [3]. On the other hand, the absorption spectra of the Ag and Eu³⁺ co-doped glasses, display in addition to the Eu³⁺ absorption band, a broad band at 319 nm ascribed to absorption of Ag molecular-like (ML-Ag) species. The photoluminescence spectra upon 350 nm excitation of the Ag and Eu co-doped glasses, exhibit a broad band around 450 and 540 nm such emissions is originated by the superposition of the species Ag⁺-Ag⁰ and Ag⁰+Ag⁺, respectively [4]. At the same time, the Eu³⁺ exhibits emissions bands at 579 nm (⁵D₀ → ⁷F₀), 592 nm (⁵D₀ → ⁷F₁), 611 nm (⁵D₀ → ⁷F₂), 652 nm (⁵D₀ → ⁷F₃) and 701 nm (⁵D₀ → ⁷F₄). Thus, by varying the Ag and Eu³⁺ relative concentrations, it is possible to tune emissions from bluish-white to white and white-warm regions.

References

- [1] L. Aquino-Meneses, et al. Journal of Non-Crystalline Solids 480 (2015) 26-31.
- [2] J.Tauc, Amorphous and Liquid Semiconductors, Plenum Press, New York, N. Y. USA, 1979.
- [3] W.T Carnall, P.R.Fields, K. Rajnak, J. Chem.Phys. 49 (1968) 4424.



XII -ICSMV

September 23rd to 27th, 2019 / San Luis Potosí, México

[4] M. Seshadri, et al. J. of Luminescence. 210 (2019) 444.

[LPM-509] Luminescent hybrid lead halide perovskite films

Jesus Uriel Balderas-Aguilar (jesus.balderas@cimav.edu.mx)¹, Eduardo Martínez-Guerra

¹, Ciro Falcony-Guajardo², Francisco Servando Tostado-Aguirre¹

*¹ Centro de Investigación en Materiales Avanzados, Unidad Monterrey, Av. Alianza Norte
202, PIIT, Apodaca, Nuevo León, México.*

*² Centro de Investigación y de Estudios Avanzados del IPN, Departamento de Física, Av.
Instituto Politécnico Nacional 2508, San Pedro Zacatenco, Gustavo A. Madero CDMX,
07360, México*

Lead halide perovskites have emerged as highly attractive alternatives for the fabrication of optoelectronic devices. Nevertheless, the synthesis of luminescent perovskite films by low-cost, scalable, and air-processing conditions is still challenging. Here we demonstrate a scalable, single-step ultrasonic-assisted spray method for luminescent methylammonium lead dibromo chloride (MAPbBr_2Cl) perovskite films with high deposition rates under atmospheric pressure. The photoluminescence properties and quality of the films were enhanced by simply modulating the ratio of the reactants in the precursor solutions. Our results demonstrate a promising approach for perovskite films processing with controlled luminescent, structural, and morphological properties.



XII -ICSMV

September 23rd to 27th, 2019 / San Luis Potosí, México



[LPM-675] Tunable white light emission in zinc phosphate glasses activated with Ag_m⁽ⁿ⁺⁾ clusters and Sm³⁺

W. Romero-Romo (*william.romero@alumno.buap.mx*) ², O. Soriano-Romero ², R.L. Flores-Cruz ¹, R. Lozada-Morales ², U. Caldiño ⁵, C. Falcony ⁴, S. Cármoma-Téllez ³, I. Camarillo ⁵, A. Méndez-Blas ⁶, A.N. Meza-Rocha (*abraham.meza@fcfm.buap.mx*) ³

¹ Benemérita Universidad Autónoma de Puebla, Facultad de Ciencias Físico-Matemáticas

² Benemérita Universidad Autónoma de Puebla, Postgrado en Física Aplicada, Facultad de Ciencias Físico-Matemáticas

³ CONACYT- Benemérita Universidad Autónoma de Puebla, Postgrado en Física Aplicada, Facultad de Ciencias Físico-Matemáticas

⁴ Centro de Investigación y de Estudios Avanzados del IPN, Departamento de Física

⁵ Departamento de Física, Universidad Autónoma Metropolitana-Iztapalapa

⁶ Instituto de Física, Benemérita Universidad Autónoma de Puebla

Zinc phosphate glasses, activated with clusters and Sm³⁺, were prepared by the conventional melt-quenching method. The X-Ray diffraction patterns revealed that the samples remain amorphous for Ag and Sm³⁺ contents up to 3.0 and 1.0 mol%, respectively. The Raman and FTIR spectra showed that the main vibrational modes are associated with P-O bonds. The absorption spectrum of the Ag singly doped glass sample displayed a broad band centered at 318 nm, related to clusters, whereas those co-doped with Sm³⁺ showed, in addition to the cluster absorption, the well-known Sm³⁺ absorptions at 360, 374, 388, 401, 415, 438, 465 and 477 nm. The photoluminescence excitation spectrum of the Ag singly doped glass sample exhibited a broad band from 200 to 400 nm, assigned to superposition of the Ag⁺: 4d¹⁰ → 4d⁹s transition and clusters, being the excitation into the clusters attractive for W-LEDs applications. The photoluminescence emission spectra of the Ag singly doped glass sample, upon cluster excitations at 340, 350 and 360 nm, displayed cold white light tonality, with (0.279, 0.300) CIE1931chromaticity coordinates of 9453 K and bluish white light tonality with (0.264, 0.276) and (0.259, 0.270) CIE1931 chromaticity coordinates and correlated color temperature values of 12901 and 14201 K, respectively. The global emission of the Ag and Sm³⁺ co-doped glass samples was, upon 340, 350 and 360 nm excitations, gradually tuned from the bluish and cold white region to the warm white one, as the Sm³⁺ content was increased, with correlated color temperatures in the 14201-2691 K range. The Sm³⁺ emission bands, under excitations at 340 and 350 nm, were attained at expense of radiative and non-radiative energy transfer from the clusters, as revealed respectively by the sinks mounted on the cluster emission bands and the emission decay profile shortening in presence of Sm³⁺. Analysis of the cluster emission intensity and decay profiles, with the Dexter and Burstein models, showed that the non-radiative energy transfer process might be dominated by an electric quadrupole-quadrupole interaction.



[LPM-688] Study of luminescent metal-organic frameworks (MOFs) using benzene carboxylic acids for synthesis

GILBERTO ALARCON-FLORES (*galarcon@ipn.mx*)⁴, ANAID CARRO GASTELUM⁴, SANDRA LOERA-SERNA¹, RAUL IVAN SANCHEZ -ALARCÓN⁴, SALVADOR CARMONA-TELLEZ², MIGUEL A. AGUILAR-FRUTIS⁴, ISMAEL A. GARDUÑO-WILCHES³

¹ 2Departamento de Ciencias Básicas, Universidad Autónoma Metropolitana Azcapotzalco, Ciudad de México, México.

² Cátedras Conacyt/Benemérita Universidad Autónoma de Puebla, Posgrado en Física Aplicada, Facultad de Ciencias Físico-Matemáticas, Av. San Claudio y Av. 18 sur, Col. San Manuel Ciudad Universitaria, Puebla Pue C. P. 72570, México

³ Cátedras Conacyt/Instituto Politécnico Nacional, Centro de Investigación en Ciencia Aplicada y Tecnología Avanzada, Calzada Legaria 694, Col. Irrigación, Alcaldía Miguel Hidalgo, C.P. 11500 Ciudad de México, México

⁴ Instituto Politécnico Nacional, Centro de Investigación en Ciencia Aplicada y Tecnología Avanzada, Calzada Legaria 694, Col. Irrigación, Alcaldía Miguel Hidalgo, C.P. 11500 Ciudad de México, México

The structural and luminescent properties of Metal-Organic Frameworks (MOFs) derived from benzenecarboxylic acids with terbium such as Tb2 (BDC)3, Tb (BTC) and Tb2 (TDC)3 are reported. These MOFs were synthesized by the microwave-assisted solvothermal method and show the characteristic green emission of the Tb³⁺ ion. The photoluminescent emission is due to the antenna effect where the energy is transferred from the ligands, singlet levels in benzenecarboxylic acids, to the excited level 5D4 of the Tb³⁺ from which the energy decays to its basal levels 7FJ (J = 6, 5, 4, 3). Surprisingly, the emission intensity in all samples increases by two orders of magnitude (from 104 to 106), when they are thermally treated. The excitation spectra obtained by PL confirm that the excitation of the MOFs is by means of the organic sensitizers. XRD measurements confirm the presence of crystalline MOFs. By FTIR, the vibrations corresponding to the carboxylate functional groups were determined, in addition to the metal-oxygen bond. The Nitrogen adsorption isotherms denote the presence of porosity in the MOFs and a thermogravimetric analysis (TGA) was also carried out. SEM images are obtained for all samples indicating the formation of large crystals

Acknowledgements

Authors acknowledge the partial financial support of projects: SIP-IPN #20181597, SIP-IPN #20181456, CB-2015/253342 and 871(2017) and 572(2018) of Cátedras Conacyt



XII -ICSMV
September 23rd to 27th, 2019 / San Luis Potosí, México

LUMINESCENCE PHENOMENA:
MATERIALS AND APPLICATIONS (LPM)
POSTER SESSIONS



[LPM-125] Synthesis and Thermoluminescent Response of Materials based on Magnesium Borates for Dosimetric Applications

Carina Oliva Torres-Cortés (califetorres7@gmail.com)², Héctor René Vega-Carrillo⁶, Luis Hernández-Adame¹, María Leticia Pérez-Arrieta⁵, Luis Octavio Solís-Sánchez⁴, Ángel García-Durán³

¹ CONACyT-Centro de Investigaciones Biológicas del Noreste

² Programa de Doctorado de Ingeniería y Tecnología Aplicada, Universidad Autónoma de Zacatecas

³ Programa de Doctorado en Ciencias Básicas, Universidad Autónoma de Zacatecas

⁴ Programa de Doctorado en Ingeniería y Tecnología Aplicada, Universidad Autónoma de Zacatecas

⁵ Unidad Académica de Física, Universidad Autónoma de Zacatecas

⁶ Unidad Académica en Estudios Nucleares, Universidad Autónoma de Zacatecas

Thermoluminescence (TL) is a potential technique in the nuclear area within the dosimetry of radiation, in the dating by luminescence and computerized radiography mainly. Magnesium borates have desirable chemical and physical properties for various applications, such as thermoluminescent dosimeter (TLD). The MgB₄O₇ doped with rare earths and alkaline elements has been of interest in several studies, due to the excellent characteristics that it presents; high sensitivity, low fading, detection of X-rays, gamma-rays, beta particles and neutrons, and effective atomic number close to that of human tissue. In this work, two TL materials were synthesized based on Magnesium Borate doped with Dy and Dy, Na, to evaluate their TL response to exposure to gamma-rays and neutrons. The concentration of Dy was 0.1 mol% and for Na it was set at 0.5 mol%. The synthesis was carried out by means of the wet reaction method assisted by thermal treatment. The materials were characterized by techniques of Scanning Electron Microscopy (SEM) and X-Ray Diffraction (XRD) to determine their morphology and crystallographic phases, respectively. In the dosimetric study, TL's materials were irradiated with a source of ¹³⁷Cs with an estimated dose of 6.8±0.415 mGy to evaluate their response to gamma-ray exposure; for neutrons, a source of ²⁴¹AmBe (estimated dose of 3.10±0.072 mGy) was used. The results indicate that the TLD's have a higher TL response for gammas. According to the characterization by XRD, a mixture of three phases, Mg₂(B₂O₅), MgB₄O₇ and DyBO₃ was obtained, in mayor percentage the first (not yet reported for dosimetric applications), however, its TL response is considerable. The codoped TL material has a higher TL response of 88.07 nC when is irradiated with 0.66 MeV photons. In the neutrons exposure case, the two TL's exhibited low response, possibly due to the degree of crystallinity, phase mixing and the defects of the host matrix. In the glow curves, the MBO:Dy, Na 0.1,0.5 mol% shows its main peak at a temperature of about 222 °C and for MBO:Dy 0.1 mol% at about 250 °C. For neutrons, the peaks are not well defined, however, the two TL materials have similar behavior in the glows curves. In addition, comparing the TLD-100 and the material with higher TL response for gamma rays, this latter is 1.9 times more sensitive.

Keywords: Thermoluminescent Dosimeter, Magnesium Borates, Gamma-rays, Neutrons.



XII -ICSMV

September 23rd to 27th, 2019 / San Luis Potosí, México

[LPM-180] Microphotoluminescence of thin films of GaSeTe

Osvaldo Del Pozo Zamudio (osvaldo.delpozo@uaslp.mx)², Jacob Adrián Collazo Vázquez², Raúl Balderas Navarro², Andrei Gorbatchev², Jorge Puebla-Nuñez¹, Edgar Armando Cerdá Méndez²

¹ *Center for Emergent Matter Science, RIKEN, Wako, Saitama 351-0198, Japan*

² *Instituto de Investigación en Comunicación Óptica, Universidad Autónoma de San Luis Potosí, 78210 San Luis Potosí, S.L.P., Mexico*

The study of layered materials has attracted prominent attention of the scientific community since the isolation and discovery of remarkable properties of a single layer of graphite (graphene) in 2004. Inspired by this studies, an intense research to different types of materials similar to graphite started, such as transition metal dichalcogenides (TMDCs), hexagonal boron nitride, metallic oxides and, to a lesser extent, gallium chalcogenides [1]. In this work we present a study of a ternary material which belongs to the latter: $\text{GaSe}_{0.5}\text{Te}_{0.5}$. In its bulk form, this material is a semiconductor with a bandgap (E_g) of 1.89 eV. The thin films (<250 nm) were obtained by micromechanical exfoliation and studied by means of spatially resolved microphotoluminescence (uPL) spectroscopy. In contrast with TMDCs, the uPL signal intensity decreases together with film thickness, which indicates a transition from direct to indirect bandgap. Furthermore, a tuning of the E_g is observed also depending on the film thickness. This study is motivated by the potential of this layered material to be used in devices based on van der Waals heterostructures.

References:

[1] Del Pozo-Zamudio, O., et al. 2D Materials 2.3 (2015): 035010.



[LPM-185] Color centers in boron nitride microparticles as single-photon emitters at room temperature

Osvaldo Del Pozo-Zamudio (osvaldo.delpozo@uaslp.mx)³, Fabiola Armenta-Monzón², Amparo Rodriguez-Cobos³, David Ariza-Flores³, Manuel García-Pimentel², César E. García-Ortiz¹, Edgar Armando Cerdá Méndez³

¹ *Centro de Investigación Científica y de Educación Superior de Ensenada, Baja California. Unidad Monterrey, 66629, Apodaca, N. L., México*

² *Facultad de Ciencias Físico Matemáticas, Universidad Autónoma de Nuevo León, 66451 San Nicolás de los Garza, N.L., México*

³ *Instituto de Investigación en Comunicación Óptica, Universidad Autónoma de San Luis Potosí, 78210 San Luis Potosí, S.L.P., México*

The fabrication of devices based on single-photon emitters (SPEs) is a field with intense activity nowadays. The SPEs are essential for applications focused on the transmission of quantum information in a safe and fast way. There is a wide diversity of systems where single-photon emission can be produced, such as semiconductors quantum dots, vacancies in diamonds and, recently, two-dimensional materials [1]. Hexagonal boron nitride (hBN) is a layered material that exhibits bright and narrowband single-photon emission at room temperature in the spectral range of 570-700 nm. The single-photon emission is a consequence of vacancy defects in the crystal lattice of the hBN [2], similar to color centers in diamond. Microparticles of hBN powder constitute a highly attractive alternative because of its low-cost, inertness, and easy dissolution with common and harmless solvents. In this work, we study the segregation of hBN microparticles in the form of powder in different substrates and solvents using spin coating. The microparticles have sizes between 1 and 5 mm. We show that it is possible to efficiently isolate single particles by this technique using ethanol or photoresist as solvents. By means of micro-Raman and micro-photoluminescence studies of the isolated microparticles it is possible to locate the ones with color centers which are potential single photon emitters (SPE). The use of photoresist allows the fabrication of plasmonic devices deterministically on the particles containing them. This technique opens the door to robust and functional nanophotonic devices for the enhancement of the emission and collection efficiency of SPEs [3].

References:

- [1] Aharonovich et al., Nature Photonics 10, 631-641, 2016.
- [2] Tran et al., Nature Nanotechnology 11, 37-42, 2016.
- [3] Li et al., ACS Nano, 2019.



[LPM-299] UPCONVERSION AND DOWNSHIFT LUMINESCENT PROPERTIES IN $(\text{HfO}_2)(\text{SiO}_2)$ HOST CO-DOPED WITH Tb - Yb

Vicente Vargas García (chentever@hotmail.com)⁴, Jesús Uriel Balderas¹, Salvador Carmona², Roberto Vázquez Arreguín⁵, Zacarias Rivera Alvarez³, Ciro Falcony Guajardo (cfalcony@fis.cinvestav.mx)³

¹ CIMAV Monterrey, Sin departamento, Mexico

² CONACYT-Benemérita Universidad Autónoma de Puebla, Facultad de Ciencias Físico Matemáticas, Mexico

³ Centro de Investigación y de Estudios Avanzados del IPN - CINVESTAV, Física, Mexico

⁴ Centro de Investigación y de Estudios Avanzados del IPN - CINVESTAV, Nanociencia y Nanotecnología, Mexico

⁵ Escuela Superior de Computación del IPN - ESCOM, Mexico

In this work we present the synthesis and luminescence properties of $(\text{HfO}_2)(\text{SiO}_2)$ using the spray pyrolysis technique, hollow spherical particles with a diameter ranging from a few nanometers to a couple of microns were obtained. The shells, nevertheless, have a few nanometers thick and the distribution of diameters have a maximum of around 700nm. XRD analysis has shown that the particles are mainly composed by nanocrystals of hafnium oxide domains with sizes of about 14.36nm. The incorporation of the ions within the host allows the cooperative transfer of energy between them, it is also possible to excite with a wavelength of 980nm and obtain the characteristic terbium spectrum with a maximum of emission at 545nm which is known as the upconversion process. When exciting with a wavelength of 270nm and obtain a maximum of emission at 977nm, since the ytterbium ion does not have resonant states at 270nm the cooperative process of excitation and emission on $(\text{HfO}_2)(\text{SiO}_2)$ host between terbium and ytterbium was confirmed, which is known as the downconversion process. When the decay times were measured and adjusted, we were able to calculate the quantum efficiency of the downconversion process, obtaining a maximum of 137%. So these properties can make this material an excellent candidate to function both as a biological marker and to increase the efficiency of a solar cell.



[LPM-342] Photoluminescent properties of crystalline vanadates doped with lanthanides.

Maria Yesica Espinosa Cerón (yess93.ec@hotmail.com)¹, Rosendo Lozada Morales (rlozada@fcfm.buap.mx)¹, Abraham Meza Rocha¹

¹ Posgrado Física Aplicada, FCFM-BUAP

According to suitable stoichiometric ratios, crystalline powders of type , and , initially with , were synthesized by solid state reaction. The luminescent properties of vanadates were studied, which are due to energy transfers within the tetrahedron, the basic unit of this type of compounds. The emission spectra obtained showed that has a very intense yellow emission, located around 580 nm. Additionally, the vanadates that presented intrinsic luminescence were doped with different lanthanide ions in order to producing modulatable emissions in the visible and infrared range, assisted by energy transfer as a consequence of the overlap of the emission with the absorption of lanthanides.

The emission band of zinc orthovanadate was modified by doping the matrix with different percentages of Neodymium. The broad emission located around 580 nm was decomposed into two different emission bands, due to the overlap with the main absorption band of the neodymium, located in the same area. On the other hand, infrared emissions due to neodymium were monitored, and it was found that, in fact, after absorbing photons emitted by , the neodymium showed characteristic emission bands located at 880 nm and 1060 nm.



[LPM-350] Structural and optical properties of SiCxOy films grown by HFCVD

A. Coyopol (acoyopol@gmail.com) ¹, G. García-Salgado ¹, T. Diaz-Becerril ¹, R. Romano-Trujillo ¹, E. Rosendo ¹, M. Vásquez-Agustín ¹, F. G. Nieto-Caballero ¹, C Morales-Ruiz ¹, R. Galeazzi ¹

¹ Benemérita Universidad Autónoma de Puebla

In this work, we present results of a strong emission of visible light in the visible region (3.35 to 1.72 eV) from non-stoichiometric silicon oxycarbide films (SiC_xO_y). The SiC_xO_y films were deposited by Hot Filament Chemical Vapor Deposition (HFCVD) on silicon (100) p-type substrates. The atomic carbon concentration in the SiC_xO_y films was measured quantitatively by XPS measurements, obtaining concentrations between 2 and 10 at.% as hydrogen flow increase. From FTIR analysis, the increase in carbon content favors the formation of Si-C bonds located at about 816 cm^{-1} , however of low intensity respect to Si-O-Si vibrations located at around $1050\text{-}1070 \text{ cm}^{-1}$ associated to a SiO_x network. For low carbon concentrations in the SiC_xO_y films the photoluminescence (PL) intensity is very high compared with the films with high carbon concentrations. This novel method allows us to obtain a promising material for fabricating light emitting diodes silicon based.



[LPM-413] Structural analysis and luminescent characteristics in ZnS:Mn 2+ nanoparticles obtained by the hydrothermal method

Berenice Villaneda Saldivar (*bere.fisica@gmail.com*)¹, María Concepción Muñoz Ramírez¹, María Leticia Pérez Arrieta¹, José Juan Ortega Sigala¹, Hugo Tototzintle Huitle¹, José de Jesús Araiza Ibarra¹

¹ Unidad Academica de Fisica, Universidad Autonoma de Zacatecas,

The work carried consisted in establishing the conditions to prepare nanocrystalline powders of Zinc Sulfide and ZnS: Mn²⁺ by the hydrothermal method. In this method, aqueous solutions placed inside a stainless steel autoclave were used and subjected to temperatures that go above 100 °C, reaching pressures ranging from 2 to 3 MPa. In the synthesis of ZnS and ZnS: Mn²⁺ nanoparticle particles, temperatures of 220 °C and pressures of 2 MPa were used. In the samples obtained, the conventional structural characterization techniques were applied, such as X-ray diffraction (XRD), scanning electron microscopy (SEM) and chemical composition, such as Dispersed Energy Spectroscopy (EDS).

The results indicate the obtaining of the compound ZnS with structure Zinc Blenda (cubic). The nanoparticles showed different sizes and shapes. It was possible to obtain particle sizes that vary from 30 to 50 nm with hexagonal and spherical morphology. The doping with manganese in ZnS varied from 4% to 12% atomic. However the EDS analysis indicates a very small incorporation of manganese impurities (~ 2% at). Finally, the characterization of Photoluminescence (FL) was used as a technique with the aim of being able to identify the transition that takes place between a defect state of the surface and the dopant impurity (Mn²⁺)¹T₄, which can be observed as a change of emission.

The outstanding result of this work was the obtaining of pure ZnS, free of the ZnO phase, commonly when other methods of synthesis are used.

- [1] Z. Li., J. Wang, X. Xu, X. Ye, "The evolution of optical properties during hydrothermal coarsening of ZnS nanoparticles", Matt.Lett. 62, 3862-3864 (2008).
- [2] X. Wu, K. W. Li, H. Wang, "Facile synthesis of ZnS nanostructured sphere and their photocatalytic properties". J. Alloys Compd. 487, 537-544 (2009).



[LPM-495] Detection of irradiated cocoa bean by luminescence methods

Ivonne Berenice Lozano Rojas (ivonne.berenice@gmail.com)³, Jesus Roman Lopez ¹,
Cinthya Nataly Quiroz Reyes ², José Antonio Irán Díaz Góngora ², Jesus Israel Guzmán
Castañeda ⁴

¹ CONACYT-Instituto de Ciencias Nucleares, Universidad Nacional Autónoma de México,
A.P.70-543, 04510 Ciudad de México

² Instituto Politécnico Nacional, Centro de Investigación en Ciencia Aplicada y Tecnología
Avanzada, Unidad Legaria, 11500 Ciudad de México

³ Instituto Politécnico Nacional, Centro de Investigación en Ciencia Aplicada y Tecnología
Avanzada, Unidad Legaria, 11500 Ciudad de México,

⁴ Instituto Politécnico Nacional, Escuela Superior de Ingeniería Química e Industrias
Extractivas, Edificio 6, Unidad Profesional Adolfo López Mateos, 07738 Ciudad de México

We analyzed two group of organic cacao bean raw: forastero (FC) and criollo (CC) cacao bean, the forastero bean is the most important commercial type of cacao and accounts for the bulk of the world cacao production. FC and CC were provided from Tabasco (México), they have been analyzed by mean of the EN 1788 protocols. The minerals were separated from organic material, according to the superficial morphology and X-ray diffraction (XRD), FC and CC mineral composition is made up of quartz and feldspars. The luminescence methods of pulsed photo-stimulated luminescence (PPSL) and thermoluminescence (TL) were used for identification of non-irradiated and irradiated. The minerals were irradiated with ⁹⁰Sr beta particles and ¹³⁷Cs gamma rays in range dose absorbed (5 – 1kGy) and (5- 3kGy) respectively. A complex TL glow curve composed of three peaks were exhibited at 80, 112 and 327 °C. After 150 days of storage, the FC and CC cacao minerals showed TL emissions for their identification as irradiated.



[LPM-496] Efficient near-infrared quantum cutting in Ag-Nd³⁺ and Ag-Yb³⁺ co-doped zinc phosphate glasses

Omar Soriano Romero (omar.soriano.romero@gmail.com) ², Rosendo Lozada Morales ²,
Salvador Carmona Telléz ², Antonio Méndez Blas ¹, Abraham Meza Rocha ²

¹ Benemérita Universidad Autónoma de Puebla, Instituto de Física Luis Rivera Terrazas, Av. San Claudio y Av. 18 sur, Col. San Manuel Ciudad Universitaria, Puebla, Pue. C.P. 72570, México

² Benemérita Universidad Autónoma de Puebla, Postgrado en Física Aplicada, Facultad de Ciencias Físico- Matemáticas, Av. San Claudio y Av. 18 sur, Col. San Manuel Ciudad Universitaria, Puebla, Pue. C.P. 72570, México

Keywords: ZnO-P₂O₅, Ag-Nd³⁺ and Ag-Yb³⁺ emission, Absorption

Zinc-phosphate glasses doped with Ag+-Ag0, Ag+-Ag+ and trivalent Nd³⁺ and Yb³⁺ ions were high-temperature melt-quenching technique. X-ray diffractions (XRD) patterns confirm their amorphous structure. FTIR and Raman spectroscopy suggest that the phosphate network is composed by tetrahedral Zn₃(PO₄)₂ in amorphous phase[1]. From optical absorption data, the band gap energy calculated by The Tauc equation [2], result to be around 3.7 eV. The absorption spectra for Nd³⁺ and Yb³⁺ doped glasses display the, Nd³⁺: 349 nm (⁴I_{9/2} → ²D_{3/2}+⁴D_{5/2}+⁴D_{1/2}+²I_{11/2}), 430 nm (⁴I_{9/2} → ²P_{1/2}), 476 nm (⁴I_{9/2} → ²G_{9/2}+²D_{3/2}+⁴G_{11/2}+²K_{15/2}), 525 nm (⁴I_{9/2} → ⁴G_{7/2}+⁴G_{9/2}+²K_{13/2}), 583 nm (⁴I_{9/2} → ⁴G_{5/2}+²G_{7/2}), 628 nm (⁴I_{9/2} → 2H_{11/2}), 682 nm (⁴I_{9/2} → 4F_{9/2}), 745 nm (⁴I_{9/2} → 4F_{7/2}), 802 nm (⁴I_{9/2} → 4F_{5/2}), 873 nm (⁴I_{9/2} → 4F_{3/2}) and Yb³⁺: (²F_{7/2} → ²F_{5/2}) [3]. On the other hand, the absorption spectra of the Ag-Nd³⁺ and Ag-Yb co-doped glasses, display in addition to the Nd³⁺ and Yb³⁺ absorptions bands, a broad band at 319 nm ascribed to absorptions of Ag molecular-like (ML-Ag) species. The photoluminescence spectra upon 350 nm excitation of the Ag and Nd³⁺ co-doped glasses, exhibit a broad band at 450 nm and 540 such emission is originated by the superposition of the species Ag+-Ag0 and Ag+-Ag+, respectively [4]. At the same time, two several hollows are observed at 525 nm (⁴I_{9/2} → ⁴G_{7/2}+⁴G_{9/2}+²K_{13/2}) and 583 nm (⁴I_{9/2} → ⁴G_{5/2}+²G_{7/2}), ascribed to absorptions of Nd³⁺. Furthermore, Ag-Nd³⁺ co-doped system shows three bands in the near-infrared region Nd³⁺: 875 nm (⁴F_{3/2} → ⁴I_{9/2}), 1052 nm (⁴F_{3/2} → ⁴I_{11/2}) and 1322 nm (⁴F_{3/2} → ⁴I_{13/2}). While, the photoluminescence spectra upon 350 nm excitation of the Ag and Yb³⁺ co-doped glasses, displays a broad band at 450 nm and 540 such emission is originated by the superposition of the species Ag+-Ag0 and Ag+-Ag+, respectively [4], those bands decrease while increasing the molar concentration of Yb³⁺ in the system. Simultaneously, Ag-Yb³⁺ co-doped glasses presents a broad band at 975 nm (²F_{5/2} → ²F_{7/2}) associated to Yb³⁺ emission.



References

- [1] R. Hussin, M.A. Salim, N.S. Alias, M.S. Abdullah, S. Abdullah, S.A.A. Fuzi, S. Hamdan, M.N.M. Yusu, Vibrational Studies of Calcium Magnesium Ultraphosphate Glasses, *J. Fund. Sci.* 5 (2009) 41-53. <https://doi.org/10.11113/mjfas.v5n1.286>
- [2] J.Tauc, Amorphous and Liquid Semiconductors, Plenum Press, New York, N. Y. USA, 1979.
- [3] W.T Carnall, P.R.Fields, K. Rajnak, *J. Chem.Phys.* 49 (1968) 4424.
- [4] M. Seshadri, et al. *J. of Luminescence.* 210 (2019) 444.



[LPM-578] Screen evaluation of visual devices by photoacoustic spectroscopy

Edgar Omar López de León (optoedg@gmail.com)², Claudia Hernandez Aguilar², Flavio Arturo Dominguez Pacheco², Ángel Morales Gonzalez¹

¹ *ESCOM, Av. Juan de Dios Bátiz s/n esq. Av. Miguel Othón de Mendizabal. Colonia Lindavista. Alcaldía: Gustavo A. Madero. C. P. 07738. Ciudad de México*

² *Ingenieria de sistemas, Instituto Politecnico Nacional ESIME ZACATENCO, Manuel de Andía Barredo Edificio 5, 3er piso, Unidad Profesional Adolfo López Mateos, ZACATENCO 07738, Gustavo A. Madero, CDMX*

Spending a lot of time in front of LED screens (light emitting diodes) of various visual devices such as computers, electronic tablets and mobile phones increases eye fatigue and with it the triggering of other eye symptoms such as dry eye. The dry eye in the users of various visual devices has been linked to the reduction of tear film tear time.

The objective of the research work is to evaluate the absorption of blue light by visual device screens such as computers, electronic tablets and mobile phones. The technique used is by photoacoustic spectroscopy, which consists of 3 fundamental processes: absorption of light radiation, transformation of electromagnetic energy and diffusion of heat generated through the evaluated material until the establishment of a temperature field whose periodic oscillations are waves thermal

As a result it is shown that all the screens of the devices fulfill the function of protection against blue light. But it is the screens of the mobile phone 2, the electronic tablet 2 and the computer that have the highest range of protection among the spectrum of blue light, compared with those of the mobile phone 1 and electronic tablet 1. Therefore, it is possible to conclude that there are visual devices with better protection to the blue light that emit their screens, depending on the material that they are made.

**[LPM-581] Enhancement of NIR and red photoluminescent emission, and Burstein Moss effect in CdO-V₂O₅-P₂O₅: Er³⁺ : Yb³⁺ co-doped glass system**

Erika Cervantes Juárez (*k_eri13@hotmail.com*) ¹, Rosendo Leovigildo Lozada Morales ¹,
Abraham Nehemías Meza Rocha ¹

¹ FCFM, BUAP, Prol. 24 sur esq. Av. San Claudio, Ciudad Universitaria Col. San Manuel

CdO-V₂O₅-P₂O₅:Er³⁺:Yb³⁺ co-doped glass system has been studied through its structural, optical and photoluminescent properties as a function of the incorporation of Yb³⁺ ions. Using the melt-quenching method, a group of ten samples was synthesized. The composition 90-5-5: 2.5 % mol of CdO-V₂O₅-P₂O₅: Er³⁺ was used like a host matrix and the Yb³⁺ ions were added from 0.5 to 4.0 % mol, increasing by steps of 0.5 % mol. From XRD and Micro Raman Spectroscopy was possible to determine that in spite of the incorporation of Yb³⁺, the complete serie is largely made up by amorphous phase of Cd₂V₂O₇ and other compounds composed by VO₄ and PO₄ units which exhibit Raman modes at 923, 850, 637 cm⁻¹. The calculated optical band gaps by Tauc's Plot Method, were obtained in the range from 2.4-2.6 eV exhibiting a behavior identified as a Burstein Moss effect. Also, were calculated the Urbach energies, which are in the range from 0.70 to 0.35 eV displaying an inverse line shape respect to the band gaps. The incorporation of Yb³⁺ as co-doping ion, increase the emission of the Er³⁺ transitions $^4I_{13/2} \rightarrow ^4I_{15/2}$ localized at 1534 nm in the NIR and the ($^2H_{11/2}$, $^4S_{3/2} \rightarrow ^4I_{15/2}$ and $^4F_{9/2} \rightarrow ^4I_{15/2}$ transitions in the green to red visible region.



[LPM-584] Thermoluminescence emissions of polyminerals extracted from ancho and chipotle chile peppers

Jesús Román López (jesus.roman@nucleares.unam.mx)¹, Ivonne Berenice Lozano Rojas², Mónica Samanta Monroy Arellano⁴, José Antonio Irán Díaz Góngora², Jesús Israel Guzmán Castañeda³, Epifanio Cruz Zaragoza⁴

¹ CONACYT-Instituto de Ciencias Nucleares, Universidad Nacional Autónoma de México,
A.P.70-543, 04510 Ciudad de México, México

² Instituto Politécnico Nacional, Centro de Investigación en Ciencia Aplicada y Tecnología Avanzada, Unidad Legaria, 11500 Ciudad de México, México

³ Instituto Politécnico Nacional, Escuela Superior de Ingeniería Química e Industrias Extractivas, Edificio 6, Unidad Profesional Adolfo López Mateos, 07738 Ciudad de México

⁴ Instituto de Ciencias Nucleares, Universidad Nacional Autónoma de México, A.P.70-543,
04510 Ciudad de México, México

In this work, polyminal fraction of ancho and chipotle chile peppers were extracted and studied by thermoluminescence (TL). Scanning Electron Microscopy (SEM) images showed that the polyminal grains of both chile samples have different sizes greater than 100 µm. The polyminal fraction of ancho chile, analyzed by X-ray difraction, shows a composition of quartz and anorthoclase (alkali feldspars), whereas the chipotle chile polyminal are mainly quartz. Energy Dispersive Spectroscopy (EDS) analyses exhibited the presence of Si, O, Na, Al, K, Fe, Cu and Zn elements in both polyminal samples. The TL glow curves of both polyminal chile samples depicted two peaks around 84 and 180 °C. Chipotle chile polyminal fraction is 1.3 times more sensitive to ¹³⁷Cs radiation than ancho chile polyminal. The TL properties of both polyminal chile samples, such as dose-response, reproducibility, fading and sun light bleaching (direct and indirect), were determined. From TL₁/TL₂ ratio the ancho and chipotle chile peppers could be detected as irradiated or not.



**[LPM-599] Preparation and characterization of SiO₂: Ge/Cu
thermoluminescent (TL) dosimeters.**

*Rogelio Fragoso Soriano (rogelio@fis.cinvestav.mx)¹, G. L. Jiménez, ** Family Name(s) **
1, A. Guillen ** Family Name(s) **¹, B. E. Zendejas ** Family Name(s) **¹, C. Vázquez -
López ** Family Name(s) **¹, I. Golzarri ** Family Name(s) **², G. Espinosa ** Family
Name(s) **²*

¹ CINVESTAV-DEPTO FISICA

² INSTITUTO DE FÍSICA UNAM

Nanostructured powders of SiO₂: Ge were prepared using commercially available optical fibers. The powders were immersed into Cu adhesive tape normally used for SEM análisis.

The samples showed a linear response of the TL signal after beta irradiation from a ⁹⁰ Sr source. Morphology characterization of the dosimeters was obtained by SEM and AFM. Confocal Micro-Raman spectra were also obtained and analyzed.



[LPM-659] Correlation between spectroscopy and microscopy of SRO-HFCVD films.

Haydee Patricia Martínez Hernández (*pathaymh@yahoo.com*)², José Alberto Luna López¹, José Álvaro David Hernández de la Luz¹, Adán Luna Flores¹, Karim Monfil Leyva¹, Godofredo García Salgado¹, Roberto Morales Caporal³, Raquel Ramírez Amador (*newraq77@hotmail.com*)¹

¹ Centro de Investigación en Dispositivos Semiconductores (CIDS-ICUAP), Benemérita Universidad Autónoma de Puebla (BUAP), Av. San Claudio y 14 sur, Edif. 103C C.U., Col. San Manuel, Puebla 72570, México.

² Centro de Investigación en Dispositivos Semiconductores (CIDS-ICUAP), Benemérita Universidad Autónoma de Puebla (BUAP), Av. San Claudio y 14 sur, Edif. 103C C.U., Col. San Manuel, Puebla 72570, México. Departamento de Ingeniería Eléctrica y Electrónica

³ Departamento de Ingeniería Eléctrica y Electrónica, Instituto Tecnológico de Apizaco (ITA), Fco I Madero s/n, Barrio de San José, 90300 Apizaco, Tlaxcala, México.

This work correlates the results of the spectroscopy and microscopy obtained of the monolayer and bilayer Silicon-Rich Oxide films, obtained by Hot-Filament Chemical Vapor Deposition system, on Quartz and Silicon substrates. The molecular hydrogen fluxes used for the deposit of the films were 25 and 100 sccm with a distance between source and substrate of 8 mm. Thermal annealing was subsequently applied at 1000°C for 60 minutes in Nitrogen ambient. The nanometric thicknesses of the monolayer films are of 296±7.72 nm and bilayer films are of 577.3±16.7 nm which decreased, the same that the refractive indexes after thermal annealing both measured by null ellipsometry. X-ray Photoelectron Spectroscopy also has shown a decrease in excess silicon in the monolayers at 5% after thermal annealing and in their oxidation states the disappearance of Si⁰⁺ (Si) is observed and predominate Si⁴⁺ (SiO₂). For Fourier Transform Infrared Spectroscopy, in addition to presenting the three characteristic vibratory modes, flexion = 458 cm⁻¹, balancing = 812 cm⁻¹ and stretching = 1082 cm⁻¹ of the Si-O-Si bonds in SiO₂, also it presents other vibrating modes of Si-H, Wagging = 614.5 ±4.5 cm⁻¹, Bending = 880.5±0.5 cm⁻¹ and Stretching = 2258.5±0.5 cm⁻¹, which disappear after thermal annealing, indicating a better stoichiometry in the films, besides a shift to higher wavenumber is observed. Using UV-Vis spectroscopy, the transmittance of the Silicon Rich Oxide films on quartz was obtained, which increases and moves to smaller wavelengths after thermal annealing in all films. From this, is obtained the absorbance and the absorption coefficient SRO films, to obtain the optical bandgap energy that increased with thermal annealing, this was used to theoretically calculate the diameter size of the silicon nanocrystal, which with thermal annealing decreased of 1.94±0.19 nm to 1.61 ± 0.14 nm. In the photoluminescent spectra, a higher intensity is observed after thermal annealing in the SRO films as well as a change to higher wavelengths. The maximum peaks of the spectra photoluminescent were used to theoretically calculate the diameter size of the silicon nanocrystal, which has an average of 1.645 ± 0.015 nm in the optical bandgap energy located with Tauc. Therefore, the decrease in thickness, refractive index and size of the silicon nanocrystal after thermal annealing are correlated with the disappearance of hydrogen in the FTIR spectra and the disappearance and increase of photoluminescent spectra of the films in different optical bandgap energy. On the other hand, microscopes confirm the thicknesses of 320nm films without thermal annealing at 309 nm with thermal annealing and the diameter of the silicon nanocrystal of 2.1±0.6 nm with scanning electron microscopy and high-resolution transmission electron microscopy respectively.



[LPM-680] Electroluminescent characterization of commercial solar panels.

Lorena Rodríguez Salas (loresalas@yahoo.com)¹, Oscar Fernando Núñez Olvera¹, Alfonso Lastras²

¹ IICO Av. Karakorum # 1470 Lomas 4a sección San Luis Pososi S.L.P.Mexico

² IICO Av. Karakorum # 1470 Lomas 4a sección San Luis Potosí

Electroluminescence (EL) has become a very convenient tool to evaluate the quality of Si solar panels. The EL emission in a directly polarized p-n junction is generated by the recombination of minority carriers injected into the neutral regions adjacent to the junction. In comparison to direct gap materials like GaAs, the electroluminescent emission of Si is weak due to its indirect band gap nature. It is, nevertheless, measurable with infrared detectors sensitive to wavelengths around the band gap of Si (1.15 μm), including CCD cameras.

Fuyuki et al obtained EL images of a polycrystalline Silicon cell and found a linear relationship between the intensity of the EL emission and the diffusion length of minority carriers [1]. Because of its indirect band gap, the lifetime of minority carriers in Silicon is dominated by recombination through deep levels (Shockley-Read-Hall recombination). The concentration of deep levels is thus directly related to the local diffusion length and a map of the EL intensity across the cell surface would give a measure of cell uniformity and cell quality.

Here, we report on EL images of polycrystalline and monocrystalline Si commercial panels (polycrystalline panels Solartec 250 W, Solarnorte 265 W, Canadian Solar 250 W and monocrystalline Q Cells panels 370 W). Such images were obtained with a commercial photographic camera (EOS 50D Canon) by removing its infrared filter to enhance IR sensitivity. These images are of good quality and allow us to evaluate the homogeneity of the p-n union of a cell, as well to map the distribution of crystalline defects across the cells that comprise the solar panel.

Our results indicate that it is possible to obtain EL images of solar panels of good quality employing instrumentation with a moderate cost. This make the technique affordable for an ample range of applications, including the quick characterization of commercial panels. It also allows its use in teaching laboratories for didactic purposes.

[1] Takashi Fuyuki, Hayato Kondo, Tsutomu Yamazaki, Yu Takahashi, and Yukiharu Uraoka, Photographic surveying of minority carrier diffusion length in polycrystalline silicon solar cells by electroluminescence, *Appl. Phys. Lett.* 86, 262108 (2005).



XII -ICSMV

September 23rd to 27th, 2019 / San Luis Potosí, México

MICROELECTRONICS AND MEMS (MEM)

Chairmen: Norberto Hernandez Como (Centro de Nanotecnología, IPN)
Israel Mejia Silva (CIDESI)



XII -ICSMV

September 23rd to 27th, 2019 / San Luis Potosí, México

MICROELECTRONICS AND MEMS (MEM) ORAL SESSION



[MEM-90] Design and Manufacturing of a Microvalve-pump Array for Flow Control in a Microfluidic System

Mauricio Calderón Zamora (mauricio.calderon@inaoep.mx)¹, Claudia Reyes-Betanzo (creyes@inaoep.mx)¹, Adrián Itzmoyotl Toxqui¹, Victor Aca Aca¹, Armando Hernández Flores¹

¹ Electronics Department, National Institute for Astrophysics, Optics and Electronics - INAOE, Luis Enrique Erro No. 1, Sta. María Tonantzintla, 72840, Puebla, Mexico

The design and manufacturing of a microvalve-pump system for microfluidics control is presented. The proposed design is based in electrostatic transduction of a flexible membrane made with silicon carbide (α -SiC) (1 um of thickness) generating volume changes inside the pump chamber to displace the working fluid across the system. Nozzle/diffuser elements were used as fluid rectifiers to promote the fluid displacement in a preferential direction. COMSOL Multiphysics was used to simulate the behaviour of the proposed model and to obtain results about the output flow rate and the membrane maximum deflection (5um for 20V) during the operation of the device. For device manufacturing, two substrates were used, a silicon substrate containing the fluid channels, the passive valves and the pumping chamber, and a glass substrate containing inlet and outlet of fluid, and the flexible membrane. Both substrates were bonded to complete the whole device.



[MEM-502] A study of the threshold voltage variations on IGZO TFTs.

*Luis Carlos Alvarez Simón (alvarez.simon.dr@gmail.com)¹, Rodolfo Zolá García Lozano¹,
Gerardo Gutierrez Heredia², Ovidio Rodríguez López², Walter Voit²*

¹ *Universidad Autónoma del Estado de México, Ecatepec*

² *University of Texas*

Variations in the threshold voltage due to process variations and the effect of electrical stress on Thin Film Transistors (TFTs) are the main constraints in the development of applications with this technology. Currently, an important area of research is the analysis and design of digital and analog circuits using TFTs in order to apply this technology beyond liquid crystal displays. In the literature, various methods have been proposed to counteract the effect of electrical stress, from the continuous development of new materials to the use of circuit techniques. However, there is a lack of studies showing the magnitude of the spatial variations of the threshold voltage along a wafer in conjunction with the effect of electrical stress.

In this paper are presented the results obtained by the characterization and the study of the threshold voltage variations on indium-gallium-zinc-oxide (IGZO) based TFTs. Providing an analysis of the spatial variations of the threshold voltage in conjunction with the effects of electrical stress. The above allows obtaining a key overview in order to design high performance integrated circuits with this technology.



[MEM-618] Design of an Inclinometer based on Bismuth Hall Probes

*Edgar Iván Sierra Maya (esierra@posgrado.cidesi.edu.mx)¹, Rodolfo Sánchez Fraga¹,
Horacio Estrada Vázquez²*

¹ *Centro de Ingeniería y Desarrollo Industrial, CIDESI Querétaro*

² *University of North Carolina at Charlotte, UNC Charlotte*

The considerations for the design of an inclination sensor based on the Hall-Effect, with bismuth as sensitive layer, are presented. Bismuth is a semimetal that shows interesting electronic properties for this application, such as the highest Hall coefficient among metals and semimetals ($R_H = -0.5 \text{ cm}^3/\text{C}$) and negligible surface depletion effects, which is a limiting factor for the miniaturization of semiconductor-based Hall sensors. Usually, the practical utility of magnetic sensors for several applications relies on its miniaturization and compatibility with microelectronics and microdevices. In this cases, the use of bismuth enables the fabrication of miniaturized Hall probes with submicrometer layers that can be driven with higher currents, than semiconductor sensitive layers, to improve the sensitivity. In addition, Bismuth thin films can be processed with standard microelectronic facilities with less difficulties than semiconductors. In this work, an inclination sensor to measure the tilting referenced to gravity is evaluated using several geometries of Hall sensors and considering the properties of bismuth deposition.

Acknowledgements: This work has been supported by CONACYT-FORDECyT through the project FORDECyT-297497.



XII -ICSMV

September 23rd to 27th, 2019 / San Luis Potosí, México

[MEM-621] Fast and Low-Cost Water Quality Analysis through Optic Biosensors for Microbial Contamination

Claudia Carolina Baltazar Méndez (carolina_bm77@hotmail.com)¹, Jesús Javier Alcantar Peña (jesus.alcantar@cidesi.edu.mx)¹, Elienai Simon Mier¹, Luis David Velarde Díaz¹, Jesús Israel Mejía Silva¹

¹ Division of Microtechnologies, Center for Engineering and Industrial Development, CIDESI, Queretaro 76125, Mexico

One of the main causes of contamination in drinking water is microorganisms. Total and fecal coliform bacteria including *E. coli* are indicators of microbial contamination. Traditionally, determination of these microorganisms requires laboratory analysis which can take more than 18 hours accordingly limits an early intervention in contamination events. Therefore, the development of sensors that allow *in situ* identification of these microorganisms represents an excellent alternative to reduce time, reagents, operators and cost of the process. Fluorescence spectrophotometry offers a rapid detection technique since tryptophan is a common fluorophore in natural surface waters that is related to the activity of the biological community. Tryptophan- like fluorescence (peak T₁) occurs at $\lambda_{\text{ex}}/\text{em}$ 275–296/330–378 nm (Hudson *et al.*, 2008) and has an excellent correlation with BOD₅ (Biochemical Oxygen Demand) which is another parameter of water quality. The aim of this work is to develop multi-wavelength through-flow fluorescence sensors to determinate multiple water parameters to integrate them into an embedded system that can evaluate in real time the drinking water.



XII -ICSMV

September 23rd to 27th, 2019 / San Luis Potosí, México

[MEM-654] DEP-SAW Design and Simulation for Cell Sorting Applications

L.D. Velarde-Díaz¹, C.C. Baltazar-Méndez¹, V.M. Hurtado-Pájaro¹, E. Simon-Mier¹, D.E. Guzmán-Caballero (david.guzman@cidesi.edu.mx)¹, I. Mejía¹

¹ Center for Engineering and Industrial Development, CIDESI, Division of Microtechnologies, 76125, Queretaro, Mexico

Cell sorting of a mixture of biological cells has a potential application on medical diagnostics, cell therapies, regenerative medicine, blood transfusions and others in pharmaceutical industry. Unfortunately, traditional cell-separation processes such as density-based methods or cytometers are expensive and take long time of reaction. Lab-on-a chip devices as Dielectrophoresis Surface Acoustic Wave (DEP-SAW) sensors can sort cells based on their dielectric properties. This kind of devices have several advantages since their size allowing reduction of materials, reagents, reaction times and easy design compared with traditional equipment. In this work, we report the design and simulation of DEP-SAW sensors by using Finite Element Method (FEM) to find the optimal device performance for their potential application in cell sorting. AT cut, ST cut and SAW grade piezoelectric substrates, waveguide layers and the comb-shaped electrodes of the interdigital-transducers are evaluated to operate at different frequencies.



XII -ICSMV
September 23rd to 27th, 2019 / San Luis Potosí, México

MICROELECTRONICS AND MEMS (MEM) POSTER SESSIONS



[MEM-80] Semi-empirical Electrical Model of inter-metallic connections into a RF-CMOS fabrication process

Carlos Alberto Sanabria Díaz¹, Mónico Linares Aranda (mlinares@inaoep.mx)¹, Luis Hernández Martínez¹

¹ Instituto Nacional de Astrofísica, Óptica y Electrónica

The technological scaling and increase of the operation frequency can alter the behavior of the parasitic elements of devices and circuits to RF applications, showing effects that are unusual in the low frequency range. Today, the interconnections are one of the principal sources of the parasitics in the complex electronic systems implementation and in particular the vertical connections or vias (intermetallic connections), are a special case for the analysis of parasitic elements. In integrated circuits (ICs) for RF applications, vias are generally considered as simple resistive-capacitive (RC) elements; this approximation is valid for local interconnections and low operating frequencies where the optimization of RC characteristics can be achieved with the use of via arrays with larger connection area. However, at high frequency, it is necessary to consider the impact of the transmitted signal in the electrical parasites for its mitigation. As the operation frequency of ICs increases, the inductive behavior of On-Silicon Vias (OSV) and vertical interconnections should be considered in a similar way to Printed Circuit Board (PCB), Redistribution Layer (RDL), and Through-Silicon Vias (TSV) technologies.

The present work proposes an experiment-based characterization and modeling approach for interconnection channels (via-stacks as vertical transitions) using a Daisy chain structure which was manufactured in an *180nm RF-CMOS 1.8Volts, Single-Poly 6-Metal (1P6M) layers fabrication process*. The electrical model presents a maximum average error of 5.1% for the return loss when it is compared with experimental data. The usefulness of the model is shown by assessing the impact of the vias in a practical resonant rotary-traveling wave oscillator (RTWO). It is shown that the operation frequency of the designed RTWO is reduced 13.7% when the via-stack effects are included.



[MEM-135] SCHOTTKY BARRIER DIODES FABRICATED WITH IGZO/AgOx METAL OXIDES.

Luis Alonso Santana Dorantes (coster_8@hotmail.com)², Miguel Angel Aleman¹, Luis Martín Reséndiz M.², Aarón I. Díaz Cano², Francisco J. Hernandez Cuevas¹, Norberto Hernandez Como¹

¹ CNMN-IPN. Centro de Nanociencias y Micro y Nanotecnologías, Instituto Politécnico Nacional, México. Av. Luis Enrique Erro s/n, Nueva Industrial Vallejo, 07738 Ciudad de México, CDMX

² SEPI-UPIITA. Unidad Interdisciplinaria de Ingeniería y Tecnologías Avanzadas, Instituto Politécnico Nacional, México. Avenida Instituto Politécnico Nacional No. 2580, Col Barrio la Laguna Ticomán, Gustavo A. Madero, Ciudad de México, C.P. 07340.

In this work, Schottky barrier diodes were fabricated using silver oxide (AgO) as the Schottky contact and amorphous indium gallium zinc oxide (a-IGZO) as the n-type semiconductor. The devices were fabricated with four photolithography steps on glass substrates. The materials used for the fabrication were: 150nm thick Indium tin oxide (ITO) as the cathode, 45 nm thick IGZO layer deposited by sputtering, 500nm thick SU-8 layer as passivation layer, 40 nm thick AgO layer deposited by reactive sputtering and 70 nm thick Au capping layer deposited by e-beam evaporation as the anode. The fabricated Schottky barrier diodes area was 80um x 160um . From the current-voltage characteristics, based on thermionic emission theory, the following electrical parameters were obtained: an ideality factor of 1.71 ± 0.14 , rectification ratio of 1.38×10^9 , Schottky barrier height of 1.14 ± 0.01 eV, as well as the saturation current density $4.5 \times 10^{-13} \text{A/cm}^2$. The fabricated diodes are intended for use in metal-semiconductor field effect transistors (MESFETs), temperature sensors and ultra-fast IGZO Schottky diodes applications.



[MEM-270] Field Effect Transistors in horizontal architecture with carbon allotropes contacts

Juan Pablo Aguilar Gonzalez (norbac_pablo@hotmail.com)¹, Ramón Gómez Aguilar²,
Jaime Ortiz López¹

¹ Department of Physics, ESFM-Instituto Politécnico Nacional, U.P.A.L.M. Zacatenco,
Mexico CDMX, C.P. 07738.

² UPIITA-Instituto Politécnico Nacional, U.P.A.L.M., Av IPN N° 2580, Col. Barrio la Laguna
Ticomán, México CDMX, C.P. 07340

Organic Field Effect Transistors (OFETs) are promising devices for future development of variety of low-cost and large-area electronics applications. These typically consist of three metallic contacts or electrodes (Source, Drain and Gate), a semiconductor material and a dielectric material. In this work, we propose, manufacture and characterize OFETs in horizontal architecture, using P3HT as semiconductor material, PDMS as dielectric material and carbon allotropes contacts, such as: Laser-Induced Graphene (LIG) and reduced Graphene Oxide (rGO). This was done with the purpose of establishing the contribution of contact materials (LIG and rGO) in this type of devices and to compare them with respect to traditional contacts, such as indium tin oxide (ITO).

The devices were characterized by obtaining their I-V curves: transfer and output. These curves were obtained with a gate voltage (V_{GS}) in the range of 15 to 45V and the voltage between the contacts Source-Drain (V_{SD}) of the device took values from 0 to 15 V. From the transfer curves and using the mathematical models for field effect mobility (μ_{FET}) in OFETs, we found that for LIG and rGO contacts there is a maximum field effect mobility of $\mu_{FET}=5.3 \times 10^{-3} \text{ cm}^2/\text{Vs}$ and $\mu_{FET}=3.2 \times 10^{-3} \text{ cm}^2/\text{Vs}$ respectively, presenting n-channel OFETs for both contacts. On the other hand, the output curves show that devices with LIG and rGO contacts have output currents of $I_{DS}=290 \mu\text{A}$ and $I_{DS}=2.2 \mu\text{A}$ respectively. From which it can be concluded that the contacts of rGO and LIG take better advantage of the mobility of the polymer P3HT, overcoming the ITO contacts that provide $\mu_{FET}=8 \times 10^{-4} \text{ cm}^2/\text{Vs}$. The performance of OFETs is evaluated in terms of mobility, on/off current ratio and threshold voltage.

Keywords: LIG, GO, rGO



XII -ICSMV

September 23rd to 27th, 2019 / San Luis Potosí, México

[MEM-276] Fabrication of thin film transistors based on Al₂O₃/IGZO.

Pablo Toledo Guizar (*gilardomagno@hotmail.com*)², Luis Reséndiz Mendoza², Francisco Hernández Cuevas¹, Miguel Aleman¹, Norberto Hernández Como
(*nohernandezc@ipn.mx*)¹

¹ CNMN-IPN

² UPIITA-IPN

In this work, we report the development of a microfabrication process for thin film transistors (TFTs) based on the dielectric/semiconductor junction Al₂O₃/IGZO. A bottom-gate structure was designed with a channel width (W) of 150 μm and a channel length (L) of 80 μm. Five steps of photolithography were used to manufacture the devices. Cr/Au bilayer was used as gate, Al₂O₃ as gate dielectric, IGZO as semiconductor, SU-8 as passivation layer and Ti/Au bilayer for the source and drain contacts. After fabrication, a thermal treatment was carried out on the TFTs at a temperature of 150°C for one hour. The extraction parameters were performed in the linear regime of the square root of the drain current. The devices presented threshold voltages of 2.75V and field effect mobility of 3.3cm²/V-s.

Acknowledgments

This work was supported by SIP-IPN under grant 20190189.



[MEM-306] Design, fabrication and electrical characterization of thin-film electronic devices

Norberto Hernandez-Como (nohernandezc@ipn.mx)², Miguel Lopez-Castillo³, Pablo Toledo-Guizar⁴, Alonso Santana⁴, Luis Alvarez¹, Rodolfo Garcia¹, Francisco Hernandez-Cuevas², Miguel Aleman²

¹ *Centro Universitario Ecatepec, Universidad Autónoma del Estado de México, México*

² *Centro de Nanociencias y Micro y Nanotecnologías, Instituto Politécnico Nacional, México*

³ *Escuela Superior de Ingeniería Química e Industrias Extractivas, Instituto Politécnico Nacional, México*

⁴ *Unidad Profesional Interdisciplinaria en Ingeniería y Tecnologías Avanzadas, Instituto Politécnico Nacional, México*

The development of semiconductor fabrication technologies in Mexico have been growing in the last 10 years with the establishment of several national laboratories (CIDESI, CIO, CNyN-UNAM, CNMN-IPN, CIDETEQ, etc.) with their own cleanroom infrastructure. These laboratories aim to fabricate devices for several applications including sensors based on MEMs, optical devices, nanoelectronic devices, thin-film electronic devices, biosensors, microfluidics, etc. In this work, we report the advances in the development of the fabrication of three basic devices: the capacitor, the Schottky diode and the transistor using our own technology based on thin films of metal-oxides. The three fabrication processes used glass substrates, full photolithography steps and wet and dry etching. We also used the combination of several deposition techniques such as sputtering, e-beam and thermal evaporation, atomic layer deposition and spin coating. For the capacitor, the Schottky diode and the NMOS thin-film transistor the following stack were fabricated: ITO/Al₂O₃/Al, ITO/IGZO/AgO/Au and ITO/Al₂O₃/IGZO/Ti/Au, respectively. The electrical characterization led to the following results: dielectric constant for Al₂O₃ of 8; an ideality factor of 1.71±0.14, rectification ratio of 1.38 x10⁹, Schottky barrier height of 1.14±0.01 eV, as well as the saturation current density 4.5 x10⁻¹³A/cm² for the diodes; and a mobility of 3 cm²/V-s and VT of 2.7V for the transistors. Our fabrication processes used a SU-8 film as etch-stop, passivation and interconnection layer for future integration of the three devices in a single substrate.



[MEM-357] Nanostructure for Bio-Sensing Applications featuring NEMS and MOS as a Hybrid Structure

Mario Alberto García Ramírez (seario@gmail.com) ¹, Miguel Angel Bello Jiménez ⁴, Orfil González Reynoso ³, Estela Adriana Castellanos Alvarado ¹, Everardo Vargas Rodríguez ²

¹ Departamento de Electrónica, CUCEI, Universidad de Guadalajara, Blvd. Marcelino García Barragan 1421, Guadalajara, Jalisco, México

² Departamento de Estudios Multidisciplinarios, DICIS, Universidad de Guanajuato, Guanajuato, Mexico

³ Departamento de Química, CUCEI, Universidad de Guadalajara, Blvd. Marcelino García Barragan 1421, Guadalajara, Jalisco, México

⁴ Instituto de Investigación en Comunicación Óptica, Universidad Autónoma de San Luis Potosí, Av. Karakorum 1470, Lomas 4ta Secc., San Luis Potosí, S.L.P. 78210, México

A numerical analysis of a hybrid nano-structure is performed for bio-sensing applications that features the co-integration of nano-electromechanical systems (NEMS) with the well known metal-oxide-semiconductor (MOS) technology. The hybrid structure features a MOSFET as a readout element and an double-isolated beam from the substrate by a thin air-gap and by a tunnel oxide layer. The beam structure is functionalised aiming to detect bio,molecules such as enzymes or bacterias. In here, a 3D finite element analysis is performed in order to study the behaviour of the doubly-clamped functionalised beam. Preliminary results for the fabrication and characterisation processes of the nanostructure shows a promising structure for key bio-applications.



[MEM-411] Development of capacitive pressure sensors for aquifers monitoring in Mexico

Jesús Armando León Gil (jesus.leon@cidesi.edu.mx)¹, Jesús Javier Alcantar Peña¹, Israel Mejía Silva¹

¹ Division of Microtechnologies, Center for Engineering and Industrial Development, CIDESI. Av. Playa Pie de la Cuesta No. 702, Desarrollo San Pablo, C.P. 76125 Santiago de Querétaro, Qro. México.

Recently, capacitive pressure sensors are acquiring an increasing interest since their characteristics as to high-pressure tolerance, lower power consumption, and temperature-invariant performance. Furthermore, capacitive pressure sensors have a wide field of applications such as automotive, aerospace, medical and chemical industries. A capacitive sensor transduces the variation in the position or dielectric properties into an electrical response. Latter capacitive phenomena can be employed to monitor the liquid level in water reservoirs. Nowadays in Mexico, the over-exploitation of aquifers has been growing during the last decades. Therefore, an alternative to control the water level of local aquifers can be achieved by developing national pressure sensor technology that is needed to reduce international dependence and implementation costs.



[MEM-412] A novel flexible wireless sensor for intracardiac blood pressure monitoring

Natiely Hernández Sebastián (natiely@inaoep.mx) ¹, Daniela Díaz Alonso ², Francisco Javier Renero Carrillo ³, Wilfrido Calleja Arriaga ¹

¹ Electronics Department, National Institute of Astrophysics, Optics and Electronics (INAOE)

² MEMS Department, Center for Engineering and Industrial Development (CIDESI)

³ Optics Department, National Institute of Astrophysics, Optics and Electronics (INAOE)

This work, addresses the development of a novel flexible wireless pressure sensor for full-range continuous monitoring of intracardiac blood pressure. The device is designed for implantation into left ventricle using a catheter-based delivery system. By utilizing surface micromachining techniques and flexible electronics, a variable capacitor and a dual-layer inductor (with 3D approach) were implemented in the sensor as a RCL resonator for wireless pressure sensing and signal retrieving. The sensor is fabricated using biocompatible polymeric films, polyimide-2611, as the substrate material and Polyimide-2610 as coating film. The sensor is characterized according the following parameters, sensitivity, capacitance, response time and operating pressure range, such parameters were validated and simulated using the CoventorWare® software. The sensitivity was approximately 0.21pF/mmHg; capacitance, measured in the 0 to 300 mmHg range, was 2.4 pF to 28.7 pF; and the simulated minimum response time was 0.3 seconds per cardiac cycle. The wireless pressure sensing performance was evaluated based on the finite element method and the near field approximation, using the software Comsol Multiphysics and ANSYS HFSS. The simulated results indicated that the power transmission efficiency, for the wireless system, changes from 92% to 74%, as the resonant frequency varied from 13.65 MHz to 4.41 MHz, due to performance changes in sensor capacitance. Finally, the specific absorption rate (SAR) was simulated across a 3.5 cm-thick compound biological tissue; showing a SAR lower than 1.6 W/Kg, which suggests that the wireless pressure sensor can be safely implanted for intracardiac blood pressure measurement.



[MEM-528] Wireless biodevice for the Stimulation Electrical of the Cornea (CES)

Iván de Jesús Flores Cerón (ivan.jfc@inaoep.mx) ¹, Wilfrido Calleja Arriaga ¹

¹ Electronics department, National institute of astrophysics, optics and electronics (INAOE)

The stimulation electrical of the cornea (CES), is a promising therapy to reduce the damage caused to the visual system derived from retinal diseases, such as: retinitis pigmentosa, central arterial occlusion of the retina and macular degeneration. This therapy has the purpose of causing a rehabilitation effect in the retinal cell tissues, by applying controlled low potentials using an electrode positioned on the surface of the cornea. According to different investigations reported, the CES promotes the recovery of lost visual abilities, using as comparison parameters, electroretinography exams and visual fields, performed before and after the CES therapy protocols. This work, presents the novel development of a wireless biodevice for CES. The complete system consists of two passive RCL modules: a transmitter module and a stimulator set. The stimulator set, consists of an array of microelectrodes and a multilevel inductor electrically interconnected to a capacitor element to form the RCL circuit. In this design, the two inductive-coupling modules are calculated considering proper electromagnetic alignment properties and the following: (a) a radiation distance of 10 cm, (b) an operating frequency of 13.56 MHz to avoid tissue damage by radiation or heating and (c) a core composed of air. The proposed system is validated and modeled using the COMSOL Multiphysics software, showing a self-inductance of 61 μ H, electrical resistance of 270 Ω and mutual inductance of 70.5 μ H. Finally, this design is supported by advanced manufacturing techniques, based on microelectromechanical systems (MEMS) and flexible electronics, which allows to obtain devices with high efficiency, ergonomics and low cost. Also, due to the versatility of design and fabrication techniques used, an experimental model applied to the eye of rat is developed as part of the characterization and in-vivo validation of the device.



[MEM-582] Comparison of CdSe-based thin film transistors with hybrid and inorganic gate dielectric layers.

Maria de la Soledad de Urquijo Ventura (maria.urquijo@cinvestav.mx)², Rafael Ramirez Bon², Manuel A Quevedo Lopez³, Eneftali Flores Garcia¹, Javier Meza Arroyo², Gouri Syamala Rao mullapudi²

¹ *Centro de Ingeniería y Desarrollo Industrial, sede Querétaro*

² *Centro de Investigación y de Estudios Avanzados del IPN, Unidad Querétaro*

³ *Department of Materials Science and Engineering, The University of Texas at Dallas*

In this work, we synthesized two hybrid dielectrics Al_2O_3 -PMMA (150C) and SiO_2 -PVP (200C) by low temperature sol-gel process and they are compared with two commercial inorganic dielectrics SiO_2 and HfO_2 . To test the electrical properties, these dielectric layers were applied as gate dielectric and fabricated MIS devices with Cadmium Selenide (CdSe) as semiconductor channel layer by RF sputtering. The dielectric thin films demonstrated decent dielectrical properties with good gate capacitance and leakage current density. Finally, we fabricated n-type CdSe TFTs by using these different hybrid and inorganic gate dielectrics and the best TFT electrical performance was achieved with SiO_2 -PVP hybrid gate dielectric with high field effect electron mobility (μ_{FE}) $22.1 \text{ cm}^2/\text{V.s}$, low threshold voltage (V_t) of 1.1, low subthreshold swing (SS) of 0.47 and current $I_{ON}/I_{OFF} 10^4$ respectively. Whereas the other TFT with hybrid Al_2O_3 -PMMA gate dielectric show μ_{FE} $2.38 \text{ cm}^2/\text{V.s}$, V_t of 1.67, SS of 0.53 and $I_{ON}/I_{OFF} 10^4$ respectively. Subsequently, the fabricated TFTs electrical response with inorganic based HfO_2 and SiO_2 gate dielectrics indicating deprived electrical performance when compared with TFTs contains hybrid gate dielectrics. Here, the signifying electrical response of CdSe TFTs observed with hybrid dielectrics comparatively with inorganic gate dielectrics is expected due to compatible dielectric/semiconductor interface, also we calculated the charge carrier taps at this interface and the observed value is low while for the others is relatively high.



XII -ICSMV

September 23rd to 27th, 2019 / San Luis Potosí, México

[MEM-586] UV photoassisted chemical deposition of CdSe.

Fernando Garibay-Martinez (fgaribay@cinvestav.mx)¹, Eneftali Flores-Garcia², Iker Chavez-Urbiola³, Rafael Ramirez-Bon¹

¹ CINVESTAV, Unidad Queretaro

² Centro de Ingenieria y Desarrollo Industrial, cede Queretaro

³ University of Texas at Dallas

Semiconductors can be synthesized either by physical or chemical methods. Chemical methods usually involve a trigger that boosts or promotes the reaction, such as a temperature range, a chemical component addition or radiation with a specific wavelength. In this work the effect of UV radiation in the growth of CdSe films deposited by an ammonia free, chemical bath process was evaluated. The reaction vessels were irradiated with UV lamps at room temperature for 5 hours during film deposition at different wavelengths. Subsequently, the deposited films were analyzed crystallographically by means of X-ray diffraction (XRD) as well as morphologically through scanning electron microscopy (SEM). The XRD spectra agrees with PDF:19-0191, corresponding to the diffraction lines of cubic CdSe. A direct relationship was observed between the crystallite size, estimated by FWHM, and the intensity of the irradiated light. Tauc plots was used to determine the optical band gap of the deposited CdSe films.



[MEM-665] Design and Simulation of High Sensitivity MEMS Strain Sensors based on Capacitive Effect

R. Sánchez-Fraga¹, D.E. Guzmán-Caballero (david.guzman@cidesi.edu.mx)¹, J.A. León-Gil¹, I. Mejía¹

¹ Center for Engineering and Industrial Development, CIDESI, Division of Microtechnologies, 76125, Queretaro, Mexico

Design and manufacture of MEMS strain sensors are required in automotive industry to monitor the applied stress and strain on mechanical components. This monitoring is critical when the vehicle must guarantee stability to different phenomena. In this work, we report the design and simulation of a MEMS strain sensor based on capacitive effect by using Finite Element Method (FEM). The current strain sensor converts the strain applied on automotive components into a capacitive change by using an interdigitated comb capacitor suspended by buckle-beams. The design and simulation of the MEMS capacitive sensor includes considerations related to mechanical amplification of the packaging system, the suspended buckle-beams and different sizes of the comb structure. This device was designed to operate at least 200,000 cycles with deformations up to 7000 μ Strains. Using a differential approach, a sensitivity of 0.02 fF/ μ Strain is estimated which is suitable, with an appropriate signal conditioning, for quasistatic large strain sensing applications.



XII -ICSMV
September 23rd to 27th, 2019 / San Luis Potosí, México

NANOSTRUCTURES (NSN)

Chairmen: Yenny Casallas (UPIITA-IPN)

Ángel Gabriel Rodríguez Vázquez (CIACYT -UASLP)



XII -ICSMV
September 23rd to 27th, 2019 / San Luis Potosí, México

NANOSTRUCTURES (NSN) ORAL SESSIONS



XII -ICSMV

September 23rd to 27th, 2019 / San Luis Potosí, México

**[NSN-18] GATE-TUNABLE EMISSION OF EXCITON-PLASMON POLARITONS IN HYBRID
MoS₂-GAP-MODE METASURFACES**

*ANDRES DE LUNA BUGALLO (ALUNA@CINVESTAV.MX)¹, PEINAN NI², VICTOR ARELLANO
ARREOLA¹, MARIO FLORES SALAZAR¹, PATRICE GENEVET²*

¹ CINVESTAV - UNIDAD QUERETARO

² CRHEA - CNRS

The advance of in designing arrays ultrathin two-dimensional optical nano-resonators, known as metasurfaces, is currently enabling a large variety of novel flat optical components. The remarkable control over the electromagnetic fields offered by this technology can be further extended to the active regime in order to manipulate the light characteristics in real-time. In this contribution, we couple the excitonic resonance of atomic thin MoS₂ monolayers with gap-surface-plasmon (GSP) metasurfaces, and demonstrate selective enhancement of the exciton-plasmon polariton emissions. We further demonstrate tunable polaritonic emissions by controlling the charge density at interface through electrically gating in MOS structure. Straddling two very active fields of research, this demonstration of electrically tunable polaritonic light-emitting metasurfaces enables manipulation of light-matter interactions at the extreme subwavelength dimensions in real time.



[NSN-34] Exfoliation of Layered Crystals: The Key Role of the Solvent Properties

Antonio Esau Del Rio Castillo (antonio.delrio@iit.it) ¹

¹ Istituto Italiano di Tecnologia

The discovery of graphene in 2004[1] triggered the research of two dimensional (2D) materials. The outstanding properties of these thin materials awoke the imagination of hundreds of scientists. Giving as a result, multiple possible applications for these materials, ranging from polymer composites for aircraft to quantum computers, through applications in biology, electronics, and medicine.[2] It was clear that the announced 2D revolution requires efficient production methods and bring to the market commercial applications. Although many production techniques developed[2] the most promising methods for large scale production of 2D materials relies on liquid phase exfoliation (LPE).[3] The process consists of mixing the bulk material in a solvent, and give energy to the mixture. Usually, the energy is applied in the form of sonic waves (or shear forces).

Up to now, the production of two-dimensional (2D) crystals is facing critical issues related to the transition from the lab to the industry,[2] e.g., heterogeneity of the flake size distribution, random type of defect, low-production rate, and so forth.[4] Recently, the high-pressure homogenisers (HPH) have emerged as attractive options for the large scale production of 2D crystals,[5,6] overcoming the low-production rate characteristic of the LPE methodologies.[5] Additionally, in the HPH, the solvent flow reaches shear-rates $> 10^6 \text{ s}^{-1}$, and the exfoliation process occurs in a short time (μs), thus reducing the impact of cavitation (explosion-implosion of solvent bubbles). These phenomena promote the peeling-off of large flakes (up to few μm in lateral size) and reduce the damage induced in the flakes during the exfoliation.[7] However, the control of the flake sizes and defects (from the exfoliation) have not been demonstrated yet.

A possible route to achieve the size and defect tuning is to adjust the parameters that affect the shear rate and cavitation, i.e., the solvent viscosity, density, and vapour pressure.

In this talk will be presented the state-of-the-art results on the large scale exfoliation of layered materials (i.e., production rate more than 20 g h^{-1}) in the wet-jet mill,[5] a commonly used HPH technique in the industry. Additionally, the first steps towards the on-demand control of the flakes morphology and defects, obtained by selecting solvents with different viscosities and vapour pressures will be presented. Finally, the last studies regarding the physicochemical process involved during the exfoliation and the importance of size selection will also be discussed.

1. Novoselov, et al., *Science*, **306** (2004) 666.
2. Ferrari, et al., *Nanoscale*, **7** (2015) 4598.
3. Hernandez, et al., *Nat. Nano.*, **3**, (2008) 9, 563., Nicolosi, et al., *Science*, **340**, (2013) 6139., Paton, et al., *Nat. Mat.*, **13** (2014) 624
4. Del Rio and Bonaccorso. *Manuscript in preparation*
5. Del Rio, et al., *Mater. Horizon*, **5** (2018) 890



6. Del Rio, et al, FlatChem, 2019. Accepted manuscript

7. Del Rio, et al. Manuscript in preparation

[NSN-46] Ferroelectric properties G-ZnO nanocomposite thin films studied by Piezoresponse Force Microscopy

Raquel Ramírez Amador (newraq77@hotmail.com) ², José Juan Gervacio Arciniega ³, Salvador Alcántara Iniesta ², Leonardo Morales de la Garza ⁴, José Joaquín Alvarado Pulido ², Yasmín Esqueda Barrón ⁴, Gabriel Alonso Núñez ⁴, David Dominguez ⁴, Mario Farias Sánchez ⁴, Primavera López Salazar ², Raquel Ramírez Amador ¹, Yesmin Panecatl Bernal ²

¹ Carrera de Mecatrónica, Universidad Tecnológica de Huejotzingo (UTH), Real San Mateo 36B, Segunda Secc, Santa Ana Xalmimilulco, Puebla 74169, México.

² Centro de Investigación en Dispositivos Semiconductores (CIDS-ICUAP), Benemérita Universidad Autónoma de Puebla (BUAP), Av. San Claudio y 14 sur, Edif. 103C C.U., Col. San Manuel, 72570 Puebla, Puebla, México.

³ Conacyt-Facultad de Ciencias de Físico Matemáticas (FCFM), Benemérita Universidad Autónoma de Puebla (BUAP), Av San Claudio, Edif. FM6, C. U., Jardines de San Manuel, 72572 Puebla, Puebla, México.

⁴ Universidad Nacional Autónoma de México, Centro de Nanociencias y Nanotecnología, Carretera Tijuana-Ensenada km107, Playitas, 22860 Ensenada, Baja California, México.

Piezoelectric and ferroelectric materials are a class of important functional materials applied in high-voltage sources, sensors, vibration reducers, actuators, motors, non-volatile memory, technology in mobile communications and so on [1]. Zinc oxide (ZnO) is an environmental-friendly semiconducting, piezoelectric, and plays an essential role for applications in microelectromechanical systems (MEMS) [2]. So, in this work, it was studied the piezoelectric and ferroelectric properties of thin films of G-ZnO composite. In this case, the thin films of G-ZnO composite were deposited by Ultrasonic Spray Pyrolysis (USP). The structure and morphology of ZnO and G-ZnO samples were characterized using powder X-ray diffraction (XRD), Raman spectroscopy, X-ray photoelectron spectroscopy (XPS), and AFM techniques. The piezoelectric and ferroelectric behavior was through the analysis of piezoresponse force microscopy (PFM) measurements, revealed a local piezoelectric coefficient of $d_{eff} = 113 \text{ pm/V}$ and with the application of the external electrical field polarization in the G-ZnO thin films can be switched. These results are compared with previous works [3].

Acknowledgments: R. Ramírez-Amador acknowledges the financial support CONACYT by a doctoral scholarship and the facilities given by VIEP-BUAP and CIDS-ICUAP. Also, the authors would like to thank the facilities given by laboratory equipment of department of Nanocharacterization of UNAM.

References



[1] Zhang, Y., Sun, D., Gao, J., Hua, X., Chen, X., Mei, G., & Liao, W. (2019). A semiconducting organic-inorganic hybrid perovskite-type non-ferroelectric piezoelectric with excellent piezoelectricity. *Chemistry—An Asian Journal*.

[2] Tao, K., Yi, H., Tang, L., Wu, J., Wang, P., Wang, N., ... & Chang, H. (2019). Piezoelectric ZnO thin films for 2DOF MEMS vibrational energy harvesting. *Surface and Coatings Technology*, 359, 289-295.

[3] Xiao, J., Herng, T. S., Ding, J., and Zeng, K. (2017). Polarization rotation in copper doped zinc oxide (ZnO:Cu) thin films studied by Piezoresponse Force Microscopy (PFM) techniques. *Acta Materialia*, 123, 394-403.

[NSN-81] TEMPERATURE INFLUENCE IN THE SYNTHESIS OF CARBON SPHERES FROM NAPHTHALENE

Carmen Judith Gutiérrez- García⁴ , Jael Madaí Ambriz-Torres⁴ , Diana Litzajaya García-Ruiz⁴ , Jaime Abraham Guzmán-Fuentes⁴ , José de Jesús Contreras-Navarrete¹ , Francisco Gabriel Granados-Martínez² , Luis Fernando Ortega-Varela⁴ , Patricia Castillo-Ocampo³ , Arlette Richaud³ , Francisco Méndez³ , Lada Domratcheva-Lvova (ladamex@yahoo.es)⁴

¹ Instituto Tecnológico de Morelia, Avenida Tecnológico 1500, 58120 Morelia, Michoacán

² UNAM Escuela Nacional de Estudios Superiores Unidad Morelia ,Antigua Carretera a Pátzcuaro 8701, 58190 Morelia, Mich., México

³ Universidad Autónoma Metropolitana, Av. San Rafael Atlixco N° 186, Vicentina, Iztapalapa, 09340, Ciudad de México.

⁴ Universidad Michoacana de San Nicolás de Hidalgo, Gral. Francisco J. Múgica S/N, Felicitas del Río, 58030 Morelia, Mich., México.

Several forms of carbon nanostructures have become a continuous research object such as fullerenes (C_{60}). Since the discovery of C_{60} a greatly impact on the understanding of carbon bonding has made. It is expected that carbon spheres with closed shell structure to have analogous chemical characteristics as C_{60} . Carbon spheres (CSs) are classified according to size, growth kind and graphitization degree. CSs could be applying in several application like nanodevices, absorbent material, energy storage, catalysts, electrodes in supercondensors and lubricants due their chemical and physical properties. The carbon spheres have properties which can be influence by their different parameters such as diameter, chemical composition, bulk structure and crystallinity. Some CSs synthesis methods have been developed. The Chemical Vapor Deposition (CVD) compared to other synthesis methods has some advantages: low synthesis temperature, low cost, process control and ease to use, etc. The aim of this research was analyze the temperature influence in the carbon sphere growth from naphthalene as carbon source by CVD method. CS were grown on stainless steel



core onto a tubular quartz reactor. The synthesis temperatures were 750, 800 and 850 °C. Reaction time was 60 minutes. Argon was used as carrier gas at 10 ml/min. After cooling down, the samples were analyzed by Field Emission Scanning Electron Microscopy (FESEM), Energy Dispersive Spectroscopy (EDS), Fourier Transform Infrared Spectroscopy (FTIR), and Raman Spectroscopy. SEM micrographs showed a spherical morphology at 800 and 850°C with 0.8 - 3 micrometer diameters. At these temperatures spheres were the unique kind of morphology. At 750 °C it is possible to observe carbon nanomaterials with different morphologies like carbon nanotubes, some spheres, moreover carbon beads in the extremes of carbon bars. These beads could be the seeds of carbon sphere growth, however this temperature is not enough to the formation of perfect spherical bodies. The carbon content is high for all samples. FTIR spectra showed a peak around 3400 cm⁻¹ corresponding to OH vibrations and also the presence of C=O in a range among 1590 and 1706 cm⁻¹. The D and G bands were observed by Raman spectroscopy around 1300 and 1600 cm⁻¹ respectively. In conclusion, the temperature is an overriding parameter in the growth of carbon spheres, just up to 800 °C is possible the sphere formation and below this temperature carbon nanotubes prevailed, for these synthesis conditions. The characterization techniques showed the carbon spheres produced from naphthalene contain 100% carbon and they are completely solid. **Acknowledgement** to Scientific Research Coordination of UMSNH and CONACyT for the financial support.



[NSN-258] SYNTHESIS OF HELICAL CARBON NANOTUBES GROWN OVER THIN COPPER FOIL BY CHEMICAL VAPOR DEPOSITION SYSTEM

Juan Luis Fajardo Díaz (juan.fajardo@ipicyt.edu.mx)¹, Emilio Muñoz Sandoval¹,
Florentino López Urias¹

¹ Advanced Materials Division, IPICYT, San Luis Potosí, México

Helical carbon nanotubes (H-CNT) were synthesized in an aerosol assisted chemical vapor deposition system (AACVD) using a copper foil as catalyst and substrate and ethanol vaporized as precursor. The copper foils were cleaned and pre-treated with ethanol, isopropanol and acetone in sonication bath during one hour each to obtain a surface modification. The AACVD was carried in one tubular furnace at 980 °C where several copper foils of 0.25 mm thickness were placed inside the reactor from the highest to the coolest temperature zone. These carbon nanostructures were characterized by scanning electron microscopy (SEM), transmission electron microscopy (TEM), X-ray diffraction, Raman spectroscopy, atomic force microscopy (AFM) and cyclic voltammetry. Carbon nanostructures with different morphologies were found passing from the formation of graphite at high temperature to the synthesis of H-CNT and stacked graphene carbon nanofibers SG-CNF where the temperature drops. The H-CNT are helical structures with no practically gap between each coil with a pitch of ~27 nm by a tubular structure with ~20 graphitic layer in each wall, in the case of the SG-CNF the graphitic layers are almost perpendicular to the CNT axis similar to a stacked short graphene layers directed outwards the structure that leads to the edge formation. Raman characterization illustrates differences between the graphitic carbon structures found at early stages from those at the dropping temperature zone where at the higher temperature mainly graphite the relation of the ID/IG bands is 0.88, while for the H-CNT the ID/IG relation is 1.79 indicative of high defective graphitic structure which is related with the "herringbone structure" of stacked graphitic structure and high edge formation. In the case of the coolest zone the Raman spectra is characteristic of low sp³ amorphous carbon (ID/IG of 0.67). The cyclic voltammetry results indicate that the sample with the H-CNT structures becomes more capacitive in a quasi-reversible process with practically no modification of the standard oxide-reduction potential for Cu, while for the other sections this oxide-reduction potential increases. Another aspect of the sample with the H-CNT is its hydrophobic surface with a contact angle of 122 °. With this work we demonstrate that Cu foils are effective substrates to the production of H-CNT structures. The temperature and position of the Cu-foils inside tubular furnace and surface roughness are determinant parameters in the growing of the H-CNT, also the shape of the copper nanoparticle influence the type of carbon nanostructure catalyzed over the copper substrate.



[NSN-263] Chemical vapor deposition of MoSe₂ monolayers using metal alkali halides

Mario Flores Salazar (mario.flores@cinvestav.mx) ¹, Víctor Arellano Arreola ¹, Andrés de Luna Bugallo ¹

¹ Cinvestav Unidad Querétaro

Currently, research on transition metal dichalcogenides (TMDs) has attracted extensively attention due to unique properties in their two-dimension form. Particularly, MoSe₂ present a narrow and direct band gap, high optical absorbance, and relatively high carrier mobility making it a suitable ultra-thin semiconductor material for different applications such as field effect transistors (FETs), photodetectors, quantum emitters, etc. However, one of the principal challenges is to obtain large area TMDs films, specifically the synthesis of MoSe₂ is difficult due to the low reactivity of selenium. Recently, the use of alkali salts has been demonstrated as an attractive route to grow large area TMDs monolayers semiconductors like WS₂ and WSe₂, nevertheless the consequences of using alkali promoters during the growth should be understood.

Herein, we show the synthesis of MoSe₂ monolayers by atmospheric pressure chemical vapor deposition (APCVD) using MoO₂, Se as precursors and KBr, KCl, NaCl as promoters. Optical and scanning electron microscopy images show large crystal domains up to 100 microns. MoSe₂ monolayers and few layered crystals were characterized by Raman spectroscopy. All the samples show the two characteristic peaks A_{1g} (out-of-plane) and E_{2g} (in-plane) centered around 241, 295 cm⁻¹ respectively. However, using resonant Raman spectroscopy we found a prominent peak around 250 cm⁻¹ (2ZA) only for MoSe₂-KBr samples, which can be attributed to a high-quality crystallinity. This result was further confirmed by photoluminescence (PL) measurements, while MoSe₂-KBr crystals show high PL intensity, MoSe₂-NaCl and MoSe₂-KCl monolayers presented an important PL reduction up to 70%. In addition, PL mapping revealed good homogeneity in MoSe₂-KBr compared to KCl and NaCl samples.

To summarize, we showed that the use of alkali salts represents an attractive solution to MoSe₂ synthesis, in particular the employment of KBr during APCVD growth of MoSe₂ not only promotes large domain growth, also present excellent optical properties in comparison with MoSe₂-NaCl and MoSe₂-KCl.



[NSN-307] Thermally and optically stimulated luminescence characteristics of detonation micro and nanodiamonds

*María Claudia Calderón Martínez³, María Inés Gil Tolano², Susana Álvarez García², Carlos F. Ruiz Valdez¹, Rodrigo Meléndrez², Valery Chernov², Marcelino Barboza Flores
(mbarboza@cifus.uson.mx)²*

¹ Departamento de Física, Posgrado en Nanotecnología, Universidad de Sonora,
Hermosillo, Sonora 83000, México

² Departamento de Investigación en Física, Universidad de Sonora, Hermosillo, Sonora
83000, México

³ Posgrado en ciencias (física), Departamento de Investigación en Física, Universidad de
Sonora, Hermosillo, Sonora 83000, México

We report on the TL/OSL properties of high quality synthetic detonation microdiamond (10-600 μm) and nanodiamond (60-600 nm) particles to assess their potential application as ionizing radiation detectors and dosimeters. This issue is important in the designing of dosimeters suitable to perform in an environment of high-energy photons and beam particles radiotherapy procedures. We investigate and compare the thermoluminescence (TL) and optically stimulated luminescence properties (OSL) of synthetic microdiamond and nano diamond particles. The diamond particles exhibited a typical photoluminescence under excitation with 488 nm laser light, demonstrating the presence of $[\text{NV}]^0$ and $[\text{NV}]^-$ centers at 575 and 637 nm; respectively, along with a well-defined Raman peak at 1332 cm^{-1} characteristic of high quality crystalline diamond. The TL glow curves of microdiamond samples under study are composed of several overlapped peaks in the 300-623 K temperature range with maximum around 460 K after beta irradiation at doses of 0.1 - 3400 Gy, with noticeable differences in peak intensities for different diamonds sizes. The nanodiamond samples showed a TL with a maximum peak around 590-653 K. The TL/OSL as a function of dose was found to be highly reproducible for the samples indicating the good perspective of these microdiamonds and nanodiamonds particles as TL/OSL dosimeters for ionizing radiation



[NSN-343] III-V Semiconductor Device Integration on Si using Van der Waals Epitaxy

Isaac Martinez-Velis (sissa85@gmail.com)², Yazeed Alaskar¹, Koichi Murata¹, Kang L. Wang¹, Isaac Martinez-Velis¹

¹ Department of Electrical Engineering, University of California at Los Angeles, California 90095, USA

² Facultad de ciencias Químicas, Universidad Juárez del Estado de Durango, Durango, México

Integration of arsenide based III-V compound semiconductors on silicon (Si) has been the focus of significant research to integrate light sources on silicon, enabling an integrated optical solution for chip-chip interconnects in future computing systems, as well as to make cost-effective and efficient multi-junction solar cells. We present a novel approach to grow high-quality single-crystal GaAs layers on silicon substrates that uses 2D material as buffer layer. The Van der Waals forces are dominant in the vertical direction decreasing the restraints of lattice and thermal expansion coefficients mismatches. In this work, GaAs/2D heterostructures are grown on vicinal silicon (111) substrates with 4 degrees miscut to facilitate nucleation on the silicon substrate. As-grown GaAs exhibits a superior quality compared to those grown directly on silicon substrates with a narrow FWHM of the surface-normal reflection, indicating a low defect density. In addition, room temperature Photoluminescence (PL) reveals that a narrow FWHM of the PL signal was achieved, indicating we achieved the best crystal quality of GaAs with lowest defect density of GaAs grown directly on Si to date, making this work a remarkable step towards GaAs/2D/Si layers of sufficient quality to serve as optical emitters in silicon micro-circuits.



[NSN-377] UNZIPPING CARBON NANOTUBE SPONGES

Alejandro J. Cortés-López (alejandro.cortes@ipicyt.edu.mx) ¹, Emilio Muñoz-Sandoval ¹,
Florentino López-Urías ¹

¹ División de Materiales Avanzados, IPICYT, Camino a la Presa San José 2055, Lomas 4a
Sección, San Luis Potosí, S.L.P., 78216, México

Carbon nanotube sponges are a three-dimensional type structure with attractive properties such as superhydrophobicity, elasticity, compressibility, and electrical conductivity. Such properties make them as potential material for applications in Li-ion batteries, electrodes, trapping nanoparticles, and oil absorption. Different physical and chemical treatments have been reported to develop new materials of carbon nanotubes and enhance its properties. Such treatments comprise chemical methods with oxidizing agents, the intercalation-exfoliation involving agents as ammonia, lithium and acids, and catalytic methods using metal nanoparticles to cut longitudinally surface of carbon nanotubes¹⁻⁴. In the present work, we report unzip of carbon nanotube sponges by acid treatment using a solution of H₂SO₄/HNO₃. Carbon nanotube sponges were characterized after and before of acid treatment by scanning electron microscopy, X-ray diffraction, thermal analysis and Raman spectroscopy. Carbon nanotube sponges are formed by entangled carbon nanotubes exhibiting high hydrophobicity before acid treatment. Then acid treatment carbon nanotube sponge shows hydrophilic behavior and longitudinal unzip of nanotubes exposing graphitic layers, increasing presence of edges and defects, and decreasing of graphitization degree.

Kosynkin D.M., Higginbotham A.L., Sinitskii A., Lomeda J.R., Dimiev A., Price B.K., Tour J.M. Longitudinal unzipping of carbon nanotubes to form graphene nanoribbons. *Nature* 458 (2009) 872-876.

Terrones M. Sharpening the Chemical Scissors to Unzip Carbon Nanotubes: Crystalline Graphene Nanoribbons. *ACS Nano* 4 (2010) 1775-1781.

Sinitskii A., Dimiev A., Kosynkin D.V., Tour J. Graphene Nanoribbon Devices Produced by Oxidative Unzipping of Carbon Nanotubes. *ACS Nano* 4 (2010) 5405-5413.

Wu K.-H., Wang D.-W., Gentle I.R. Revisiting oxygen reduction reaction on oxidized and unzipped carbon nanotubes. *Carbon* 81 (2015) 295-304.



[NSN-503] Many-electron interaction in nanostructures under the effect of an external electric field

Reyna Méndez Camacho (reyna129b@hotmail.com) ¹, Esteban Cruz Hernández ¹, Ramón Castañeda Priego ²

¹ Coordinación para la Innovación y la Aplicación de la Ciencia y Tecnología, CIACYT-Universidad Autónoma de San Luis Potosí, UASLP, Sierra Leona 550, San Luis Potosí, S. L. P., México.

² División de Ciencias e Ingenierías, Campus León, Universidad de Guanajuato, Loma del Bosque 103, León, Guanajuato, México.

A topic of fundamental importance is the electron-electron (e – e) interaction in nanostructures such as one-dimensional (1D) quantum wires (QWRs) or zero-dimensional (0D) quantum dots (QDs), which show unique and interesting properties of great relevance both experimentally and theoretically. One example of these interactions is the Wigner crystallization, which is one of the most remarkable many-body effects in QWRs where electrons spontaneously form a self-organized lattice.

Even when several studies addressing the problem of few electrons confined in QWRs have predicted the formation of such 1D electronic structure, and some experimental signatures of the Wigner crystal have already been reported, when many electrons interacting in nanostructures are considered, the problem becomes very challenging.

This challenge arises because when many-body forces are explicitly included in large structures (such as QWRs), long computational times and complex mathematical calculations are required. Recently, we have proposed a simple approach to deal with this problem of many electrons confined in QWRs by solving numerically the Schrödinger equation for two non-relativistic electrons without spin, confined in QWRs of infinite barriers and interacting effectively through a Yukawa-like potential. This model allowed us to explore some new features of the Wigner molecule formation and it also showed density correlations of a nearly perfect 1D Wigner crystal that are fully consistent with experimental reports.

In the work, we report the derivation and use of a Yukawa-based effective potential that is able to describe the effects of the spatial confinement and the e- e interaction. As a working model, we report a square cross-sectional GaAs structure embedded into an $\text{Al}_x\text{Ga}_{1-x}\text{As}$ matrix. The resulting effective potential is compared with the Yukawa potential model and with experimental results associated to the Wigner crystallization in QWRs reported in a previous work.



[NSN-650] Core/Shell Magnetite and Silicon Nanoparticles: Synthesis and Characterization

JESUS ROBERTO VARGAS ORTIZ (*jvargas12@alumnos.uaq.mx*)², MARINA VEGA GONZALEZ³, RODRIGO VELÁZQUEZ CASTILLO², MARIA DEL CARMEN GONZALEZ CASTILLO¹, KAREN ESQUIVEL ESCALANTE (*karen_esq_2001@yahoo.com*)²

¹ Faculty of Chemistry Sciences Autonomous University of San Luis Potosí, Av. Dr. Manuel Nava No.6 - Zona Universitaria, S.L.P.

² Faculty of Engineering, Autonomous University of Queretaro, Carr. A Chichimequillas S/N, Terrenos Ejidales Bolaños, Qro.

³ Geosciences Center Autonomous National University of Mexico, Boulevard Juriquilla 3001, 76230 Juriquilla, Qro

Nanotechnology is rapidly advancing, covering an important part of daily and industrial fields, such as the treatment and diagnostics of diseases in medicine. The selective targeting of afflicted tissue or cells is one of the major issues in treating diseases like cancer, which the regular treatments fail to achieve, causing damage to cancerous cells and healthy cells alike[1]. On this regard, magnetic core – shell nanoparticles (Ferrous-Diferric Oxide ($\text{Fe}^{2+}\text{Fe}^{3+}_2\text{O}_4$)), also mistakenly referred to as Iron Oxide coated with Silica (MNP), have recently caught the attention of researchers because of its unique ferromagnetic properties, this means that these particles not only respond to an external magnetic field, but generate their own, producing positive results in different treatment applications[2]. Nevertheless, as it happens with all newly developed pharmaceutical assets, it is still unknown how it will react inside the body once its application is completed and given the size of nanostructures (10^{-9} meters) they are easily transported through cellular membranes and carried away in the bloodstream. Although different toxicological assays exist to test several materials and reagents, nanostructure compounds behave differently given their unique properties attributable to their size, composition, and reactivity. The magnetic nanoparticles (MNP) were synthesized using a modified sonochemical - assisted chemical co - precipitation method with basic pH conditions (NH_4OH) and later coated with Silica using a tetraethoxysilane (TEOS) solution as Silica source to produce the core - shell magnetic nanoparticles ($\text{Fe}^{2+}\text{Fe}^{3+}_2\text{O}_4@\text{SiO}_2$) treated by ethanol extraction and low temperature calcination[3]. The MNP were characterized by XRD, Raman, Zeta potential technology, and SEM. Results show that the as-prepared $\text{Fe}^{2+}\text{Fe}^{3+}_2\text{O}_4$ and $\text{Fe}^{2+}\text{Fe}^{3+}_2\text{O}_4@\text{SiO}_2$ nanoparticles have indeed the desire magnetite “spinel” structure and the core - shell structure without losing its magnetic structure providing the appropriate properties for its targeting applications, proving the sonochemical treatment promising to obtaining and maintaining its magnetic properties, evidencing that the obtained MNP are useful for the subsequent medical application.

- [1] W. N. Missaoui, R. D. Arnold, and B. S. Cummings, “Toxicological Status of Nanoparticles: What We Know and What We Don’t Know,” *Chem. Biol. Interact.*, 2018.
- [2] J. Liu, S. Z. Qiao, Q. H. Hu, and G. Q. Lu, “Magnetic nanocomposites with mesoporous structures: Synthesis and applications,” *Small*, vol. 7, no. 4, pp. 425–443, 2011.
- [3] D. M. de Santiago Colín *et al.*, “Sonochemical coupled synthesis of Cr-TiO₂ supported on Fe₃O₄ structures and chemical simulation of the degradation mechanism of Malachite Green dye,” *J. Photochem. Photobiol. A Chem.*, vol. 364, no. May, pp. 250–261, 2018.



[NSN-653] Release of aromatic essences encapsulated in graphene micro-sponges through an electric potential

Jonathan Soto Soto³, José de Jesús Pérez Bueno (*jperez@cideteq.mx*)¹, Víctor Hugo Castrejón Sánchez³, María Luisa Mendoza López²

¹ Centro de Investigación y Desarrollo Tecnológico en Electroquímica (CIDETEQ), S.C., Pedro Escobedo, Querétaro, CP 76703, México.

² Tecnológico Nacional de México, Instituto Tecnológico de Querétaro, Av. Tecnológico s/n Esq. Mariano Escobedo, Col. Centro, C.P.76000, Querétaro, Qro. México

³ Tecnológico de Estudios Superiores de Jocotitlán, Carretera Toluca-Atlacomulco KM 44.8 Ejido de San Juan y, San Agustín, 50700 Jocotitlán, México.

The aromatic essences have compounds that can be lost due to their high volatility and their oxidation in different environments either in heat or with the air, hence the importance of implementing new methods of encapsulation and release of aromatic essences that give you more lifetime when deposited in certain products.

Graphene micro-sponges are absorbent materials of aromatic essences and due to their capabilities such as thermal conduction, as well as their electrical properties, the essences can be released through the Joule effect, generated by adding a potential difference. This phenomenon can be manipulated to have a controlled release of aromatic essences.

Graphene micro-sponges were functionalized by the Hummers method, but they lose much of their absorption capacity, from absorbing 23 to 25 times their weight, they only absorb 10 times their weight, but with functionalization their conductivity increases electrical since it was found that to release the aromatic essences, a smaller potential difference is needed than that applied to the non-functionalized graphene micro-sponges.

In the case of functionalized graphene micro-sponges, the affection by these phenomena does not occur. With functionalized micro graphene sponges, the potential difference can be manipulated without any problem.

It was observed that despite releasing 100% of the aromatic essences retained in the normal and functionalized graphene micro sponges using the difference in potential functional groups of the essences, this is added to the structure of the micro-sponges, due to the free electrons of the carbon chain of these.

The graphene micro sponges turned out to have greater thermal stability than those that were functionalized since the first ones remain stable until a temperature of 630 °C, reaching combustion at a temperature of 938 °C which is where the sponges are finished degrade. While the functionalized micro sponges remain thermally stable at a temperature of 534 °C and end of degradation at a temperature of 850 °C and even after adding EA to the two types of sponge.

Another phenomena in the tests was the union of graphene micro-sponges to be releasing aromatic essences by applying a voltage. This commonly occurred after exceeding 15 mA, this union in the graphene micro sponges took the form of a filament, and while increasing the intensity of current in the filament it became more incandescent, going from a reddish tone to a white touch when a current intensity greater than 1.70 A was reached and a very intense heat shedding was generated. The analysis with Ocean Optics spectrometry was measured from the wavelength of light emitted by the filaments and this ranges from a wavelength of 350 to 800 nm. The filaments, after a few seconds, broke down attributed to the interaction with oxygen.



XII -ICSMV

September 23rd to 27th, 2019 / San Luis Potosí, México

NANOSTRUCTURES (NSN)

POSTER SESSIONS



[NSN-12] QUASI-INSTANTANEOUS SYNTHESIS OF AuX (X=Cu,Pt) BIMETALLIC NANOPARTICLES AT ROOM TEMPERATURE

Osnaider Rocha Rocha (osnaider.1007@gmail.com) ¹, Mario Flores Acosta ¹, Manuel Cortez Valadez ¹, Raúl García Llamas ¹

¹ Departamento de Investigación en Física, Universidad de Sonora, Blvd. Luis Encinas y Rosales, Hermosillo, Colonia Centro C.P. 8300

In this work, we present a simple and low toxicity method for to obtain bimetallic nanoparticles of AuCu and PtAu. The optical absorption properties were analyzed and an absorption band was observed in the Uv-Vis spectrum centered at 540 nm, associated with localized surface plasmons resonance (LSPR). The location of the LSPR of the nano-alloy was at an intermediate value to the reported for the AuNp and CuNp. Vibrational bands of Raman activity of AuCu nanoparticle clusters were observed between 130-300 cm⁻¹. The structural and optical analyzes of synthesized nanoparticles confirmed the presence of the Au-Cu bond, with spherical geometries and sizes between 5-10 nm. The EDS spectrum showed the coexistence of gold and copper in the samples without the oxidation of copper. For AuPt two absorption bands were observed in the Uv-Vis spectrum around at 300 and 375 nm, both associated with LSPR of nano-alloy of Au and Pt. These optical response were at an intermediate value to the reported for the AuNp and PtNp. The images TEM shown quasi-spherical geometries.

An absorption band was observed in the Uv-Vis spectrum centered at 525 nm for Pt core-Au shell nanoparticles. We did a comparison with the numerical results obtained by means of a computational code that we developed for core-shell nanoparticles with spherical geometries.



XII -ICSMV

September 23rd to 27th, 2019 / San Luis Potosí, México

[NSN-21] Role of the plasmon modes on the optical properties of graphene-metallic film metamaterials

GERARDO Gonzalez de la Cruz (bato@fis.cinvestav.mx)¹

¹ Departamento fr Fisica, CINVESTAV-IPN Apartado Postal14-740, 07000 Ciudad de Mexico,
Mexico

In recent years, the tunable plasmon modes in the terahertz region of a multilayer graphene structure interacting with a metallic film substrate have attracted significant interest motivated by the graphene's unique optical and electronic properties and the possibility to enhance light-matter interaction. In this work, the plasmon waves in graphene layered systems on a conducting thin film are investigated, the hybrid graphene-metal metasurface is surrounded by two semi-infinite materials with different dielectric properties ϵ_1 and ϵ_2 , respectively. The dispersion relations of electronic collective excitations of the structure are calculate by the zeros of an effective dielectric constant obtained from a recursive relation for the amplitudes associated with the electric field between graphene layers in the metasurface. Long-range Coulomb interactions based on the hybrid plasmonic graphene-metal metasurfaces lead a new set spectrum of collective excitations. At long wavelength ($q>0$) the optical modes ($w\sim q^{1/2}$) depend on the two-dimensional carrier density, the metallic thickness, the metallic substrate plasmon frequency, the number of the graphene layers and the dielectric constants in which the hybrid graphene-metal structure is embedded. This latter plays an important role in a wide range of applications such a surface plasmon resonance biological sensors and terahertz surface plasmons in optically pumped graphene metasurfaces.



XII -ICSMV

September 23rd to 27th, 2019 / San Luis Potosí, México

[NSN-22] Ab-initio study of geometric, magnetic and electronic properties of AuxPty ($x + y \leq 5$) clusters.

Pedro Gilberto Alvarado-Leyva (pal@fciencias.uaslp.mx)¹, Elisa Marina Sosa-Hernández (elisasosah@gmail.com)¹

¹ Facultad de Ciencias, Universidad Autónoma de San Luis Potosí. Álvaro Obregón 64, c.p. 78000 San Luis Potosí, S.L.P., México

Employing first-principles methods, based on density functional theory as implemented in VASP code, we present the ground state geometric and electronic structures of binary atomic clusters Au_xPt_y ($x + y \leq 5$). Our results show all the bimetallic clusters present magnetic behavior. In structures with 5 atoms, some global minimum clusters correspond to pure Pt_4 but capped with Au atom. We study the electronic properties such as the ionization potential, electronic affinity and the chemical hardness as an index for catalytic activity.



[NSN-26] Bioconjugation of highly luminescent CdS-dextrin QDs with doxorubicin

Patricia Rodriguez Fragoso (prodriiguez@fis.cinvestav.mx)², Areli Mastache Juarez⁴, Yolanda Elinor Bravo Garcia³, Gerardo Gonzalez de la Cruz¹, Julio Gregorio Mendoza Alvarez¹

¹ Departamento de Física, CINVESTAV-IPN, Apartado Postal 14-740, 07000 México, Ciudad de México.

² Departamento de Física, CINVESTAV-IPN, Apartado Postal 14-740, 07000 México, Ciudad de México.

³ Facultad de Ciencias de la Electrónica, BUAP, Puebla, Puebla. 72000, México

⁴ Facultad de Farmacia, Universidad Autónoma del Estado de Morelos, Cuernavaca, 62210, México

Semiconductor quantum dots (QDs) are a new class of advanced nanomaterials, which provide them with extraordinary physical and chemical properties. QDs are an important tool to realize a great number of biomedical applications. Bioconjugation process involves the reaction of one functional group with another, resulting in the formation of a covalent bond. QDs needed to be conjugated with biological molecules without unsettling the biological function of these molecules. Biomolecules including peptides, proteins, oligonucleotides, and drugs have been successfully linked to QDs. CdS QDs were prepared with one-step aqueous synthesis method. Dextrin was used as capping agent for their effectiveness in limiting the particle growth. In this work, our goal is to conjugate the doxorubicin with dextrin coated CdS QDs. The morphology and the crystalline structure were measured by transmission electron microscopy (TEM) and x-ray diffraction (XRD), respectively. The hydrodynamic diameter distributions of the CdS-dextrin QDs bioconjugated with doxorubicin was estimated by Dynamic light scattering (DLS). Fourier transform infrared (FTIR) spectra was performed to establish the attachment of the Doxorubicin molecule on the CdS-dextrin QDs in the bioconjugation process. The size of the particles obtained from these experiments correlates well with the TEM and Scherrer's formula from XRD patterns. These CdS-dextrin QDs bioconjugated with doxorubicin are in an average range of 5 nm in size, and exhibit an intense fluorescence emitting in the green and red spectrum, which benefited the fluorescence imaging on cells.



[NSN-29] ENHANCE OF ANTIMICROBIAL PROPERTIES OF AMINO ACID CHELATED COPPER NANOPARTICLES PRODUCED BY USING A SOY EXTRACT

Idania De Alba Montero (didania@hotmail.com)¹, Griselda Mayela Loredo Becerra¹, Martha E. Compean Jasso¹, Nereyda Niño Martínez¹, Ana Ketzaly Calvillo Anguiano¹, Alejandra Durán Almendárez¹, Facundo Ruiz¹

¹ *Facultad de Ciencias, Universidad Autónoma de San Luis Potosí*

In this work, I report a new eco-friendly pathway to synthesize a high stable copper-amino acid chelates using a soy extract with potent antibacterial properties against *Escherichia coli*, *Staphylococcus aureus*, and *Enterococcus faecalis*. These copper-amino acids chelates were synthesized by using a soybean aqueous extract and copper nanoparticles were produced using as a starting material the copper-amino acids chelates species. The antibacterial activity of the samples was evaluated by using the standard microdilution method (CLSI M100-S25 January 2015). In the antibacterial activity assays copper ions and copper-EDTA chelates were included as references, so that copper- amino acids chelates can be particularly suitable for acting as an antibacterial agent, so they are excellent candidates for specific applications such as agricultural use, medical therapy, algaecide, food, pest control, fertilizers, paints, irrigation and water treatment. Additionally, to confirm the antimicrobial mechanism on bacterial cells, MTT assay (3-[4,5-dimethylthiazol-2-yl]- 2,5-diphenyltetrazolium bromide) was carried out. Its results would eventually lead to better utilization of copper-amino acids chelate for specific application where copper nanoparticles can be not used.



XII -ICSMV

September 23rd to 27th, 2019 / San Luis Potosí, México

[NSN-33] EVALUATION OF A CHITOSAN HYDROGEL WITH SILVER NANOPARTICLES PREPARED WITH GREEN SYNTHESIS

Aarón Milo Alvarez (ingmilo370z@gmail.com) ¹, Gabriel Alejandro Martínez Castañon ¹,
Nereyda Niño Martínez ¹, Facundo Ruiz ¹

¹ Facultad de ciencias, Universidad Autonoma de San Luis Potosí, San Luis Potosí, México

Chitosan hydrogels and silver nanoparticles were prepared. The silver nanoparticles were synthesized by means of green synthesis, aqueous extract of the Camelia Sinensis plant (White tea) and the Helianthus annuus plant (sunflower). The silver nanoparticles were characterized by DLS, FTIR, SEM, XRD and UV-Vis spectroscopy. The chitosan gel was prepared in combination with the silver nanoparticles, the acidity of the hydrogel was evaluated with pH strips and the viscosity by the propagation test method. Finally, its bactericidal property in S. Mutans bacteria was evaluated by measuring its inhibition halo. The best sizes of nanoparticles were obtained for the synthesis of Helianthus annuus extract, obtaining sizes between 20 and 30 nm. The result was the best inhibition halo of chitosan in combination of AgNps with sunflower extract with a halo of 29.9 mm.



[NSN-36] SYNTHESIS AND CHARACTERIZATION OF BIOCHAR FOR USE AS SUPPORTS FOR ELECTROCHEMICAL CO₂ REDUCTION

R. Rocío García Rocha (*yo_fr7@hotmail.com*) ¹, Salvador Palomares Sanchez ¹, Ismailia L Escalante García ²

¹ Doctorado Institucional en Ingeniería y Ciencia de Materiales, UASLP, San Luis Potosí, México.

² Unidad Académica de Ciencias Químicas, UAZ, Zacatecas

Year after year, the damages caused by global warming have been increasing, as there is a pressing need to reduce greenhouse gases, which cause CO₂, so efforts have been made in several disciplines to not only reduce emissions, but convert them into a source of energy such as hydrocarbons (HC) to alcohols and acids[1], trying to valorize the use of CO₂. So electrocatalysis is seen as an excellent option to achieve this goal. Electrocatalysts are organic or inorganic molecules dissolved in electrolytes with unique active centers that interact with CO₂ molecules. Transition materials are commonly used, such as Platinum, which increased their cost considerably, and therefore work has been carried out that allows not only the reduction of these costs as the increase in efficiency.

One of these efforts has focused on synthesizing nanoparticles capable of replacing the expensive platinum and supports that in addition to increasing the active surface of the catalyst stabilize said nanoparticles in order to reduce CO₂ to significant amounts of hydrocarbons such as methanol and methane under pressure and room temperature.

The present work uses agricultural waste for the synthesis of coals, which will be used as supports in an electrocatalyst, with the intention of reducing the effects of the synthesis of the supports in the environment, in addition to without sacrificing efficiency and using economic precursors and low impact that represent an alternative to harmful solvents, which are used in some traditional synthesis methods. The resulting coals were characterized by Raman spectroscopy, electron scanning microscopy, X-ray diffraction, surface area and adsorption isotherms as well as electrochemically. [1] Yoshio Hori, Akira Murata and Ryutaro Takahashi, 1989, Formation of Hydrocarbons in the Electrochemical Reduction of Carbon Dioxide at a Copper Electrode in Aqueous Solution, J. Chem. SOC., Faraday Trans.



[NSN-53] Trimetallic nanocatalysts with increased activity and durability for the ORR of Pt₂NiCo/C

Hilda Margarita Alfaro López (hilmari105@hotmail.com) ¹, Miriam Marisol Tellez Cruz ², Heriberto Cruz Martínez ², Hugo Rojas Chavez ³, Miguel Adrián Padilla Islas ², Omar Solorza Feria ²

¹ *1 Departamento de Química, Cinvestav, Av. Instituto Politécnico Nacional 2508, San Pedro Zacatenco, Gustavo A. Madero, Ciudad de México, C.P. 07360, Mexico, 2 Escuela Superior de Ingeniería Mecánica y Eléctrica – Departamento de Ingeniería Eléct*

² *Departamento de Química, Cinvestav, Av. Instituto Politécnico Nacional 2508, San Pedro Zacatenco, Gustavo A. Madero, Ciudad de México, C.P. 07360, Mexico*

³ *Tecnológico Nacional de México, Instituto Tecnológico de Tláhuac II, Camino Real 625, Col. Jardines del Llano, San Juan Ixtayopan. Tláhuac, CDMX, C.P. 13508, Mexico.*

The synthesis, physical characterization, and electrochemical evaluation of the carbon dispersed Pt₂NiCo nanocatalyst are analyzed toward the oxygen reduction reaction (ORR) in an acid electrolyte. Here, a novel ternary electrocatalyst synthesized by a chemical route using a mixture of benzyl ether, oleylamine, and oleic acid as dissolvent, as well as tungsten hexacarbonyl as reducing agent, is reported. The physical properties of the Pt₂NiCo/C nanocatalyst were investigated using XRD, EDXS-SEM, and TEM, while the catalytic properties of the Pt₂NiCo/C and commercial Pt/C nanocatalysts were determined through CV, CO-stripping, and RDE electrochemical techniques. XRD and EDXS-SEM corroborated the presence of the three metals in the nanoparticles; while through TEM, the Pt₂NiCo nanoparticles of ~ 10 nm were observed. The measured specific activity for the synthesized nanocatalyst is ~ 6.4 times higher than Pt/C, while its calculated mass activity is ~ 2.2 times higher than Pt/C. The specific and mass activity of the synthesized material is maintained after the accelerated stability test, whereas for Pt/C, these catalytic properties decrease.



[NSN-64] Effect of Light on the Wettability of Assembled SiO₂ and Fe₂O₃ Particles

César Márquez Beltrán (*cmarquez@ifuap.buap.mx*) ¹, Jesús Iván Peña Flores
(*jesuspf@ifuap.buap.mx*) ¹, Enrique Sánchez Mora ¹

¹ Instituto de Física Luis Rivera Terrazas, Benemérita Universidad Autónoma de Puebla

We report an experimental study of the influence of consecutive irradiation with visible and UV light on the wettability of films made by the assembly of SiO₂ or α-Fe₂O₃ particles in the sub-micrometre range. X-ray diffraction (XRD), Raman spectroscopy, Fourier transform infrared (FTIR) were used to examine the structural, and optical properties of the particles. Additionally, we have characterized the colloidal stability through Z potential measurements of the particles, varying the pH in the solution, in order to optimize the conditions for the film formation using a dip coating technique, and a sessile drop experiment serves us for the measurements of contact angle (surface wettability). The results of AFM showed similar surface roughness and topography for both assembled particles but obtaining different wettability character: superhydrophilic ($\theta_W = 8^\circ$) in the SiO₂ case and hydrophilic ($\theta_W = 40^\circ$) in the case of α-Fe₂O₃. The difference of wettability for each system is related to their own surface physicochemical properties rather than the changes on the surface structure, as predicted by the Wenzel equation. The contact angle (CA) of drop water onto the α-Fe₂O₃ surface is changing when is irradiated by visible (2.7 eV) and UV (4.2 eV) light, i.e., from $\theta_W = 37^\circ$ (hydrophilic) to 15° (highly hydrophilic), respectively. This behavior is attributed to the amount and the mechanism of the recombination of electron-hole pair that interacting with organic molecules as well as the dissociative adsorption of water from moisture. This work could provide new insights to control the wettability on complex geometries and structures of hydrophilic surfaces when is irradiated with light at different wavelengths

**[NSN-66] ZrO₂ Nanopowders synthesized by means the polyol method.**

Guillermo Juárez-López (gjuarezl@hotmail.com) ⁴, Rafael Martínez-Martínez ⁴, Bernardo Macedas-García ⁴, E. Isac Velazquez-Cruz ⁴, Edgardo Yescas-Mendoza ⁴, Gilberto Alarcón-Flores ³, Salvador Carmona-Téllez ², Miguel Ángel Aguilar-Frutis ³, Ciro Falcony-Guajardo ¹

¹ CINVESTAV-IPN Zacatenco, Av. National Polytechnic Institute # 2508, Mexico City, CDMX.

² CONACyT-BUAP

³ Instituto Politécnico Nacional, Centro de Investigación en Ciencia Aplicada y Tecnología Avanzada, Legaría 694 Colonia Irrigación, Mexico City C.P. 11500, Mexico.

⁴ Technological University of the Mixteca, Road Acatlima km 2.5, Huajuapan de León, Oaxaca.

Zirconia (ZrO₂) nanopowders were obtained by means of the Polyol method, using as precursor reagent Zirconium Oxynitrate (IV) hydrated [ZrO(NO₃)₂·xH₂O], using diethylene glycol as a reaction medium for the reduction of the precursor, as a stabilizing agent and solvent. Deionized water was added in order to obtain more elements of oxygen, and achieve the formation of zirconia to observe its influence in obtaining nanometric crystals sizes. By means of this methodology, it was possible to carry out the synthesis of Zirconium Oxide and obtain a white and fine powder after submitting a thermal treatment at 300°C, 500°C and 700°C with a constant flow of oxygen since 3 to 5 LPM. The structural characterization of ZrO₂ by XRD it was determined the coexistence of the monoclinic and tetragonal phases with a grain size between 12 to 16 nm, using the Scherrer's formula. The micrographs obtained through SEM, it is known that the surface consists of a rough relief formed by dense semi-spherical agglomerates and nanometric sizes, it is emphasized that with a concentration of deionized water the particles are more united. The composition of the ZrO₂ samples obtained by EDS was determined according to the variation de-ionized water concentrations, resulting in the presence of zirconium ions and a large amount of oxygen, having a small proportion of nitrogen coming from the precursor agent, it was possible to find a minimum concentration of carbon. The thermograms do not display a relationship between the heat exchange with the loss of mass with respect to the increase in temperature, the mass quantity of the samples remain unchanged throughout this analysis, reaching the temperature up to 700°C indicating that the crystalline phases of ZrO₂ are complete.



[NSN-68] IMMUNOSENSORS BASED ON CARBON NANOSTRUCTURES FOR CHRONIC-DEGENERATIVE DISEASES DIAGNOSIS

ANTONIO ROWLAND RAMOS-DÍAZ (*ing.rowalnd@gmail.com*)³, RAMON GÓMEZ-AGUILAR (*rgomez@ipn.mx*)⁴, HUGO MARTÍNEZ-GUTIÉRREZ¹, JAIME ORTIZ-LÓPEZ², GERARDO ORTEGA-CERVANTEZ²

¹ Instituto Politécnico Nacional, CNMN, Av. Luis Enrique Erro s/n, 07738 Ciudad de México, México.

² Instituto Politécnico Nacional, ESFM, Av. Instituto Politécnico Nacional, 07738 Ciudad de México, México.

³ Instituto Politécnico Nacional, ESIQIE, Av. Instituto Politécnico Nacional s/n, 07738 Ciudad de México, México.

⁴ Instituto Politécnico Nacional, UPIITA, Av. Instituto Politécnico Nacional, 07340 Ciudad de México, México.

In this work we present the manufacture and characterization of immunosensors based on carbon nanostructures and semiconductor polymers, using an impedance transducer that allows the quantification of protein markers associated with chronic-degenerative diseases, by means of electrochemical detection. The design and optimization of manufacturing of this type of sensors based on carbon nanostructures is the main objective of our work. From reduced graphene oxide and multiple wall carbon nanotubes, impedometric transducers were constructed that were electrically characterized to look for reproducibility, specificity and sensitivity for the detection of compounds in electroactive solutions. The results obtained allow us to conclude that the devices constructed from the aforementioned nanostructures are feasible in 80% as immunosensors, the foregoing proposes a rapid, low cost and sensitive analysis for the detection and diagnosis of diseases such as cancer.



[NSN-77] Synthesis of ZnO inverse opal photonic crystals

Mónica Paola Vega García (paoola_495@hotmail.com)³, Karina Cruz Martínez³, Bernabé Rebollo Plata⁵, Gerardo Francisco Pérez Sánchez¹, Mercedes Portillo Sampedro³, Jesús Rodríguez Mera³, Maribel Méndez Otero², Gregorio Hernández Cocoletzi⁶, Mirna López Fuentes⁴, Benito Zenteno Mateo⁴, Estefanía Yañez Mota²

¹ Departamento de Investigación de Fisicoquímica de Materiales, Instituto de Ciencias de la Universidad Autónoma de Puebla, Benemérita Universidad Autónoma de Puebla, Val 3, Independencia O 2 Sur 50, San Pedro Zacachimalpa, Puebla, México

² Facultad de Ciencias Físico Matemáticas, Benemérita Universidad Autónoma de Puebla, Avenida San Claudio y 14 Sur, Ciudad Universitaria, Puebla, Puebla, C.P. 72570, México

³ Facultad de Ingeniería Química, Benemérita Universidad Autónoma de Puebla, Avenida San Claudio y 18 Sur, Ciudad Universitaria, Puebla, Puebla, C.P. 72570, México

⁴ Facultad de Ingeniería, Benemérita Universidad Autónoma de Puebla, Boulevard Valsequillo s/n, Ciudad Universitaria, Puebla, Puebla, C.P. 72570, México

⁵ Instituto Tecnológico Superior de Irapuato, km 12.5 Carretera Irapuato-Silao, Irapuato, Guanajuato, C.P. 36821, México

⁶ Instituto de Física, Benemérita Universidad Autónoma de Puebla, Avenida San Claudio y 18 Sur, Edificio 14-B, Ciudad Universitaria, Puebla, Puebla, C.P. 72570, México

Zinc oxide (ZnO) inverse opal photonic crystals (PhCs) structures were fabricated on a seed layer using three-dimensional (3D) colloidal crystal templates. The 3D colloidal crystal templates were fabricated from poly (methyl methacrylate) sphere (PMMA) by a free radical chain-growth polymerization. Result of the scanning electron micrograph (SEM) technique show that the ZnO inverse opals (PhCs) are formed with spheres of 235.29 nm in diameter ordered in fcc structure with (111) planes parallel to the surface of the sample. From results of reflectance measurements structures possess the photonic band gaps in the near-ultraviolet range. Fourier transform infrared (FT-IR) absorption spectra of pure PMMA. Pure PMMA showed an IR absorption band at 1513 cm⁻¹ due to asymmetric bending vibration (CH₃) of methyl group. The band at 1282 cm⁻¹ was due to -OCH₃ stretching. A sharp band located at 1754 cm⁻¹ was ascribed to the carbonyl group. The band located at 1098 cm⁻¹ was attributed to the C-O group.

The technology can effectively increase efficiency for the applications of sensors.



[NSN-86] Theoretical study of the effects of surface lithiation on the structural and electronic properties of Si nanowires

Jacqueline Rebollo Paz ¹, Margarita C. Crisóstomo ², David Fernández Lara ³, Fernando Salazar Posadas (fsalazarp@ipn.mx) ³, Miguel Cruz-Irisson ³

¹ CECyT C.V.M., Instituto Politécnico Nacional, Ciudad de México, México

² CECyT N.B.G., Instituto Politécnico Nacional, Ciudad de México, México

³ ESIME-Culhuacán, Instituto Politécnico Nacional, Ciudad de México, México

In this work, we present a density functional theory study of the mechanical and electronic properties of silicon nanowires (SiNWs) grown along the [111] and [001] crystallographic directions with a diamond structure and surface passivated with hydrogen (H) and lithium (Li) atoms. The study is performed within the local density approximation by applying the supercell method. The results indicate that the energy gap is a function of the Li concentration for both studied directions. The binding energy is almost independent of the concentration of Li atoms and stay almost constant for both studied directions. Furthermore, the Young's modulus (Y), increases as function of the Li concentration at the surface leads to a larger Y value compared to the Y value of the completely H-passivated SiNWs. These results indicate that it is possible to simultaneously control the energy gap and the Young's modulus by tuning the Li concentration on the surface of the SiNWs and could help to understand the structural changes that the silicon nanowire arrays experience during the lithiation process in Li batteries.

This work was supported by IPN projects 2018-1669, 1937, and PAPIIT-DGAPA-UNAM IN107717. The supercomputing resources were given through LANCAD-UNAM-DGTIC-180 project and Abacus-CINVESTAV.



XII -ICSMV

September 23rd to 27th, 2019 / San Luis Potosí, México

[NSN-97] ZIF and HUSK structural MOF derived carbón materials embedded with NiCo alloy nanoparticles.

Ana de Monserrat Navarro Tellez ¹, Cesar Máximo Oliva González ¹, Boris Ildusovich Kharissov (bkhariss@hotmail.com) ¹, Yolanda Peña Méndez ¹

¹ Facultad de Ciencias Químicas, Universidad Autónoma de Nuevo León, Ave. Universidad S/N, Cd. Universitaria, San Nicolás de los Garza N.L. México, C.P. 66455.

The use of MOF (metal-organic structures) as templates to prepare carbon-based composites have favorable morphological characteristics for a wide variety of applications including adsorption, catalysis and electronics. In this work, we report on the synthesis and characterization of carbon structures nanoporous compounds with Co and Ni nanoparticles, by direct pyrolysis of metal-organic structures (MOF) of Co / Ni with nitrogen flow at different temperatures (300 ° C, 500 ° C and 700 ° C.), using as ligands 1-methylimidazole for ZIF type structures and Trimesic acid (H3BTC) for HUSK type structures.

The synthesized composites showed great advantages in terms of morphology, revealing greater agglomeration of particles as the pyrolysis temperature increases and the presence of metal oxide nanoparticles, concluding with an average particle size of 80 nm, demonstrating great potential as low cost materials. All these results were obtained by characterization using methods such as powder X-ray diffraction (XRD), Fourier transform infrared spectrometry (FT-IR), scanning electron microscopy (SEM) and energy dispersive X-ray spectroscopy (EDX).



[NSN-147] Type I $\text{In}_{0.145}\text{Ga}_{0.855}\text{As}_y\text{Sb}_{1-y}$ alloys: Structural, chemical and optical properties.

A.L. Martínez-López (anlomartinez@esimez.mx)², G. Villa-Martínez², M. Ramírez López², P. Rodríguez-Fragoso¹, J.G. Mendoza-Álvarez¹, J.L. Herrera-Pérez², Y.L. Casallas-Moreno²

¹ Physics Department, Centro de Investigación y de Estudios Avanzados del IPN, C.P. 07360, México.

² Unidad Profesional Interdisciplinaria en Ingeniería y Tecnologías Avanzadas-Instituto Politécnico Nacional, Av. IPN 2580, Col. Barrio la Laguna Ticomán, Gustavo A. Madero, C.P. 07340, México.

Antimonide family has become one of the most potential semiconductor materials to develop a new generation of applications in the infrared, such as laser diodes, light-emitting diodes (LEDs), thermophotovoltaic cells and detectors. These devices are promising for a large variety of biomedical, environmental and industrial applications. Among the antimonide family, the $\text{In}_x\text{Ga}_{1-x}\text{As}_y\text{Sb}_{1-y}$ alloy covers a wide electromagnetic spectrum from near infrared (1.7 μm) to medium infrared (3.5 μm), with a direct band gap [1,2]. In this study we showed the changes of the crystalline quality and of the infrared emission, as well as the growth mechanism of the $\text{In}_{0.145}\text{Ga}_{0.855}\text{As}_y\text{Sb}_{1-y}$ alloys by varying the arsenic (As) content. These quaternary alloys were grown by liquid phase epitaxy (LPE) on intrinsic GaSb (100) substrates. The alloys presented a tensile strain over the substrate, which increases with the As content. Furthermore, we found a nearly lattice-matched between the alloys and the GaSb substrates of $\Delta a/a \approx 10-4$, allowing a stable configuration of the $\text{In}_{0.145}\text{Ga}_{0.855}\text{As}_y\text{Sb}_{1-y}$. The alloys showed excitonic transitions evidencing the high crystalline quality, whose energy decreases with the As content. Additionally, we have also identified that the stable atomic arrangement of the quaternary alloy is mainly formed by two compounds, Ga-Sb and In-As, such as was proved by X Ray Photoelectron Spectroscopy (XPS).

[1] An, N.; Ma, L.; et. Al. Structure Design and Analysis of 2 μm $\text{InGaAsSb}/\text{AlGaAsSb}$ Muti-Quantum Well Laser Diode with Carrier Blocking Layer. *Appl. Sci.* 2019, 9, 1-7.

[2] Borca-Tasciuc T; Song, D. W.; et. Al. Thermal conductivity of $\text{AlAs}_{0.07}\text{Sb}_{0.93}$ and $\text{Al}_{0.9}\text{Ga}_{0.1}\text{As}_{0.07}\text{Sb}_{0.93}$ alloys and $(\text{AlAs})_1/(\text{AlSb})_{11}$ digital-alloy superlatticess. *J. Appl. Phys.* 2002, 92, 4994-4998.

**[NSN-174] ZrO₂:Eu³⁺ thin films obtained by the pyrosol technique**

Guillermo Juárez-López (gjuarezl@hotmail.com) ⁴, Rafael Martínez-Martínez ⁴, Edgardo Yescas-Mendoza ⁴, E. Isac Velazquez-Cruz ⁴, Gilberto Alarcón-Flores ³, Salvador Carmona-Téllez ², Miguel Ángel Aguilar-Frutis Aguilar-Frutis ³, Ciro Falcony-Guajardo ¹

¹ CINVESTAV-IPN Zacatenco, Av. National Polytechnic Institute # 2508, C.P. 07360. Mexico City, CDMX.

² CONACyT-BUAP

³ Instituto Politécnico Nacional, Centro de Investigación en Ciencia Aplicada y Tecnología Avanzada, Legaria 694 Colonia Irrigación, Mexico City C.P. 11500, Mexico.

⁴ Technological University of the Mixteca, Road Acatlima km 2.5, Huajuapan de Leon, Oaxaca.

ZrO₂:Eu³⁺ photoluminescent films were successfully obtained by the pyrosol technique, from the zirconium acetylacetone [Zr(C₅H₇O₂)₄] as precursor, doped with Europium (Eu³⁺) deposited on Corning glass substrates. Using different concentrations of the precursor [Zr(C₅H₇O₂)₄] 3, 5 y 7 Molar, as well as different concentrations of the Eu³⁺ dopant ions using from 1% to 15% with increases of 2% in relation to the molar mass of the precursor. The deposit conditions were explored by varying the temperature from 300°C to 550°C in increments of 50°C, using dimethylformamide HCON(CH₃)₂ and methyl alcohol CH₃-OH as a solvent in a 4:1 ratio, respectively. The best experimental deposit conditions to obtain ZrO₂:Eu³⁺ photoluminescent films were at a temperature of 450 ° C, with precursor at 5% Molar and 9% Eu³⁺, distance nozzle-substrate 1 cm, Nitrogen flow 10 LPM, deposit time 20 min, with a piezoelectric frequency of 0.8 MHz, thus generating films with good adherence and transparency. The dependence of the photoluminescence properties on the annealing temperature was examined, the excitation spectra of Eu³⁺ doped ZrO₂ with a monitoring emission wavelength at 615nm, obtaining in these conditions an excitation wavelength at 286 nm. According to these result, the emission spectra of Eu³⁺ doped ZrO₂ were measured with an excitation wavelength at 286 nm, that consisted of four emission peaks with the emission centre at 590 nm, 598 nm, 615nm and 627 nm, respectively.



XII -ICSMV

September 23rd to 27th, 2019 / San Luis Potosí, México

[NSN-177] Spectroscopic and surface study of commercial aluminum foil for using as a SERS substrate

José Guadalupe Morales Méndez (jose_gmm@hotmail.com)², José Rafael Godínez Fernández¹, Emmanuel Haro Poniatowski²

¹ *UAM Izt. Department of electrical engineering San Rafael Atlixco No. 186, Col. Vicentina, Iztapalapa CDMX Mexico*

² *UAM Izt. Physics department San Rafael Atlixco No. 186, Col. Vicentina, Iztapalapa CDMX Mexico*

Three commercial brands of aluminum foil available in Mexico (Reinolds, Avilés, Great Value) are studied. In this work, we have obtained experimental results which demonstrate that commercial aluminum foil enhances the Raman signal. The Raman signal enhancement of methylene blue at a concentration of 1×10^{-6} M has been analyzed by placing a drop (6 uL) onto samples of the three commercial brands of aluminum foil and the reference. Preliminary results show that Raman enhancement has been observed in the Great Value samples. Microchannels on the surface of the three commercial brands of aluminum foil have been observed via SEM; their origin is possibly due to the aluminum foil manufacturing process. We hypothesize that these microchannels give rise to the Raman enhancement of methylene blue.



[NSN-261] ZINC NANOSTRUCTURES FOR THE SAFE TREATMENT OF NITROAROMATICS

Ma. Guadalupe García Valdivieso (guadalupe.valdivieso@uaslp.mx)², Brenda Acosta Ruelas (brenda.acosta@uaslp.mx)³, Karí Martínez Reyna², Andrey Simakov¹, Hugo Ricardo Navarro Contreras²

¹ *Centro de Nanociencias y Nanotecnología de la UNAM, Ensenada, B.C., México*

² *Coordinación para la Innovación y Aplicación de la Ciencia y la Tecnología (CIACYT-UASLP), Av. Sierra Leona #550, Col. Lomas 2a. Sección, CP 78210, San Luis Potosí, S.L.P., MÉXICO.*

³ *Cátedra CONACYT, CIACYT- Universidad Autónoma de San Luis Potosí, San Luis Potosí, México*

Zinc-based nanostructures have been widely used in many scientific fields related to materials development. The synthesis assisted by microwave is a revolutionary method for the preparation of homogeneous products with good yield and purities. Among the advantages of this method are the fast heating of reaction mixtures, even seconds, and quick reach high pressures and temperatures. Zinc nanostructures prepared via microwave have been characterized with several shapes, such as porous nanonodules, nanorods, nanoneedles, nanodisk, nanocandles, nanonuts, nano/microstars, etc., by simple control in the irradiation methods.

The aim of this study is to synthesize novel zinc-based nanostructures, in both morphology and physicochemical properties, with carbon nanotubes (CNT), via microwave assisted synthesis with remarkable performance in adsorption, photodegradation and catalytic transformation of nitroaromatic compounds. Obtained nanostructures were characterized by UV-Vis and Raman spectroscopy, TEM, SEM. The photodegradation, adsorption and the catalytic performance were evaluated using 4-nitrophenol as a model molecule and monitored by in situ UV-Vis spectroscopy.

The positive interaction between ZnO and CNT in photodegradation and adsorption of dangerous nitroaromatics was revealed. The microwave assisted synthesis favors the homogenous formation in both size and distribution of ZnO on the surface of CNT. The physicochemical properties of the obtained ZnO/CNT composites are comparable with that achieved by other methods. The synergistic effect of ZnO/CNT composite results are potentially advantageous in catalytic applications.



[NSN-279] pH influence on properties and Kinetics of CdS_{1-x}Sex nanoparticles grown by controlled precipitation

Elvia Angelica Sanchez-Ramirez (saraelan2411@hotmail.com) ¹, Daniela Carrillo-Medina

¹, Isaias Daniel Peralta-Vazquez ¹, Luis Ramon Arellano-Piña ¹, Cesar Vazquez-Morales

², Maria de los Angeles Hernandez-Perez ²

¹ Departamento de Ingeniería Metalúrgica - UPIIZ, Instituto Politécnico Nacional,
Zacatecas, 98160, Mexico,

² Departamento de Ingeniería en Metalurgia y Materiales - ESIQIE, Instituto Politécnico
Nacional, Ciudad de México, 07738, Mexico

Last years, research of semiconductor II-VI materials has been amply developed because of the potential applications; such as optoelectronic devices, solar cells, sensors and photovoltaic cells. The main interest is by focusing on the improvement optical, electrical, photoelectrochemical properties. These materials can be obtain on different presentations e.g. quantum dot, core shell, nanoparticles and films. Semiconductors can be synthetized by different techniques like as laser ablation, sol gel, sputtering and controlled precipitation among others. CdS exhibit cubic and hexagonal phases, some papers report a mixture of these structures, have a bandgap (E_g) of 2.42. Precipitation is an easy and economic technique, it is not necessary a sophisticated equipment, reaction occurs at low temperature in solution, most of the times in alkalin medium. On this paper, CdS nanoparticles were prepared varying the pH on the solution of 4 to 11, at 30 min and at 75°C by using controlled precipitation method that allows the control on the properties. In this work, the conditions of the grown were pH varying the quantity of NH₄OH and HCl. The analysis were realize using X ray Diffraction (XRD), scanning electron microscopy (SEM) and UV-VIS Spectroscopy. The main objective was establish the influence of pH on the structural and optical properties and reaction efficiency.

The properties of CdS particles are strongly affected by pH. Studies on semiconductors II-VI report that this material present cubic or hexagonal phase some of them say that it is possible a mixture of both phases. XRD patterns shows that the CdS particles are polycrystalline and exhibit hexagonal phase, in the case of particles growth in acid medium but for particles synthetized with pH≥9.2 the crystal structure is a mixture of cubic and hexagonal phase. Cadmium impurities are observed for some materials that is obtained of secondary reactions affecting the reaction yield. The quantity of the impurities decreases in acid medium. Crystal size was calculated according to the Scherrer's equation using the full width at half maximum (FWHM) of (111) and (002) planes. Crystal size oscillate between 6± 2 nm without show a clear tendency. Surface morphology of CdS is formed by nanocluster of particles that increase on size from 20 to 500 nm in function of pH, i.e. bigger nanocluster are obtained in alkaline medium. The kinetics of the growth changes with pH, reaction yield increase as augment pH, on the contrary band gap decrease as pH increases.



[NSN-280] CHARACTERIZATION OF SILVER –ACRYLIC NANOCOMPOSITES TO BE USED IN 3D PRINTING.

José Luis Luna Sánchez (jluis.lunas@gmail.com)³, José Luis Jiménez Pérez (jimenezp1957@gmail.com)³, Alfredo Cruz Orea², Marcos Macías Mier², Mario Perez Gonzalez⁴, Zormy Nacary Correa Pacheco¹

¹ *3. CONACYT-Instituto Politécnico Nacional. Centro de Desarrollo de Productos Bióticos. Carretera Yautepec-Joxtla, km. 6, Calle CEPROBI, No. 8, San Isidro, Yautepec, C.P. 62731, Morelos. México*

² *Physics Department, CINVESTAV-IPN, AP 14-740, 07360 Mexico City, Mexico*

³ *Unidad Profesional Interdisciplinaria en Ingeniería y Tecnologías Avanzadas-Instituto Politécnico Nacional, Av. Instituto Politécnico Nacional No. 2580, Col. Barrio la Laguna Ticomán, Del. Gustavo A. Madero, C.P. 07340 Ciudad de México, Mexico.*

⁴ *Área Académica de Matemáticas y Física, Instituto de Ciencias Básicas e Ingeniería, Universidad Autónoma del Estado de Hidalgo, Carr. Pachuca-Tulancingo Km 4.5, Col. Carboneras, C. P. 42184, Mineral de la reforma, Hidalgo, México.*

Among the materials used to print 3D prototypes, composites gather important interest due to their properties that sometimes can be modified on demand. In this research, composites formed by a photosensitive Acrylic Resin and Silver nanostructures; were compounded. The Silver nanostructures were Silver Nanowires (AgNW), synthesized by the polyol method; and Silver Nanoparticles (AgNPs), synthesized by a green method. The nanostructures were analyzed by Transmission Electron Spectroscopy (TEM) to determine shape and size dispersion and by X-Ray Diffraction (XRD) to determine its structure. Fourier Transform Infrared Spectroscopy (FTIR) analyses were performed on pure resin and the composites to observe changes in resonance spectra. Characteristic curing time for the composites will be determined employing a photoacoustic spectroscopy open cell (PA-OPC) experimental set up.



[NSN-284] The role of structural defects in the growth of ZnTe nanorods by mechanochemical synthesis

H. Rojas Chávez (huroch@gmail.com)⁶, Rurik Farías⁶, H. Cruz Martínez⁷, J.L. González Domínguez³, N. Daneu¹, J.M. Juárez García², A. Ávila García⁴, R. Román Doval⁵

¹ Advanced Materials Department, Jožef Stefan Institute, Jamova cesta 39, SI-1000 Ljubljana, Slovenia

² Centro Nacional de Metrología, km 4.5 carretera a Los Cués, Municipio del Marqués, Santiago de Querétaro, 76246 Qro., Mexico

³ Departamento de Física, Centro de Investigación y de Estudios Avanzados del Instituto Politécnico Nacional, Av. Instituto Politécnico Nacional 2508, Col. San Pedro Zacatenco, Gustavo A. Madero, 07360, CDMX, Mexico

⁴ Departamento de Ingeniería Eléctrica-SEES, Centro de Investigación y de Estudios Avanzados del Instituto Politécnico Nacional, Av. Instituto Politécnico Nacional 2508, Col. San Pedro Zacatenco, Gustavo A. Madero, 07360, CDMX, Mexico

⁵ Facultad de Química, Universidad Autónoma de Querétaro, Centro Universitario, Santiago de Querétaro, 76010, Qro., Mexico

⁶ Instituto de Ingeniería y Tecnología, Departamento de Física y Matemáticas, Universidad Autónoma de Ciudad Juárez, Av. del Charro 450 Col. Romero Partido, 32310 Juárez, Chihuahua, Mexico

⁷ Tecnológico de Monterrey, School of Engineering and Sciences, Atizapán de Zaragoza, Estado de México, 52926, Mexico

The high-energy milling process offers a versatility to synthesize almost any desired phase composition of any kind of alloy or compound. However, provided that one understands how to control process variables, the morphology of the final as-milled product can also be controlled. If one considers the nature of precursors (which are strongly dependent on their deformation mechanisms) as a variable of the milling system, then the response of precursors to deformation, due to crystalline defects, can be used as a strategy to control the final morphology of the as-milled powders. In this work, the mechanochemical synthesis of ZnTe nanorods is promoted by a structural-defect approach, which has been sequentially traced –by means of transmission electron microscopy (TEM)– as an evolution from highly deformed nanoparticles to multi-twinned nanoparticles and thereof to ZnTe nanorods. The effect of the ZnTe nanorods is discussed in terms of its photoluminescence (PL) spectrum. TEM results confirm that when the as-milled powders underwent all kind of deformation mechanisms and once this point is overpassed, the multi-twinned nanoparticles broke down along the twin boundaries giving way to nanorods. Finally, the aspect ratio and related optical properties of ZnTe nanorods are discussed based on TEM and PL results.



[NSN-295] SUPER-FLUIDIFICATION ADDITIVE BASED ON POLYCARBOXYLATE AND NANOPARTICLES OF SiO₂ FOR USE IN HYDRAULIC CONCRETE

Manuel de Jesus Ungsson Nieblas (manuel_ungsson@hotmail.com)², Jorge Luis Almaral Sánchez (jalmaral@uas.edu.mx)², Efraín Rubio Rosas¹, Andres Castro Beltrán², Carlos Augusto López Lazcano², Gibran Guadalupe Martínez Falomir²

¹ *Benemérita Universidad Autónoma de puebla, Prolongación de la 24 Sur y Av. San Claudio, Ciudad Universitaria, Col. San Manuel C.P. 72570 Puebla, Puebla, México*

² *Facultad de Ingeniería Mochis, Universidad Autónoma de Sinaloa, Fuente Poseidón y A. Flores s/n, C.U., Los Mochis, Sin. C.P.81223*

The basic components of hydraulic concrete are cement, water, fine and coarse aggregate, any other ingredient in its preparation is considered as an additive, which is added to the concrete before, during or after mixing, to improve its properties, such as mechanical, physical-chemical, chemical or physical. The superfluidifying additives used today are synthetic water-soluble polymers, called polycarboxylates, reach water reductions up to 40%, while the nano-powders most commonly used are nano-SiO₂, nano-Al₂O₃ and nano-Fe₂O₃, where fluidizers have become one of the indispensable ingredients in concrete formulations, which functions as a dispersing agent for cement grains and increases the fluidity of cement mixes without additional water demanded, called plasticizing effect, being understood that the dispersing effect is closely related to its adsorption on the surface of cement, with adding silica nanoparticles increases the development of the compressive strength of mortars, small size of the particles of nano-SiO₂ provides a larger area, which accelerates the rate of hydration of cement and pozzolanic reactions with crystals of calcium hydroxide producing C-S-H gel, Therefore, the size and quantity of calcium hydroxide crystals are significantly reduced. In this study, polycarboxylate and SiO₂ nanoparticles (PCNPS) were used to improve the fluidity and strength of the hydraulic concrete. The addition of PCNPS resulted in an increase in resistance of 18% according to reference mixtures, in fluidity tests at the first minutes, it was possible to improve its fluidity by 10%, less absorption in the mixtures with additive, having a lower number of pores in the specimens of the concrete.



[NSN-300] Green fabrication of Au nanoparticles incorporated on mesoporous TiO₂ (TiO₂/Au NPs) for catalytic reduction of 4-nitrophenol

Siva Kumar Krishnan (*sivakumar@ifuap.buap.mx*) ¹, Mou Pal ², Andrés Guzmán Cruz (*aguzman@ifuap.buap.mx*) ²

¹ CONACYT-Instituto de Física, Benemérita Universidad Autónoma de Puebla, Av. San Claudio y Blvd 18 sur Col. San Manuel Ciudad Universitaria C.P 72570 Puebla, México.

² Instituto de Física, Benemérita Universidad Autónoma de Puebla, Av. San Claudio y Blvd 18 sur Col. San Manuel Ciudad Universitaria C.P 72570 Puebla, México.

In the present work, we report a facile, and ecofriendly approach to fabricate mesoporous titanium dioxides (TiO₂) decorated with gold nanoparticles (Au NPs) using deep eutectic solvent (DES) based on choline chloride/Urea (ratio 1:2) for efficient catalytic reduction of 4-nitrophenol. Specifically, the mesoporous TiO₂ was obtained using solvothermal method at 180°C for 15 h, subsequently a thermal treatment step was applied without oxygen flow at 500 °C in a muffle furnace for 3 h to achieve anatase crystalline phase. In the second step, the Au NPs was incorporated onto TiO₂ surface by reducing HAuCl₄ precursor using sodium citrate as reducing agent at 95 °C in a thermal bath. Different techniques were used to study their chemical composition, structural, optical, phase crystalline, morphology, superficial area and porosity. The X-ray diffraction (XRD) and Raman scattering analysis revealed that the both TiO₂ and TiO₂/Au NPs samples present in anatase phase. The optical results suggest the good light absorption capacity in the ultraviolet region for pure TiO₂ whereas TiO₂/Au NPs exhibit the absorption peak at 548.0 nm associated to the characteristic surface plasmon resonance (SPR) due to Au NPs. In addition, the estimated band gap values were 3.16 eV for the TiO₂ and 3.0 eV for the TiO₂/Au NPs sample, while the E_g of un-annealed TiO₂ had a band gap of the 3.42 eV. Finally, the resultant samples were investigated for the catalytic reduction of 4-nitrophenol by NaBH₄. The results revealed that the Au/TiO₂ catalyst manifests higher catalytic performance in comparison with the pristine TiO₂ sample. The present environmental friendly, and efficient approach for the controlled fabrication of mesoporous TiO₂, and TiO₂/Au NPs provide exciting opportunities for the fabrication other hybrid nanostructures for efficient catalysis. Acknowledgments. This work was partially supported by the CONACyT and, VIEP-BUAP (Grant # 100523733). Andrés Guzmán Cruz (CVU # 862151) is thankful to CONACyT for extending doctoral scholarship.



[NSN-303] Electronic transport in nanowire Y-junctions

Elihu Sánchez-Martínez (elihuuhazels@yahoo.com.mx) ¹, Esteban Cruz-Hernández ¹, Reyna Méndez-Camacho ¹, John Eder-Sánchez ¹

¹ Coordinación para la Innovación y la Aplicación de la Ciencia y la Tecnología (CIACYT-UASLP), Sierra Leona 550, C. P. 78210, San Luis Potosí, S.L.P., México

One of the challenges in nanoelectronics is the miniaturization of components used in electronic devices. Nowadays there are some investigations that seek to overcome the barriers presented by this miniaturization. One of such investigations is the electronic transport in carbon nanotube Y-junctions, which exhibit a switching behavior that make it potential candidates for a new class of transistors [1]. However, this kind of switching behavior could be advantageous for nanoelectronic applications if semiconductor materials could be used instead.

In this work, we present an experimental and theoretical study of the electronic transport in semiconductor nanowire Y-junctions. The synthesis of these one-dimensional nanostructures was carried out by molecular beam epitaxy (MBE). 12 nm-thick GaAs layers sandwiched between AlGaAs barriers were grown on GaAs (631) substrates by varying the growth temperature (640 °C, 690 °C and 720 °C). The Y-junction GaAs structures were self-assembled as described elsewhere [2]. The n-type doping of the nanostructures was carried out with Si by using two delta doping layers inside the AlGaAs barriers. The surface characterization of the samples was performed in-situ by RHEED and, at the end of the growths, by using atomic force microscopy (AFM) to verify the formation of the Y-junctions at the GaAs/AlGaAs interface. Platinum metal contacts were placed on the nanostructure employing the Gas Injection System tool coupled to a scanning electron microscope (SEM). Electrical transport measurements and the development of a theoretical description of the Y-junction systems, that are currently in progress, will be presented.[1] P. R. Bandaru, C. Daraio, S. Jin and A. M. Rao, Nat. Mater., 2005, 4, 663–666. [2] R. Méndez-Camacho, M. López-López, V. H. Méndez-García, D. Valdez-Pérez, E. Ortega, A. Benitez, A. Ponce and E. Cruz-Hernández, RSC Adv., 2017, 7, 17813-17818



XII -ICSMV

September 23rd to 27th, 2019 / San Luis Potosí, México

[NSN-337] Nano graphene oxide functionalized by green reduction for biomedical applications

Andrés Rodolfo Serrano Castro (mmendezg07@yahoo.com.mx)¹, Arturo García Borquez
¹, María Magdalena Méndez-González¹

¹ Physics department, ESFM-IPN, U.P. Adolfo López Mateos, Edif. 9, Lindavista 07738 CDMX, México

Graphene oxide possesses great surface energy, due to its unsaturated bonds and its high reactivity, so it needs to be reduced by epigallocatechin-3-gallate for biomedical uses. The green reduction uses methods friendly to the environment and to biological systems that ensure their null toxicity. The UV-vis spectra obtained in the method of thermal reduction at 95 °C with ascorbic acid show a greater displacement compared to the method by reduction by ultrasonic bath. Changes in the properties of optical transmission with respect to its initial constituents are evident in the functionalized graphene oxide spectrum. This suggests a strong interaction at the molecular level of the graphene oxide network with the epigallocatechin-3-gallate molecule. The functionalized nanometric graphene oxide, due to its size, can easily be introduced into the cytoplasm of the tumor cell, freeing the cell restriction, to then exert its anti-cancer effect.



[NSN-339] Structural of nano-sized hydroxyapatite synthesized by hydrothermal system, using Cetyl Trimethyl Ammonium Bromide as a cationic template

Manuel Alejandro Valdés Madrigal², Susana Elisa Sánchez Méndez¹, María Magdalena Méndez-Gonzalez³

¹ Industrial Engineering Department, UPIICSA-IPN, CDMX, Mexico

² Mechatronics and Nanotechnology Engineering Department, ITSCH, Michoacán, México

³ Physics department, ESFM-IPN, U.P. Adolfo López Mateos, Edif. 9, Lindavista 07738 CDMX, México

Structural characterization of nanometric hydroxyapatite was obtained by X-ray diffraction, Fourier transform infrared spectroscopy, X-ray energy dispersion spectroscopy and transmission electron microscopy. It was synthesized by hydrothermal system, using as cationic template Cetyl Trimethyl Ammonium Bromide (CTAB), with the purpose of regulating the nucleation and growth of crystals. Human tooth root was used as a reference for the parameters and properties required. The only crystalline phase present in the nanometric hydroxyapatite was the non-stoichiometric hydroxyapatite, with different degrees of crystallinity and molar ratio very close to the value of the human dental root. Due to the coincidence of the functional groups and similar characteristics of the nanometric hydroxyapatite with the human dental root, it is proposed to use it in the odonto-keratoprosthesis technique for corneal transplantation.



[NSN-340] Morphology and adhesion of osteoblasts of poly-hydroxyethyl methacrylate hydrogel coatings with nanocrystalline hydroxyapatite and nanophilic peptide nanoparticles deposited on Ti6Al4V

Fernando Francisco Ríos Pimentel¹, Samuel Sánchez Méndez², María Magdalena Méndez-González³

¹ *Nanosciences and nanotechnology, CINVESTAV-IPN, Av IPN 2508, San Pedro Zacatenco, 07360, CDMX, México*

² *National Preparatory School 6, UNAM, Corina 27, Del Carmen, 04100, CDMX, México*

³ *Physics department, ESFM-IPN, U.P. Adolfo López Mateos, Edif. 9, Lindavista 07738 CDMX, México*

Hydrogel coatings of poly-hydroxyethyl methacrylate (pHEMA) with nanocrystalline hydroxyapatite (nHA) and amphiphilic peptide particles (APnPs) were obtained by immersion technique, deposited on metallic Ti6Al4V substrates. The morphology and adhesion of osteoblasts of the coated substrates was observed by X-ray diffraction, Fourier transform infrared spectroscopy, scanning electron microscopy, X-ray energy dispersion spectroscopy and transmission electron microscopy. By individually adding both nanocrystalline hydroxyapatite or amphiphilic peptide particles, the density of osteoblasts is not increased and significantly increased by adding nanocrystalline hydroxyapatite and nanoparticulate peptide nanoparticles to the hydro-hydroxyethylmethacrylate hydrogel, so that the metal substrates of Ti6Al4V coated with pHEMA + nHA + APnPs have better bone-integration.



[NSN-344] PHYSICOCHEMICAL PROPERTIES OF TITANATE NANOTUBES CALCINED AT DIFFERENT TEMPERATURES AND THEIR EFFECT ON THE REMOVAL OF POLLUTANTS

Ana Laura Ruiz Castillo (anacasru@gmail.com)¹, Mariana Hinojosa Reyes¹, Facundo Ruiz¹

¹ Facultad de Ciencias, Universidad Autónoma de San Luis Potosí. Av. Parque Chapultepec 1570, 78210. San Luis Potosí, S.L.P.

Hydrogen titanate nanotubes were successfully synthetized by the hydrothermal method using P25-Degussa as a precursor. The obtained materials were calcined at temperatures between 100-500°C and characterized by X-ray diffraction, transmission electron microscopy, nitrogen physisorption, zeta potential, X-ray photoelectron, DRIFTS and UV-Vis spectroscopy. The effects of calcination on phase structure, morphology and surface area were discussed. Results showed that materials with calcination temperatures between 100-300°C possess a nanotubular structure with a $H_2Ti_3O_7$ phase. Temperatures above 300°C cause the collapse of the tubular structure and materials are transformed into anatase nanoparticles. The adsorption capacity of the nanotubes was evaluated using safranin dye as a model pollutant. The titanate nanotube sample treated at 100°C showed the highest adsorption capacity, up to 94% of safranin was removed using an optimum dose of 100 mg/L with 80% being adsorbed in the first 5 minutes. Kinetic studies and desorption tests were performed to elucidate the mechanisms involved in safranin adsorption. UV-Vis and diffuse reflectance Fourier transformed infrared spectroscopy provided a better insight of the interactions between the functional groups of safranin and titanate nanotubes. Titanate nanotubes were also evaluated for photocatalysis using caffeine as a model organic compound. Titanate nanotube sample calcined at 500°C achieved the highest caffeine degradation of 73% with 500 mg/L. The photocatalytic activity of nanotubes is closely related to the crystalline phases and OH groups in the samples. While calcination temperature has an opposite effect on adsorption and photocatalysis, titanate nanotubes calcined at 300°C can efficiently adsorb safranin and degrade caffeine. Results in this study showed that titanate nanotubes can be applied efficiently for treatment of wastewater containing complex chemical pollutants.



[NSN-352] LIGHT-MATTER INTERACTION ENHANCEMENT OF WSe₂ MONOLAYERS THROUGH GAP-PLASMON STRUCTURES

Bárbara Alejandra Muñiz Martínez (barbara.muniz@cinvestav.edu.mx) ¹, Andrés De Luna Bugallo (aluna@cinvestav.mx) ¹

¹ CINVESTAV Unidad Querétaro

Tungsten diselenide monolayer (WSe₂) is a member of transition metal dichalcogenides (TMDs) family which has shown great potential for diverse applications in electrical, optical and quantum devices due to its intrinsic mobility, direct band gap and electronic structure. However, the extreme thickness (around 8 Å) presented in WSe₂ single layers remains a challenge to integrate this material in devices due to its weak light-matter interaction.

In this work, we demonstrate an enhancement of light-matter interaction in WSe₂ single layers using a gap-plasmon structure. First, WSe₂ monolayers were synthesized on SiO₂ (300 nm)/Si substrates by chemical vapor deposition. Scanning electron microscopy images show triangular shapes with lengths up to ~20 μm. The thickness found through atomic force microscopy (~7 Å) while Raman spectroscopy shows the out-of-plane vibrational mode A_{1g} centered at ~250 cm⁻¹ confirming the presence of WSe₂ monolayers.

In order to increase the optical absorption in WSe₂ single layers, we prepared a Fabry-Perot cavity composed by 100 nm of silver and 50 nm of HfO₂ dielectric deposited by sputtering and atomic layer deposition respectively on SiO₂ substrates. WSe₂ flakes were then transferred on top of the cavity using wet-transfer method. Photoluminescence spectroscopy was performed on WSe₂ single layers located out and inside the Fabry-Perot cavity, both spectra show a main contribution located at 1.63 eV associated with direct optical transition from the highest spin-split valence band to the lowest conduction band at the K point of the Brillouin zone. However, we observe a significant increase of the emission of the WSe₂ flakes laying on top the Fabry-Perot cavity in comparison with WSe₂ single layers outside the cavity. We attributed this enhancement to the multiple photon reflection in Fabry-Perot cavity and the electric field confinement on the surface leading to an important optical absorption in the WSe₂ monolayers.

This study is applicable to enhance the light-matter interaction of TMDs for applications in potential devices such as lasers, light-emitting devices and photodetectors.



[NSN-374] Enhancement of nonlinear refraction index with copper nanoparticles prepared by pulsed laser ablation (PLA)

Rubén Gutiérrez-Fuentes⁴, José Luis Jiménez-Pérez (jimenezp@fis.cinvestav.mx)⁵, Genaro Gamboa-López⁶, Zormy Nacary Correa-Pacheco¹, José Luis Luna-Sánchez⁵, Miguel Angel Camacho-López², Marco Antonio Camacho-López³

¹ CONACYT- Centro de Desarrollo de Productos Bióticos del Instituto Politécnico Nacional, Carretera Yautepec-Joxtla, Km. 6, Calle CEPROBI No. 8, Col. San Isidro, C.P. 62731, Yautepec, Morelos, Mexico.

² Facultad de Medicina, Universidad Autónoma del Estado de México, Jesús Carranza y Paseo Tollocán s/n. C.P. 50120, Toluca, Mexico.

³ Facultad de Química, Universidad Autónoma del Estado de México, Paseo Colón y Tollocán 50110, Toluca, Mexico

⁴ Instituto Tecnológico de Ciudad Cuauhtémoc, Av. Tecnológico # 137, C.P. 31500, Ciudad Cuauhtémoc, Chihuahua, Mexico.

⁵ Unidad Profesional Interdisciplinaria en Ingeniería y Tecnologías Avanzadas-Instituto Politécnico Nacional, Av. Instituto Politécnico Nacional, No. 2580, Col. Barrio la Laguna Ticomán, Gustavo A. Madero, C.P. 07340, Mexico City, Mexico.

⁶ Universidad Politécnica del Valle de Toluca, Km. 5.6. Carretera Toluca-Almoloya de Juárez, Santiaguito Tlalcilalcali, C.P. 50904, Lamoloya de Juárez, Mexico.

The present work explores the non-linear refractive index of copper nanoparticles as a function of ablation time of nanoparticle growth by the use of the Z-scan technique. In the Z-scan technique, the measurements were carried out using a diode laser as a continuous source of excitation with a wavelength of 534 nm and power of 40 mW. The modulation of the pulses was interrupted by a chopper with a frequency of 14 Hz. With the use of a lens, the excitation laser was focused and the sample was moved around the excitation laser focus, where the transmittance changes as a function of the position of the sample. The synthesis of the copper nanoparticles was obtained by different ablation times between 1 to 6 minutes in a copper disc, immersed in a liquid or solvent medium, such as acetone. For the process of ablation, an Nd: YAG laser was used with wavelength emission of 1064 nm at a frequency of 15 Hz and with a pulse energy of 47 mJ and pulses of 7 to 2 ns. The copper nanoparticles showed high non-linear refractive indices between 0.61 to $3.73 \times 10^{-8} \text{ cm}^2/\text{W}$, in which a non-linear increase of the non-linear refractive index was observed as a function of the ablation time. The colloidal solutions synthesized were analyzed with UV-visible spectroscopy and the shape and size of the nanoparticles were obtained by transmission electron microscopy (TEM). The usefulness of this work has possible applications in the study of nanomaterials for high power compact solid-state laser gain amplifier systems.



[NSN-378] Preparation of the nanocrystalline phase TiO₂ by sol-gel for its use in medical applications

Georgina García Pacheco (ggpacheco@outlook.com) ², Rosa Estrella Ruiz Miranda ³,
Héctor Francisco Mendoza León ¹, Salvador Mendoza Acevedo ¹

¹ CNMN, Instituto Politécnico Nacional, Ciudad de México, México

² ESIME Ticomán, Instituto Politécnico Nacional, Ciudad de México, México

³ ESIME Zacatenco, Instituto Politécnico Nacional, Ciudad de México, México

The TiO₂ phase has different crystalline structures, tetragonal (anatase and rutile) and orthorhombic (brookite). Initially, the first applications were directed to applications where coloration is required, such as pigments. At the beginning of this century, new uses were found, such as photocatalysis, gas sensors, solar cells and batteries, among others. However, one of the most promising applications is in medical sensors for the early detection of chronic degenerative diseases. The latter is the motivation of the present work, to synthesize the TiO₂ nanostructure phase (anatase), by the sol-gel method. And evaluate, its memrsistive property on its interaction of DNA from blood samples. The precursors of the synthesis were the isopropoxide Ti(O₄C₁₂H₂₈) (I) and ethanol C₂H₅OH (I), in a volumetric ratio of 5: 1. The chemical reaction was promoted by ultrasonic waves, from an ultrasonic bath operated at 40 kHz, at 3 different process times: 1, 2 and 3 h, respectively. The precipitated solid was separated by centrifugation and subsequent decantation. The wet powders were dried at 80° for 2 h. Finally, these were subjected to a thermal treatment of 350 ° C, for 1 h. The samples were initially characterized by X-ray diffraction, using a Cu-Ka radiation of 1.54060 Å, with a scanning speed of 0.01° / s from 20 to 100 °. The results show that, for the 3 process times, the reaction was completed and the final phase was anatase. However, the broadening of the diffraction peaks for 3 hours is noticeably greater than the shorter times, which is a qualitative indication that the refinement of the crystallite size is smaller for this time.



XII -ICSMV

September 23rd to 27th, 2019 / San Luis Potosí, México

[NSN-379] Synthesis and characterization of multi-walled nanotubes doped with nitrogen

V.L Medina-Llamas (veronica.medina@ipicyt.edu.mx)², F Lopez-Urías², E Muñoz-Sandoval², E Muñoz-Sandoval¹

¹ Department of Chemical Engineering, Natural and Exact Sciences Division, University of Guanajuato. Noria Alta S/N, Guanajuato, Guanajuato, México 360503

² División de Materiales Avanzados, IPICYT, Camino a la presa San José 2055, Col. Lomas 4a sección, San Luis Potosí S.L.P., 78216, México

In this work, results are reported on the production of multi-walled carbon nanotubes doped with nitrogen (N-MWCNT) using the chemical vapor deposition (CVD) method. A solution of benzylamine and dichlorobenzene was used as precursors in the CVD experiment, the synthesis time was: 120, 180 and 240 minutes. The N-MWCNT were characterized by scanning electron microscopy (SEM), transmission electron microscopy (TEM), Raman and X-ray spectroscopy, thermogravimetric analysis and cyclic voltammetry. The SEM and TEM characterizations revealed that the samples are formed by corrugated N-MWCNTs. The N-MWCNT also showed a bamboo-type structure due to the incorporation of nitrogen in the graphitic network.



[NSN-402] Production of nitrogen-doped multiwall carbon nanotubes using Fe-rich Leptosol from Sierra de Álvarez, San Luis Potosí, México.

Felipe de Jesus Barraza Garcia (felipe.barraza@ipicyt.edu.mx)², Nelia Martinez Villegas², Florentino Lopez Urias³, Emilio Muñoz Sandoval (ems@ipicyt.edu.mx)¹

¹ Department of Chemical Engineering, Natural and Exact Sciences Division, University of Guanajuato. Noria Alta S/N, Guanajuato, Guanajuato, México 360503

² División de Geociencias Aplicadas, IPICYT, Camino a la Presa San José 2055, Col Lomas 4a sección, San Luis Potosí S.L.P., 78216, México

³ División de Materiales Avanzados, IPICYT, Camino a la Presa San José 2055, Col Lomas 4a sección, San Luis Potosí S.L.P., 78216, México

Due to the large distribution of carbon nanotubes for being a material with very exceptional physical and chemical properties, the search of cheap and natural abundant catalysts for the large and low-cost production of this carbon nanomaterial has become an important research field. In the present work we use a Fe-rich Leptosol powder (ball milled and oxidized) as a catalyst for large production of nitrogen-doped multiwalled carbon nanotubes (N-MWCNTs) in an aerosol assisted catalytic chemical vapor deposition (AACCVD) system. The morphology and composition of the Leptosol powders as well as the synthesized N-MWCNT samples were analyzed by scanning electron microscopy (SEM), transmission electron microscopy (TEM), X-ray diffraction (XRD), X-ray fluorescence (XRF), Raman spectroscopy and thermogravimetric analysis (TGA). We also investigate the synthesis process by reducing the soil at different times. The characterizations by XRD revealed that the Leptosol was composed of quartz, kaolinite, iron and titanium oxides. Also XRF composition analysis showed that the composition of iron oxides was only behind the silicon oxides. Those result was also confirmed by SEM. To evaluate the applications of our synthesized materials, its structure was characterized by SEM, TEM, DRX, Raman and TGA, in addition, the morphology of the N-MWCNT, which shows a structure similar to a sponge, is also presented, showing a sponge-like structure. The efficiency of 93.54% wt / wt in production yield of N-MWCNTs was obtained by oxidized Leptosol pouders. Finally, due to the very low cost and ecological impact of soil as a catalyst, it will accelerate the growth of industrial production of carbon nanotubes.



XII -ICSMV

September 23rd to 27th, 2019 / San Luis Potosí, México

[NSN-409] Temperature effect on the control of morphology of Pt/C Nanotubular Heterostructures by a Simple Vapor Deposition Method

Eunice Jiménez Marín (eunice_jmarin@hotmail.com)², Jorge Roberto Vargas García ¹

¹ Centro de Nanociencias y Micro y Nanotecnologías del Instituto Politécnico Nacional,
Ciudad de México, 07738, México

² Depto. Ing. Metalurgia y Materiales, ESIQIE, Instituto Politécnico Nacional, 07300
México, DF, México

Nanotubular carbon heterostructures is becoming a promising area of research due their potential applications in nanoelectronics devices, fuel cells and optoelectronic devices. The nanotubular carbon heterostructures properties can be modulated by fitting their composition, morphology and size. In this work, the authors report uniform Pt/C nanotubular hetetrostructures obtained by a novel simple vapor decomposition method consisting in two-steps procedure. In an initial step, a mixture of Pt precursor (Pt-acac) and f-NTC was heated in a quartz reactor at 180 °C for 10 min at 560 torr. In a second step, the temperature was increased at 400, 450, 500, 600 and 700 °C for 10 min in flowing Ar (100 cm³/min). The functionalization of CNTs was achieved with HNO₃ (60% v/v) to generated oxygen functional groups. Pt incorporation was favored as a consequence of the functionalization treatment. These results suggest that functional groups served as nucleation sites for Pt phase on the surface of CNTs. X-ray diffraction, Raman, SEM and TEM results reveled that temperature has a significant effect on the total control in morphology of Pt. Whereas dispersed Pt nanocrystals of about 3 nm in size were deposited at 400 °C forming a continuous phase. When the temperature increase the Pt crystal also increase distorting the tubular shape of the CNTs and carbon is eliminated at 700 °C. Pt morphology was controlled as a function of the working temperature.



[NSN-508] ELECTRICAL CONDUCTIVITY OF GRAPHENE NANOPLATELET/EPOXY COMPOSITES

Luis Alberto Becerril Landeros (beceland25@gmail.com)², Naria Adriana Flores Fuentes

², Ángel Adalberto Durán Ledezma ¹

¹ ESCOM, Instituto Politécnico Nacional, Av. Juan de Dios Bátiz S/N, Col. Nueva Industrial Vallejo, Alcaldía Gustavo A. Madero, CP 07738, CDMX, México

² ESIME U.P Ticomán, Instituto Politécnico Nacional, Av. Ticomán No. 600, Col. San José Ticomán, Alcaldía Gustavo A. Madero, CP 07340, CDMX, México.

The aerospace material composites have a low electrical conductivity. Therefore, to avoid thermal damage when a light hits a vehicle of this type, lightning protection systems (LPS) are required. However, the current LPS contribute considerably to the weight of the structure, which is reflected in an increase in fuel consumption. In this work an epoxy resin material reinforced with graphene nanoplatelets (GnPs) is presented to increase the electrical conductivity properties of the polymer in exchange for low amounts of reinforcement added. The materials were fabricated with two types of GnPs and different percentages of weight (%wt) of such particles, this to increase the properties of electrical conductivity. Each of the morphologies was characterized by Fourier Transform Infrared spectroscopy (FTIR) and Raman spectroscopy to determine the morphology and composition of the reinforcement. For the dispersion of the nanoparticles no solvents are used to avoid the degradation of the mechanical properties. Accordingly, mechanical dispersion methods of sonication and High-Speed Mixer (HSM) were used to disperse said particles. The dispersion process used was 4000 RPM for 30 min for HSM and 30 min for sonication. The electrical conductivity of each compound was evaluated to find the percolation threshold (f_c) of each system. For nanocomposites with M25 particles the percolation threshold is less than 1 %wt, while for compounds with C300 particles this value is between 10 and 15 %wt. The results show that the morphology and the composition of the particles have a considerable influence on the conductivity properties of the material. We believe that our work could be the basis for long fiber composite materials that do not need LPS to avoid thermal damage caused by a phenomenon of this type in exchange for a low weight percentage of GnPs.



[NSN-515] Monolayers of lipids deposited by the Langmuir-Blodgett technique on nanostructured substrates.

Enrique Esparza Alegría (espaleg@ciencias.unam.mx)², José Guadalupe Morales Mendez², Emmanuel Haro Poniatowski³, Gregorio Sánchez- Balderas¹, Luis Hernandez Adame¹, Elías Pérez¹

¹ *Instituto de Física, UASLP, Álvaro Obregón 64, San Luis Potosí S.L.P. 78000, México.*

² *Posgrado en Ciencias (Física), Universidad Autónoma Metropolitana Unidad Iztapalapa (UAMI), Av. San Rafael Atlixco 186, Leyes de Reforma 1ra Secc, México C.D.Mx., C.P. 09340.*

³ *Universidad Autónoma Metropolitana Unidad Iztapalapa (UAMI), Av. San Rafael Atlixco 186, Leyes de Reforma 1ra Secc, México C.D.Mx., C.P. 09340.*

Surfaces of glass slides and silicon wafers were modified by silanization to create hydrophobic and hydrophilic surfaces onto which a thin film of amphiphilic (lipids) molecules was deposited by the Langmuir-Blodgett technique (LBT). These samples were characterized by AFM microscopy and ellipsometry measurements. A lipid monolayer was observed. A second set of glass slides and silicon wafers served as substrates for depositing nanostructured silver islands by pulsed laser ablation (PLA). Subsequently a lipid monolayer was deposited by LBT. Raman Spectroscopy was done in both sets of samples. Preliminary results are presented in order to detect Surface Enhanced Raman signal in the nanostructured substrates.



[NSN-530] Study of the properties of nano-structures of ZnO obtained by the vapor-solid method at atmospheric pressure and photocatalytic activity

Carlos Bueno (cba3009@gmail.com)⁴, René Perez¹, Mauricio Pacio², Adán Luna¹,
Jose Alberto Alvarado², Héctor Juárez², Jose Toledo³

¹ Benemérita Universidad Autónoma de Puebla, Facultad de Ingeniería Química, Av. Sn. Claudio y 18 sur, Jardines de San Manuel, 72570, Puebla, México

² Benemérita Universidad Autónoma de Puebla, Centro de Investigación en Dispositivos Semiconductores, , 14 Sur and Av. San Claudio, San Manuel, 72000, Puebla, México

³ Centro de Estudios Universitarios Rudolph Diesel, 13 Poniente No.707 y 713, Centro, 72000 Heróica Puebla de Zaragoza, Pue

⁴ Instituto Tecnológico de Apizaco, Benemérita Universidad Autónoma de Puebla, Carretera Apizaco – Tzompantepec esquina con Avenida instituto Tecnológico S/N. Conurbado Apizaco – Tzompantepec, 90300, Tlaxcala, México.

Nano and micro-structures of ZnO were synthesized by the vapor-solid method at 600, 700 and 800 °C in atmospheres of argon and air, at atmospheric pressure. The structural characterization XRD shows that the nano-structures synthesized in air atmosphere at 600 °C, there is still presence of metallic Zn on the surface of the pellet. In SEM it is found that the morphologies go from nano-wires to micro-tubes. When cathodoluminescence is measured in micro-tubes there is a shift of the neard band edge of the ZnO towards red, this is due to structural defects in the ZnO network. This result is corroborated with panchromatic CL measurements where a difference in brightness between in the micro-tubes is exhibited. Furthermore, in EDS measurements, it is shown that there is an atomic quantity ratio of Zn-O different from the stoichiometric in the micro-tubes.

The photocatalytic activity of three types of structures, nano-wires, micro-tubes and micro-rods under UV irradiation using methylene blue as a model pollutant were evaluated. The best response was obtained for nanowires, not only because they have a larger surface area but because of the present defects.



[NSN-545] Robustness of the enhanced magnetic anisotropy in Ni nanowires regardless of the deposition potential

Yenni Velázquez Galván (yenni.velazquez.g@gmail.com)¹, Joaquin de la Torre Medina³,
Armando Encinas¹, Luc Piraux²

¹ : Departamento de Materiales Avanzados, Instituto Potosino de Investigación Científica y Tecnológica A. C., Camino a la Presa 2055, 78216 San Luis Potosí, SLP, México.

² Institute of Condensed Matter and Nanoscience, Université catholique de Louvain, Place Croix du Sud 1, B-1348, Louvain-la-Neuve, Belgium

³ Instituto de Investigaciones en Materiales/ Unidad Morelia, Universidad Nacional Autónoma de México, Antigua Carretera a Pátzcuaro No. 8701 Col. Ex Hacienda de San José de la Huerta, 58190 Morelia, México

The effect of the deposition potential on the structural and magnetic properties of Ni nanowire arrays with a diameter of 40 nm has been studied with particular interest in the enhanced uniaxial magnetic anisotropy obtained in very long Ni nanowires (NWs). To this end, Ni NWs with lengths varied from 16 up to 56 mm grown in PC (Polycarbonate) and AAO (anodic aluminum oxide) were considered. Our results are consistent with a two crystal structures, where a polycrystalline phase grows first followed by a single crystalline stage with a preferential orientation in the [110] direction, parallel to the NWs axis. This two-stage growth mechanisms leads to an enhanced anisotropy. This anisotropy reaches values as high as 1.6×10^6 erg/cm³ that is comparable with the value due to the magnetostatic anisotropy contribution ($\approx 5 \times 10^6$ erg/cm³) and as high as the effective magnetic anisotropy of Co (1.4×10^6 erg/cm³) [1, 2]. Furthermore, the results show that for the longest NWs this large anisotropy is practically insensitive to the deposition potential. On the contrary, shorter NWs grown in PC membranes, where the second stage of the polycrystalline segment is not reached, the enhancement of the anisotropy is not observed. However, the length of this segment increase with the deposition potential that relate to their magnetic properties. Therefore, the large uniaxial magnetic anisotropy in arrays of Ni NWs it is independent of the deposition potential and has an inherent relation with their size and confinement, this is, it is a robust effect. Understanding particular properties of the nanocomposites on the magnetic properties is of prime interest for the development of novel devices with materials with high anisotropy.

References

- [1] H. Pan, B. Liu, J. Yi, C. Poh, S. Lim, J. Ding, Y. Feng, C. H. A. Huan, and J. Lin, *J. Phys. Chem. B*, **109**, 3094-3098, 2005
- [2] A. Encians, M. Demand, J.M. George, and L. Piraux, *IEEE Trans. Magn.*, **38**, 2574-2576, 2002.



[NSN-549] Ge nanocrystals embedded within a germanium nitride film grown by PLD

J.G. Quiñones-Galván (jose.quinones@academicos.udg.mx)¹, E. Campos-González², E. Camps², A. Pérez-Centeno¹, M.A. Santana-Aranda¹, G. Gómez-Rosas¹, A. Chávez-Chávez¹

¹ Departamento de Física, Centro Universitario de Ciencias Exactas e Ingenierías, Universidad de Guadalajara, Boulevard Marcelino García Barragán 1421, Guadalajara, Jalisco, México, C.P. 44430

² Departamento de Física, Instituto Nacional de Investigaciones Nucleares, Apdo. Postal 18-1027, México DF 11801, Mexico

Germanium nitride has been studied in the last decades due to its interesting properties such as high hardness, photocatalytic activity or dielectric properties, which make it a functional material. On the other hand, semiconductor nanocrystals embedded in different kind of matrices, could result in enhanced properties own to quantum confinement effects.

The growth of Ge nanocrystals embedded in a germanium nitride matrix by means of pulsed laser ablation of Ge in a nitrogen reactive atmosphere is presented in this study. Films were grown onto Si and quartz substrates at room temperature. The density and mean kinetic energy of the Ge ions present in the plasma were determined by Langmuir probe measurements.

Working pressures of 1 and 2 Pa of pure N₂ were used for the experiments, the plasma parameters were adjusted to be the same for both pressure values. Samples were structurally characterized by TEM, XRD and Raman Spectroscopy. It was found that Ge nanocrystals were grown into a GeN matrix. By means of UV-Vis spectroscopy, the band gap was found to change with pressure. Surface morphology was observed by SEM. The chemical composition of the films was analyzed by XPS measurements.



[NSN-553] Analytical magnetostatic model for 2D arrays of interacting magnetic nanocylinders

Yenni Velázquez Galván (yenni.velazquez.g@gmail.com) ¹, Armando Encinas ¹

¹ División de Materiales Avanzados, Instituto Potosino de Investigación Científica y Tecnológica A. C., Camino a la Presa San José 2055, 78216 San Luis Potosí, SLP, México.

Two-dimensional arrays of nanocylinders, both nanotubes and nanowires, are known to possess a very interesting and rich effective magnetic anisotropy properties which are due to their main geometrical parameters: nanocylinder outer and inner diameters, their height and the distance between them. Just these four parameters define the magnitude and the preferred orientations of the nanocylinder shape anisotropy and the dipolar interaction between nanocylinders. At present, there are models capable of providing an accurate account for these two effects, however such models, typically micromagnetic, require intensive computing resources and depending on the approximations used, the degree of complexity in the programming can vary. This has led to the difficulty of having easy and accessible models to analyze, interpret and make predictions of the anisotropy properties of these systems. In this contribution we present a fully analytical model to describe the magnetic properties of these 2D nanocylinder arrays. The model allows calculating the components of the effective demagnetizing field as a function of the cylinder height, inner diameter and center-to-center distance, all normalized by the cylinder outer diameter. From these components it is possible to calculate the shape anisotropy of the cylinder and the dipolar interaction between them, thus the total magnetostatic energy. The model allows performing calculations very simply, using basically a spread sheet or open access software such as Geogebra. Amongst the most interesting findings is that the model describes naturally the magnetization easy-axis reorientation transition induced by the dipolar interaction, for which a general phase diagram has been calculated for both tubes and wires. For the case of nanowires, our results show a very good agreement with previous published results. Finally, the model predicts that the magnetization easy-axis reorientation transition is frustrated in nanotubes as the nanotube wall thickness decreases and reaches a critical value.



XII -ICSMV

September 23rd to 27th, 2019 / San Luis Potosí, México

[NSN-574] Method to determine the intrinsic switching field distribution from the end points of the descending and ascending parts of a minor loop in arrays of magnetic nanowires

*Kevin Hintze Maldonado (kevin_hintze@ipicyt.edu.mx)¹, Juan Manuel Martínez Huerta¹,
Armando Encinas¹*

¹ División Materiales Avanzados, IPICYT, Camino a la Presa de San José 2055, Lomas 4ta Secc, 78216 San Luis, S.L.P.

Arrays of magnetic nanowires have been used as a model system of a 2D array of nanomagnets with perpendicular magnetic anisotropy that interact dipolarly between them, in order to propose and validate a simple method to determine the intrinsic switching field distribution using standard minor loop measurements. The method is based on the field asymmetry of the end points of the descending and ascending parts of a minor loop. A simple identification of the expression that describes the field asymmetry allows obtaining a function that corresponds to the intrinsic switching field distribution shifted along the field axis by a quantity equal to the average value of the interaction field. The model has been tested and validated by performing computer simulations first for an idealized case of the mean field approximation in which all the particles (nanowires) in the array are subjected to the same average interaction field value and then for a more realistic case that considers a fluctuating interaction field, or an interaction field dispersion. The results show that the model works extremely well within the mean field approximation, whereas some discrepancies appear as the interaction field is let to fluctuate. However, these discrepancies are only noticeable near saturation and are a well-known effect related to the interaction field dispersion.



[NSN-591] Physicochemical properties of ZnTiO₃ powder for photocatalytic applications

Constanza Ibeth Coop-Santa², Araceli Sanchez-Martínez (sanmtz49@gmail.com)¹,
Hector Guillen-Bonilla², Walter Ramirez-Meda², Milton Oswaldo Vazquez-Lepe², Víctor
Manuel Rangel-Cobián², Oscar Ceballos-Sánchez (ceballos0516@gmail.com)²

¹ CONACYT-Departamento de Ingeniería de Proyectos, CUCEI, Universidad de Guadalajara,
Av. José Guadalupe Zuno # 48, Industrial los Belenes, Zapopan, Jalisco 45157, México

² Departamento de Ingeniería de Proyectos, CUCEI, Universidad de Guadalajara, Av. José
Guadalupe Zuno # 48, Industrial los Belenes, Zapopan, Jalisco 45157, México

For decades, different semiconductors have been studied for photocatalytic applications due to their ability for the dyes degradation and energy production.[i] In particular, the heterogeneous photocatalysis is an alternative to address environment issues as water pollution, and air pollution from the excessive use of fossil fuels.[ii] From the photogenerated electron-hole pairs is possible to produce radicals (OH^\bullet , $\text{O}_2^{\bullet-}$), which are responsible to produce secondary reactions that lead to the photodegradation of organic compounds. ZnTiO₃ is a perovskite with a high potential for applications such as microwave dielectrics, gas sensors, dye degradation and paint pigments.[iii] The synthesis of this material has been carried out by different methods such as sol-gel, hydrothermal, solid state and molten salts. According to the synthesis method and synthesis route, the physicochemical properties of this material can be varied (band gap, grain size, and superficial area). In this work, ZnTiO₃ powder was prepared by molten salts method in order to study its physicochemical properties for photocatalytic applications. Analysis by X-ray diffraction (XRD) was carried out to study the crystal structure. The morphology and grain size were analyzed by scanning electron spectroscopy (SEM). The chemical states and elemental composition were assessed by X-ray photoelectron Spectroscopy (XPS). On the other hand, the photocatalytic activity was studied by the RhB degradation under UV and visible light.

[I] R.S. Raveendra et. al., "Synthesis, structural characterization of nano ZnTiO₃ ceramic: An effective azo dye adsorbent and antibacterial agent", Journal of Asian Ceramic Societies 2 (2014) 357–365.

[II] Xin Yan et al. "Synthesis and characterization of ZnTiO₃ with high photocatalytic activity", Trans. Nonferrous Met. Soc. China 25 (2015) 2272-2278.

[III] Ji-ZhouKong et. al., "Preparation, characterization and photocatalytic properties of ZnTiO₃ powders", / Journal of Hazardous Materials 171 (2009) 918–923.



XII -ICSMV

September 23rd to 27th, 2019 / San Luis Potosí, México

[NSN-597] Simagna: an open-source code for simulating magnetic nanoparticles

*Victor Hugo Carrera-Escobedo (victor.carrera@ipicyt.edu.mx)¹, Armando Encinas¹,
Antonio Capella²*

¹ *División de materiales avanzados, IPICYT, Camino a la presa San José 2055, San Luis Potosí, SLP*

² *Instituto de Matemáticas, UNAM, Cto. Bicipuma, C.U., 04510 Ciudad de México, CDMX*

In the present work we present a method for simulating the equilibrium magnetization of a finite system of magnetic particles with several characteristics. The equilibrium magnetization is calculated by minimizing the micromagnetical energy. The minimization process is carried out by a BFGS algorithm in which one has previously found the gradient of the micromagnetic energy with respect to the magnetization of the system. This tool can handle both: periodic systems of a finite number of magnetic particles per unit cell or systems of magnetic particles with zero boundary conditions. The particles may have an arbitrary geometry but must be of the single domain type. This tool will be available online for free as an open-source code.



[NSN-598] TITANIA-SILICA-COPPER SUPPORT FOR INFRARED SPECTROSCOPY SIGNAL ENHANCEMENT

Daniela Solorio-Grajeda², Fernando Soto-Nieto (al145882@alumnos.uacj.mx)², Simon Yobanny Reyes-López (yobannyr@yahoo.com.mx)², Rurik Farias², Miguel Melendez-Lira¹

¹ Physics Department, CINVESTAV-IPN

² Universidad Autónoma de Ciudad Juárez

The infrared spectroscopy technique represents a classical tool for materials identification and characterization, distinguished by its high specificity and sensitivity, as well as easy handling. Some of the disadvantages that may attenuate its performance, such as the presence of spectral noise or weakness in the signal can be efficiently treated through the implementation of strategies as Surface Enhanced Infrared Absorption Spectroscopy (SEIRAS). The development of substrates for infrared signal enhancement contributes to the quality improvement of the analysis by this method in terms of resolution. Nevertheless, the production of these kind of substrates using conventional processing turns out to be complex and its commercial acquisition, expensive. In this work a titania-silica based nanostructured substrate doped with copper nanoparticles was obtained. After a thermal treatment, the fibers obtained by the sol-gel method and electrospinning presented an average diameter of 331 ± 76 nm. The composite was fixed on a conductive plastic membrane of indium tin oxide (ITO) and was doped by electrodeposition at 0.75, 1, 2 and 5 minutes using a voltage of 19.27 V. The several doping times led to the formation of nanoparticles with needle, dendrite and bow-like morphologies which at longer exposition became large clusters of copper species. The signal enhancement evaluation was carried out with solutions of pyridine 1 nM, methyl violet 1 mM and concentrated pyridine (99.7%). The 2-minutes doped support exhibited an enhancement factor of 1.94 for the band localized at 3331 cm^{-1} of the 1 nM pyridine solution.



[NSN-603] Ag nanoparticles embedded in Zeolite A4: HR-TEM tomography study and their catalytic performance in the 4-nitrophenol reduction to 4-aminophenol

Patricia Horta Fraijo (*hfpatricia@gmail.com*)⁴, Brenda Acosta², Miguel A. Vidal⁴,
Andrey Simakov¹, Miguel José-Yacaman³

¹ Centro de Nanociencias y Nanotecnología de la UNAM

² Cátedra CONACYT, CIACYT- Universidad Autónoma de San Luis Potosí

³ Department of Physics and Astronomy, University of Texas at San Antonio

⁴ Laboratorio Nacional CIACYT-Universidad Autónoma de San Luis Potosí

We are reporting the tomography reconstruction of a complex – system (silver – nanoparticles / zeolites A4) by using high resolution transmission electron (HR-TEM) tomography to determine the real position of the nanoparticles in the zeolite. The determination of the specific positions of the Ag NPs through advanced high-resolution electron microscope techniques allows to obtain, with high accuracy, a 3D model that describe the whole system. The high-resolution images were acquired with a JEOL ARM 200F, equipped with a CEOS probe corrector for spherical aberration operated at 80 kV, where the sample is loaded within an electron tomography holder (Fishione 2030 with high tilt range from -50° to +50°). The images acquired were obtained by tilting the goniometer in tilt steps around 5°. The reconstruction was carried out using the 3D WBP algorithm (weighted back-projection) in the GATAN module for image reconstruction. Additionally, we are presenting the structural, morphologic, chemical analysis, and optical absorption of the nanostructured system. Furthermore, it is presented the catalytic properties of the obtained metallic silver nanoparticles (~2 nm) deposited on the crystalline hydrated aluminosilicate (zeolites) using the reduction of 4-nitrophenol to 4-aminophenol as model reaction. Undoubtedly, the results here shown will allow us to determine the physical-chemical properties that allows to elucidate the optical, antibacterial and catalytic properties where these systems are being employed nowadays.



[NSN-611] Relaxation and shape study of InAs quantum dots grown on strained modulated GaAs(100) films

Jesus Hernandez-Medina ³, Miriam Favila-Castañeda ³, Lendy M. Hernandez-Gaytán ², J. Pablo Olvera-Enriquez ², Christian Alejandro Mercado-Ornelas ², Leticia Ithsmel Espinosa-Vega ², Irving Eduardo Cortes-Mestizo ¹, Victor Hugo Mendez-García
(victor.mendez@uaslp.mx) ²

¹ CONACYT-CIACYT, Universidad Autónoma de San Luis Potosí, San Luis Potosí, México

² Coordinación para la Innovación y Aplicación de la Ciencia y la Tecnología - Laboratorio Nacional, Universidad Autónoma de San Luis Potosí Av. Sierra Leona #550, Col. Lomas 2a. Sección, C.P.: 78210, San Luis Potosí, México

³ Unidad Académica de Física, Universidad Autónoma de Zacatecas “Francisco García Salinas” Zacatecas, México

Nanotechnology is today one of the milestones of science and has represented a radical change in the mankind lifeway from everyday aspects to a complete revolution in the industry. Likewise, one of the most promising achievements nanotechnology has reached is the development of quantum dots (QDs). QDs are semiconductor particles with few nanometers in size, having optical and electronic properties that differ from larger particles. For example, semiconductor QDs give rise to the development of more efficient solar cells, optoelectronic devices, and also quantum computing. QDs can be self-assembled with molecular beam epitaxy (MBE) technique which is the ordered growth of a monocrystalline layer that maintains a defined relationship with respect to the lower crystalline substrate. In Stranski-Krastanov growth mode the InAs/GaAs system self-assemblage process occurs since the GaAs lattice constant is 7% smaller than the InAs lattice. Thus, at the initial stages of the growth the InAs adopts the GaAs lattice constant, but elastic strain (E) is generated in the deposited film. e is accumulated as the InAs thickness is increased. So, the thickness reaches a point (called as critical thickness, H_c) at which the structure collapses and instead of forming a flat 2D surface, 3D nano-islands are assembled that finally make up the QDs. Since the QDs are nucleated due to the tension of the film on which it grows, one can assume that by modifying it, the self-assembling would change too. In this report it is presented an analysis of H_c and geometry of InAs quantum dots grown on InGaAs. The E was modulated by inserting a layer of GaAs of thickness Sm between the InAs and InGaAs. The in-situ RHEED characterization showed that H_c changes significantly with Sm . In order to explain the results we took the dependence of H_c with E as developed for Mathews et al. [1] and extended the equations to simulate the dependence of H_c with Sm . Fittings of $H_c(Sm)$ to the experimental data were obtained, with the exception for the sample grown at $Sm=0$, which is explained as a possible In segregation from the InGaAs film to the QDs. Additionally, we investigated the effects of the strain on the QDs morphology. As it is known, the QDs usually assume the rhombic pyramidal geometry whose faces are crystallographic planes. The shape of RHEED chevron like intensity spots close to the 2D-3D transition changes. In particular, we followed the evolution of the (002) streaks spot (chevron angle) and found that the QD facets undergoes through the previously reported family planes {531}, {631} and {731} during self-assembling. In spite that H_c was noticeably modulated with Sm , the faceting appeared to be independent of it, indicating that the huge diffusion of the adatoms close to the transition 2D-3D may have to govern the shape of the QDs. **Acknowledgments:** The authors acknowledge the financial support from FRC-UASLP, C19-FAI-05-18.18 and CONACYT-Mexico through grants: CB 2015-257358, PNCPN2014-01-248071 and Catedras CONACyT Project No. 44. Hernández-Medina and M. Favila-Castañeda would like to thank the “Verano de la Ciencia Regional 2019” program.



[1] J. W. Matthews, S. Mader, and T. B. Light, Journal of Applied Physics **41**, 3800 (1970).

[NSN-612] Influence of ferrocene concentration, carrier flux and temperature in the structure of N-MWCNTs: CVD method

Brenda Irais Orea Calderon (*bioc_0695@hotmail.com*)¹, Brenda Irais Orea Calderon²,
Florentino Lopez Urías¹, Emilio Muñoz Sandoval¹

¹ Advanced Materials Division, IPICYT, San Luis Potosí, México.

² Faculty of Chemical Engineering, Materials Division, Autonomy University of Puebla, 18
sur S/N, Puebla, Mexico.

The research of carbon nanotube (CNT) growth mechanism using different precursors is an issue constantly addressed in diverse publications. The study of the morphology and physic-chemical properties of obtained CNT allow us design carbon nanomaterials for specific applications. In this work, the effect of low catalyst concentration on the growth of nitrogen-doped multi-wall carbon nanotubes (N-MWCNTs) by the aerosol assisted chemical vapor deposition method is investigated. The thermal decomposition of a benzylamine/ferrocene mixture was used as a source of carbon, nitrogen and as a source of the catalytic particle. The AACVD experiment was developed in an Ar gas flow range of 0.6 L/min at 3.6 L/min at temperatures of 800 °C and 850 °C. The N-MWCNTs were characterized by scanning electron microscopy (SEM), transmission electron microscopy (TEM), thermogravimetric analysis (TGA), Raman spectroscopy and X-ray diffraction (XRD). Our results showed that low concentrations of ferrocene led to the growth of N-MWCNTs with an internal morphology of bamboo type. Additionally, a electrochemical characterization was performed to test its in electrochemical sensors.



[NSN-616] InAs quantum dots grown on GaAs (AlGaAs) and enclosed with AlGaAs (GaAs) upper barriers by MBE.

Christian Alejandro Mercado-Ornelas (*cmercado@estudiantes.uaslp.edu.mx*)², Felipe Eduardo Perea-Parrales², Leticia Ithsmel Espinosa-Vega², Irving Eduardo Cortes-Mestizo¹, Victor Hugo Mendez-Garcia (*victor.mendez@uaslp.mx*)²

¹ CONACYT-CIACYT, Universidad Autónoma de San Luis Potosí, San Luis Potosí, México

² Coordinación para la Innovación y Aplicación de la Ciencia y la Tecnología, Av. Sierra Leona #550, Col. Lomas 2a Sección, CP 78210, UASLP, San Luis Potosí, México

Low dimensional systems (LDS) have demonstrated to create unique quantum confinement, which increases the density of states and consequently may improve the devices performance. Examples of LDS applications are high efficiency LEDs, lasers, storage devices and solar cells. In the later the implementation of LDS leads to unique quantum confinement states allowing to produce greater amount of photogenerated carriers. [1] Among the variety of LDS, one of the most promising and intriguing systems are the InAs quantum dots (QDs), which are also known as zero-dimensional structures. However, in order to apply InAs QDs heterostructures into a device, it is necessary to possess multiple bands and consequently a sequence of stacking QDs. It is known that the formation of multilayers comprises two interesting effects: 1) as the number of stacked layers increases, the strain is also augmented; 2) intermixing between QDs and capping materials occurs, which may change the islands geometry and optical properties. In this work the variation of InAs critical thickness during the QDs stacking and the capping effects with GaAs and AlGaAs was studied. The QDs capped with GaAs (AlGaAs) were grown on AlGaAs (GaAs), defining asymmetric LDS. The samples were synthesized by molecular beam epitaxy (MBE).The QDs nucleation process for each stacked layer was analyzed by in-situ reflection high-energy electron diffraction (RHEED) patterns and the equation proposed in [2], which links the InAs critical thickness H_c and the adatoms diffusion length (λ), related to the nanostructures density (δ) [2]. It was observed that H_c increased slightly as the number of stacking layers increases, independently of the QDs capping material. On the hand λ during the QDs nucleation increased for the growth on AlGaAs, but it decreases for GaAs, even if the lattice mismatch is almost the same. The variation of λ suggest that the QDs density will be affected. In the particular case of InAs/GaAs a greater value of δ is expected, compared with the ternary alloy. After the selfassembling of the QDs the RHEED patterns showed typical chevron like spots, and at the end of the capping processes, linear RHEED patterns were recovered. However, faster evolution towards a flat surface was observed for AlGaAs capping as compared with the GaAs cap.

ACKNOWLEDGMENTS: The authors acknowledge the financial support from CEMIE-SOL 22, FRC-UASLP and CONACYT-Mexico through grants: CB 2015- 257358 and PNCPN2014-01-248071.

References:

- [1] Rakhlin, M. V., Belyaev, K. G. Klimko, G. V., Mukhin, I. S., Kirilenko, D. A., Shubina, T. V., Ivanov, S. V., Toropov, A. A. Scientific Reports 5299 - 8, 1, (2018). <https://doi.org/10.1038/s41598-018-23687-7>
- [2] E. Eugenio-López, et. al. Physica E: Low-dimensional Systems and Nanostructure. 95, (2018) 022-26. <https://doi.org/10.1016/j.physe.2017.08.013>



[NSN-624] Self-assembly process optimization of GaAs (631) quantum wire geometry.

*Felipe Eduardo Perea Parrales*³, *Leticia Ithsmel Espinoza Vega*³, *Christian Alejandro Mercado Ornelas*³, *Irving Eduardo Cortes Mestizo*², *Donato Valdez*⁴, *Andrei Gorbachev*⁵, *Victor Hugo Mendez Garcia (vyktormen@hotmail.com)*³, *David Rubin de Celis Leal*¹
¹ *Applied Artificial Intelligence Institute, Deakin University, Locked bag 2000, Geelong, VIC, Australia.*

² *CONACYT-Center for the Innovation and Application of Science and Technology, Universidad Autónoma de San Luis Potosí, Av. Sierra Leona #550, Col. Lomas 2a Secc. 78210, México.*

³ *Center for the Innovation and Application of Science and Technology, Universidad Autónoma de San Luis Potosí, Av. Sierra Leona #550, Col. Lomas 2a Secc. 78210, México.*

⁴ *Instituto Politécnico Nacional, Unidad Profesional Adolfo López Mateos, Av. Luis Enrique Erro s/n, Edif. Z-4 3er Piso, Ciudad de México 07738, México.*

⁵ *Instituto de Investigación en Comunicación Óptica, Universidad Autónoma de San Luis Potosí, Av. Karakorum 1470, Lomas 4^a Sección 78210, México.*

The fabrication of superlattices (SL) by molecular beam epitaxy is a matter of special importance regarding the design of optoelectronics (e.g. lasers, solar cells and transistors) in behalf of the ability to handily design the electron's wave function and energy nested in these heterostructures. Experimentation is central to the discovery and development of these kinds of high complexity heterostructures involving a myriad of decisions for the system configuration [1], design and growth parameters. Thus, the manufacture success is determined by the design of the experiment (DoE), the hypothesized governing principles, broad approximations and the expert's intuition [2]. As the multi-variable complexity increases the task of identifying the best combination of processes and layer-material settings to achieve a proper device output becomes complex, time and resource consuming. By these reasons, there have been development efforts in experimental optimization aided by new technologies like machine learning, artificial intelligence and adaptive experimental optimization. Even in present days big technological and theoretical advances are able to be made in this area of research [3]. This work presents a novel interdisciplinary theoretical tool for the optimization of self-assembling of GaAs (631) quantum wire-like (QWR) nanostructures. Specifically, Rapid Bayesian Optimization (RBO) has been employed for the synthesis of new materials that involves numerous decisions concerning the process of design, operation, and material characteristics, making RBO suitable for application in MBE self-assembly processes. The input variables $\{x_{1:t}, \dots, x_{n;t}\}$ are the III-V BEP ratio, growth temperature and molecular beams-substrate setup, and the output $\{y_{1:t}, \dots, y_{n;t}\}$ values to be computed are the terrace relative height, width and nanowire length. The best approach to study the self-assembling utilizing this method is found to be throughout the implementation of a Gaussian process where with a kernel function: . The output obtained consist of a series of inter-related variables that gives insight for the experimental setup of the growth parameters to achieve the synthesis of QWRs arrangements, with cost-effective characteristics.

REFERENCES

¹Fisher, S.R.A. et al. vol. 1 1906.

²Cheng Li Scientific Reports vol. 7; 5683 2017.

³Mockus J. Journal of Global Optimization, 4, 347-365 1994.



[NSN-625] Synthesis of Hybrid Carbon Nanostructures Co-Doped With Nitrogen and Sulfur

Cristina de Lourdes Rodríguez Corvera (cristina.rodriguez@ipicyt.edu.mx)¹, Florentino López-Urías (flo@ipicyt.edu.mx)¹

¹ *División de Materiales Avanzados, IPICYT, Camino a la Presa San José 2055, Lomas 4ta sección 78216, San Luis Potosí, S.L.P. , México.*

In this work, three kinds of nanostructures were synthesized varying the setup temperature. We synthesized hybrid graphene nanowalls on carbon nanofibers, carbon nanofibers decorated with iron sulfide and iron sulfide nanoparticles covered by nanoflakes of carbon. The samples were synthesized by aerosol-assisted chemical vapor deposition (AACVD) through the decomposition of thiourea ($\text{CH}_4\text{N}_2\text{S}$), n-hexane (C_6H_{14}) and ferrocene ($\text{Fe}(\text{C}_5\text{H}_5)_2$) using two furnaces, the temperature of the first one was varied from 180 °C, 230°C to 290 °C. The temperature of the second was fixed at 850 °C under a flow of H_2/Ar . The samples were characterized by scanning electron microscopy (SEM), transmission electron microscopy (TEM), Raman spectroscopy, X-ray diffraction (XRD), thermogravimetric analysis (TGA), and in attempt to probe this material as lithium-sulfur cathode, cyclic voltammetry was performed.



[NSN-635] Chemical and electronic characterization of graphene obtained by liquid-phase exfoliation

*Andrea Guadalupe Villalpando (andrea_hasel@hotmail.com)¹, Mildred Quitana Ruiz²,
Mariela Bravo Sanchez¹*

¹ *Universidad de Guadalajara, Centro Universitario de Ciencias Exactas e Ingenierías,
Departamento de Física, Boulevard Marcelino García Barragán 1421, Olímpica, 44430
Guadalajara, Jal., México*

² *Centro de Investigación en Ciencia de la Salud y Biomedicina, Universidad Autónoma de
San Luis Potosí, Av. Sierra Leona 550, 78201, San Luis Potosí, S. L. P.*

Graphene has become one of the most studied materials due its unique properties. Being a carbon sheet with an atom of thickness, graphene has given us a completely different vision of the future for applications in diverse areas of human life: from electronics to health and environment.

The step towards applications requires a deep control in production methods yielding qualities and quantities according with particular applications. Generally, it is desirable for practical industrial applications, high quantities with high quality, ensuring in this way reliability of their properties.

In this work, we have studied chemical and electronic properties of graphene obtained with the liquid-phase exfoliation method, considered for production of pure graphene with reasonable equilibrium between quality, cost aspect, purity, and yield. The method consists on mixing a source of graphene in an aqueous solution under sonication or high shear mixing. In our case, under sonication, we mixed the organic solvent N-Methyl-2-pyrrolidone (NMP) and two different sources of graphene: graphite of electrochemical grade and graphite of a local mine from San Luis Potosí, S.L.P., México, obtaining in this way two liquid samples: PGE (pure graphene from graphite of electrochemical grade) and PGM (pure graphene from mine). During the sonication of both solutions a cavitation phenomenon through sound waves is carried out. The phenomenon of cavitation is defined as a hydrodynamic effect that results in the formation of voids or bubbles in water or any fluid. These bubbles reach a maximum size where they implode, which leads to the rise of separations of layers in the graphite, giving place to graphene.

According to the characterization with TEM, we obtained graphene with areas of up to 20 nm and 50 nm for PGE and PGM, respectively. Chemical properties have been evaluated using XPS, Raman and electronic properties were assessed by Kelvin method, and UPS to show valence band.



[NSN-642] Efficient photocatalytic degradation of Methyl Orange through TiO₂-ZrO₂ photocatalysts

Victor Ruiz Santoyo (ruizsvictor@gmail.com) ⁴, Virginia F. Marañón Ruiz (vmaranon@culagos.udg.mx) ⁴, Alejandro Pérez Larios ¹, Juan Felipe Moreno Torres ⁴, Rita Judit Patakfalvi ³, Héctor Pérez Ladrón de Guevara ², Jesús Castañeda Contreras ², Rubén Arturo Rodríguez Rojas ²

¹ Centro Universitario de los Altos Universidad de Guadalajara Av. Rafael Casillas Aceves no. 1200 Tepatitlán de Morelos Jalisco.

² Centro Universitario de los Lagos, Universidad de Guadalajara, Av. Enrique Díaz de León no. 1144, Col. Paseos de la Montaña, Lagos de Moreno, Jalisco, CP 47460, Mexico

³ Departamento de Ciencias de la Tierra y de la Vida, Centro Universitario de los Lagos, Universidad de Guadalajara, Av. Enrique Díaz de León no. 1144, Col. Paseos de la Montaña, Lagos de Moreno, Jalisco, CP 47460, Mexico

⁴ Laboratorio de Ciencias Químicas/Área de Química Orgánica CA: Tecnología de Materiales 674/Laboratorio Tecnología de Materiales Universidad de Guadalajara Centro Universitario de los Lagos Enrique Diaz de León 1144 Col. Paseo de la Montaña C.P. 474 Efficient photocatalytic degradation of Methyl Orange through TiO₂-ZrO₂ photocatalysts

Water conservation due to the strong dependence that humans have on it has generated a deep interest in developing technologies to conserve it with high quality standards. Among technologies proposed for contaminated water treatment, the advanced oxidation processes appear as one of the most attractive possibilities [1]. Many and different photocatalytic systems based on metal oxides have been studied and designed in various nanostructured shapes for their application in the photodegradation of polluting dyes [2]. Therefore, in this work were synthesized TiO₂-ZrO₂ photocatalysts to study their physicochemical characteristics as well as the effect on the photocatalytic degradation of an azo dye. The synthesis of TiO₂-ZrO₂ with 1, 3, and 5 % wt. of ZrO₂ was carried out through sol-gel method. The crystalline structure of photocatalysts was confirmed by X-ray diffraction analysis and the morphologies of samples were observed by SEM. Furthermore, chemical properties of photocatalysts were characterized via FTIR and UV-Vis spectrophotometry analyses. The photocatalytic activities of the photocatalysts were investigated using methyl orange (MO), an azo dye with high presence in contaminated water from textile industries. The results showed that all photocatalysts presented high crystallinity according to X-ray analysis as well as a semi-globular shape and a uniform agglomeration among nanoparticles with an average size between the 300 and 600 nm. The photocatalytic degradations showed that TiO₂-ZrO₂ exhibited higher photocatalytic activity than the TiO₂ nanoparticles. The photodegradations achieved for TiO₂-ZrO₂-1 %, TiO₂-ZrO₂-3 % and TiO₂-ZrO₂-5% after five hours of reaction were 96%, 92% and 90% respectively. Those differences were attributed to absorption in the visible light region, smaller crystal sizes and more surface OH groups, which resulted in a lower band gap energy.

[1] M.C. Collivignarelli, A. Abbà, M. Carnevale Miino, S. Damiani, Treatments for color removal from wastewater: State of the art, *J. Environ. Manage.* 234 (2019) 727–745. doi:10.1016/j.jenvman.2018.11.094.

[2] M. Anjum, R. Miidad, M. Waqas, F. Gehany, M.A. Barakat, Remediation of wastewater using various nano-materials, *Arab. J. Chem.* (2016). doi:10.1016/j.arabjc.2016.10.004.



[NSN-646] Structural study of the phases of cobalt nanowires and their relationship with the properties of magnetic anisotropy

Maria Fernanda Ruiz Villegas (maria.ruiz@ipicyt.edu.mx)¹, Armando Encinas (armando.encinas@ipicyt.edu.mx)¹

¹ División de Materiales Avanzados, Instituto Potosino de Investigación Científica y Tecnológica, San Luis Potosí, México.

Electrodeposition of Cobalt into nanoporous templates to produce nanowire arrays is known to have a strong dependence on the pH of the electrolyte. In particular, a vast number of reports have shown that the microstructure of the Co deposits can be controlled by adjusting the pH. At pH values near 2.0 the growth of Co is such that it can't grow in its usual HCP structure, instead several reports have shown that it grows dominated by stacking faults. Whereas at pH values in the 3.5 up to 5.5 it grows with a textured HCP structure such that the c-axis is practically perpendicular to the growth direction and for pH values above 6.0 a strong texture with the HCP c-axis oriented parallel to the growth direction is observed. Most of these studies employ well-defined parallel pores in anodized alumina or polycarbonate membranes. [1,2]

In the present study we are interested in the effects of using a deposite angle commercial grade membranes where the cylindrical pores are known to be not parallel to each other and are characterized by a large pore orientation dispersion. For these types of membranes, we want to assess the effect of the electrolyte pH on the microstructure of Co deposits and correlate them with their magnetic properties. For the present study commercial grade Polycarbonate and Polyester membranes with cylindrical pores of 125 and 200 nm, respectively have been used. Deposits have been made at pH values of 3.5 and 6.5 in order to favor the HCP structure with the c-axis nominally oriented perpendicular and parallel to the growth direction. The samples have been characterized using X ray diffraction and room temperature vibrating sample magnetometry. The results show that the most dominant effect follows from the electrolyte pH value and that the orientational disorder of the pores has little effect. Cobalt wires grown at pH values of 3.5 always show a clear HCP texture with the c-axis oriented perpendicular to the growth direction. While for pH=6.5, a preferential orientation of the c-axis along the growth direction. While, on the other hand, the hysteresis loops show that membranes with different pore orientational disorder show little changes between Co samples grown at the same pH value. However, the rotation of the c-axis from the direction perpendicular (pH=3.5) to parallel (pH=6.5) results in clear changes in the magnetic properties of the nanowire arrays. [3]

References

1. J. Phys. D: Appl. Phys. 37, 1411 (2004)
2. Physical Review B 77, 014417 (2008)
3. *Journal of Physics D: Applied Physics* — Vol. 39, no. 23, p. 5025-5032 (2006).



[NSN-652] WIRE FABRICATION AND 3D PRINTING OF POLYMER/GRAPHENE FOAM FOR THE ENCAPSULATION OF ESSENTIAL OIL

Alma Delfina Arenas Flores², José de Jesús Pérez Bueno (*jperez@cideteq.mx*)¹, Gustavo Alvarado Kinnell², María Luisa Mendoza López³

¹ Centro de Investigación y Desarrollo Tecnológico en Electroquímica (CIDETEQ), S.C., Pedro Escobedo, Querétaro, CP 76703, México.

² Tecnológico Nacional de México, Instituto Tecnológico de Orizaba, Oriente 9, Emiliano Zapata, 94320 Orizaba, Veracruz, México.

³ Tecnológico Nacional de México, Instituto Tecnológico de Querétaro, Av. Tecnológico s/n Esq. Mariano Escobedo, Col. Centro, C.P.76000, Querétaro, Qro. México

According to research carried out in recent years, the inclusion of graphene in plastic materials used for the generation of filaments, useful in 3D printing processes, tends to improve the qualities of thermal conductivity and fusion of the process to the material, in addition to benefiting the macroscopic properties of the product formed.

In this work, filaments were obtained of the polymers Poly (methyl methacrylate) PMMA and Acrylonitrile-butadiene-styrene ABS, mixed with graphitic materials such as carbon black, graphene and graphene foam at different concentrations. The fundamental part of this study consisted of the preparation of filaments with graphene foam and its use in the encapsulation of oils of essences.

This research was carried out in different stages; the first was to develop filaments with PMMA mixed with different graphene materials, at different concentrations, and different temperatures for extrusion. The second stage was to obtain ABS filaments with different temperature and concentration parameters. Then, the encapsulation of the essential oil. Finally, the last stage contemplates the characterization of the filaments obtained.

A double screw extruder was used in the ABS NH and Graphene foam composite samples. Thermoplastic polymeric materials were prepared using the melt mixing technique, with the help of an extruder where particles of a carbon derivative, carbon black, and graphene foam were applied, varying the concentrations thereof, to then perform a 3D print.

The comparative study, at different concentrations and temperatures in the PMMA, shows as the adequate concentration that of about 1% of the graphene material since the pigmentation on the polymer was better. In the case of the temperature, it was better extracted at 160 °C since if the temperature was increased, the filament came out faster in the die and had more deformities.



[NSN-656] SYNTHESIS TEMPERATURE SIMULATION OF STAINLESS STEEL BAR CATALYST IN CARBON NANOSTRUCTURES GROWTH

José de Jesús Contreras-Navarrete², José de Jesús Contreras-Navarrete¹, Víctor García-García¹, Carmen Judith Gutiérrez-García², Jael Madaí Ambriz-Torres², Francisco Gabriel Granados-Martínez², Francisco Gabriel Granados-Martínez³, Diana Litzajaya Garcia-Ruiz², Omar Aguilar-García¹, Ezequiel Huipe-Nava², Lada Domratcheva-Lvova²

¹ *Instituto Tecnológico de Morelia, Avenida Tecnológico 1500, 58120 Morelia, Michoacán*

² *Universidad Michoacana de San Nicolás de Hidalgo, Gral. Francisco J. Múgica S/N, Felicitas del Río, 58030 Morelia, Mich., México.*

³ *Universidad Nacional Autónoma de México, Campus Morelia, Antigua Carretera a Pátzcuaro 8701, 58190 Morelia, Mich., México*

The carbon nanostructures formation is influenced by several internal and external factors. Precursor, gas flow, reaction time, catalyst, temperature and others are considered as the most common factors of influence in the carbon nanostructures synthesis. The temperature influence over stainless steel bar (used as catalyst) and how this factor affects the carbon nanostructures growth over the catalyst was analyzed in this research using simulation. Carbon nanostructures were obtained by CVD technique using hexane as carbon source and stainless steel bar as catalyst. Two temperatures reaction (700 and 750 °C) and two reaction times (30 and 40 minutes) were carried out. Heat transfer process between quartz tube, argon, argon/hexane and a stainless steel bar was simulated using ANSYS Mechanical software. Considering internal laminar flow, the heat transfer coefficients were calculated for argon and hexane. The results show that temperature synthesis distribution reaches its highest value at the middle of the bar with temperatures around 620 °C for 30 and 40 minutes. Bar edges present values over 205 °C. According to the simulation results, the synthesis temperature of the experiments affects over all the bar mainly in the middle and it is one of the principal reasons of carbon nanostructures growth in this zone of the stainless steel bar. Simulation provides the possibility to predict how the experimental conditions affect carbon nanostructures growth with the possibility of cost minimization and synthesis optimization.

Acknowledgment:

Acknowledgment to CIC of Universidad Michoacana de San Nicolás de Hidalgo, Instituto Tecnológico de Morelia y CONACYT México for the financial support.



XII -ICSMV

September 23rd to 27th, 2019 / San Luis Potosí, México

[NSN-657] A nanocomposite for increasing hydrophobicity of clothes

Hugo Valdemar Galindo Cuevas (okhariss@mail.ru) ¹, Oxana V. Kharissova
(okhariss@mail.ru) ¹

¹ FCFM, Universidad Autónoma de Nuevo León, Monterrey, Nuevo León, México

One of the most important properties of clothes in the textile industry is that they repel all water, or at least delay it in a very significant way. All this is to avoid spillage accidents and not to get dirty or store odors, making it not necessary to wash or change so frequently. In this work, a composite containing silicon oxide, MTMS, APTES, MSDS and PMDS nanoparticles was added to different clothes such as polyester and suede. In each of them, the initial and final contact angles were observed to study the hydrophobicity. The initial angles without the coating were 70-80°; after applying the composite, the contact angles increased up to 140°, showing good hydrophobic properties of textiles.



XII -ICSMV

September 23rd to 27th, 2019 / San Luis Potosí, México

[NSN-658] Use of carbon nanotubes as an alternative method of cleaning water contaminated by oil spills

Jonathan Gerardo Martínez Quiroz¹, Oxana V. Kharissova (okhariss@mail.ru)¹

¹ FCFM, Universidad Autónoma de Nuevo León, Monterrey, Nuevo León, México

Oil spills negatively affect maritime ecosystems and, over time, various inefficient methods and some harmful to the environment have been designed for their elimination. In this work, several tests of an alternative methodology for the cleaning of the drinking and saline water, contaminated with oil, were carried out with the aid of multiwall carbon nanotubes containing iron nanoparticles. As a main result, almost total elimination of oil has been achieved by using small quantities of iron-doped carbon nanotubes at room temperature without any other additives or additional treatments. In addition, iron nanoparticles possess weak antibacterial properties, preventing multiplication of bacteria in treated environmental samples.



XII -ICSMV

September 23rd to 27th, 2019 / San Luis Potosí, México

[NSN-660] Optical tweezers for the characterization of functionalized gold nanoparticles

Antonio Sotelo-López (ant.sotelo.l@gmail.com)¹, José Abraham Balderas-López¹

¹ UPIBI - IPN. Photothermal Techniques Laboratory.

Optical tweezers systems have been used traditionally for the tridimensional trapping of micrometer objects, leading mostly to biological applications. Only in recent years, optical forces have been reported to be used for applications in the nanoscale range and few of them about plasmonic nanoparticles. In this work, we study the use of optical tweezers with linear polarized laser for the measuring of physical properties of functionalized gold nanoparticles, registering the formation of arrays around the laser irradiation area depending on the light polarization and the interparticle interaction.



[NSN-661] Synthesis of iron selenide (FeSe_2) nanoparticles and their self-assembly into stacked nanoplatelets

MANUEL ALEJANDRO PEREZ GUZMAN (maperez@cinvestav.mx)⁵, ALVARO GUZMAN CAMPUZANO⁴, JAIME SANTOYO SALAZAR¹, REBECA ORTEGA AMAYA³, ENRIQUE CAMPOS GONZALEZ², MAURICIO ORTEGA LOPEZ⁴

¹ DEPARTAMENTO DE FISICA, CINVESTAV. AV. IPN 2508 COL. SAN PEDRO ZACATENCO, GUSTAVO A. MADERO, CIUDAD DE MEXICO 07360

² DEPARTAMENTO DE FISICA, ININ. CARR. MEXICO TOLUCA-LA MARQUESA S/N, OCOYOACAC, EDO. MEX. C.P. 52750

³ DEPARTAMENTO DE FISICA, UAM IZTAPALAPA. AV. SAN RAFAEL ATLIXCO 186, COL. VICENTINA, CIUDAD DE MEXICO 09340

⁴ DEPARTAMENTO DE INGENIERIA ELECTRICA, CINVESTAV. AV. IPN 2508 COL. SAN PEDRO ZACATENCO, GUSTAVO A. MADERO, CIUDAD DE MEXICO 07360

⁵ PROGRAMA DE DOCTORADO EN NANOCIENCIAS Y NANOTECNOLOGÍA CINVESTAV. AV. IPN 2508 COL. SAN PEDRO ZACATENCO, GUSTAVO A. MADERO, CIUDAD DE MEXICO 07360

Nanocrystals of the transition-metal chalcogenides display a variety of useful physical and chemical properties for applications in the technological areas of electronic, nanomedicine, energy storage and conversion, etc. Recent studies on the several crystalline phases of FeSe and FeTe and their alloys have indicated that promising superconductors can be obtained. Furthermore, Fe_xSe_y and FeS have suitable electrical and optical properties as those of better light absorber material of thin film solar cells. Fe_xSe_y develops various crystalline phases, including $\text{Fe}_{1.01}\text{Se}$ (superconducting), Fe_5Se_8 (hard magnetic) and FeSe_2 (direct band gap p-type semiconductor). Due to its electrical and optical properties, FeSe_2 is being tested as the absorber material of thin film solar cells. The present work describes the synthesis of FeSe_2 and their self-assembly into stacked layers, the FeSe_2 nanoparticles were synthesized by a polyol method. We monitored the FeSe_2 nanostructures (morphology, structure and chemical possible changes) at different times from 1 h to 96 h. The resultant FeSe_2 dispersions produce the above-mentioned nanostructures and thin films when it is used as the starting solution in the spray pyrolysis process.



[NSN-666] Shape Control, Chemical Ordering and Structural Characterization of Nanoalloys

Ruben Mendoza Cruz (rumecc21@gmail.com)², Lourdes Bazan Diaz ¹

¹ Materials Research Institute, UNAM.

² University of Texas at San Antonio

As the case of ancestral bulk alloys, nanoalloys have opened field of research of paramount importance due to their enhanced properties arisen from the finite size and synergic effects between their components. These properties appear not only by the mixed nature of the particles, but also in their structural arrangement, and they are highly dependent of the particle size and shape. Nanoalloys possess properties with great applicability in catalysis, optoelectronics, mechanical engineering, biomedical engineering, etc., and these properties can be highly improved by changing their relative composition and atomic arrangement (ordering/segregation). Hence, the study of their structure, as well as the correlation with the observable properties is of great importance. Among the characterization techniques, transmission electron microscopy has proven to be an excellent alternative for an integral characterization of nanoscale materials, since very fine local information and the complete structure can be directly obtained. In this talk, an electron microscopy study of the effect of the chemical composition and ordering/segregation on the final structure of different metallic nanoalloys is presented. The importance of controlling the experimental conditions during the synthesis is discussed, aiming the control on the size and shape of the bimetallic nanoparticles.



[NSN-668] Facile preparation of g-C₃N₄/WO₃ for evaluation of its photocatalytic properties in the degradation of emerging pollutants

Julio César Vallejo Márquez (cesarvallejo28@outlook.com) ¹, Daniel Sánchez Martínez (cesarvallejo28@outlook.com) ¹, Diana Berenice Hernández Uresti (cesarvallejo28@outlook.com) ¹, Elvira Zarazúa Morín (cesarvallejo28@outlook.com) ¹

¹ Av. Universidad S/N Cd. Universitaria, apartado postal 17

The g-C₃N₄/WO₃ composites were obtained by physical mixing at different weight ratios. The characterization of the materials was using X-ray diffraction analysis (DRX), where it was observed that the composites are made up of both materials. The characterization was complemented by scanning electron microscopy (SEM), where it was observed that carbon nitride and tungsten oxide have a morphology of thin sheets and flakes, respectively [1]. The banned band energy (Eg) of the composites had a value between 2.6 and 2.7 eV [2,3]. The surface area values ranged from 9 to 36 m²g⁻¹. Photocatalytic tests were performed to evaluate the activity of the composites in the degradation of different emerging pollutants (Acetaminophen and Ibuprofen) under simulated sunlight (Xe lamp 6000K). The sample that presented the best photocatalytic activity was the compound with a ratio of 95% g-C₃N₄ / 5% WO₃, with both contaminants. This sample was used to perform stability tests. In turn, medicine mineralization tests were performed, said the test was determined by analysis of total organic carbon (TOC).

1. Ken-ichi Katsumata, Ryosuke Motoyoshi, Nobuhiro Matsushita, Kiyoshi Okada, Journal of Hazardous Materials (2013).
2. Xin Liu, Ailing Jin, Yushuai Jia, Tonglin Xia, Chenxin Deng, Meihua Zhu, Changfeng Chen, Xiangshu Chen, Applied Surface Science (2017)
3. Bo Chai, Chun Liu, Juntao Yan, Zhandong Ren, Zhou-jun Wang, Applied Surface Science (2018)



[NSN-676] Numerical analysis of spiral nanocapacitors with gold nanoparticles

Brhayllan Mora Ventura (bmora.ventura@gmail.com)¹, Gabriel González Contreras (gabriel.gonzalez@uaslp.mx)¹, Alexander Cuadrado Conde², Javier Alda², Francisco Javier González¹

¹ *Universidad Autónoma de San Luis Potosí, Sierra Leona, 550, Lomas 2da Sección, Building CIACYT, 78210 San Luis Potosí, México.*

² *University Complutense of Madrid, Faculty of Optics and Optometry, Applied Optics Complutense Group, Avenue, Arcos de Jalón, 118, 28037 Madrid, Spain.*

A spiral nanocapacitors are analysed using numerical simulation. The performance of the capacitor is evaluated with and without a doping with gold nanoparticles improving its electrical properties. The results show that spiral capacitors present an increment in their capacitance when are doped with gold nanoparticles. These results show that the overall capacitance efficiency can be increased by the combination of geometry and the quantity of metal nanoparticles. Fractal and square spiral capacitors have been fabricated by electron beam lithography.

Capacitors are crucial electronic devices that play an important role in many applications that range from domestic devices, telecommunications systems, medical instrumentation, power systems, energy harvesting and others applications. With the constant miniaturization of electronic devices area efficient capacitors are desirable. One of the approaches for the area efficiency problem was to employ a fractal geometry in the capacitor design [1]. Fractal objects are described by a specific mathematical formulation that undergoes a recursive iteration generating the fractal which is scale-invariant and self-similar. Several designs of fractal geometry have been presented to improve the capacitance per unit area [2]. Capacitors based on fractal geometry such as Hilbert [1], Peano, etc, are area-efficient but unfortunately have low capacitance. One solution for increasing the capacitance of the fractal capacitor is to dope the fractal capacitors with nanoparticles. Recently, it has been shown that the capacitance of an interdigital capacitor increases with colloidal gold nanoparticles [3].

References

- [1] Kumar PA, Rao NB. Fractal spiral capacitor for wireless applications. 2016;52(6).
- [2] Sagan H. Space-Filling Curves. New York, USA: Springer-Verlag; 1994.
- [3] Zeinabad HA, Ghourchian H. Ultrasensitive interdigitated capacitance immunosensor using gold nanoparticles. Nanotechnology. 2018.



XII -ICSMV

September 23rd to 27th, 2019 / San Luis Potosí, México

[NSN-677] DESIGN, FABRICATION AND CHARACTERIZATION OF BOWTIE ANTENNA DEVICE IN RANGE OF SUB-TERAHERTZ

LUIS ISAAC LUGO PEREZ (*luisaac.lugo@gmail.com*)¹, FRANCISCO JAVIER GONZÁLEZ CONTRERAS¹, GABRIEL GONZÁLEZ CONTRERAS¹

¹ LANCYTT-CIACYT, UASLP, SLP, MEXICO

The main objective of this work is to show a Bowtie Antennas (BTA) as devices to detect the electromagnetic spectrum in the range of sub-terahertz (sub-THz). The device fabricated were an array of BTA over a substrate. The design of the antenna were calculated with the dipole relation (, where λ is the wavelength and ϵ_r is the relative permittivity of the substrate), then a simulation of the antenna were made by the Finite Element Method (FEM) using the software COMSOL MULTIPHYSICS. The antenna fabrication was made by the Electron Beam Lithography (EBL) technique. For substrates, and **polyamide tape** were used. Once the antenna array were impressed on the substrate, a material deposition were made by the Sputtering technique, the material choosed for the antenna was silver (Ag). For characterizaion and study of the the BTA array a FTIR analysis was selected looking for the antenna frequency response.



[NSN-683] Study of nanostructured gallium oxynitride thin films

Orlando zelaya-angel¹, Elizabeth Galván-Flores³, Gerardo González de la Cruz², Mario Fidel García-Sánchez⁴

¹ Departamento de Física, CINVESTAV-IPN,

² Departamento de Física, CINVESTAV-IPN

³ Departamento de Nanociencias, CINVESTAV-IPN

⁴ Unidad Profesional Interdisciplinaria en Ingeniería y Tecnologías Avanzadas- (IPN),
C.P. 07340, México DF, México.

Thin films of gallium oxynitride have been prepared on glass substrates by the r.f. sputtering technique at room temperature. A target with a mix of gallium nitride and high purity nitrogen and oxygen gases were employed. The structure and morphology were studied by X-ray diffraction (XRD), scanning electron microscopy (SEM), atomic force microscopy (AFM), Raman, photoluminescent and UV-Vis optical absorption spectroscopies. XRD measurements show that the obtained films were composed by gallium oxynitride and some secondary phases, and from peak reflections an average crystal size of 5 ± 1 nm was determined. UV-Vis absorbance allows to calculate the direct energy band gap with a 4.1 eV value. The Raman spectra also reveal the presence of other phases into the films. PL measurements, in the range of 360-630 nm, show wide bands identified with emission centered in the blue region of the visible light spectrum, which are associated with levels of defects into the forbidden energy band gap.



XII -ICSMV

September 23rd to 27th, 2019 / San Luis Potosí, México

PLASMA AND VACUUM (PLV)

**Chairmen: José G. Quiñones-Galván, (CUCEI, UdeG)
Miguel Ángel Santana-Aranda, (CUCEI, UdeG)**



XII -ICSMV
September 23rd to 27th, 2019 / San Luis Potosí, México

PLASMA AND VACUUM (PLV) ORAL SESSION



XII -ICSMV

September 23rd to 27th, 2019 / San Luis Potosí, México

[PLV-94] Characterization of hybrid plasmas for deposition of nanostructured thin films

ENRIQUE CAMPOS GONZALEZ (enrique.campos.conacyt@inin.gob.mx)¹, ENRIQUE CAMPS C.²

¹ Departamento de Física > Instituto Nacional de Investigaciones Nucleares (ININ) > Carretera México-Toluca s/n. La Marquesa > Ocoyoacac, Estado de México, México > C.P. 52750

² Departamento de Física, Instituto Nacional de Investigaciones Nucleares (ININ) > Carretera México-Toluca s/n. La Marquesa Ocoyoacac, Estado de México, México C.P. 52750

The use of plasmas for the modification of the properties of different materials is a topic that has been known for several decades and has attracted the attention of specialists because, through the exposure to plasmas of different materials, it is possible to modify mechanical, electrical and magnetic properties. The main aim of this work is to report the study of the combination of continuous plasma, formed by a microwave discharge and pulsed plasma of laser ablation which allow studying the formation of materials in the form of thin films with elements that are obtained from solids, combined with the continuous plasma formed from gases. In this way the background gas will be plasma, instead of a neutral gas. In this way we can study materials that in each of the plasmas separately, are not possible to obtain or is too complicated. Plasma parameters were measured by a Langmuir probe. The chemical species contained in the plasma were analyzed by optical emission spectroscopy (OES). In this work we report the formation of TiO₂ films using the pulsed plasma of laser ablation. The obtained films were subsequently treated in continuous nitrogen plasma formed in the microwave discharge. The structure and chemical composition of the nitride TiO₂ films results are reported.



[PLV-132] Synthesis of nitrides via reactive magnetron sputtering: Analysis of different deposition parameters by optical emission spectroscopy

Roberto Sanginés (sangines@cnyn.unam.mx)¹, Itayeé Sierra-Cruz², Genaro Soto Valle Angulo², Julio Cruz², Noemí Abundiz Cisneros¹, Juan Águila Muñoz¹, Roberto Machorro Mejía²

¹ CONACyT, Centro de Nanociencias y Nanotecnología, Universidad Nacional Autónoma de México

² Centro de Nanociencias y Nanotecnología, Universidad Nacional Autónoma de México

Direct-Current reactive magnetron sputtering (DC-RMS) is one of the most popular techniques to deposit high-quality thin films of compounds. It is preferred because it can produce thin films with controllable stoichiometry, it has a relatively high deposition rate and can be escalated to industrial applications. One major drawback of this technique is the so called target poisoning which is the formation of compounds on the target surface and may result in unwanted thin film composition and/or low deposition rate. Although this is a well established deposition technique still some questions arise on how the optimal deposition conditions can be identified for a particular deposition system.

In DC-RMS, deposition of metallic nitrides could potentially become a difficult task, as a result of the lower affinity of nitrogen to metals with respect to oxygen. Then, even for low residual oxygen within the chamber, it is likely that some oxygen incorporation occurs at the thin film.

In this work we propose a method to optimize the synthesis of nitrides films via reactive magnetron sputtering. We used optical emission spectroscopy (OES) to monitor, in real time, the plasma produced during the deposition process in DC-RMS. A detailed analysis of the OES results for different deposition parameters gave that the intensity ratios of specific transitions can be correlated to the properties of growing film. Three materials were studied to illustrate this optimization: Silicon nitride (Si₃N₄), Aluminium nitride (AlN) and Titanium nitride (TiN).



[PLV-305] DC, P-DC and RF sputtering of titanium and graphite targets, with and without magnets in the cathode

Stephen Muhl (muhl@unam.mx)², Sandra E. Rodil², Luis E. Sanchez-Balanzar³, Enrique Camps¹

¹ *Depto. de Fisica, ININ*

² *IIM-UNAM, CDMX*

³ *UNAM, CDMX*

Magnetron sputtering is extensively used to fabricate thin film coatings for a very broad range of applications. It is well known that the magnetic field close to the surface of the magnetron cathode traps electrons and produces an increased ionization of the gas, and that this increases the plasma density allowing sputtering at lower pressures, higher sputtering rates and also can produce an increased bombardment of the deposit. The optimal value of the magnetic field strength depends on a combination of the sheath width and the target voltage. If the electron cyclotron radii are significantly less than, or much larger than, the sheath width then little increase in the ionization is produced. Various groups have proposed that when RF or pulsed DC (P-DC) are used the overvoltage associated with restarting the plasma in each cycle, plus the varying target voltage means that the magnetron provides little benefit, i.e. that the magnetic field is only effective for a small part of each cycle. To study this idea, we prepared thin films from carbon and titanium targets by low pressure argon magnetron sputtering, with and without the magnets, using the same experimental conditions, but with DC, RF or 250 kHz P-DC excitation. Without the magnets the maximum plasma power which could be used was < 80 W for the RF and < 200 W for the P-DC, using the graphite target, and 300 W RF and 200 W P-DC using the titanium target. Attempts to use higher powers resulted in very unstable plasmas and/or plasma extinction. Without the magnets the deposition rates were decrease to about half that of the normal value, independent of the target or type of high frequency excitation, and the DC deposition rates were 2 - 3 times the high-frequency rates. The thickness uniformity, hardness, adhesion and properties of the films were strongly dependent on the type of electrical power used.



[PLV-546] Synthesis and characterization of thin films deposited by the laser ablation of a MoS₂ target at different fluence values

J.G. Quiñones-Galván (jose.quinones@academicos.udg.mx)¹, E. Campos-González², E. Camps², A. Pérez-Centeno¹, M.A. Santana-Aranda¹, G. Gómez-Rosas¹, A. Chávez-Chávez¹, J.S. Arias-Cerón³

¹ Departamento de Física, Centro Universitario de Ciencias Exactas e Ingenierías, Universidad de Guadalajara, Boulevard Marcelino García Barragán 1421, Guadalajara, Jalisco, México, C.P. 44430

² Departamento de Física, Instituto Nacional de Investigaciones Nucleares, Apdo. Postal 18-1027, México DF 11801, Mexico

³ Departamento de Ingeniería Eléctrica, Sección de Estado Sólido, CINVESTAV-IPN, Apdo. Postal 14-740, México D.F. 07360, México.

Recently, molybdenum disulfide has attracted attention due to it can be grown as a 2D material. Its optoelectronic properties make it interesting for solar cells or photocatalysis applications.

The physical properties of thin films grown by the laser ablation of a bulk MoS₂ target on vacuum are reported.

The samples were grown at fluence values of: 1, 4 and 23 J/cm² at a substrate temperature of 100 °C. The plasma parameters (mean kinetic energy and density) were determined by TOF curves obtained from Langmuir probe measurements. It was found that both mean kinetic energy and density of Cu ions increase with increasing fluence.

The crystalline structure of the films was characterized by XRD and Raman spectroscopy. Raman spectroscopy results show the typical vibrational modes of MoS₂, however, XRD measurements revealed the presence of only one peak that could be assigned to metallic Mo, which would imply Mo segregation or highly sulfur deficient MoS_x thin films. UV-Vis spectroscopy was used to analyze the optical properties of the samples.

Surface morphology was observed by SEM. XPS was used to study the chemical composition and oxidation states of Mo and S.



XII -ICSMV

September 23rd to 27th, 2019 / San Luis Potosí, México

PLASMA AND VACUUM (PLV) POSTER SESSIONS



[PLV-107] CuS films by pulsed laser deposition: Effect of laser fluence on structural and optical properties grown at different wavelengths

Paola Elideth Rodríguez Hernández (prodriuezh89@gmail.com)³, José G. Quiñones Galván², José Santos Cruz³, Miguel Meléndez Lira¹, Sandra A. Mayén Hernández³, Francisco J. de Moure Flores (fcomoure@hotmail.com)³

¹ CINVESTAV, Departamento de Física

² Centro Universitario de Ciencias Exactas e Ingenierías, Universidad de Guadalajara

³ Universidad Autónoma de Querétaro

The importance of alternative energy sources has increased in significance both energy supply and ecological conservation reasons. An example of this, is solar energy, where a natural resource has been used through photovoltaic devices. In recent years, solar cells based on cadmium and selenium have been developed. However, the use of these materials has being questioned due to their toxicity. In order to elaborate nontoxic solar cells, alternative materials have been studied. Metal chalcogenides such as Cu_xSe, Cu_xS, ZnS and CdS, have had a great interest in the last few decades, specially in semiconductor films due to their physical and chemical properties. Among them, copper sulfide is a commonly used material because of their constituent materials (Cu and S) are non-toxic and abundant in nature and it is well-know Cu_xS thin films properties are depended on their diverse stoichiometric composition ranging from copper-poor to copper-rich.

Several methods have been used for growing Cu_xS films, such as chemical bath deposition (CBD), spray pyrolysis, atomic layer deposition (ALD), chemical vapor deposition (CVD) vacuum evaporation, among others. In order to improve and control some stoichiometric phases, several physical techniques have been used. However, stoichiometry transfer from the target to the substrate is difficult to obtain with evaporation or magnetron sputtering using a single target. Pulsed laser deposition (PLD) is an alternative deposition technique to fabricate high quality thin films of materials with a complex stoichiometry, or sandwich structure from a target with similar composition. In addition, a lot of variables can be manipulated in order to improve the properties of the films in the PLD technique, such as laser incident energy, background gas pressure and substrate temperature.

In this work, Cu_xS films were prepared onto soda-lime glass substrates by PLD, changing the wavelength and the distance between the target and lens. Results are presented according to the laser fluence.



[PLV-153] Structural, optical and electrical properties of antimony doped zinc oxide thin films deposited by DC magnetron sputtering.

Javier Alejandro Berumen Torres (jberumentorres@hotmail.com) ², José Juan Ortega Sigala ², José de Jesús Araiza Ibarra ², Fernando Avelar Muñoz ², Efraín Grarcía Jaramillo ², José Guadalupe Quiñones Galván ¹, María Leticia Pérez Arrieta ²

¹ Departamento de Física, Centro Universitario de Ciencias Exactas e Ingenierías, Universidad de Guadalajara, Boulevard Marcelino García Barragán 1421, Guadalajara, Jalisco, México, C.P. 44430

² Unidad Académica de Física, Universidad Autónoma de Zacatecas, Calzada Solidaridad esq. paseo la Bufa s/n. C.P. 98060. Zacatecas, Zac., México

Thin films of antimony doped zinc oxide were deposited by DC magnetron sputtering. A mixture of ZnO and Sb powders was used as target material. The relative concentration of Sb in the target used was 0, 2, 4, 6, 8 and 10 at. %. The films were deposited onto glass and silicon substrates. In order to study the kinetics of the material the used DC power was 30 and 45 W. The structural characterization was carried out by X-ray diffraction, also, the optical properties were obtained by UV-Vis and Raman spectroscopy. Chemical composition was obtained by EDS and finally the electrical properties were measured by Hall effect using Van der Pawn method.



[PLV-169] Physical properties of Sb and Ag co-doped zinc oxide thin films deposited by DC magnetron sputtering.

Susana Abigail González Florez (susanaglez@live.com) ¹, Javier Alejandro Berumen Torres (jberumentorres@hotmail.com) ³, José Juan Ortega Sigala ³, José de Jesús Araiza Ibarra ³, Fernando Avelar Muñoz ³, Juan Ortiz Saavedra ³, José Guadalupe Quiñones Galván ²

¹ *Coordinación de Ingeniería Industrial, Universidad Politécnica de Zacatecas. Plan de Pardillo s/n, Parque Industrial, Fresnillo, Zac. México*

² *Departamento de Física, Centro Universitario de Ciencias Exactas e Ingenierías, Universidad de Guadalajara, Boulevard Marcelino García Barragán 1421, Guadalajara, Jalisco, México, C.P. 44430*

³ *Unidad Académica de Física, Universidad Autónoma de Zacatecas, Calzada Solidaridad esq. paseo la Bufa s/n. C.P. 98060. Zacatecas, Zac., México*

Thin films of antimony and silver co-doped zinc oxide were deposited by DC magnetron sputtering. A mixture of ZnO and Sb powders was used as primary target material, as secondary target, silver 99.999% pure was used. The relative concentration of Sb on the primary target used was 0, 2, 6 and 10 at. %. The films were deposited onto glass and silicon substrates. The used DC power was 30 W. The structural characterization was carried out by X-ray diffraction, also, the optical properties were obtained by UV-Vis and Raman spectroscopy. Chemical composition was obtained by EDS and XPS spectroscopy. SEM measurements were made to obtain micrographs of the material; and finally, the electrical properties were measured by Hall effect using Van der Pauw method.



[PLV-541] CuxS thin films grown at different mean kinetic ion energies of plasmas produced by the pulsed laser ablation of a CuS target

P. E. Rodríguez-Hernández ⁴, E. Campos-González ², E. Camps ², A. Pérez-Centeno ¹, J.S. Arias-Cerón ³, M.A. Santana-Aranda ¹, G. Gómez-Rosas ¹, A. Chávez-Chávez ¹, F. de Moure-Flores ⁴, J.G. Quiñones-Galván (jose.quinones@academicos.udg.mx) ¹

¹ Departamento de Física, Centro Universitario de Ciencias Exactas e Ingenierías, Universidad de Guadalajara, Boulevard Marcelino García Barragán 1421, Guadalajara, Jalisco, México, C.P. 44430

² Departamento de Física, Instituto Nacional de Investigaciones Nucleares, Apdo. Postal 18-1027, México DF 11801, Mexico

³ Departamento de Ingeniería Eléctrica, Sección de Estado Sólido, CINVESTAV-IPN, Apdo. Postal 14-740, México D.F. 07360, México.

⁴ Facultad de Química, Materiales, Universidad Autónoma de Querétaro, Querétaro, 76010, México.

Cu_xS thin films are of interest for solar cell applications due to it can possibly substitute CdTe, it has a p-type conductivity and band gap ranging from 1.2 to 2.5 eV depending on the composition.

In the present work, thin films were deposited by the pulsed laser ablation of a solid CuS target under different fluence values in order to produce plasmas with two different mean kinetic energies. The films were deposited on glass substrates at room temperature. The physical properties of the films depend on the plasma energy.

Plasma mean kinetic energy was estimated from the TOF curves obtained from Langmuir planar probe measurements, using a 6 mm electrode biased at -48 V and connected to a 20 Ohm resistor.

Samples were structurally characterized by X-Ray diffraction and Raman spectroscopy. Optical characterization was carried out by means of UV-Vis spectroscopy. Surface morphology was observed by scanning electron microscopy.



XII -ICSMV

September 23rd to 27th, 2019 / San Luis Potosí, México

[PLV-631] Electronic, Structural and Optical Properties of ZnO:Ag,N

Efraín García Jaramillo (egarcia@fisica.uaz.edu.mx)², Javier Alejandro Berumen Torres², María Teresa Alejos Palomares³, Julio César López Domínguez², Juan Ortiz Saavedra², Ciro Falcony Guajardo¹, Roberto Gómez Rosales², Fernando Avelar Muñoz², José Juan Ortega Sigala², José de Jesús Araiza Ibarra (araiza@fisica.uaz.edu.mx)²

¹ Departamento de Física, CINVESTAV-IPN

² Unidad Académica de Física, Universidad Autónoma de Zacatecas

³ Unidad Académica de Ingeniería I, Universidad Autónoma de Zacatecas

ZnO:Ag, N thin films were deposited by DC-sputtering and the crystalline structure of doped Ag, N: ZnO in a supercell was analyzed by AB Initio using Quantum Espresso suite. The results and analysis for AB-Initio calculations as band structure, DOS and dielectric function, directly and with a reescalation were realized to establish a predictive behaviour with the structural, optical and electrical characterizations from the experimental X-ray diffraction and UVVis spectroscopy, EDS and electrical measurements. It is found that the ZnO is p-type when nitrogen and silver is incorporated in the structure, giving states near to the valence band. These effects are clear for composition below 20% of N2 in the structure in the deposited films and with Ag-contents lower than 5%. The density of states per energy (DOS) were obtained in the AB Initio calculations initially, from which the band gap energy was determined and corroborated with the optical characterization, using the Tauc equation. Finally, some the effects previously observed for ZnO:N and ZnO: Ag are compared with the observed results from the supercell proposed for Ag, N:ZnO and correlated to the XRD calculated from the AB Initio relaxed structure and latter XRD measured results. The electrical obtained properties are measured by Hall effect. The films used for these purposes (ZnO:Ag, N) had p-type carrier concentration between 10^{16} to 10^{20} cm⁻³.



XII -ICSMV

September 23rd to 27th, 2019 / San Luis Potosí, México

[PLV-647] Spectroscopic analysis of TiN thin films deposited by DC and pulsed reactive magnetron sputtering

Miriam Peralta (mperalta@cicese.edu.mx)², Noemí Abundiz (nabundiz@gmail.com)¹, Roberto Sanginés¹, Juan Águila¹, Roberto Machorro³

¹ CONACYT, Centro de Nanociencias y Nanotecnología, Universidad Nacional Autónoma de México. Apartado Postal 14, Ensenada, B.C., 22800, México

² Centro de Investigación Científica y de Educación Superior de Ensenada, Carretera Ensenada-Tijuana No. 3918, Zona Playitas, C.P. 22860, México

³ Centro de Nanociencias y Nanotecnología, Universidad Nacional Autónoma de México. Apartado Postal 14, Ensenada, B.C., 22800, México

TiN is a transitional metal compound showing covalent and ionic properties, especially TiN films, exhibit excellent physical and chemical properties, such as low resistivity, high hardness, thermal resistivity. Because of these properties, TiN films are extensively applied in many fields.

In this work, we present a study of the growth of titanium nitride thin films (TiN) deposited by DC and pulsed reactive magnetron sputtering. The emission of the plasma is analyzed in real time by optical emission spectroscopy (OES) and TiN films were measured by in-situ ellipsometric-spectroscopy to obtain the optimal deposition parameters to make a comparison between deposits made by DC and DC pulsed. . Finally, this work focuses on the correlations between the plasma species and the properties and structure of the thin film.



XII -ICSMV

September 23rd to 27th, 2019 / San Luis Potosí, México

RENEWABLE ENERGY: MATERIALS AND DEVICES (RWE)

Chairmen: Issis Claudette Romero Ibarra (UPIITA-IPN)

Mario Fidel García Sánchez (UPIITA-IPN)



XII -ICSMV

September 23rd to 27th, 2019 / San Luis Potosí, México

RENEWABLE ENERGY: MATERIALS AND DEVICES (RWE) ORAL SESSIONS



[RWE-44] BORON DOPED NANOCRYSTALLINE DIAMOND FILMS ON SILICON BY MPCVD AND THERMAL DIFFUSION

Rafael Garcia Gutierrez (rgarcia@cifus.uson.mx)¹, Pablo Tirado Cantu¹

¹ Departamento de Investigación en Física, Universidad de Sonora, Hermosillo, Sonora, 83000, México

This presentation will focus on describing the results from research and development of a novel process for Boron doping large area NCD films by thermal diffusion after growth, thus eliminating the problem of Boron contamination of the diamond film growth chamber. The research is focused on understanding the chemical, structural and electrical properties of the NCD films before and after doping with Boron by thermal diffusion. The NCD films were grown by Microwave Plasma Chemical Vapor Deposition (MPCVD) technique on Si (100) substrates. Afterwards, a 200 nm thick Boron containing film was deposited, as a B source, on the NCD film's surface via spin coating followed by annealing in an atmospheric oven at 200°C for 20 minutes in order to evaporate any excess solvent. The diffusion process was carried in a Jetfirst 200 Rapid Thermal Processor (RTP) in a low oxygen atmosphere at 800 °C, 900 °C, and 1000 °C for 180s. Once the diffusion process was over, the NCD films were ultra-sonically cleaned with acetone, methanol and isopropanol in order to remove any remaining Spin on Dopant film from the surface. The boron doped films were characterized by Raman, XRD, XPS and Hall effect measurements. Raman and XRD characterizations were done to confirm that there was no induced graphitization or damage in the films during the diffusion process, while XPS, and Hall effect characterizations were carried to confirm the boron doping and the change in electrical properties (sheet resistance, charge carrier concentration) during the diffusion process. This new process to produce B-doping of NCD films can in principle be extended to MCD films to explore the development of a new generation of diamond based electronics.



[RWE-51] Optical properties of TiO₂ thin films deposited by DC sputtering and their photocatalytic performance in photoinduced process

Maria Alfaro Maria Alfaro (alfachio@gmail.com) ¹, Daniel Sanchez ¹, Leticia Torres ¹

¹ Universidad Autónoma de Nuevo León, Facultad de Ingeniería Civil, Departamento de Ecomateriales y Energía, Av. Universidad S/N Ciudad Universitaria, San Nicolás de los Garza, Nuevo León, C.P. 66455, México

TiO₂ thin films were deposited by DC Sputtering varying the deposit time. The optical properties of TiO₂ thin films with different thickness influenced their photocatalytic behavior in two photoinduced processes. When TiO₂ thin films were irradiated with a UV light, midgap states were generated and the electrons were placed in lower energies than its band gap, favoring the photocatalytic hydrogen production and CO₂ photoreduction. From PL technique analyses it was observed that electrons occupied midgap states between the bands, with lower energies than the band gap. With these results, it was possible to propose an energy diagram in order to correlate with photoinduced processes results. The presence of Ti³⁺ species was reconfirmed by means of XPS analyses. These species could be found in the midgap states, generated by the interaction between the UV irradiation and the film surface, which contributed to the photocatalytic activity of the films.

Keywords: TiO₂, thin films, optical properties, photocatalysis, photoinduced process



XII -ICSMV

September 23rd to 27th, 2019 / San Luis Potosí, México

[RWE-349] Fabrication of organic electrodes for application in storage and energy generation devices.

Roman Lopez-Sandoval (sandov@ipicyt.edu.mx)², Eduardo Tovar-Martinez², Jorge Valentin Cabrera-Salazar², Marisol Reyes-Reyes¹

¹ IICO-UASNL^P

² IPICYT

Recently, it has increased the interest in the fabrication of organic electrodes for the replacement of metals or metal oxides as electrodes. These applications range from its use as a transparent electrode, in the case of solar cells, and its use as an electrode in energy storage devices such as batteries, electric double layer capacitors and supercapacitors. The advantage in the use of organic electrodes is the low cost of organic materials and their easy processing. In addition, organic materials provide an excellent opportunity to further improve energy generation and storage technologies and are a versatile platform for developing new technologies. Organic materials are abundant, relatively cheap, and their synthesis can be designed such that it does not demand too much money and generates little waste. In this talk, we will present our contribution in this area.



[RWE-373] Synthesis route effect of ATiO₃ (A = Zn, Cd, Pb) perovskites and their application on photocatalytic water splitting

Omar A. Carrasco-Jaim (carrascolqi@gmail.com) ², Leticia M. Torres-Martínez (letterresg@yahoo.com) ¹, Edgar Moctezuma ²

¹ Universidad Autónoma de Nuevo León, Facultad de Ingeniería Civil, Departamento de Ecomateriales y Energía, Av. Universidad S/N Ciudad Universitaria, San Nicolás de los Garza, Nuevo León, C.P. 66450, México.

² Universidad Autónoma de San Luis Potosí, Facultad de Ciencias Químicas, Av. Manuel Nava 6, Zona Universitaria, San Luis Potosí, C.P. 78290, México.

In this work, the photocatalytic properties for hydrogen production of the perovskites with the general formula ATiO₃ (A = Zn, Cd, Pb) synthesized by solid-state and solvo-combustion methods were investigated. The CdTiO₃ and PbTiO₃ materials prepared by solid-state exhibited almost 3-times superior photocatalytic hydrogen production from pure water under UV irradiation (254 nm) compared to those obtained by solvo-combustion. The solid-state method allowed an enhancement of the photogenerated charge transfer due to higher crystallinity and homogeneous particle size evidenced by photoluminescence (PL) and electrochemical impedance spectroscopy (EIS) analysis. In the case of ZnTiO₃, the solvo-combustion synthesis allowed a 5-times increment of the hydrogen generation compared with the solid-state reaction, attributed to the presence of TiO₂ traces on this material which was acting as an *in-situ* co-catalyst during the photocatalytic reaction. In addition, through the photoelectrochemical characterization it was possible to determine the influence of the synthesis route over the semiconductor nature for all materials, which plays an important role for the internal recombination process directly associated to the photocatalytic efficiency.



XII -ICSMV

September 23rd to 27th, 2019 / San Luis Potosí, México

[RWE-510] SOLAR CELLS RESEARCH AND DEVELOPMENT IN MEXICO; THE CdTe SOLAR CELL CASE

Jaime MIMILA-ARROYO (jmimila@cinvestav.mx) ¹

¹ CINVESTAV-IPN-Zacatenco

The ever increasing appetite for energy in the actual global society and the deleterious byproducts of its production utilizing non-renewable primary sources have, since several decades, favored a vigorous revival of the research, development, production and applications of the renewable energy sources, particularly the solar cells. Extremely promising new materials and solar cells structures are proposed almost permanently. Notwithstanding the sometimes spectacular success of a very few of those new propositions, others, now classical ones, are currently struggling in the market place. Such is the case of the thin film CdTe solar cell. Forcefully, semiconductor materials and electronic devices specialists around the world, mainly in non-high tech societies try to follow the trends and the hot points of this research activity. Mexico, as one of those non high tech societies, has devoted time and resources to develop this solar cell. Its effort over the last 30 years has involved the activity of around 200 local specialist of the semiconductors and its devices, belonging to 40 different research groups throughout the country, involving 18 national institutions collaborating with more than 60 foreign researchers from 11 countries.

In this presentation, the results that this activity has produced, considering only those published in international journals, are reviewed and discussed. The findings are convincing enough to invite a reflection on the approach that has been followed in this research activity.



[RWE-536] Simplified continuum electrochemical model to describe fabrication of Li-ion batteries at different active/inactive cathode compositions

*Jorge Vazquez-Arenas (jorge_gva@hotmail.com)*¹

¹ *Universidad Autónoma Metropolitana-Iztapalapa*

Li-ion batteries (LiB) still represent one of the last steps restricting the use of competitive energy storage systems to replace fossil fuels, particularly, in terms of power and energy densities, cycle-life and safety. A tremendous effort is currently involved to design and synthesize novel LiB components (e.g. cathode, anode, electrolyte, and separator). However, this technology has met a critical point where synergism should be established along with materials science to optimize the vast number of existing components in the market. In this regard, fabrication process requires improving composite configuration and assembly methods, as well as enhancing the cooperation between solid and liquid phases. Indeed, this effort can demand a considerable amount of time if conducted under trial and error or statistically at the experimental level. Thus, the following study proposes a simplified analytical model intended to assist battery fabrication process at different active/inactive component ratios. Particularly, the main objective is to develop an efficient, robust, fast and easy industrial application tool to optimize the properties of a lithium battery during its manufacturing process. A simplified phenomenological mathematical model is derived, based on balances of matter and energy. The simplified nature of this model is obtained through the correct application of integral current balances; the application of theoretical equations to adjust the conductivity of the electrolyte phase (which provides a better fit than the typical polynomial equations typically used in the literature); and integral material balances in both the electrolyte phase and the solid phase of the electrode particles. Although the model accounts for the physics of LiFePO₄ phase, it can be extrapolated for the analysis of other cathode materials or larger domains. It is expected that it can pave the way as a rapid tool to perform optimization of battery properties during fabrication.



XII -ICSMV

September 23rd to 27th, 2019 / San Luis Potosí, México

[RWE-543] COMPARING THE EFFECT OF INSERTING DIFFERENT CARBON NANO-ALLOTROPES ON HYBRID PEROVSKITE SOLAR CELLS

Alejandra Castro-Chong (alejandra.castro@cinvestav.mx)², Mildred Quintana¹, Gerko Oskam²

¹ Centro de Investigación en Ciencias de la Salud y Biomedicina, CICSaB Universidad Autónoma de San Luis Potosí. San Luis Potosí, SLP.

² Department of Applied Physics, CINVESTAV-IPN, Mérida, Yucatán, México.

Hybrid halide perovskites have demonstrated to be one of the most promising materials for third-generation solar cells. While several issues remain to be addressed regarding device stability, the incorporation of carbon-based nanostructures has lead to significant advances. Carbon-derived materials are used as electron transport layer (ETL), hole transport layer (HTL), conducting, semi-transparent electrodes, or as an additive in the perovskite layer. The main benefits associated to the incorporation of carbon-based materials in perovskite solar cells relate to the stability and more efficient electron extraction.

In the present work, we develop a route for inserting graphene oxide and carbon nanotubes as interlayers in PSCs. Dispersions were obtained in appropriate solvents and deposited by the spin-coating method. To cast light into the charge carrier dynamics we performed photoluminescence measurements. We characterized the photovoltaic parameters under solar simulator (AM 1.5G).

**[RWE-588] Stability of the bilayer CdS/CdS:O to apply in CdTe solar cells**

Juan Luis Peña Chapa ¹, Mariely Loeza Poot (mariely_lop@hotmail.com) ¹, Ricardo Mis Fernandez ¹, Eduardo Camacho Espinosa ¹, Ivan Rimmaudo ¹

¹ Applied Physics Department, CINVESTAV-IPN, Apdo. Postal 73, Mérida, Yucatán, 97310, México

During decades, the CdS has been considered the best candidate to be applied as a window layer in thin film solar cells, especially in CdTe. However, due to the CdS has a band gap value of 2.42 eV, it shows a remarkable light absorption in the short wavelength region (less than 520 nm). Therefore, photon lights with energy higher than 2.42 eV don't contribute to the solar cell performance. Base on this, some research groups have doped the CdS in order to improve its optical properties. Resulting that the oxygenated CdS (CdS:O) film with an easier band gap value to tunable, depending on the oxygen percentage used during the CdS deposition [1]. In this work, we propose the use of CdS/CdS:O structure as a window layer in solar cells. This was analyzed during three processes to which this layer is subjected: 1) as deposited, 2) under CdTe deposition condition, and 3) with a CdTe deposit. The structure was characterized by optical, structural, chemical, and morphological techniques. By these analyses, we corroborated the stability of this window layer. Depth-profile XPS demonstrated that oxygen loss and a high CdS-CdTe interfusion can be avoided using a 35-mn CdS film.

[1] X. Wu, Y. Yan, R. Dhere, Y. Zhang, J. Zhou, C. Perkins and B. To, "Nanostructured CdS:O film: preparation, properties, and application," *Physica Status Solidi C*, vol. 1, no. 4, pp. 1062-1066, 2004.

ACKNOWLEDGMENTS:This work has been supported by CONACYT-SENER (México) under the project Consolidación del Laboratorio de Energía Renovable del Sureste (LENERSE) 254667. M. Loeza-Poot acknowledges CONACYT-México for scholarship (number 556332) in the Applied Physics Department of Cinvestav Mérida. Also, the authors gratefully acknowledge D. Huerta and W. Cauich for technical support and L. Pinelo for its secretarial assistance.



[RWE-596] Sodium Zincsilicates as a novel catalyst for reactions of environmental concern

Ricardo Iván Rodríguez Ramírez (argentum130@gmail.com)¹, Jorge Gabriel Vázquez Arenas², Issis Claudette Romero Ibarra (issisromero@gmail.com)¹

¹ Laboratory of Advanced Materials for Energy and Environment, UPIITA, IPN, Av. Instituto Politécnico Nacional 2580, La Laguna Ticomán, 07340 Ciudad de México

² Mexican Center for a Cleaner Production. IPN. Av. Acueducto S/N, Ticomán, 07340 Ciudad de México, CDMX

Capturing and preventing the emissions of CO₂ and other greenhouse gasses can offer a novel alternative to prevent climate change effects, but it demands the research and development of specialized materials to consolidate this process at large scales. Following this direction, biofuels are intended to reduce the dependency on fossil fuels while mitigating the carbon footprint. To this concern, biodiesel is one of the most promising transition fuels with closed carbon cycle, high energy efficiency and adequate compatibility with diesel engines but it requires alkaline catalysts for its production.

Zinc-based heterogeneous catalysts (specially Sodium Zincsilicate) seem to possess the required catalytic features, while being affordable, abundant on earth's crust and with low toxicity. Particularly, basicity is a desired property for these applications, which has been scarcely described on sodium silicate phases. Thus, this study aims to synergically synthesize and characterize sodium zincsilicates, to obtain low cost and stable catalysts via scalable synthesis methods.



[RWE-613] Novel design of Multi-Quantum Well Heterostructure Solar Cell based on GaNAs Highly Mismatched Alloys

Victor Hugo Mendez-Garcí (victor.mendez@uaslp.mx)², Yuliano Jarrouj-Zoudi², Jose Angel Espinoza-Figueroa², Christian Alejandro Mercado-Ornelas², Felipe Eduardo Pereira-Parrales², Alfredo Belio-Manzano², Leticia Ithsmel Espinosa Vega², Irving Eduardo Cortes-Mestizo¹, Cristo M. Yee-Rendón³

¹ CONACYT- CIACYT, Universidad Autónoma de San Luis Potosí, San Luis Potosí, México

² Center for the Innovation and Application of Science and Technology, Universidad Autónoma de San Luis Potosí, Av. Sierra Leona #550, Col. Lomas 2a Secc. 78210. San Luis Potosí, Mexico

³ Facultad de Ciencias Físico-Matemáticas, Universidad Autónoma de Sinaloa, Culiacán, Sinaloa, México

In recent years, extensive theoretical and experimental studies have been reported with the aim to contribute to improve the efficiency of photovoltaic devices, which has conducted to the proposal of novel materials and new designs of solar cells (SC). Up to the present time, the highest power conversion efficiencies have been achieved with tandem or multi-junction solar cells. These technologies comprise the simultaneous absorption of photons of different wavelengths, allowing through this mechanism the capture of a wider region of the solar spectrum, as compared with a simple pn junction. An alternative approach to achieve this same objective is the utilization of highly mismatched alloys (HMA) where the decoupling in electronegativity and size of the atomic radios of the constituting atoms, generates a splitting of the host material conduction band. The lower energy band is frequently called as the intermediate band (IB). Thus, the splitting allows for the absorption of photons via three different transitions: i) valence band (VB) - IB, ii) IB - conduction band (CB) and iii) VB-CB. An important advantage of the HMA-SCs compared to tandem SCs is that the multiple absorptions of photons are achieved in a single layer. Nevertheless, despite the simplicity involved in these devices, the concept has not been crystallized in the generation of profitable efficiency HMA-SCs, which is attributed to the limited activation of the so-called E+ CB. In this work, a novel proposal of SC based on the HMA GaNAs is presented. The alloy was inserted within the intrinsic layer of a p-i-n SC as part of a multi-quantum well (MQW) heterostructure. The details of the sequence layers are depicted in [1]. The physics and drawbacks of the single GaNAs layers SC are revisited and the advantages of the construction of MQW HMA SCs is explored. It is shown that this novel photovoltaic device assembly improves the SC efficiency up to an order of magnitude, as compared with a conventional HMA SC.

[1] IMPI MX/a/2019/001156, Patent#29697 “Dispositivo de celda solar basada en semiconductores GaNAs-GaAs con barreras de AlGaAs”.

Acknowledgments: The authors acknowledge the financial support from CEMIE-SOL 22, FRC-UASLP and CONACYT-Mexico through grants: INFR-2015-01-255489, CB 2015- 257358 and PNCPN2014-01-248071.



[RWE-614] Asymmetric quantum well solar cells AlGaAs/InAs/GaAs grown by MBE

Christian Alejandro Mercado Ornelas (cmercado@estudiantes.uaslp.edu.mx)², Felipe Eduardo Perea-Parrales², Leticia Ithsmel Espinosa Vega², Irving Eduardo Cortes-Mestizo¹, Andrei Yu-Gorbachev⁴, Gregorio Sánchez-Balderas³, Victor Hugo Mendez-Garcia (victor.mendez@uaslp.mx)²

¹ CONACYT- Coordinación para la Innovación y Aplicación de la Ciencia y la Tecnología, Av. Sierra Leona #550, Col. Lomas 2a Sección, CP 78210, UASLP, San Luis Potosí, México

² Coordinación para la Innovación y Aplicación de la Ciencia y la Tecnología, Av. Sierra Leona #550, Col. Lomas 2a Sección, CP 78210, UASLP, San Luis Potosí, México

³ Doctorado Institucional en Ingeniería y Ciencia de Materiales. Universidad Autónoma de San Luis Potosí. Sierra Leona 530, San Luis Potosí, S. L. P. 78210, México

⁴ Instituto de Investigación en Comunicación Óptica, Universidad Autónoma de San Luis Potosí, Av. Karakorum #1470, Lomas 2^a Secc. C.P. 78210, San Luis Potosí, México

In recent years, variety of proposals have been published to increase the Shockley–Queisser limit for the efficiency of a solar cell. One of the most attractive routes to accomplish this task is the implementation of intermediate bands (IBs) in the solar cells, more specifically by using low dimensional semiconductors heterostructures, like quantum dots (QDs). A superlattice array of QDs leads to discrete energy levels of unique confinement states, this results in a set of minibands within the band gap of the host semiconductor. It is estimated that the implementation of IBs will allow to increase the efficiency of a solar cell up to 63%. In this work the insertion of QDs within the intrinsic layer of p-i-n solar cells (SCs) is proposed. Two multi quantum well (MQW) heterostructures are studied in this work: AlGaAs/InAs/GaAs and GaAs/InAs/AlGaAs. Note that for the particular layered growth and InAs QDs self-assembling allowed by molecular beam epitaxy (MBE) the crucial difference in the proposed samples is the surrounded material of the QD; i.e. its boundary is mostly covered with AlGaAs or GaAs. This difference is not trivial, since the energy gap of these materials is different and so the quantum confinement states will be changed, which are very important for carrier photogeneration. Additionally, the intermixing i.e. the strain of the QD will change with the variation of the capping material, conducting to differences in QDs geometry and adatoms diffusion. And finally, the interface band-bending and electric field will vary with the direction of the anisotropic MQW, which are crucial for the transport of the photo-generated carriers. These differences were corroborated using numerical simulations where the band diagrams and quantum states have been estimated. Photoluminescence (PL) measurements showed the QDs transitions at 1.09 and 1.15, both sustaining FWHM close to 70 meV, possibly related to the size dispersion of the nanostructures. The I-V characteristics of the QDs solar cells were obtained, which showed good electrical performance, obtaining the following: $J_{SC}=196 \text{ mA/cm}^2$ and $V_{OC}=0.67 \text{ V}$ for the AlGaAs/InAs/GaAs sample, and $J_{SC}=156 \text{ mA/cm}^2$ and a $V_{OC}=0.55 \text{ V}$ for the GaAs/InAs/AlGaAs heterostructure. It was seen in the I-V curves that the first sample showed a better response, demonstrating that the high-energy barrier facing the p-type layer is more suitable for asymmetric MQWs SCs. It is worth to mention that these type of heterostructures still present increase values of V_{OC} compared with conventional QDs In(Ga)As/GaAs samples. External quantum efficiency (EQE) was measured from 350-1200nm, through the photocurrent was determined within



XII -ICSMV

September 23rd to 27th, 2019 / San Luis Potosí, México

this range. The electrical and optical performance of our novel QDs SCs proposal exhibited a very promising solar cell behavior.

Acknowledgments: The authors acknowledge the financial support from CEMIE-SOL 22, FRC-UASLP and CONACYT-Mexico through grants: CB 2015- 257358 and PNCPN2014-01-248071



[RWE-632] Stage Upgrade of System Control of Molecular Beam Epitaxy, by a Microcontroller

Ismael Lara Velázquez (ishma_lara@hotmail.com)², Carlos Enrique Leandro Martínez², Antonio Gonzalez Nicolas², Victor Hugo Mendez García¹, Felipe Perea Parrales¹, Leticia Espinoza Vega¹, Ramón Diaz de León Zapata²

¹ *Coordinación para la Innovación y Aplicación de la Ciencia y la Tecnología, Universidad Autónoma de San Luis Potosí, Av, Sierra Leona #550, Col. Lomas 2a Secc., 78210, México*

² *Instituto Tecnológico de San Luis Potosí, Tecnológico Nacional de México, Soledad de Graciano Sánchez, San Luis Potosí, Av. Tecnológico S/N . Col. UPA 78437, México*

The control systems are widely used in different fields of research, in this case in the branch of nanoparticles, being precise and complex applications, the operation must be very precise, for this reason the idea of automation this process was raised, in addition to needing precision in the filling process, it is very difficult to achieve the exact precision of a filling making it manual way.

This project aims to automate the opening of shutters. To carry out the project, we have the following predetermined resources a 12 V power supply with an output current of 10A and a unipolar stepper motor, which requires a current of 4A. To control this system it was proposed to use an 18F4550 microcontroller, since it is capable of working at the speed we need to move the motor step by step with the precision that is required.

This system also has intermediate elements to achieve the desired control and complete the system, for example the different power stages, for example to obtain the voltage and current suitable for the stepper motor a cd-cd buck converter module was used, to reduce the voltage of the power supply. A second buck module was also used, with less current capacity for the power supply of the pic 18F4550 microcontroller. To isolate the signals sent and received by the Microcontroller, an L298N driver module was used. In addition to being a closed loop control system, we also use a optoelectronic sensor, to have a reference of the starting position of the motor.



XII -ICSMV

September 23rd to 27th, 2019 / San Luis Potosí, México

[RWE-672] Light intensity modulated impedance Spectroscopy in Perovskite Solar Cells

Osbel Almora (osbel.almora@fau.de) ¹

¹ *i-MEET-FAU*

Potentiostatic impedance spectroscopy (IS) is a well established characterization technique for elucidating the electric resistivity and capacitive features of materials and devices. In the case of solar cells, by applying a small voltage perturbation the current signal is recorded and the recombination processes and defect distributions are among the typical outcomes in IS studies. In this work a new photoimpedance approach is introduced by recording the individual photocurrent and photovoltage signals due to a small light perturbation. The from-here-on-called "light intensity modulated impedance spectroscopy" (LIMIS) technique informs on carrier generation process and identifies bulk/interface phenomena. A first approach theory is presented, and experimental data is analyzed in several types of solar cells, including state-of-the-art perovskite solar cells.



[RWE-678] MoO₂ flakes for catalysis and surface enhanced Raman applications

Osvaldo de Melo (odemelo@gmail.com) ³, Estrella Ramos ², Ateet Dutt ², Goldie Oza ¹,
Emilia Margarita Mendoza ¹, C. Arjona ¹, Guillermo Santana ²

¹ Centro de Investigación y Desarrollo Tecnológico en Electroquímica (CIDETEQ), Parque Tecnológico Querétaro s/n, Sanfandila, Pedro Escobedo, C.P. 76703, Querétaro, Qro, Mexico

² Instituto de Investigaciones en Materiales, Universidad Nacional Autónoma de México, Cd. Universitaria, A.P. 70-360, Coyoacán 04510, México D. F.

³ Physics Faculty, University of Havana 10400 La Habana (also at Instituto de Investigaciones en Materiales, Universidad Nacional Autónoma de México, Cd. Universitaria, A.P. 70-360, Coyoacán 04510, México D. F.)

Presently, molybdenum oxides are the subject of intense research efforts because their interesting properties and promising applications in different areas. They cover catalysis, energy storage and harvesting, computing and biomedical applications.[i] For applications in catalysis, for example, the crystal surface plays a decisive role, reason why the study of molybdenum oxide flakes has become a subject of interest. Also, it has been demonstrated[ii] that the surface of MoO₂ flakes exhibits a very good performance for Surface Enhanced Raman Spectroscopy (SERS).

Recently, a technique has been reported[iii] to prepare pure MoO₂ films in a chemically driven isothermal close space vapor transport configuration (CD-CSVT) under a flow of reductive H₂ atmosphere and using MoO₃ as the source. In the present communication, the CD-CSVT growth of micrometer sized MoO₂ flakes is presented. It was observed that flakes orientation and growth strongly change when they are grown on different substrates. The crystalline direction and the orientation of the flakes facets deposited on sapphire c-cut, sapphire a-cut, Si (100) and Si (111) substrates were determined using different techniques. Triangular, standing rectangular, rhombic, “kite” shaped or not clearly faceted flakes including nano-belts and nanowires were obtained depending on the used substrate. An interesting case is the MoO₂ growth onto sapphire c-cut substrate in which epitaxial growth of both lying and standing flakes were grown. Density functional theory (DFT) calculations of the strain energy of the elemental lattice cell of MoO₂ for the different expected film-substrate epitaxial relationships allowed to predict the favored orientations of the flakes. It was demonstrated that strain state is the driven mechanism for the growth of one or the other crystalline orientation. Preliminary results of Raman enhanced properties of the flakes are reported using rhodamine as testing substance.

[i] I. A. de Castro, R. S. Datta, J. Z. Ou, A. Castellanos-Gomez, S. Sriram, T. Daeneke and K. Kalantar-zadeh, *Adv. Mater.* 2017, 29, 1701619

[ii] H. Wu, X. Zhou, J. Li, X. Li, Baowen Li, W. Fei, J. Zhou, J. Yin, and W. Guo, *Small* 2018, 14, 1802276, DOI: 10.1002/smll.201802276

[iii] O. de Melo, L. García-Pelayo, Y. González, O. Concepción, M. Manso-Silván, R. López-Nebreda, J. L. Pau, J. C. González, A. Climent-Font, V. Torres-Costa, *J. Mater. Chem. C*, 2018, 6, DOI: 10.1039/C8TC01685B



XII -ICSMV

September 23rd to 27th, 2019 / San Luis Potosí, México

RENEWABLE ENERGY: MATERIALS AND DEVICES (RWE) POSTER SESSIONS



[RWE-27] High stability of PtNiCu catalyst supported on graphene oxide

Miguel Adrian Padilla Islas (adrianmapi@gmail.com)¹, Miriam Marisol Tellez-Cruz¹,
Omar Solorza-Feria¹

¹ Química, CINVESTAV, Av. Instituto Politécnico Nacional 2508, Ciudad de México, C.P.
07360, México,

Nano-catalyst of NiCu is synthesized by two steps; reduction of non-noble metals as nuclei and decoration of platinum (shell) by galvanic displacement. New synthesis of catalysts for the reduction reaction of oxygen by the adequate amount of oleylamine and oleic acid and precursor salts of non-noble metals, Cu (acac)₂ and Ni(acac)₂, and using morpholine borane as a reducing agent is present. The prepared NiCu@Pt octahedral core-shell were characterized by TEM, octahedral nanoparticles have narrow size distribution, with a measured average edge length of 30 ± 5 nm. The EDX analysis by elemental mapping show that three elements were found homogeneously distributed throughout nanoparticles. The XRD pattern shows characteristic peaks, it suggests that CuNi is decorated whit Pt. The metallic core inherits the crystal structure of its composing elements, i.e., the face-centeredcubic (FCC) structure. The diffraction peaks at can be assigned to (1 1 1), (2 0 0), (2 2 0) and (3 1 1) crystallographic planes, respectively, which correspond to FCC phase. The electrochemical performance of NiCu decorate with Pt/C was evaluated by cyclic voltammetry, CO stripping and rotating disk electrode in HClO₄ as electrolyte. NiCu@Pt/ shows better catalytic activity in terms of mass activity 311mA/cm² and specific activity, which is 246 mA/cm², respect to commercially available 20-wt% Pt/C-Etek® with mass activity of 105 mA/cm² and specific activity of 184 mA/cm².

Therefore, this finding suggests a methodology for producing an oxide graphene supported octahedral nanocatalyst, which could be used as a cathode electrode in a PEM fuel cell.



[RWE-55] Influence of the deposition parameters on copper sulfide thin films by SILAR method as semiconductor material

Rocío Yazmín Mendoza-Cristán (*rocio.mendoza@uadec.edu.mx*)³, Luis Alfonso García-Cerda¹, Marco Arturo García-Rentería³, Sergio García-Villarreal³, Lazaro Abdiel Falcón-Franco³, Josefina García-Guerra³, Norberto Hernández-Como², Victor Hugo Martínez-Landeros (*vmartinezlanderos@uadec.edu.mx*)³

¹ Centro de Investigación en Química Aplicada, Blvd. Enrique Reyna Hermosillo #140, C.P. 25294, Saltillo, Coahuila, México.

² Centro de Nanociencias y Micro y Nanotecnologías, Instituto Politécnico Nacional, México City 07738, México.

³ Facultad de Metalurgia, Universidad Autónoma de Coahuila, Carr. 57, km. 5, C.P. 25720, Monclova, Coahuila, México.

Copper sulfide (CuS) is a very important metal chalcogenide and it is considered as p-type semiconductor material, it has a hexagonal crystal structure. This compound as thin film is an excellent candidate for use in photovoltaic energy investigation, which is due to the abundance and low cost of the starting materials. These thin films of copper sulfide were made on top of glass substrates, the synthesis route was by following the Successive Ionic Layer Adsorption and Reaction (SILAR) chemical method, which is very simple and economical to carry out. The chemical deposition consisted by using two precursor solutions: copper chloride as a cationic source and thioacetamide as the anionic source; also, two rinsing steps in deionized water were employed after immersion in each precursor. The optimum conditions by adjusting the parameters of the chemical deposition were identified as the number of deposition cycles, time and temperature of the deposition, pH and molar concentration of the precursors as well as a final rinsing step and post annealing. The CuS thin films obtained were characterized by X-ray diffraction (XRD), scanning electron microscopy (SEM), ultraviolet-visible spectroscopy (UV-vis), X-ray energy dispersion spectrometry (EDS), four points (Kelvin method) and Hall effect. These analyses were done to identify the structural, morphological, optical, chemical and electrical properties of the resulting semiconductor material, and to study the potential application as possible candidate for absorber semiconductor material in photovoltaic technologies.

Keywords: copper sulfide, semiconductor, chalcogenide, SILAR, solar cells.



[RWE-91] Development of Cu₂ZnSnS₄ films from a non-toxic molecular precursor ink and theoretical investigation for application in solar cells

David Mora-Herrera (dmora@ifuap.buap.mx) ¹, Rutilo Silva-González ¹, Mou Pal ¹

¹ Instituto de Física, BUAP, Av. San Claudio y Blvd. 18 Sur Col. San Manuel, Ciudad Universitaria, C.P. 72570 Puebla, México.

In this work, we reported a facile and cost effective way to deposit Cu₂ZnSnS₄ (CZTS) film using a non-toxic precursor ink and photovoltaic performance of single junction Cu₂ZnSnS₄ solar cell by implementing experimentally obtained optical and electrical parameters of our CZTS film in a simulation program known as SCAPS-1D (Solar cell capacitance simulator in one dimension). The ink was deposited over glass substrates by drop casting method and the as-deposited films were subjected to thermal annealing in N₂ atmosphere to obtain the kesterite CZTS annealed at 450 °C with 30 and 45 minutes. XRD and Raman spectra have shown the polycrystalline nature of CZTS films with tetragonal kesterite phase. The values of optical band gap (E_g) were found to vary in between 1.26-1.37 eV depending on the annealing time as determined by diffuse reflectance spectroscopy. Both films showed p-type electrical conductivity. The films possess good electrical properties with the resistivity (ρ) in the range of 60.4-190 Ωcm, carrier concentration (n) = 6.65x10¹⁶ - 2.58x10¹⁷ cm⁻³ and mobility (μ) = 1.41-10.6 cm²/Vs which is directly related to the surface morphology. Numerical simulation of CZTS film solar cells with CdS buffer layer was modeled through SCAPS-1D (Solar cell capacitance simulator in one dimension) using the experimentally obtained parameters of CZTS films fabricated in this work. The simulation reveals that the CZTS film annealed for 45 min is ideal for solar cell applications, with a maximum efficiency of 14.127 % considering all possible defects.

Acknowledgement

D. Mora-Herrera is thankful for the doctoral scholarship in Materials Science granted by Consejo Nacional de Ciencia y Tecnología (CONACYT, México). Financial helps offered by CONACYT though the grant Bilateral #266406 is acknowledged.



**[RWE-290] Study of the catalytic activity and stability of Pt₃Fe/C catalyst;
towards the RRO for PEMFC**

*Miriam Marisol Tellez-Cruz (mtellez@cinvestav.mx)¹, Miguel Adrian Padilla-Islas¹,
Heriberto Cruz-Martinez¹, Omar Solorza-Feria¹*

¹ *Chemistry, Cinvestav, Av. Instituto Politécnico Nacional 2508, Ciudad de México, C.P.
07360, México*

The synthesis of octahedral nanocatalyst of Pt₃Fe for oxygen reduction reaction (ORR) in acid media is presented. The catalyst was prepared through chemical reduction of precursor salts Pt(acac)₂ and Fe(acac)₃ with a variable amount of oleylamine and oleic acid. Subsequent, the catalyst was dispersing in a carbon matrix (Vulcan Carbon) previously thermally treated. XRD proved the presence of the alloy Pt₃Fe in the nanoparticles. STEM micrographs showed the morphology of the nanoparticles with an average 7-9 nm in size. The electrochemical performance of Pt₃Fe/C was evaluated by cyclic voltammetry, CO stripping and rotating disk electrode in HClO₄ as the electrolyte, showing better mass activity and specific activity than commercially available 20-wt% Pt /C-Etek® catalyst. Finally, the stability of the catalyst is evaluated, showing high resistance to corrosion.



[RWE-341] Photoelectrodes based on semiconductor nanoparticles of BiOI and BiVO₄ for the photogeneration of hydrogen photoelectrodes

Paola Gisel Jimenez Ortiz (gisjimort@gmail.com)², Guillermo Alam Moctezuma Salazar², Mildred Quintana (mildred@ifisica.uaslp.mx)², Mildred Quintana¹

¹ Centro de Investigación en Ciencias de la Salud y Biomedicina (CICSaB), Universidad Autónoma de San Luis Potosí (UASLP), Av. Sierra Leona 550, Lomas de San Luis, 78210 San Luis Potosí, SLP.

² Facultad de Ciencias, Universidad Autónoma de San Luis Potosí (UASLP), Av. Parque Chapultepec 1570, 78210 San Luis Potosí, SLP.

In the future it is intended to use hydrogen as an important carrier of energy and a great potential to reduce the dependence on energy sources such as oil. The conversion of light into hydrogen by water splitting is of immense interest as a source of clean, storable and renewable energy. If this process is assisted by photocatalysis, obtaining hydrogen can become more efficient and self-sustaining. But it is necessary to find efficient and resistant materials. BiOI and BiVO₄ semiconductors can be the solution, since they have high chemical stability, good photocatalytic activity, and low production cost.

In this work, photoelectrodes for the reduction and oxidation of water were produced with BiOI and BiVO₄ nanoparticles supported on graphene oxide. The photoelectrodes were made by making a paste with the nafion polymer on ITO substrates. The quantum efficiency of all the photoelectrodes was measured in a solar simulator.



[RWE-363] Numerical design and fabrication of (Al,Ga)As-based thin-film solar cells by TCAD and MBE

L.M. Hernandez-Gaytan ¹, J.P. Olvera-Enriquez ¹, L.I. Espinosa-Vega ¹, J. Hernández-Medina ³, M. Favila-Castañeda ³, C.A. Mercado-Ornelas ¹, F.E. Perea-Parrales ¹, V.H. Méndez-García ¹, I.E. Cortes-Mestizo (irving.cortes@uaslp.mx) ²

¹ CIACYT, Universidad Autónoma de San Luis Potosí, San Luis Potosí, México

² CONACYT-CIACYT, Universidad Autónoma de San Luis Potosí, San Luis Potosí, México.

³ UAF, Universidad Autónoma de Zacatecas, Zacatecas, México

The development of photovoltaic systems based in GaAs thin-film technology has been investigated over the past several years reaching efficiencies above 28%, which is close to the theoretically predicted 33.5% Shockley–Queisser efficiency limit for single junction solar cells [1]. In this work the authors showed the design of (Al,Ga)As-based thin-film solar cells through Technology Computer-Aided Design (TCAD), which main objective is to determine the experimentally realizable optimal (Al,Ga)As-based layer sequence of solar cell structure with efficiency above 20%. Optical and electrical transport models have been employed in the numerical process. The effect of the semiconductor-metal junction was including by the contact resistance and the Schottky barrier in order to analyze electrical losses. Recombination losses were considered by modeling the Auger, radiative, SRH, and surface recombination processes. A non-optimized simple p-n junction solar cell was proposed with the aim to explore loss mechanisms that might reduce the efficiency, being the SRH and surface recombination processes the major responsible for the low 7% theoretical exhibited efficiency. Solar cells heterostructures were designed based on the insertion of the capping, FSF and BSF (Front Surface Field and Back Surface Field) layers with the aim to reduce the losses that in conjunction with the appropriate doping/thickness relationship of the active layers may rise the theoretical efficiency around 50% with respect to the reference structure. Finally, a strategy to implement the capping layer to reduce the electrical losses and the surface recombination by the appropriated doping and passivation procedure is shown, increasing the efficiency of designed solar cell up to 25%. The non- and the numerically-optimized solar cells were grown by molecular beam epitaxy (MBE) in order to compare our numerical study with the experiments. The best optimized structure exhibited 10 times better electrical response than the p-n solar cell, demonstrating that the doping/thickness optimization process is satisfactory.

Acknowledgments: The authors acknowledge the financial support from CEMIE-SOL 22, FRC-UASLP, C19-FAI-05-18.18 and CONACYT-Mexico through grants: INFR-2015-01-255489, CB 2015-257358, PNCPN2014-01-248071 and the Catedras CONACyT (Project No. 44).

[1] Arpad Kosa et al., J. of Elec. Eng., 67(5), 377–382 (2016).

Author for correspondence: irving.cortes@uaslp.mx



[RWE-364] NaBiO₃ as heterogeneous catalyst to obtain biodiesel by direct transesterification

Gabriela Elizabeth Mijangos Zúñiga ¹, Issis Claudette Romero Ibarra ¹

¹ Instituto Politécnico Nacional, Unidad Profesional Interdisciplinaria en Ingeniería y Tecnologías Avanzadas , Av. Instituto Politécnico Nacional 2580 La Laguna Ticoman, 07340, Ciudad de México

Biodiesel has emerged as an alternative fuel, produced from renewable biomass because it is an attractive way to mitigate CO₂ emissions. It is a renewable biofuel, is biodegradable and sulphur free. The biodiesel is obtained industrially with homogeneous, heterogeneous and enzymatic catalyst. Recent studies report that heterogeneous catalyst Na-based are commonly used in transesterification reaction due the characteristic that presents as the basic character, chemical stability, high activity at room temperature, etc. In this work the synthesis and characterization of *sodium bismuthate* were analyzed. Additionally, direct transesterification was implemented to evaluate the catalyst. Direct transesterification is a novel method to obtain biodiesel from seeds. In this process the extraction of the oil from *ricinus communis* [1] and its subsequent transesterification are carried out in *one-pot* in the same reactor. This sustainable alternative to produce biodiesel has been reported using *sodium bismuthate* as heterogeneous catalyst [2].

[1] A. Martínez, G. E. Mijangos, I. C. Romero-Ibarra, R. Hernández-Altamirano, V. Y. Mena-Cervantes, and S. Gutiérrez, *J. Clean. Prod.*, vol. 196, 340–349, 2018.

[2] A. Martínez, G. E. Mijangos, I. C. Romero-Ibarra, R. Hernández-Altamirano, and V. Y. Mena-Cervantes, *Fuel*, vol. 235, 277–287, 2019.



[RWE-367] HETEROGENEOUS DIRECT TRANSESTERIFICATION TO OBTAIN BIODIESEL FROM RICINUS COMMUNIS SEEDS USING Na₂SiO₃ AS CATALYST.

Uriel Salvador Zarate Luna (U.ZarateL@hotmail.com)¹, Uriel Salvador Zarate Luna², Issis Claudette Romero Ibarra (iromero@ipn.mx)¹, Gabriela Elizabeth Mijangos Zúñiga¹

¹ *Unidad Profesional Interdisciplinaria de Ingeniería y Tecnologías Avanzadas, Instituto Politécnico Nacional, Av. IPN No 2580, Gustavo A. Madero, C.P. 07340, México D.F*

² *Universidad Tecnológica De Tecámac, Carretera Federal México - Pachuca, KM 37.5, Col. Sierra Hermosa, C.P. 55740, Tecámac, Estado de México.*

Abstract

The relationship between energy and the environment has become a fundamental issue due to the extremely negative implications related to the excessive use of hydrocarbons to obtain energy, especially in developing countries. Renewable energies as a whole represent an alternative that will reduce the consumption of hydrocarbons in the short and medium term. Bioenergy is interesting because biofuels are generated that directly impact the consumption of hydrocarbons. For example, products such as biogas, biohydrogen, bioethanol or biodiesel can be obtained directly from biomass. The latter is the object of our study. Biodiesel is obtained from vegetable oils, animal fats or algae oil and by means of the transesterification reaction a triglyceride molecule is reacted with three molecules of a short chain alcohol in the presence of a catalyst that can be homogeneous or heterogeneous. In this work, we propose the heterogeneous direct transesterification, in which the oil is extracted and reacted in a single step using methanol as a solvent and as a reagent. In this way, the oil extraction step is saved. We use an inedible seed, *Ricinus communis*, methanol and a heterogeneous basic catalyst such as sodium silicate (Na₂SiO₃) obtaining methyl esters, glycerol and biomass that contains the residue of the seed and the catalyst. Results shown yields higher than 90%. Direct transesterification is a new alternative for biodiesel production.

Acknowledgment:

The authors acknowledge financial support for this work from IPN with project 20196667 and 20196708; CONACyT under project PN 1373 and “Red Temática de Almacenamiento”; and SECITI/071/2016



[RWE-371] Electrochemical performance of nanostructured ceria thin films prepared by spray pyrolysis

Inti Zumeta Dubé¹, Gabriela Mariela Reyes Chaparro (mreys.gaby@gmail.com)¹, José Manuel García Rangel¹, Mario Fidel García Sánchez¹

¹ Unidad Profesional Interdisciplinaria en Ingeniería y Tecnologías Avanzadas. Instituto Politécnico Nacional, Av. I.P.N. 2580, Gustavo A. Madero, 07340, Ciudad de México, México.

In this work, nanostructured ceria thin films have been prepared on FTO substrates by ultrasonic spray pyrolysis using cerium acetylacetone as metallo-organic precursor dissolved in anhydrous methanol. The temperature of the heating plate (Ts) was fixed at 450 °C, the deposition time (td) was 30 min, and the carrier and director gas flow rates, air in both cases, were fixed at 1.0 L/min and 1.5 L/min respectively. The morphology, structure, optical and electrical properties were studied using scanning electron microscopy, X-ray diffraction (XRD), Raman spectroscopy, UV-Vis and electrochemical impedance spectroscopy (IS). The influence of thermal annealing at 500 °C on the structural properties of films was studied. Thermal annealing do not modified the morphology and texture of films, but reduce the oxygen vacancies concentration. The band gap was 3.23 eV for as grown samples and 2.98 eV for treated films. Photoelectrochemical measurements indicate variations in the Voc higher than 0.1 eV when 360 nm UV-LEDs light is turn on. The flat-band potential was calculated from the Mott-Schotky relation with values of -0.36 V in dark and -0.47 V for the illuminated sample. Films was evaluated in the photoelectrocatalytic hydrogen production.

The authors acknowledge financial support for this work from IPN with projects 20181399 and 20181907; CONACyT under project PN 1373 and “Red Temática de Almacenamiento”; and SECITI/071/2016.



[RWE-376] Photocatalytic evaluation for the rhodamine B degradation using thin CeO₂ films

José Manuel García Rangel (*ing.manuel.3007@gmail.com*) ², Mario Fidel García Sánchez (*mgarciasan@ipn.mx*) ², Inti Zumeta Dubé ², Issis Claudette Romero Ibarra ², Ulises Garduño Terán ², José Francisco Malagón García ¹, Ernesto Espinoza Hernández ², Guillermo Santana Rodríguez ¹

¹ Instituto de Investigaciones en Materiales, U.N.A.M., A.P. 70-360, Coyoacán, C.P. 04510, Ciudad de México, México

² Unidad Profesional Interdisciplinaria en Ingeniería y Tecnologías Avanzadas. Instituto Politécnico Nacional, Av. I.P.N. 2580, Gustavo A. Madero, 07340, Ciudad de México, México

In this work, cerium oxide thin films have been prepared by ultrasonic spray pyrolysis on glass substrates using cerium acetylacetone as a metalloorganic precursor dissolved in anhydrous methanol. The morphology, structure and optical properties were studied by scanning electron microscopy (SEM), X-ray diffraction (XRD), Raman spectroscopy and UV-vis spectroscopy. The photocatalytic study was carried out with an artificial UV light of 360 nm, in a solution of rhodamine B with a molarity of 10^{-3} mol/L. The degradation process of rhodamine B using the CeO₂ films was monitored with UV-vis spectroscopy at different time intervals. The optimal films in the degradation of rhodamine B also showed the characteristic of absorbing the dye. The effective film in the photocatalysis was subjected to a chemical treatment with NaBH₄ which favored the absorption of rhodamine B but it impairs its photocatalytic activity, canceling out its effect. CeO₂ films have potential in the application of photocatalysis for the treatment of contaminated water using visible light irradiation.

The authors acknowledge financial support for this work from IPN with projects 20196667 and 20196708; SECITI/071/2016 and CONACYT under project PN 1373 and “Red Temática de Almacenamiento”.



[RWE-407] Synthesis and characterization of nanostructured YSZ thin films with applications in solid oxide fuel cells.

Ernesto Espinoza Hernández (ernst.esp.hdz@hotmail.com) ¹, Mario Fidel García Sánchez

¹, Ulises Garduño Terán ¹, José Manuel García Rangel ¹, Inti Zumeta Dumbé ¹

*¹ Unidad Profesional Interdisciplinaria en Ingeniería y Tecnologías Avanzadas Avenida
Instituto Politécnico Nacional No. 2580, Col Barrio la Laguna Ticomán, Gustavo A. Madero,
Ciudad de México, C.P. 07340.*

Decrease the operating temperatures of solid oxide fuel cells (SOFC) is the most important aspect in the commercialization of these devices. Recently has been demonstrated that decreased the grain size of ionic conductors to nanometric scale (< 50nm) increase the conductivity of these materials. In this work, nanostructured thin films of yttria stabilized zirconia (YSZ) have been prepared on crystalline silicon substrates and glass substrates by ultrasonic spray pyrolysis using zirconium acetylacetone and yttrium acetylacetone hydrate as metallo-organic precursors. The flow rate, substrate temperature and Y concentration was varied in order to evaluate its effect on the morphology and electrical properties of films. The morphology, structure, optical and electrical properties were studied by X-ray diffraction, scanning electron microscopy, UV-Vis and impedance spectroscopy (IS). The substrate temperature was optimized for obtaining smooth, dense and homogeneous nanocrystalline films with grains sizes lower than 20 nm. The films obtained are good candidates for electrolytes in solid oxide fuel cells (SOFC) operating at lower temperatures. The authors acknowledge financial support for this work from IPN with projects 20196667; SECITI/071/2016 and CONACYT under project PN 1373 and "Red Temática de Almacenamiento".



[RWE-494] Development of Phase Change Materials impregnated in construction materials for save energy

Daniel Jimenez (*dje_86@hotmail.com*)¹, Lilia Narvaez², Juana Maria Miranda²

¹ DICIM - UASLP

² HABITAT - UASLP

The use of Phase Change Materials (PCM) in construction has created effective solutions for the control of the internal microclimate in buildings around the world. PCMs are those that, when they pass from the liquid to the solid state (crystallization), transfer energy to their environment, releasing the accumulated latent heat in the process of passing from the solid to the liquid state (fusion). The aim is to develop a PCM based on coconut oil and paraffin to be impregnated in porous materials that will be added to the concrete. The mixtures of coconut oil and paraffin were made in proportions (coconut/paraffin) 100/0, 99/1, 98/2, 97/3, 96/4 and 95/5, evaluating their melting points in search of temperatures close to the human thermal comfort zone, as well as the fusion and crystallization enthalpies which generate the latent heat in the mixtures. As porous materials, the pumice stones of the central region of Mexico and the recycling of concrete blocks were used as coarse aggregates, density, pore volume and absorption were evaluated, determining the maximum impregnation capacity of the stones. The impregnation of the stones with PCM was carried out under the vacuum impregnation method at a temperature of 90°C for 40 minutes, with a pressure of 1.00 Pa, evaluating the impregnation capacity in the coarse aggregates. It is observed that the mixtures of coconut oil and coconut/paraffin 99/1, 98/2 and 97/3 have melting points between 23.5°C and 26°C suitable for research, in addition they generate enthalpies in the crystallization process of approximately 87 J / g suitable for thermal comfort control. The absorption capacity of the pumice stone is high, with averages greater than 150% of weight gain; the concrete block only has a maximum absorption capacity of 11%. Vacuum impregnation for 40 minutes proved to be the adequate time to reach the maximum absorption capacity of the PCM in the coarse aggregates, obtaining an impregnation of 125% for the pumice stone and 10.5% for the concrete block. Therefore, the use of coconut oil/paraffin proves to be an excellent alternative to be used as PCM impregnated in pumice stone.



[RWE-497] Synthesis and characterization of cerium oxide thin films as electrolyte in solid oxide fuel cells.

Ulises Garduño Terán (ulgarduno@gmail.com)¹, Mario Fidel García Sánchez¹, José Manuel García Rangel¹, Inti Zumeta Dubé¹, Ernesto Espinoza Hernández¹

¹ Unidad Profesional Interdisciplinaria en Ingeniería y Tecnologías Avanzadas-Instituto Politécnico Nacional. Av. IPN No. 2580, Gustavo A. Madero, C.P. 07340, Ciudad de México, México

Nowadays, electricity production is one of the greatest problems of humanity. Current production depends almost entirely on fossil fuels. However, It is very difficult to justify the use of these fuels due to their rapid exhaustion and the irreparable damage to the planet that they producing. Then, the implementation of clean and renewable energies is actually a necessity. Within these energies, one that is gaining great interest is hydrogen. The devices for obtaining electrical energy from hydrogen are called fuel cells, and among these cells are the so-called solid oxide (SOFC). This work proposes the application of thin films of cerium oxide as electrolyte in solid oxide fuel cells, since it has been reported that they have excellent properties of ionic conductivity and low operating temperatures. To obtain the thin films, the Ultrasonic Pyrolytic Spray technique is used, as it is an accessible and easily scalable method, in addition to which it allows obtaining dense and homogeneous films. The films were optimized varying the flow rate, the substrate temperature and the Gd concentration. Films were characterized by X-ray diffraction, UV-vis spectroscopy, ellipsometry, scanning electron microscopy and impedance spectroscopy. Variations in temperature and flow rates modified the morphology, grain size and the texture of films. The nanometric grain size increase the conductivity of these materials, which allows the reductions of operating temperature in SOFC.

The authors acknowledge financial support for this work from IPN with project 20181399; CONACyT under project PN 1373 and “Red Temática de Almacenamiento”; and SECITI/071/2016.



[RWE-507] INFLUENCE OF NATURAL FIBER ON THE COMPRESSIVE STRENGTH AND WATER ABSORPTION OF ADOBES STABILIZED WITH ZEOLITE

Angelica Lara Ojeda (arq.angielara@gmail.com)¹, Juana María Miranda Vidales², Lilia Narvaez Hernandez²

¹ Doctorado Institucional en Ingeniería y Ciencia de Materiales, Sierra Leona No. 550 Col. Lomas 2da. Sección, Planta Baja

² Facultad del Hábitat, Avenida Niño Artillero 150, Zona Universitaria, 78290 San Luis, S.L.P.

The use of building materials generates a high energetic and environmental cost. Therefore, traditional building materials such as the adobe, have been demonstrated being a viable alternative due to the proximity, availability and geographical location of the raw material. Furthermore, the manufacturing process of adobes does not generate pollution by greenhouse gases, it is economical and biodegradable. Nevertheless, the adobe has certain disadvantages such as low compressive strength (2-4 MPa) and its vulnerability to humid environments. To face these problems, additives like cement, lime, pozzolans and their combinations are added to adobes in order to stabilize them. Moreover, the addition of natural fibers is common in order to improve their compressive strength.

This work evaluates the compressive strength and water absorption of adobes manufactured with materials from the center region of Mexico. Specimens for this investigation were prepared with stabilized soil with 15% lime and 15% zeolite. The dimension of the specimens was 5x5x5 cm, reinforced by 0.5% and 1.0% (by weight of dry soil) of ixtle fibers. Dry and wet compressive strength of all specimens (with or without fibers) and water absorption tests were made after a period of 28 days, 90 days and 180 days of curing.

The results show an increase of compressive strength of the specimens with both fiber percentages. This increase is due to cementing compounds formations, which can bind the soil particles together and reduce water absorption. As well, small quantities of fiber show a better distribution, which leads to a greater cohesion of the fiber with the matrix. On the other hand, specimens with large quantities of fibers (1.0%) show higher water absorption. The affinity to absorb water and the low cohesion of the fibers generates large pores in the matrix, which leads to a decrease in the mechanical properties. This study concludes that stabilization with zeolite and lime, next to the addition of ixtle fibers in low quantities (0.5%), increases the compressive strength of the adobes and reduces their water absorption, thus showing a viable, economic and ecological alternative for manufacturing adobes for construction.



[RWE-518] Development of heterostructure TCO/Cds/ Ce0.95 Gd0.05 O1.75 /Pb6 Bi2 S9/PbS for photovoltaic device.

Harumi Moreno García (harumi.moreno@uaslp.mx)¹, José Gabriel Roberto Hernández Arteaga (robertojg_13@hotmail.com)¹

¹ *Facultad de Ciencias, Universidad Autónoma de San Luis Potosí Av. Manuel Nava No. 6, C.P. 78260, San Luis Potosí, S.L.P., MÉXICO.*

The development of photovoltaic devices, mainly solar cells (SCD) of emerging materials has taken on greater importance in recent years due to the interest of prove with new materials based on abundant elements and a simple fabrication processes. Lead Sulfide (PbS) is a material that when applied in the development of solar cells allows conversion efficiency arround 9.88% . On the other hand cerium oxide (CeO₂), which has a band gap (E_g) of 3.1 to 3.6 eV depending on the growth technique has optical and electrical properties compatible with the development of solar cells.

In the present work a device was made from emergent materials such as the CeO₂ doped with gadolinium (Gd), PbS and a new ternary compound of lead bismuth sulfide (Pb₆Bi₂S₉) that is proposed as absorber material. The films were grown by spin coating and chemical deposition techniques. Different configurations were implemented varying the deposition times of the Pb₆Bi₂S₉ film and the influence of Ce0.95Gd0.05O1.75 as a buffer layer to optimize the performance of the device. The structural, optical and electrical characterization was carried out from different techniques such as X-ray diffraction, Raman spectroscopy and optical reflection and transmission spectroscopy . For the characterization of the solar cell, the current versus voltage (I-V) curve was measured. The values of open circuit voltage (V_{oc}) of 334mV, short circuit current (I_{sc}) 1 mA and series resistance of 13.5 Ω were determined.



[RWE-554] Photocatalytic Degradation of Methylene blue (MB) on Graphene decorated Titanium Dioxide (TiO₂) under visible light irradiation.

Marco Aurelio Acosta Esparza (macostae4@outlook.com)², Jose Guadalupe Quiñones Galván (jose.quinones@academicos.udg.mx)¹

¹ *Departamento de Física, Centro Universitario de Ciencias Exactas e Ingeniería, Universidad de Guadalajara, Boulevard Marcelino García Barragán 1421, Guadalajara, Jalisco, México, C.P. 44430.*

² *Departamento de Física, Unidad Académica de Física, Universidad Autónoma de Zacatecas, Calzada Solidaridad esq. Paseo de la Bufa s/n, Zacatecas, Zacatecas, Mexico, C.P. 98060.*

Titanium Dioxide (TiO₂) is an excellent photocatalyst in the Uv region however, for the visible region there is no interaction with visible light due to its wide band-gap(3.2eV), in order to activate Titanium Dioxide in the visible range, it can be combined with different materials, for example Graphene. Three samples of Titanium Dioxide powders of approximately 50 nanometers have been synthesized by hydrothermal and mixed with Graphene powders. The powder combination of TiO₂ and graphene treated at different temperatures (100 and 200 °C) was investigated with the aim to evaluate their photocatalytic MB degradation. All samples were analyzed by Raman Spectroscopy and X-ray diffraction. The material photocatalytic activity with the semiconductor could accelerate the process of degradation in the Uv-region and do it in the visible region. The powders were mixed with methylene blue and bidistilled water to be exposed to ultraviolet and visible light. The photocatalytic activity of the samples under Uv and visible radiation was evaluated by Uv-vis spectroscopy as a function of time. Significant photocatalytic degradation was observed for visible radiation reaching a value of 46 percent.



[RWE-622] Effect of the pressure on CdTe films grown on thin metallic substrate by Close Space Vapor Transport

Ana María Salomón Preciado (asalomonp@gmail.com)¹, István González Valdés¹, Osvaldo Vigil Galán¹, Jorge Ricardo Aguilar Hernández¹, Gerardo Silverio Contreras Puente¹

¹ Escuela Superior de Física y Matemática, Instituto Politécnico Nacional, México

Cadmium Telluride (CdTe) is a semiconductor with a band gap of 1.5 eV at room temperature and high absorption coefficient ($> 5 \times 10^5 \text{ cm}^{-1}$), which indicates that few micrometers of materials are capable of absorb most of the incident photons¹. These properties make it ideal for solar cell application. For this reason, CdTe semiconductor films were grown on molybdenum flexible substrates of 100 μm thick. The metallic substrates were cleaned with $\text{NH}_4\text{OH}:\text{H}_2\text{O}$, deionized water, isopropyl alcohol and deionized water, 5 minutes for each cleaning component. The CdTe film deposition was carried out at 650°C for the source temperature and 500°C for the substrate temperature; during 15 minutes in an atmosphere of (Ar/O₂ 50/50 %)² using a chamber pressures of 80 and 100 mTorr².

The thickness of the CdTe film obtained was: ~27 μm for the film deposited with pressure of 80 mTorr; and ~11 μm for the film deposited with pressure of 100 mTorr. The mean grain sizes were estimated at 20 μm and 7 μm , for 80 mTorr and 100 mTorr, respectively. The optical band gap theoretically calculated using was 1.48 eV for both films. The morphology and structural properties of the CdTe films as grown were investigated by X-Ray diffraction, scanning electron microscopy and atomic force microscopy. Our results shown that, the structural properties and morphology of CdTe as grown by CSVT are optimized in order to have semiconductor films suitable for applications as flexible solar cells.

Acknowledgments: We acknowledge the financial support of SIP-IPN under project number 20190173.

[1] A Seth, G.B Lush, J.C McLure D Flood. "Growth and characterization of CdTe by Close space sublimation on metal substrates. Solar Energy Materials & Solar cells. (1999) 35-49.

[2] G. Contreras-Puente et al. "Influence of the growth conditions in the properties of the CdTe thin films deposited by CSVT". Thin solid Films. 387, (2001) 50-53.



[RWE-637] Design and synthesis of bismuth-based nanoparticles to obtain Hydrogen via water splitting.

Luis G. Flores Larrea (*luisgfloreslarrea@gmail.com*)¹, Diego Torres¹, Mildred Quintana (*quintanamildred@gmail.com*)¹, Esmeralda Mendoza¹, Socorro Oros-Ruiz²

¹ CICSAB

² UAM

In an effort to decrease the global impact by fossil fuels and our dependency in them, hydrogen promises to be a solution as it can work as fuel and an electricity generator. Thus, the production of hydrogen via Water Splitting has become ideal because it is green, cheap and simple so an escalation might be convenient.

In this work BiVO₄ and BiOI are proposed to work under solar radiation directly and visible ideally. The synthesis and optimization of each material it is taken for further enhance changing variables such as heat treatment, ratio between reagents all this to improve crystallinity and particle size, then the most challenging factor would be the addition of graphene oxide to promote photogenerated carriers migration. A complex device where these particles are incorporated it is proposed to finally obtain hydrogen self-sufficient.



[RWE-638] Scalable solar chimney for passive cooling through dimensionless Physics

Enya Licea Suazo ¹, Alejandro Molina Bermúdez ², Andrea Tsam Nieto Encarnación ²,
Rafael Gómez Sánchez ², Manolo Ramírez López (mrlopez.ipn@gmail.com) ²

¹ Instituto Politécnico Nacional, ENCB, Prolongación de Carpio y Plan de Ayala s/n, Santo Tomás, Nueva Industrial Vallejo, 11340 Miguel Hidalgo, Ciudad de México

² Instituto Politécnico Nacional, UPIITA, Av. I.P.N. 2580 Barrio la Laguna Ticomán, Gustavo A. Madero, 07340, Ciudad de Mexico, México

Corresponding email: mrlopez.ipn@gmail.com, mramirezlo@ipn.mx

Keywords : Solar chimney, Heat Transfer, Passive Cooling, Stack Effect, Buckingham's Theorem.

World population growth requires unsustainable energy consumption whose origin comes mainly from fossil fuels, which generate a negative impact in the environment and extreme climatic conditions. In semiarid geographic regions, intensive use of air conditioning systems is required in order to achieve thermal comfort inside of rooms, which consumes between 1-2 kW per room, being one of the home devices with highest energy consumption. In this work, a scalable model and a prototype of a solar chimney were developed, where solar radiation is absorbed inducing air movement along chimney connected to a scale room for reduce its internal temperature by passive cooling. The chimney consists of a rectangular pipeline formed by an absorber, a glazed wall, and an angular system that allows to vary its orientation and the gap between absorber and glazing surfaces (d_c). Main function of the absorber is to absorb the heat of solar radiation and transfer it to the air for generate stack effect. Absorber is conformed by a metal plate with a coating of metallic microspheres, while the glazing has a transparency of 96 % to solar radiation. The scaling model was developed by applying Buckingham's theorem. Kinetic energy of air ($mv^2/2$), density (ρ), gravity (g), irradiance per unit of heat capacity (I/C_p), thermal expansion coefficient (β), and the system gap (d_c) were considered as the 6 mainly physical variables that describe the phenomena and depend on four fundamental dimensions (length, mass, time and temperature). Therefore the expressions of two dimensionless parameters (Π_1, Π_2) were calculated, whose dependence were determinated by measuring the air speed for different values of solar irradiance in our prototype. Physical dependence of $\Pi_1=f(\Pi_2)$ corresponds to a power law with experimental results of $\Pi_1 = 1.49(\Pi_2)^{1.27}$. Last expression allows to determine scaling factors (physical and geometric parameters) of the solar chimney to achieve the necessary air changes per hour (~6ACH) for thermal comfort of a room with volume V in a environment with solar irradiance I_0 [1].

[1] Jyotirmay M. et. al., *experimental investigations on solar chimney for room ventilation*, Solar Energy, **80**, Issue 8 (2006), p.p. 927-935.

This work was partially supported by SIP-IPN project No. 20195413 and 2019 Innovation Project of Instituto Politecnico Nacional.



[RWE-685] Evaluation of potassium ferrate as heterogeneous catalyst for biodiesel production using jatropha curcas L. oil.

Adriana Nahúm Gutiérrez López (adriana.ngl.91@gmail.com)¹, Adriana Nahúm Gutiérrez López², Raúl Hernández Altamirano (rhaltamirano@gmail.com)¹, Raúl Hernández Alta-mirano², Jorge Gabriel Vázquez Arenas¹

¹ Centro Mexicano para la Producción más Limpia

² Laboratorio Nacional de Desarrollo y Aseguramiento de la Calidad en Biocombustibles

Fossil fuels are the most used energy source; however, its combustion causes atmospheric pollution and adverse effects on human health. A supplementary fuel for diesel engines is the biodiesel, which has shown to be environmentally safe, technically feasible, economically viable and is produced by triglyceride transesterification using an alcohol and a catalyst to form esters and glycerol.

Heterogeneous catalysts are separable from the reaction mixture and are reusable, they do not generate carboxylates (soaps) or washing wastewater, in contradistinction to homogeneous catalysis. For these reasons, the main objective for this project is to synthesize, characterize and test potassium ferrate VI (K_2FeO_4) as a new heterogeneous catalyst for biodiesel production using inedible oilseeds of *Jatropha curcas L.* Potassium ferrate is a low-cost material made from abundant precursors, is not toxic and can be easily separated due to its magnetic properties.



XII -ICSMV

September 23rd to 27th, 2019 / San Luis Potosí, México

SCIENCIE DIVULGATION (SCD)

Chairmen: Wilfrido Calleja (INAOE),
Dolores García Toral (BUAP)
Josefina Robles Aguilar (BUAP)
Dalia Alejandra Mazón Montijo (CIMAV-Monterrey)



[SCD-619] Materiales avanzados para remediación ambiental

ISSIS CLAUDETTE ROMERO IBARRA (*IROMERO@IPN.MX*)¹

¹ Unidad Profesional Interdisciplinaria en Ingeniería y Tecnologías Avanzadas-Instituto Politécnico Nacional. Av. IPN No. 2580, Col Barrio La Laguna Ticomán, Gustavo A. Madero 07340, Ciudad de México.

Una de las grandes problemáticas que enfrentamos en la actualidad es el aumento de las emisiones de gases de efecto invernadero (GEI) en la atmósfera, lo cual afecta el medio ambiente y la salud humana. En materia de energía y cambio climático México propone en el Plan Verde “reducir las emisiones de gases de efecto invernadero, impulsar y fortalecer el mercado de las energías renovables y realizar acciones de adaptación al cambio climático para la población”. Para lograr este objetivo es necesario el desarrollo y uso de nuevos materiales aplicables a tecnologías enfocadas en energías renovables y ambientales.

En esta plática se presentan estrategias para la síntesis y evaluación de materiales que por medio de un proceso de quimisorción puedan capturar CO₂ (un gas de efecto invernadero), que funcionen como catalizadores heterogéneos en la generación de energéticos limpios (biodiesel y gas de síntesis, CO + H₂), tratamiento de agua y que puedan ser usados como cátodos en dispositivos de almacenamiento de energía como baterías de ion litio. Los materiales se caracterizaron estructural y microestructuralmente por medio de diversas técnicas espectroscópicas. Además, se presentan resultados de la evaluación de cada uno de estos materiales en diversas aplicaciones ambientales y energéticas.

Agradecimientos: Se agradece el financiamiento de la SECITI con el proyecto 071/2016, al proyecto SIP 20196708 y a la Red de Almacenamiento de Energía.



XII -ICSMV

September 23rd to 27th, 2019 / San Luis Potosí, México

[SCD-640] Semiconductores contra el calentamiento global*

Miguel Melendez-Lira (mlira@fis.cinvestav.mx) ¹

¹ *Departamento de Fisica, CInvestav-IPN, Zatenco, CDMX, Mexico*

Comparando el tiempo de vida estimado para el sol y el de los seres humanos podemos considerar que el sol es una fuente inagotable de energía. La vida en la tierra debe su origen a la energía recibida del sol. Sin embargo, un desarrollo acelerado sin respeto por un sano equilibrio con la naturaleza puede hacer que la humanidad sea inviable debido al cambio climático. Éste tiene su origen básicamente en la quema indiscriminada de combustibles fósiles por lo que es necesario desarrollar fuentes confiables de energía limpia [1]. La tierra recibe del sol partículas cargadas y radiación que puede ser aprovechada para producir energía al transformar luz visible y calor en energía eléctrica. Los semiconductores son materiales que tienen las características idóneas para producir energía limpia. En esta charla describiremos aplicaciones de semiconductores en la producción de energía limpia y el gran potencial que estas aplicaciones representan para contribuir a disminuir el calentamiento global.

*: trabajo apoyado parcialmente por CONACyT

[1]: Gurevich, Yuri, and G. Miguel Meléndez Lira. Fenómenos de contacto y sus aplicaciones en celdas solares. Fondo de Cultura Económica, 2013.



[SCD-309] Almacenamiento de energía y energías renovables

*Mario Fidel García Sánchez (mgarciasan@ipn.mx)*¹

¹ Unidad Profesional Interdisciplinaria de Ingeniería y Tecnologías Avanzadas, Instituto Politécnico Nacional, Av. IPN No 2580, Gustavo A. Madero, C.P. 07340, CDMX, México

La necesidad de impulsar el desarrollo de energías que minimicen el daño que provocamos al planeta ha creado un gran interés en el desarrollo de fuentes renovables de energía. Pero la mayor parte de estas fuentes son intermitentes, o sea, la generación de energía depende de aspectos no controlables como la velocidad del viento, o la luz del sol. Por tanto, uno de los grandes retos en la actualidad es el almacenamiento de energía. En este contexto se trabaja fundamentalmente el desarrollo de baterías, lo que provocará una transición en el futuro cercano a coches eléctricos, por ejemplo. Pero para poder extender esto al transporte público y a las grandes plantas de generación se requieren otras fuentes de almacenamiento. Es aquí donde el hidrógeno juega un papel muy importante. En esta plática se mencionará el funcionamiento de las baterías y sus principales ventajas y desventajas, a la vez que se expondrán de forma general las distintas etapas y problemáticas que tiene la transición a una “economía del hidrógeno”; desde la obtención del hidrógeno y su almacenamiento, hasta el diseño de celdas de combustible para su transformación en energía eléctrica. Se comentarán algunas aplicaciones del hidrógeno en el transporte público y las perspectivas del transporte a futuro. Finalmente, mencionaremos brevemente algunas investigaciones que hacemos en México con el fin de contribuir al desarrollo de estas tecnologías.

Agradecimientos:

Se agradece al CONACyT el financiamiento de este trabajo a través de la Red de Almacenamiento de Energía y del proyecto 1373 de la Convocatoria de Problemas Nacionales. Se agradece también el apoyo del Instituto Politécnico Nacional a través del proyecto SIP 20196667 y la SECITI 071-2016.



[SCD-664] BioMEMS: Posibilidades de Desarrollo para la Ingeniería Biomédica

Wilfrido Calleja Arriaga (wcalleja@inaoep.mx)¹

¹ CD-MEMS INAOE wcalleja@inaoep.mx

En la actualidad la Electrónica se desarrolla en base a la tecnología de los chips (Microelectrónica), la gran mayoría de las aplicaciones se desarrollan con la ingeniería de software como herramienta, a esta combinación se le llama sistemas electrónicos, por lo que actualmente diversos tipos de modernos sistemas están presentes en nuestro entorno. Algunos ejemplos de sistemas son las pantallas inteligentes, los hornos de microondas y los teléfonos celulares, por mencionar algunos. Los sistemas electrónicos inteligentes siguen evolucionando siempre basados en los avances de la Microelectrónica, esta tecnología se desarrolla con la física, química y las ciencias de materiales, principalmente. Así los chips evolucionan en forma de diversos microcomponentes llamados sensores y actuadores (dispositivos con dimensiones de micrómetros).

Actualmente el término "Internet de las cosas" (Internet of Things) representa un concepto bastante amplio en las telecomunicaciones, que también se utiliza para describir el protocolo de intercomunicación y control de un arreglo de sensores colocados sobre el cuerpo de una persona, para el seguimiento continuo de los signos vitales. Estos nuevos sistemas son el producto de una fase más de desarrollo combinando chips, sensores e ingeniería de software. De aquí surge un nuevo concepto en los sistemas electrónicos: los Sistemas MicroElectroMecánicos (MEMS, MicroSistemas), como una nueva tecnología interdisciplinaria, a partir de la ya consolidada industria de la Microelectrónica.

En sus inicios, los MEMS presentaron aplicaciones restringidas hacia áreas de electromecánica: pero posteriormente, con el desarrollo de nuevos materiales compatibles con los chips, los Microsistemas se han diversificado hacia áreas tales como biología, óptica, fluídica, medicina, comunicaciones, Internet de las cosas, entre otras. Hasta la fecha, los prototipos MEMS con amplio uso industrial son enfocados hacia aplicaciones específicas, algunos ejemplos clásicos son los acelerómetros que detonan las bolsas de aire cuando ocurre una colisión vehicular, los cartuchos para inyección de tinta en las impresoras y recientemente los dispositivos microfluídicos para el análisis portátil de la sangre.

En un contexto general de investigación y desarrollo, los MEMS representan un amplio campo de estudio. En otro contexto de salud pública, los dispositivos MEMS para aplicaciones médicas (BioMEMS) representan un campo de desarrollo estratégico porque se proyecta como un mercado con potencial muy alto. La tecnología de BioMEMS permite el desarrollo de nuevos sensores con posibilidades de interacción con el cuerpo humano, utilizando nuevos polímeros y metales nobles para evitar rechazo biológico (lograr biocompatibilidad). En la actualidad, los trabajos de investigación en BioMEMS han derivado en una gran variedad de procedimientos en síntesis de materiales y métodos de fabricación, que utilizando técnicas de miniaturización de fluidos han conducido al desarrollo de la tecnología denominada "Lab on a chip" (mini-laboratorio contenido en un chip). Este tipo de tecnología incrementa la precisión en el análisis bioquímico, posibilitando nuevas capacidades de análisis clínico de tipo ambulatorio.

En el contexto tecnológico ya descrito, en esta conferencia se abordará la siguiente pregunta:

¿Puede la Microelectrónica ofrecer soluciones para la Ingeniería Biomédica



XII -ICSMV
September 23rd to 27th, 2019 / San Luis Potosí, México

SEMICONDUCTORS (SEM)

Chairmen:
Salvador Gallardo (CINVESTAV-DF)



XII -ICSMV
September 23rd to 27th, 2019 / San Luis Potosí, México

SEMICONDUCTORS (SEM) ORAL SESSION



XII -ICSMV

September 23rd to 27th, 2019 / San Luis Potosí, México

[SEM-45] Light emitters and photodetectors based on AlN/Ga(AlIn)N short period superlattices.

Sergey Nikishin (sergey.a.nikishin@ttu.edu)¹

¹ Department of Electrical and Computer Engineering, Nano Tech Center, Texas Tech University, Lubbock, TX 79401, USA

AlN/Ga(AlIn)N short period superlattices (SPSLs), whose period does not exceed ~ 2 nm grown on (0001) oriented sapphire and AlN substrates as well as on (111) oriented Si substrates are very attractive for design and fabrication of light-emitters and photodetectors operating in deep UV range of wavelengths. Such SPSLs can be grown using both plasma assisted and ammonia-based molecular beam epitaxy. The electrical and optical properties of such SPSLs, as well as the properties of deep UV light-emitters and photo-detectors will be described and discussed.



[SEM-69] Effect of Metal Halide Salts on optical properties of MoS₂ crystals grown by CVD

Victor Manuel Arellano Arreola (varellano@cinvestav.mx) ¹, Mario Flores Salazar ¹,
Andrés De luna Bugallo ¹

¹ Cinvestav unidad Querétaro

Single layered semiconductor molybdenum disulfide (MoS₂) has shown great potential for optoelectronics, mechanical, thermal, and other applications. One of the important challenges for two-dimensional (2D) materials is to develop a reliable growth technique to respond the industrial demand, including large areas deposition and high crystallinity. It has been recently shown that the use of metal halide salts (MHS) in diverse growth techniques lead to a significant area growth of transition metal dichalcogenides (TMDs) including MoS₂. However, the use of these promoters can have an important impact on the properties of these materials. In this work we compared the optical and structural properties between pristine MoS₂ singles layers and MoS₂ monolayers grown using metal halide salts during the growth[1,2,3].

Pristine and MHS-assisted MoS₂ flakes were grown using atmospheric pressure chemical vapor deposition on SiO₂/Si substrates, while the growth of pristine samples was carried out using only MoO₃ and sulfur as precursors, on the other hand, NaCl, KBr and KCl were included as promoters to carry out the MHS-assisted MoS₂ growth. All samples were grown at 750°C using 100sccm of argon as a carrier gas. Optical and SEM images revealed triangular shapes for all the cases, however we found that crystal sizes increase for MHS MoS₂ flakes.

MoS₂ optical properties were studied by means of Raman and Photoluminescence (PL) spectroscopy. For pristine samples the A1g and E2g modes at the Gamma point of the hexagonal Brillouin Zone are located at 384.54 and 405.6 cm⁻¹. However, a redshift of A1g mode on NaCl and KCl MoS₂ single layers can be appreciated, suggesting a residual doping during the growth. On the other hand, the position of KBr A1g mode remains unchanged while E2g peak presents a Raman downshift by 1.24 cm⁻¹ likely due to tensile strain inside the MoS₂ single layers. PL revealed the near band-edge emission (NBE) or exciton A located around 1.82eV and the exciton B peaked at 1.95eV for all samples. Nevertheless, PL emission intensity presented on pristine and KBr MoS₂ SL is comparable while the intensity of MoS₂-NaCl and MoS₂-KCl layers considerably quenches by 4 and 23 times respectively.

Finally, the structural properties of pristine and MHS assisted MoS₂ crystals was studied using x-ray photoemission spectroscopy (XPS). Mo3d and S2P signals indicates high chemical quality, however, KCl spectra show additional contributions located at lower energies suggesting the presence of the meta stable 1T structure.

References

Shape Evolution of Monolayer MoS₂ Crystals Grown by Chemical Vapor Deposition, Shanshan Wang, Youmin Rong, Ye Fan, Mercè Pacios, Harish Bhaskaran, Kuang He, and Jamie H. Warner Chemistry of Materials 2014 26 (22), 6371-6379 DOI: 10.1021/cm5025662



XII -ICSMV

September 23rd to 27th, 2019 / San Luis Potosí, México

Suppressing Nucleation in Metal–Organic Chemical Vapor Deposition of MoS₂ Monolayers by Alkali Metal Halides, HoKwon Kim, Dmitry Ovchinnikov, Davide Deiana, Dmitrii Unuchek, and Andras Kis Nano Letters 2017 17 (8), 5056-5063 DOI: 10.1021/acs.nanolett.7b02311

Considerations for Utilizing Sodium Chloride in Epitaxial Molybdenum Disulfide, Kehao Zhang, Brian M. Bersch, Fu Zhang, Natalie C. Briggs, Shruti Subramanian, Ke Xu, Mikhail Chubarov, Ke Wang, Jordan O. Lerach, Joan M. Redwing, Susan K. Fullerton-Shirey, Mauricio Terrones, and Joshua A. Robinson ACS Applied Materials & Interfaces 2018 10 (47), 40831-40837 DOI: 10.1021/acsami.8b16374



[SEM-145] Synthesis and characterization of ZnO/TiO₂ composite by mechanochemical milling for photocatalysis applications

Sofia Estrada Flores (sofiaestrada@uadec.edu.mx)¹, Antonia Martínez Luévanos (aml15902@uadec.edu.mx)¹, Catalina María Pérez Berumen², Elsa Nadia Aguilera González¹, Yuliana Elizabeth Ávila Alvarado¹, Yuliana Elizabeth Ávila Alvarado³

¹ Departamento de Materiales Cerámicos Avanzados y Energía, Facultad de Ciencias Químicas de la Universidad Autónoma de Coahuila, Blvd. V. Carranza s/n Col. República Oriente, Saltillo, Coahuila

² Departamento de Química Orgánica, Facultad de Ciencias Químicas de la Universidad Autónoma de Coahuila, Blvd. V. Carranza s/n Col. República Oriente, Saltillo, Coahuila

³ Facultad de Sistemas de la Universidad Autónoma de Coahuila, Carretera a México Km 13, Arteaga, Coahuila

In present the decreasing of potable water sources has moved the scientific community to develop new technologies of water treatment and photocatalysis has been proved to be an efficient process to obtain clean water. Photocatalysts are materials used in this type of process and they must have suitable characteristics such as high porosity, a low band gap and high absorption of light. The photocatalytic activity of a material can be improved through several strategies, some of these are through its doping or forming a composite with another material. The ZnO has a band gap value of 3.13 eV and presents light absorption in the ultraviolet region. ZnO can interact with TiO₂ forming a composite with improved optical and photocatalytic properties. In this work a composite material of ZnO/TiO₂ was obtained by mechanochemical milling; the infrared spectra present the characteristic bands of the Zn-O bonds and the Ti-O bonds into the region of 400 to 1200 cm⁻¹. The XRD pattern of the composite indicates the presence of zincite and anatase, a displacement in the 2θ values of the ZnO sample shows the modification of the cell parameters due to an interaction with the TiO₂. The band gap of ZnO/TiO₂ composite (3.08 eV) is lower than the pure ZnO (3.13 eV) due to the incorporation of anatase sample. The ZnO/TiO₂ composite presents higher light absorption in the UV region than the ZnO, which makes it a good photocatalyst if it is activated under UV light. The last was corroborated through photodegradation tests of a model dye (methylene blue) with 2 g/L of photocatalyst under UV light. The results indicate that ZnO/TiO₂ composite degrades a greater amount of dye than pristine ZnO.

Keywords: band gap, mechanochemical milling, photocatalyst, TiO₂, ZnO



[SEM-178] Effect of the growth method on the physical properties of the cubic In_xGa_{1-x}N/GaN quantum wells

Marlene Camacho Reynoso (marlene.camacho@cinvestav.mx) ³, Cristo Manuel Yee Rendón ², Máximo López López ⁴, Yuriy Kudriavtsev ¹, Yenny Lucero Casallas Moreno ⁵

¹ Electrical Engineering Department SEES, Centro de Investigación y de Estudios Avanzados del IPN, Apartado Postal 14-740, 07360 Ciudad de México, México.

² Facultad de Ciencias Físico- Matemáticas, Universidad Autónoma de Sinaloa, Cd Universitaria, C.P. 80010, Culiacán, Sinaloa, México.

³ Nanotechnology and Nanosciences Program, Centro de Investigación y de Estudios Avanzados del IPN, Apartado Postal 14-740, 07360 Ciudad de México, México.

⁴ Physics Department, Centro de Investigación y de Estudios Avanzados del IPN, Apartado Postal 14-740, 07360 Ciudad de México, México.

⁵ Unidad Profesional Interdisciplinaria en Ingeniería y Tecnologías Avanzadas, Instituto Politécnico Nacional, Av. IPN 2580, Gustavo A. Madero, 07340 Ciudad de México, México.

Optoelectronic devices based on group III-nitrides have had a great impact on technological development, due to that they can operate in hostile environments and at high processing temperatures [1,2]. Recent research focuses on applications such as Light Emitting Diodes (LEDs) and laser diodes, which are grown with the GaN heterojunction and the InGaN alloy in the blue-green spectral region. In this work, we present the optical, chemical and structural characterization of the cubic InGaN/GaN quantum wells (QWs) on GaAs (100) substrates by varying the Indium (In) content in the ternary alloy. The QWs were grown by Beam-Assisted Molecular Beam Epitaxy (PA-MBE). For the growth of the QWs, two methods were used, the first one is called Migration Enhanced Epitaxy (MEE) and the second one is Conventional Molecular Beam Epitaxy (MBE). Thicknesses of 10 and 30 nm for the InGaN QWs and the GaN barriers, respectively, were measured by Secondary Ions Mass Spectroscopy (SIMS). Emissions between 2.17 to 3.10 eV for the QWs were obtained by photoluminescence (PL) measurements at 20 K, which correspond to green, blue and violet wavelengths. This information was contrasted with photoreflectance (PR) measurements at the same temperature of the PL measurements, in which the cubic phase of the grown quantum wells was also observed. Additionally, the solution of the Schrödinger equation for a rectangular well potential was determined analytically. This potential was used as a first approximation for determining the transitions corresponding to the first energy states, in order to compare with the experimental values obtained. The binding energies of the InGaN QWs and the GaN barriers were also found by Spectroscopy of photoelectrons emitted by X-rays (XPS).

[1] Ding, S. A., Barman, S. R., Horn, K., Appl Phys Lett., **70**, 2407 (1997).

[2] Dewan, S., Tomar, M., Tandon, R.P., et. al., Vacuum., **164** (2019) 72-76.



[SEM-265] Electronic, Structural, Optical and Electrical Properties of ZnO:N

José De Jesús Araiza Ibarra Araiza Ibarra (araiza@fisica.uaz.edu.mx)³, Javier Alejandro Berumen Torres (jberumentorres@hotmail.com)³, José Juan Ortega Sigala³, Fernando Avelar Muñoz³, José Luis Rodríguez López², Juan Ortiz Saavedra³, Roberto Gómez³, Ángel Guillén Cervantes¹, Salvador Gallardo Hernández¹, Ciro Falcony Guajardo¹

¹ Departamento de Física, CINVESTAV-IPN

² IPICYT, A. C.

³ Unidad Académica de Física, Universidad Autónoma de Zacatecas

In this work, ZnO:N in a 32 atoms supercell were analyzed by AB Initio at different doping concentrations and ZnO:N thin films were deposited by DC-sputtering. The results and analysis for AB-Initio calculations as band structure, DOS and dielectric function, directly and with a reescalation were realized to establish a predictive behaviour with the structural, optical and electrical characterizations from the experimental X-ray diffraction, UV-Vis spectroscopy, EDS and electrical measurements. It is found that the ZnO is p-type when nitrogen is incorporated in the structure, giving states near to the valence band. These effects are clear for composition below 20% of N₂ in the structure in the deposited films. The density of states per energy (DOS) were obtained in the AB Initio calculations initially, from which the band gap energy was determined and corroborated with the optical characterization, using the Tauc equation.

Finally, some interesting effects are observed from the supercell proposed to the XRD calculated from the AB Initio relaxed structure and latter XRD measured results. The electrical obtained properties are measured by Hall effect and Seebeck effect. The films used for these purposes (ZnO:N) had p-type carrier concentration between 10¹⁶ to 10¹⁹ cm⁻³.



[SEM-282] Polaritonics in hybrid semiconductor microcavities

Edgar Armando Cerdá Méndez (edgar.cerda@uaslp.mx)⁴, Hector Francisco Lara Alfaro⁴, Oscar Ruiz Cigarrillo⁴, Francisco Javier Rocha Reina⁴, Osvaldo del Pozo Zamudio⁴, Ángel Andrés Torres Rosales⁴, Raul Eduardo Balderas Navarro⁴, Augusto David Ariza Flores⁴, Alfonso Lastras Martínez⁴, Andrés de Luna Bugallo¹, Antonio del Rio Portilla³, Vivechana Agarwal², Klaus Biermann⁵, Paulo Santos⁵

¹ CINVESTAV unidad Querétaro, Libramiento Norponiente #2000, Fracc. Real de Juriquilla.
76230 Santiago de Querétaro, Qro. México

² Centro de Investigación en Ingeniería y Ciencias aplicadas, Universidad del Estado de Morelos, Av. Universidad 1001, Colonia Chamilpa 62209 Cuernavaca Morelos, México

³ Instituto de Energías Renovables, Universidad Nacional Autónoma de México, Priv. Xochicalco S/N 62580 Temixco, Morelos, México

⁴ Instituto de Investigación en Comunicación Óptica, Universidad Autónoma de San Luis Potosí, Av. Karakorum 1470, CP 78216 San Luis Potosí, México

⁵ Paul-Drude-Institut für Festkörperelektronik, Hausvogteiplatz 5-7, 10117 Berlin, Germany

Polaritons are quasi-particles created by a quantum superposition of excitons in a semiconductor and photons in an optical microcavity (MC). The superposition occurs in the so called strong-coupling light-matter regime. Polaritons have been the subject of intense research in the last years due to their interesting properties such as Bose-Einstein condensation up to room temperature and strong non-linear interactions which allow superfluid behavior and the formation of solitons, for example.[1]–[3] These properties make polaritons strong candidates for the implementation of novel optoelectronic devices. In this work, we present two novel approaches for the fabrication of polaritonic devices based on a hybrid architecture. The structure is composed by two so-called de Bragg reflectors (DBR; stacks of thin layers with alternating refraction index) embedding a thin spacer layer, which acts as the cavity, with a few quantum wells (QWs) in it. The photon is confined in the cavity and is repeatedly absorbed by the excitons and reemitted into the cavity mode. Spatial manipulation of the polaritons in the cavity plane may be achieved by patterning or by acoustic fields. Traditionally, quasi-single mode MCs based on III-V semiconductors such as (Al,Ga)As are monolithic heterostructures grown by molecular beam epitaxy (MBE). The first approach of our proposal consists in substituting the top DBR by a porous silicon (PSi) DBR, which is separately grown by an electrochemical process, separated from the substrate, and mechanically deposited at the surface of an MBE-grown III-V half-MC. This allows for novel functionalities such as embedding a metallic pattern polariton confinement and application of electric fields. The second approach consists in using bidimensional semiconductor monolayers of transition metal dichalcogenides (DMT) deposited on a porous silicon DBR and covered by a second PSi DBR. The large exciton binding energy in TMD allows the existence of polaritons at room temperature, in contrast to traditional polaritons in III-V heterostructures, which can only be observed at cryogenic temperatures (10-15 K) due to the low binding energy of the exciton in GaAs QWs. Additionally, the particular symmetry lattice of the TMD, where the spin of the electrons is coupled to their momentum, opens the door to a new generation of polaritonics. [4], [5] Our work envisions a novel generation of hybrid polaritonic devices where the fabrication process is simplified and where novel functionalities may be implemented.

[1] D. Sanvitto and S. Kéna-Cohen, “The road towards polaritonic devices,” *Nat. Mater.*, vol. 15, no. 10, pp. 1061–1073, Oct. 2016.

[2] E. A. Cerdá-Méndez, D. N. Krizhanovskii, M. S. Skolnick, and P. V. Santos, “Quantum fluids of light in acoustic lattices,” *J. Phys. Appl. Phys.*, vol. 51, no. 3, p. 033001, 2018.

[3] E. A. Cerdá-Méndez *et al.*, “Exciton-Polariton Gap Solitons in Two-Dimensional Lattices,” *Phys. Rev. Lett.*, vol. 111, no. 14, p. 146401, Oct. 2013.

[4] Y.-J. Chen, J. D. Cain, T. K. Stanev, V. P. Dravid, and N. P. Stern, “Valley-polarized exciton–polaritons in a monolayer



XII -ICSMV

September 23rd to 27th, 2019 / San Luis Potosí, México

semiconductor," *Nat Photon*, vol. 11, no. 7, pp. 431–435, Jul. 2017.

[5] J. R. Schaibley *et al.*, "Valleytronics in 2D materials," *Nat. Rev. Mater.*, vol. 1, p. 16055, Aug. 2016.



[SEM-511] HARDENING THE AlGaN/GaN HEMT NANOMETRIC STRUCTURE BY ITS DEUTERIUM PASSIVATION

*Jaime MIMILA-ARROYO (jmimila@cinvestav.mx)¹, Alma Sofia ARREOLA-PINO
(asmcom2@gmail.com)¹*

¹ CINVESTAV-IPN-Zacatenco

Gallium nitride based devices made on epitaxial layers grown on foreign substrates suffer of the presence of threading dislocations (TD) with densities in the range of 10^8 - 10^{11} cm $^{-2}$, degrading their performance. Although TDs concentration can be controlled through the growth conditions, it is quite complicated, time consuming, and to now they have not been completely suppressed. Dislocations degrade the performance of every device produced with this semiconductor. By another way, it has been widely demonstrated that dislocations and some other GaN native defects can be passivated, at least partially, in an important way by in-diffusing hydrogen. Such hydrogenation improves in an important way the electrical and opto-electronical properties of the GaN epitaxial layers. For the case of the AlGaN/GaN high electron mobility transistors (HEMT), which involves several layers of nano-metric dimensions, such hydrogenation, properly realized, strongly improves the device capacity to handle current as well as other important parameters. Improvements due to the increase of the two dimensional electron gas concentration, their mobility and the homogeneity of the physical properties of the structure throughout the wafer. Notwithstanding all these benefits resulting of hydrogen passivation of defects in the HEMT structure studies assessing its stability have not been realized and are badly needed to decide on its industrial application.

Here we report on a detailed study on the stability of hydrogen passivated HEMT structure. This has been done monitoring the behavior of two different types of HEMT; "As grown" and hydrogenated, both taken from the same wafer and processed simultaneously. The stability have been, explored through the realization of thermal anneals simultaneously on both types of samples, looking for the out-diffusion of the introduced hydrogen. Our results allow to identify that the degradation mechanisms are completely different for each type of sample. The activation energy for each one of them has been determined being, as well, quite different. The main result being that the introduced hydrogen hardens this HEMT structure making it much more stable than the "as grown" one, i.e., without controlled introduced hydrogen. All the details will be given in this presentation.



XII -ICSMV
September 23rd to 27th, 2019 / San Luis Potosí, México

SEMICONDUCTORS (SEM)

POSTER SESSIONS



[SEM-5] CONSTRUCTION OF A MIS STRUCTURE BASED ON TWO-DIMENSIONAL ZnO NANOSTRUCTURES BY CHEMICAL ROUTES

Rubén Jonatan Aranda García (jonatan_izucar@hotmail.com) ¹, Mirian Yoceline Herrera Herrera ¹, Angélica María Barrientos Valeriano ¹

¹ Facultad de Ingeniería Química, Benemérita Universidad Autónoma de Puebla

Because of its physical properties, ZnO is considered a potential semiconductor compound for fabricating electronic and optoelectronic devices. In this regard, several growth techniques have been developed to ensure the required control for manufacturing commercial devices based in this semiconductor. On the pathway for improving the performance of the current devices, low-dimensional ZnO structures seem to be a promising alternative.

Here, we report the fabrication of a metal-insulator-semiconductor (MIS) structure based on ZnO nanostructures grown on the surface of an anodized aluminum substrate (ZnO/Al₂O₃/Al) by chemical routes. Namely, while the ZnO nanostructures were obtained through a low-temperature hydrothermal route, the Al₂O₃/Al substrate was obtained by electropolishing and anodizing of aluminum foil. The used electrochemical techniques for obtaining the substrate involve soft reaction conditions, short reaction times, low cost and easy processing. The obtained ZnO/Al₂O₃/Al architecture was studied by x-ray diffraction (XRD), scanning electron microscopy (SEM), micro-Raman spectroscopy (μRS) and electrical measurements. The voltage-time plot acquired during the anodizing process indicates the formation of an insulating barrier (Al₂O₃) on the metallic substrate (Al). The SEM analysis reveals that the semiconductor layer grown on the insulator film is nanostructured in nature, constituted by leave-like structures with an average thickness of ~ 50 nm. According with the Raman spectrum, these ZnO nanostructures are well-crystalline. The formation of Al₂O₃ and ZnO phases was further confirmed by means of XRD. Finally, the characteristic rectifying response of a metal-oxide-semiconductor junction is observed in the curves I-V and C-V of the obtained architecture, indicating that it is possible to build a MIS structure based on ZnO nanostructures using exclusively chemical routes.



[SEM-119] ZnO nanorods and nanotubes: Optical, electrical and electrochemical properties

Fernanda Retana (fernanda.rb92@gmail.com)¹, Boris Kharissov¹, Yolanda Peña¹, Idalia Gómez¹, Thelma Serrano (thelma.serranoqzd@uanl.edu.mx)¹

¹ Laboratorio de Materiales I, Universidad Autónoma de Nuevo León, Facultad de Ciencias Químicas, Av. Pedro de Alba s/n, Ciudad Universitaria, C.P. 66455, San Nicolás de los Garza, Nuevo León, México.

ZnO is a widely used semiconductor as the electron acceptor in the inorganic phase within hybrid solar cells. On the other hand, one-dimensional (1D) nanostructures provide properties and useful characteristics for this approach such as transparency and conductivity. The most common morphologies for 1D nanomaterials include nanorods and nanotubes. It is the aim of this work, the comparison of the optical, electrical and electrochemical properties between ZnO nanorods and nanotubes. ZnO nanorods and nanotubes were obtained by an electrochemical method. The nanostructures were grown on ITO substrates applying a stationary potential of -0.8 and -1.0 V vs Ag/AgCl. While ZnO nanotubes are obtained through a selective etching process at 1.0 V vs Ag/AgCl varying the time. The structural, optical, electrical and electrochemical properties were studied. Both nanostructures exhibit a single wurtzite crystalline structure, an enhancement in the visible range absorption associated to its anisotropic nature, the band gap was estimated in a range of 3.35-3.45 eV for ZnO nanorods and nanotubes, respectively. Nanorods and nanostructures show low intensity of photoluminescence that improves charge separation and transportation. Moreover, the nanostructures have a cylindrical shape with a uniform size of 150-300 nm. The ZnO nanotubes exhibited a correlation between its diameter and length size with its optical properties. The electrical conductivity was estimated in a range of 10⁻³ to 10⁻⁵ S/cm. The diameter and length size has an important correlation with the optical and electrical properties for this kind of 1D nanostructures. Furthermore, ZnO nanotubes showed an enhancement in the properties since the exciton are more confined than nanorods.



[SEM-143] Type I In_{0.145}Ga_{0.855}As_ySb_{1-y} alloys: Structural, chemical and optical properties.

A.L. Martínez López (*anlomartinez@esimez.mx*) ², G. Villa-Martínez ², M. Ramírez López ², J.G. Mendoza-Álvarez ¹, J.L. Herrera-Pérez ², Y.L Casallas-Moreno ²

¹ Physics Department, Centro de Investigación y de Estudios Avanzados del IPN, C.P. 07360, México.

² Unidad Profesional Interdisciplinaria en Ingeniería y Tecnologías Avanzadas-Instituto Politécnico Nacional, Av. IPN 2580, Col. Barrio la Laguna Ticomán, Gustavo A. Madero, C.P. 07340, México.

Antimonide family has become in potential semiconductor materials to develop a new generation of applications in the infrared, such as laser diodes, light-emitting diodes (LEDs), thermophotovoltaic cells and detectors. These devices are promising for a large variety of biomedical, environmental and industrial applications. Among the antimonide family, the In_xGa_{1-x}As_ySb_{1-y} alloy covers a wide electromagnetic spectrum from near infrared (1.7 μm) to medium infrared (3.5 μm), with a direct band gap [1,2]. In this study we showed the changes of the crystalline quality and of the infrared emission; as well as the growth mechanism of the In_{0.145}Ga_{0.855}As_ySb_{1-y} alloys by varying the arsenic (As) content. These quaternary alloys were grown by liquid phase epitaxy (LPE) on intrinsic GaSb (100) substrates. The alloys presented a tensile strain over the substrate, which increases with the As content. Furthermore, we found a nearly lattice-matched between the alloys and the GaSb substrates of $\Delta a/a \approx 10^{-4}$, allowing a stable configuration of the In_{0.145}Ga_{0.855}As_ySb_{1-y}. The alloys showed excitonic transitions evidencing the high crystalline quality, whose energy decreases with the As content. Additionally, we have also identified that the stable atomic arrangement of the quaternary alloy is mainly formed by two compounds, Ga-Sb and In-As, such as was proved by X Ray Photoelectron Spectroscopy (XPS).

[1] An, N.; Ma, L.; Wen, G.; Liang, Z.; Zhang, H.; Gao, T.; Fan, C. Structure Design and Analysis of 2 μm InGaAsSb/AlGaAsSb Muti-Quantum Well Laser Diode with Carrier Blocking Layer. *Appl. Sci.* 2019, 9, 1-7.

[2] Borca-Tasciuc T.; Song, D. W.; Meyer, J. R.; Vurgaftman, I.; Yang, M.-J.; Noshio, B. Z.; Whitman, L. J.; Lee, H.; Martinelli, R. U.; Turner, G. W.; Manfra, M. J.; Chen, G. Thermal conductivity of AlAs_{0.07}Sb_{0.93} and Al_{0.9}Ga_{0.1}As_{0.07}Sb_{0.93} alloys and (AlAs)₁/(AlSb)₁₁ digital-alloy superlattices. *J. Appl. Phys.* 2002, 92, 4994-4998.



[SEM-163] Synthesis of high-quality mono and multilayer graphene by the LPCVD technique.

Ana Karen Susana Rocha Robledo (anarocha@cinvestav.mx)¹, Andrés de Luna Bugallo (aluna@cinvestav.mx)¹

¹ Cinvestav, Unidad Querétaro

Among the most interesting low dimensional materials, we can find that graphene has attracted a lot of attention due to its unique properties and a great versatility to be used in different areas including electronics, photonics, medicine, biology etc. However, in the specific case of graphene synthesis, obtaining significant quantities with low defect density is still a challenge that must be addressed to develop graphene-based products at industrial scale.

In this work we present the synthesis and study of mono and multilayer graphene using low pressure chemical vapor deposition at low pressures (LPCVD) technique on copper substrates. In order to obtain graphene, the substrate is first cleaned with HNO_3 and sonicated with acetone and isopropanol to remove organic and inorganic contaminants then the substrate is placed inside tubular reactor with a starting vacuum of 1-0.01 torr, the system is heated up to temperatures between 1000 to 1050 °C, at this temperature the substrate is subjected to a flow of H_2 for a defined time, finally the graphene growth starts in the presence of CH_4 and ends with the cooling of the system.

To determine the presence of graphene we perform spectroscopy Raman after the growth on copper and on SiO_2 substrates, all spectra present typical bands D, G and G' located around 1350, 1580 y 2700 cm^{-1} respectively, it is well known that the intensity relation between the G' and G () indicate the number of layers while the D and G relation gives a good idea about the quality of the layers. We detected in our samples, the presence of graphene monolayer for samples grown at 1005°C and 1050°C, in addition, we found relations of =0.40 for 1005°C and 0.20 for 1050°C, indicating a decrease in the defect density when the growth temperature is higher. Furthermore, we observed the morphology of the mono and multilayer graphene through SEM and AFM technique.

Our results show that temperature plays a crucial role on quality graphene monolayers obtained by LPCVD technique, by increasing 45 degrees we found a considerable reduction of defect density, which is highly desirable for the development of graphene-based devices.



[SEM-176] Grown and characterization of ZnO thin films doped with Zr obtained by RF-sputtering technique.

Andrea Herrera Sánchez (andykiru13@gmail.com)³, Sergio Joaquín Jimenez Sandoval¹, Francisco Rodríguez Melgarejo¹, Martín Adelaido Hernández Landaverde¹, Olexandr Bondarchuck², Iván René Corrales Mendoza³, Julián Javier Carmona Rodríguez³

¹ *Centro de Investigación y de Estudios Avanzados del IPN, Unidad Qro., Querétaro, Qro., 78001, México.*

² *División de Estudios de Posgrado, Universidad Tecnológica de la Mixteca, Huajuapan de León, Oaxaca, 69000, México.*

³ *Instituto de Física y Matemáticas, Universidad Tecnológica de la Mixteca, Huajuapan de León, Oaxaca, 69000, México.*

Zr doped ZnO thin films at 0, 0.1, 0.5, 1.0, 2.0 y 2.5 at% were grown on to glass slides and Si substrates at room temperature by radiofrequency sputtering. The samples were characterized by energy dispersive X-ray spectroscopy (EDS), X-ray diffraction (XRD), and UV-vis spectroscopy.

Chemical composition was obtained by EDS analysis, the results show that all the samples grew with excess of oxygen (~ 56 at%) and the incorporation of Zr in the samples induces a decrease the at% of Zn.

XRD diffraction patterns show that all the samples are polycrystalline with wurtzite structure and the highest intensity peak in all the thin films is associated to diffraction plane (002), according to table PDF 79-0208 by ICCD database. As the Zr concentration increases, the thin films show a displacement at low angles due to an increase in interplanar distance. This displacement could be associated to Zr⁴⁺ replaces Zn²⁺ in ZnO lattice. In the samples with 2.0 and 2.5 at% peaks with low intensity around 2theta ~ 31° were observed and could be correspond to formation of ZrO₂.

UV-vis spectra show that the transparency of the samples is improved with the increase of Zr. The ZnO sample shows transmittance lower than 80% and the incorporation of Zr increases transmittance around 85%, this value corresponds to sample doped with 2.5%at Zr.



XII -ICSMV

September 23rd to 27th, 2019 / San Luis Potosí, México

[SEM-272] Characterization of GaAs/GaP micro-pyramids grown by Liquid Phase Epitaxy

Francisco Rocha-Reina (fjrochar.22@gmail.com)², Edith Castillo-Baldivia², Osvaldo Del Pozo-Zamudio², Andrés de Luna-Bugallo¹, Edgar Cerdá-Méndez², Raúl Balderas-Navarro², Michourny Viatcheslav², Andrei Gorbatchev (andre@cactus.iico.uaslp.mx)²

¹ Cinvestav, 76230 Santiago de Querétaro, Qro. México

² Instituto de Investigación en Comunicación Óptica, Universidad Autónoma de San Luis Potosí, 78210 San Luis Potosí, S.L.P., México.

The manufacture of micro and nano-structures for the development of low-cost devices for applications in the Near Infrared region has been one of the main challenges at present. In this work we show micro-photoluminescence (μ PL) and X-ray diffraction measurements of truncated pyramidal micro-structures of GaAs on a GaP (001) substrate. These pyramids were grown by Liquid Phase Epitaxy (LPE) for wetting times of 1, 5 and 15 seg the sizes of the structures are 5-10 μ m. Through the two characterization techniques observed that we have some concentration of phosphorus atoms (P) in the pyramid structures. We also observed the absence of planar epitaxial layers that confirms the results of thermodynamic analysis. We show that in the GaP-GaAs system in the case of a great lattice mismatch with the substrate, the thin epitaxial layers can only be formed with reduced elastic energies.



[SEM-287] Fabrication and characterization of hybrid (Al,Ga)As - porous silicon microcavities for operation at cryogenic temperatures

Hector Francisco Lara Alfaro ¹, Edgar Armando Cerdá Méndez ¹, Oscar Ruiz Cigarrillo ¹, Francisco Javier Rocha Reina ¹, Ángel Andrés Torres Rosales ¹, Augusto David Ariza Flores ¹, Alfonso Lastras Martínez ¹, Klaus Biermann ², Paulo Santos ²

¹ Instituto de Investigación en Comunicación Óptica, Universidad Autónoma de San Luis Potosí, Av. Karakorum 1470, CP 78216 San Luis Potosí, México

² Paul-Drude-Institut für Festkörperferelektronik, Hausvogteiplatz 5-7, 10117 Berlin, Germany

In this work, we show a study of the fabrication and characterization of hybrid microcavity (MC) devices for the strong light-matter coupling regime (SLMC). MCs operating in the SLMC regime are interesting since they sustain bosonic light-matter quasiparticles called polaritons, which show interesting properties such as Bose-Einstein Condensation and strong nonlinearities.[1], [2] A MC is composed of two reflectors and a spacer layer (the actual cavity) with quantum wells (QWs) embedded in it. While the reflectors confine the photons, the QW confines excitons. In semiconductor MCs, the reflectors, known as de Bragg reflectors (DBR), are stacks of layers of thicknesses equal to $\lambda/4n$ with alternated index of refraction n. The alternating change in n favors the reflection of light in one direction of propagation by interference of the reflected waves in the multiple interfaces. The reflectance amplitude and spectral bandwidth of the DBRs can be thus engineered by controlling the thicknesses and n of the layers. The SLMC regime is achieved when the quality factor Q (i.e. the ratio between the storage and losses rates) is high enough ($Q>1000$) so that the confined photons are absorbed and reemitted by an exciton in the QW. Semiconductor MCs with high Q can be achieved with (Al,Ga)As heterostructures grown by Molecular Beam Epitaxy (MBE). In our device, the top DBR in an (Al,Ga)As MC is substituted by a porous silicon (PSi) one.[3] The Psi DBR is separately grown by an electrochemical process and separated from the substrate by electropolishing. We show that with this architecture it is possible to embed a metallic pattern previously deposited on the half-MC, with which one can create arbitrary confinement potentials for the polaritons as deep as 10 meV. The latter is impossible to do in a monolithic MC grown by MBE. Also, the metallic layer allows to directly apply current or voltage to the active layer for manipulation by electric fields, bypassing the important constraint inherent of the monolithic structure of having to apply the current or voltage through the thick resistive top-DBR. We present detailed calculations and experimental studies of the reflectance at temperatures down to 10K. Interestingly, the SiP DBRs show unexpected energy shifts when separated from the substrate, probably due to the release of built-in strain, as shown in Raman studies. Our work opens a novel architecture for the implementation of polaritonic devices with new functionalities.

[1] E. A. Cerdá-Méndez, D. N. Krizhanovskii, M. S. Skolnick, and P. V. Santos, "Quantum fluids of light in acoustic lattices," *J. Phys. Appl. Phys.*, vol. 51, no. 3, p. 033001, 2018.

[2] A. Amo and J. Bloch, "Cavity Polaritons: Crossroad Between Non-Linear Optics and Atomic Condensates," *Strong Light-Matter Coupling At. Solid ...*, 2014.

[3] V. Agarwal, "Porous Silicon Multilayers and Superlattices," in *Handbook of Porous Silicon*, L. Canham, Ed. Cham: Springer International Publishing, 2014, pp. 1–9.



[SEM-289] Structural analysis of ZnO thin films doped with Zr annealed in air and nitrogen atmospheres

Jeeniffer Herrera Ramírez (jeenifferherrera@gmail.com)², Sergio Joaquín Jiménez Sandoval¹, Francisco Rodríguez Melgarejo¹, Martín Adelaido Hernández Landaverde¹, Abraham Israel Calderón Martínez¹, Julián Javier Carmona Rodríguez²

¹ Centro de Investigación y de Estudios Avanzados del IPN, Unidad Querétaro, Querétaro, Qro, 78001, México.

² Instituto de Física y Matemáticas, Universidad Tecnológica de la Mixteca, Huajuapan de León, Oax, 69000, México.

Zr doped ZnO thin films at different Zr content (0, 0.1, 0.5, 1.0, 2.0 y 2.5 at%) were successfully deposited at room temperature on to glass substrates by RF magnetron sputtering. Two sets of samples were annealed at 450°C for 1 hour, the first set in air atmosphere and second set in nitrogen atmosphere. The effect of doping and annealing in different atmospheres on thin films structure have been analyzed by X-ray diffraction (XRD). X-ray diffraction patterns indicate that samples as-grown and annealed are polycrystalline and correspond to hexagonal structure. The growth was mainly oriented in the direction of the plane (002) for all samples. Samples with 2.0 and 2.5 at% Zr the presence of ZrO₂ is observed. The interplanar distance in the samples without annealed is increased from 2.615 Å (0 at% Zr) to 2.637 Å (2.5 at% Zr) and after of the heat treatments is reduced to 2.613 Å (0 at% Zr) to 2.614 Å (2.5 at% Zr) annealed in air and 2.606 Å (0 at% Zr) to 2.607 Å (2.5 at% Zr) annealed in N₂. The grain size is increased for ZnO sample, however the samples doped with high concentration of at% Zr no substantial changes were observed.



[SEM-365] Optical analysis of nitrogen-induced localized levels of Ga(N,As) thin films grown by molecular beam epitaxy

I.E. Cortes-Mestizo (irving.cortes@uaslp.mx)², L.I. Espinosa-Vega¹, J.A. Espinoza-Figueroa¹, C.M. Yee-Rendón³, L. Zamora-Peredo⁴, A.G. Rodríguez-Vázquez¹, C.A. Mercado-Ornelas¹, F.E. Perea-Parrales¹, V.H. Méndez-García¹

¹ CIACYT, Universidad Autónoma de San Luis Potosí, San Luis Potosí, México

² CONACYT- CIACYT, Universidad Autónoma de San Luis Potosí, San Luis Potosí, México

³ FCFM, Universidad Autónoma de Sinaloa, Culiacán, Sinaloa, México

⁴ MICRONA, Universidad Veracruzana, Boca del Río, Veracruz, México

The use of Ga(N,As) ternary materials systems has been recently developed in order to take advantage of the fact that their energy band gap is reduced by incorporation of small amounts mole fractions of N in the GaAs host crystal structure, making this material very useful to the development of GaAs-based devices such as light-emitting and solar cells, avoiding problems related to the use of traditional arsenides and phosphides [1]. Incorporation of N into GaAs modifies the crystal composition of this dilute nitride compound, altering their band structure and changing the optical and electrical properties. In this work, the authors shown the optical analysis $\text{GaN}_x\text{As}_{1-x}/\text{GaAs}$ system grown by molecular beam epitaxy where the nitrogen concentration of the Ga(N,As) layer has been varied from $X \sim 0.2$ to 2%. Photoreflectance spectroscopy (PR) of the samples exhibited three groups of spectral signatures in the range of 1 to 2 eV. Temperature dependent PR characterization with two modulation sources of 325 and 572 nm was realized in order to determine the type and origin of the PR spectra signatures. It was found that the observed transition can be associated to nitrogen-induced levels (E_- and E_+) and energy levels of the host material (GaAs band to band, E_0 , and $E_- + \Delta_{SO}$). At room temperature and for relatively low concentration values (X between 0.2 to 0.6%) signals mixing among E_- and E_0 and for E_+ and $E_- + \Delta_{SO}$ occurs, making difficult to distinguish the precise location of them and making mandatory the use of numerical analyses based in Aspnes' third derivate functional form. Low temperature PR facilitates the analyses of the Ga(N,As) band structure by the bifurcation of the energy levels. Ellipsometry spectroscopy (ES) was employed in order to contrast with both the numerical results and the PR characterization. The behavior of the pseudo-dielectric function of the GaNAs/GaAs given by the ES spectrum was analyzed. The Lorentzian-like signals are exhibited around the energy position where the standard critical point model predicted the presence of nitrogen-induced localized levels in the ES spectrum. With this investigation the numerical and experimental procedure to determine the E_- and E_+ nitrogen-induced localized levels is reported, which is a main demand to understand the bulk properties of the G(N,As) compound and the first step to improve the use of GaNAs in nanostructures.

[1] Hidetoshi Suzuki et al., Journal of Crystal Growth 384, 5 (2013).

Acknowledgments: The authors acknowledge the financial support from CEMIE-SOL 22, FRC-UASLP, C19-FAI-05-18.18 and CONACYT-Mexico through grants: INFR-2015-01-255489, CB 2015-257358, PNCPN2014-01-248071 and the Catedras CONACyT (Project No. 44).

+ Author for correspondence: irving.cortes@uaslp.mx



[SEM-504] Many-electron interacting into semiconductor nanowire Y-Junctions

Reyna Méndez Camacho (reyna129b@hotmail.com)¹, Elihu Hazel Sánchez Martínez¹,
Esteban Cruz Hernández¹

¹ Coordinación para la Innovación y la Aplicación de la Ciencia y Tecnología, CIACYT-Universidad Autónoma de San Luis Potosí, UASLP, Sierra Leona 550, San Luis Potosí, S. L. P., México.

To maintain the accelerated technological growth of the last decades, new nanoelectronic systems are required to do the functions of transistors, logic gates, etc., or for the development of completely novel components. A basic element to develop more complex elements is a union of quantum wires (QWRs) to form a structure in form of Y (Y-Junctions).

The electronic interaction between quantum wires (QWRs) that build the Y-Junctions are important to study unique one dimensional (1-D) quantum effects such as evanescent coupling, negative Coulomb drag, electromagnetically induced transparency, etc.

In this work, we explore the use of a Yukawa-like potential to describe in a simplified way the interaction of two or even 10^{24} e/cm^3 in Y-junction QWRs. In addition, by establishing an electric potential along the axis-wire, the model is able to describe the external electric field effect on the electronic distribution in the Y-junctions. In addition to the theoretic results, we present some advances in the experimental measurement of the carrier transport by an external voltage in GaAs/AlGaAs Y-junctions.



**[SEM-506] Optical and structural properties of SiO₂/C/SiO₂ and
SiO₂/Si/SiO₂ heterostructures deposited by reactive RF sputtering.**

Mario Cervantes Contreras (*calculo1fm1@gmail.com*) ¹, Miguel Meléndez Lira ², Orlando Zelaya Ángel ²

¹ Departamento de Ciencias Básicas, Unidad Profesional Interdisciplinaria de Biotecnología - Instituto Politécnico Nacional. Av. Acueducto s/n Col. Barrio la Laguna Ticomán, C. P. 07340, Gustavo A. Madero, México City, México.

² Departamento de Física, CINVESTAV-IPN, , Apdo. Postal 14-740, México, DF 07000, México

The roughness associated with the sputtering deposition process has been employed to explore the possibility to produce C and Si nanoparticles embedded within a silicon oxide matrix on soda-lime glass and p-silicon substrates. Silicon dioxide, silicon and carbon films were deposited employing silicon and carbon targets. An oxygen rich working plasma was employed. Oxygen content of the working plasma was modulated through argon partial pressure. A sequential deposition of SiO₂/C/SiO₂ films was employed; SiO₂ layer was produced at room temperature by 30 minutes while deposition of C layer was produced at room temperature by 2 minutes. The heterostructure of SiO₂/Si/SiO₂ was produced under the same conditions. Results of the optical and structural properties are presented. Results X-ray diffraction and Raman characterization are correlate with Photoluminescence emission, absorbance and reflectance spectra.



[SEM-576] BiOI nanostructures and their visible light photocatalytic activity

John Fredy Florez Rios (jofflorezri@gmail.com)¹, Jesús Fernando Zamudio García², José Guadalupe Quiñones Galván¹, Miguel Ángel Santana Aranda¹, Arturo Chávez Chávez¹, Armando Pérez Centeno¹

¹ Departamento de física, Universidad de Guadalajara (CUCEI), Blvd. Gral. Marcelino García Barragán 1421, Olímpica, 44430 Guadalajara, Jal.

² Departamento de ingeniería en nanotecnología, Universidad Politécnica de Sinaloa, Carretera Municipal Libre Mazatlán Higueras Km 3, 82199 Mazatlán, Sin.

Recently, bismuth based semiconductors have attracted attention due to their outstanding physical and chemical properties, non-toxicity, stability and potential photocatalytic activities at visible radiation. In particular, BiOI semiconductor could be used on visible light photocatalysis since its band gap is around 1.9 eV. The BiOI photocatalytic activity depends on the morphology and structure properties, in turn they depend on the Bi precursor used during the synthesis, among others variables.

In this work, BiOI nanostructures were synthetized thought hydrothermal synthesis using bismuth acetate (BiAc) and bismuth subsalicylate (BiSs) as bismuth sources. Optical properties were studied by UV-Vis spectroscopy. X-ray diffraction and Raman spectroscopy were used to study structural properties and scanning electron microscopy to study their morphology. In order to study its photocatalytic activity, measurements of dye concentration versus exposure time of UV and Visible radiation were carried out. As reference sample, standard P25 TiO₂ was used. We found that there is a significant improvement of photocatalytic activity of BiOI when using visible light radiation.

Acknowledgements

Authors thanks to UDG ProSNI and CONACYT-scholarships program for the partial financial support. Also, we thank to Sergio Oliva for his technical assistance.



[SEM-580] Synthesis, characterization and glass formation area of CuCl₂–CdO–V₂O₅ ternary system

Rosendo Leovigildo Lozada Morales (*rlozada@fcfm.buap.mx*) ¹, Erika Cervantes Juárez (*k_eri13@hotmail.com*) ¹, María Fernanda Hernández Rodríguez ¹

¹ FCFM,BUAP,Prol. 24 sur esq. Av. San Claudio, Ciudad Universitaria Col. San Manuel

Glass formation area in the CuCl₂–CdO–V₂O₅ ternary system was determined. The synthesis was carried out by melt quenching method. At 1200 °C during 30 minutes and followed by a thermal shock at room temperature. The structural and optical properties for all the samples were characterized by X-ray diffraction, Raman spectroscopy and Diffuse Reflectance Spectra. The X-ray patterns of amorphous samples presented a broad band around $2\theta=30^\circ$ while the obtained for crystalline samples, presented the diffraction peaks of crystalline Cd₂V₂O₇. The Raman spectra of the complete series of samples, exhibited a first group of peaks

located at 873, 845, and 818 cm⁻¹ modes and a second one with maximums at 474, 349, 310 and 255 cm⁻¹ which are related to stretching and symmetry modes respectively of Cd₂V₂O₇ compound. By diffuse reflectance spectra and using the Tauc's law was estimated the optical band gap. According to the content of CuCl₂, when it is increased the optical band gap is reduced from 2.4 to 1.7 eV. The variation of the glass properties and structural changes were studied in terms of the glass composition. The glass formation area was localized at high content of CdO and small amounts of V₂O₅ and CuCl₂. Surrounding this area the compound Cd₂V₂O₇ in crystalline structure, was identified.



[SEM-583] Evaluación de una celda MHD operada con soluciones electrolíticas

Steffanie Jimenez-Flores (sjimenez286@gmail.com)¹, J. Guillermo Perez-Luna²

¹ *Centro de Investigación en Dispositivos Semiconductores, BUAP Prolongación 14 Sur, Edificio IC5, San Manuel, 72570 Puebla, Pue.*

² *FCE-BUAP Ciudad Universitaria, San Manuel, Puebla, Pue., CP 72570*

Una celda magnetohidrodinámica (MHD) es un dispositivo que genera energía eléctrica a partir de la interacción entre un fluido conductor con alta energía cinética y un campo magnético. Para propósitos de este trabajo, se diseñó y fabricó una celda MHD que opera con flujo de soluciones electrolíticas de NaCl y KOH. El aumento de la velocidad del flujo se genera mediante un panel solar que lo hace fluir hacia la celda MHD en condición de lazo cerrado. Para realizar la evaluación de la celda MHD, se desarrolló una interfaz que se acopla a un sistema de adquisición de datos el cual se opera con el programa Lab View. La interfaz permite evaluar el comportamiento eléctrico de la celda MHD en tiempo real y con bajo ruido. Los resultados obtenidos muestran que la conversión de energía se lleva a cabo mediante la presencia del efecto MHD. También se muestra que, la celda MHD con electrolito de KOH es capaz de generar corrientes del orden de uA, y que la impedancia interna de la celda es de tipo resistivo y reactivo capacitivo.



[SEM-610] Linear metamorphic $\text{In}_x\text{Ga}_{1-x}\text{As}$ layers grown by MBE for THz emitters

Alfredo Belio-Manzano³, Leticia Ithsmel Espinosa-Vega³, Irving Eduardo Cortes-Mestizo¹, Christian Alejandro Mercado-Ornelas³, Salvador Gallardo-Hernández⁴, V. Damian Compean-Garcia¹, Jorge L. Regalado-de la Rosa², Enrique Castro-Camus², Victor Hugo Mendez-García (victor.mendez@uaslp.mx)³

¹ CONACYT- CIACYT, Universidad Autónoma de San Luis Potosí, San Luis Potosí, México

² Centro de Investigaciones en Óptica A.C., Loma del Bosque 115, Lomas del Campestre, León, Guanajuato 37150, México

³ Coordination for the Innovation and Application of Science and Technology (CIACYT), Autonomous University of San Luis Potosí, San Luis Potosí, 78210 Mexico

⁴ Physics Department, Centro de Investigación y de Estudios Avanzados del IPN, Apartado 14470, D.F. México

The development of new mechanisms that allows for the generation of radiation at terahertz (THz) frequencies represents a new and interesting area of work and research due to the enormous impact that THz technologies would have in various modern scientific areas [1]. Besides of the most commonly used THz emitters based on photoconductive antennas, alternative THz radiation sources have been proposed [2]. In this work, we have studied the epitaxial growth of linear metamorphic layers of $\text{In}_{1-x}\text{Ga}_x\text{As}$ on SI GaAs (100) substrates by molecular beam epitaxy (MBE) with the aim to improve the near-surface band bending and the generation of THz radiation. Additionally, two samples with $x = 1$ and 0 were grown for reference. The concentration of In registered by SIMS corroborates the formation of linear metamorphic layers in complete agreement with the HRXRD rocking curves. In reference samples only the InAs and GaAs bandgap transitions are observed by photoluminescence (PL) spectroscopy. On the contrary, the metamorphic layers spectra show several broad transitions, which are indicative of the growth of InGaAs alloys with different In concentration. The electron mobility and carrier concentration of these samples are comparable to those used for THz radiation emitters. While still preliminary, our measurements show a significant increase in the emission of the x from 1 to 0 (ie. GaAs on the surface) structure with respect to the GaAs layer. This increase is attributed to the band bending caused by the bandgap variation along the growth direction.

[1] A.G Davies, E.H Linfield and M.B Johnston, Phys. Med. Biol. 47, 3679 (2002).

[2] M. Alfaro-Gomez and E. Castro-Camus. App. Phys. Lett. 110, 042101 (2017).

ACKNOWLEDGMENTS: The authors acknowledge the financial support from CEMIE-SOL 22, FRC-UASLP and CONACYT-Mexico through grants: CB 2015- 257358 and PNCPN2014-01-248071.



[SEM-643] Development of nanometric photocatalysts of BiOI and BiVO₄ on a graphene oxide support for an application in water splitting

Guillermo Alam Moctezuma Salazar (toroalam@gmail.com) ², Paola Gisel Jimenez Ortiz
³, Mildred Quintana (quintanamildred@gmail.com) ³, Mildred Quintana ¹

¹ Centro de Investigación en Ciencias de la Salud y Biomedicina (CICSaB), Universidad Autónoma de San Luis Potosí (UASLP), Av. Sierra Leona 550, Lomas de San Luis, 78210 San Luis Potosí, SLP.

² Coordinación para la Innovación y Aplicación de la Ciencia y la Tecnología (CIACYT), Universidad Autónoma de San Luis Potosí, San Luis Potosí C. P. 78210, San Luis Potosí.

³ Facultad de Ciencias, Universidad Autónoma de San Luis Potosí (UASLP), Av. Parque Chapultepec 1570, 78210 San Luis Potosí, SLP.

In recent years photocatalysis has acquired great interest in research, mainly in the area of carbon-based materials as a support for semiconductor photoelectrodes. It is intended to take advantage of these improvements in photoelectrodes for water splitting application. In this work, semiconductors of BiOI and BiVO₄ were used as photoelectrodes since they have high chemical stability, good photocatalytic activity, and low production cost; and they were put on a graphene oxide support. Characterizations of Raman spectroscopy, TEM images and solar simulator measurements were made.



[SEM-651] Use of individualized solutions on SILAR deposited Cu₂ZnSnS₄ thin films

*Laura Isabel Hernandez-Ramirez*³, *Gilberto Jafet Zetina-Banderas*⁴, *José Santos-Cruz*²,
*Armando Pérez-Centeno*¹, *José Guadalupe Quiñones-Galván*¹, *Gilberto Gómez-Rosas*¹,
*Miguel Ángel Santana-Aranda (msantana.aranda@academicos.udg.mx)*¹

¹ Departamento de Física, CUCEI, Universidad de Guadalajara

² Facultad de Química, Universidad Autónoma de Querétaro

³ Licenciatura en Ciencia de Materiales, CUCEI, Universidad de Guadalajara

⁴ Posgrado en Ciencia de Materiales, CUCEI, Universidad de Guadalajara

Most of the materials used today for thin film photovoltaic technology are expensive, toxic and rare on the earth's crust; as the Indium, Gallium and Tellurium. The quaternary Cu₂ZnSnS₄ (CZTS) is composed of earth abundant elements, which are low cost and friendly to the environment. On the other hand, the technique of successive ionic layer adsorption and reaction (SILAR) is a process of low cost and energy consumption; it operates by sequential and cyclic immersion of the substrate in cationic and anionic solutions, rinsing mediated, for a controlled reaction. In this work, thickness optimization is explored, with fixed number of cycles, looking for variations that keep good film density and crystalline quality; starting from experimental conditions, which has previously shown deposition of CZTS with low content of secondary phases.



[SEM-662] Physicochemical conditions for ZnO films deposited by microwave chemical bath deposition

Bertha Luisa Rivera Flores (dubhe_1@yahoo.com.mx)¹, Reina Galeazzi Isasmendi¹,
Isidro Juvencio González Panzo¹, Tomás Díaz Becerril¹, Crisóforo Morales Ruiz¹

¹ Benemérita Universidad Autónoma de Puebla. CIDS-ICUAP. Av. San Claudio y 14 Sur s/n
C.U. Puebla, Pue., 72570, México.

Physicochemical analysis was carried out to obtain the species distribution diagrams (SDDs) for the deposition of ZnO films as a function of OH⁻ ion concentration ([OH⁻]) in the reaction solution. The study of SDDs predicts nucleations and ZnO films growth by means of the dominant species at a given pH value. To confirm this, a series of experiments were made varying the [OH⁻] in the reaction solution and keeping the others parameters constant. Structured zinc oxide (ZnO) films were obtained on glass substrates by microwave chemical bath deposition (MWCBD). Structural, optical and morphological ZnO film properties were investigated as a function of [OH⁻]. X-Ray diffraction technique (XRD) measurements show multiple diffraction peaks, indicating the polycrystalline nature of ZnO films. Scanning Electron Microscopy (SEM) images of ZnO showed morphological changes with the variation of [OH⁻]. The stoichiometry of the structures changed as the [OH⁻] was varied in solution. From Raman spectra, it was observed that the [OH⁻] of the reaction mixture strongly affects the crystal quality of ZnO structures. A reaction pathway for the synthesis of structures based on our results is proposed. Experimental results are consistent with the physical-chemical analysis.



XII -ICSMV

September 23rd to 27th, 2019 / San Luis Potosí, México

[SEM-669] PHOTODEGRADATION OF METHYLENE BLUE AND ORANGE G BASED ON THIN FILMS OF METAL OXIDE SEMICONDUCTOR

*Maria del Rosario Maria del Rosario Herrera Rivera (sharol4@gmail.com)¹, Heber Vilchis
Bravo¹, Jacob Morales Bautista², María de la Luz Amador Olvera²*

¹ *IIIER-UNICACH Libramiento Norte Poniente 1150, Col. Lajas Maciel, Tuxtla Gtz, Chiapas
Mex*

² *SEES-Cinvestav Ave. INP 2508 Col San Pedro Zacatenco, CdMx*

Semiconductor oxides as thin films playing an important role in applications such as microelectronics, and the opto-electronic devices, due to their electronic and optical properties. In recent years, the oxides more studied are zinc oxide (ZnO), titanium oxide (TiO_2), tin oxide (SnO_2), gallium oxide (Ga_2O_3), among others due to their short wavelength, chemical stability and low cost fabrications. In this paper a study of the photocatalytic activity of three thin films type is presented: Zinc Oxide (ZnO), titanium oxide (TiO_2), and gallium oxide (Ga_2O_3). The films were obtained by spray pyrolysis technique. The structural, morphological and optical properties of the samples synthesized were obtained by X-Ray Diffraction (XRD), Atomic Force Microscope (AFM), Scanning Electron Microscopy (SEM) and UV-vis spectroscopy, respectively. The photocatalytic activity was measured with the photobleaching of an aqueous solutions of methylene blue (MB) and orange G (OG) after irradiation with UV lamp.



[SEM-670] Ferromagnetism in Vanadium doped CdTe nanostructured thin films

Marcelino Becerril (becerril@fis.cinvestav.mx)¹, Agustín Conde-Gallardo¹, Miguel Meléndez-Lira¹, Salvador Gallardo-Hernández¹, Sergio Tomás¹, Orlando Zelaya-ängel (ozelaya@fis.cinvestav.mx)¹

¹ Department of Physics, CINVESTAV-IPN, Av. IPN 2508 Col. San Pedro Zacatenco, Apdo. Postal 14-740, CP 07000, México City

The Vanadium (V) ferromagnetic transition element was cosputtered with the II-VI semiconductor Cadmium Telluride (CdTe) by employing an Ar plasma, onto glass substrates at room temperature. The aim was to prepare a based CdTe diluted magnetic semiconductor using V as magnetic impurity. Son after the samples were submitted to thermal annealing at 300 °C for 1 hour in N₂ atmosphere. Morphological analysis shows that the nanocrystalline films are constituted of flat agglomerates of 2-4 μm-size containing 12 ± 2 nm of average diameter nanoparticles (NP's). X ray diffraction patterns reveal that films crystallize in both cubic zinc blende (ZB) and hexagonal wurtzite (WZ) phases, with ZB as the predominant structure. Atomic electron dispersion energy studies do not reveal the presence of V, which is signal of a doping level presence of V. Raman and X ray photoelectron spectroscopies analyses confirm that the film material is mainly constituted by CdTe. From UV-Vis optical absorbance data an 1.5 eV direct band gap energy was calculated by means of the Tauc's method. Hall effect measurements indicate negative carrier concentration (n) of 5.5x10¹⁸ cm⁻³. Magnetic properties of the CdTe:V at 3 temperatures in the 10-300 K range were carried out. For 10K the sample shows a ferromagnetic phase, whereas for 100 and 300 K the material presents a paramagnetic phase.



[SEM-679] Cubic InGaN nanostructures grown by PAMBE

Orlando Hernández Vázquez (orlandohv81@hotmail.com) ¹, Edgar López Luna ¹, M. Ángel Vidal Borbolla ¹, V. Damián Compean García ¹, Sergio A. García Hernández ¹

¹ Universidad Autónoma de San Luis Potosí (UASLP), Alvaro Obregón 64, San Luis Potosí, SLP 78000, México.

The critical thickness for the relaxation of cubic $\text{In}_x\text{Ga}_{1-x}\text{N}$ layers grown on cubic (002) GaN/MgO, for an indium content of 18, 44 and 70% have been determined experimentally. The layers were grown by plasma-assisted molecular beam epitaxy (PAMBE). In all samples studied, the critical thickness of the pseudomorphic layer was measured with a frame by frame analysis of RHEED patterns. After the critical thickness, RHEED patterns could identify the growth mode transition during layer growth, from layer by layer or 2D to three-dimensional 3D growth mode by changing from a streaky to a spotty pattern. The experimental critical thickness h_c value of c- $\text{In}_x\text{Ga}_{1-x}\text{N}$ on c-GaN is compared to values calculated from the Fisher model. Self-assembling epitaxial nanostructures of c- $\text{In}_{0.44}\text{Ga}_{0.56}\text{N}$ nanostructures were successfully grown in the Stranski-Krastanov growth mode with a critical thickness of 1.2 ± 0.2 nm. The c- $\text{In}_{0.44}\text{Ga}_{0.56}\text{N}$ nanostructures showed a variation in morphology and density depending on the deposition time. Self-assembled nanodots and nanobars depending on deposition time were confirmed by atomic force microscopy (AFM). The optical properties of $\text{In}_{0.44}\text{Ga}_{0.56}\text{N}$ nanobars show photoluminescent transitions centered at 1.72 eV, this is 0.07 eV higher than in bulk cubic $\text{In}_x\text{Ga}_{1-x}\text{N}$ with $x = 0.45$ (1.79 eV). This energy blue shift may be attributed to the lateral confinement in the β -InGaN nanobars.

The XPS results determine the presence of nitrogen, indium, and gallium over the samples obtained. Also, the intensity dependence with the take-off angle shows a weak indium segregation in InGaN nanostructures.



XII -ICSMV
September 23rd to 27th, 2019 / San Luis Potosí, México

SURFACES AND INTERFACES (SIF)

Chairmen: Leonardo Morales de la Garza (CNyN-UNAM)
Mario Farás Sánchez (CNYN-UNAM)



XII -ICSMV
September 23rd to 27th, 2019 / San Luis Potosí, México

SURFACES AND INTERFACES (SIF) ORAL SESSION



[SIF-2] Crystalline Tantalum Pentoxide Films for Electrochromic Devices: Study of Chemical and Physical Properties

Israel Perez (israel.perez@uacj.mx)³, Victor Sosa¹, Fidel Gamboa¹, Jose Elizalde², Diana Carrillo², Rurik Farias², Ruben Abenuz², Jose Enriquez², Pierre Mani², Manuel Ramos²

¹ *Applied Physics Department, CINVESTAV Unidad Mérida, Km 6 Ant. Carretera a Progreso A.P. 73, C.P, 97310, Mérida, Yucatán, Mexico*

² *Department of Physics and Mathematics, Institute of Engineering and Technology, Universidad Autónoma de Ciudad Juárez, Av. Del Charro 450 Col. Romero Partido, C. P. 32310, Juárez Chih. México*

³ *National Council of Science and Technology (CONACYT)-Department of Physics and Mathematics, Institute of Engineering and Technology, Universidad Autónoma de Ciudad Juárez, Av. Del Charro 450 Col. Romero Partido, C. P. 32310, Juárez Chih. México*

The search for materials to improve the efficiency in electrochromic devices (ECD) is of great importance in materials science. These devices are composed of a pile of layers of transition metal oxides combined with an electrolyte layer. Their electrochromic properties largely depend on the materials used and how the different layers interact among each other. However, a deep understanding of the electrochromic effects would be impossible if one tries to analyze the whole pile all at once. For this reason it is crucial to study the physical and chemical properties layer by layer. In this research we carry out an investigation of the physical and chemical properties of crystalline Ta₂O₅ films (one of the component layers in ECD) grown by radio frequency magnetron sputtering. The samples were found to be crystalline with orthorhombic structure and exhibit a granular morphology resembling the powder version. After growth, the samples were exposed to Ar ion bombardment for several time intervals and their chemical properties were investigated by X-ray photoelectron spectroscopy. We observe the generation of several Ta oxidation states as a function of the sputtering time. To understand the effects of sputtering in the films we performed a simulation of the irradiation process. It is found that the sputtering yield of O is much greater than that one of Ta. This results in the generation of vacancies and Frenkel defects that destabilize the crystalline structure leading to the formation of tantalum suboxides. We determined that the high oxygen yield has two contributions related to oxygen: the low surface binding energy and the low atomic number. We observed that the suboxides are unstable and the original phase is restored after exposing the films to an oxygen environment.



[SIF-32] Ultra-thin films epitaxial growth of Mn₅Ge₃ on GaAs(111) substrates: dependence on initial growth conditions.

Gutierrez Ojeda Ssandra Julieta (julietago.14@gmail.com)³, Oliveira Ronei. C.¹, Ponce-Pérez Rodrigo², Guerrero Sanchez Jonathan⁴, Mosca Dante¹, H. Cocoletzi Gregorio³, Varalda Jose (varalda@fisica.ufpr.br)¹

¹ Laboratório de Superfícies e Interfaces, Universidade Federal do Paraná , C. P. 19044, CEP 81531-990 Curitiba, Paraná , Brazil

² Universidad Autónoma de Coahuila, Facultad de Ciencias Químicas, Ing. J. Cárdenas Valdez, Republica, 25280 Saltillo, Coahuila, México

³ Universidad Autónoma de Puebla, Instituto de Física, Apartado Postal J-48, Puebla 72570, México

⁴ Universidad Nacional Autónoma de México, Centro de Nanociencias y Tecnología, Ensenada, Baja California, México

Spintronic devices make use of electrical conductance along the ferromagnetic metallic element for applications. For the device fabrication recent studies have been focused on the deposition on Ge substrates [1, 2]. These structures have demonstrated good matching and may allow integration into the Si technology. On the other hand, a few studies are focused on GaAs technology integration in spite of the fact that GaAs substrates diminish parallel conductance effects when compared with Ge at room temperatures [3]. This fact has motivated us to investigate the deposit on surface. The study consisted in applying molecular beam epitaxy (MBE) to grow ultra-thin films under different initial conditions. Substrate temperature was set at

200° during Mn and Ge deposition. All growth films were annealed at 300°C to characterize them by *In situ* reflection high-energy electron diffraction (RHEED), X-ray photoelectron spectroscopy (XPS) and *ex situ* X-ray diffraction (XRD). RHEED pattern showed disorder on the sample under higher concentration of Mn however crystalline order is conserved as Mn coverage decreases. The epitaxial relationship between the deposited alloy film and the substrate is $\sqrt{3} \times \sqrt{3}$ with and $\sqrt{3} \times \sqrt{3}$. XRD pattern shows the (111) and (222) characteristics planes. Concentration and components for the Mn 2p, Ge 3d, Ga2p and As3d were determinate by XPS.



[SIF-271] Use of amino acids as an ecological alternative as corrosion inhibitor for mild steel in CO₂ saturated brine

Juan Pablo León González (*jpleonglez@gmail.com*) ¹, Edgar Onofre Bustamante (*eonofre@ipn.mx*) ¹, Francisco Javier Rodríguez Gómez ², Greta de Monserrat Tavarez Martínez ¹, Adriana Montiel García ¹, Sandra Edith Benito Santiago ¹

¹ Instituto Politécnico Nacional. CICATA-Altamira. Km14.5 Carretera Tampico-Puerto Industrial Altamira, Altamira, México.

² Universidad Nacional Autónoma de México. Facultad de Química. Departamento de Metalurgia. Circuito de los Institutos S/N Ciudad Universitaria, Ciudad de México.

The extraction in an oil well can be separated in two steps, the first one when the well is full and its pressure is enough to extract the petroleum, and the second is when the pressure falls and it needs to be added water with CO₂ to increase the pressure in the well to keep extracting oil, during this second step, the corrosion phenomenon is a problem associated to the low pH due to the presence of H₂CO₃ and, to counteract this, the use of corrosion inhibitors is needed, for this reason, together with the environmental problematic that have afflicted humanity, in this work it is proposed the use of amino acids as an ecological and biodegradable alternative as corrosion inhibitors to prevent the degradation of pipelines during oil extraction and transportation. Phenylalanine, Leucine and Valine are the amino acids used in the investigation, with concentrations of 0, 10, 100 and 250 ppm in a brine solution NACE saturated with CO₂ in continuous immersion during 24 h, the mild steel is an AISI 1018 alloy. The molecules presented high efficiencies above 90%, associated with the adsorption over the surface, covering the metal and preventing the contact between the substrate and the electrolyte, besides enhancing the charge transfer resistance and thus the polarization resistance, leading to lower corrosion rates.



XII -ICSMV

September 23rd to 27th, 2019 / San Luis Potosí, México

[SIF-288] Two-dimensional electron gas with spin-orbit coupling in metal/oxide interfaces

Jose Manuel Flores-Camacho (jmflores@actus.iico.uaslp.mx)³, Jorge Puebla¹, Florent Auvray¹, Florent Auvray², Yoshichika Otani¹, Yoshichika Otani², Raul Balderas-Navarro³

¹ Center for Emergent Matter Science, RIKEN, Wako, Saitama 351-0198, Japan

² Institute for Solid State Physics, University of Tokio, Kashiwa, Chiba 277-8581, Japan

³ Instituto de Investigación en Comunicación Óptica, Universidad Autónoma de San Luis Potosí

Here we report an optical study, based on infrared spectroscopic ellipsometry, of nonmagnetic metal and amorphous semiconducting oxide (Cu/Bi₂O₃) with sharp interfaces where the formation of a high mobility two-dimensional electron gas (2DEG) with spin-orbit coupling (SOC) is detected. In addition, Fano resonances which are attributed to the coupling of 2DEG quantum confined states with continuum of interface bulk-like states are also observed. In particular, the line shape of the interfacial 2DEG dielectric function resolved in free-electron (Drude) and Lorentz components resulted very similar to theoretical predictions of a 2DEG confined in the normal direction of perovskite interfaces. Although the original constituent materials do not possess spin-orbit coupling, the resulting interfacial hybridization of such states induce material-specific asymmetric wave functions. This work demonstrates the detection of 2DEG in amorphous crystals allowing to study its challenging interfacial phenomena such as SOC and interface-bulk coupling, overcoming an experimental impediment which has hold for decades important advancements for the understanding of 2DEGs in amorphous materials.



[SIF-601] Modification of MLM for a quantitative ARXPS analysis of ultra-thin iron oxide films

Jesús Fernando Fabian-Jocobi (jesus.fabian@cinvestav.mx)¹, Orlando Cortazar-Martínez¹, Abraham Cardona-Cardona¹, Joaquín Raboño-Borbolla¹, Alberto Herrera-Gomez¹
(aherrerag@cinvestav.mx)¹

¹ Materiales, Cinvestav - Querétaro, Libramiento Norponiente #2000 Fraccionamiento Real de Juriquilla CP 76230, Querétaro, Querétaro, México.

The increasing scope of transition metals and their oxides in nanostructure-related applications in turn increases the relevance of their characterization through X-ray photoelectron spectroscopy (XPS). The latter provides information about the chemical structure and film thickness. In this work, we propose a modification for the multilayer model (MLM) used for the characterization by angle resolved (ARXPS) of different iron oxidations to quantitative study the oxidation state and the oxidation mechanisms of metallic iron films.

Metallic iron films were deposited in an ultra-high vacuum system through sublimation using a background pressure of 1.5×10^{-7} Torr and a sublimation pressure of 1.1×10^{-6} Torr. The growing rate was measured with a MASTEK TM-350 (0.1 Å/s) and the total thickness was 1 nm. Oxidation of the metallic film were done under an oxygen-controlled. The film was characterized with an XPS instrument with a monochromatic X-ray aluminum source (XR5, from ThermoFisher) and a 7-channeltron hemispherical spectrometer (Alpha110, from ThermoFisher).

Metallic iron films have shown a complex multiplet structure and a strong contribution to the background. Special care was given to the modeling of the background of the metallic iron and its oxide. We use the block approach as well as the MLM for a precise composition of the thin oxide layer [1, 2]. Nevertheless, it is not possible to make calculations with MLM because iron oxide is not growing as a layer, instead, it grows in the form of clusters. The proposed modification to the MLM calculation was done by considering a non-homogeneous layer of metallic iron and iron oxide. Calculations obtained with the new model gives a thickness of 4 Å for the oxide and a composition of Fe₂O₃ which shows concordance with the growth kinetics of a metal oxide.

[1] A. Herrera-Gomez, F.-S. Aguirre-Tostado, P. Pianetta, Formation of Si1+ in the early stages of the oxidation of the Si[001] 2 × 1 surface, Vacuum Sci. Tecnol. A Vacuum, Surfaces, Film. 34 (2016) 020601. doi:10.1116/1.4936336.

[2] A. Herrera-Gomez, Internal Report. CINVESTAV-Unidad Querétaro. "Self-consistent ARXPS analysis for multilayer conformal films with abrupt interfaces," 2008.



[SIF-634] In situ monitoring of AlGaAs/GaAs (631) nanoterraces for the control on the self-assembling of 1D systems.

Felipe Eduardo Perea Parrales³, Christian Alejandro Mercado Ornelas³, Leticia Ithsmel Espinosa Vega³, Irving Eduardo Cortes Mestizo², Donato Valdez⁴, Andrei Gorvachev¹, Victor Hugo Mendez Garcia (vyktormen@hotmail.com)³

¹ *2: Instituto de Investigación en Comunicación Óptica, Universidad Autónoma de San Luis Potosí, Av. Karakorum 1470, Lomas 4^a Sección 78210, México*

² *CONACYT-Center for the Innovation and Application of Science and Technology, Universidad Autónoma de San Luis Potosí, Av. Sierra Leona #550, Col. Lomas 2a Secc. 78210, México.*

³ *Center for the Innovation and Application of Science and Technology, Universidad Autónoma de San Luis Potosí, Av. Sierra Leona #550, Col. Lomas 2a Secc. 78210, México.*

⁴ *Instituto Politécnico Nacional, Unidad Profesional Adolfo López Mateos, Av. Luis Enrique Erro s/n, Edif. Z-4 3er Piso, Ciudad de México 07738, México.*

Within the framework of wave function engineering one dimensional (1D) structures have particular relevance due to the unique set of phenomena arising from them [1]. Self-assembly growth processes of MBE have been used throughout the last decades to obtain quantum dots (QDs) and quantum wires (QWs) nanostructures, even though the latter are harder to accomplish owing to the complexity of their nucleation and self-organization requirement conditions. In the last few years we have been working in the synthesis of nanostructures and quantum wire superlattices grown over the anisotropic high index (631) plane. The intrinsic anisotropic and kinetic properties of this template are ideal to achieve nanocorrugation and 1D QWs, whose geometry essentially depends on the growth temperature and III/V BEP ratio [2]. To be able to determine a precise geometry onto the QWs in the AlGaAs/GaAs heterostructure system is fundamental for the design of functional optoelectronic devices. Nevertheless, up to date the evaluation of the 1D character of these systems has been mainly performed after growth, having no mechanisms to assess the 1D order and characteristics during the self-assembling process itself. In this work, we report an unprecedented in-situ analysis of the nanoterraces self-assembling through the reflection high-energy electron diffraction technique (RHEED). Superlattice AlGaAs/GaAs heterostructures were prepared and the growth front was monitored process along the [8 -19 9] direction in order to analyze the cross-sectional dimensions of the terraces and their evolution as a function of the layer thickness and growth rates of well and barrier materials. Layer thickness dependence portrays the diffusion length of adatoms along the terrace edges and the kink formation distinctive of this surface. It has been found that ternary and binary material growth processes have inverse effects over the terrace geometry. Ternary material elongates the terraces width whilst shrinks the relative height amongst terraces at 1:13 with respect the layer thickness, the opposite is true for the binary at 1:8. Nevertheless, this process is anything but continuous; a step bunching process is noticeable from the discontinuities and hops in the streak dimension during the growth process. The step bunching has been identified as a B2-type according to Staneva et al. classification [3]. The subtle contribution of the kink-rich surface to the streak's intensity of a step-like RHEED pattern, quantified by equation (1), granted copious information about the constitution of the terrace's edges. For instance, the intensity $I(s)$ is found to hardly oscillate along [-1 1 3] due to the existence of wavy borders, contrary to the particular characteristics of low index vicinal surfaces that holds flat all along the step edges.

REFERENCES



1S. Tomonaga, Prog. Theor. Phys. 5,544 (1950).

2E. Cruz-Hernandez, S. Shimomura and V.H. Mendez-Garcia, App. Phys. Letters 101, 073112 (2012)

3D. Staneva, B, CR de l'Academie Bulgare des Sciences, in press

ACKNOWLEDGMENTS: The authors acknowledge the financial support from CEMIE-SOL 22, FRC-UASLP and CONACYT-Mexico through grants: CB 2015- 257358 and PNCPN2014-01-248071.



XII -ICSMV
September 23rd to 27th, 2019 / San Luis Potosí, México

SURFACES AND INTERFACES (SIF)

POSTER SESSIONS



[SIF-52] Texturization of soda-lime glass and amorphous SiO₂ irradiated with Si ions

Cristian Felipe Cruz Garcia (*rebeca@fisica.unam.mx*)², Rebeca Trejo Luna (*rebeca@fisica.unam.mx*)², Miguel Angel Garcia Cruz¹, Jorge Rickards², Jacqueline Cañetas-Ortega², Luis Ricardo De la Vega³

¹ Instituto de Ciencia de Materiales de Madrid, Consejo Superior de Investigaciones Científicas (CSIC), Cantoblanco 28049, Madrid, Spain

² Instituto de Física, Universidad Nacional Autónoma de México Apartado Postal 20-364, Cd. de México, Mexico

³ Universidad Autónoma de la Ciudad de México Avenida la Corona 320, Ap. Postal 07160 Cd. de México, Mexico

The modification of soda lime glass microscope slides and high-purity amorphous silicon dioxide (SiO₂) surfaces by 1 MeV Si ion bombardment at 70° was studied. Values for the ion implantation fluence varied between 1.3'10¹⁷ ions cm⁻² and 4.0'10¹⁷ ions cm⁻², while beam currents were set between 0.5 μA and 1.3 μA. The obtained surface topographies were studied using scanning electron microscopy (SEM) and atomic force microscopy (AFM). Two different studies were carried out: the first compares the effects of the ion implantation in both materials, for a high current , while the second, compares these effects for low and high current, only for soda-lime glass. The formation of surface structures on these two materials depends on the ion current, suggesting a temperature effect. Within the ion beam current values utilized: a) texturization appears in SiO₂ before soda lime, b) formation of surface waves and their associated height increase with ion fluence, c) in both materials, near a fluence of 2'10¹⁷ ions cm⁻² surface wave structures transform into cells with flake-like borders, and d) at even higher fluences surface wave structures are again recovered. The authors acknowledge the technical assistance of Francisco Jaimes, Mauricio Escobar and Juan Gabriel Morales. This work was financially supported by DGAPA-UNAM under PAPIIT IN 111717. M. A. Garcia acknowledges the support of CONACyT for the Postdoctoral Fellowship stay at Instituto de Ciencia de Materiales de Madrid (CSIC).



[SIF-139] Quantitative ARXPS study of the metallic titanium in a Ti/Al structure

Orlando Cortazar Martinez (orlando.cortazar@cinvestav.mx) ¹, Abraham Carmona Carmona ¹, Yuri Chipatecua Godoy ¹, Joaquín Raboño Borbolla ¹, Alberto Herrera-Gomez ¹

¹ Cinvestav-Unidad Queretaro, Querétaro, Querétaro, México

Titanium is a transition metal with a strong chemical affinity for oxygen which allows a fast formation of TiO_2 films on its surface. Properties of Ti and TiO_2 allow them to be used for many applications in the aerospace, military, chemical and medical field. Because of its affinity for oxygen, an angle-resolved X-ray photoelectron spectroscopy (ARXPS) analysis cannot be done if the deposition system is not directly attached to an XPS equipment. If is not the case XPS analysis require ion etching in order to remove oxidation or contamination from the surface layer. However, etching could change the very near-surface composition.

In this work we present the XPS analysis of titanium films with an ultra-thin film of aluminum (< 5 nm) on the top. Aluminum also has a high chemical affinity for oxygen, for that, this film can be used as barrier against oxygen protecting the titanium film from oxidation. In this way, high-resolution XPS spectrum of pure metallic core levels of the Ti 2p can be acquired because aluminum XPS peaks does not interfere with the main peaks of Ti 2p or either their satellites.

We prepared titanium and aluminum metal films using an ultra-high vacuum (UHV) sputtering system and a DC magnetron sputtering mode applied in the titanium and aluminum targets (99.995% and 99.9995% pure Kurt J. Lesker). The background pressure in the processing chamber was 1.3×10^{-7} Torr and the pressure during the sputtering process was 3×10^{-3} Torr. The film was characterized with an XPS instrument with a monochromatic X-ray aluminum source (XR5, from ThermoFisher) and a 7-channeltron hemispherical spectrometer (Alpha110, from ThermoFisher) assembled by Intercovamex.

The quantification of the composition of the as deposited Ti/Al structure exposed to atmospheric conditions was done employing XPS data. We employed the multilayer method (MLM) [2] to analyze the angular dependency and obtain the chemical depth distribution as well as the thickness of the Al layer. XPS analysis shows the Ti 2p_{3/2} peak at 454.12 eV, Ti 2p_{1/2} at 460.39 eV and two satellites at 469.96 and 473.7 eV. The Al 2p shows a peak at 72.58 eV corresponding to the metallic aluminum and a peak at 75.34 eV corresponding to the Al_2O_3 . Finally, the O 1s has a peak at 532.67 eV and C 1s at 285.6 eV. Results show that a thin layer of oxide is formed at the surface of the structure forming an aluminum oxide layer. Also, it shows that the titanium layer has no interaction with the oxygen which can be analyzed as a clean metallic film.

[1] Grzegorz Greczynski, Ivan Petrov, J. E. Greene, and Lars Hultman “Al capping layers for nondestructive x-ray photoelectron spectroscopy analyses of transition-metal nitride thin films”, Journal of Vacuum Science & Technology A: Vacuum, Surfaces, and Films 33, 05E101 (2015).

[2] A. Herrera-Gomez, Internal Report. CINVESTAV-Unidad Querétaro. “Self-consistent ARXPS analysis for multilayer conformal films with abrupt interfaces,” 2008.



[SIF-150] Determination of the anticorrosive properties of the synergic effect of valine and isoleucine as ecological corrosion inhibitors on steel AISI 1018 in sweet médium.

*David Luevano Valdez (da.luevano@outlook.com)*¹

¹ CICATA-IPN, Carretera Tampico-Puerto Industrial Altamira Km 14.5, Industrial Altamira, 89600 Altamira, Tamaulipas, México

Abstract

The problem of corrosion refers to all hydrocarbon industries as it deteriorates due to the effects of this phenomenon, the risk of oil pipeline accidents, human losses, industrial breakdowns due to breakage, environmental pollution, among others. At present, it is not only necessary to investigate the development of new ecological materials, but also to continue to deepen the fundamentals of corrosion processes in order to avoid them, it is proposed to study the corrosion inhibiting properties of valine and isoleucine as biodegradable ecological alternative. To do this, tests will be carried out in a static system, using the AISI 1018 steel as a support, carry out a continuous immersion of 0, 6, 12 and 24 hours, in concentrations of 10, 100, 250 ppm of the amino acids in a médium "sweet", medium consisting of a solution NACE + CO₂ (g). Likewise, an electrochemical characterization will be done by the techniques (OCP, LRP, EIS) to determine its corrosion rate, resistance in the system and its protection mechanisms.



[SIF-188] Evaluation of ErGO coatings on CoCrMo alloy by conventional and localized electrochemical techniques

Greta de Monserrat Tavarez Martínez², Edgar Onofre Bustamante (eonofre@ipn.mx) It is estimated that 75% of failures in the articular prosthesis is due to bone resorption, caused by osteolysis due to the presence of wear particles that occur in the daily wear process of the components of the implanted joint. Particles,) ², María Cristina García Alonso ¹, María Lorenza Escudero Rincón ¹, Juan Pablo León González ², Adriana Montiel García ², Sandra Edith Benito Santiago ²

¹ Centro Nacional de Investigaciones Metalúrgicas, Consejo Superior de Investigaciones Científicas

² Instituto Politécnico Nacional, CICATA- UA

It is estimated that 75% of failures in the articular prosthesis is due to bone resorption, caused by osteolysis due to the presence of wear particles that occur in the daily wear process of the components of the implanted joint. Particles, traces and/or ions are accumulated in the surrounding tissues, interacting with cells and even incorporating into the bloodstream.

Recent research to surfaces of removed prostheses submitted to a tribocorrosión, have revealed the presence of sp3-sp2 hybridization carbon structures from of fluid synovial denaturation that seem to be involved in the reduction of tribological damage in the articular metal implants. Based on this, films composed of Electrochemically Reduced Graphene Oxide (ErGO) and ErGO functionalized, will be deposited on the substrates CoCrMo. The optimum conditions of synthesis, composition, morphology, roughness and, electrochemical, tribological performance and biocompatibility in vitro.

ErGO films were deposited by cyclic voltammetry and CoCrMo substrates, which was detected by Raman spectroscopy, in where seems are deposited in agglomerates form. Said films provide corrosion protection to CoCrMo substrate, films deposited from -2.1 V to -0.5V by 10 cycles to 60 mV/min has better benefits.



[SIF-260] Quantitative ARXPS chemical state assessment of the early stages of oxidation of iron oxide

Orlando Cortazar Martinez (orlando.cortazar@cinvestav.mx)¹, Jesús Fernando Fabian-Jacobi¹, Abraham Carmona Carmona¹, Joaquín Raboño-Borbolla¹, Alberto Herrera-Gomez¹

¹ *Cinvestav-Unidad Queretaro, Querétaro, Querétaro, México*

Iron has proven to be the most used metal because its properties allow it to be used for multiple applications within many industries. In this work we present the quantitative analysis for chemical assessment as well as the calculation of the iron oxide thin film.

We prepared thin iron metal films through sublimation employing a tungsten filament with metallic iron (99.995% pure Sigma Aldrich). The background pressure in the processing chamber was 1.4×10^{-7} Torr and the pressure during sublimation was 2.1×10^{-6} Torr. The growing rate (measured with a MASTEK TM-350) was 0.2 Å/s and the total thickness was 30 nm. The film was characterized with an X-ray photoelectron spectroscopy (XPS) instrument with a monochromatic X-ray aluminum source (XR5, from ThermoFisher) and a 7-channeltron hemispherical spectrometer (Alpha110, from ThermoFisher) assembled by Intercovamex.

Films of metallic iron were oxidized under an oxygen-controlled environment at 1 kL, 10 kL, 100 kL, 1 ML, 10 ML and 100 ML. The quantification of the composition of clean metallic iron exposed to oxygen was done employing XPS data. For an appropriate fitting we employ the block method [1] to analyze the oxidized Fe 2p spectra considering the differences on background properties between pure metallic and oxidized iron. We employed the multilayer method [2] to analyze the composition to obtain the chemical composition and thickness of the oxide layer.

[1] A. Herrera-Gomez, F. S Aguirre Salgado, Y. Sun, P. Pianetta, Z. Yu, D. Marschall, R. Droopad, W. E. Spicer, "Photoemission from the Sr/Si(001) interface", Journal of Applied Physics, Vol. 90, 12, p. 6070, 2001

[2] A. Herrera-Gomez, Internal Report. CINVESTAV-Unidad Querétaro. "Self-consistent ARXPS analysis for multilayer conformal films with abrupt interfaces," 2008.



[SIF-297] On the Usefulness of the Equation of State Approach for Interfacial Tensions on Rough Surfaces

*Gregorio Sánchez Balderas (gbalderas@ifisica.uaslp.mx)¹, José Elías Pérez López
(elias@ifisica.uaslp.mx)²*

¹ *Doctorado Institucional en Ingeniería y Ciencia de Materiales, Universidad Autónoma de San Luis Potosí, Sierra Leona 530, C. P. 78210, San Luis Potosí, S.L.P., México*

² *Instituto de Física, Universidad Autónoma de San Luis Potosí, Av. Manuel Nava #6, Zona Universitaria, C. P. 78290, San Luis Potosí, S. L. P., México*

The equation-of-state (EQS) approach has been used successfully to calculate the surface tension of solids, however, its scope has been limited to ideal surfaces where the effects of the tensions involved are dominant. In this work we use the EQS approach in homogeneous rough surfaces. These surfaces are characterized topographically by atomic force microscopy (AFM) and their roughness is quantified with the area factor (A_f). We observe that the "effective" surface tension calculated on rough surfaces decreases and has a smooth tendency with the increase of the area factor. In this way we propose the validity of the EQS approach in homogeneous rough surfaces to calculate an effective surface tension that involves roughness and structure surface effects.



[SIF-335] ADSORPTION OF THE IMIDAZOLE ON COPPER SINGLE CRYSTAL

Mayra Paulina Hernández Sánchez (mayrap@imre.uh.cu)², Jesús Antonio Díaz Hernández (olaf@cnyn.unam.mx)¹, Michelle Ivonne Cedillo Rosillo¹, José Valenzuela Benavides¹, Yasmín Esqueda Barrón¹, Mario Humberto Farías Sánchez¹, Armando Paneque Quevedo²

¹ Centro de Nanociencias y Nanotecnología, UNAM

² Instituto de Ciencia y Tecnología de Materiales, Universidad de La Habana

Imidazole and imidazolate ions of considerable interest for both biology and chemistry. Their role as ligands for transition metal ions, and some of their metal complexes have been used as model compounds in the study of electronic interactions between proteins and transition metal centers in biological system. Also, they are well known to be efficient corrosion inhibitors^{1,2}. However, the atomic scale mechanism of how organic corrosion inhibitors work is usually not known. It is therefore important to characterize the molecule–surface bonding as one aspect towards the atomic-scale understanding of corrosion protection mechanisms. These studies has also been receiving considerable attention due to its importance in many other technological applications. In the current work, we investigate the bonding of imidazole on a copper (100) single crystal surface by XPS measurements and STM imaging. The copper single-crystal was prepared by cycles of suitable laser ablation treatment and annealing (570K) until no copper oxide could be detected by XPS measurements. Imidazole was deposited on copper surface by vacuum sublimation from imidazole powder (99.999%). The measured binding energies of the N1s and C1s are attributed to imidazole-metal complexes. The Raman measurements confirmed the adsorption of the molecule on Cu (100) surface. The STM images showed irregular surfaces with adsorbed species on terraces but also decorating step edges. Deprotonation and coordination with free copper atoms at step edges and surface defects readily occurs, allowing chemisorption of species.

Acknowledgments

We would like to thank the support of PREI-DGAPA for the invited professor to MPHS

1 Y. I. Kuznetsov and L. P. Kazansky, Russ. Chem. Rev., 2008, 77, 219–232.

2 M. M. Antonijevic, S. M. Milic and M. B. Petrovic, Corros. Sci., 2009, 51, 1228–1237.



[SIF-604] Sorption isotherm of chestnut flour (*Artocarpus altilis* (Parkinson) Fosberg)

Isaac Abraham Reyes-Cruz², Ignacio Concepción-Brindis², Fulgencio Eduardo Torres-Hernández¹, Laura Mercedes Lagunes-Gálvez², Pedro García-Alamilla²

¹ Departamento de Ingeniería Química, Instituto Tecnológico de Villahermosa, Carretera Villahermosa-Frontera km. 3.5, 86010, Centro, Tabasco, México.

² División Académica de Ciencias Agropecuarias, Universidad Juárez Autónoma de Tabasco., Carretera Villahermosa-Teapa km 25, 86298, Centro, Tabasco, México.

Sorption isotherms were made for chestnut powder *Artocarpus altilis* (Parkinson) Fosberg at 30, 40 and 50 °C by the gravimetric method. Chestnut dried, crushed and sieved samples to obtain a particle size greater than 70 mesh. The range of water activity was controlled by sales in a range of 0.05 to 0.96. The results of equilibrium moisture versus water activity showed a type III behavior according to Brunauer, which indicates that the interactions are adsorbent-adsorbent at higher ratios of water activity in the monolayer. A temperature effect was found, showing a cross effect of the moisture content of the equilibrium, which has been reflected to a water activity around of 0.6. The experimental data were adjusted to the equations of BET, GAB, Freundlich, Smith, Peleg, Oswin, Halsey, Page, Two terms and Caurie. The BET model was the only one that obtained a value of R^2 less than 0.70, while the best model was adjusted to the experimental data of the Caurie model with an R^2 greater than 0.89. The difference between the value of the monolayer and the result of the equations of BET and GAB is function by high adsorption capacity of chestnut flour at the monolayer level, the which is related to the high carbohydrates content and to its typical sorption properties.



[SIF-606] Thermodynamic properties of chestnut flour estimated from moisture sorption isotherm

*Ignacio Concepción-Brindis¹, Jose Luis Rivera-Armenta², Ricardo García-Alamilla²,
Laura Mercedes Lagunes-Gálvez¹, Pedro García-Alamilla¹*

¹ *División Académica de Ciencias Agropecuarias, Universidad Juárez Autónoma de Tabasco, Carret. Villahermosa-Teapa Km 25 Ra. La Huasteca. Villahermosa, Tab. C.P. 86280, México.*

² *Instituto Tecnológico de Ciudad Madero, Av. 1° de Mayo y Sor Juana I. de la Cruz, Col. Los Mangos, Cd. Madero, Tam. C.P. 89440, México.*

The equilibrium moisture content of chesnut flour (*Artocarpus altilis* (Parkinson) Fosberg) was determined using the static gravimetric method at temperatures of 30, 40 and 50 °C in the 0.05 to 0.89 water activity range. The sorption curves show a decrease in equilibrium content as the temperature increasing. The Guggenheim, Anderson, and de Boer (GAB) equation was used to determine the thermodynamic properties of water sorption. The isosteric heat and the differential entropy were determined by applying Clausius-Clapeyron and Gibbs-Helmholtz equations, respectively. The monolayer moisture content values decreased like function of temperature, while that values of energy constants increased and decreased respectively. The net integral enthalpy values for chestnut flour were lesser to other flour reported. The relation of differential enthalpy versus entropy was satisfied according to the enthalpy-entropy compensation theory.



[SIF-649] COMPARATIVE STUDY OF PHOTO CATALYTIC DEGRADATION BEHAVIOR OF SURFACES PRODUCED FROM SONOCHEMICAL AND SOL-GEL PROCEDURES RESPECTIVELY

Dwight Acosta (dacosta@fisica.unam.mx)¹, Paul Alavarado³, Arturo Maldonado²

¹ IFUNAM

² Instituto Politécnico Nacional

³ Universidad Nacional de Ingeniería, Lima, Perú

SnO_2 nanoparticles with quantum dots size dimensions were produced by ultrasonic agitation; then after filtering and drying processes, were dispersed with a specific preparation method on silica glasses previously covered with a FTO thin film. The degradation of methylene blue (MB) by the photocatalytic process of the SnO_2 nanoparticles deposited on metallic glass substrates, and by sol-gel methods, were tested by measuring the corresponding discoloration (change in MB dye concentration C/Co) of $1 \times 10^{-5}\text{M}$ (MB) dissolved in water. The measurements were done by immersing the deposited coated substrate, (with an exposed area of $25 \times 0.8 \text{ mm}^2$), facing the illumination source, into six quartz cell, each containing 3 ml of MB solution. Then, the cells were irradiated with a vertical UV lamp (G15T8 germicidal 15 W, with prevailing emission at 254 nm) inside a light-isolated chamber. The sample-to-lamp distance was kept at 4 cm. The optical absorbance of the solution was continuously monitored with an UV-Vis spectrophotometer, in intervals of 30 min, during 150 min. The residualconcentration of MB was calculated by measuring the variation in the peak height located at 664 nm, as this condition is reported as the MB maximum absorption peak. It is worthy to note that the sol-gel film was manufactured with 16 immersions in the Sn containing solution. On the other hand, nano-particles covering only required 4 immersion in the corresponding solution. After 150 min of UV-Vis exposure, remains less than 20% of the original methylene blue solution. The performance of nanoparticles of SnO_2 was similar to the sol-gel deposited film, manufactured with different film thickness. In fact, the nanoparticle covering does not waste too much material as compared with the processing of sol-gel film, with a significant saving of precursor and energy.

Acknowledgement. Financial support of Project DGAPA-UNAM IN 102419 is highly appreciated and recognized



XII -ICSMV

September 23rd to 27th, 2019 / San Luis Potosí, México

THEORY AND SIMULATION OF MATERIALS (TSM)

Chairmen: Raul Esquivel (IF-UAM)
María Teresa Romero de la Cruz (FCFM-UAdE)
Ariadna Sanchez Castillo (UAEH)



XII -ICSMV
September 23rd to 27th, 2019 / San Luis Potosí, México

**THEORY AND SIMULATION OF
MATERIALS (TSM)
ORAL SESSION**



[TSM-6] Development and characterization of nanofilms for applications in electrochromic devices

Juan Rubén Abenuz Acuña (sanmaikel23@gmail.com) ¹, Israel Omar Pérez López ², José Trinidad Elizalde Galindo ¹, José Rurik Farías Mancilla ¹, José Luis Enríquez Carrejo ¹, Manuel Antonio Ramos Murillo ¹, Pierre Giovanni Mani González ¹

¹ Department of physics and mathematics Institute of Engineering and Technology, Universidad Autónoma de Ciudad Juárez, Av. Plutarco Elías Calles #1210, Fovissste Chamizal, C.P. 32310 Ciudad Juárez, Chihuahua, México.

² National Council of Science and Technology (CONACyT)-Department of physics and mathematics Institute of Engineering and Technology, Universidad Autónoma de Ciudad Juárez, Av. Plutarco Elías Calles #1210 , Fovissste Chamizal, C.P. 32310 Ciudad Juárez,

In this research we show the partial progress about the fabrication, simulation and characterization of nanofilms based on transition metal oxides for applications in all-solid-state electrochromic devices. Electrochromic devices are composed of several layers of different materials of transition metal oxides and in this work NiO and Ta₂O₅ have been proposed for the development of these devices. Nanofilms of these materials were manufactured by RF magnetron sputtering technique. In order to acquire a better understanding in the properties of the nanofilms, simulation and characterization were performed to study their crystalline structure, morphology, as well as the chemical, electronic, and electrochromic properties. We also discuss the future work to achieve the development of an electrochromic device.

Key Words: Nanofilms, Transition metal oxide, Electrochromic devices.

References

- [1] G. Atak and Ö. D. Coşkun, "Annealing effects of NiO thin films for all-solid-state electrochromic devices," *Solid State Ionics*, vol. 305, pp. 43-51, 2017/07/01/ 2017.
- [2] H. Moulki *et al.*, "Electrochromic performances of nonstoichiometric NiO thin films," *Thin Solid Films*, vol. 553, pp. 63-66, 2014/02/28/ 2014.



XII -ICSMV
September 23rd to 27th, 2019 / San Luis Potosí, México



[TSM-70] DFT calculation for OH formation on SrTiO₃(110):Bi and its interaction with Methylene blue

Reyes Garcia-Diaz (reyes_garcia@uadec.edu.mx) ², María Teresa Romero de la Cruz ³,
Raúl Ochoa Valiente ³, Gregorio Hernández Cocoletzi ¹

¹ Benemérita Universidad Autónoma de Puebla, Instituto de Física “Ing. Luis Rivera Terrazas”, Apartado Postal J-48, Puebla 72570, México

² Catedra CONACyT-Facultad de Ciencias Físico Matemáticas, Universidad Autónoma de Coahuila, Unidad Camporredondo, Edif. A, 25000, Saltillo, Coahuila, México

³ Facultad de Ciencias Físico Matemáticas, Universidad Autónoma de Coahuila, Unidad Camporredondo, Edif. A, 25000, Saltillo, Coahuila, México

Total energy density functional theory (DFT) calculations were carried out in order to investigate the OH formation on Bismuth (Bi) decorated strontium titanate (SrTiO₃) 110 surface. After OH formation the interaction with methylene blue (MB) is studied. MB is a water contaminant and understand it interaction with reactive species can help us to develop better water treatment process. We study the OH adsorption on SrTiO₃(001):Bi using a supercell with slab geometry. Minimum energy path (MEP) for the OH formation was calculated using the nudged elastic band (NEB) method. After the OH radical is formed the interaction with the MB is studied without the substrate in order to reduce computational cost. HOMO-LUMO plots help us to find reactive sites for OH interaction. The calculations were carried out using the PWscf code of the Quantum ESPRESSO Package. Adsorption energies and activation energies were calculated for different configurations. Electronic properties were studied by calculating the density of states (DOS), projected density of states (PDOS), Löwdin charges and isosurfaces. Results show different types of interactions between the OH radical and the MB molecule.



[TSM-186] Mapping of structural energy in surface reconstructions for a GaAs binary system.

Isaac Azahel Ruiz Alvarado (azahel.ruiz@hotmail.com)², Alfonso Lastras Martínez (alastras@gamil.com)², Milton Muñoz Navia¹

¹ CONACyT-IFUASLP, Av. Dr. Manuel Nava 6, Zona Universitaria, 78290 San Luis, S.L.P. Mexico.

² IICO-UASLP, Av. Karakorum 1470 Lomas 4a. 78210 San Luis Potosí, SLP México.

Tailoring materials properties nowadays requires alloying individual properties. Due to its open scientific questions and technological implications, combining Ga and As (GaAs) is a long standing binary system of interest. Recently, the Reflectance Difference Spectroscopy (RDS), has reemerge as a powerful technique to characterize and monitor the specific *in situ* growth in surfaces. However, for the system of interest (GaAs), in the literature several possible surface reconstructions are proposed. The physics behind the optical anisotropies related to the surfaces is an open question and not yet resolved with (RDS). Understanding the physics that gives rise to the reconstruction of GaAs (2x4) surface, and its implications in the (RDS), is interesting from a scientific and technological point of view. In this work, we discussed the structural energy landscape of several possible reconstructions in GaAs (2x4) surface. In the framework of a density functional theory using projector-augmented-wave method, with an exchange correlation potential in the form of the generalized gradient approximation (GGA), the electronic structure of the different surface reconstructions (namely α , α_1 , β , β_2 and β_3) are obtained. Our results show that the energy landscape of the surface reconstructions of the GaAs system can be discuss in terms of the layer by layer mobility influence, the proclivity of the As dimerization (affected by the dimer relative orientation with respect the neighboring plane) and the dependence in the concentration (As or Ga rich structure). Within our results we observe a charge distribution in the different layers of the structures, affected by the surface reconstruction. Furthermore we discuss how the charge distribution yields a new surface dipoles and how this differ for different surface reconstructions.



XII -ICSMV

September 23rd to 27th, 2019 / San Luis Potosí, México

[TSM-277] Enantiospecific adsorption of chiral amino acids on chiral carbon nanotubes

José de Jesús Pelayo Cárdenas (josedejesus_pelayo@uaeh.edu.mx)¹, Dante Fernando Hernández Andrade¹, Ariadna Sánchez Castillo¹

¹ Escuela Superior de Apan, Universidad Autónoma del Estado de Hidalgo, Chimalpa Tlalayote, Municipio de Apan, Hidalgo 43920, México.

Carbon nanotubes are very interesting and promising structures thanks to their properties and potential applications in many fields such as material science, energetic systems and medicine, to name a few.

Chirality is very important in carbon nanotubes, in fact some of their properties, such as conductivity, change with it. Although the interaction of amino acids with single walled carbon nanotubes (SWNTs) has already been studied to some extent, the effects of the chirality of the SWNTs and the amino acids (most of them are chiral) has not.

In this work we use first principles calculations based on the density functional theory (DFT) to study the enantiospecific adsorption of several chiral amino acids on chiral SWNTs, from structural, energetic, and vibrational stand points.



XII -ICSMV

September 23rd to 27th, 2019 / San Luis Potosí, México

[TSM-623] Ab initio study of growth of MnN on GaN(001)-(2x2) surface

Gloria Elizabeth Rodríguez García (rodriguez.elizabeth81@gmail.com)¹, Rodrigo Ponce Pérez¹, María Teresa Romero de la Cruz (teresa.romero.cruz@uadec.edu.mx)¹

¹ Facultad de Ciencias Físico Matemáticas, Universidad Autónoma de Coahuila, Unidad Camporredondo, Edif. A, 25000, Saltillo, Coahuila, México

First-principles calculations have been developed to study epitaxial growth of MnN on GaN(001)-(2x2). The calculations were carried out using the Quantum ESPRESSO package that works within the framework of the Density Functional Theory (DFT). Ultrasoft pseudopotentials were used to model the electron-ion interaction. The exchange-correlation functional was treated by the generalized gradient approximation (GGA) with the parametrization of Perdew-Burke-Ernzerhof (PBE). Different high symmetry sites were considered for the adsorption and incorporation of Mn on GaN(001)-(2x2) surface. Several Mn coverage were considered, from a Mn atom per supercell to a bilayer. The fcc site is the most stable to the all calculated configurations. The formation energy was calculated for each configuration in order to study the structural stability for all the took into account Mn coverages. Two phases of MnN were considered to study the epitaxial growth. The zincblende phase is more stable than the tetragonal phase.

Keyword: MnN, GaN, epitaxial growth.



[TSM-674] STRUCTURAL, ELECTRONIC AND TRANSPORT PROPERTIES OF
SILICON NANOWIRES GROWTH IN [001], [110], AND [111]
CRYSTALLOGRAPHIC DIRECTIONS: AN AB INITIO DENSITY FUNCTIONAL
THEORY STUDY

Alejandro Herrera-Carbajal², Ariadna Sánchez-Castillo (ariadna.s.castillo@gmail.com)¹,
Juan Hernández-Ávila², Ventura Rodríguez-Lugo²

¹ Escuela Superior de Apan - Universidad Autónoma del Estado de Hidalgo, Carretera
Apan-Calpulalpan Km.8, Col.Chimalpa, 43920 APAN, Hgo.

² Instituto de Ciencias Básicas e Ingeniería, Área Académica de Ciencias de la Tierra y
Materiales, Ciudad del Conocimiento, Carretera Pachuca- Tulancingo Km. 4.5, Col.
Carboneras

In this work, structural, electronic and transport properties of six H-terminated silicon nanowires (with two wires of different diameter per direction) were studied by using ab initio density functional theory. Calculations were computed with SIESTA code which is based in Density Functional Theory, a local density approximation potential was employed to approximate the exchange–correlation (XC) energy functional. Particularly, electronic band structure, density of states, and phonon thermal conductivity are reported. The study was carried out in three parts. In the first part, ground state structure was calculated for each silicon wire (SiNWs), this calculation was done by a conjugate-gradient type calculation varying the A, B (which define the distance between the closest atoms of hydrogen of consecutive SiNWs) and C (who defines the periodicity) parameters until the structure with lowest energy was reached. In the second part, the force constants matrix and vibrational modes were calculated at Γ -point and at a path from Γ to X (high symmetry point along the wire) by applying a FC type calculation. Finally, transmittance and phonon thermal conductivity were calculated (in channels defined inside the SiNWs) applying Landauer formula, Kubo Formalism and Bose-Einstein Distribution Function. It can be concluded that the magnitude of bandgap increased while diameter decreases at any growth direction, this behavior can be attributed to the confinement effect of the nanowire, also the transition from valence to conduction band of SiNWs growth in direction [111] changed from direct transition bandgap Γ - Γ (in $d = 11.7 \text{ \AA}$) to indirect transition bandgap Γ -70%X (in $d = 7.2 \text{ \AA}$). On the other hand, it can be seen that transmittance is susceptible to the features of systems (e.g, masses and force constants), therefore, it can be stated that thermal transport can be controlled. At last, we can say that phonon thermal conductivity rises linearly at low temperatures and converges to a constant value for high temperatures due to the harmonic approximation.

Keywords: Local Density Approximation, Silicon Nanowires, Landauer Formalism.



XII -ICSMV

September 23rd to 27th, 2019 / San Luis Potosí, México

THEORY AND SIMULATION OF MATERIALS (TSM) POSTER SESSIONS



[TSM-267] Electronic and Optical Properties of ZnO:Ag

Juan Andrés Orozco Dueñas (juan.orozco@fisica.uaz.edu.mx)², Olga SánchezGarrido¹,
Javier Alejandro Berumen Torres², Juan Ortiz Saavedra², José Juan Ortega Sigala², José
de Jesús Araiza Ibarra (araiza@fisica.uaz.edu.mx)²

¹ Instituto de Ciencia de Materiales de Madrid-CSIC

² Unidad Académica de Física, Universidad Autónoma de Zacatecas

In this work, it is reported the theoretical study of ZnO systems using first principles calculation based on density function theory for a pseudopotential (PP) under the generalized gradient approximation using the Perdew-Burke-Erzenhof approximation (GGA-PBE) for Zn and O, with the presence of silver as a single impurity. Different configurations for two impurity concentrations (3.25% and 6.5% of Ag-doping) were used. Important effects on the structure were observed, the induction of stress depending on the inclusion of the Ag impurity. Likewise, the impurity induces states on the band gap near to the valence band, but it also does it in the middle of the band gap and near to the conduction band, although its amount of state is lower in these last two cases. Finally, the optical analysis shows the effect of the Ag on the imaginary dielectric permittivity, and from these data, the absorption and finally the absorptivity was used to determine, by means of Tauc law, the optical band gap energy. As it is expected, the calculated band gap is underestimated to be 0.745 eV for pure ZnO, which is attributed to the well-known intrinsic factor of DFT. Considering this underestimation, the transition states located in the band gap energy due to the Ag in ZnO, were determined.



[TSM-311] THEORETICAL STUDY OF A CATALYST AND ITS APPLICATION IN THE OXIDATION OF ENVIRONMENT POLLUTANTS

Roberto Mejia-Olvera (rmejia_cinvestav@hotmail.com)², María Edith Lemus-Hernandez², Sandy María Pacheco-Ortíz¹, Esther Agacino-Valdes¹

¹ Facultad de Estudios Superiores Cuautitlán UNAM

² Tecnológico de Estudios Superiores de Cuautitlán Izcalli

Iron oxides are among the most common oxides on earth and are found in rocks, ores, or soils in nature. These kind of oxides are also products of iron corrosion and can be easily synthesized. In the last decade, progress in the development of experimental techniques and theoretical methods has allowed to gain insight on the fundamental properties of small iron oxides clusters.

The study of the electronic and catalytic properties of FeO_2 adsorbed on a $\text{MgO}(100)$ surface which shows potential as a novel low-cost and low-temperature CO nanocatalyst in an overall exothermic reaction. The CO oxidation may be separated into two steps, namely (1) oxidation of CO by the metal oxide leaving a reduced metal oxide and (2) oxidation of the reduced metal by oxygen to regenerate the active metal oxide. It is found that CO and O_2 adsorption energies are the driving force for the CO oxidation by providing the energy required to surmount the activation energies along the reaction path. All the calculations were made with the code deMon2K.



[TSM-408] Catalytic reactivity of silicates in the biodiesel obtaining process.

Crstina Cuautli (cristy141201@hotmail.com) ¹, Issis C. Romero-Ibarra ¹

¹ Unidad Profesional de Interdisciplinaria en Ingenierías y Tecnologías Avanzadas, Instituto Politécnico Nacional. Av. Instituto Politécnico Nacional 2580, Col. Barrio la Laguna Ticoman. 07340, Gustavo A. Madero. CDMX. México.

13 643 252 ktoe (thousand tonnes of oil equivalent) was the amount of energy consumed in 2015 in the world, as a by-product 32 104 million tonnes of CO₂ -mean greenhouse gas- were produced from fossil fuel burning¹. These figures highlight the challenge nowadays: the search for sustainable energy resources. Biofuels are a promising solution.

In our research group we work in improve the efficiency of biodiesel obtaining from non-food feedstocks. One important step in the process is the transformation of triglycerides (from vegetable oils) and alcohols into the biodiesel through the transesterification reaction in the presence of a catalyst. The right choice of the catalyst is essential. In this work we analyze the activity of sodium and lithium silicates as heterogeneous catalysts from a theoretical point of view, the starting point are experimental results obtained in our group^{2,3}.

With DFT periodic calculations, we analyze the electronic structure and the energetics of the clean exposed surfaces -determined by X-ray diffraction- and the same surfaces with the molecular species involved in the transesterification reaction absorbed (methanol and triacetin) in order to clarify some aspects of the mechanisms behind this process and contribute to an intelligent design of future catalysts.

Financial Supporting from Instituto Politecnico Nacional through SIP-20196708 project is gratefully anknowlede.

C.C. thanks to "Apoyo otorgado por el fondo sectorial CONACYT-SENER de energía-hidrocarburos".

¹ International energy agency. <https://www.iea.org/>

² Martinez A.; Mijangos G. E.; Romero-Ibarra I. C.; Hernández-Altamirano R.; Mena-Cervantes V. Y. Fuel 235 (2019), 277-287.

³ Martínez, A.; Mijangos, G. E.; Romero-Ibarra, I. C.; Hernández-Altamirano, R.; Mena-Cervantes, V. Y.; Gutiérrez S. J. Clean. Prod. 196 (2018) 340-349.



[TSM-671] Modeling 1s Exciton in GaN/InGaN quantum wells using Genetic Algorithms and Particle Swarm Optimization.

Arturo Yee-Rendón ², Ana J. Yee-Rendón ³, Oscar J. Velarde-Escobar ¹, Gelacio Atondono-Rubio ¹, Cristo M. Yee-Rendon (cristo@uas.edu.mx) ¹

¹ Facultad de Ciencias Físico-Matemáticas, Universidad Autónoma de Sinaloa, Av. de las Américas y Blvd. Universitarios, Cd. Universitaria, Culiacán, Sinaloa C.P. 80010

² Facultad de Informática Culiacán, Universidad Autónoma de Sinaloa, Josefina Ortiz de Dominguez s/n, Ciudad Universitaria, Culiacán, Sinaloa C.P. 80013.

³ Unidad Académica Preparatoria Hermanos Flores Magón, Universidad Autónoma de Sinaloa, Gral. Antonio Rosales #353, Culiacán, Sinaloa Col. CC.P. 80000

In the present work a comprehensive study of Genetic Algorithms (GA) and Particle Swarm Optimization (PSO) for computing the energy of an 1s like exciton in a GaN/InGaN quantum wells on Zinc-Blende structure. The lattice mismatch of the InGaN/GaN induces a deformation potential that removes the degeneracy of the valence band. In particular the effect of the biaxial strain is computed as function of the In concentration using the Van der Waals formalism of the model-solid. The conduction and valence band potentials are computed and the Schrödinger equations are solved using numerical methods for the electron and holes in the quantum well. The exciton is normally modeled with a wavefunction that is the combination of the electron, the hole and hydrogenic like wavefunction. In the particular we considered the 1s function with two parameters one is λ which is the effective Bohr radius of the exciton and second parameter β related with the deformation of the spherical symmetry it exhibits a 3D exciton in bulk when it is forced to be in quantum well. The problem is then formulated as minimization of the energy of the exciton as function of λ and β and GA and PSO are used for finding these two parameters. The results are then compared to the reported in the case of the three dimensional and two-dimensional excitons.



XII -ICSMV

September 23rd to 27th, 2019 / San Luis Potosí, México

[TSM-3] Study of the electronic properties of the superconductor Y_{3x}Sm₃(1-x)Ba₅Cu₈O₁₈ (0≤x≤1) by the LAPW + lo method.

Tomas Santillán Gómez (tomas.santillan@fisica.uaz.edu.mx)¹, Felipe Puch Ceballos¹,
Hugo Tototzintle Huitle¹, Leticia Perez Arrieta¹

¹ UAZ

The density of electronic states (DEE) around the fermi energy (Ef) were calculated for the superconducting family of high critical temperature (high-Tc) and Y_{3x}Sm₃(1-x)Ba₅Cu₈O₁₈ (0≤x≤1). In order to find the variation of the DEE in the Ef (which will give us an idea of the T_c), with respect to the composition x. The DEE is also calculated for the Cu-O planes of the material, because by varying the composition of an atom of Sm by one of Y, the DEE is affected around Ef, due to the contribution of the orbitals f of the atom of Ye; This contribution is not reflected in the DEE of the Cu-O chains of the material, due to the distance of these with the atoms of Y or Sm. To calculate the DEE, the first principles LAPW + lo method is used. The Perdew and Burke generalized gradient approach of 1996 was used for the exchange-correlation potential. For the calculation of the variation of the network parameters (a, b and c) with the variation of the component x an experimental law known as the law of vegard was used.



[TSM-58] On the Quest of the Lowest-Energy Structure in Cu Clusters Using a Modified Kick Algorithm

Jorge Isaac Díaz Hernández (*jidh0812@gmail.com*)¹, J. Oscar C. Jimenez-Halla¹, José Luis Cabellos², Alvaro Posada-Amarillas (*posada@cifus.uson.mx*)²

¹ Departamento de Química, División de Ciencias Naturales y Exactas, Universidad de Guanajuato, Noria Alta s/n 36050, Guanajuato, Gto.

² Departamento de investigación en Física, Universidad de Sonora, Blvd. Luis Encinas & Rosales, 83000, Hermosillo, Son.

Finding the lowest-energy configuration for a molecular system is a problem that has attracted significant attention in both chemistry and physics. Despite its complexity, a number of methods have been proposed and applied. Based on a modified kick algorithm, an automated and parallel computational package called *Guglosac* is presented to explore the potential energy surface (PES) of a given aggregate of atoms, and obtain the lowest-energy structure. Our methodology is capable of using any electronic structure method, like DFT as implemented in *Gaussian*, to calculate the total energy of the atomic arrangement. *Guglosac* is simple to use, efficiently searching the isomers on the PES. In this work, we have scanned the PES of Cu_n (n=2-10) clusters as a test case, successfully locating the minima in energy isomers. A comparison with previous reported works is presented.

References

Posada-Amarillas A. Ab initio molecular electrostatic potential of hexanuclear Cu, Ag, and Au clusters. In: APS March Meeting Abstracts. 2016. p. T1.023.



[TSM-71] Magnetic moment of bulk iron-cobalt alloy ($\text{Fe}_{1-x}\text{Co}_x$; $x = 0.0, 0.05, 0.10, \dots, 1.0$) with DFT theory.

GABRIEL RAMIREZ-DAMASO (*gramirezd@ipn.mx*)², FRANCISCO CABALLERO³, ADRIAN PINEDA-JIMENEZ (*pija880712@gmail.com*)², JULIE ROBERGE², EZEQUIEL ROJAS-HERNANDEZ², OSCAR CANO-AGUILA², MISael SOLORZA-GUZMAN¹

¹ ESCOM, INSTITUTO POLITECNICO NACIONAL

² ESIA TICOMAN, INSTITUTO POLITECNICO NACIONAL

³ FES ZARAGOZA, UNAM

In this work, we study iron-cobalt alloy ($\text{Fe}_{1-x}\text{Co}_x$; $x = 0.0, 0.05, 0.10, \dots, 1.0$), considering crystal structure bcc for pure iron and fcc for pure cobalt. Iron and cobalt have ferromagnetic properties, with 3d electrons of the periodic table. First of all, we optimize the bulk crystal structures of these alloys to obtain the state of minimum energy or the optimum geometry. With Density Functional Theory (DFT) we estimate their electronic density of states of the electrons with spin up and electrons with spin down, for values of energy less or equal than the level of Fermi energy. Once bulk electronic density of states is calculated, we proceed to calculate the magnetic moment as the difference between electrons with spin up and spin down. In our calculations we used the module CASTEP of the molecular simulation program Materials Studio and our results are in good agreement with experimental results of magnetic moment reported in the literature.



[TSM-109] Hydrogen adsorption on nitrogen-doped Single Walled Carbon Nanotubes using DFT theory

Adrian Pineda-Jiménez (*pija880712@gmail.com*)², Gabriel Ramírez-Dámaso (*pija880712@gmail.com*)², Ezequiel Rojas-Hernández (*pija880712@gmail.com*)², Fernando Caballero (*pija880712@gmail.com*)¹

¹ Carrera de Ingeniería Química, Facultad de Estudios Superiores Zaragoza C. II UNAM, Batalla 5 de Mayo s/n, Col. Ejército de Oriente, C.P. 09320, Iztapalapa CDMX, México

² Escuela Superior de Ingeniería y Arquitectura “Unidad Ticomán” del Instituto Politécnico Nacional (SEPI), Av. Ticomán No. 600, Col. San José Ticomán, C. P. 07340, Del. Gustavo A. Madero, CDMX, México

In this work we studied the hydrogen adsorption process on a single walled carbon nanotube pristine (p-CNT) with dimension mxn (3x6) and carbon nanotube doped with nitrogen (N₁-CNT) with the same dimensions (3x6). First of all, we realize the geometric optimization or state of minimum energy, of the carbon nanotube pristine. Then we optimize the structure of the carbon nanotube doped with nitrogen, with DFT theory. The next step is adding hydrogen molecules on the external surfaces of the p-CNT and N₁-CNT, identifying the effect of the variation from physical properties like his diameter or the stability of the hydrogen molecule on his surface. Finally, we observed that a SWCNT with 83 carbon atoms and one nitrogen atom can storage 12 hydrogen molecules. In our calculations we used the module Dmol3 of the molecular simulation program Materials Studio.



[TSM-127] Electronic and magnetic properties of H-passivated Ge-NWs on a LaTiO₃ slab

José Miguel Cervantes Cervantes (*josemiguel.cervantes.gin2013@gmail.com*)², Erika Alva Suárez², Margarita Clarisaila Crisóstomo Reyes¹, Raúl Oviedo-Roa³, Eliel Carvajal Quiroz (*eliel.carvajal@gmail.com*)²

¹ CECyT 8 Narciso Bassols, Instituto Politécnico Nacional, Av. De las Granjas 618, 02530 Ciudad de México, México.

² ESIME Culhuacan, Instituto Politécnico Nacional, Av. Santa Ana 1000, 04440 Ciudad de México, México.

³ Instituto Mexicano del Petróleo, Eje Central Lázaro Cárdenas Norte 152, 07730 Ciudad de México, México.

Energy storage or energy generation devices require designs to avoid the current degradation problems. Among other proposals, there are some based on nanostructured systems which can provide more interaction surface. For this work were modelled some systems based on perovskite-like oxides and semiconductor materials with a diamond-like structure: H-passivated Ge nanowires (Ge-NWs) on LaTiO₃ slabs, which can offer an alternative for an electrode-electrolyte interface for Li-ion batteries. Calculations for the lower energy configurations, and the electronic and magnetic properties of such systems, were made on the Density Functional Theory (DFT) frame. Results shown that deformation of the Ge-NWs' cross-section is a function of the relative orientation of the NW and the electrolyte. Besides, all systems shown metallic behaviour and ferrimagnetic configurations. There are electronic charge transfers between the Ge-NWs and the LaTiO₃ slab; for that case where the LaTiO₃ slab surface is LaO terminated, Ge-NWs exhibit an electronic charge loss while the slab's O atoms gain an electron, which is linked to binding type nature. On the other hand, when Ge-NWs interact with the atoms which define the TiO₂ termination, there are electronic charge concentrations at the NW/slab interphase, which also are linked to the nature of the binding between atoms. Acknowledgments: This work was partially supported by the multidisciplinary project IPN-SIP-2019-6659. J. M. Cervantes and E. Alva acknowledge the scholarship from CONACYT.



[TSM-134] Effect of La³⁺/Sr²⁺ ordering on the magnetic properties of La_{2/3}Sr_{1/3}MnO₃ by first principles calculations

H Linh H mők (hlinh.hmok@gmail.com)⁴, Espiridión Martínez Aguilar⁴, Jordi Ribas Ariño², Jesús María Siqueiros Beltrones¹, José Luis Sánchez Llamazares³, Oscar Raymond Herrera¹

¹ Centro de Nanociencias y Nanotecnología, Universidad Nacional Autónoma de México, Apdo. Postal 14, Ensenada 22860, Baja California, México.

² Departament de Ciència de Materials i Química Física and IQTCUB, Universitat de Barcelona, Martí i Franquès 1, 08028 Barcelona, Spain.

³ Instituto Potosino de Investigación Científica y Tecnológica A. C., Camino a la Presa San José 2055, Col. Lomas 4a, San Luis Potosí 78216, México.

⁴ Posgrado en Física de Materiales, Centro de Investigación Científica y de Educación Superior de Ensenada, Carretera Tijuana-Ensenada No. 3918, Zona Playitas, Ensenada 22860, Baja California, México.

The La_{2/3}Sr_{1/3}MnO₃ (LSMO) material is a promising candidate for Spintronics as a source of spin-polarized electron current. To date, many theoretical works have been focused on describing the physical properties of La_{1-x}Sr_xMnO₃ with cubic and/or tetragonal perovskite structure. However, a detailed discussion on the effect of the Sr distribution on the magnetic properties of LSMO is still missing in the literature. In this work, using DFT+U formalism, we investigate the effect of the order-disorder in the A-site occupation by La³⁺ and Sr²⁺ on the stability of the ferromagnetic order in LSMO bulk with *R3c* symmetry. For this purpose, we employ structural models corresponding to rhombohedral *R3csymmetry* consisting of 120 atom supercells constructed according to the precise stoichiometry of the compound. Two configurations, describing randomized and ordered occupation of the La³⁺ and Sr²⁺ ions, are evaluated. The electronic structure of these configurations has been studied by means of an analysis of their density of states, band structure, electron density and electron localization function. We have demonstrated that the ferromagnetic arrangement of the LSMO with La³⁺ and Sr²⁺ ions randomly distributed is more stable than that with an ordered A-site occupation. We find that with the random configuration, it is not possible to distinguish between Mn³⁺ and Mn⁴⁺ ions, thus favoring the double-exchange mechanism, which in turn is enhanced by the high degree of covalence in the Mn-O bonds near the Fermi level between the *spin-up* Mn-eg orbitals with the O-p orbitals.

Acknowledgments

This work was partially supported by PAPIIT-DGAPA-UNAM Grants IN107918 and IN105317. The authors thank the computer support thorough Projects LANCAD-UNAM-DGTIC-351. The authors thank A. G. Rodriguez Guerrero and P. Casillas for their technical assistance. H' Linh H mők and E. Martínez-Aguilar thank CoNaCyt for Scholarship Grant 290784 and 290934, respectively.



XII -ICSMV

September 23rd to 27th, 2019 / San Luis Potosí, México

[TSM-179] SWNT interactions with chiral amino acids.

Dante Fernando Hernandez Andrade (dante.guitar.09@gmail.com)¹, José de Jesus Pelayo Cardenas¹, Ariadna Sánchez Castillo¹

¹ Escuela Superior de Apan, Universidad Autónoma del Estado de Hidalgo, Chimalpa Tlalayote, Municipio de Apan, Hidalgo 43920, México.

Single Walled Carbon Nanotubes (SWNTs) have been widely studied because of their potential applications in many fields including conductive and high-strength composites, energy storage and energy conversion devices, sensors, field emission displays, hydrogen storage media, etc.

This work studies the interaction between a chiral (6,4) SWNT and a chiral amino acid (arginine, cysteine, alanine and asparagine), and determines through first principles calculations based in the density functional theory (DFT) the enantiomer of each amino acid which interacts best with the SWNT, based on structural, energetic and vibrational properties.



[TSM-505] Monolithic integration of GaAs on high index Si substrates: A DFT study.

Reyna Méndez Camacho (reyna129b@hotmail.com)¹, Esteban Cruz Hernández¹

¹ Coordinación para la Innovación y la Aplicación de la Ciencia y Tecnología, CIACYT-Universidad Autónoma de San Luis Potosí, UASLP, Sierra Leona 550, San Luis Potosí, S. L. P., México.

The crystalline surfaces of high index (HI) are energetically unstable planes. In the epitaxial growth they tend to generate facets by minimizing their surface free energy, which makes them attractive to be used in the self-assembly of nanometric templates to fabricate highly ordered nanostructures. In a previous work, we have reported the finding of a criterion that unifies and explain the facet formation in HI substrates of GaAs. In that work we describe how the HI planes could be used also to modify the way the layers can growth on such substrates.

In the present work, we explore the use of HI Silicon substrates to growth III-V compounds. The results were obtained by using the Density Functional Theory (DFT). With DFT, information such as minimum energy configurations, interface stress, charge distribution, density of states, reconstructions and dislocations in the interface of specific HI-Si planes and GaAs layers were obtained. The results show that under the correct choice of the HI-Si orientation an almost perfect epitaxial growth of GaAs layers can be achieved.



[TSM-514] 3D SIMULATION OF GAS PHASE REACTIONS BY HOT FILAMENT VAPOR DEPOSITION TO OBTAIN SIO_X FILMS

XOCHITL ALEYDA MORAN MARTINEZ (xochitlmoran@gmail.com) ¹, JOSE ALBERTO LUNA LOPEZ ¹

¹ Benemérita Universidad Autónoma de Puebla, 14 sur y Av. San Claudio, Col. San Manuel, Ciudad Universitaria, Edificio IC6, Posgrado en Dispositivos Semiconductores, C.P. 72570, Puebla, México

The non-stoichiometric silicon oxide (SiO_X) films have been widely studied to exhibit photoluminescent properties which are required in optoelectronic applications. In this work is presented a three-dimensional (3D) simulation of gas phase reactions by Hot Filament Vapor Deposition (HFCVD) to produce SiO_X films. The 3D simulation of the HFCVD process solves the continuity, momentum and energy equations in steady state by means of a commercial software Comsol. The gas phase reaction in the HFCVD was introduced in the 3D model by means of Chemkin-Pro. The results obtained were the temperature and the velocity in the reactor. The temperature was evaluated for different flow rates of hydrogen (25,50,75, 100 sccm) and different temperature substrate. The calculated temperature was compared with the experimental measurements obtained with a thermocouple. The theoretical study of the gas phase reaction was investigated at atmospheric pressure and varied from 300°C to 2000°C. The mechanism of gas phase reactions was taken of the literature. The results obtaining allow to evaluate the mass-fraction concentration of the main precursor species in the reactor. The concentration mass-fraction in the filaments and in the deposit zones is relevant to propose a mechanism of surface reaction for the deposit of SiO_X films.



[TSM-627] Dissociation of NO₂ and SO₂ adsorption on Cu/ZnO(0001): DFT study

Erika Camarillo Salazar (*erikacamarillo@uadec.edu.mx*)³, Reyes García Díaz¹, Yuliana Elizabeth Avila Alvarado⁴, María Teresa Romero de la Cruz (*teresa.romero.cruz@uadec.edu.mx*)²

¹ Cátedra CONACyT, Facultad de Ciencias Físico Matemáticas, UAdeC, Unidad Camporredondo, Edif. A, 25000, Saltillo, Coahuila, México

² Facultad de Ciencias Físico Matemáticas, UAdeC, Unidad Camporredondo, Edif. A, 25000, Saltillo, Coahuila, México

³ Facultad de Ciencias Químicas, UAdeC, Blv. Venustiano Carranza e Ing. José Cárdenas, 25080, Saltillo, Coahuila, México

⁴ Facultad de Sistemas UAdeC, Ciudad Universitaria, Blvd. Fundadores Km 13, 25350, Arteaga, Coahuila, México

Due to the importance of reducing environmental pollution, especially NO₂ and SO₂, we have studied the adsorption of these contaminants for their elimination in the atmosphere. We perform ab initio calculations of NO₂ and SO₂ adsorption on pristine and copper deposited zinc oxide (0001) surface. The calculations were carried out by means of computational modeling using the Quantum ESPRESSO package that works within the framework of the Density Functional Theory (DFT). Ultrasoft pseudopotentials were used to model the electron-ion interaction. The exchange-correlation functional was treated by the generalized gradient approximation (GGA) with the parametrization of Perdew-Burke-Ernzerhof (PBE). Several high symmetry sites were tested for the adsorption of the molecules. The electronic properties (DOS, PDOS and charge density maps) of the most stable configurations for each molecule were calculated. The adsorption energies values show that chemisorption takes place for both molecules. Nudged elastic band (NEB) calculations were performed in order to study NO₂ and SO₂ dissociation. The activation energy for NO₂ first dissociation process on clean ZnO surface is more favorable compared to Cu deposited case. On the other hand, for the second dissociation process, the activation energy for the Cu deposited system is lower than on the pristine surface. The SO₂ molecule is dissociated on the surface, although is more favorable without Cu.

Keywords: Cu, DFT, NO₂, SO₂, ZnO.



[TSM-628] Ab initio study of adsorption of C₇H₆O₂ and CH₃COOH on
pristine graphene and graphene with vacancies.

Adrián Alberto Arroyo Escareño (adrianarroyo@uadec.edu.mx) ³, Aidé Sáenz Galindo ³,
María Teresa Romero de la Cruz (teresa.romero.cruz@uadec.edu.mx) ², Jonathan
Guerrero Sánchez ¹

¹ Centro de Nanociencias y Nanotecnología, Universidad Nacional Autónoma de México,
Apartado 5 Postal 14, Ensenada Baja California, 22800, Ensenada, Baja California, México.

² Facultad de Ciencias Físico Matemáticas, Universidad Autónoma de Coahuila, Unidad
Camporredondo, Edif. A, 25000, Saltillo, Coahuila, México

³ Facultad de Ciencias Químicas, Universidad Autónoma de Coahuila, Blvd. Venustiano
Carranza e Ing. José Cardenas, 25080, Saltillo, Coahuila, México

The graphene is considered a material with innumerable applications, this due to its chemical structure, it consists entirely of carbon, however, its re-arrangement and its arrangement between carbon atoms make this material unique, presents sp₂ hybridization, which, among other characteristics, makes it highly electrically and calorically conductive. Although 2D materials provide a large specific surface area for the adsorption of molecules, the interaction between molecules and pristine graphene is weak. However, the presence of vacancies in graphene can increase the interaction with the adsorbates. We performed ab initio calculations of C₇H₆O₂ and CH₃COOH adsorption on pristine graphene and graphene with vacancies. The calculations were developed using the Quantum ESPRESSO package that works within the framework of the Density Functional Theory (DFT). Ultrasoft pseudopotentials were used to model the electron-ion interaction. We used the generalized gradient approximation (GGA) with the parametrization of Perdew-Burke-Ernzerhof (PBE) to treat the exchange-correlation functional. Several sites were considered for the adsorption of the molecules. The electronic properties of the most stable configurations were calculated.



[TSM-648] Nickel nanostructure formation on the AlN (0001)-(2x2) surface: ab-initio studies

Aracely del Carmen Martínez Olguín (amartinez@ifuap.buap.mx)³, Rodrigo Ponce Perez², Carlos Antonio Corona García³, Do Minh Hoat¹, Leonardo Morales de la Garza⁴, Gregorio Hernandez Cocoletzi (cocoletz@ifuap.buap.mx)³

¹ Advanced Institute of Materials Science, Ton Duc Thang University

² Universidad Autónoma de Coahuila, Facultad de Ciencias Químicas

³ Universidad Autónoma de Puebla, Instituto de Física

⁴ Universidad Nacional Autonoma de Mexico, Centro de Nanociencias y Nanotecnologia

Structural, electronic and magnetic properties of the nickel deposit and incorporation in the AlN(0001)-(2x2) surface are investigated by ab-initio total energy calculations. Studies have been performed within the spin polarized periodic density functional theory (DFT) according to the PWscf code of the quantum espresso. Provided that Ni is a transition metal it contains highly correlated electrons, therefore the Hubbard-U theory is invoked in the calculations. In addition this material displays magnetic properties, so different magnetic alignments are considered: nonmagnetic (NM), ferromagnetic (FM) and antiferromagnetic (AF). First, we investigate the Ni deposit at four high symmetry sites with the coverage varying from $\frac{1}{4}$ monolayer (ML) to a full ML. The $\frac{1}{4}$ ML most stable structure corresponds to the H3 site. In the $\frac{1}{2}$, $\frac{3}{4}$ and 1 ML coverage the adsorption relaxes into dimers, trimers and tetramers, respectively. In the Ni incorporation the most stable structures relax into the T4 site. To determine the most favorable geometry the surface formation energy formalism (SFE) is applied. According to the SFE, under Al-rich condition the most favorable structure is the adsorption of $\frac{1}{4}$ ML of Ni on top of the surface at the H3 site. However under N-rich conditions the most favorable geometry is the deposit of one ML of Ni on the N terminated surface with adsorption site being the H3 indicating epitaxial growth. Electronic properties have been investigated with the density of states (DOS) and projected density of states (PDOS), with results indicating that the most stable structures display metallic behavior. A magnetic behavior was observed on the Ni deposit from $\frac{1}{2}$ to a full ML with magnetic moments changing from $0.80 \mu_B$ to $2.33 \mu_B$.



XII -ICSMV

September 23rd to 27th, 2019 / San Luis Potosí, México

THIN FILMS (THF)

Chairman: Alberto Duarte Moller, Universidad de La Salle Bajío



XII -ICSMV

September 23rd to 27th, 2019 / San Luis Potosí, México

THIN FILMS
(THF)
ORAL SESSIONS



[THF-56] ZnO-Gd₂O₃ THIN FILMS OBTAINED BY CO-SPUTTERING

Carlos Augusto López-Lazcano (carlos.alazcano@hotmail.com) ², Gibran Guadalupe Martínez Falomir ², María Isabel Pintor-Monroy ¹, Xavier Mathew ³, Manuel Ángel Quevedo-Lopez ¹, Jorge Luis Almaral-Sánchez ²

¹ Department of Material Science and Engineering, The University of Texas at Dallas, Richardson, Texas, 75080, USA

² Facultad de Ingeniería Mochis, Universidad Autónoma de Sinaloa, Fuente de Poseidón y Ángel Flores s/n, 81223, Los Mochis, Sinaloa, México

³ Instituto de Energías Renovables, Universidad Nacional Autónoma de México, 62580, Temixco, Morelos, México

In this work we are presenting the preliminary results on ZnO-Gd₂O₃ thin films (~100 nm) deposited by co-sputtering of individual targets of ZnO and Gd₂O₃ on glass, quartz and silicon substrates at room temperature, under Ar atmosphere. The percentage of Gd₂O₃ in the films was controlled by varying the deposition power on the Gd₂O₃ target while keeping the power fixed for ZnO.

The resulting thin films were studied using different characterization techniques such as Scanning Electron Microscope (SEM), Atomic Force Microscope (AFM), X-ray diffraction (XRD), Raman spectroscopy and Ultraviolet-visible spectroscopy (UV-Vis). The ZnO rich films are polycrystalline, transitioning to amorphous as the percentage of Gd₂O₃ in the films increased. Raman spectroscopy indicated the presence of both materials in the films. According to AFM, all films are highly smooth, with a ~ 2-4 nm roughness. The band gap increased from 3.2 eV of the pure ZnO to 3.9 eV as the percentage of Gd₂O₃ increases, due to Gd₂O₃ wide band gap. All films were highly transparent.

Co-sputtering technique was successful in obtaining high quality, smooth ZnO-Gd₂O₃ thin films, allowing the homogenous introduction of Gd₂O₃ in the ZnO matrix at low Gd₂O₃ percentages with a transition from polycrystalline to amorphous as Gd₂O₃ becomes more dominant and the ZnO structure is lost.

Acknowledgements: This work was partially supported by Conacyt scholarship #295768 and Conacyt Becas Mixtas Ago 17-Jun 18, at Universidad Autónoma de Sinaloa-DGIP by project PROFAPI2015/011, at UTD by AFOSR grants FA9550-18-1-0019 and NSF/PFI:AIR TT 1701192.

Keywords: Co-sputtering, ZnO-Gd₂O₃, Thin-Film.



[THF-60] Deposition of Methylammonium Lead Bromide Perovskite by Close Space Sublimation

Gibrán Guadalupe Martínez Falomir (gibran.mfalomir@hotmail.com)², Carlos Augusto López Lazcano², Iker Rodrigo Chávez Urbiola¹, María Isabel Pintor Monroy¹, Jorge Luis Almaral Sánchez², Xavier Mathew¹, Manuel A. Quevedo Lopez¹

¹ Department of Materials Science and Engineering, University of Texas at Dallas, Richardson, TX, 75080, USA

² Facultad de Ingeniería Mochis, Universidad Autónoma de Sinaloa, Fuente de Poseidón y Prol. Ángel flores S/N, C.P. 81223, Los Mochis, Sinaloa, México

A novel and scalable method to deposit thick methylammonium lead bromide ($\text{CH}_3\text{NH}_3\text{PbBr}_3$) perovskite thin films is discussed in this work. In a two-step close space sublimation (CSS) process, the precursors lead bromide (PbBr_2) and methylammonium bromide (MABr) were sublimed sequentially onto glass substrates at pre-determined source and substrate temperatures. The *in-situ* formed $\text{CH}_3\text{NH}_3\text{PbBr}_3$ film had trace amounts of the precursor PbBr_2 . A post-annealing at high pressure and temperature (hot-press) was developed to reduce the surface roughness as well as to achieve full conversion into $\text{CH}_3\text{NH}_3\text{PbBr}_3$. Films as thick as 3 um with surface roughness \sim 10 nm were developed by the described CSS deposition and the subsequent hot-press process. The films were characterized for structure, morphology, optical, and spectroscopic properties. The polycrystalline $\text{CH}_3\text{NH}_3\text{PbBr}_3$ film has a cubic structure with optical band gap 2.28 eV. The surface roughness decreased from 55 nm to \sim 10 nm after hot-press anneal at 100°C for 3 hours under 5000 psi pressure. Photoluminescence (PL) spectra show a shoulder band at low energy side of the excitonic band, which can be due to surface defects, impurities, grain size inhomogeneity, etc. Intensity of the shoulder band show a tendency to diminish with increasing the pressure during hot-press anneal, which indicates that the shoulder band can be related with surface defects.

Acknowledgements: This work was partially supported by Conacyt scholarship #295770 and Conacyt Becas Mixtas Ago 17-Jun 18, at Universidad Autónoma de Sinaloa-DGIP by project PROFAPI2015/011, worked at University of Texas at Dallas and by AFOSR grants FA9550-18-1-0019 and NSF/PFI:AIR TT 1701192.

Keywords: $\text{CH}_3\text{NH}_3\text{PbBr}_3$, perovskite film, close space sublimation



[THF-122] Low-Temperature Deposition of Inorganic-Organic HfO₂-PMMA Hybrid Gate Dielectric Layers for High Mobility ZnO Thin-film Transistors

Gouri Syamala Rao Mullapudi (mullapudi.gouri@gmail.com) ¹, Gonzalo Alonso Velazquez-Nevarez ², Rafael Ramirez-Bon ¹, Manuel Angel Quevedo-Lopez ³, Carlos Avila-Avendano ³, Jorge Alejandro Torres-Ochoa ¹

¹ Cinvestav, Unidad Queretaro

² Depto. Ing. Metalurgia y Materiales, Escuela Superior de Ingeniería Química e Industrias Extractivas-ESIQUE, Instituto Politécnico Nacional-IPN, Ciudad de México

³ University of Texas at Dallas

In this work, we developed a novel inorganic-organic HfO₂-PMMA hybrid material as gate dielectric by an efficient and ecofriendly sol-gel method. The hybrid thin films deposited by a simple spin coating technique and converted into thin films at very low annealing temperatures of 185 °C. The successful hybrid thin film formation was investigated systematically by FTIR and XPS analysis respectively. Then, the surface morphology of hybrid thin films was observed by atomic force microscopy (AFM) through tapping mode and it was revealed that the film surface is homogenous with a very low surface roughness of 0.8 nm. In addition, it was found that the hybrid films are hydrophilic with a high surface energy of 59.9 mJ/m² as measured by contact angle technique. The insulating properties of this hybrid film, studied by I-V and C-V measurements, showed very low leakage current density under 1 nA/cm² at -5V, high gate capacitance of 106 nF/cm² and high dielectric constant of 11.3 at 1 kHz. With such dielectric properties, the hybrid thin films were employed as dielectric gate layers in room temperature sputtered ZnO thin film transistor (TFTs). The analysis of the electrical response of the ZnO-based TFTs with the hybrid gate dielectric show that they achieve low operating voltage, less than 5 V, with high saturation field effect mobility of 15.5 cm² V⁻¹ s⁻¹, very low threshold voltage, 0.5 V, high on/off current ratio of 10⁶ and low subthreshold slope of 0.37 V/dec respectively.



[THF-123] Low-Temperature Deposition of Inorganic-Organic HfO₂-PMMA Hybrid Gate Dielectric Layers for High Mobility ZnO Thin-film Transistors

Gouri Syamala Rao Mullapudi (mullapudi.gouri@gmail.com) ², Gonzalo Alonso Velazquez-Nevarez ³, Rafael Ramirez-Bon ¹, Manuel Angel Quevedo-Lopez ⁴, Carlos Avila-Avendano ⁴, Jorge Alejandro Torres-Ochoa ²

¹ Cinvestav, Unidad Queretaro

² Cinvestav, Unidad Queretaro, Mexico.

³ Depto. Ing. Metalurgia y Materiales, Escuela Superior de Ingeniería Química e Industrias Extractivas-ESIQUE, Instituto Politécnico Nacional-IPN, Ciudad de México, Mexico.

⁴ University of Texas at Dallas, United States

In this work, we developed a novel inorganic-organic HfO₂-PMMA hybrid material as gate dielectric by an efficient and ecofriendly sol-gel method. The hybrid thin films deposited by a simple spin coating technique and converted into thin films at very low annealing temperatures of 185 °C. The successful hybrid thin film formation was investigated systematically by FTIR and XPS analysis respectively. Then, the surface morphology of hybrid thin films was observed by atomic force microscopy (AFM) through tapping mode and it was revealed that the film surface is homogenous with a very low surface roughness of 0.8 nm. In addition, it was found that the hybrid films are hydrophilic with a high surface energy of 59.9 mJ/m² as measured by contact angle technique. The insulating properties of this hybrid film, studied by I-V and C-V measurements, showed very low leakage current density under 1 nA/cm² at -5V, high gate capacitance of 106 nF/cm² and high dielectric constant of 11.3 at 1 kHz. With such dielectric properties, the hybrid thin films were employed as dielectric gate layers in room temperature sputtered ZnO thin film transistor (TFTs). The analysis of the electrical response of the ZnO-based TFTs with the hybrid gate dielectric show that they achieve low operating voltage, less than 5 V, with high saturation field effect mobility of 15.5 cm² V⁻¹ s⁻¹, very low threshold voltage, 0.5 V, high on/off current ratio of 10⁶ and low subthreshold slope of 0.37 V/dec respectively.



[THF-149] Structural characterization of graphene by using a near field scanning optical microscope

Luis Felipe Lastras-Martinez (lflm@cactus.iico.uaslp.mx) ¹, Daniel Medina-Escobedo ¹,
Gabriela Flores-Rangel ¹, Raul Balderas-Navarro ¹, Oscar Ruiz-Cigarrillo ¹, Ricardo
Castro-Garcia ¹, Maria del Pilar Morales-Morelos ¹, Jorge Ortega-Gallegos ¹, Maria
Losurdo ²

¹ *Instituto de Investigación en Comunicación Óptica, Universidad Autónoma de San Luis Potosí, Alvaro Obregón 64, CP 78000, San Luis Potosí SLP, Mexico*

² *Institute of Nanotechnology, CNR-NANOTEC, Department of Chemistry, via Orabona 4, 70126 Bari, Italy*

We report on differential reflectance contrast (DRC) sub-microscopic images measured of graphene layers deposited on different substrates by using a near field scanning optical microscope (NSOM) with a spatial resolution of 40 nm. The DRC signal is obtained by taking the numerical difference between the reflectivity coming from a region with no graphene (substrate) and a region containing graphene. DRC in the near field limit is a very useful technique to characterize the thickness and shape of flakes and nanostructures in the sub-microscopic scale. The results open the possibility to use this optical technique for the structural characterization in the sub-micrometer scale of 2D materials.



XII -ICSMV

September 23rd to 27th, 2019 / San Luis Potosí, México

[THF-151] Characterization of MoO₃ thin films obtained by laser ablation

CARLOS VIRGILIO RIVERA RODRIGUEZ (carlos.rivera@inin.gob.mx)¹, ENRIQUE CAMPOS GONZALEZ², ENRIQUE CAMPS CARVAJAL²

¹ Departamento de Estudios del Ambiente, Instituto Nacional de Investigaciones Nucleares Apdo. Postal 18-1027, México DF 11801, México.

² Departamento de Física, Instituto Nacional de Investigaciones Nucleares. Apdo. Postal 18-1027, México DF 11801, México.

Molybdenum oxide in thin film form, shows a great electrochromic efficiency, property that allows inaddition to change of coloration reversible by the application of a certain voltage difference, modular optical transmittance, reflectance, absorbance and in some cases emittance, with a Band Gap of approximately 3.2 eV, according to the literature. Furthermore, the surface of these MoO₃ films shows high catalytic activity so they can be used to promote total or partial oxidation-reduction reactions of nitrites and organic molecules. For this reason we took on the task of generating and characterizing samples in the form of thin films from high purity molybdenum target, within an oxidizing atmosphere of argon/oxygen, by laser ablation technique, on quartz substrates. Maintaining the operating parameters of the system constant except for the working pressure during the growth of the thin film, subsequently, each sample was thermally treated at 450 °C, under normal atmospheric conditions. X-ray diffraction results of each thin film obtained, show an orthorhombic structure associated with molybdenum trioxide, which are corroborated by Raman spectroscopy, where bands belonging to the alpha phase of said compound are clearly located. However, in the transmittance spectra recorded by UV-Visible Spectroscopy could be observed some displacement of the absorbance edge, which leads to a variation of tenths of the Band Gap. Finest studies of X-ray Photoemission Spectroscopy, showed a certain molecule rearrangement, resulting in a second stoichiometric composition.



[THF-152] Characterization of MoO₃ thin films obtained by laser ablation

CARLOS VIRGILIO RIVERA RODRIGUEZ (carlos.rivera@inin.gob.mx)¹, ENRIQUE CAMPOS GONZALEZ², ENRIQUE CAMPS CARVAJAL²

¹ Departamento de Estudios del Ambiente, Instituto Nacional de Investigaciones Nucleares Apdo. Postal 18-1027, México DF 11801, México.

² Departamento de Física, Instituto Nacional de Investigaciones Nucleares. Apdo. Postal 18-1027, México DF 11801, México.

Molybdenum oxide in thin film form, shows a great electrochromic efficiency, property that allows inaddition to change of coloration reversible by the application of a certain voltage difference, modular optical transmittance, reflectance, absorbance and in some cases emittance, with a Band Gap of approximately 3.2 eV, according to the literature. Furthermore, the surface of these MoO₃ films shows high catalytic activity so they can be used to promote total or partial oxidation-reduction reactions of nitrites and organic molecules. For this reason we took on the task of generating and characterizing samples in the form of thin films from high purity molybdenum target, within an oxidizing atmosphere of argon/oxygen, by laser ablation technique, on quartz substrates. Maintaining the operating parameters of the system constant except for the working pressure during the growth of the thin film, subsequently, each sample was thermally treated at 450 ° C, under normal atmospheric conditions. X-ray diffraction results of each thin film obtained, show an orthorhombic structure associated with molybdenum trioxide, which are corroborated by Raman spectroscopy, where bands belonging to the alpha phase of said compound are clearly located. However, in the transmittance spectra recorded by UV-Visible Spectroscopy could be observed some displacement of the absorbance edge, which leads to a variation of tenths of the Band Gap. Finest studies of X-ray Photoemission Spectroscopy, showed a certain molecule rearrangement, resulting in a second stoichiometric composition.



[THF-259] Modelling the spatial distribution of silicon oxide thin films grown by reactive magnetron sputtering

julio cruz (juliocruz@cnyn.unam.mx)², roberto sanginés¹, noemí abundiz-cisneros¹, stephen muhl³, roberto machorro-mejía²

¹ CONACYT, CNyN-UNAM

² Departamento de Materiales Avanzados. CNyN-UNAM

³ Departamento de Materiales de Baja Dimensionalidad. IIM-UNAM

Target poisoning in reactive sputtering is one of the biggest problems in the coatings industry. There are several research groups that have made great advances in the subject, among them are the groups of S. Berg and D. Depla. These groups have developed models to shed light on the phenomenon, taking into account most of the physical phenomena that would occur when a reactive gas atom reaches the surface of the racetrack to subsequently achieve the so called hysteresis cycle.

In this work, we use the Co-Sputtering Simulation Reactive mode software, Co-SS Rm, to present a different solution of the compound formation both on the target and on the substrate, based on the comparison of the simulations with the thickness measurements of the films deposited at different flows of reactive gas. In the simulations, Co-SS analyse the sputtering yield as a function of the reactive gas amount, in addition to providing the angular distribution of compound or metallic species ejected from the target. The experimental parameters for the deposition thin films by reactive sputtering on a 2" diameter Si (99.99%) target were: constant supplied power of 50 Watts, working pressure at 6.8 mTorr, target-substrate distance 4.5 cm, Ar and O₂ mass flow rates at 10 sccm, and from 0.2 to 3.0 sccm correspondingly. All experiments had a constant deposition time of 30 min.

Results indicate that the target surface poisoning suffers an evolution ejecting metallic atoms and silicon oxide until the whole racetrack area is covered by silicon oxide, but at the same time, there is a reduction in the racetrack area due to the growth of several monolayers of silicon oxide. Spectroscopic ellipsometry analysis showed the formation of SiO₂ in the thin films in almost all the reactive gas flows. Simulation results were validated by thickness measurements of actual thin films and plasma optical emission spectroscopy, OES; by analysing emission transitions from the target species (Si).



[THF-264] 3-D CARBON NANOSTRUCTURED BELTS GROWN BY Co-Cu THIN FILMS USED AS CATALYST IN A CHEMICAL VAPOR DEPOSITION SYSTEM

Juan Luis Fajardo Diaz (juan.fajardo@ipicyt.edu.mx)¹, Emilio Muñoz Sandoval¹,
Florentino López Urías¹

¹ Advanced Materials Division, IPICYT, San Luis Potosí, México

A 3-D nitrogen doped carbon nanostructured belt (N-CNBs) were grown over Co/Cu thin films using an aerosol assisted catalytic chemical vapor deposition (ACCVD) system. Co/Cu films were deposited on Si/SiO₂ substrates using the magnetron sputtering technique under argon atmosphere. The ACCVD was carried out by two tubular furnaces configuration at different temperatures (750 °C and 850 °C). Benzylamine, ethanol and thiophene were employed as carbon, nitrogen and sulfur sources. Transmission electron microscopy (TEM), scanning electron microscopy (SEM), Raman spectroscopy and X-ray diffraction were performed to elucidate the growth mechanism of such nanostructures. A N-CBs consists of a strap built with complex elongated carbon nanostructure accommodated one after another. These N-CNBs probably grow in two steps as follow: first, due the interaction between Co-Cu nanoparticles with sulphur and oxygen that led to the formation of Co@CuO-CuS nanosystems which acts as catalyst; second, the structure of N-CNBs is formed by a self-assembly process promoted by sulfur and nitrogen. Characterizations reveals that N-CNBs presents both sp² and sp³ carbon hybridizations with large amount of disordered graphitic material (ID/IG = 1.17). DRX shows the existence of CuO, Cu₂S and CxNySx structures. Interaction between Co and CuO-Cu₂S probably is obstructing the vertical growth of the graphite layers and promoting their horizontal growth, this could explain the complex structures that are the building blocks of the N-CNBs. The findings indicate the production of a novel carbon material with several structural defects that could serve as electrode in ORR systems.



[THF-513] TIN SULFIDE FILMS DEPOSITED ON COPPER SUBSTRATES BY CBD FOR SOLAR CELL APPLICATIONS

MARIA MONTSERRAT OROPEZA SAUCEDO (montserrat.oropeza@hotmail.com)², ROMAN ROMANO TRUJILLO², ENRIQUE ROSENDO ANDRES², RUTILIO SILVA GONZALEZ¹

¹ Benemérita Universidad Autónoma de Puebla, 14 Sur y Av. San Claudio, Col. San Manuel, Ciudad Universitaria, Edificio IF-2, Instituto de Física, C.P. 72570 Puebla, México

² Benemérita Universidad Autónoma de Puebla, 14 Sur y Av. San Claudio, Col. San Manuel, Ciudad Universitaria, Edificio IC-6, Posgrado en Dispositivos Semiconductores, C.P. 72570 Puebla, México

Tin sulfide (SnS) is a semiconductor compound from the IV–VI groups. SnS exhibits a p-type conductivity and its band gap generally is between 1.1 and 1.6 eV. Furthermore, SnS is abundant, non-toxicity, inexpensive and with a large absorption coefficient ($\alpha > 10^4 \text{ cm}^{-1}$), and due to this characteristics is an attractive compound as absorber in solar cells applications. In this work, SnS thin films were deposited on copper substrates to analyze its formation and growth by chemical bath deposition (CBD). The parameters of deposition such as temperature and time were varied to obtain films with a good adherence. Also ammonia hydroxide concentration contributes to form SnS on copper substrates due to the pH increase. Precursors used to obtain SnS were tin chloride and thioacetamide as source of Sn ions and S ions respectively. The deposition temperature was kept at 70°C during 3 hours. SnS films exhibited an orthorhombic structure and a crystal size of 15 nm. The films morphology for SnS was rice shape properly for this material. Optical characterization of SnS films on copper substrates were carried out by diffuse reflectance and the gap value for SnS was 1.17 eV. The thickness of SnS films was around of 1.7 micrometers which is an appropriate value for applications as absorber material in solar cells.



XII -ICSMV

September 23rd to 27th, 2019 / San Luis Potosí, México

[THF-535] Syntesis and Characterization of hybrid perovskite thin films for optoelectronic applications

Francisco Servando Aguirre-Tostado (servando.aguirre@cimav.edu.mx)¹

¹ Centro de Investigacion en Materiales Avanzados, S.C., Unidad Monterrey, Apodaca, Nuevo León, México

Hybrid perovskites (HPV) have recently emerged as highly efficient optoelectronic materials and are currently being intensively investigated as alternative active layer materials for photodetectors, light-emitting diodes, laser devices, sensors and X-ray detectors, among others. Since HPV are direct band gap materials with high optical absorption coefficients ($\sim 10^5 \text{ cm}^{-1}$) the majority of publications have been dedicated to hybrid organic-inorganic solar cells with certified efficiencies over 20%. However, the realization of a long-lasting device implies the understanding of chemical and structural stability of HPV materials and their interface with electron and hole transport layers (ETL and HTL, respectively). This presentation will show detailed XPS analyses of the chemical stability of the transition metal and transition metal oxides with ABX₃ hybrid perovskites for A=MethylAmmonium (MA), B=Pb, and X=Cl, I, and Br. HTL/HPV interface is not trivial as the reactivity of halogen group elements forms an unstable high resistance interlayer at the charge transport layer interface compromising the optimum operation of the device. The electrical characterization and work function measurements will be discussed and correlated to the chemistry and crystalline structure of the materials of interest.



[THF-592] Synthesis of Mo-Si-B Alloy and Development of Thin Films by DC Sputtering

JORGE MORALES HERNÁNDEZ (*jmorales@cideteq.mx*)², JULIO AGUIRRE DELGADO²,
JOSÉ MARTÍN YAÑES LIMÓN¹

¹ CENTRO DE INVESTIGACIÓN Y DE ESTUDIOS AVANZADOS

² CENTRO DE INVESTIGACIÓN Y DESARROLLO TECNOLÓGICO EN ELECTROQUÍMICA

Metal-ceramic alloys are one possibility to resist high temperature oxidation. Mo-Si-B alloys have excellent oxidation resistance in the temperature range of 800-1300° C, associate with the formation of boro-silicates of molybdenum of high density such as Mo_5Si_3 , Mo_5SiB_2 , Mo_2B_5 and MoB_2 .

Mo_5SiB_2 and MoB_2 phases have been obtained after 30 h of Mechanical Alloying (MA) under argon atmosphere, with an acicular morphology and crystal size of 22.7 nm. With a uniaxial load of 60 MPa, a target of 5.08 mm (2 in) in diameter and 5 mm of thickness was obtained. Sintering process in the target, to improve the density and stability of the phases was made in a tube furnace for 2 h in an argon continues flow at 1150° C.

Thin films of the phases Mo_5SiB_2 and MoB_2 with an average thickness of 1.5 μm , were deposited on 316 stainless steel, with a working vacuum of 1.1×10^{-2} Torr, 30 ccm of argon, 150 W of power and 50 minutes of growth.

AFM Characterization with a contact mode, showed pentagonal crystals at the surface, overlapped in the same growing way. SEM micrographs confirmed the pyramidal crystals growth at the surface with a nanometric structure and with the minimum distance between each pyramidal structure.

Keywords: Mechanical Alloying, High Temperature Oxidation



[THF-687] TITANIUM DIOXIDE (TiO_2) THIN FILMS STUDY, DEPOSITED BY LASER ABLATION ON GLASS SUTRATES, IN THE FORM OF PRISMATIC FIGURES TYPE PYRAMIDAL

Martín López García (mlopezg1600@alumno.ipn.mx)¹, Fabio Felipe Chalé Lara¹

¹ CICATA Altamira IPN - Km. 14.5 Carretera Tampico-Puerto Industrial Altamira, 89600 Altamira, Tamaulipas

This research paper is about a study of thin films of titanium dioxide (TiO_2), deposited by laser ablation, on glass substrates in the form of prismatic figures. The main objective was to confine the plasma plume, to force it to produce a continuous trail with varying thicknesses that could be analyzed; the films were prepared under conditions of low vacuum between 17 and 21 mtorr at 25 °C temperature, with laser pulses of 7 ns and 1064 nm wavelength, 20 hertz frequency, energies of 100 and 200 mJ, applied on circular areas of 0.3 mm in diameter in a target of TiO_2 at 99% purity in rutile phase, without substrate heating, using a Quantel laser equipment, model Q-smart 450 from Nd-Yag. The growth times were 5, 10, 15, 20 and 30 minutes, obtaining films that exhibited a colours pattern related to the expected thickness variation, except for the 5 minute films that did not reach the thicknesses required to display a color. The characterization process was carried by: X-ray diffraction (DRX) to know the structure, ultraviolet-visible spectroscopy (UV-VIS) to verify the variation of thicknesses, X-ray emitted photoelectron spectroscopy (XPS) to verify the composition and scanning electron micrograph (SEM) to accurately measure the thicknesses. The theory of optical interference was applied to the continuous trace to calculate the thicknesses, finding a problem in the spectral behavior of the colours pattern; This fact manifested itself by showing a defect in the first appearance of the violet color, which caused the optical interference equations to fail in sequence. The problem arises when the thickness for the initial presentation of the purple color is calculated, using the first reflection or the value of π for the phase change, this data is logical in order, since the thickness trail is continuous, the conflict is resolved by starting the calculations with the second reflection or 3π for the phase. The details of this phenomenon are explained in the development of the presentation.



XII -ICSMV

September 23rd to 27th, 2019 / San Luis Potosí, México

THIN FILMS (THF) POSTER SESSIONS



[THF-72] GaInAsSbN epitaxial layers growth on GaSb by LPE

VICTOR HUGO COMPEÁN JASSO (*compean9@gmail.com*) ¹, FRANCISCO JAVIER DE ANDA SALAZAR ², ANDREI GORBATCHEV ², VIATCHESLAV MISHURNYI ², CLAUDIA VERONICA SILVA JUAREZ ², ULISES ZAVALA MORAN ²

¹ CÁTEDRA CONACYT adscrito al Instituto de Investigación en Comunicación Óptica, UASLP

² Instituto de Investigación en Comunicación Óptica, Universidad Autónoma de San Luis Potosí.

Incorporation of Nitrogen in epitaxial layers with LPE technique at temperatures under 1000 °C used to be quite difficult because of the very low segregation of GaN on In or Ga. In this work, we tried to grow GaInAsSbN on n type GaSb tellurium doped substrate with liquid phase epitaxy technique at temperatures below 550 °C. We compare 3 different samples and analyze some difference between them. Sample S1 was grown with polycrystalline GaN powder always in contact with the liquid phase system Ga-In-As-Sb. Sample S2 was grown with a previous reaction of drops of nitric acid (HNO₃) with some Gallium and Indium pieces and then join them after the reaction with the rest of materials to make the alloy Ga-In-As-Sb. Sample S3 is just a well known GaInAsSb growth. The 3 samples were grown by LPE technique on Sapphire boat at the same growth temperature and with the same composition of materials in liquid phase. Here we compare photoluminescence spectrum measures of each one.



[THF-104] Deposit of Zn-Sn-O thin films by Magnetron Co-Sputtering and their performance as photocatalyst in hydrogen production

Maria Rocio Alfaro Cruz (alfachio@gmail.com)¹, Anakaren Saldaña-Ramírez², Isaias Juárez-Ramírez²

¹ CONACYT- Universidad Autónoma de Nuevo León, Facultad de Ingeniería Civil, Departamento de Ecomateriales y Energía, Av. Universidad S/N Ciudad Universitaria, San Nicolás de los Garza, Nuevo León, C.P. 66455, México

² Universidad Autónoma de Nuevo León, Facultad de Ingeniería Civil, Departamento de Ecomateriales y Energía, Av. Universidad S/N Ciudad Universitaria, San Nicolás de los Garza, Nuevo León, C.P. 66455, México

Zinc Tin Oxide (ZTO) is a ternary oxide n-type semiconductor with high electron mobility and interesting optical properties, which make it suitable for gas sensors, solar cells, lithium-ion batteries, and photocatalytic applications. Regarding photocatalytic applications, Zinc Tin Oxide has proven to be efficient in different photocatalytic processes, such as the degradation of organic dyes and hydrogen production. In this sense, Zn-Sn-O thin films were deposited by Magnetron Co-Sputtering varying the deposit conditions and their effect on the final film properties. These films were deposited from a metallic Zn and Sn target, at different working pressures. When the work pressure decrease, the structural properties of the films were modified, influencing their photocatalytic efficiency. Zn-Sn-O thin films were characterized by X-ray diffraction (XRD), UV-Vis spectroscopy, Scanning Electron Microscopy (SEM), Atomic Force Microscope (AFM) and Photoluminescence spectroscopy (PL). The thin film photocatalytic activity was evaluated using a chromatograph with a thermal conductivity detector (TCD). Results will be discussed.

Keywords: Zn-Sn-O, thin films, Co-Sputtering, photocatalysis, hydrogen production



[THF-126] Synthesis and characterization of ZnS coatings chemically deposited by a simple and non-toxic method

E.A. Ordaz-Fernández (malexordaz@hotmail.com) ¹, D.L. García-Antonio ¹, M.B. Ortúñoz-López (mbortuno@mail.itq.edu.mx) ¹, G. Barreiro-Rodríguez ¹, R. Flores-Farías ², J.M. Yáñez-Limón ², R. Ramírez-Bon ², A.L. González-Rostro ¹, V. Chávez-Guzmán ¹, J.A. Navarro-Martínez ³

¹ Departamento de Metal-Mecánica; Tecnológico Nacional de México / I. T. Querétaro; Av. Tecnológico s/n esq. Gral. Mariano Escobedo. Colonia Centro Histórico C.P. 76000, Querétaro, Qro.

² Laboratorio Nacional de Investigación y Desarrollo Tecnológico de Recubrimientos Avanzados, LIDTRA; CINVESTAV; Libramiento Norponiente #2000, Fracc. Real de Juriquilla. C.P. 76230, Querétaro, Qro. México

³ Universidad Autónoma de Querétaro; Centro Universitario (CU) Cerro de las Campanas. Cerro de las Campanas s/n, Querétaro, Qro. C.P. 76100.

In this work is proposed a chemical bath deposition (CBD) method for growth of high quality ZnS thin films. ZnS has a wider band gap, non toxicity and abundance in nature, reasons why ZnS thin films prepared by CBD method can be a better option than CdS thin films, for the buffer layer of thin film solar cells based Cu(InGa)Se₂, and other photovoltaic or optoelectronic devices. A CBD method simple, cheap and environmental friendly has developed, using an ammonia free reaction solution and low deposition temperature. The films were fabricated, and then characterized by XRD, Perfilometry, Uv-Vis Spectroscopy, Fluorescence Spectroscopy and Resistivity analyses. It was proved the formation of ZnS and their high potential, studying some structural, morphological, optical and electrical properties, such as: crystalline structure, thickness, transmission and emission of radiation, band gap and electric resistivity.



[THF-131] Effect of complexing agent and sulfur source on Cu₂SnS₃ thin films obtained by chemical bath deposition

Johan A. Vargas Rueda (*andhy312@gmail.com*) ², Mónica A. Botero Londoño ⁵, Alejandro R. Alonso Gómez ³, M. Meléndez-Zamudio ⁶, J. Cervantes ⁶, S. Y. Reyes-Lopez ⁴, Orlando Zelaya ¹, Miguel A. Meléndez Lira ¹

¹ Centro de Investigación y de Estudios Avanzados del Instituto Politécnico Nacional,
Departamento de Física

² Universidad Autónoma Metropolitana

³ Universidad Autónoma Metropolitana, Departamento de Ingeniería Química

⁴ Universidad Autónoma de Ciudad Juárez, Instituto de Ciencias Biomédicas

⁵ Universidad Industrial de Santander, Escuela de Ingeniería Eléctrica, Electrónica y de
Telecomunicaciones

⁶ Universidad de Guanajuato: División de Ciencias Naturales y Exactas

Currently, semiconductors from non-toxic metal chalcogenide family have aroused great interest as candidate for absorbing layer in thin film solar cell due to their physical properties such as band gap energy, absorption coefficient, high photo-stability, low cost and earth abundant. Among those, Cu₂SnS₃ (CTS) is the material with most suitable photovoltaic properties as absorber layer as p-type conductivity, high absorption coefficient (10^5 cm^{-1}), band gap in a range of 1.1-1.5 eV and environmentally friendly. This work involves the synthesis and characterization of Cu₂SnS₃ (CTS) thin films. The films were prepared on glass substrates by simple and inexpensive chemical bath deposition method at a bath temperature of 90°C. Films were produced using three different complexing agents -ethanolamine, triethanolamine and sodium citrate- and two sulfide ion source - thiourea and sodium thiosulfate-. The structural and optical properties were studied by GIXRD and Raman spectroscopy. Experimental results indicate that Cu₂S is the predominant compound but there are also presence of Sn₃S₄, SnS₂ and Cu₂SnS₃ compounds. The species distribution of Sn(II)-citrate and Cu(II)-citrate are investigated and the results presented as speciation diagrams. The dependence of phase and dominant species in citrate ion and bisulfide concentration depending on pH were studied. The results allow us to report the synthesis conditions for the formation of CTS films employing sodium citrate as complex agent and thiourea as source of bisulfide.



[THF-133] Equipment manufacturing and some results of successive deposition of SnO layers

Antonio Del Rio-De Santiago (adelrio22@gmail.com)⁶, Karla María Méndez Martínez², Flavio Manuel Nava-Maldonado³, Victor Hugo Méndez-García¹, Marlen Hernández-Ortiz⁴, David Armando Contreras-Solorio⁵, Juan Carlos Martínez-Orozco⁵

¹ Center for the Innovation and Application of Science and Technology UASLP

² Unidad Académica de Ciencias Nucleares, Universidad Autónoma de Zacatecas

³ Unidad Académica de Ciencias Químicas, Universidad Autónoma de Zacatecas

⁴ Unidad Académica de Economía, Universidad Autónoma de Zacatecas

⁵ Unidad Académica de Física, Universidad Autónoma de Zacatecas

⁶ Unidad Académica de Ingeniería, Universidad Autónoma de Zacatecas

Acquiring thin film deposit equipment involves a large investment, and depending on the chosen technique, appropriate facilities and possibly electricity supply, refrigeration, compressed air and vacuum equipment are required. The sources of financing are each time more scarce, so the design and own-making equipment becomes an option in this days. The study and deposit of transparent conductive films is an active field of physics and chemistry, for its use in electronic devices, such as flat screen televisions and solar cells. Transparent conductive films have wide bandwidth whose energy value is greater than those of visible light and are normally used as electrodes when a situation requires low resistance electrical contacts without blocking the light. As such, these materials do not absorb photons with energies below the band gap value and visible light passes through them. The possibility of implementing semi-transparent solar cells in the windows of the houses increases the need for these materials. The technique of Successive Ionic Layer Adsorption and Reaction (SILAR) has the advantage of being able to scale according to the needs and be carried out at atmospheric pressure conditions. In this work we show the results of making our own SILAR equipment and the conductivity and absorbance of SnO₂ films deposited on glass, with the aim of using this material for the aforementioned purposes, achieving average conductivities of 0.002-0.14671 (Ω-cm)⁻¹. Characterization by Uv Vis produces values at 400-460 nm for the band interval depending on the concentration of tin. The deposit and electrical characterization equipment was manufactured at the Autonomous University of Zacatecas.

Keywords: SILAR, Deposition of materials, Photovoltaic applications.



[THF-137] "Synthesis and simulation of thin films with the software SIMTRA, RSD2013 and Co-SS"

Karla León Zúñiga (karlaxlzu@gmail.com)², Julio Cruz Cárdenas (juliocruz@cnyn.unam.mx)¹, Roberto Sangines De Castro¹, Roberto Machorro Mejía¹

¹ Universidad Nacional Autónoma de México

² Universidad Tecnológica De Querétaro

Growing thin films with the sputtering technique, is very popular among the different methods of deposition for laboratories and the industry of coatings. Its highlights are the capacity to deposit several elements and compounds, giving good thin films properties, for example, density, adhesion to the substrate, resistivity, refractive index, among others. Its applications range from medical, decorative, mechanical, tribological, electrical, magnetic, optical, surface energy, biocompatibility, etc.

The Simulation Transport code (SIMTRA¹) was developed to simulate the flow of metal during the sputtering process; using predefined surfaces for a geometric representation giving conditions such as position, energy and direction based on the atoms sputtered from the target. Reactive Sputter Deposition 2013 (RSD2013²) simulates the process of reactive sputtering in function of parameters (voltage, current, flow and pumping speed), focused on the hysteresis cycle. Co-Sputtering Simulation (Co-SS³), reactive mode (Co-SS Rm³), models the thickness distribution of a thin film and the angular distribution of the atoms sputtered from the target.

In this work the sputtering process was simulated. Data input were, for a circular target of 2", a substrate of 1" x 2", and a distance target-substrate of 4.5 cm. The parameters used for SIMTRA were the type of surface by binary collision Monte Carlo. In RSD2013, the parameters were the reactive gas flow, pumping speed, voltage and current. And, finally, for Co-SS: sputtering yield, angular distribution and atoms sputtered from the target, geometry and size of the racetrack, the material contribution to the racetrack area, or quantity of material making up the target (for targets composed from 2 elements), target-substrate distance and the area where the compound is formed on the racetrack, oxide o nitride (for reactive sputtering).

We compared simulations from these codes taking into account the angular distribution of the sputtered atoms from the target, thickness distribution and sputtering yield, the similarity with the data obtained from experimental deposits was analyzed.

- [1] D.Depla & W.P.Leroy. (2012). Magnetron sputter deposition as visualized by Monte Carlo modeling. Elsevier: volume 520, Issue 20, 1 August 2012, Pages 6337-6354
- [2] K Strijckmans and D Depla. (2014). A time-dependent model for reactive sputter deposition. Journal of Physics D: Applied Physics, Volumen 47. 1-23.
- [3] J. Cruz, E. Andrade, S. Muhl, C. Canto, O. de Lucio, E. Chávez, M.F. Rocha, E. Garcés-Medina (2016). Ion beam analysis and co-sputtering simulation (CO-SS) of bi-metal films produced by magnetron co-sputtering. Elsevier: volume 371, 15 March 2016, Pages 268-272



XII -ICSMV

September 23rd to 27th, 2019 / San Luis Potosí, México

[THF-283] Physical Properties of Sputtered CdTe:O Films Deposited on Flexible Transparent and glass slide Substrate

Marcelino Becerril (becerril@fis.cinvestav.mx)¹, Miguel Meléndez¹, Alejandra García¹,
Orlando Zelaya¹

¹ Departamento de Física, Centro de Investigación y de Estudios Avanzados, Instituto Politécnico Nacional (IPN), Apartado Postal 14-740, D.F. 07300, México

Oxygenated amorphous cadmium telluride (n-CdTe:O) thin films were grown on polyethylene naphthalate (PEN) and glass slide substrates at room temperature by radio frequency magnetron sputtering technique in a controlled plasma (N-O). Photoluminescence and optical absorption spectra show that the bandgap Eg of the films depends on the oxygen concentration. Moreover X-rays and Raman spectra show that films of CdTe:O are strongly affected on the oxygen concentration insomuch that explode when removed from the growth chamber. The films on PET there is explosion and on the glass slide not. Eg can be changed in a controlled way in the range from 1.5 eV to 1.8 eV. The film composition was determined by Energy Dispersive Spectroscopy (EDS).



[THF-336] Growth of superconducting tantalum nitride thin films on MgO substrates by pulsed laser deposition

Michelle Ivonne Cedillo Rosillo², Jesús Antonio Díaz Hernández (*olaf@cnyn.unam.mx*)²,
Víctor Manuel Quintanar Zamora¹, Óscar Edel Contreras López²

¹ Centro de Investigación Científica y de Educación Superior de Ensenada

² Centro de Nanociencias y Nanotecnología, UNAM

Since their discovery at 1911 by Kamerlingh Onnes, the superconductivity has been a promising property of specific materials that is important for scientist and engineers. Particularly, the superconducting materials have applications in lossless energy power supply, transport levitation and development of nanometric electronic devices. In this last, efficient fabrication of materials with a low superconductive energy gap and an intermediate transition temperature (T_c), results essential for the development and enhance of superconductive electronic devices in the GHz range. TaN thin films have previously showed superconductive transition temperatures up to 10.4 K with a superconductive energy gap lower than NbN, the most commonly used material for single photon detectors in the GHz range. The T_c of tantalum nitride depends strongly of the crystallinity and stoichiometry of the thin films. In the present work, the superconductive thin films of tantalum nitride grown on MgO (100) substrates by using laser ablation technique with a Nd-YAG laser on a Ta target (99.95%) varying the N₂ (99.999%) partial pressure in the chamber as well as substrate temperature were obtained. X-Ray Diffraction Spectroscopy with a Panalytical X'pert Pro MRD (DRX) and Transmission Electron Microscopy with a JEOL JEM-2100F (STEM), X-Ray Photoelectron Spectroscopy (XPS) with a X-ray monochromatic source and semispherical analyzer from SPECS, were obtained in order to study the crystallography and stoichiometry respectively. The R vs T curve of the films were obtained by using Van der Pauw method.

Acknowledgments

We would like to thank E. Aparicio, I. Gradilla, E. Murillo and D. Domínguez for the characterization of the samples. This work was supported by CONACyT-FORDECyT project 272894.



[THF-512] Bismuth vanadate BiVO₄ thin films deposited by pulsed laser deposition

F. Gonzalez-Zavala (fernngoz@hotmail.com)³, D. A. Solis-Casados¹, L. Escobar-Alarcon²,
E. Haro-Poniatowski³

¹ Centro Conjunto de Investigación en Química Sustentable UAEM-UNAM, Carretera Toluca-Atlacomulco Km 14.5, Unidad San Cayetano, Toluca, Estado de México, 50200, México

² Departamento de Física, Instituto Nacional de Investigaciones Nucleares. Carretera México-Toluca s/n, La Marquesa, Ocoyoacac, Edo. de México, C. P. 52750, México

³ Departamento de Física. Universidad Autónoma Metropolitana Iztapalapa. San Rafael Atlixco No. 186, Col. Vicentina, Iztapalapa, 09340, México

Thin films of bismuth vanadate BiVO₄ were prepared by pulsed laser deposition technique. High purity vanadium and bismuth targets were ablated using a Nd:YAG (355 nm) laser in vacuum at working pressures close to 5×10^{-5} torr. During experiments the plasma parameters, mean ion kinetic energy and plasma density, of vanadium and bismuth remain approximately constant. Ratios of ablation time in the two targets were varied in order to obtain different bismuth/vanadium content in the deposited thin film. Glass and silicon substrates were employed. Afterwards, the thin films were subjected to thermal treatment at 450 °C/120 min to obtain crystalline oxides. XPS characterization reveals that the composition of the thin films were mainly composed of bismuth and vanadium in oxidate state, oxygen and adventitious carbon. Raman spectroscopy shows that the thin films were composed by mixtures of Bi₂O₃ and BiVO₄ in different proportions as well as the presence of V₂O₃ for the films prepared with higher vanadium content. UV-vis spectroscopy reveals a red shift displacement as the vanadium content increases. These films could have potential applications for photocatalytic applications.



[THF-575] Effects of target's precursors in optical and structural properties of CZTS thin films grown by pulsed laser deposition

Javier Issac Vega Hernández (javier.issac.vega@gmail.com)⁴, Paola Rodríguez Hernández³, Miguel Meléndez Lira², José Santos Cruz³, Miguel Ángel Santana Aranda¹, Armando Pérez Centeno¹, Gilberto Gómez Rosas¹, Arturo Chávez Chávez¹, José Guadalupe Quiñones Galván (jose.quinones@academicos.udg.mx)¹

¹ Departamento de Física, Centro Universitario de Ciencias Exactas e Ingenierías, Universidad de Guadalajara, Boulevard Marcelino García Barragán 1421, Guadalajara, Jalisco, México, C.P. 44430

² Departamento de Ingeniería Eléctrica, Sección de Estado Sólido, Cinvestav-IPN, Apdo. Postal 14-740, Ciudad de México, 07360, México

³ Facultad de Química, Materiales, Universidad Autónoma de Querétaro, Querétaro, 76010, México

⁴ Maestría en Ciencia de Materiales, Departamento de Ingeniería de Proyectos, Centro Universitario de Ciencias Exactas e Ingenierías, Universidad de Guadalajara, Boulevard Marcelino García Barragán 1421, Guadalajara, Jalisco, México, C.P. 44430

The structural and optical properties of Cu₂SnSnS₄ (CZTS) thin films of CZTS deposited by pulsed laser deposition were studied as a function of the precursors used for the target. Two targets were created by manually compacting CuS, Zn, SnS, S and Sn powders. In the first, a mixture of CuS, Zn, S and SnS was used; while in the second a mixture of CuS, ZnS, Sn, S having both targets molar ratio of 2:1:1:1 respectively. The films were deposited using a Nd: YAG laser with a wavelength of 1064 and 532 nm on glass substrates. The distance between the target and the substrate was varied from 4 to 5 cm while the working pressure and the deposition time remained constant. The films were structurally characterized using the techniques of X-ray diffraction and Raman spectroscopy. The optical characterization was carried out by UV-Vis spectroscopy.

**[THF-681] Study of the mechanical properties of cubic InGaN.**

Sergio Agustín García Hernández (sergioagustin.ghdz@gmail.com)², Miguel Ángel Vidal Borbolla², Vicente Damián Compeán García¹, Edgar López Luna²

¹ CONACyT—Coordinación para la Innovación y la Aplicación de la Ciencia y la Tecnología (CIACYT), Universidad Autónoma de San Luis Potosí, Álvaro Obregón 64, 78000 San Luis Potosí, S.L.P., México

² Coordinación para la Innovación y la Aplicación de la Ciencia y la Tecnología (CIACYT), Universidad Autónoma de San Luis Potosí, Álvaro Obregón 64, 78000 San Luis Potosí, S.L.P., México

The use of semiconductors in optoelectronic and electronic devices is having a significant impact at present, the GaN semiconductor in cubic phase is one of the most important for which it seeks to increase its efficiency, strength, and durability. In this work, a series of InGaN thin film samples were grown with concentrations ranging from 27% to 72%, on cubic GaN layers by plasma-assisted molecular beam epitaxy (PAMBE)¹. The XRD results show a dominant diffraction peak for the plane (002) of the zinc-blend InGaN structure, and atomic force microscopy shows a mosaic morphology associated with the cubic crystalline structure. Employing the Nanoindentation technique, with a Berkovich type diamond tip, the load-displacement curves were obtained. These curves were analyzed using the method proposed by Oliver-Pharr² to obtain the Hardness and Young's Modulus, which is the main interest of this research because these mechanical properties have not been studied experimentally for β -GaN and β -InGaN (cubic phase). Elastic-plastic transition phenomena (pop-in) were observed in only a range of depth of the load-displacement curve during loading; these transitions are mainly due to dislocations nucleation.

The hardness and Young's modulus for InN was 12.6 ± 0.4 GPa and 358.8 ± 6.7 , respectively. For GaN, the values of hardness and Young's modulus were 21.5 ± 1.1 GPa and 292.9 ± 11.7 GPa, respectively. The InGaN thin films vary the mechanical properties between GaN and InN, according to the concentration of In.

Keywords: Nanoindentation, PA-MBE, Hardness, Elasticity, Gallium nitride.

¹V. D. Compeán García, I. E. Orozco Hinostroza, A. Escobosa Echavarría, E. López Luna, A. G. Rodríguez, and M. A. Vidal, "Bulk lattice parameter and band gap of cubic $\text{In}_x\text{Ga}_{1-x}\text{N}$ (001) alloys on MgO (100) substrates," *J. Cryst. Growth*, vol. 418, pp. 120–125, 2015.

²W. C. Oliver and G. M. Pharr, "Measurement of hardness and elastic modulus by instrumented indentation: Advances in understanding and refinements to methodology," *J. Mater. Res.*, vol. 19, no. 1, pp. 3–20, 2004.



XII -ICSMV
September 23rd to 27th, 2019 / San Luis Potosí, México

TRIBOLOGY

(TRB)

Chairmen: Enrique Camps Carvajal (ININ)
Giovanni Ramirez (Bruker Nano Surfaces)



XII -ICSMV

September 23rd to 27th, 2019 / San Luis Potosí, México

[TRB-79] Tribological properties of AlSiN and SiON thin films deposited by laser ablation

Enrique Camps (*eecamps2@hotmail.com*)³, Enrique Campos³, Stephen Muhl¹, Laura Rivera²

¹ IIM, UNAM

² IIM-UNAM

³ ININ, Depto. de Física

Multifunctional materials are of great interest for academic or industrial purposes, as they can combine at least two properties in the same material. In the present work AlSiN and SiON compounds in the form of thin films deposited by the laser ablation technique are studied in terms of their mechanical and tribological properties. In both compounds the energy band gap can be modulated so as to obtain a highly transparent material. For the case of the AlSiN films this transparency can be combined with a high hardness (up to 30 GPa). For the case of the SiON films the transparency can be combined with a moderated hardness of about 14 GPa, and an intense visible photoluminescence. The properties of each compound depend on the experimental conditions used for their fabrication. The AlSiN compound varies its properties as a function of the silicon content and the SiON compound varies its properties as a function of the nitrogen working pressure. Scratch tests were carried out on samples prepared with different experimental conditions and a correlation of the tribological properties with the mechanical and optical properties is presented.



[TRB-83] Tribology and Impedance testing of natural rubber pristine and filler with carbon nanostructures

Diana Litzajaya García-Ruiz³, Jael Madaí Ambriz-Torres³, Carmen Judith Gutiérrez-García³, Jaime Abraham Guzmán-Fuentes³, Francisco Gabriel Granados-Martínez⁴, José de Jesús Contreras-Navarrete², Nelly Flores-Ramirez³, Luis Zamora-Pereido¹, Ricardo Orozco-Cruz¹, Leandro García-González¹, Lada Domratcheva-Lvova
(ladamex@yahoo.es)³

¹ Centro de Investigación en Micro y Nanotecnología, Universidad Veracruzana, Veracruz Boca del Río, México.

² Instituto tecnológico de Morelia, Avenida Tecnológico 1500, 58120 Morelia, Michoacán

³ Universidad Michoacana de San Nicolás de Hidalgo, Av. Francisco J. Mújica S/N, Morelia, Mich., México, 58030, México.

⁴ Universidad Nacional Autónoma de México, ENES, Campus Morelia, 58190 Morelia, Michoacan

Nowadays rubber has wide applications in engineering as vibration dampers, packing materials and electrical applications. Moreover as polymer composites, consisting of an insulating matrix reinforced with suitable conducting or semi-conducting particles, it finds application in several electrical and electronic systems. Besides acting as conducting and semi-conducting materials in electronic industries, polymer composites are also used for electromagnetic and microwave shielding applications. The carbon nanostructures were synthesized by chemical vapor deposition using isopropanol as precursor. The aim of the present work is to obtain composites of natural rubber with nanostructures to enhance the rubber properties and application. The composites contain 1% to 3% carbon nanostructures respect to rubber (phr). Composite films were obtained through natural rubber as polymeric matrix and carbon nanostructures in acetone dissolution. The solution was heated at 100 °C during 8 hours to evaporate the solvent and complete the vulcanization. Samples obtained via this process were analyzed by Scanning Electron Microscope and Raman Spectroscopy. The Raman spectra showed the characteristic G and D band of the nanostructure and some rubber bands lightly displaced. Tribology friction and impedance properties were evaluated by Microtribometer and Pontentiostat/Galvanostat respectively. The tribological properties of, cis-1,4-polyisoprene (natural rubber), and this reinforced with nanostructures (1 to 3% wt.) were examined. The effect of adding carbon nanostructures (CNS) on the friction characteristics and impedance was evaluated. Dry friction tests were carried out using pin-on-cylinder tribometer (100Cr6) under different operating conditions such as applied normal load (1 and 2 N), sliding speed (0.3–1.5 m/s) and sliding distance (90–500 m). Our experimental results showed that the addition of CNS was significantly affected the friction characteristics of natural rubber to reduce the abrasion weight loss up to 35% respect to unfilled rubber, depending on the CNS concentration. The friction coefficient of natural rubber was decreased about 12.5% upon the addition of 2 phr CNS, compared to unfilled natural rubber. The impedance analysis has been studied as a function of filler loading. The effect of frequency (8.0 to 12.5 GHz) on electrical characteristics has also been depicted. The nanostructures obtained contained metallic nanoparticles which joined to the nanocomposites improve the application of the sensors due to their electrical conductivity.

Acknowledgment of “UMSNH”, “MICRONA-UV” and to “CONACYT”.



[TRB-375] Tribological characterization of UHMWPE coated with Ti and Ti/TiN deposited by DC magnetron sputtering.

Ernesto García (edgb007@hotmail.com)¹, Sandra Violeta Guzmán Ayón², María del Pilar Jadige CEBALLOS MUEZ², Martín Flores Martinez⁴, Stephen Muhl³

¹ Cátedras-CONACyT, Universidad de Guadalajara, CUCEI, Depto. De Ingeniería de proyectos, Guadalajara, Jalisco, México.

² Instituto Tecnológico y de Estudios Superiores De Occidente, Tlaquepaque, Jalisco, México.

³ Universidad Autónoma de México, Instituto de Materiales, Coyoacan, Ciudad de México, México.

⁴ Universidad de Guadalajara, CUCEI, Depto. De Ingeniería de proyectos, Guadalajara, Jalisco, México.

The application of the polymer material in tribological field is very important, especially in the industry and biomedical applications, where these materials are including such as gears, sliding surfaces and artificial devices into the human body. The transference of materials when a polymeric surface to polymeric and not polymeric surfaces are on contact and relative motion is one of the main problems in the polymer tribological application. This work presents the tribological characterization of Ti and two Ti/TiN films on UHMWPE polymer substrate produced by DC-magnetron sputtering. The films were deposited on UHMWPE and Si wafer substrate obtained from a commercial source. A Ti target of 2" of diameter with a 40 W of power and 60 min of time deposition was used to produces the Ti and the Ti/TiN bilayers. The Ti/TiN bilayers were deposited with 40 and 20 min of Ar plasma and 20 and 40 min of N₂/Ar plasma, respectively. The films were structural, chemical, topographic and morphology characterized using X-ray diffraction, EDS and SEM, respectively. The adhesion of the layers to the polymer substrate was studied using a scratch test under incremental load performance from 0.2 to 10 and 40 N. The tribological characterization was carried out in a sliding-contact test under reciprocating movement at 1, 2 and 3 N, using a ZrO₂ counterbody of 5 mm of diameter with 1800 time and 1 Hz per sliding test. The friction force produced during the sliding-contact test was registered in real-time, while the wear tracks were characterized by contact profilometry and optical and electronic microscopy. The structure of the films on both substrates presented the peak of Ti phase. The wear produced on the UHMWPE with the Ti film did not present polymer damages while on Ti/TiN film was observed high abrasion wear marks.



AUTHORS

Abenuz Ruben *SIF-2*
Abenuz Acuña Juan Rubén *TSM-6*
Abundiz Noemi *PLV-647*
Abundiz Cisneros Noemí *PLV-132*
Abundiz Cisneros Noemi *CHM-61, CHM-274*
Abundiz Cisneros Noemi *CHM-39, CHM-63*
abundiz-cisneros noemí *THF-259*
Aca Aca Victor *MEM-90*
Acosta Brenda *NSN-603*
Acosta Dwight *SIF-649*
Acosta Esparza Marco Aurelio *RWE-554*
Acosta Ruelas Brenda *NSN-261*
Agacino-Valdes Esther *TSM-311*
Agarwal Vivechana *SEM-282*
Aguila Juan *CHM-61*
Aguila Muñoz Juan *CHM-63, CHM-274, CHM-39*
Aguilar Frutis Miguel *LPM-93, LPM-73*
Aguilar Gonzalez Juan Pablo *MEM-270*
Aguilar Hernández Jorge Ricardo *RWE-622*
AGUILAR-FRUTIS MIGUEL A. *LPM-688*
Aguilar-Frutis Miguel Ángel *NSN-66*
Aguilar-Frutis Miguel Ángel Aguilar-Frutis *NSN-174*
Aguilar-García Omar *NSN-656*
Aguilera González Elsa Nadia *SEM-145*
AGUIRRE DELGADO JULIO *THF-592*
Aguirre Tostado Francisco Servando *ALD-301*
Aguirre Tostado Francisco Servando *ALD-291*
Aguirre Tostado Servando *ALD-266*
Aguirre-Tostado Francisco Servando *THF-686, THF-535*
Alarcón Flores Gilberto *LPM-281*
Alarcón-Flores Gilberto *NSN-174, NSN-66*
Alarcon Flores Gilberto *LPM-73*
Alarcon Flores Gilberto *LPM-93*
ALARCON-FLORES GILBERTO *LPM-688*
Alaskar Yazeed *NSN-343*
Alavarado Paul *SIF-649*
Alcantar Peña Jesús Javier *MEM-411*
Alcantar Peña Jesús Javier *MEM-621*
Alcántara Iniesta Salvador *NSN-46*



Alda Javier *NSN-676*
Alejos Palomares María Teresa *PLV-631*
Aleman Miguel *MEM-306, MEM-276*
Aleman Miguel Angel *MEM-135*
Alfaro Cruz Maria Rocio *THF-104*
Alfaro López Hilda Margarita *NSN-53*
Almaral Sánchez Jorge Luis *THF-60*
Almaral Sánchez Jorge Luis *NSN-295*
Almaral-Sánchez Jorge Luis *THF-56*
Almora Osbel *RWE-672*
Alonso Gómez Alejandro R. *THF-131*
Alonso Núñez Gabriel *NSN-46*
Alva Suárez Erika *TSM-127*
Alvarado Elizabeth *BIO-531*
Alvarado Jose Alberto *NSN-530*
Alvarado Estrada Ahtziry Guadalupe *CHM-617*
Alvarado Gómez Elizabeth *BIO-577*
Alvarado Kinnell Gustavo *NSN-652*
Alvarado Pulido José Joaquín *NSN-46*
Alvarado Veloz Mario Alberto *CHM-106*
Alvarado-Leyva Pedro Gilberto *NSN-22*
Alvarez Carlos *BIO-630*
Alvarez Luis *MEM-306*
Alvarez Marco Antonio *BIO-630*
Alvarez Sánchez Daniela *BIO-667*
Alvarez Simón Luis Carlos *MEM-502*
Alvarez Vera Melvyn *CHM-140*
Alvarez-Ortega Oskar *BIO-587*
Alvarez-Ortega Oskar Alejandro *BIO-602, BIO-607*
Ambriz-Torres Jael Madaí *NSN-81, NSN-656, BIO-82, CHM-85, TRB-83*
Ananthakumar Soosaimanickam *LPM-73*
Anaya Garza Karelly *BIO-78*
Anzueto Álvaro *CHM-617*
Araiza Ibarra José de Jesús *PLV-169, LPM-413, PLV-153*
Araiza Ibarra José de Jesús *PLV-631, TSM-267*
Araiza Ibarra José De Jesús Araiza Ibarra *SEM-265*
Aranda García Rubén Jonatan *AMC-187, SEM-5*
Aranda González Erick Saúl *BIO-278*
Arellano Arreola Víctor *NSN-263*
ARELLANO ARREOLA VICTOR *NSN-18*
Arellano Arreola Victor Manuel *SEM-69*
Arellano-Piña Luis Ramon *NSN-279*



Arenas Flores Alma Delfina *NSN-652*
Arias San Elías Alejandra *CHM-30*
Arias-Cerón J.S. *PLV-541, PLV-546*
Ariza Flores Augusto David *SEM-287, SEM-282*
Ariza-Flores David *LPM-185*
Arizmendi Morquecho Ana *ALD-372*
Arjona C. *RWE-678*
Armenta-Monzón Fabiola *LPM-185*
Arredondo-León Yesenia *BIO-82*
ARREOLA-PINO Alma Sofia *SEM-511*
Arreola-Reyes Adán Eduardo *BIO-24*
Arroyo Escareño Adrián Alberto *TSM-628*
Atanacio-Gelover A.L. *BIO-262*
Atondo- Rubio Gelacio *TSM-671*
Atzori Marco *BIO-636*
Auvray Florent *SIF-288*
Avelar Muñoz Fernando *SEM-265, PLV-631, PLV-169, PLV-153*
Avila Alvarado Yuliana Elizabeth *TSM-627*
Avila Herrera Carlos Alberto *AMC-645*
Avila-Avendano Carlos *THF-123, THF-122*
Águila Juan *PLV-647*
Águila Muñoz Juan *PLV-132*
Álvarez García Susana *NSN-307*
Álvarez Vera Melvyn *CHM-106, CHM-108*
Ávila Alvarado Yuliana Elizabeth *SEM-145*
Ávila García A. *NSN-284*
Bach Horacio *BIO-17*
Balderas Jesús Uriel *LPM-299*
Balderas Jesus Uriel *ALD-301*
Balderas Uriel *LPM-310*
Balderas Aguilar Jesús Uriel *ALD-266*
Balderas Navarro Raúl *LPM-180*
Balderas Navarro Raul Eduardo *SEM-282*
Balderas-Aguilar Jesus Uriel *LPM-509*
Balderas-López José Abraham *NSN-660*
Balderas-Navarro Raúl *SEM-272*
Balderas-Navarro Raul *SIF-288, THF-149*
Baltazar Méndez Claudia Carolina *MEM-621*
Baltazar-Méndez C.C. *MEM-654*
Barboza Flores Marcelino *NSN-307*
Barraza Garcia Felipe de Jesus *NSN-402*
Barreiro-Rodríguez G. *THF-126*



Barrera del Ángel David *CHM-617*
Barrientos Valeriano Angélica María *SEM-5*
Bautista-Baños Silvia *BIO-59*
Bazan Diaz Lourdes *NSN-666*
Becerra Rodríguez María Blanca *BIO-67*
Becerril Marcelino *SEM-670, THF-283*
Becerril Landeros Luis Alberto *NSN-508*
Belio-Manzano Alfredo *RWE-613, SEM-610*
Bello Jiménez Miguel Angel *MEM-357*
Benito Santiago Sandra Edith *SIF-188, SIF-271*
Bermúdez Jiménez Carlos Omar *BIO-17*
Bermúdez Jiménez Carlos Omar *BIO-17*
Berumen Torres Javier Alejandro *PLV-631, TSM-267*
Berumen Torres Javier Alejandro *PLV-169, PLV-153, SEM-265*
Betancourt-Reyes J. Israel *AMC-533*
Biermann Klaus *SEM-287, SEM-282*
Bondarchuk Olexandr *SEM-176*
Botero Londoño Mónica A. *THF-131*
Bravo García Yolanda Elinor *NSN-26*
Bravo Sanchez Mariela *NSN-635*
Bravo-Rangel C. *BIO-262*
Bueno Carlos *NSN-530*
Cañetas-Ortega Jaqueline *SIF-52*
Caballero Fernando *TSM-109*
CABALLERO FRANCISCO *TSM-71*
Cabellos José Luis *TSM-58*
Cabrera-Salazar Jorge Valentin *RWE-349*
Calderón Martínez Abraham Israel *SEM-289*
Calderón Martínez María Claudia *NSN-307*
Calderón Zamora Mauricio *MEM-90*
Caldiño U. *LPM-675*
Caldiño Ulises *LPM-369*
Calleja Arriaga Wilfrido *MEM-528, MEM-412*
Calleja Arriaga Wilfrido *SCD-664*
Calvillo Anguiano Ana Ketzaly *NSN-29*
Camacho Espinosa Eduardo *RWE-588*
Camacho Martínez Daniel Esteban *BIO-547*
Camacho Reynoso Marlene *SEM-178*
Camacho-López Marco Antonio *NSN-374*
Camacho-López Miguel Angel *NSN-374*
Camarillo I. *LPM-675*
Camarillo Salazar Erika *TSM-627*



Campos Enrique *TRB-79*
CAMPOS GONZALEZ ENRIQUE *NSN-661, THF-151, THF-152*
CAMPOS GONZALEZ ENRIQUE *PLV-94*
Campos-González E. *NSN-549, PLV-546, PLV-541*
Camps E. *PLV-541, NSN-549, PLV-546*
Camps Enrique *PLV-305*
Camps Enrique *TRB-79*
CAMPSC. ENRIQUE *PLV-94*
CAMPSCARVAJAL ENRIQUE *THF-152, THF-151*
CANO-AGUILA OSCAR *TSM-71*
Capella Antonio *NSN-597*
Carbajal-Valdés Rigoberto *CHM-130*
Cardona-Cardona Abraham *SIF-601*
Carmona Salvador *LPM-299*
Carmona Carmona Abraham *SIF-260, SIF-139*
Carmona Carmona Abraham Jorge *ALD-121*
Carmona Rodríguez Julián Javier *SEM-289, SEM-176*
Carmona Téllez Salvador *LPM-281*
Carmona Telléz Salvador *LPM-496, LPM-369*
Carmona-Téllez Salvador *NSN-174, NSN-66*
CARMONA-TELLEZ SALVADOR *LPM-688*
Carrasco-Jaim Omar A. *RWE-373*
Carreón Aguiñaga Noé Martín *BIO-537*
Carrera-Escobedo Victor Hugo *NSN-597*
Carrillo Diana *SIF-2*
Carrillo Flores Diana Maria *AMC-551*
CARRILLO FLORES DIANA MARIA *AMC-682*
Carrillo-Castillo Amanda *BIO-24, BIO-35, BIO-25*
Carrillo-Medina Daniela *NSN-279*
CARRO GASTELUM ANAID *LPM-688*
Carvajal Quiroz Eliel *TSM-127*
Casallas Moreno Yenny Lucero *CHM-639, SEM-178*
Casallas-Moreno Y.L *SEM-143*
Casallas-Moreno Y.L. *NSN-147*
Castañeda Contreras Jesús *NSN-642*
Castañeda Priego Ramón *NSN-503*
Castanedo-Pérez Rebeca *AMC-645, CHM-347*
Castellanos Alvarado Estela Adriana *MEM-357*
Castillo Dulce Natalia *BIO-28*
Castillo Jhonathan *ALD-353*
Castillo Jhonathan *ALD-353*
Castillo-Baldivia Edith *SEM-272*



Castillo-Ocampo Patricia NSN-81
Castrejón Sánchez Víctor Hugo NSN-653
Castro Beltrán Andres NSN-295
Castro-Camus Enrique SEM-610
Castro-Chong Alejandra RWE-543
Castro-Garcia Ricardo THF-149
Caval-Velarde Javier G. AMC-533
Cazares-Montañez Javier THF-686
Cármona-Téllez S. LPM-675
CEBALLOS MUEZ Maria del Pilar Jadige TRB-375
Ceballos-Sánchez Oscar NSN-591
Cedeño Enrique CHM-138
Cedillo Rosillo Michelle Ivonne SIF-335, THF-336
Cerda Méndez Edgar Armando LPM-185, LPM-180, SEM-287
Cerda Méndez Edgar Armando SEM-282
Cerda-Méndez Edgar SEM-272
Cerna Cortez Jorge Raúl BIO-148
Cervantes J. BIO-298, THF-131
Cervantes Cervantes José Miguel TSM-127
Cervantes Contreras Mario SEM-506
Cervantes Juárez Erika LPM-581, SEM-580
Chalé Lara Fabio Felipe THF-687
Chavez-Urbiola Iker MEM-586
Chávez Chávez Arturo SEM-576, THF-575
Chávez Urbiola Iker Rodrigo THF-60
Chávez-Chávez A. PLV-546, PLV-541, NSN-549
Chávez-Guzmán V. THF-126
Chernov Valery NSN-307
Chipatecua Godoy Yuri SIF-139
Chirvony Vladimir LPM-73
Cira-Esquivel Juan Ignacio CHM-629
Cisneros Carrillo Hermenegildo CHM-633, CHM-641
Collazo Vázquez Jacob Adrián LPM-180
Compean García V. Damián SEM-679
Compean Jasso Martha E. NSN-29
Compean-Garcia V. Damian SEM-610
COMPEÁN JASSO VICTOR HUGO THF-72
Compeán García Vicente Damián THF-681
Compeán Jasso Martha Eugenia BIO-615
Compeán Jasso Martha Eugenia BIO-615
Concepción-Brindis Ignacio SIF-606, SIF-604
Conde Díaz Jorge Evaristo SEM-669



Conde-Gallardo Agustín *SEM-670*
Contreras López Óscar Edel *THF-336*
Contreras Puente Gerardo Silverio *RWE-622*
Contreras-Navarrete José de Jesús *NSN-81*
Contreras-Navarrete José de Jesús *NSN-656, TRB-83, CHM-85, BIO-82*
Contreras-Solorio David Armando *THF-133*
Coop-Santa Constanza Ibeth *NSN-591*
Corona García Carlos Antonio *TSM-648*
Corrales Mendoza Iván René *SEM-176*
Correa Pacheco Zormy Nacary *NSN-280*
Correa-Pacheco Zormy Nacary *BIO-59, NSN-374, CHM-130, CHM-129*
Cortazar Martínez Orlando *ALD-121, ALD-124*
Cortazar Martinez Orlando *SIF-260, SIF-139*
Cortazar-Martínez Orlando *SIF-601*
Cortés-López Alejandro J. *NSN-377*
Cortés-Mendoza A. *BIO-262*
Cortes Mestizo Irving Eduardo *SIF-634, NSN-624*
Cortes Vega Fernando Daniel *AMC-360*
Cortes-Mestizo I.E. *SEM-365, RWE-363*
Cortes-Mestizo Irving Eduardo *SEM-610, RWE-613, NSN-611, NSN-616, RWE-614*
Cortez Valadez Manuel *NSN-12*
Coyopol A. *LPM-350*
Crisóstomo Margarita C. *NSN-86*
Crisóstomo Reyes Margarita Clarisaila *TSM-127*
Cristo Yee *NSN-1*
Cruz Julio *PLV-132*
cruz julio *THF-259*
Cruz Cardenas Julio *CHM-63, CHM-61, CHM-39*
Cruz Cárdenas Julio *CHM-274*
Cruz Cárdenas Julio *THF-137*
Cruz Gabarain Lorena Conchita *CHM-39*
Cruz Gabarain Lorena Conchita *CHM-61*
Cruz Gaona Roel *BIO-537*
Cruz Garcia Cristian Felipe *SIF-52*
Cruz González Daniel *AMC-187*
Cruz Hernández Esteban *TSM-505, NSN-503, SEM-504*
Cruz Martínez H. *NSN-284*
Cruz Martínez Heriberto *NSN-53*
Cruz Martínez Karina *NSN-77*
Cruz Orea Alfredo *CHM-617, NSN-280*
Cruz Zaragoza Epifanio *LPM-584*
Cruz-Hernández Esteban *CHM-304, NSN-303*



Cruz-Irisson Miguel *NSN-86*
Cruz-Martinez Heriberto *RWE-290*
Cruz-Orea Alfredo *CHM-130*
Cuadrado Conde Alexander *NSN-676*
Cuautli Crstina *TSM-408*
Cuevas-González Juan Carlos *BIO-607, BIO-609*
Daneu N. *NSN-284*
Dante Mosca *SIF-32*
David Luevano Valdez David Luevano Valdez *SIF-150*
Díaz Alonso Daniela *MEM-412*
Díaz Becerril Tomás *SEM-662*
Díaz Cano Aarón I. *MEM-135*
Díaz Góngora José Antonio Irán *LPM-495, LPM-584*
Díaz Hernández Jesús Antonio *SIF-335, THF-336*
Díaz Hernández Jorge Isaac *TSM-58*
De Alba Montero Idania *BIO-615*
De Alba Montero Idania *NSN-29*
De Anda Gil Jessica *LPM-310*
DE ANDA SALAZAR FRANCISCO JAVIER *THF-72*
De la Cruz Terrazas Edna Carina *SIF-150*
de la Luz Merino Samuel *BIO-181*
de la Torre Medina Joaquin *NSN-545*
De la Vega Luis Ricardo *SIF-52*
De luna Bugallo Andrés *SEM-69, SEM-282, ALD-124, NSN-263, ALD-164*
De Luna Bugallo Andrés *NSN-352, SEM-163*
DE LUNA BUGALLO ANDRES *NSN-18*
de Luna-Bugallo Andrés *SEM-272*
de Melo Osvaldo *RWE-678*
de Moure Flores Francisco J. *PLV-107*
de Moure-Flores F. *PLV-541*
de Urquijo Ventura Maria de la Soledad *MEM-582*
del Pozo Zamudio Osvaldo *SEM-282*
Del Pozo Zamudio Osvaldo *LPM-180*
Del Pozo-Zamudio Osvaldo *SEM-272*
Del Pozo-Zamudio Osvaldo *LPM-185*
Del Rio Castillo Antonio Esau *NSN-34*
del Rio Portilla Antonio *SEM-282*
Del Rio-De Santiago Antonio *THF-133*
Diaz de León Zapata Ramón *RWE-632*
Diaz-Becerril T. *LPM-350*
Dilielgros-Godines Carolina Janani *CHM-347*
Domínguez Crespo Miguel Antonio *BIO-78*



Domínguez Pacheco Flavio Arturo *CHM-641, CHM-633*
Dominguez David *NSN-46*
Dominguez Pacheco Flavio Arturo *LPM-578*
Domratcheva-Lvova Lada *BIO-82, NSN-656*
Domratcheva-Lvova Lada *NSN-81, CHM-85, TRB-83*
Donohué-Cornejo Alejandro *BIO-607, BIO-609*
Durán Almendárez Alejandra *NSN-29*
Durán Ledezma Ángel Adalberto *NSN-508*
Durruthy-Rodríguez María Dolores *AMC-645*
Dutt Ateet *RWE-678*
Eder-Sánchez John *NSN-303*
Elizalde Jose *SIF-2*
Elizalde Galindo José Trinidad *TSM-6*
Elizalde Galindo Jose Trinidad *AMC-551*
ELIZALDE GALINDO JOSE TRINIDAD AMC-682
Encinas Armando *BIO-547, BIO-577, NSN-553, NSN-597, NSN-545, NSN-574, BIO-531*
Encinas Armando *NSN-646*
Encinas Oropesa Armando *BIO-615*
Enríquez Carrejo José Luis *TSM-6*
Enríquez Valdés Edwin Alejandro *CHM-617*
Enriquez Jose *SIF-2*
Escalante Álvarez Marcos Alfredo *BIO-136*
Escalante García Ismailia L *NSN-36*
Escobar Garcia Diana *BIO-532*
Escobar-Alarcon L. *THF-512*
Escudero Rincón María Lorenza *BIO-146, SIF-188*
Esparza Alegría Enrique *NSN-515*
Esparza García Alma *THF-137*
ESPERICUETA GONZÁLEZ DIANA LETICIA AMC-663
ESPERICUETA GONZÁLEZ DORA ERIKA AMC-663
Espinosa G. *LPM-599*
Espinosa Cerón María Yesica *LPM-342*
Espinosa Cristóbal León Francisco *BIO-529*
Espinosa Vega Leticia Ithsmel *RWE-613, SIF-634, RWE-614*
Espinosa-Cristóbal León Francisco *BIO-608, BIO-609, BIO-607*
Espinosa-Cristobal Leon *BIO-602*
Espinosa-Vega L.I. *RWE-363, SEM-365*
Espinosa-Vega Leticia Ithsmel *SEM-610, NSN-611, NSN-616*
Espinoza Hernández Ernesto *RWE-497, RWE-376*
Espinoza Hernández Ernesto *RWE-407*
Espinoza Vega Leticia *RWE-632*
Espinoza Vega Leticia Ithsmel *NSN-624*



Espinoza-Cristóbal León *BIO-587*
Espinoza-Figueroa J.A. *SEM-365*
Espinoza-Figueroa Jose Angel *RWE-613*
Esqueda Barrón Yasmín *SIF-335, NSN-46*
ESQUIVEL ESCALANTE KAREN *NSN-650*
Estrada Flores Sofia *SEM-145*
Estrada Vázquez Horacio *MEM-618*
Estrella Núñez Jocelyne Marissa *AMC-644*
Fabian-Jacobi Jesús Fernando *SIF-260*
Fabian-Jocobi Jesús Fernando *SIF-601*
Fajardo Díaz Juan Luis *NSN-258*
Fajardo Diaz Juan Luis *THF-264*
Falcón-Franco Lazaro Abdiel *RWE-55*
Falcony C. *LPM-675*
Falcony Ciro *LPM-281*
Falcony Guajardo Ciro *PLV-631, LPM-310, SEM-265*
Falcony Guajardo Ciro *LPM-299*
Falcony-Guajardo Ciro *NSN-174, NSN-66, LPM-509*
Farías Rurik *NSN-284*
Farías Mancilla José Rurik *TSM-6*
Farías Sánchez Mario Humberto *SIF-335*
Farias Rurik *NSN-598, AMC-593, AMC-600, SIF-2*
Farias Rurik *AMC-551*
FARIAS MANCILLA JOSE RURIK *AMC-682*
Farias Sánchez Mario *NSN-46*
Favila-Castañeda M. *RWE-363*
Favila-Castañeda Miriam *NSN-611*
Fernández Lara David *NSN-86*
Fierro-Ruiz César D. *AMC-551*
Flores Acosta Mario *NSN-12*
Flores Cerón Iván de Jesús *MEM-528*
Flores Fuentes Naria Adriana *NSN-508*
Flores Garcia Eneftali *MEM-582*
Flores Larrea Luis G. *RWF-637*
Flores Martinez Martín *TRB-375*
Flores Reyes Héctor *BIO-537*
Flores Reyes Hector *BIO-532*
Flores Salazar Mario *SEM-69, NSN-18*
Flores Salazar Mario *NSN-263*
Flores-Camacho Jose Manuel *SIF-288*
Flores-Cruz R.L. *LPM-675*
Flores-Farías R. *THF-126*



Flores-Farias Rivelino *AMC-644*
Flores-Garcia Eneftali *MEM-586*
Flores-Hernández C.G. *BIO-262*
Flores-Ramírez Nelly *BIO-82*
Flores-Ramirez Nelly *TRB-83*
Flores-Rangel Gabriela *THF-149*
Flores-Ruiz Francisco Javier *CHM-347*
Flores-Ruiz Francisco Javier *CHM-348*
Florez Rios John Fredy *SEM-576*
Gabarain Cruz Lorena *CHM-63*
GALARZA GALARZA ENRIQUE *CHM-75, CHM-76*
Galeazzi R. *LPM-350*
Galeazzi Isasmendi Reina *SEM-662*
Galindo Cuevas Hugo Valdemar *NSN-657*
GALINDO IDROGO ITZEL ESTEFANIA *CHM-75*
GALINDO IDROGO ITZEL ESTEFANIA *CHM-76*
Gallardo Hernández Salvador *SEM-265*
Gallardo-Hernández Salvador *SEM-670, SEM-610*
Galván-Flores Elizabeth *NSN-683*
Gamboa Fidel *SIF-2*
Gamboa-López Genaro *NSN-374, CHM-129*
García Alejandra *THF-283*
García Ernesto *TRB-375*
García Alonso María Cristina *SIF-188*
García Borquez Arturo *NSN-337*
García Cabrera Amaidaly *CHM-274*
García Díaz Reyes *TSM-627*
García Hernández Sergio A. *SEM-679*
García Hernández Sergio Agustín *THF-681*
García Jaramillo Efraín *PLV-631*
García Llamas Raúl *NSN-12*
García Lozano Rodolfo Zolá *MEM-502*
García Pacheco Georgina *NSN-378*
García Ramírez Mario Alberto *MEM-357*
García Rangel José Manuel *RWE-371, RWE-407*
García Rangel José Manuel *RWE-376*
García Salgado Godofredo *LPM-659*
García Sánchez Mario Fidel *RWE-407, RWE-497, RWE-371*
García Sánchez Mario Fidel *RWE-376, SCD-309*
García Valdivieso Ma. Guadalupe *BIO-74*
García Valdivieso Ma. Guadalupe *NSN-261*
García-Alamilla Pedro *SIF-604, SIF-606*



García-Alamilla Ricardo *SIF-606*
García-Antonio D.L. *THF-126*
García-Casillas Perla Elvia *BIO-25*
García-Cerda Luis Alfonso *RWE-55*
García-Durán Ángel *LPM-125*
García-Gallegos Jesús *AMC-31*
García-García Víctor *NSN-656*
García-González Leandro *TRB-83*
García-Guerra Josefina *RWE-55*
García-Jacobo Rubén *CHM-184*
García-Ortiz César E. *LPM-185*
García-Pimentel Manuel *LPM-185*
García-Rentería Marco Arturo *RWE-55*
García-Ruiz Diana Litzajaya *BIO-82*
García-Ruiz Diana Litzajaya *NSN-81*
García-Ruiz Diana Litzajaya *TRB-83, CHM-85*
García-Salgado G. *LPM-350*
García-Sánchez Mario Fidel *NSN-683*
García-Vázquez Felipe de Jesús *CHM-184*
García-Villarreal Sergio *RWE-55*
García-Zaldivar Osmany *CHM-347*
Garcia Rodolfo *MEM-306*
Garcia Cruz Miguel Angel *SIF-52*
Garcia Gutierrez Rafael *RWE-44*
Garcia Rangel José Manuel *RWE-497*
Garcia Rocha R. Rocío *NSN-36*
Garcia-Diaz Reyes *TSM-70*
Garcia-Ruiz Diana Litzajaya *NSN-656*
Garduño Terán Ulises *RWE-407, RWE-376*
Garduño Terán Ulises *RWE-497*
Garduño Wilches Ismael Arturo *LPM-93*
GARDUÑO-WILCHES ISMAEL A. *LPM-688*
Garibay Vicente *BIO-630*
Garibay Alvarado Jesús Alberto *BIO-529*
Garibay-Alvarado Jesús Alberto *AMC-600, BIO-607, AMC-538*
Garibay-Martinez Fernando *MEM-586*
GÁRATE-VÉLEZ LORENA *BIO-293, BIO-294*
Gárate-Vélez Lorena *BIO-636*
Golzarri I. *LPM-599*
Gómez Idalia *SEM-119*
Gómez Luz del Carmen *BIO-28*
Gómez Roberto *SEM-265*



Gómez Aguilar Ramón *MEM-270*
Gómez Rosales Roberto *PLV-631*
Gómez Rosas Gilberto *THF-575*
Gómez Sánchez Rafael *RWE-638*
Gómez-Rosas G. *PLV-546, PLV-541, NSN-549*
Gómez-Rosas Gilberto *SEM-651*
GÓMEZ-AGUILAR RAMON *NSN-68*
GENEVET PATRICE *NSN-18*
Gervacio Arciniega José Juan *NSN-46*
Gil Tolano María Inés *NSN-307*
Godínez Fernández José Rafael *NSN-177*
GONZALEZ CASTILLO MARIA DEL CARMEN *NSN-650*
Gonzalez de la Cruz Gerardo *NSN-26*
Gonzalez de la Cruz GERARDO *NSN-21*
Gonzalez Nicolas Antonio *RWE-632*
Gonzalez-Zavala F. *THF-512*
GONZÁLEZ CONTRERAS FRANCISCO JAVIER *NSN-677*
GONZÁLEZ CONTRERAS GABRIEL *NSN-677*
González Contreras Gabriel *NSN-676*
González de la Cruz Gerardo *NSN-683*
González Domínguez J.L. *NSN-284*
González Florez Susana Abigail *PLV-169*
González Morgado María Guadalupe *BIO-338*
González Panzo Isidro Juvencio *SEM-662*
González Reynoso Orfil *MEM-357*
González Valdés István *RWE-622*
González-Castro Brayan *CHM-629*
González-Rostro A.L. *THF-126*
Gorbachev Andrei *NSN-624*
GORBATCHEV ANDREI *THF-72, LPM-180*
Gorbatchev Andrei *SEM-272*
Gorvachev Andrei *SIF-634*
Granados-Martínez Francisco Gabriel *BIO-82, TRB-83, NSN-656, NSN-81, CHM-85*
Grarcía Jaramillo Efraín *PLV-153*
Gregorio H. Cocoletzi *SIF-32*
Gudiño Cabrera Graciela *BIO-136*
Guerrero Sánchez Jonathan *TSM-628*
Guerrero-Serrano Azdrubal L. *AMC-533*
Guillen A. *LPM-599*
Guillén Cervantes Ángel *SEM-265*
Guillen-Bonilla Hector *NSN-591*
Gutiérrez Hernández José Manuel *BIO-136*



Gutiérrez López Adriana Nahúm *RWE-685*
Gutiérrez López Adriana Nahúm *RWE-685*
Gutiérrez- García Carmen Judith *NSN-81*
Gutiérrez-Castañeda Emmanuel José *CHM-184*
Gutiérrez-Fuentes Rubén *NSN-374*
Gutiérrez-García Carmen Judith *NSN-656, CHM-85, BIO-82, TRB-83*
Gutierrez Heredia Gerardo *MEM-502*
GUZMAN CAMPUZANO ALVARO *NSN-661*
Guzmán Ayón Sandra Violeta *TRB-375*
Guzmán Bucio Dulce María *ALD-121*
Guzmán Bucio Dulce María *ALD-124*
Guzmán Castañeda Jesús Israel *LPM-584*
Guzmán Castañeda Jesus Israel *LPM-495*
Guzmán Chapa Kevin *BIO-278*
Guzmán Cruz Andrés *NSN-300*
Guzmán-Bucio Dulce Maria *ALD-164*
Guzmán-Caballero D.E. *MEM-665, MEM-654*
Guzmán-Fuentes Jaime Abraham *NSN-81, CHM-85, BIO-82, TRB-83*
H mők H Linh *TSM-134*
Haro Poniatowski Emmanuel *NSN-515, NSN-177*
Haro-Poniatowski E. *THF-512*
Hernandez Adame Luis *NSN-515*
Hernandez Aguilar Claudia *LPM-578*
Hernandez Andrade Dante Fernando *TSM-179*
Hernandez Cocoletzi Gregorio *TSM-648*
Hernandez Como Norberto *MEM-135*
Hernandez Cuevas Francisco J. *MEM-135*
HERNANDEZ DE LA CRUZ TERESA *CHM-84*
Hernandez Marquez Jesus Alfredo *ALD-516*
Hernandez-Como Norberto *MEM-306*
Hernandez-Cuevas Francisco *MEM-306*
Hernandez-Gaytan L.M. *RWE-363*
Hernandez-Gaytán Lendy M. *NSN-611*
Hernandez-Medina Jesus *NSN-611*
Hernandez-Perez Maria de los Angeles *NSN-279*
Hernandez-Ramirez Laura Isabel *SEM-651*
Hernández Aguilar Claudia *CHM-641, CHM-633*
Hernández Altamirano Raúl *RWE-685*
Hernández Altamirano Raúl *RWE-685*
Hernández Andrade Dante Fernando *TSM-277*
Hernández Arteaga José Gabriel Roberto *RWE-518*
Hernández Cocoletzi Gregorio *TSM-70, NSN-77*



Hernández Como Norberto *MEM-276*
Hernández Cuevas Francisco *MEM-276*
Hernández de la Luz José Álvaro David *LPM-659*
Hernández Flores Armando *MEM-90*
Hernández García Héctor Manuel *CHM-106*
Hernández Hernández Arturo *BIO-67*
Hernández Landaverde Martín Adelaido *SEM-289, SEM-176*
Hernández Martínez Luis *MEM-80*
Hernández Méndez Miguel Ágel *CHM-108*
Hernández Rodríguez María Fernanda *SEM-580*
Hernández Rosas Francisco *CHM-617*
Hernández Rosas Juan *CHM-617*
Hernández Sánchez Mayra Paulina *SIF-335*
Hernández Sebastián Natiely *MEM-412*
Hernández Uresti Diana Berenice *NSN-668*
Hernández Vázquez Orlando *SEM-679*
Hernández-Adame Luis *LPM-125*
Hernández-Aguilar Claudia *CHM-130*
Hernández-Ávila Juan *TSM-674*
Hernández-Como Norberto *RWE-55*
Hernández-Cristóbal Orlando *BIO-82*
Hernández-García Moisés *AMC-645*
Hernández-López Susana *AMC-551*
Hernández-Medina J. *RWE-363*
Hernández-Ortiz Marlen *THF-133*
Hernández-Rufino Z. I. *BIO-262*
Herrera Gómez Alberto *ALD-124, ALD-121*
Herrera Herrera Mirian Yoceline *SEM-5*
Herrera Herrera Mirian Yoceline *AMC-187*
Herrera Pérez Jose Luis *CHM-639*
Herrera Ramírez Jeeniffer *SEM-289*
Herrera Rivera Maria del Rosario *SEM-669*
Herrera Sánchez Andrea *SEM-176*
Herrera-Carbajal Alejandro *TSM-674*
Herrera-Gómez Alberto *ALD-164*
Herrera-Gomez Alberto *SIF-260, SIF-139*
Herrera-Gomez Alberto *SIF-601*
Herrera-Pérez J.L. *SEM-143, NSN-147*
Hinojosa Reyes Mariana *NSN-344*
Hintze Maldonado Kevin *NSN-574*
Hoat Do Minh *TSM-648*
Horley Paul *ALD-301*



Horta Fraijo Patricia *NSN-603*
Hortua Diaz Omar Camilo *BIO-89*
Hughes Gregory *ALD-346, ALD-516*
Huipe-Nava Ezequiel *CHM-85, BIO-82, NSN-656*
Hurtado-Pájaro V.M. *MEM-654*
Isidro Ojeda Michel Alonso *CHM-105*
Isidro-Ojeda Michel *CHM-138*
Itzmoyotl Toxqui Adrián *MEM-90*
Izquierdo-Almaguer Tania Beatriz *AMC-593*
Izquierdo-Almaguer Tania Beatriz *AMC-600*
Jarrouj-Zoudi Yuliano *RWE-613*
Jasso Jasso María Fernanda *ALD-266*
Javier González Francisco *NSN-676*
Jiménez G.L. *LPM-599*
Jiménez Marín Eunice *NSN-409*
Jiménez Pérez José Luis *NSN-280*
Jiménez Sandoval Sergio Joaquín *SEM-289*
Jiménez-Pérez José Luis *CHM-130, NSN-374*
Jiménez-Pérez Jose Luis *CHM-129*
Jimenez Daniel *RWE-494*
Jimenez Ortiz Paola Gisel *SEM-643*
Jimenez Ortiz Paola Gisel *RWE-341*
Jimenez Sandoval Sergio Joaquín *SEM-176*
Jimenez-Flores Steffanie *SEM-583*
Jimenez-Halla J. Oscar C. *TSM-58*
Jonathan Guerrero Sanchez *SIF-32*
José García Sergio Osbaldo *CHM-617*
José-Yacaman Miguel *NSN-603*
Jose Varalda *SIF-32*
Juarez-Sanchez M.A. *BIO-298*
Juárez Héctor *NSN-530*
Juárez García J.M. *NSN-284*
Juárez-López Guillermo *NSN-174, NSN-66*
Juárez-Ramírez Isaias *THF-104*
Kessels W.M.M. (Erwin) *ALD-673*
Kharissov Boris *SEM-119*
Kharissov Boris Ildusovich *NSN-97*
Kharissova Oxana V. *NSN-657, NSN-658*
Kudriavtsev Yuriy *SEM-178*
Kumar Krishnan Siva *NSN-300*
Lagunes-Gálvez Laura Mercedes *SIF-606, SIF-604*
Lahtonen K. *ALD-346*



Lang-Salas Michelle Gerardo *BIO-607*
Lara Alfaro Hector Francisco *SEM-287, SEM-282*
Lara Ojeda Angelica *RWE-507*
Lara Velázquez Ismael *RWE-632*
Lastras Alfonso *LPM-680*
Lastras Martínez Alfonso *SEM-287, SEM-282*
Lastras Martínez Alfonso *TSM-186*
Lastras-Martinez Luis Felipe *THF-149*
López de León Edgar Omar *LPM-578*
López Domínguez Julio César *PLV-631*
López Fuentes Mirna *NSN-77*
López García Martín *THF-687*
López Granada María Guadalupe *BIO-67*
López Lazcano Carlos Augusto *THF-60, NSN-295*
López López Máximo *SEM-178*
López Luna Edgar *THF-681, SEM-679*
López Salazar Primavera *NSN-46*
López Urías Florentino *NSN-258, THF-264*
López-Lazcano Carlos Augusto *THF-56*
López-Urías Florentino *NSN-377*
López-Urías Florentino *NSN-625, NSN-626*
Leandro Martínez Carlos Enrique *RWE-632*
León Gil Jesús Armando *MEM-411*
León González Juan Pablo *BIO-146*
León Gonzalez Juan Pablo *SIF-150*
León González Juan Pablo *SIF-188*
León González Juan Pablo *SIF-271*
León Zúñiga Karla *THF-137*
León-Gil J.A. *MEM-665*
Lemus-Hernandez María Edith *TSM-311*
Licea Suazo Enya *RWE-638*
Linares Margarita *BIO-630*
Linares Aranda Mónico *MEM-80*
LOBO GUERRERO AZDRUBAL *AMC-663*
Lobo-Guerrero Azdrubal *AMC-31*
LOERA-SERNA SANDRA *LPM-688*
Loeza Poot Mariely *RWE-588*
Lopez Urías Florentino *NSN-612*
Lopez Urias Florentino *NSN-402*
Lopez-Castillo Miguel *MEM-306*
Lopez-Sandoval Roman *RWE-349*
Lopez-Urías F *NSN-379*



Loredo Becerra Griselda Mayela NSN-29
Losurdo Maria THF-149
Lozada Morales Rosendo LPM-496
Lozada Morales Rosendo LPM-342
Lozada Morales Rosendo Leovigildo LPM-281, LPM-581
Lozada Morales Rosendo Leovigildo SEM-580
Lozada-Morales R. LPM-675
Lozada-Morales Rosendo LPM-369
Lozano Rojas Ivonne Berenice LPM-584
Lozano Rojas Ivonne Berenice LPM-495
LUGO PEREZ LUIS ISAAC NSN-677
Luis Arnulfo BIO-28
Luna Adán NSN-530
Luna Flores Adán LPM-659
Luna López José Alberto LPM-659
LUNA LOPEZ JOSE ALBERTO TSM-514
Luna Sánchez José Luis NSN-280
Luna-Sánchez José Luis CHM-130, NSN-374
Luna-Sánchez Jose Luis CHM-129
Lundy Ross ALD-346
MACÍAS LÓPEZ DR. FERNANDO CHM-655
Macías Mier Marcos NSN-280
Macedas-García Bernardo NSN-66
Machorro Roberto PLV-647
Machorro Mejía Roberto CHM-63, PLV-132, THF-137
Machorro Mejia Roberto CHM-61, CHM-39
Machorro Mejia Roberto CHM-274
machorro-mejía roberto THF-259
Malagón García José Francisco RWE-376
Maldonado Arturo SIF-649
Mani Pierre SIF-2
Mani Gonzalez Pierre Giovanni ALD-516
Mani González Pierre Giovanni TSM-6
Mani-Gonzalez Pierre Giovanni ALD-346
Mani-Gonzalez Pierre Giovanni ALD-346
Mansanares Antonio Manoel CHM-138
Marañón Ruíz Virginia F. NSN-642
Marín Moares Ernesto CHM-105
Marcelo Ademir Martínez Puente Marcelo Ademir Martínez Puente ALD-266
Maria Alfaro Maria Alfaro RWE-51
Marin Ernesto CHM-138
Marquéz Beltrán César BIO-148



MARTÍNEZ-GUTIÉRREZ HUGO NSN-68
Martínez Aguilar Espiridión *TSM-134*
Martínez Castañón Gabriel Alejandro *BIO-17*
Martínez Castañon Gabriel Alejandro *NSN-33*
Martínez Falomir Gibran Guadalupe *NSN-295, THF-56*
Martínez Falomir Gibrán Guadalupe *THF-60*
Martínez Guerra Eduardo *ALD-183, ALD-182, ALD-291, ALD-266, ALD-372*
Martínez Guerra Eduardo *ALD-301*
Martínez Hernández Haydee Patricia *LPM-659*
Martínez Huerta Juan Manuel *NSN-574*
Martínez López A.L. *SEM-143*
Martínez Luévanos Antonia *SEM-145*
Martínez Olgún Aracely del Carmen *TSM-648*
Martínez Pastor Juan *LPM-73*
Martínez Pastor Juan P. *LPM-92*
Martínez Puente Marcelo Ademir *ALD-291, ALD-301*
Martínez Puente Marcelo Ademir *ALD-183, ALD-182*
Martínez Quiroz Jonathan Gerardo *NSN-658*
Martínez Reyna Karí *NSN-261*
Martínez Reyna Karí Guadalupe Hortensia *BIO-74*
Martínez Rodríguez Lucio *BIO-181*
Martínez-Guerra Eduardo *THF-686, LPM-509*
Martínez-López A.L. *NSN-147*
Martínez-Martínez Rafael *NSN-174, NSN-66*
Martínez-Orozco Juan Carlos *THF-133*
Martel-Estrada Santos Adriana *BIO-35*
Martel-Estrada Santos Adriana *BIO-24, BIO-25*
Martinez Eduardo *ALD-353*
Martinez Marcelo *ALD-353*
MARTINEZ MENDOZA JOSÉ REFUGIO *AMC-663*
Martinez Villegas Nadia *NSN-402*
Martinez-Landeros Victor Hugo *RWE-55*
Martinez-Velis Isaac *NSN-343*
Martinez-Velis Isaac *NSN-343*
Mastache Juarez Areli *NSN-26*
Mateos David *ALD-353*
Mathew Xavier *THF-60, THF-56*
Mayén Hernández Sandra A. *PLV-107*
Mayorga Garay Marisol *ALD-121, ALD-124*
Mayorga-Garay Marisol *ALD-164*
Márquez Beltrán César *NSN-64*
Méndez Francisco *NSN-81*



Méndez Blas Antonio *LPM-496*
Méndez Camacho Reyna *TSM-505, SEM-504, NSN-503*
Méndez Martínez Karla María *THF-133*
Méndez Otero Maribel *NSN-77*
Méndez-Blas A. *LPM-675*
Méndez-Blas Antonio *LPM-369*
Méndez-Camacho Reyna *NSN-303*
Méndez-García V.H. *SEM-365, RWE-363*
Méndez-García Victor Hugo *THF-133*
Méndez-Gonzalez María Magdalena *NSN-339*
Méndez-González María Magdalena *NSN-340, BIO-338, NSN-337*
McGlynn Enda *ALD-346*
Medellín-Castillo Nahum *AMC-538*
Medina-Escobedo Daniel *THF-149*
Medina-Llamas V.L *NSN-379*
Medina-Ochoa Liliana *BIO-608*
Medina-Ochoa Liliana *BIO-602*
Mejía I. *MEM-654, MEM-665*
Mejía Gonzalez Diego *CHM-63*
Mejía Silva Israel *MEM-411*
Mejía Silva Jesús Israel *MEM-621*
Mejia Gonzalez Diego G. *CHM-61*
Mejia Gonzalez Diego Germain *CHM-39*
Mejia-Olvera Roberto *TSM-311*
Meléndez Miguel *THF-283*
Meléndez Estrada Idahli Alejandra *BIO-529*
Meléndez Lira Miguel *THF-575, SEM-506, PLV-107*
Meléndez Lira Miguel A. *THF-131*
Meléndez-Estrada Idahli Alejandra *BIO-587, BIO-608*
Meléndez-Estrada Idahli Alejandra *BIO-609*
Meléndez-Lira Miguel *SEM-670*
Meléndez-Zamudio M. *THF-131*
Meléndrez Rodrigo *NSN-307*
Melendez-Lira M. *BIO-298*
Melendez-Lira Miguel *NSN-598, AMC-593*
Melendez-Lira Miguel *SCD-640*
Melendez-Zamudio M. *BIO-298*
Menchaca Jiménez Rubén *CHM-269, CHM-268*
Mendez García Victor Hugo *RWE-632*
Mendez Garcia Victor Hugo *NSN-624, SIF-634*
Mendez-Garcí Victor Hugo *RWE-613*
Mendez-García Victor Hugo *NSN-611, SEM-610*



Mendez-Garcia Victor Hugo *RWE-614, NSN-616*
Mendivil Isabel *ALD-353*
Mendivil Palma María Isabel *ALD-291, ALD-301*
Mendoza Emilia Margarita *RWE-678*
Mendoza Esmeralda *RWE-637*
Mendoza Acevedo Salvador *NSN-378*
Mendoza Alvarez Julio Gregorio *NSN-26*
Mendoza Álvarez Julio G. *CHM-639*
Mendoza Cruz Ruben *NSN-666*
Mendoza López María Luisa *CHM-57*
Mendoza López Maria Luisa *NSN-652, NSN-653*
MENDOZA LÓPEZ MARÍA LUISA *CHM-84*
Mendoza León Héctor Francisco *NSN-378*
Mendoza-Álvarez J.G. *NSN-147, SEM-143*
Mendoza-Cristán Rocío Yazmín *RWE-55*
Mendoza-delaRosa Luis Alberto *CHM-269, CHM-268*
Mendoza-Duarte Mónica *BIO-25*
Mendoza-Zubia Edgar Eduardo *BIO-35*
Mercado Ornelas Christian Alejandro *SIF-634, NSN-624*
Mercado Ornelas Christian Alejandro *RWE-614*
Mercado-Ornelas C.A. *RWE-363, SEM-365*
Mercado-Ornelas Christian Alejandro *NSN-611, SEM-610, RWE-613*
Mercado-Ornelas Christian Alejandro *NSN-616*
Meza Arroyo Javier *MEM-582*
Meza Rocha Abraham *LPM-369, LPM-496, LPM-342*
Meza Rocha Abraham Nehemías *LPM-281, LPM-581*
Meza-Rocha A.N. *LPM-675*
Mijangos Zúñiga Gabriela Elizabeth *RWE-367, RWE-364*
Milo Alvarez Aarón *NSN-33*
MIMILA-ARROYO Jaime *RWE-510, SEM-511*
Mirabal-García Manuel *AMC-31*
Miranda Juana Maria *RWE-494*
Miranda Vidales Juana María *RWE-507*
Mis Fernandez Ricardo *RWE-588*
MISHURNYI VIATCHESLAV *THF-72*
Moctezuma Edgar *RWE-373*
Moctezuma Salazar Guillermo Alam *RWE-341*
Moctezuma Salazar Guillermo Alam *SEM-643*
Molina Bermúdez Alejandro *CHM-639, RWE-638*
Molina Torres Andres Felipe *ALD-372*
Mondragon-Sanchez María de Lourdes *CHM-85*
Monfil Leyva Karim *LPM-659*



Monroy Arellano Mónica Samanta *LPM-584*
Montiel García Adriana *BIO-146, SIF-271, SIF-188*
Mora Ventura Brhayllan *NSN-676*
Mora-Herrera David *RWE-91*
Morales Bautista Jacob *SEM-669*
Morales Caporal Roberto *LPM-659*
Morales de la Garza Leonardo *TSM-648, NSN-46*
Morales Gonzalez Ángel *LPM-578*
MORALES HERNÁNDEZ JORGE *THF-592*
Morales Méndez José Guadalupe *NSN-177*
Morales Mendez José Guadalupe *NSN-515*
Morales Ruiz Crisóforo *SEM-662*
Morales-Morelos Maria del Pilar *THF-149*
Morales-Ruiz C *LPM-350*
MORAN MARTINEZ XOCHITL ALEYDA *TSM-514*
Moreno García Harumi *RWE-518*
Moreno Torres Juan Felipe *NSN-642*
Morris Michael *ALD-346*
Moya Canul Karla Mariela *AMC-644*
Muñoz Arroyo Rita *CHM-108*
Muñiz Martínez Bárbara Alejandra *NSN-352*
Muñoz Navia Milton *TSM-186*
Muñoz Ramírez María Concepción *LPM-413*
Muñoz Ruiz Abraham Israel *BIO-532*
Muñoz Sandoval Emilio *NSN-258, THF-264, NSN-612*
Muñoz Sandoval Emilio *NSN-402*
Muñoz-Escobar Antonio *BIO-587, BIO-602, BIO-609*
Muñoz-Sandoval E *NSN-379*
Muñoz-Sandoval Emilio *NSN-377*
muhl stephen *THF-259, TRB-375, TRB-79*
Muhl Stephen *PLV-305*
mullapudi Gouri Syamala Rao *MEM-582*
Mullapudi Gouri Syamala Rao *THF-122, THF-123*
Murata Koichi *NSN-343*
Narvaez Lilia *RWE-494*
Narvaez Hernandez Lilia *RWE-507*
Nava Pineda Antonio Joaquin *BIO-67*
Nava-Maldonado Flavio Manuel *THF-133*
Navarrete-Meza Zulema *CHM-129*
Navarro Arenas Juan *LPM-73*
Navarro Contreras Hugo Ricardo *NSN-261*
Navarro Contreras Hugo Ricardo *BIO-74*



Navarro Tellez Ana de Monserrat NSN-97
Navarro-Martínez J.A. THF-126
Núñez Olvera Oscar Fernando LPM-680
Nedev Nicola ALD-353
NERI-GÓMEZ TERESA BIO-294, BIO-293
Netzahual-Lopantzi Angel CHM-129
NI PEINAN NSN-18
Niño Martínez Nereyda NSN-33, BIO-17, NSN-29, BIO-615
Nieto Encarnación Andrea Tsam RWE-638
Nieto-Caballero F. G. LPM-350
Nikishin Sergey SEM-144, SEM-45
O'Connor Robert ALD-516
O'Connor Robert ALD-346
Ochoa Valiente Raúl TSM-70
Ojeda-Galván Joazet CHM-304
Oliva González Cesar Máximo NSN-97
Olivares-Ochoa Diego Javier BIO-25
Olivas-Armendáriz Imelda BIO-24, BIO-35
Olvera Amador María de la Luz SEM-669
Olvera-Enriquez J. Pablo NSN-611
Olvera-Enriquez J.P. RWE-363
Onofre Bustamante Edgar SIF-150, BIO-146
Onofre Bustamante Edgar SIF-271
Onofre Bustamante Edgar SIF-188
Ordaz-Fernández E.A. THF-126
Orea Calderon Brenda Irais NSN-612
Orea Calderon Brenda Irais NSN-612
ORNELAS GUTIERREZ CARLOS ELIAS AMC-682
OROPEZA SAUCEDO MARIA MONTSERRAT THF-513
Oros-Ruiz Socorro RWE-637
Orozco Dueñas Juan Andrés TSM-267
Orozco-Cruz Ricardo TRB-83
ORTEGA AMAYA REBECA NSN-661
Ortega García Beatriz ALD-291
ORTEGA LOPEZ MAURICIO NSN-661
Ortega Sigala José Juan SEM-265, PLV-631, PLV-169, LPM-413, PLV-153, TSM-267
ORTEGA ZARZOSA GERARDO AMC-663
ORTEGA-CERVANTEZ GERARDO NSN-68
Ortega-Gallegos Jorge THF-149
Ortega-Varela Luis Fernando NSN-81
Ortiz López Jaime MEM-270
ORTIZ MONRROY LUIS SANTIAGO CHM-76



ORTIZ MONRROY LUIS SANTIAGO CHM-75
Ortiz Saavedra Juan SEM-265, PLV-169, TSM-267, PLV-631
Ortiz-Alvarez Maria Raquel CHM-19
ORTIZ-LÓPEZ JAIME NSN-68
Ortuño-López M.B. THF-126, BIO-262
Oskam Gerko RWE-543
Otani Yoshichika SIF-288
Oviedo-Roa Raúl TSM-127
Oza Goldie RWE-678
Pacheco-Ortíz Sandy María TSM-311
Pacio Mauricio NSN-530
Padilla Islas Miguel Adrian RWE-27
Padilla Islas Miguel Adrián NSN-53
Padilla-Islas Miguel Adrian RWE-290
Padilla-Robles Artemio S. AMC-551
Pal Mou NSN-300, RWE-91
Pal Umapada BIO-28
PALESTINO-ESCOBEDO ALMA GABRIELA BIO-294, BIO-293
Palomares Sanchez Salvador NSN-36, AMC-345
Palomares-Sánchez Salvador A. AMC-533
Panecatl Bernal Yesmin NSN-46
Paneque Quevedo Armando SIF-335
PANTOJA RODRIGUEZ ISAAC AMC-682
Patakfalvi Rita Judit NSN-642
Pérez Elías NSN-515
Pérez Arrieta María Leticia PLV-153, LPM-413
Pérez Berumen Catalina María SEM-145
Pérez Bueno José de Jesús NSN-652, NSN-653
Pérez Centeno Armando SEM-576, THF-575
Pérez Ladrón de Guevara Héctor NSN-642
Pérez Larios Alejandro NSN-642
Pérez López Israel Omar TSM-6
Pérez López José Elías SIF-297
Pérez Sánchez Gerardo Francisco NSN-77
Pérez-Arrieta María Leticia LPM-125
Pérez-Centeno A. PLV-546, PLV-541, NSN-549
Pérez-Centeno Armando SEM-651
Pérez-González Mario CHM-130
Pérez-Medina Gladys Yerania CHM-184
Pérez-Rodríguez Felipe NSN-620
PÉREZ BUENO J CHM-84
Peña Yolanda SEM-119



Peña Chapa Juan Luis *RWE-588*
Peña Flores Jesús Iván *NSN-64*
Peña Méndez Yolanda *NSN-97*
Pelayo Cardenas José de Jesus *TSM-179*
Pelayo Cárdenas José de Jesús *TSM-277*
Peralta Miriam *PLV-647*
Peralta Arriola Miriam *CHM-63*
Peralta-Vazquez Isaias Daniel *NSN-279*
Perea Garduño Alberto Ignacio *CHM-269, CHM-268*
Perea Parrales Felipe *RWE-632*
Perea Parrales Felipe Eduardo *SIF-634, NSN-624*
Perea-Parrales F.E. *SEM-365, RWE-363*
Perea-Parrales Felipe Eduardo *RWE-613, NSN-616, RWE-614*
Perez Israel *SIF-2*
Perez René *NSN-530*
Perez Arrieta Leticia *TSM-3*
Perez Gonzalez Mario *NSN-280*
PEREZ GUZMAN MANUEL ALEJANDRO *NSN-661*
Perez-Luna J. Guillermo *SEM-583*
Pineda-Jiménez Adrian *TSM-109*
PINEDA-JIMENEZ ADRIAN *TSM-71*
Pinna Nicola *LPM-93*
Pintor Monroy María Isabel *THF-60*
Pintor- Monroy Maria Isabel *THF-686*
Pintor-Monroy Maria Isabel *THF-56*
Piraux Luc *NSN-545*
Plaza Ma. Guadalupe *CHM-57*
Polanco-Martagón Said *CHM-19*
Ponce González Abigail *BIO-493*
Ponce Pérez Rodrigo *TSM-623*
Ponce Perez Rodrigo *TSM-648*
Portillo Sampedro Mercedes *NSN-77*
Posada-Amarillas Alvaro *TSM-58*
Pozos Amaury de Jesús *BIO-630*
Pozos Guillén Amaury de Jesús *BIO-537*
Pozos Guillen Amaury *BIO-532*
Precious-Ayanwale, Ayodeji *BIO-587*
Puch Ceballos Felipe *TSM-3*
Puebla Jorge *SIF-288*
Puebla-Nuñez Jorge *LPM-180*
Quevedo Lopez Manuel A *MEM-582*
Quevedo Lopez Manuel A. *THF-60*



Quevedo-López Manuel *THF-686*
Quevedo-Lopez Manuel Angel *THF-123, THF-122*
Quevedo-Lopez Manuel Ángel *THF-56*
Quiñones Galván José G. *PLV-107*
Quiñones Galván José Guadalupe *PLV-153, SEM-576, PLV-169*
Quiñones Galván José Guadalupe *THF-575*
Quiñones Galván Jose Guadalupe *RWE-554*
Quiñones-Galván J.G. *NSN-549, PLV-541, PLV-546*
Quiñones-Galván José Guadalupe *SEM-651*
Quintana Mildred *SEM-643, BIO-532, RWE-341, RWE-543*
Quintana Mildred *RWE-341*
Quintana Mildred *SEM-643, RWE-637*
QUINTANA RUIZ MILDRED *BIO-293*
QUINTANA RUIZ MILDRED *BIO-294*
Quintana-Ruiz Mildred *BIO-636*
Quintanar Zamora Víctor Manuel *THF-336*
Quiroz Reyes Cinthya Nataly *LPM-495*
Quitana Ruiz Mildred *NSN-635*
Raboño Borbolla Joaquín *SIF-139*
Raboño Borbolla Joaquín Gerardo *ALD-124*
Raboño-Borbolla Joaquín *SIF-260, SIF-601*
Ramírez Amador Raquel *NSN-46*
Ramírez Amador Raquel *LPM-659, NSN-46*
Ramírez López M. *NSN-147, SEM-143*
Ramírez López Manolo *CHM-639, RWE-638*
Ramírez-Bon R. *THF-126*
Ramírez-Dámaso Gabriel *TSM-109*
Ramirez Bon Rafael *MEM-582*
Ramirez Elias Victor Alfonso *BIO-89*
Ramirez-Bon Rafael *THF-123, MEM-586, THF-122*
RAMIREZ-DAMASO GABRIEL *TSM-71*
Ramirez-Meda Walter *NSN-591*
Ramos Estrella *RWE-678*
Ramos Manuel *SIF-2*
Ramos Murillo Manuel Antonio *TSM-6*
RAMOS-DÍAZ ANTONIO ROWLAND *NSN-68*
Ramos-García Margarita de Lorena *BIO-59*
Rangel-Cobián Víctor Manuel *NSN-591*
Rangel-Rivera J. *BIO-298*
Raymond Herrera Oscar *TSM-134*
Ríos Pimentel Fernando Francisco *NSN-340*
Rebollo Paz Jacqueline *NSN-86*



Rebollo Plata Bernabé *NSN-77*
Regalado-de la Rosa Jorge L. *SEM-610*
Renero Carrillo Francisco Javier *MEM-412*
Reséndiz M. Luis Martín *MEM-135*
Reséndiz Mendoza Luis *MEM-276*
Retana Fernanda *SEM-119*
Reyes Chaparro Gabriela Mariela *RWE-371*
Reyes Esqueda Jorge Alejandro *AMC-551*
Reyes Ixta Fatima Paloma *ALD-301*
Reyes Ixta Fátima Paloma *ALD-266*
Reyes López Simón Yobanny *BIO-529*
Reyes-Betanzo Claudia *MEM-90*
Reyes-Blas Hortensia *BIO-24, BIO-35*
Reyes-Cruz Isaac Abraham *SIF-604*
Reyes-López Simón Yobanny *BIO-587, AMC-538*
Reyes-López Simón Yobanny *BIO-608, AMC-600, BIO-607, BIO-602*
Reyes-López Simon Yobanny *NSN-598, AMC-593*
Reyes-Lopez S. Y. *THF-131*
Reyes-Lopez S.Y. *BIO-298*
Reyes-Reyes Marisol *RWE-349*
Ribas Ariño Jordi *TSM-134*
Richaud Arlette *NSN-81*
Rickards Jorge *SIF-52*
Rimmaudo Ivan *RWE-588*
Rivera Laura *TRB-79*
Rivera Alvarez Zacarias *LPM-299*
Rivera Flores Bertha Luisa *SEM-662*
RIVERA RODRIGUEZ CARLOS VIRGILIO *THF-151, THF-152*
Rivera-Armenta J.L. *BIO-262*
Rivera-Armenta Jose Luis *SIF-606*
Rivera-Mayorga José Antonio *CHM-629*
Rivera-Rios Lorena *BIO-35*
ROBERGE JULIE *TSM-71*
Rocha Reina Francisco Javier *SEM-282, SEM-287*
Rocha Robledo Ana Karen Susana *SEM-163*
Rocha Rocha Osnaider *NSN-12*
Rocha-Rangel Enrique *CHM-19*
Rocha-Reina Francisco *SEM-272*
Rodil Sandra E. *PLV-305*
RODRÍGUEZ CABRERA ING. CECILIA *CHM-655*
Rodríguez Canto Pedro Javier *LPM-73*
Rodríguez Corvera Cristina de Lourdes *NSN-625*



Rodríguez Fragoso Patricia *CHM-639*
Rodríguez García Gloria Elizabeth *TSM-623*
Rodríguez Gómez Francisco Javier *SIF-271*
Rodríguez Hernández Paola *THF-575*
Rodríguez Hernández Paola Elideth *PLV-107*
Rodríguez López José Luis *SEM-265*
Rodríguez López Ovidio *MEM-502*
Rodríguez Melgarejo Francisco *SEM-289, SEM-176*
Rodríguez Mera Jesús *NSN-77*
Rodríguez Ramírez Ricardo Iván *RWE-596*
Rodríguez Rojas Rubén Arturo *NSN-642*
Rodríguez Salas Lorena *LPM-680*
Rodríguez-Chávez Jorge Antonio *CHM-184*
Rodríguez-Corvera Cristina de Lourdes *NSN-626*
Rodríguez-Fragoso P. *NSN-147*
Rodríguez-García Jose Amparo *CHM-19*
Rodríguez-González Claudia Alejandra *BIO-25, BIO-24, BIO-35*
Rodríguez-Hernández P. E. *PLV-541*
Rodríguez-Lugo Ventura *TSM-674*
Rodríguez-Vázquez A.G. *SEM-365*
Rodrigo Ponce-Pérez *SIF-32*
Rodriguez Ramón *CHM-274*
Rodriguez Fragoso Patricia *NSN-26*
Rodriguez López Ramon *CHM-63*
Rodriguez-Cobos Amparo *LPM-185*
Rojas Chavez Hugo *NSN-53*
Rojas Chávez H. *NSN-284*
ROJAS-HERNANDEZ EZEQUIEL *TSM-71*
Rojas-Hernández Ezequiel *TSM-109*
Roman Lopez Jesus *LPM-495*
ROMANO TRUJILLO ROMAN *THF-513*
Romano-Trujillo R. *LPM-350*
Román Doval R. *NSN-284*
Román López Jesús *LPM-584*
Romero de la Cruz María Teresa *TSM-70*
Romero de la Cruz María Teresa *TSM-627, TSM-628, TSM-623*
Romero Ibarra Issis Claudette *RWE-364, RWE-376*
ROMERO IBARRA ISSIS CLAUDETTE *SCD-619, RWE-367*
Romero Ibarra Issis Claudette *RWE-596*
Romero-Ibarra Issis C. *TSM-408*
Romero-Romo W. *LPM-675*
Romney Marc G. *BIO-17*



Ronei. C. Oliveira *SIF-32*
Roque-Ruiz José Hafid *AMC-538*
Rosendo E. *LPM-350*
ROSENDO ANDRES ENRIQUE *THF-513*
RUÍZ MONDRAGÓN DR. JOSÉ JORGE *CHM-655*
Ruíz Santoyo Victor *NSN-642*
Ruíz Valdez Carlos F. *NSN-307*
Ruíz-Ramírez Mónica Cecilia *BIO-24*
Rubin de Celis Leal David *NSN-624*
Rubio Rosas Efraín *NSN-295*
Ruiz Facundo *NSN-33, BIO-615, NSN-29, AMC-345, NSN-344*
Ruiz Alvarado Isaac Azahel *TSM-186*
Ruiz Castillo Ana Laura *NSN-344*
Ruiz Cigarrillo Oscar *SEM-282, SEM-287*
Ruiz Miranda Rosa Estrella *NSN-378*
Ruiz Villegas Maria Fernanda *NSN-646*
Ruiz-Cigarrillo Oscar *THF-149*
Ruvalcaba-Martínez Zabdy Jaqueline *AMC-593*
Ruvalcaba-Martínez Zabdy Jaqueline *AMC-600*
Saari J. *ALD-346*
Saenz Hernández Renee Joselin *ALD-372*
Salazar Posadas Fernando *NSN-86*
Salazar-Muñoz Verónica E. *AMC-533*
Saldaña-Garcés Rocio *CHM-184*
Saldaña-Garcés Rocio *CHM-184*
Saldaña-Ramírez Anakaren *THF-104*
Salomón Preciado Ana María *RWE-622*
Sanabria Díaz Carlos Alberto *MEM-80*
Sanchez Daniel *RWE-51*
SANCHEZ -ALARCÓN RAUL IVAN *LPM-688*
Sanchez-Balanzar Luis E. *PLV-305*
Sanchez-Martínez Araceli *NSN-591*
Sanchez-Ramirez Elvia Angelica *NSN-279*
Sandoval Ramos José Victor *BIO-181*
Sanginés Roberto *PLV-647, THF-259*
Sanginés Roberto *PLV-132*
Sanginés de Castro Roberto *CHM-274, CHM-63*
Sangines de Castro Roberto *CHM-61, THF-137, CHM-39*
Santana Alonso *MEM-306*
Santana Guillermo *RWE-678*
Santana Aranda Miguel Ángel *SEM-576, THF-575*
Santana Dorantes Luis Alonso *MEM-135*



Santana Rodríguez Guillermo *RWE-376*
Santana-Aranda M.A. *PLV-546, PLV-541, NSN-549*
Santana-Aranda Miguel Ángel *SEM-651*
Santillán Gómez Tomas *TSM-3*
Santos Paulo *SEM-287, SEM-282*
Santos Cruz José *THF-575, PLV-107*
Santos-Cruz José *SEM-651*
Santos-López Fabiola *AMC-31*
SANTOYO SALAZAR JAIME *NSN-661*
Sáenz Galindo Aidé *TSM-628*
Sánchez Alarcón Raúl Iván *LPM-93, LPM-73*
Sánchez Alarcón Raúl Iván *LPM-281*
Sánchez Arroyo Juan Francisco *LPM-73*
Sánchez Balderas Gregorio *SIF-297*
Sánchez Castillo Ariadna *TSM-277, TSM-179*
Sánchez Fraga Rodolfo *MEM-618*
Sánchez Llamazares José Luis *TSM-134*
Sánchez Martínez Daniel *NSN-668*
Sánchez Martínez Elihu Hazel *SEM-504*
Sánchez Méndez Samuel *NSN-340*
Sánchez Méndez Susana Elisa *NSN-339*
Sánchez Mora Enrique *NSN-64*
Sánchez Torres Rene *SIF-150*
Sánchez- Balderas Gregorio *NSN-515*
Sánchez-Balderas Gregorio *RWE-614*
Sánchez-Castillo Ariadna *TSM-674*
Sánchez-Dena Oswaldo *AMC-551*
Sánchez-Fraga R. *MEM-665*
Sánchez-Martínez Elihu *CHM-304, NSN-303*
SánchezGarrido Olga *TSM-267*
Serralta-Macias Jesus *AMC-644*
Serrano Thelma *SEM-119*
Serrano Castro Andrés Rodolfo *BIO-338*
Serrano Castro Andrés Rodolfo *NSN-337*
Shiel Kyle *ALD-516*
Sierra Maya Edgar Iván *MEM-618*
Sierra Romero Noé *CHM-617*
Sierra-Cruz Itayeé *PLV-132*
SILVA GONZALEZ RUTILO *THF-513*
Silva Guajardo Luis Antonio *CHM-268, CHM-269*
Silva Holguín Pamela Nair *BIO-529, BIO-608*
Silva Holguin Pamela Nair *BIO-609*



SILVA JUAREZ CLAUDIA VERONICA THF-72
Silva Vidaurri Luis Gerardo ALD-183, ALD-182
Silva-González Rutilo RWE-91
Silva-Holguín Pamela Nair BIO-602
Simakov Andrey NSN-261, NSN-603
Simón Yobanny Simón Yobanny BIO-609
Simon Mier Elienai MEM-621
Simon-Mier E. MEM-654
Siqueiros Beltrones Jesús María TSM-134
Snelgrove Matthew ALD-516, ALD-346
Solís-Sánchez Luis Octavio LPM-125
Solis-Casados D. A. THF-512
Solorio-Grajeda Daniela NSN-598
Solorza Feria Omar NSN-53
Solorza-Feria Omar RWE-27, RWE-290
SOLORZA-GUZMAN MISael TSM-71
SoriaBotello Ana Patricia CHM-140
Soriano Rogelio Fragoso LPM-599
Soriano Romero Omar LPM-496, LPM-369
Soriano-Romero O. LPM-675
Sosa Victor SIF-2
Sosa-Hernández Elisa Marina NSN-22
Sotelo-López Antonio NSN-660
Soto Soto Jonathan NSN-653
Soto Valle Angulo Genaro PLV-132
Soto-Nieto Fernando NSN-598
Ssandra Julieta Gutierrez Ojeda SIF-32
Tacumá Garzón Anyi Maritza BIO-148
Tapia Jesús Iván BIO-577
Tapia Jesús Iván BIO-531
Tavarez Martínez Greta de Monserrat SIF-271, SIF-188, BIO-146
Tellez Cruz Miriam Marisol NSN-53
Tellez-Cruz Miriam Marisol RWE-27
Tellez-Cruz Miriam Marisol RWE-290
Tirado Cantu Pablo RWE-44
Toledo Jose NSN-530
Toledo Guizar Pablo MEM-276
Toledo-Guizar Pablo MEM-306
Tomás Sergio SEM-670
Toriz González Guillermo BIO-136
TORRES ALBERTO CHM-75
Torres Leticia RWE-51



TORRES CASTILLO ALBERTO *CHM-76*
Torres Castro Jaime Agustín *BIO-136*
Torres Castro Jaime Agustín *BIO-136*
Torres Huerta Aidé Minerva *BIO-78*
Torres Rosales Ángel Andrés *SEM-287, SEM-282*
Torres-Castillo A. Alberto *AMC-533*
Torres-Cortés Carina Oliva *LPM-125*
Torres-Delgado Gerardo *AMC-645, CHM-347*
Torres-Hernández Fulgencio Eduardo *SIF-604*
Torres-Martínez Leticia M. *RWE-373*
Torres-Ochoa Jorge Alejandro *THF-123, THF-122*
Torres-Pérez Jonatan *AMC-538*
Torrres Diego *RWE-637*
Tostado-Aguirre Francisco Servando *LPM-509*
Tototzintle Huitle Hugo *LPM-413, TSM-3*
Tovar-Martinez Eduardo *RWE-349*
Trejo Luna Rebeca *SIF-52*
Ungsson Nieblas Manuel de Jesus *NSN-295*
Urbano Peña Maria de los Angeles *AMC-345*
URBINA-RODRÍGUEZ RUBÉN OMAR *BIO-294, BIO-293*
Valdés Madrigal Manuel Alejandro *NSN-339*
Valdez Benjamín *ALD-353*
Valdez Donato *NSN-624, SIF-634*
Valenzuela Benavides José *SIF-335*
Vallejo Márquez Julio César *NSN-668*
Vargas García Jorge Roberto *NSN-409*
Vargas García Vicente *LPM-299*
VARGAS ORTIZ JESUS ROBERTO *NSN-650*
Vargas Rodríguez Everardo *MEM-357*
Vargas Rueda Johan A. *THF-131*
Vargas-Requena Claudia Lucía *BIO-24, BIO-35*
Vazquez-Arenas Jorge *RWE-536*
Vazquez-Lepe Milton Oswaldo *NSN-591*
Vazquez-Morales Cesar *NSN-279*
Vásquez-Agustín M. *LPM-350*
Vázques Arenas Jorge Gabriel *RWE-596*
Vázquez Arenas Jorge Gabriel *RWE-685*
Vázquez Arreguín Roberto *LPM-299*
Vázquez Lepe Milton *BIO-278*
Vázquez-Lepe Milton *CHM-629*
Vázquez – López C. *LPM-599*
Vega García Mónica Paola *NSN-77*



VEGA GONZALEZ MARINA NSN-650
Vega Hernández Javier Issac THF-575
VEGA VALDES EDGAR DE JESUS CHM-76, CHM-75
Vega-Carrillo Héctor René LPM-125
Velarde Díaz Luis David MEM-621
Velarde-Díaz L.D. MEM-654
Velarde-Escobar Oscar J. TSM-671
Velazquez-Cruz E. Isac NSN-174, NSN-66
Velazquez-Nevarez Gonzalo Alonso THF-122, THF-123
VELÁZQUEZ CASTILLO RODRIGO NSN-650
Velázquez Galván Yenni NSN-553, NSN-545
Velázquez Hernández Ruben BIO-67
Velázquez Nevárez Gonzalo Alonso ALD-291
Viatcheslav Michourny SEM-272
Vidal Miguel A. NSN-603
Vidal Borbolla M. Ángel SEM-679
Vidal Borbolla Miguel Ángel THF-681
Vigil Galán Osvaldo RWE-622
Vigueras-Santiago Enrique AMC-551
Vilchis Bravo Heber SEM-669
Vilchis Sanchez Sofia BIO-547
Villa Martínez Gerardo CHM-639
Villa-Martínez G. NSN-147, SEM-143
Villagómez Carlos J. AMC-551
Villalpando Andrea Guadalupe NSN-635
Villaneda Saldivar Berenice LPM-413
Voit Walter MEM-502
Wang Kang L. NSN-343
Yañez Limon J. Martin AMC-360
Yañez Mota Estefanía NSN-77
Yañez-Limón Jose Martín AMC-644
YAÑES LIMÓN JOSÉ MARTÍN THF-592
Yadav Pravind Kumar ALD-346
Yáñez-Limón J.M. THF-126, BIO-262
Yáñez-Limón José Martín AMC-645
Yee Rendón Cristo Manuel SEM-178
Yee-Rendón Ana J. TSM-671
Yee-Rendón Arturo TSM-671
Yee-Rendón C.M. SEM-365
Yee-Rendón Cristo M. RWE-613
Yee-Rendon Cristo M. TSM-671
Yescas-Mendoza Edgardo NSN-66, NSN-174



XII -ICSMV

September 23rd to 27th, 2019 / San Luis Potosí, México

Yu-Gorbatchev Andrei *RWE-614*
Zamora-Peredo L. *SEM-365*
Zamora-Peredo Luis *TRB-83*
Zamudio García Jesús Fernando *SEM-576*
Zarate Luna Uriel Salvador *RWE-367*
Zarate Luna Uriel Salvador *RWE-367*
Zarazúa Morín Elvira *NSN-668*
ZAVALA MORAN ULISES *THF-72*
Zárate Elvia *BIO-302*
Zelaya Orlando *THF-131, THF-283*
Zelaya Ángel Orlando *SEM-506*
zelaya-angel Orlando *NSN-683*
Zelaya-ängel Orlando *SEM-670*
Zendejas B. E. *LPM-599*
Zendejas Leal Blanca Estela *CHM-617*
Centeno Mateo Benito *NSN-77*
Zetina-Banderas Gilberto Jafet *SEM-651*
Zumeta Dubé Inti *RWE-376, RWE-497, RWE-371*
Zumeta Dumbé Inti *RWE-407*



